

CROP AND NUTRITIONAL WATER PRODUCTIVITY OF SWEET POTATO AND TARO

Report to the
Water Research Commission

by

**R Kunz¹, K Reddy¹, T Mthembu¹, S Lake¹,
T Mabhaudhi², V Chimonyo² and V Naiken¹**

¹Centre for Water Resources Research

²School of Agricultural, Earth and Environmental Sciences
University of KwaZulu-Natal, Pietermaritzburg, South Africa

WRC Report No. 3124/1/24
ISBN 978-0-6392-0599-1

March 2024



**UNIVERSITY OF
KWAZULU-NATAL™**

**INYUVESI
YAKWAZULU-NATALI**

Obtainable from

Water Research Commission
Bloukrans Building, Lynnwood Bridge Office Park
4 Daventry Street
Lynnwood Manor
PRETORIA

orders@wrc.org.za or download from www.wrc.org.za

This is the final report for WRC project no. C2019/2020-00088.

DISCLAIMER

This report has been reviewed by the Water Research Commission (WRC) and approved for publication. Approval does not signify that the contents necessarily reflect the views and policies of the WRC, nor does mention of trade names or commercial products constitute endorsement or recommendation for use.

EXECUTIVE SUMMARY

BACKGROUND & MOTIVATION

Indigenous root and tuber food crops (RTCs) exhibit broad agro-ecological adaptability to marginal environments, flexibility in mixed farming systems, ability to produce reasonable yields where most crops cannot, and thus are suitable for production by resource-poor farmers. In addition, their capacity to provide high levels of carbohydrates and nutrients makes RTC production the basis for improving food and nutrition security, particularly at the smallholder household level. Despite the many perceived benefits of producing RTCs, these crops remain side-lined and forgotten, i.e. underutilised.

In the past, research attention has been mainly focused on cereal crops such as wheat, rice and maize, despite the importance of RTCs in sub-Saharan Africa. Furthermore, RTC production and trade has been neglected in favour of other cash crops such as tea, coffee, cotton and cocoa. The neglect of RTCs has also led to the prolonged use of traditional landraces and production techniques that are not necessarily suited to producing high yields. Disproportionate attention has also been given to individual RTCs regarding research on water use characterisation. For example, there has been extensive research on potato and cassava, with some work done on sweet potato. However, information on the water use of taro, tannia and yam remains scarce. The range in water use figures reported in the literature for certain RTCs is large, with taro emerging as having high crop water use.

PROJECT AIMS

The project's overall objective was to measure and model the water use, yield and nutrient content of selected RTCs where little or conflicting information currently exists. Knowledge gaps were identified from a literature review of five RTCs (Aim 1; cf. **Chapters 2 & 3**), which were then addressed through field work (Aim 2; cf. **Chapters 4 & 5**) that focused on (i) an orange flesh sweet potato (OFSP; cultivar 199062.1), and (ii) an upland, eddoe type taro landrace called Dumbe dumbe. A crop simulation model was partially calibrated and used to model crop evapotranspiration (ET) and yield (Y) of each crop (Aim 3; cf. **Sections 4.3.7 & 5.3.7**). The model was then run at a national scale to estimate Y and ET, from which crop water productivity (CWP) was calculated as Y/ET . The product of CWP and nutrient content provided another useful metric called nutritional water productivity (NWP). Maps showing the spatial variability in Y, CWP, NWP, crop cycle and risk of crop failure were developed to improve existing knowledge on these two RTCs (Aim 5; cf. **Chapter 6**). Model simulations were also used to develop land suitability maps for both crops (Aim 4; cf. **Chapter 8**) and to derive site-specific crop coefficients. The latter were used as input for a hydrological model to assess the impact of crop production on downstream water availability (Aim 6; **Chapter 7**). This final project report represents Aim 7, a synthesis of the above information to help promote the sustainable production of OFSP and taro.

OVERVIEW OF INDIGENOUS ROOT & TUBER FOOD CROPS

There is a need to diversify marginal farming systems, and to produce more crop and nutrient yield using less water. A noteworthy strategy is to grow crops that have economic potential and are drought-tolerant and nutrient-dense. RTCs, which are also referred to as "drought insurance" crops, have emerged as a plausible option in addressing food and nutrition insecurity under climate variability and change. RTCs produce underground food and include sweet potato (*Ipomoea batatas*), cassava (*Manihot esculenta*), taro (*Colocasia esculenta*), tannia (*Xanthosoma spp.*) and yam (*Dioscorea spp.*). Their broad agro-ecological adaptability, especially in marginal environments and mixed farming systems, make them central to addressing malnutrition in poor rural households.

Of these five RTCs, sweet potato and taro have been prioritised for further research in South Africa. Sweet potato and taro are mostly cultivated in the Limpopo, North West, Mpumalanga, KwaZulu-Natal and Eastern Cape provinces. Commercial producers regard sweet potato as a cash crop, whereas smallholder farmers produce it mainly for household consumption, but sell the surplus to local markets. Although the literature review highlighted the suitability of RTCs to a wide range of agro-ecologies, it did not provide the amount of water required for their successful production. Research on crop water use of RTCs is scarce in comparison to legume and cereal crops. This has led to a lack of credible values of crop water requirements and water productivity of RTCs. The lack of information has limited the extent to which these crops can be recommended for production in new areas. If these crops are to form part of crop choices for farmers, knowledge is required on production systems and food value chains, crop water use, water productivity, nutrition and health, as well as future production scenarios under projected climate change concerning water availability.

The nutrient content of RTCs is becoming a key component towards their mainstreaming, especially in terms of improving dietary diversity. Nutritional composition requires consideration of both proximate and mineral composition, as well as bioactive compounds. This information was extracted from the available literature and summarised in tables presented in this report, which highlight numerous desirable nutritional and health benefits of RTCs. The tables show a wide range of reported nutrient contents, which highlights the need to study linkages between different growing environments and nutrient composition. Nutrient contents are needed for the calculation of NWP for evaluating impacts of agricultural production on food and nutrition security, especially under limited water availability.

The national policy on Food and Nutrition Security recognises the role of underutilised crops that are nutrient-dense for improving dietary diversity in South African households. Taro has high nutritional value, especially in terms of protein digestibility and mineral composition. Sweet potato provides more protein, carbohydrates and fibre than cassava and its mineral composition (e.g. Mg, K & P) is also superior to that of cassava. More importantly, orange flesh sweet potato (OFSP) can help address vitamin A deficiency in women and children in South Africa. Hence, of the five underutilised RTCs, OFSP and taro exhibit the most potential for addressing national priorities such as poverty alleviation, unemployment and inequality, by creating new value chains in rural areas. OFSP and taro have therefore been prioritised for further research in South Africa. New research projects that target these two RTCs are required to address existing knowledge gaps. The funding of this research project highlights the Water Research Commission's commitment to this strategy. The literature review was then extended, focusing specifically on OFSP and taro.

OVERVIEW OF SWEET POTATO & TARO

Prior to the start of this project, evidence-based research that provided credible estimates of taro's water requirements in South Africa were almost non-existent. The literature review identified only two studies on taro's water use, thus highlighting the fact that taro is one of the most under-researched RTCs. A wide range of crop water requirements have been reported in the literature, based largely on anecdotal evidence. The variability in crop water requirements is largely due to genotype differences in taro. Lowland taro (KwaNgwanase) has higher optimum crop water requirements compared to upland taro (e.g. Umbumbulu landrace), because the latter genotype exhibits greater stomatal control. Hence, yields and CWP are generally higher for upland taro compared to lowland taro.

As noted previously, sweet potato is more nutritious than cassava and has a shorter growing season. When compared to white flesh sweet potato, orange flesh cultivars contain much higher levels of (β -carotene (β -c), and thus their cultivation should be promoted to alleviate vitamin A deficiency, especially in rural households. Although sweet potato is more drought tolerant than taro, mechanisms that allow for drought avoidance usually have a high yield penalty. Despite this, sweet potato can produce good yields with high higher amounts of β -c under water limited conditions, which results in high CWP and

NWP. The latter was higher for most elements (especially β -c) under water-limited conditions, compared to optimum conditions, as shown in numerous studies.

Both sweet potato and taro are regarded as dual-purpose crops, since both their leaves and tubers can be consumed. Furthermore, CWP increases with decreasing water application for both crops. It is clear that more research has been conducted on sweet potato than taro in South Africa. In addition, crop parameters have been developed for both sweet potato and taro, which is important to note, as it facilitated the crop modelling work undertaken by this project. Based on the evidence mentioned above, this project focused its attention on the two prioritised RTCs.

MEASUREMENT OF WATER PRODUCTIVITY: SEASON 2

Introduction

Field trials were conducted at Fountainhill Eco-estate (Wartburg, KwaZulu-Natal) with sufficient fetch to facilitate crop evapotranspiration measurements using two micrometeorological techniques. In the first season (2020/21), the taro trial was abandoned because it was initially affected by excessive weed growth, then severely damaged by animals (bush pigs). Sweet potato was not planted because a postgraduate student decided not to pursue his MSc study due to concerns related to the COVID-19 pandemic. In the second season (2021/22), crop water use, yield and nutrient content of sweet potato and taro were measured at two trial sites at Fountainhill. A brief summary of the methodology and main findings are presented next.

Materials and methods

Crop establishment: Planting of taro corms and OFSP vines was completed at site 1 and 2 on 19 November and 14 December 2021, respectively. Both trials were planted at a target density of 20,000 plants ha^{-1} . At each site, an organic fertiliser was applied at a rate based on fertility results for nitrogen.

Crop water use: Crop water use was estimated using the eddy covariance (EC) and surface renewal (SR) methods. The EC method is considered the “gold” standard, and thus provides the most reliable estimate of crop water use. Since SR is calibrated against EC, it provides similar results. Sensible heat flux was estimated using (i) the classic method, and (ii) dissipation theory.

Crop yield and water productivity: For each trial, a total of 15 plants were harvested from two representative rows. Plants were separated into leaves, vines and storage roots/tubers. Each component was weighed to obtain fresh mass, then air/oven dried to obtain dry mass. CWP in dry kg m^{-3} was determined as the ratio of yield (dry kg ha^{-1}) to crop ET (m^3). CWP was estimated using crop ET measured using the EC method, since it is more accurate than the SR method.

Nutritional water productivity: NWP in dry g m^{-3} was calculated as the product of CWP (dry kg m^{-1}) and nutrient content (g kg^{-1}). The latter was measured for root/tuber and leaf samples in a laboratory. In addition to total C, N and S, the following elements were measured: β -carotene, B, Ca, Cu, Fe, K, Mg, Mn, Mo, Na, P and Zn.

Crop modelling: Both the AquaCrop and SWB models were evaluated for their ability to simulate the water use and yield (biomass and root storage) of OFSP. Existing crop parameter values were sourced from the literature. A partial calibration was done, where measured data was used to adjust (i.e. fine-tune) certain crop parameters (e.g. phenological growth stages) to better represent local landrace and growing conditions. Climate data required by AquaCrop was measured by each EC tower and a nearby automatic weather station at Fountainhill. All soil-related model inputs (i.e. soil water retention parameters and saturated hydraulic conductivity) were measured in the laboratory. Both models were evaluated by comparing simulated vs observed above-ground biomass and storage root growth over the growing season and at harvest using four statistical measures.

Results and discussion

Yield measurements: The harvested fresh and dry storage root yield of OFSP (at 118 DAP) was 34.89 and 12.12 t ha⁻¹ respectively, resulting in a fresh:dry ratio of 2.88 and a dry harvest index (HI) of 55%. Due to the threat of animal damage, OFSP was harvested prematurely, which may have affected the yield. For taro, the harvested fresh and dry tuber yields (at 217 DAP) were 11.79 and 4.91 t ha⁻¹ respectively. Hence, the fresh:dry ratio was 2.40 and the HI was of 76%. The nutrient composition of OFSP leaves was higher than for the storage roots for almost all minerals, especially Ca, Mg and Mn.

Crop water use: Taro's canopy cover development is slower than for OFSP, which means less surface shading and higher soil water evaporation rates in the initial growth stage. Taro can take up to 49 days to emerge, which highlights the need to keep taro plantings weed free for two months after planting. Despite the difference in season length, the EC method provided similar ET measurements of 354 vs 358 mm, compared to 322 and 330 mm from the SR methods. Both the EC and SR methods account for the evaporation of intercepted water, which is not considered by the soil water balance method. CWP was higher for OFSP than taro (3.42 vs 1.37 dry kg m⁻³), which is important to note.

Crop modelling: Although the SWB model performed slightly better at simulating above-ground biomass than AquaCrop, it substantially under-estimated root yield. Hence, SWB significantly under-estimated CWP when compared to AquaCrop. NWP was also under-estimated due to poor simulation of CWP. Hence, the decision was made to use AquaCrop for modelling the water productivity of both RTCs.

MEASUREMENT OF WATER PRODUCTIVITY: SEASON 3

Introduction

In the third season (2022/23), crop water use, yield and nutrient content for OFSP and taro were measured in a greenhouse at UKZN. Both crops were grown under water-stressed (deficit irrigation) and non-stressed (fully irrigated) conditions. A brief summary of the methodology and main findings are presented next.

Materials and methods

Experimental setup: OFSP and taro were planted in four raised beds (two beds per crop) in a greenhouse on 27 October 2022. In each bed, two rows (0.60 m apart) were planted at a spacing of 0.30 m between plants, i.e. 55,556 plants ha⁻¹. Prior to planting, an organic fertiliser was applied to each bed at a rate determined from fertility measurements. A drip irrigation system was installed to supply two beds with 30 and 100% of OFSP's water requirement. The latter was calculated as the product of ET_o measurements and a single crop coefficient, which was adjusted to match the crop's growth stage. An automatic weather station was installed inside the greenhouse to determine daily ET_o. Kemprin® was sprayed regularly to prevent the outbreak of red spider mites, particularly in the two taro beds.

Crop development: Weekly measurements of plant height, leaf number and leaf area were made over the growing season. The latter was used to estimate canopy cover development. In addition, chlorophyll content leaf temperature and stomatal conductance were measured as indicators of plant health. Diurnal measurements of leaf water potential and stomatal conductance were also made for OFSP.

Results and discussion

During load shedding, extreme temperatures (> 55°C) were experienced in the greenhouse, which provided clear evidence that both RTCs are heat tolerant crops. OFSP's leaf number is much higher than for taro, which resulted in higher LAI (and transpiration), as well as greater biomass production. For OFSP, the initial gain in LAI for the unstressed treatment was lost midway through the growth cycle. This suggests that under water limiting conditions, sweet potato can still produce high leaf area, which is important for reducing soil water evaporation, and maintaining biomass production. Leaves exhibited

higher nutrient content than roots/tubers for most of the mineral elements tested (same result obtained in season 2). Furthermore, nutrient contents were higher when the RTCs were water stressed.

Measurements and observations from the unstressed treatment were used to fine-tune existing parameter values available for both RTCs. To further improve model performance, adjustments were made to stress-related parameters using data from the water stressed treatment. These modified parameters provided better estimates of biomass and yield for both crops when water stressed, especially for OFSP. This achievement, which represents a valuable contribution by this project, was important for the modelling work described next, especially for the rainfed model runs.

MODELLING & MAPPING OF WATER PRODUCTIVITY

Introduction

As noted previously, the AquaCrop model was selected to estimate the attainable yield of OFSP and taro. This model is ideally suited to performing multiple seasonal simulations of crop yield in environments where water availability is limited. The model has been successfully linked to the climate and soil databases for all 5,838 altitudinal zones, which facilitates simulations at the national scale.

Materials and methods

The 1,946 quaternary-level catchments were initially delineated by the Department of Water Affairs. Thereafter, each quaternary boundary was sub-divided into three smaller zones of similar altitude, resulting in less spatial variation in climate and soils. In the past, these zones were referred to as quinary sub-catchments but in this report, are called relatively homogeneous response zones (HRZs).

Climate input: Each HRZ has 50 years (1950-1999) of observed rainfall and temperature, which was revised in December 2019. Reference evapotranspiration was estimated from observed temperature, with daily wind speed set to 2 m s⁻¹. Monthly adjustment factors were used to derive rainfall estimates deemed more representative of each HRZ. Daily temperatures were adjusted using lapse rates to account for the altitude difference between the climate station and HRZ.

Soil input: For each HRZ, hydrological soil characteristics (e.g. depth, field capacity and permanent wilting point) were revised for both the A- and B-horizons in February 2022. This information was obtained from data available for each terrain unit (e.g. crest, scarp, midslope, footslope & valley bottom) within each land type. This improved the spatial accuracy of soil data for each HRZ. Saturated hydraulic conductivity was estimated for the A-horizon using well-known equations.

Planting date: For the majority of the HRZs, the first viable planting date occurs in November or December and thus, were selected as fixed planting dates for modelling purposes. The day of planting was set to the beginning of the month (not mid-month) to facilitate more accurate estimation of crop ET, and thus derivation of crop coefficients.

Plant density: Typical plant densities were obtained from the literature for each crop to represent smallholder and commercial farming. For this study, a plant density of 31,447 and 55,556 plants ha⁻¹ was selected for sweet potato. For taro, a plant density of 10,000 and 27,778 plants ha⁻¹ was selected.

Model parameters: Default model parameters for both crops were obtained from the literature. Data collected during the third season facilitated a partial calibration of the model for both crops. The validation was done by comparing simulations against observations from the previous season.

Minimising computational expense: The process of running both AquaCrop for each HRZ has been fully automated to minimise computational expense. Considerable effort was also spent on reducing model run time. In 2015, a national model run for sorghum took 62 hours to complete, which was reduced to

13 hours in 2020. For this project, the run time was further reduced to ~3 hours. However, additional effort is still required in the future to further minimise AquaCrop's run time.

Modelling approach: The automation procedure facilitated the simulation of data for 49 consecutive seasons (1950/51 to 1998/99) using daily climate data as input, from which long-term means and other useful statistics (e.g. inter-seasonal variability) were generated. AquaCrop was run for all 5,838 HRZs, regardless of whether the zone is deemed suitable for rainfed crop production. This approach facilitated the use of model output to identify areas best suited to the cultivation of OFSP and taro. For each HRZ, the crop model simulated attainable yield and accumulated ET under rainfed conditions. Model runs were then repeated for irrigated conditions to obtain maximum yield and water use, from which monthly crop coefficients were calculated for input into ACRU. Hence, four national crop model runs (i.e. for two planting dates & two plant densities) were performed for both rainfed (stressed) and irrigated (unstressed) conditions. Since AquaCrop was used to derive crop coefficients for each HRZ, the crop model runs were completed before the hydrological model runs.

Results and discussion

Crop yield modelling: Yield maps developed from AquaCrop output for rainfed conditions clearly highlight low and high potential areas for OFSP and taro production. Large parts of the country's interior region are deemed too cold for crop cultivation, whereas the western areas are too dry for rainfed cultivation. Planting date has a larger impact on crop yield than plant population and yields are generally higher when OFSP is planted in November than December. Taro planted in November produces higher yields in Limpopo, compared to a December planting for the other provinces. The risk of failure for OFSP is relatively low compared to taro.

Crop and nutritional water productivity: Maps of spatial variation in CWP indicate that taro is less water use efficient than OFSP, due to lower yield simulations. As expected, yield increases with plant density, and thus CWP and NWP are higher. CWP is lower for OFSP planted in November when compared to December. Inter-seasonal variation in CWP for both RTCs is lower for the December planting compared to November. Taro is more water efficient at producing Fe, whereas OFSP is more water efficient for K production. OFSP is most efficient at producing β -c along the coastal region of the Eastern Cape.

HYDROLOGICAL IMPACTS OF CROP PRODUCTION

Introduction

The ACRU model was used to assess the impact of OFSP and taro production on downstream water availability at the catchment scale, relative to the water use by natural vegetation. This model was the preferred choice in numerous other studies that assessed the impacts of land use change on runoff response, simply because ACRU does not require extensive parameterisation in ungauged catchments.

Materials and methods

Model inputs: The same climate and soil data available for each HRZ was again used as input for ACRU. However, reference evapotranspiration was adjusted to A-pan equivalent values using monthly pan factors available for each HRZ.

Rainfall:runoff parameters: Most of the ACRU input parameters that represent rainfall:runoff response (and the land cover/use) are physically based, and thus are measurable. Parameter values used in this project were the same as those used in the previous studies involving the HRZ configuration. However, some parameters were estimated as they were difficult to measure. For example, the coefficient of initial abstraction was calculated from rainfall seasonality and distance from the coastline.

Baseline land cover: Parameter values have been determined for 121 hydrologically relevant clusters of natural vegetation types. For example, remotely sensed values of LAI were used to derived monthly

crop coefficients for each vegetation cluster. In 2020, the Department of Water and Sanitation adopted these clusters as the new baseline against which all potential stream flow reduction activities should be assessed, thus replacing the previous Acocks veld types to represent natural vegetation. To date, the new baseline has been used to assess stream flow reduction potential of (i) sorghum and soybean in 2020, (ii) two bamboo species in 2022, (iii) 15 commercial forestry species, hybrids and clones in 2023, and (iii) OFSP and taro (this project).

Proposed land use: Parameter values were determined for OFSP and taro using approaches adopted in other similar studies to assess stream flow reduction potential. ACRU is sensitive to monthly crop coefficient inputs, and thus considerable effort was spent on deriving suitable values for both crops, as well as for the fallow period. AquaCrop was used to calculate unique crop coefficients for each HRZ, where irrigation was used to artificially remove crop water stress. The use of AquaCrop to derive a unique set of monthly crop coefficients for each HRZ is more robust than using the same monthly values obtained at Fountainhill for all HRZs. The von Hoyningen-Huene equation was used to estimate monthly interception loss using LAI measurements from season 3 for each crop. The fraction of active roots in the topsoil horizon was estimated from the topsoil depth.

Minimising computational expense: Running ACRU for all altitude zones has been computationally automated as part of previous WRC-funded projects. In the past, a national run took approximately 8.5 hours to complete. Effort was again spent on reducing model run time, with ACRU now taking ~40 minutes to complete a national run. This time saving allows for additional modelling scenarios to be considered, i.e. multiple planting dates and plant densities.

Results and discussion

With the exception of only 30 HRZs, the cultivation of OFSP or taro is unlikely to significantly affect the quantity of water available to downstream users. Furthermore, the least impact on downstream water users occurs when taro and OFSP are planted in November and December, respectively. Hence, there is little to no potential of DWS declaring these crops stream flow reduction activities.

MAPPING OF LAND SUITABILITY

Introduction

A land suitability map identifies areas deemed suitable for crop production, thus providing both smallholder and commercial farmers with alternative crop choices. AquaCrop output was analysed to determine whether each HRZ is considered suitable for rainfed production of OFSP and taro. The FAO (1976) approach was used to classify land as either suitable (S) and not suitable (N) for crop production. Suitability was further classified as either high (S1), moderate (S2) or marginal (S3). Similarly, N1 and N2 classifies a zone as either currently or permanently unsuitable for crop production, respectively.

Materials and methods

Different methods have been used to develop land suitability maps, which are categorised as either (i) traditional (i.e. simple), or (ii) modern (i.e. complex) methods. Numerous land suitability studies were assessed, of which nine are presented in this report. Very few of the reviewed studies made use of model simulations to determine land suitability. A three-tier approach was utilised to identify HRZs best suited to the cultivation of each RTC as follows:

Elimination of unsuitable areas (tier 1): HRZs deemed unsuitable for RTC production were eliminated using the following criteria and thresholds: (i) crop cycle > 365 days (too cold); (ii) mean annual rainfall < 400 mm (too dry); (iii) number of yield simulations < 20 out of 49 (too risky); (iv) high inter-seasonal variation in CWP (too variable); and (v) low CWP, thus indicating low yield potential or high water use.

Classification of suitable areas (tier 2): The remaining zones were then deemed suitable for RTC production and grouped into three suitability classes using CWP. The threshold for marginal (S3) suitability was set as half a standard deviation below the mean CWP value. Similarly, the threshold for highly suitable areas (S1) was taken as half a standard deviation above the mean. The remaining suitable zones were classified as moderately suitable (S2).

Consideration of current land use (tier 3): Land use data was also used to eliminate unsuitable crop production areas. Currently unsuitable (N1) land uses include commercial forestry and sugarcane production areas. Similarly, protected areas and large water bodies were classified as permanently unsuitable (N2) land uses.

Subsistence farming areas: The final step involved determining the portion of suitable production areas (S1, S2 and S3) located within existing subsistence farming areas.

Results and discussion

Elimination of unsuitable areas: Long crop cycles exceeding 365 days that resulted from cold temperatures eliminated the most HRZs for both RTCs (2,486-3,307 zones), followed by zones deemed too dry for rainfed crop production. Of the 5,838 HRZs, 3,694 and 4,266 did not satisfy the selected criteria and thresholds for OPSP and taro respectively, and thus were excluded from further analysis.

Classification of suitable areas: The remaining 2,144 (OFSP) and 1,572 (taro) HRZs were considered suitable for crop production. Of these, only 23% were highly suitable for OFSP and taro production. Hence, most of the production areas were classified as moderately suitable. When compared to OFSP, less areas are suited to taro production. Colder regions are better suited to OFSP production than taro.

Consideration of current land use: After considering existing land use, suitable OFSP and taro areas were reduced by 19 and 22%, respectively. This highlights the importance of eliminating unsuitable land uses, since it provides more realistic assessments of land suitability.

Subsistence farming areas: Only 68% of suitable OFSP areas were located within existing subsistence farming areas, of which the majority was classified as moderately suitable. Similarly, only 49% of existing subsistence farming areas were deemed suitable for taro production, most of which was deemed marginally suitable. These results can help guide policy makers to target specific regions for promoting increased production of RTCs under rainfed conditions.

SUMMARY & GENERAL CONCLUSIONS

The literature review focused on five RTCs, namely cassava, sweet potato, taro, tannia and yam. Of these, sweet potato and taro have been prioritised for further research in South Africa. All RTCs store edible carbohydrates (starch) in underground roots, tubers, corms, stems and rhizomes. Nutritionally, the protein content of roots and tubers is low, except for yam. Taro is superior in terms of protein digestibility and mineral composition. The upland, eddoe type uses less water than the dasheen type and can be grown in less fertile soils. The orange flesh cultivars of sweet potato contain higher amounts of β -carotene, which is a precursor of vitamin A, and thus can help alleviate vitamin A deficiency in South Africa. Sweet potato is also the most drought tolerant of the five RTCs considered in the review.

Field work conducted at Fountainhill Eco-estate therefore focused on OFSP and an upland, eddoe type of taro. In the first season, the taro trial was severely damaged by weed infestation and animals. In season 2, OFSP was harvested prematurely due to the threat of animal damage. Sweet potato produced 12.12 dry t ha⁻¹ vs 4.91 dry t ha⁻¹ for taro. Since both crops used similar amounts of water (~355 mm), which was measured using the EC and SR methods, the CWP of OFSP was much higher compared to taro (3.42 vs 1.37 dry kg m⁻³). This project also demonstrated the benefit of estimating

crop evapotranspiration using the SR method, which is far superior to the simple soil water balance approach. Crop coefficients were also determined for the fallow period, which were required as input by the ACRU hydrological model.

In season 3, OFSP and taro were grown under water stressed (deficit irrigation) and unstressed (optimum irrigation) in a greenhouse. Both crops survived extreme temperatures ($> 55^{\circ}\text{C}$) during load shedding events, and thus should be considered heat stress tolerant. For the unstressed treatment, yields of 19.35 and 8.14 dry t ha⁻¹ were obtained for OFSP and taro, respectively. AquaCrop simulated CWP of OFSP more accurately than the SWB model. Measurements from season 3 were also used to partially calibrate the AquaCrop model for both crops, which was then validated against observations from season 2. These modified parameters provided better estimates of biomass and yield for both crops under water stressed conditions, especially for OFSP.

Using the improved crop parameters, AquaCrop was run at a national scale for all 5,838 HRZs, which facilitated the development of land suitability maps for both RTCs using model simulations. The model was run for irrigated and rainfed conditions, each with two planting dates and plant densities. Maps of simulated crop yield, crop cycle and CWP were developed for both crops, which highlighted the spatial variability of these metrics. Both crops are more water use efficient along the coast and adjacent interior in the KwaZulu-Natal and Eastern Cape provinces. Nutrient content of roots/tubers and leaves was measured in a laboratory, then multiplied by CWP to map NWP. Since CWP was higher for OFSP compared to taro, NWP should also be higher. However, taro is more water efficient at producing Fe, whereas OFSP is more water efficient for K production.

AquaCrop was also run to simulate crop water use for unstressed (i.e. irrigated) conditions, from which monthly crop coefficients were calculated as input for the ACRU hydrological model. This approach facilitated the derivation of a unique set of monthly crop coefficients values for each HRZ. ACRU was then run to determine the potential reduction in runoff that may occur due to a land use change from natural vegetation to rainfed production of OFSP and taro. The results showed that neither crop has the potential to significantly impact downstream water availability.

Simulated output from AquaCrop was also used to identify potential cultivation areas using a three-tier approach. The land suitability maps showed that OFSP can be grown in more areas when compared to taro, again highlighting the potential of this OFSP. The consideration of existing land use resulted in more realistic maps highlighting areas that can be planted to both RTCs. Compared to taro, OFSP can be grown in more areas and is more water use efficient, and thus OFSP exhibits greater potential for being mainstreamed into existing agricultural systems.

Overall, the maps provide valuable information on expected crop yields and how they are influenced by planting date and plant density. They identify regions in the country with high productivity potential, where the crop is most efficient at producing storage root/tuber yield as well as nutrient yield. The risk of crop failure maps identify areas where climate variability may result in seasonal crop failures. Hence, the maps provide farmers with valuable information on alternative crop choices and expected yields.

NEW KNOWLEDGE CREATION & INNOVATION

The following outcomes were achieved for the first time in this project: (i) the water use of OFSP and taro was measured using two micrometeorological techniques; (ii) more representative climate and soil datasets were used as input for AquaCrop and ACRU; (iii) AquaCrop was run with a single-layer (not a two-layer) soil profile; (iv) improved parameter values for OFSP and taro were developed; (v) the automation procedure was revised to run AquaCrop and ACRU more efficiently at the national scale; (vi) OFSP was modelled and mapped at the national scale using AquaCrop; (vii) maps of NWP were developed for both RTCs; (viii) risk of crop failure was mapped for both crops; (ix) land suitability maps

were produced from AquaCrop output using a novel approach; (ix) land suitability maps were developed for OFSP; and (x) the hydrological impact of OFSP and taro production non downstream water availability was assessed. These outcomes further improved the validity of model simulations.

KNOWLEDGE GAPS ADDRESSED

The range in water use figures reported in the literature for RTCs is large, with taro exhibiting high water use relative to other RTCs. This project provided accurate water use values for OFSP and taro measured using two micrometeorological techniques. It also addressed knowledge gaps on: (i) spatial variability in CWP and NWP of OFSP; and taro; (ii) where OFSP can potentially be cultivated; and the (iii) hydrological impact of OFSP and taro production on downstream water availability. Revised maps of taro's yield, water productivity and crop cycle were also produced, which supersedes previous work.

RECOMMENDATIONS FOR FUTURE RESEARCH

This project has highlighted the value of national scale crop modelling. However, model accuracy depends more on input data quality, rather than on the model itself. Most importantly, model calibration and testing requires high quality measured datasets obtained from well-designed field experiments. Such experiments are needed across (i) different agro-ecological zones, and for (ii) multiple seasons. Acquiring such datasets is costly and time consuming, and thus long-term funding commitments are vitally important. Furthermore, the climate dataset for each HRZ needs to be extended beyond 1999, preferably by an additional 20 years. National assessments of agricultural and hydrological response to climate variability would provide better assessments of risk using this extended dataset. Since 2014, considerable effort has resulted in much reduced model run times for AquaCrop and ACRU, which has facilitated additional modelling scenarios to be considered. However, more work is needed to further improve model performance so that additional scenarios can be modelled.

CAPACITY BUILDING AND KNOWLEDGE DISSEMINATION

During the four year project, two Honours students and one MSc student have graduated. One part-time PhD student is expected to complete his degree in 2024. He also participated in the PhD Teacher Training Programme at UKZN. Field work conducted at Fountainhill involved the nearby Swayimane community (near Wartburg, KwaZulu-Natal) who assisted with planting and weeding. Disseminating results from this project and engaging with stakeholders was achieved via nine presentations and four popular articles. In addition, the PhD student plans to publish three chapters of his thesis.

THE WAY FORWARD

For the successful adoption of indigenous RTCs by all farmers (from subsistence to commercial), reliable estimates of water use and yield are needed, including maps that show where these crops can potentially be grown. Reliable water use estimates will also help guide future research such as breeding programmes and hopefully, reverse the current status of RTCs as being neglected and underutilised. Furthermore, increased production of RTCs is the catalyst needed to facilitate agricultural diversification. The knowledge gained in this project should also help to promote the production of RTCs (especially OFSP), thus facilitating the expansion of agricultural production in the country. This expansion will help to (i) revive and improve crop cultivation by smallholder farming in rural communities, (ii) bring underutilised arable land back into production, and more importantly, (iii) reduce the level of poverty in rural areas by creating new jobs and allowing smallholder farmers to participate in RTC food value chains. It is also envisaged that national and household food security will improve due to increased cultivation of nutrient-dense RTCs, especially those that are dual purpose (both roots/tubers & leaves are edible), such as OFSP and taro.

ACKNOWLEDGEMENTS

The research reported here formed part of a non-solicited project that was funded and managed by the Water Research Commission (WRC) in Key Strategic Area 4 (Water Utilisation in Agriculture). The project team is sincerely grateful to the WRC for their contribution to this project. The project team also acknowledges the following members of the Reference Group for their valuable contributions and guidance:

Dr L Nhamo	Water Research Commission (Chairperson)
Prof. S Mpandeli	Water Research Commission
Dr S Hlophe-Ginindza	Water Research Commission
Ms M Kapari	Water Research Commission (Intern)
Dr H Araya	Agricultural Research Council
Prof. J Asiwe (the late)	University of Limpopo
Prof. N Jovanovic	University of Western Cape
Dr C Mutengwa	University of Fort Hare
Dr K Tshikolomo	Limpopo Department of Agriculture and Rural Development

We would also like to thank the following individuals:

- Prof. Alistair Clulow (University of KwaZulu-Natal) for providing access to (i) micrometeorological equipment (two complete eddy covariance and surface renewal), and (ii) a plant canopy analyser used by this project at no cost, (iii) programming of data loggers, and for (iv) advice and guidance provided to Mr Kyle Reddy regarding his PhD study.
- Mr Vivek Naiken (University of KwaZulu-Natal) for his assistance with wiring, programming and installing instrumentation at Fountainhill Eco-estate and in the greenhouse at UKZN.
- Prof. Mark Laing (University of KwaZulu-Natal) for guidance provided on nutrient analyses.
- Dr Richard Burgdorf and Glen Cooper (Institute for Commercial Forestry Research) for their valuable advice and expertise in laboratory measurements of soil and nutritional properties.
- Prof. Albert Modi for obtaining taro material (at no cost) required for the greenhouse tunnel experiment conducted during the 2022/23 season.
- Mr Simon Lake and Mr Thando Mthembu for creating all the maps shown in this document.

Lastly, we are grateful for and acknowledge the financial contributions received from the uMngeni Resilience Project through Prof. Mabhaudhi, in particular for the taro material and fertiliser purchased for use at Fountainhill. In addition, the uMngeni Resilience Project shared travel expenses to and from Fountainhill and kindly donated six soil moisture probes for use in the second season.

This page was intentionally left blank

TABLE OF CONTENTS

EXECUTIVE SUMMARY	I
TABLE OF CONTENTS.....	XIII
LIST OF FIGURES.....	XVIII
LIST OF TABLES	XXV
LIST OF ABBREVIATIONS	XXIX
LIST OF SYMBOLS	XXXIII
REPOSITORY OF DATA.....	XXXVII
1 INTRODUCTION.....	1
1.1 BACKGROUND & RATIONALE.....	1
1.2 PROJECT OBJECTIVE & SPECIFIC AIMS	2
1.3 PROJECT SCOPE & REPORT STRUCTURE	2
2 OVERVIEW OF UNDERUTILISED ROOT & TUBER FOOD CROPS.....	5
2.1 RTC CLASSIFICATION	5
2.2 GLOBAL, REGIONAL & LOCAL PRODUCTION.....	6
2.3 RTC NEGLECT IN SSA	7
2.4 AGRONOMY OF RTC PRODUCTION	7
2.4.1 Propagation material.....	8
2.4.2 Plant density	8
2.4.3 Fertiliser recommendations	9
2.4.4 Climate and site requirements.....	9
2.5 NUTRIENT CONTENT	10
2.5.1 Proximate composition	10
2.5.2 Mineral composition.....	11
2.5.3 Bioactive compounds.....	11
2.5.4 Anti-nutritional factors	11
2.5.5 Linking nutrient content to water productivity	11
2.5.6 Converting nutrition units	13
2.6 RESEARCH AGENDA FOR UNDERUTILISED CROPS	13
2.7 SUMMARY & CONCLUSIONS	14
3 OVERVIEW OF SWEET POTATO & TARO	16
3.1 CLIMATE & SITE REQUIREMENTS	16
3.1.1 Sweet potato.....	16
3.1.2 Taro.....	17
3.2 CROP WATER USE, YIELD & WATER PRODUCTIVITY.....	18
3.2.1 Sweet potato	18
3.2.2 Taro.....	21
3.3 NUTRITIONAL WATER PRODUCTIVITY	22
3.3.1 Sweet potato	22
3.3.2 Taro.....	24
3.4 SUMMARY & CONCLUSIONS	25
4 MEASUREMENT OF WATER PRODUCTIVITY: SEASON 2.....	26
4.1 INTRODUCTION.....	26

4.2	MATERIALS AND METHODS	26
4.2.1	Site description	26
4.2.2	Planting material	27
4.2.3	Experimental design	28
4.2.4	Agronomic practices	29
4.2.5	Instrumentation	30
4.2.6	Data collection	31
4.2.7	Crop modelling.....	35
4.3	RESULTS AND DISCUSSION.....	37
4.3.1	Climate data.....	37
4.3.2	Soil properties.....	39
4.3.3	Crop development	41
4.3.4	Crop health	47
4.3.5	Crop water use and yield	50
4.3.6	Crop and nutritional water productivity	52
4.3.7	Crop modelling.....	54
4.4	SUMMARY AND CONCLUSIONS.....	60
5	MEASUREMENT OF WATER PRODUCTIVITY: SEASON 3	63
5.1	INTRODUCTION.....	63
5.2	MATERIALS AND METHODS	63
5.2.1	Planting material	63
5.2.2	Experimental design	63
5.2.3	Agronomic practices	63
5.2.4	Instrumentation	65
5.2.5	Data collection	66
5.2.6	Crop modelling.....	68
5.3	RESULTS AND DISCUSSION.....	74
5.3.1	Climate data.....	74
5.3.2	Soil properties.....	78
5.3.3	Crop development	80
5.3.4	Crop health	84
5.3.5	Crop growth and yield.....	89
5.3.6	Nutrient content	90
5.3.7	Crop modelling.....	90
5.4	SUMMARY AND CONCLUSIONS.....	98
6	MODELLING OF CROP WATER PRODUCTIVITY	101
6.1	INTRODUCTION.....	101
6.2	METHODOLOGY	101
6.2.1	Model description.....	101
6.2.2	Model inputs	103
6.2.3	Model parameters	108
6.2.4	Minimising computational expense.....	109
6.2.5	Modelling approach	109
6.3	RESULTS AND DISCUSSION.....	110

6.3.1	Yield	110
6.3.2	Crop cycle	125
6.3.3	Risk of crop failure	130
6.3.4	Crop water productivity	135
6.3.5	Nutritional water productivity.....	141
6.4	SUMMARY AND CONCLUSIONS.....	145
7	HYDROLOGICAL IMPACTS OF CROP PRODUCTION	147
7.1	INTRODUCTION.....	147
7.2	METHODOLOGY	147
7.2.1	Model description.....	147
7.2.2	Model inputs	148
7.2.3	Land cover parameters.....	148
7.2.4	Rainfall:runoff parameters	153
7.2.5	Minimising computational expense.....	154
7.2.6	Modelling approach	154
7.3	RESULTS AND DISCUSSION.....	154
7.3.1	Crop water use	155
7.3.2	Reduction in annual runoff.....	155
7.3.3	Impact on low flows	158
7.4	SUMMARY AND CONCLUSIONS.....	161
8	MAPPING OF LAND SUITABILITY	162
8.1	INTRODUCTION.....	162
8.2	REVIEW OF MAPPING TECHNIQUES.....	162
8.3	METHODOLOGY	163
8.3.1	Elimination of unsuitable area	163
8.3.2	Classification of suitable areas	165
8.3.3	Consideration of current land use.....	166
8.3.4	Production in subsistence farming areas.....	166
8.4	RESULTS AND DISCUSSION.....	166
8.4.1	Elimination of unsuitable areas.....	166
8.4.2	Classification of suitable areas	168
8.4.3	Consideration of current land use.....	171
8.4.4	Final land suitability maps.....	172
8.4.5	Production in subsistence farming areas.....	177
8.5	SUMMARY AND CONCLUSIONS.....	178
9	GENERAL CONCLUSIONS, RECOMMENDATIONS & FUTURE RESEARCH.....	180
9.1	SUMMARY OF APPROACH.....	180
9.1.1	Literature review	180
9.1.2	Experimental work	180
9.1.3	Crop and hydrological modelling	181
9.1.4	Land suitability mapping	182
9.2	SUMMARY OF MAIN FINDINGS.....	182
9.2.1	Literature review	182
9.2.2	Experimental work	183

9.2.3	Crop modelling.....	184
9.2.4	Hydrological modelling.....	184
9.2.5	Land suitability mapping	185
9.3	LIMITATIONS AND ASSUMPTIONS.....	185
9.3.1	Fallow period crop coefficients	185
9.3.2	Nutritional water productivity.....	185
9.3.3	Initial soil water content	186
9.3.4	Crop evapotranspiration	186
9.3.5	Increasing climate variability.....	186
9.3.6	Model calibration.....	186
9.3.7	Regional upscaling	187
9.4	REVISITING THE PROJECT AIMS	187
9.5	RECOMMENDATIONS AND FUTURE RESEARCH	188
9.5.1	Measuring crop water use and yield.....	188
9.5.2	Crop modelling.....	189
9.5.3	Land suitability mapping	190
9.5.4	Additional performance improvements	191
9.5.5	Development of seed systems.....	191
9.5.6	Development of agronomic guidelines	191
	REFERENCES.....	193
10	APPENDIX_A.....	212
10.1	DATA STORAGE	212
11	APPENDIX_B.....	213
11.1	CAPACITY BUILDING	213
11.1.1	Postgraduate capacity building.....	213
11.1.2	Institutional capacity building.....	216
11.1.3	Community-based capacity building.....	217
12	APPENDIX_C.....	218
12.1	TECHNOLOGY TRANSFER.....	218
12.1.1	Presentations	218
12.1.2	Popular articles	219
12.1.3	Papers.....	219
13	APPENDIX_D.....	220
13.1	SUMMARY OF LITERATURE REVIEW FINDINGS.....	220
14	APPENDIX_E.....	223
14.1	MEASURED NUTRIENT CONTENTS FROM SEASON 2.....	223
14.2	MEASURED NUTRIENT CONTENTS FROM SEASON 3.....	225
15	APPENDIX_F.....	226
15.1	Dry biomass accumulation for OFSP	226
15.2	Dry biomass accumulation for taro.....	227
16	APPENDIX_G	228
16.1	CALIBRATION & VALIDATION STATISTICS	228
16.2	DEFAULT AQUACROP PARAMETERS	229
16.3	MODEL INPUTS AND PARAMETERS: SEASON 2.....	233

16.4	MODEL INPUTS AND PARAMETERS: SEASON 3.....	234
17	APPENDIX_H.....	238
17.1	MINIMISING COMPUTATIONAL EXPENSE IN 2015.....	238
17.1.1	Background.....	238
17.1.2	Desktop PC vs laptop.....	238
17.1.3	RAM drive size.....	238
17.1.4	Automation procedure.....	239
17.1.5	Model run time.....	239
17.2	FURTHER IMPROVEMENTS MADE IN 2019.....	240
17.2.1	Desktop PC.....	240
17.2.2	Derivation of smaller tasks.....	240
17.2.3	Load balancing.....	240
17.2.4	Maximum crop cycle.....	240
17.2.5	Automation procedure.....	240
17.2.6	Model run time.....	241
17.3	ADDITIONAL IMPROVEMENTS IN 2023.....	241
17.3.1	Climate file length.....	241
17.3.2	Seasonal simulations.....	242
17.3.3	RAM drive size.....	242
17.3.4	RAM drive type.....	243
17.3.5	Maximum crop cycle.....	243
17.3.6	Sequential vs parallel runs.....	244
17.3.7	Derivation of smaller tasks.....	244
17.3.8	Load balancing: slower PC.....	245
17.3.9	WSL 1 vs WSL 2.....	246
17.3.10	Load balancing: faster PC.....	248
17.3.11	Automation procedure.....	248
17.3.12	Model run time.....	250
18	APPENDIX_I.....	251
18.1	INTER-SEASONAL VARIATION IN CWP: OFSP.....	251
18.2	INTER-SEASONAL VARIATION IN CWP: TARO.....	253
19	APPENDIX_J.....	255
19.1	TRADITIONAL METHODS.....	255
19.1.1	Case study 1: Holl et al. (2007).....	255
19.1.2	Case study 2: Jewitt et al. (2009a).....	255
19.1.3	Case study 3: Kunz et al. (2015b).....	256
19.1.4	Case study 4: Khalid et al. (2021).....	257
19.2	MODERN TECHNIQUES.....	257
19.2.1	Machine learning.....	257
19.2.2	Analytical hierarchy process.....	259
19.3	DISCUSSION AND CONCLUSIONS.....	261
20	APPENDIX_K.....	263
20.1	NATIONAL LAND COVER OF 2009.....	263
20.2	NATIONAL LAND COVER OF 2018.....	263

LIST OF FIGURES

Figure 2-1	Images of a) sweet potato plant and root, b) cassava plant and root, c) taro plant and tuber, d) tannia tuber, e) yam tuber and f) yam plant	5
Figure 2-2	Number of published articles from January 2000 to July 2020 looking at water use (WU), water productivity (WP), water use efficiency (WUE) or rain use efficiency (RUE) and drought/water stress for selected root and tuber crops	7
Figure 4-1	Propagation of (a) orange flesh OFSP (199062.1 cultivars) and (b) taro (Dumbe dumbe landrace) in raised greenhouse beds located at the University of KwaZulu-Natal in Pietermaritzburg	28
Figure 4-2	Satellite-based image showing the location of the two trial sites at Fountainhill Eco-estate (source: Google Earth®).....	28
Figure 4-3	Micrometeorological equipment installed at the (a) taro and (b) OFSP trial sites located within the Fountainhill Eco-estate.....	30
Figure 4-4	Reference evapotranspiration (ET_0) measured by the eddy covariance (EC) system compared to that obtained from the Fountainhill (FH) weather station	38
Figure 4-5	Variation in maximum (brown line) temperature, minimum (grey line) temperature, ET_0 (blue line) and rainfall (black bars) from 19 November 2021 (0 DAP) to 27 June 2022 (220 DAP) at Fountainhill Eco-estate	39
Figure 4-6	Plant height of OFSP grown under rainfed conditions over the 2021/22 growing season at Fountainhill (Mthembu, 2023).....	42
Figure 4-7	Plant height of taro grown under rainfed conditions over the 2021/22 growing season at Fountainhill (Reddy, 2024)	42
Figure 4-8	Leaf number of OFSP grown under rainfed conditions over the 2021/22 growing season at Fountainhill (Mthembu, 2023).....	43
Figure 4-9	Leaf number of taro grown under rainfed conditions over the 2021/22 growing season at Fountainhill (Reddy)	43
Figure 4-10	Leaf area index of OFSP grown under rainfed conditions over the 2021/22 growing season at Fountainhill (Mthembu, 2023).....	44
Figure 4-11	Leaf area index of taro grown under rainfed conditions over the 2021/22 growing season at Fountainhill (Reddy, 2024)	44
Figure 4-12	Estimated canopy cover of OFSP grown under rainfed conditions over the 2021/22 growing season at Fountainhill (Mthembu, 2023)	45
Figure 4-13	Estimated canopy cover of taro grown under rainfed conditions over the 2021/22 growing season at Fountainhill (Reddy, 2024).....	45
Figure 4-14	Fresh biomass accumulation of OFSP grown under rainfed conditions over the 2021/22 growing season at Fountainhill (Mthembu, 2023)	46
Figure 4-15	Dry biomass accumulation of OFSP grown under rainfed conditions over the 2021/22 growing season at Fountainhill (Mthembu, 2023)	46

Figure 4-16 Fresh biomass accumulation of taro grown under rainfed conditions over the 2021/22 growing season at Fountainhill (Reddy, 2024) 47

Figure 4-17 Dry biomass accumulation of taro grown under rainfed conditions over the 2021/22 growing season at Fountainhill (Reddy, 2024) 47

Figure 4-18 Chlorophyll content index of OFSP grown under rainfed conditions over the 2021/22 growing season at Fountainhill (Mthembu, 2023) 48

Figure 4-19 Chlorophyll content index of taro grown under rainfed conditions over the 2021/22 growing season at Fountainhill (Reddy, 2024)..... 48

Figure 4-20 Stomatal conductance and leaf temperature of OFSP grown under rainfed conditions over the 2021/22 growing season at Fountainhill (Mthembu, 2023) 49

Figure 4-21 Stomatal conductance and leaf temperature of OFSP grown under rainfed conditions over the 2021/22 growing season at Fountainhill (Mthembu, 2023) 49

Figure 4-22 Evidence of animal entry (a) and damage (b) to OFSP roots grown at Fountainhill Eco-estate (trial site 2) during the 2021/22 season 51

Figure 4-23 Oven-drying of taro (a) leaves, stems and roots, and (b) corms that were harvested on 24 June 2022 52

Figure 4-24 Comparison between simulated (AquaCrop) and observed canopy cover development for OFSP grown under rainfed conditions over the 2021/22 season at Fountainhill (after Mthembu, 2023)..... 55

Figure 4-25 Comparison between simulated (SWB) and observed leaf area index for OFSP grown under rainfed conditions over the 2021/22 season at Fountainhill (after Mthembu, 2023) 56

Figure 4-26 Comparison between simulated (AquaCrop) and observed dry above-ground biomass for OFSP grown under rainfed conditions over the 2021/22 season at Fountainhill (after Mthembu, 2023)..... 56

Figure 4-27 Comparison between simulated (SWB) and observed above-ground biomass for OFSP grown under rainfed conditions over the 2021/22 season at Fountainhill (after Mthembu, 2023)..... 56

Figure 4-28 Comparison between simulated (AquaCrop model) and observed dry storage root yields for OFSP under rainfed conditions over the 2021/22 growing season (after Mthembu, 2023)..... 57

Figure 4-29 Comparison between simulated (SWB model) and observed dry storage root yields for OFSP under rainfed conditions over the 2021/22 season at Fountainhill (after Mthembu, 2023)..... 57

Figure 4-30 Comparison between profile water content measured by CS616 probes at Fountainhill and simulations by the SWB and AquaCrop model (after Mthembu, 2023)..... 58

Figure 5-1 Sweet potato and taro grown under two water treatments (i.e. 30% and 100% of CWR) 64

Figure 5-2 Web-based monitoring of weather conditions (insider and outside), soil water content and battery status in the greenhouse at UKZN over the 2022/23 growing season 66

Figure 5-3	Parameters required by AquaCrop to simulate canopy cover development (Raes et al., 2012).....	71
Figure 5-4	Period of potential vegetative growth for determinant and indeterminate crops (Raes, 2016a).....	72
Figure 5-5	Variation in temperature (maximum & minimum) measured inside the greenhouse over the 220-day growing period in season 3.....	75
Figure 5-6	Variation in relative humidity (maximum & minimum) measured inside the greenhouse over the 220-day growing period in season 3	75
Figure 5-7	Variation in average wind speed measured inside the greenhouse over the 220-day growing period in season 3.....	76
Figure 5-8	Variation in average daily ET_o and incoming solar radiation measured inside the greenhouse over the 220-day growing period in season 3	76
Figure 5-9	Variation in reference evaporation (ET_o) explained by incoming solar radiation (R_s) measured inside the greenhouse for season 3	76
Figure 5-10	Daily air temperature measured inside a greenhouse during December 2022.....	77
Figure 5-11	Half-hourly temperatures recorded on 15 December 2022 by three sensors inside a greenhouse at UKZN, where temperatures peaked during two load shedding events....	77
Figure 5-12	(a) Healthy vs (b) heat-stressed leaves of OFSP during the 2022/23 season	78
Figure 5-13	(a) Healthy vs (b) heat-stressed leaves of taro during the 2022/23 season	78
Figure 5-14	Measured plant height for OFSP and taro for both water treatments, i.e. 30% and 100% of crop water requirement (CWR).....	80
Figure 5-15	Measured leaf number for sweet potato and taro for both water treatments (i.e. 30% and 100% of CWR).....	81
Figure 5-16	Measured leaf area index for OFSP and taro for both water treatments (30% and 100% of CWR)	82
Figure 5-17	Estimated canopy cover for OFSP and taro for water both treatments (i.e. 30% and 100% of CWR)	82
Figure 5-18	Total fresh biomass accumulation for OFSP (30% of CWR)	83
Figure 5-19	Total fresh biomass accumulation for OFSP (100% of CWR)	83
Figure 5-20	Total fresh biomass accumulation for taro (30% of CWR)	84
Figure 5-21	Total fresh biomass accumulation for taro (100% of CWR)	84
Figure 5-22	Measured chlorophyll content index for OFSP and taro for both water treatments (i.e. 30% and 100% of CWR).....	85
Figure 5-23	Measured leaf temperature for OFSP and taro for both water treatments (i.e. 30% and 100% of CWR).....	86
Figure 5-24	Measured stomatal conductance for OFSP and taro for both water treatments (i.e. 30% and 100% of CWR).....	87
Figure 5-25	Measured diurnal leaf water potential for OFSP for both water treatments (i.e. 30% and 100% CWR).....	88

Figure 5-26 Measured stomatal conductance for OFSP for both water treatments (i.e. 30% and 100% of CWR)	88
Figure 5-27 Diurnal weather conditions such as average air temperature (T_{air_avg}), average relative humidity (RH_avg) and net irradiance (R_n)	89
Figure 5-28 Comparison of simulated against observed canopy cover development for OFSP and taro (unstressed water treatment).....	95
Figure 5-29 Comparison of simulated against observed canopy cover development for OFSP and taro (stressed water treatment).....	95
Figure 5-30 Comparison of observed and simulated canopy cover development for OFSP and taro under rainfed conditions in season 2.....	98
Figure 6-1 The structural components of AquaCrop, including stress responses and the functional linkages between them (Steduto et al., 2012)	102
Figure 6-2 Depth of the A-horizon determined from the terrain unit soil polygons for all HRZs	105
Figure 6-3 Depth of the B-horizon determined from the terrain unit soil polygons for all HRZs	105
Figure 6-4 Total soil depth determined from the terrain unit soil polygons for all HRZs.....	105
Figure 6-5 Comparison of total available water between the previous (TAW_{OLD}) and revised (TAW_{NEW}) soil properties for each HRZ.....	106
Figure 6-6 Differences in total available water (TAW) between the revised (TAW_{NEW}) and previous (TAW_{OLD}) soil properties for each HRZ.....	106
Figure 6-7 The rainfall-runoff relationship as a function of the topsoil wetness (RAES, 2016a)	107
Figure 6-8 Histogram of the average planting month determined from 50 years of climate record for each of the 5,838 altitude zones (Kunz et al., 2020)	108
Figure 6-9 Averaged seasonal yield for OFSP planted in November at a density of (a) 31,447 and (b) 55,556 plants ha^{-1}	113
Figure 6-10 Averaged seasonal yield for OFSP planted in December at a density of (a) 31,447 and (b) 55,556 plants ha^{-1}	114
Figure 6-11 Averaged seasonal yield for taro planted in November at a density of (a) 10,000 and (b) 27,000 plants ha^{-1}	115
Figure 6-12 Averaged seasonal yield for taro planted in December at a density of (a) 10,000 and (b) 27,000 plants ha^{-1}	116
Figure 6-13 Relationship between non-zero seasonal yield averages for taro and the inter-seasonal variability in yield across 2,452 HRZs, as simulated by the AquaCrop model	118
Figure 6-14 Inter-seasonal variation in yield for OFSP planted in November at a density of (a) 31,447 and (b) 55,556 plants ha^{-1}	119
Figure 6-15 Inter-seasonal variation in yield for OFSP planted in December at a density of (a) 31,447 and (b) 55,556 plants ha^{-1}	120
Figure 6-16 Inter-seasonal variation in yield for taro planted in November at a density of (a) 10,000 and (b) 27,000 plants ha^{-1}	121
Figure 6-17 Inter-seasonal variation in yield for taro planted in December at a density of (a) 10,000 and (b) 27,000 plants ha^{-1}	122

Figure 6-18 Comparison of taro yields simulated using the previous (Y_{OLD}) and revised (Y_{NEW}) soil properties for each HRZ	123
Figure 6-19 Differences in taro yields simulated using the revised (Y_{NEW}) and previous (Y_{OLD}) soil properties for each HRZ	123
Figure 6-20 Comparison of taro yields simulated using the revised soils for two-layer vs one-layer soil profiles	124
Figure 6-21 Differences in taro yields simulated using the revised soils for one-layer vs two-layer soil profile in each HRZ	124
Figure 6-22 Averaged crop cycle for OFSP planted in November at a density of (a) 31,447 and (b) 55,556 plants ha^{-1}	126
Figure 6-23 Averaged crop cycle for OFSP planted in December at a density of (a) 31,447 and (b) 55,556 plants ha^{-1}	127
Figure 6-24 Averaged crop cycle for taro planted in November at a density of (a) 10,000 and (b) 27,000 plants ha^{-1}	128
Figure 6-25 Averaged crop cycle for taro planted in December at a density of (a) 10,000 and (b) 27,000 plants ha^{-1}	129
Figure 6-26 Risk of failure for OFSP planted in November at a density of (a) 31,447 and (b) 55,556 plants ha^{-1}	131
Figure 6-27 Risk of failure for OFSP planted in December at a density of (a) 31,447 and (b) 55,556 plants ha^{-1}	132
Figure 6-28 Risk of failure for taro planted in November at a density of (a) 10,000 and (b) 27,000 plants ha^{-1}	133
Figure 6-29 Risk of failure for taro planted in December at a density of (a) 10,000 and (b) 27,000 plants ha^{-1}	134
Figure 6-30 Averaged seasonal CWP for OFSP planted in November at a density of (a) 31,447 and (b) 55,556 plants ha^{-1}	137
Figure 6-31 Averaged seasonal CWP for OFSP planted in December at a density of (a) 31,447 and (b) 55,556 plants ha^{-1}	138
Figure 6-32 Averaged seasonal CWP for taro planted in November at a density of (a) 10,000 and (b) 27,000 plants ha^{-1}	139
Figure 6-33 Averaged seasonal CWP for taro planted in December at a density of 27,778 plants ha^{-1}	140
Figure 6-34 Seasonal crop water productivity (average of 49 seasons) for taro per quinary sub-catchment as simulated by AquaCrop (Kunz and Mabhaudhi, 2023)	141
Figure 6-35 NWP_{Fe} for (a) OFSP and (b) taro planted in November at the lower density	142
Figure 6-36 NWP_K for (a) OFSP and (b) taro planted in November at the lower density	143
Figure 6-37 $NWP_{\beta-c}$ for OFSP planted in November at a density of 31,447 plants ha^{-1}	144
Figure 6-38 NWP_{Zn} for taro planted in November at a density of 10,000 plants ha^{-1}	145
Figure 7-1 Structure of the ACRU agro-hydrological modelling system (Schulze, 1995)	148

Figure 7-2	Histograms of the percentage reduction in mean annual runoff (MAR) per HRZ that may result from a change in land use from natural vegetation to (a) OFSP and (b) taro cultivation	156
Figure 7-3	Location of HRZs where the reduction in mean annual runoff exceeds 10% that may occur due to a land cover change from natural vegetation to OFSP cultivation	157
Figure 7-4	Location of HRZs where the reduction in mean annual runoff exceeds 10% that may occur due to a land cover change from natural vegetation to taro cultivation.....	157
Figure 7-5	Histogram of the percentage reduction in low flows per HRZ that may result from a change in land use from natural vegetation to (a) OFSP and (b) taro cultivation	159
Figure 7-6	Location of HRZs where the reduction in runoff during the low flow period exceeds 25% that may occur due to a land cover change from natural vegetation to OFSP planted in December at the higher density.....	160
Figure 7-7	Location of HRZs where the reduction in runoff during the low flow period exceeds 25% that may occur due to a land cover change from natural vegetation to taro planted in December at the higher density.....	160
Figure 8-1	Relationship between AquaCrop simulations of stomatal stress and leaf expansion stress for taro	164
Figure 8-2	Relationship between yield and crop water productivity (CWP) for taro (1 st November at 10,000 plants ha ⁻¹), based on AquaCrop simulations	165
Figure 8-3	Relationship between water productivity and crop yield of maize produced from October 2010 to September 2011 in Morocco (Goudrian and Bastiaanssen, 2013)	165
Figure 8-4	Typical bell-shape curve showing a normal distribution of values within three standard deviations (± 3) of the mean (0) (source: Google image).....	166
Figure 8-5	Suitable areas for rainfed production of OFSP planted in November at a density of 31,447 plants ha ⁻¹	168
Figure 8-6	Suitable areas for rainfed production of taro planted in November at a density of 10,000 plants ha ⁻¹	168
Figure 8-7	Histogram showing suitability classes for OFSP planted in November at a density of 31,447 plants ha ⁻¹ , based on AquaCrop simulations of crop water productivity	169
Figure 8-8	Histogram showing suitability classes for taro planted in November at a density of 10,000 plants ha ⁻¹ , based on AquaCrop simulations of crop water productivity	169
Figure 8-9	Land suitability classification for rainfed production of OFSP planted in November at a density of 31,447 plants ha ⁻¹	170
Figure 8-10	Land suitability classification for rainfed production of taro planted in November at a density of 10,000 plants ha ⁻¹	170
Figure 8-11	Final land suitability map for rainfed production of OFSP planted in (a) November and (b) December at a density of 31,447 plants ha ⁻¹	173
Figure 8-12	Final land suitability map for rainfed production of OFSP planted in (a) November and (b) December at a density of 55,556 plants ha ⁻¹	174

Figure 8-13	Final land suitability map for rainfed production of taro planted in (a) November and (b) December at a density of 10,000 plants ha ⁻¹	175
Figure 8-14	Final land suitability map for rainfed production of taro planted in (a) November and (b) December at a density of 27,000 plants ha ⁻¹	176
Figure 8-15	Suitable production areas located within existing subsistence farming areas for OFSP planted in November	178
Figure 8-16	Suitable production areas located within existing subsistence farming areas for taro planted in November	178
Figure 15-1	Total dry biomass accumulation for OFSP (30% of CWR)	226
Figure 15-2	Total dry biomass accumulation for OFSP (30% of CWR)	226
Figure 15-3	Total dry biomass accumulation for taro (30% of CWR)	227
Figure 15-4	Total dry biomass accumulation for taro (100% of CWR)	227
Figure 17-1	Difference in average taro yield simulated by AquaCrop when the maximum allowable crop cycle was reduced from 396 to 365 days	244
Figure 17-2	Increase in AquaCrop run time to complete simulations for 14 HRZs, each with 10 years of input climate data, using the slower PC with 12 threads.....	245
Figure 18-1	Inter-seasonal variation in CWP for OFSP planted in November at a density of (a) 31,447 and (b) 55,556 plants ha ⁻¹	251
Figure 18-2	Inter-seasonal variation in CWP for OFSP planted in December at a density of (a) 31,447 and (b) 55,556 plants ha ⁻¹	252
Figure 18-3	Inter-seasonal variation in CWP for taro planted in November at a density of (a) 10,000 and (b) 27,000 plants ha ⁻¹	253
Figure 18-4	Inter-seasonal variation in CWP for taro planted in December at a density of (a) 10,000 and (b) 27,000 plants ha ⁻¹	254
Figure 19-1	Land suitability map for soybean production (Jewitt et al., 2009a)	256
Figure 19-2	Land suitability map for soybean production (Kunz et al., 2015c).....	256
Figure 19-3	Land suitability map for taro in KZN using MaxEnt (Mugiyo et al., 2022)	259
Figure 19-4	Jack-knife plot evaluating the relative importance of environmental variables for predicting suitability for taro cultivation (Mugiyo et al., 2022)	259
Figure 19-5	Land suitability map for taro based on AHP (Mugiyo et al., 2021b)	261
Figure 20-1	Location of areas considered unsuitable for crop production in South Africa (after Khomo, 2014).....	263
Figure 20-2	Unsuitable land uses for crop production based on the 2018 national land cover dataset (Lake, 2022).....	264

LIST OF TABLES

Table 1-1	Guide to the chapter that addresses each project aim.....	3
Table 2-1	Classification and origin of root and tuber crops in sub-Saharan Africa (Lebot, 2019).....	6
Table 2-2	List of nutritional constituents of root and tuber crops.....	10
Table 2-3	Conversion factors for nutritional composition data (FAO, 2012)	13
Table 3-1	Yield and water balance components per treatment for sweet potato, from which crop water use (ET) and water productivity (CWP) were estimated (Masango, 2015)	19
Table 3-2	Water use and yield components of three sweet potato cultivars (A40, A45 and 199062.1) under two ridge types (peaked and flattened) at Fountainhill (FH) and Umbumbulu (UM) (Dladla et al., 2019)	19
Table 3-3	Dry tuber yield, total biomass, ET and CWP of OFSP (Nyathi, 2019)	20
Table 3-4	Yield, harvest index and CWP of two taro landraces grown under a rainshelter at three irrigation levels over two seasons (Mabhaudhi, 2012)	21
Table 3-5	Nutritional water productivity of β -carotene ($NWP_{\beta-c}$) for OFSP (Masango, 2015)	22
Table 3-6	Nutritional water productivity (NWP) of orange and white flesh sweet potato under three water treatments (Mulovhedzi, 2017)	22
Table 3-7	Nutrient content of OFSP tubers obtained for the 2013/14 and 2014/15 growing seasons (Nyathi et al., 2019a)	23
Table 3-8	Nutrient content of three sweet potato cultivars under two water treatments (Mabhaudhi et al., 2019).....	24
Table 3-9	Nutritional water productivity of three sweet potato cultivars under two water treatments (Mabhaudhi et al., 2019).....	24
Table 3-10	Average nutritional content of taro tubers (UM landrace) under two water treatments (Shelembe, 2020)	25
Table 4-1	Climate data obtained from two automatic weather stations located at Bruyns Hill and Fountainhill	27
Table 4-2	Annual means/totals of climate variables measured by the AWS located at Fountainhill Eco-estate near Wartburg	37
Table 4-3	Annual means/totals of climate variables measured by the AWS located at Bruyns Hill near Wartburg	37
Table 4-4	Chemical properties of soil samples taken at two trial sites at Fountainhill Eco-estate in the first season	39
Table 4-5	Soil particle size distribution and textural classes for three depths at each trial site	40
Table 4-6	Measurement of soil bulk density, soil water retention and soil hydraulic conductivity for trial sites 1 and 2.....	40
Table 4-7	Calculation of soil bulk density, soil water retention and soil hydraulic conductivity for trial sites 1 and 2 using the SPAW utility.....	41
Table 4-8	Comparison between observed crop water use (ET) for OFSP and taro grown under rainfed conditions at Fountainhill Eco-estate during the 2021/22 season.....	50

Table 4-9	Monthly crop coefficients (K_c) estimated for the fallow period at Fountainhill and Baynesfield	51
Table 4-10	Comparison of nutrient content of taro tubers obtained in this project to those from Shelembe (2020) for two water treatments	53
Table 4-11	Simulated versus observed data for final root yield, total biomass and harvest index for OFSP grown under rainfed conditions at Fountainhill	58
Table 4-12	Simulated (AquaCrop and SWB) vs measured ET for OFSP	59
Table 4-13	Comparison between simulated and observed crop water productivity of OFSP grown under rainfed conditions	60
Table 4-14	Observed versus estimated NWP of OFSP for the 2021/22 season at Fountainhill	60
Table 4-15	Measured data for OFSP and taro grown in the second season (2021/22) at Fountainhill	61
Table 5-1	Estimation of irrigation demand for each water treatment.....	68
Table 5-2	Interpretation of commonly used statistical indicators of model performance (FAO, 2015)	74
Table 5-3	Monthly means/totals of climate variables measured by the AWS located inside the greenhouse at UKZN	74
Table 5-4	Soil fertility results for topsoil samples from each of the four greenhouse beds	79
Table 5-5	Soil particle size distribution and textural classes for the four beds at soil depths of 0.15 m and 0.40 m.....	79
Table 5-6	Estimation of soil water retention results using the outflow pressure method	79
Table 5-7	Calculation of soil bulk density, soil water retention and soil hydraulic conductivity for the soil in each greenhouse bed using the SPAW utility	80
Table 5-8	Final biomass, yield and harvest index obtained at the end of season 3.....	89
Table 5-9	Maximum rooting depths for OFSP and taro at the end of season 3	90
Table 5-10	β -carotene (β -c) content of OFSP storage roots grown in a greenhouse during the 2022/23 season	90
Table 5-11	Calibration statistics for canopy cover development for OFSP and taro under two water treatments.....	96
Table 5-12	Comparison of observed final biomass, yield and harvest index of OFSP and taro to AquaCrop simulations for both water treatments	96
Table 5-13	Comparison of observed final biomass, yield and harvest index of OFSP and taro at Fountainhill in season 2 to AquaCrop simulations under rainfed conditions.....	97
Table 6-1	Simulations of OFSP yield at three locations under low and high input agriculture (Nyathi et al., 2016).....	112
Table 6-2	Effect of zero yields on the coefficient of variation in seasonal yield (Y_{cv})	117
Table 7-1	Key variables (monthly values) in ACRU that account for land cover/use (Smithers and Schulze, 1995).....	149
Table 7-2	Minimum and maximum monthly crop coefficients for OFSP and taro across all 5,838 HRZs.....	150

Table 7-3	Values of the depletion fraction (p) provided by Allen et al. (1998) and Pereira et al. (2021a; 2021b).....	153
Table 7-4	Key parameters and variables in ACRU that influence rainfall:runoff response	153
Table 7-5	Absolute reduction in mean annual runoff resulting from a proposed land use change from natural vegetation to OFSP production	155
Table 7-6	Relative reduction in mean annual runoff resulting from a proposed land use change from natural vegetation to OFSP production	156
Table 7-7	Relative reduction during the low flow period (LFP) resulting from a proposed land use change from natural vegetation to OFSP production	158
Table 8-1	Variables simulated by FAO's AquaCrop model (Raes et al., 2018).....	163
Table 8-2	Criteria and thresholds used to eliminate HRZs deemed unsuitable for OFSP production	167
Table 8-3	Criteria and thresholds used to eliminate HRZs deemed unsuitable for taro production	167
Table 8-4	Thresholds of crop water productivity used to classify HRZs as marginally, moderately and highly suited to RTC production	169
Table 8-5	Reduction in suitability areas for OFSP after consideration of land use	171
Table 8-6	Reduction in suitability areas for taro after consideration of land use	171
Table 8-7	Suitable OFSP and taro production areas located within existing subsistence farming areas.....	177
Table 11-1	Individual capacity building: Postgraduate students.....	213
Table 13-1	Growth criteria, expected yields, crop water requirements and crop water productivity of selected root and tuber crops	220
Table 13-2	Proximate composition of five root and tuber crops	221
Table 13-3	Mineral composition for five root and tuber crops	221
Table 13-4	Vitamin and bioactive composition in selected root and tuber crops	222
Table 13-5	Variation in mineral content of 14 taro accessions from mostly KwaZulu-Natal (Gerrano et al., 2021).....	222
Table 14-1	Nutrient content of OFSP storage roots grown at Fountainhill during the 2021/22 season (Mthembu, 2023)	223
Table 14-2	Nutrient content of taro tubers grown at Fountainhill during the 2021/22 season (Reddy, 2024).....	223
Table 14-3	Nutrient content of OFSP leaves grown at Fountainhill during the 2021/22 season (Mthembu, 2023)	224
Table 14-4	Nutritional water productivity of OFSP (roots and leaves) and taro tubers (Reddy, 2024)	224
Table 14-5	Nutrient content of OFSP storage roots grown in a greenhouse during the 2022/23 season	225
Table 14-6	Nutrient content of taro tubers grown in a greenhouse during the 2022/23 season	225
Table 16-1	AquaCrop calibration statistics for sweet potato and taro	228

Table 16-2	AquaCrop validation statistics for sweet potato and taro	228
Table 16-3	AquaCrop parameters for sweet potato derived by Nyathi et al. (2016) and Beletse et al. (2013)	229
Table 16-4	AquaCrop parameters for sweet potato derived by Rankine et al. (2015) and compared to default parameter values for potato (Raes et al., 2018)	230
Table 16-5	AquaCrop parameters for sweet potato derived by Pushpalatha et al. (2021) and Lamaro et al. (2023).....	231
Table 16-6	AquaCrop parameters for taro derived by Mabhaudhi (2012), then modified by Mabhaudhi et al. (2014b) and Mabhaudhi et al. (2016a)	232
Table 16-7	Soil parameters for site 1 (taro) and site 2 (OFSP) at Fountainhill	233
Table 16-8	Conversion of phenological growth stages observed in calendar day (CD) format for OFSP and taro, then converted to growing degree-day (GDD) format.....	233
Table 16-9	List of important crop parameters used to run the AquaCrop model for sweet potato, with partially calibrated values highlighted in bold	233
Table 16-10	Orange flesh sweet potato crop parameters derived by Masango (2015) for SWB, together with partially calibrated values used in this project.....	234
Table 16-11	Soil parameters for the raised beds in the greenhouse at UKZN.....	234
Table 16-12	Base (T_{BSE}) and cut-off (T_{UPP}) temperatures when crop development ceases	235
Table 16-13	Updated standard crop parameters provided by Pereira et al. (2021b)	235
Table 16-14	Phenological growth stages observed in calendar day (CD) format for OFSP and taro, which were then converted to growing degree-day (GDD) format	235
Table 16-15	Comparison of sweet potato parameters derived by Rankine et al. (2015) with those obtained in this project.....	236
Table 16-16	Comparison of taro parameters derived by Mabhaudhi et al. (2016a) with those obtained in this project.....	237
Table 17-1	File size of input and output files required to run AquaCrop with 50 years of historical climate data	239
Table 17-2	Size of input and output files when running AquaCrop with 50 years of climate data ...	242
Table 17-3	Increase in RAM drive read and write performance using logical (new) vs physical (old) disk emulation.....	243
Table 17-4	Sequential vs parallel run time tests with 50 years of input climate data	244
Table 17-5	HRZ groupings to reduce the time difference between the fastest and slowest tasks (10 in total) running simultaneously on the slower PC with 30 years of input climate data	246
Table 17-6	Performance of version 2 of WSL compared to version 1 for taro using historical climate data input	247
Table 17-7	HRZ groupings to reduce the time difference between the fastest and slowest tasks (12 in total) running simultaneously on the faster PC with 30 years of input climate data	248
Table 19-1	The fundamentals for pairwise comparison (Saaty, 2008)	260

LIST OF ABBREVIATIONS

ACCI	African Centre for Crop Improvement
ACRU	Agricultural Catchments Research Unit
AGB	Above-ground biomass
AHP	Analytic Hierarchy Process
AMC	Antecedent Moisture Class
APAN	A-pan equivalent reference evaporation
APSIM	Agricultural Production Systems sIMulator
ARC	Agricultural Research Council
AWC	Available Water Capacity
AWS	Automatic Weather Station
AZ	Altitude Zone
BIN	Binary
BWP	Biomass Water Productivity
CAES	College of Agriculture, Engineering and Science
CC	Canopy Cover
CCI	Chlorophyll Content Index
CD	Calendar Day
CDC	Canopy Decline Coefficient
CGC	Canopy Growth Coefficient
CN	Curve Number
COVID-19	Coronavirus Disease 2019
CPU	Central Processing Unit
CS	Campbell Scientific
CV	Coefficient of Variation
CWP	Crop Water Productivity
CWR	Crop Water Requirement
CWRR	Centre for Water Resources Research
DAFF	Department of Agriculture, Forestry and Fisheries (now DALRRD)
DAP	Days After Planting
DALRRD	Department of Agriculture, Land Reform and Rural Development (former DAFF)
DEM	Digital Elevation Model
DFFE	Department of Forestry, Fisheries and the Environment
DIFN	Diffuse Non-interceptance
DSSAT	Decision Support System for Agrotechnology
DT	Dissipation Theory
DWA	Department of Water Affairs (now DWS)
DWS	Department of Water and Sanitation (former DWA)
EC	Eddy Covariance

ERD	Effective Rooting Depth
ET	Evapotranspiration
FAO	Food and Agricultural Organisation of the United Nations
FAO56	Food and Agriculture Organisation, Paper No. 56
FAOSTAT	Food and Agriculture Organisation Corporate Statistical Database
FC	Field Capacity
GDD	Growing Degree-day
GIS	Geographic Information System
HI	Harvest Index
HPLC	High-Performance Liquid Chromatography
HRZ	Homogenous Response Zone
ICFR	Institute for Commercial Forestry Research
IRGA	InfraRed Gas Analyser
ISCW	Institute for Soil, Climate and Water
KZN	KwaZulu-Natal
LAI	Leaf Area Index
LDARD	Limpopo Department of Agriculture and Rural Development
LINTUL	Light Interception and Utilisation
LN	Leaf Number
LSD	Least Significant Difference
LT	Leaf Temperature
LUC	Land Use Change
MAE	Mean Absolute Error
MAP	Mean Annual Precipitation
MAR	Mean Annual Runoff
MAT	Mean Annual Temperature
MaxEnt	Maximum Entropy
MCDA	Multi-Criteria Decision Analysis
MOST	Monin-Obukhov Similarity Theory
MSc	Master of Science
n.d.	no data
NIR	Near-InfraRed
NRF	National Research Foundation
NRMSE	Normalised Root Mean Square Error
NSE	Nash-Sutcliffe Efficiency Index
NV	Nutrient value
NWA	National Water Act
NWP	Nutritional Water Productivity
OFSP	Orange Flesh Sweet Potato
PAR	Photosynthetically Active Radiation

PAW	Plant Available Water
PhD	Doctor of Philosophy
PO	Porosity
PRIS	The Postgraduate Research and Innovation Symposium
PWP	Permanent Wilting Point
RAM	Random Access Memory
RCF	Risk of Crop Failure
REP	Replication
REW	Readily Evaporable Water
RMSD	Root Mean Square Deviation
RMSE	Root Mean Square Error
RRMSE	Relative Root Mean Square Error
RTC	Root and Tuber Crop
SAHS	South African Hydrological Society (formerly SANCIAHS)
SANBI	South African National Botanical Institute
SASRI	South African Sugarcane Research Institute
SAT	Saturation
SAWS	South African Weather Service
SC	Stomatal Conductance
SCS	Soil Conservation Service
SDG	Sustainable Development Goal
SED	Standard Error of Difference
SFRA	Stream Flow Reduction Activity
SPAW	Soil-Plant-Air-Water
SR	Surface Renewal
SSA	sub-Saharan Africa
SWB	Soil Water Balance
SWC	Soil Water Content
TAW	Total Available Water
UCDP	University Capacity Development Programme
UKZN	University of KwaZulu-Natal
UPS	Uninterruptible Power Supply
URP	uMngeni Resilience Project
USDA	United States Department of Agriculture
VWC	Volumetric Water Content
WaPOR	Water Productivity through Open access of Remotely sensed data
WFSP	White Flesh Sweet Potato
WP	Water Productivity
WRC	Water Research Commission
WSL	Windows Subsystem for Linux

WU Water Use
WUE Water Use Efficiency

LIST OF SYMBOLS

AET	Actual evapotranspiration (mm)
AGB	Above-ground biomass (kg ha^{-1} or t ha^{-1})
AWC	Available water capacity (mm m^{-1} or m m^{-1} or % volume)
α_s	Soil water transmission parameter (based on soil texture)
B	Accumulated biomass (g m^{-2})
$\beta\text{-c}$	Beta-carotene (g kg^{-1})
A-pan	A-pan equivalent evaporation (mm)
c	Coefficient of initial abstraction (same as COIAM in ACRU)
c	Canopy cover fraction
CAY	Monthly crop coefficient (K_c)
CC	Canopy cover (%)
CC ₀	Initial canopy cover at emergence (%)
CC _s	Green canopy cover reached (%)
CC _x	Maximum canopy cover reached (%)
CDC	Canopy decline coefficient ($\% \text{ d}^{-1}$)
CELRUN	Stream flow generated from the sub-catchment, including the contribution from all upstream sub-catchments (mm d^{-1} or mm month^{-1})
CGC	Canopy growth coefficient ($\% \text{ d}^{-1}$)
CN _{II}	Curve number for AMC class II
CO ₂	Atmospheric carbon dioxide concentration (ppmv)
COFRU	Base flow recession constant (fraction)
COIAM	Coefficient of initial abstraction (fraction)
COLON	Monthly fraction of root colonisation of the B-horizon
CONST	Fraction of plant available water at which total evaporation is assumed to drop below maximum evaporation (i.e. the onset of plant water stress)
CORPAN	Monthly APAN adjustment factors to adjust Penman-Monteith evaporation estimates to APAN equivalent evaporation (E_p/ET_0)
CORPPT	Monthly precipitation adjustment factors (e.g. to account for differences in monthly rainfall between the selected driver station and spatially averaged estimates for the sub-catchment)
CWP	Crop water productivity (kg m^{-3})
D	Drainage (mm)
D-I	Willmott's d-index
ΔS	Change in soil water content (mm)
DM	Dry matter production (g m^{-2})
E	Soil water evaporation (mm)
EFRDEP	Effective soil depth for colonisation by plant roots
E_p	A-pan evaporation (mm)
ERD	Effective rooting depth (m)
ET _A	Actual crop evapotranspiration (mm day^{-1})

ET _c	Potential (maximum) crop evapotranspiration (mm day ⁻¹)
ET _o	Reference crop evapotranspiration (mm)
EVTR	Determines whether transpiration and soil water evaporation are calculated as separate components (EVTR = 2) or combined (EVTR = 1)
FC	Field capacity (mm m ⁻¹ or m m ⁻¹ or volume %)
G	Soil heat flux (W m ⁻² s ⁻¹)
γ	Psychrometric constant (kPa °C ⁻¹)
GDD	Growing degree-days accumulated for month (°C d)
H	Sensible heat flux (W m ⁻² s ⁻¹)
HI	Harvest Index (%)
HI _o	Reference Harvest Index (%)
I	Irrigation (mm)
I _a	Initial abstraction (% or fraction)
I _a	Infiltrated water (mm; I _a = c · S)
I _c	Interception loss (mm)
k	Canopy extinction coefficient (fraction)
K _C	Crop coefficient (fraction)
K _{CB}	Basal crop coefficient (fraction)
K _{ex}	Maximum soil evaporation coefficient (fraction)
K _p	Pan factor, i.e. ET _o /E _p (fraction)
K _s	Water stress index
K _{SAT}	Hydraulic conductivity at saturation (mm d ⁻¹)
LAI	Leaf area index (m ² m ⁻²)
λ	Latent heat of vapourisation (J kg ⁻¹)
λE	Latent heat flux (W m ⁻² s ⁻¹)
MAR _{BASE}	Mean annual runoff from baseline vegetation (mm)
MAR _{CROP}	Mean annual runoff from a cropped surface (mm)
n	Number of observations
NC	Nutrient content (g kg ⁻¹)
NRMSE	Normalised root mean square error (%)
NSE	Nash-Sutcliffe efficiency index
NWP	Nutritional water productivity (g m ⁻³)
O	Observed variable (e.g. t ha ⁻¹)
p	Soil water depletion fraction
P	Predicted variable (e.g. t ha ⁻¹)
P	Precipitation (mm)
P	Soil water tension (kPa)
PAW	Plant available water (mm m ⁻¹ or m m ⁻¹ or volume %; PAW = FC – PWP)
PCSUCO	Monthly fractions (as %) of the soil surface covered by crop residue
PET	Potential evapotranspiration (mm; PET = K _c * ET _o)
P _g	Gross precipitation (mm)

PWP	Permanent wilting point (mm m ⁻¹ or m m ⁻¹ or volume %)
QFRESP	Storm flow response fraction for the catchment (fraction)
r _s	Stomatal resistance (s m ⁻¹)
R	Runoff (mm)
R ²	Coefficient of determination (fraction or %)
R _a	Extra-terrestrial radiation (MJ m ⁻² d ⁻¹)
REW	Readily evaporable water (mm)
RH	Relative humidity (%)
RH _{ave}	Average relative humidity (%)
RH _{max}	Maximum relative humidity (%)
RH _{min}	Minimum relative humidity (%)
ROOTA	Monthly fraction of roots in the A-horizon (fraction)
RMSE	Root mean square error (t ha ⁻¹)
R _N	Net radiation (MJ m ⁻² d ⁻¹)
RRMSE	Relative root mean square error (%)
R _S	Incoming solar radiation (MJ m ⁻² d ⁻¹)
RUNCO	Base flow store (mm)
S	Potential maximum storage (mm; $S = 1000/CN_{II} - 10$)
SAT	Soil water content at saturation (mm m ⁻¹ or m m ⁻¹ or volume %)
SDM	Stem dry matter yield (kg m ⁻²)
SI	Specific leaf storage (mm)
SIMSQ	Stream flow generated from the sub-catchment (mm d ⁻¹)
SMDDEP	Effective soil depth from which storm flow generation takes place (m)
TAW	Total available water (mm; $TAW = ERD * PAW$)
T _{BSE}	Base temperature (°C)
T _{MAX}	Maximum temperature (°C)
T _{MIN}	Minimum temperature (°C)
T _n	Daily minimum air temperature (°C)
Tr	Transpiration (mm)
Tr _{max}	Maximum transpiration rate (mm)
T _x	Daily maximum air temperature (°C)
T _{UPP}	Upper temperature threshold (°C)
θ	Actual soil water content (mm)
θ _{FC}	Soil water content at field capacity/drained upper limit (mm m ⁻¹ ; volume %)
θ _{PWP}	Soil water content at permanent wilting point (mm m ⁻¹ ; volume %)
θ _{SAT}	Soil water content at saturation/porosity in (mm m ⁻¹ or %)
u ₂	Wind speed at 2 m height (m s ⁻¹)
VEGINT	Monthly interception loss (mm rain d ⁻¹)
WP	Water productivity (kg m ⁻³ or g m ⁻²)
WP*	Normalised water productivity (kg m ⁻²)

WU	Water use (mm or m ³)
WUE	Water use efficiency (kg m ⁻³)
Y	Crop yield (kg or t ha ⁻¹)
Z	Effective rooting depth (m)
Z _{rmax}	Maximum rooting depth (m)
Z _{rmin}	Minimum rooting depth (m)

REPOSITORY OF DATA

For details related to the project's data, please contact:

Richard Kunz (Project Leader)
Centre for Water Resources Research
School of Agricultural, Earth and Environmental Sciences
University of KwaZulu-Natal
Private Bag X01, Scottsville 3209
Pietermaritzburg, South Africa
Email: kunzr@ukzn.ac.za

This page was intentionally left blank

1 INTRODUCTION

1.1 BACKGROUND & RATIONALE

Agriculture is important for many rural communities in South Africa, underpinning their food and nutrition security, as well as their rural socio-economic development (van Averbeke and Khosa, 2007). Considering the country is described as arid and semi-arid, more than 90% of crop production occurs under rainfed conditions (Kahinda et al., 2008). Field crops occupy 92% of the land within rural communities and maize, the nation's staple crop, accounts for more than 70% of the cropped land area under rural production. The dominance of rainfed maize production suggests that production systems within rural communities are homogenous, and water is a major limiting factor to production (Waongo et al., 2015). As a result, yields are lower ($< 1 \text{ t ha}^{-1}$) than commercially produced maize ($> 10 \text{ t ha}^{-1}$) and cannot contribute to food and nutrition security (Lahiff and Cousins, 2005). Furthermore, climate shocks in the form of floods, drought and heat waves increases the risk of crop loss within poor rural communities (Hoffman et al., 2018).

Although irrigation may seem an obvious solution to increasing agricultural water productivity in response to climate extremes (Molle and Berkoff, 2007; van Averbeke and Khosa, 2007), it is generally argued that irrigation is an expensive option and not necessarily readily accessible to most rural farmers. Water scarcity and increased climate variability necessitates technologies with high water productivity for sustainable food production. There is also a need to address malnutrition and hidden hunger in poor rural communities, thus highlighting the need to grow more nutrient-rich crops. Therefore, the challenge is to diversify current farming systems, produce more crop and nutrient yield, whilst using less water and to reduce the environmental footprint of agriculture. A noteworthy solution is to expand the production of underutilised and indigenous crops that are known to be drought-tolerant and nutrient-dense.

Root and tuber crops (RTCs), also referred to as “drought insurance” crops, have emerged as a plausible option in addressing food and nutrition insecurity under climate variability and change. Drought tolerant and water use efficient crops are considered important “future” crops because of their resilience to drier conditions and ability to produce higher yields under rainfed agriculture, whilst using less water (Chivenge et al., 2015). While the energy from RTCs is about one-third that of an equivalent weight of cereals (maize, rice and wheat), they contain more protein and fibre when compared to major cereal crops, as well as more potassium and vitamin C. Root and tubers are also considered among the most energy productive crops, producing $5,600 \text{ kcal m}^{-3}$ of energy in potato, compared to $3,860 \text{ kcal m}^{-3}$ for maize, $2,300 \text{ kcal m}^{-3}$ for wheat and $2,000 \text{ kcal m}^{-3}$ for rice (Daryanto et al., 2016). Their broad agro-ecological adaptability, especially in marginal environments and mixed farming systems and their ability to produce reasonable yields where most crops cannot, make them central to addressing malnutrition and hidden hunger in poor rural households (Palao et al., 2019). Even with their vast potential, RTCs remain underutilised and poorly researched. Available information is limited and fragmented, which prevents these crops from being front runners in drought adaptation and improved food and nutrition interventions.

Although RTCs belong to different botanical families, they all store edible starch in underground roots, tubers, roots, corms, stems and rhizomes. This project initially considered five RTCs, namely sweet potato, cassava, tannia, tannia and yam. The latter three are the most under-researched of the five RTCs. For taro, a wide range of crop water requirements have been reported in the literature, based largely on anecdotal evidence. It is against this backdrop that necessitated the interest in better understanding the water use, yield and nutrition characteristics of RTCs. Such information facilitates the calculation of two useful metrics called crop and nutritional water productivity, which represent the amount of yield and nutrients produced per unit of water consumed by the crop. This knowledge is

needed to facilitate their transition from being “the crops of the poor”, to urban foods and even industrial crops.

1.2 PROJECT OBJECTIVE & SPECIFIC AIMS

The overall objective of this project was to measure and model the water use and yield of selected RTCs currently in production, where little or conflicting information currently exists. The specific aims of this four-year project were as follows:

- 1: Review of production systems, water use and yield of indigenous root and tuber crops currently in production, as well as a review of the nutritional and health benefits of these crops.
- 2: Address major knowledge gaps through field work by measuring the water use and yield of crops where little or conflicting information currently exists.
- 3: Model the water use and yield of these crops once the crop model has been tested using field trial results.
- 4: Develop recommendations on crop suitability for production in different agro-ecological zones.
- 5: Improve existing knowledge of water use efficiency and nutritional water productivity of these crops.
- 6: Assess the hydrological impact of crop production on downstream water availability.
- 7: Synthesise the above information to help promote the sustainable production of indigenous root and tuber food crops.

All of the aims were successfully met, despite some challenges that were experienced, as discussed in the next section.

1.3 PROJECT SCOPE & REPORT STRUCTURE

In November 2019, the Centre for Water Resources Research (CWRR), based at the University of KwaZulu-Natal (UKZN) in Pietermaritzburg, was awarded a four-year project funded by the Water Research Commission (WRC). This project (No. C2019/2020-00088) is titled “Water use of indigenous root and tuber food crops”, with funding that totalled R2 million. The four-year project commenced in April 2020 and ended in March 2024. As noted in the original project proposal, this project was conducted in specific phases, each linked to a specific aim and Deliverable report, as shown in **Table 1-1**. Phase 1 focused on the planning component centred around the literature review (Aim 1) that was reported in the 1st Deliverable (September 2020). A systematic review of available literature from January 2000 to July 2020 was undertaken to meet the first aim, which is summarised in **Chapter 2**. The 2nd Deliverable represented a progress reported up to February 2021, and thus was not linked to a specific aim.

The literature review was used to guide which crops were considered for the field work (Aim 2) undertaken in Phase 2. The decision was made to focus on sweet potato and taro, considering these two crops are currently produced by many rural communities in KwaZulu-Natal. The literature review was then extended for these two crops, which is summarised in **Chapter 3**. Using the methodology described in the 3rd Deliverable (September 2021), field trials were conducted over two seasons to measure the water use, yield and nutrient content of orange flesh sweet potato (OFSP) and taro (**Chapter 4**). At the trial site (Fountainhill Eco-estate, Wartburg, KwaZulu-Natal), taro was planted during the first season (2020/21), which was initially affected by excessive weed growth, then destroyed by bush pigs. The trial site was subsequently fenced off to prevent animal damage in the second season. OFSP was not planted because an MSc student decided to deregister due to concerns related to the COVID-19 pandemic.

Table 1-1 Guide to the chapter that addresses each project aim

Phase	Aim	Deliverable	Chapter	Topic
1	1	1	2	Literature review
			3	OFSP & taro
2	2	3	4	Field trials
			5	Greenhouse experiment
3	3	4	6	Methodology:
			7	modelling & mapping
4	3	5	6	AquaCrop modelling
5	5			
6	6	6	7	ACRU modelling
	4		8	Land suitability mapping
	7	7	this report	Synthesis of all Deliverables

During the second season (2021/22), taro was re-planted and OFSP was planted for the first time at a second site. In mid-December 2021, the lattice mast and all equipment was relocated to improve the upwind fetch distance, during which the CS650 probes and/or wiring were likely damaged. The replacement of these sensors was unfortunately delayed to 9th February 2022. Despite both trials being fenced and strengthened with netting, bush pigs burrowed under the fence, which was made relatively easy at site 2 (OFSP) by the loamy sand soil texture. Due to the threat of animal damage, OFSP was harvested prematurely, and thus the observed yield may have been lower than what could have been achieved. In addition, problems in appointing and paying casual workers resulted in higher weed loads in January 2022 at both trial sites, which may have negatively affected final yields. Due to the failure of the DS-2 instrument at site 2, which performs ultrasonic measurements of wind speed at canopy level, sensible heat could not be calculated using dissipation theory.

After the Farm Manager at Fountainhill admitted that both trial sites were prone to animal damage, the decision was made to conduct the final season of experiments (2022/23) in a more controlled environment, namely a greenhouse at UKZN (**Chapter 5**). However, growing conditions in the greenhouse were severely affected by stage 6 load shedding and load reduction events, which caused air temperatures to exceed 55°C when the extraction fans stopped working. Despite the harsh conditions experienced over the growing season, both crops survived the extreme temperatures.

Phase 3 represented the modelling component (Aim 3) as described in the 4th Deliverable (November 2021) and updated in the 5th Deliverable (September 2022). Existing crop parameter files for sweet potato and taro were obtained from the literature and tested against field-based measurements from season 2. The calibration of AquaCrop was then improved using data from season 3. The model was then run to simulate the water use, yield and crop water productivity of the selected RTCs (**Chapter 6**).

Phases 4 and 5 pertained to the analysis and interpretation of crop model output, which was also discussed in previous two deliverables and summarised in **Chapter 6**. Crop water productivity (CWP) was determined from modelled output as the ratio of dry tuber yield to crop evapotranspiration accumulated over the growing season. Thereafter, nutritional water productivity was calculated as the product of CWP and nutrient content of roots/tubers (Aim 5).

In Phase 6, the hydrological impact of RTC production on downstream water availability was assessed using a hydrological model (Aim 6). The accepted and transparent methodology was described in the 4th Deliverable and updated in the 6th Deliverable. The ACRU hydrological model was run to estimate crop water use relative to that used by natural vegetation. This comparison was used to determine if OFSP or taro has the potential to significantly reduce water availability to downstream users. Initial

model results were reported in the 6th Deliverable (November 2022), with the final results presented in this report (**Chapter 7**).

A novel approach was developed to meet Aim 4, i.e. development of land suitability maps using selected output from the crop model. The methodology was first described in the 4th Deliverable, then updated in the 6th Deliverable with some initial results. The final land suitability maps for sweet potato and taro are presented in **Chapter 8**. The last aim (Aim 7) pertains to a synthesis of all Deliverables produced by this project, i.e. this final project report.

2 OVERVIEW OF UNDERUTILISED ROOT & TUBER FOOD CROPS

In this chapter, an overview is provided of underutilised indigenous root and tuber crops (RTCs), with a particular focus on their water use. The latter was used to determine which RTCs the field work would focus on. Potato is not considered an underutilised crop in South Africa, and thus was excluded from the literature review.

2.1 RTC CLASSIFICATION

RTCs are plants which store edible starch material in underground roots, tubers, corms, stems and rhizomes (**Figure 2-1**). These crops belong to different botanical families as shown in **Table 2-1**. Sweet potato (*Ipomoea batatas*) and cassava (*Manihot esculenta*) are root crops. Edible aroids store starch in corms and underground stems. They are commonly referred to as cocoyams and include taro (*Colocasia esculenta*), elephant foot yam (*Amorphophallus paeoniifolius*) and tannia (*Xanthosoma sagittifolium*). Yams (e.g. *Dioscorea alata*). are tuber crops and belong to the Dioscoreaceae family. Chandrasekara and Kumar (2016) identified other globally important root and tuber crops such as edible rhizomes, which include canna (*Canna edulis*) and arrow root (*Maranta arundinacea*).



Figure 2-1 Images of a) sweet potato plant and root, b) cassava plant and root, c) taro plant and tuber, d) tannia tuber, e) yam tuber and f) yam plant

Table 2-1 Classification and origin of root and tuber crops in sub-Saharan Africa (Lebot, 2019)

Common name	Botanical name	Family name	Centre of origin
Sweet potato (root)	<i>Ipomoea batatas</i>	Convolvulaceae	Central America
Cassava (root)	<i>Manihot esculenta</i>	Euphorbiaceae	Origins unresolved; Assumed: Brazilian-Bolivian region
Taro (corm)	<i>Colocasia esculenta</i>	Araceae	Origins unresolved; Assumed: northeast India and New Guinea
Tannia (corm)	<i>Xanthosoma spp.</i>	Araceae	Mexico, Brazil, Antilles
Yam (tuber)	<i>Dioscorea spp.</i>	Dioscoreaceae	East and West Africa

2.2 GLOBAL, REGIONAL & LOCAL PRODUCTION

Root and Tuber Crops (RTCs) are amongst the most commonly consumed food staples and provide one of the cheapest sources of energy and vital nutrients. Globally, cereals are the primary source of carbohydrates, with the secondary source being starchy RTCs. Asia is the main producer of RTCs, followed by Africa, Europe, and America. Cassava, potatoes and sweet potatoes make up 90% of global production (FAOSTAT, 2013).

Of the five RTCs discussed in **Section 2.1**, only yam is of sub-Saharan Africa (SSA) origin (Lebot, 2019). However, crop diversification and adoption in SSA has domesticated and indigenised the other five RTCs to an extent where cassava, potato and sweet potato are now the three major RTCs produced in SSA, with yam as fourth (Lebot, 2019). Of the RTCs grown across SSA, cassava currently dominates production, but the demand for the crop varies among the different regions (FAOSTAT, 2019). To date, the aggregate value of yam, cassava, potato and sweet potato exceeds all other SSA staples, including cereals which annually produce an average of 169 million tons on 108 million ha of land (Sanginga and Mbabu, 2015). In West Africa, it is grown as a cash crop, and its fresh roots exhibit higher income elasticity for demand than grain cereals. The cultivation of aroids is mainly in the coastal forest regions of West and Central Africa, as well as in the highland regions of East Africa, where they are often intercropped with bananas (Lebot, 2019). Aroids receive minimal production attention in SSA in comparison to the previously discussed RTCs (Mabhaudhi and Modi, 2015). This is primarily due to high crop water requirements and associated low tolerance to drought, which makes them unsuitable for production in the arid and semi-arid regions of SSA.

According to Allemann et al. (2004), cassava is mostly cultivated in the warmer lowveld regions of the Limpopo and Mpumalanga provinces, as well as in KwaZulu-Natal (Makhathini Flats). Since sweet potato became indigenised in South Africa, it has been grown mostly in subtropical areas (Laurie, 2010). Limpopo (Hoedspruit, Marble Hall, Burgersfort, Levubu), Mpumalanga (Nelspruit), KwaZulu-Natal and Western Cape provinces are the major production areas (Laurie et al., 2015; Motsa et al., 2015b). The estimated area under sweet potato production is 2,000-3,000 ha (Allemann et al., 2004). Although taro originated in the Indo-Malay region (Mabhaudhi, 2012), it has become a staple crop in rural households along the coastal regions of KwaZulu-Natal and the Eastern Cape. Taro is less commonly cultivated in the Mpumalanga and Limpopo provinces (Modi and Mabhaudhi, 2016), as well as the Western Cape (Modi and Mabhaudhi, 2013).

Emerging crops like sweet potato and cassava have more potential for commercialisation in the food industry. In addition, cassava can provide a source of industrial starch, including starch for bio-ethanol production in South Africa (Kunz et al., 2015a). Cassava exhibits the highest potential considering the crop produces 27-37 g of starch per 100 g of fresh weight, compared to 18-28 g for other RTCs (Olanrewaju et al., 2009). Lesser-known crops such as yam, taro and tannia remain mostly underutilised, despite also having potential as industrial crops (Allemann et al., 2004). Based on a

survey of 498 households in Sekhukhune (Limpopo province), Faber et al. (2009) found that 67.5% of the households consumed root and tuber crops. For the majority of the households, food was purchased from small trading stores (51%) and supermarkets in towns (47%).

2.3 RTC NEGLECT IN SSA

More research attention has been given to cereal crops, despite the secondary importance of RTCs in SSA, which is difficult to understand. Since the 1950s, food policy in the region has focused on achieving growth and self-sufficiency in cereals such as wheat, rice and maize. Furthermore, RTC production and trade has been neglected in favour of other cash crops such as tea, coffee, cotton and cocoa. The historical production of RTCs in SSA has been largely driven by areal expansion as opposed to yield improvements (Kenyon et al., 2006) resulting from technological innovations (e.g. improved varieties and production techniques).

Disproportionate attention has also been given to individual RTCs regarding research on water use characterisation (growth and development) and adaptation to variations in water availability. There has been extensive research on potato and cassava since they predominantly feature in semi-arid agriculture systems (**Figure 2-2**). For example, potato production in South Africa is promoted along with other staple cereals, with yield improvement emanating from both technological advancements and improved varieties. On the other hand, tannia has traditionally been a subsistence crop, grown exclusively for consumption with little or no surplus crop for trade in local markets. This explains the lack of research on the crop, scarcity of information regarding crop water use (**Figure 2-2**) and lack of tannia production statistics, particularly in South Africa. This neglect of RTCs has led to the prolonged use of (not necessarily high-yielding) traditional landraces and production techniques.

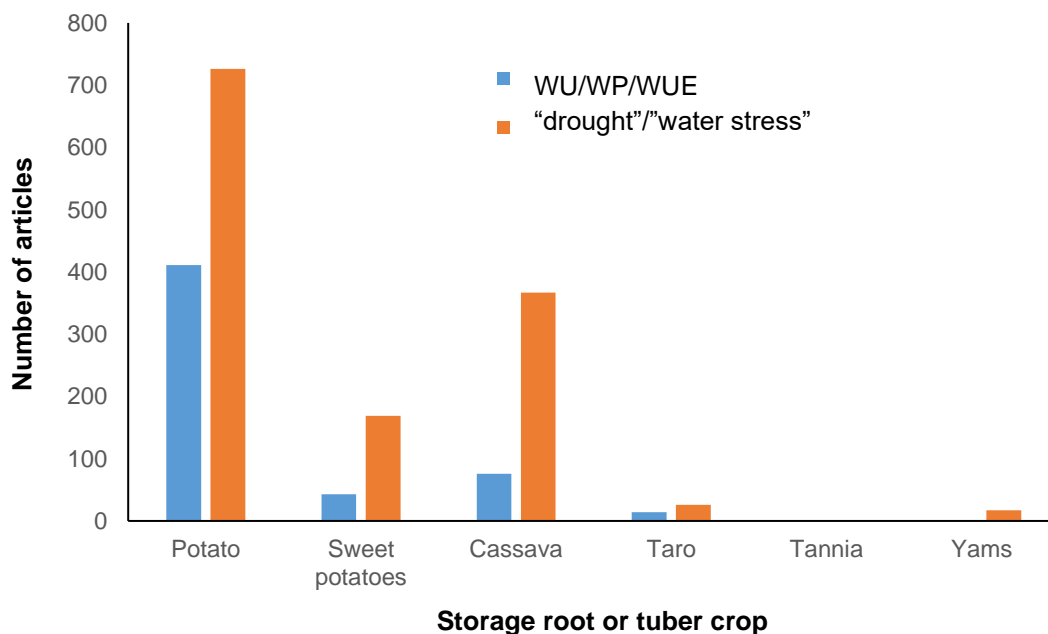


Figure 2-2 Number of published articles from January 2000 to July 2020 looking at water use (WU), water productivity (WP) or water use efficiency (WUE) and drought/water stress for selected root and tuber crops

2.4 AGRONOMY OF RTC PRODUCTION

Although most RTCs originate from hot, humid climates, they have become indigenised to the drier and cooler regions of South Africa. They have also become adapted to marginal farming areas within the

country. However, several authors have pointed out issues of poor crop establishment, low yield and poor storage and susceptibility to pests and diseases (Ray and Sivakumar, 2009; Weerathne et al., 2017). Although cultivating low input crops like RTCs on marginal lands presents many advantages, parallel disadvantages like the lack of agronomic information may restrict the promotion of major crop species within smallholder farming systems. To exploit the full potential of RTCs for food and nutrition security and rural development, research into aspects of localised crop and soil management strategies need to be formulated (Wezel et al., 2015). Generating site-specific information regarding plant densities, fertiliser application rates, planting dates, water requirements, weeding, pest and disease control, and harvest techniques is essential for upscaling production of RTCs (Wezel and Soldat, 2009). This is especially important considering that the efficient use of limited resources such as water can be enhanced through best agronomic practices. Therefore, further research is required on the various agronomic aspects of RTCs within the context of South Africa. To date, WRC-funded research has resulted in production guidelines being developed for amaranth, bambara nut, sorghum and taro (Mabhaudhi et al., 2023).

2.4.1 Propagation material

Vegetative parts can propagate RTCs and these include tubers (potato & yam), stem cuttings (cassava), vine cuttings (sweet potato), as well as side shoots, stolon, or corm-heads (taro & tannia) (Daryanto et al., 2016). This method of propagation offers an advantage to small-scale, low-income farmers who may otherwise not be able buy seed that is associated with cereals and small grain production. Also, vegetative propagation means that they can be multiplied “true to type”, i.e. their genotype is fixed (Almekinders et al., 2019). At the same time, this propagation method makes them more vulnerable to the build-up of viruses and other pathogens (Almekinders et al., 2019; Ibsa et al., 2013; Tegg et al., 2015). According to Thomas-Sharma et al. (2016), the gap between actual and potential yields is caused in part by losses to pests and diseases that accumulate in successive cycles of vegetative propagation.

In South Africa and many parts of Africa, there are no organised seed systems for cassava, sweet potato and aroids, causing the value chains to remain rudimentary due to unavailability of clean certified quality seed (seed, cuttings, tubers or stolons). Commercially, the African Centre for Crop Improvement (ACCI) used to produce cassava seedlings for the Agricultural Research Council (ARC) but has since stopped due to funding restrictions. Livingseeds® and Durandts produce and market sweet potato cuttings. For taro and tannia, farmers produce their suckers or receive them from neighbours or relatives.

Reproducing the planting materials of these crops presents complex problems and many logistical issues for their extensive use. In summary, the production of propagules is mainly an issue for smallholder farmers because of:

- absence of formal seed systems (except potato);
- lack of knowledge of phytosanitary measures and quarantine issues related to the safe movement of germplasm, plants and planting material across national borders;
- lack of consistent supplies of good quality planting material;
- variable demand for clean planting material;
- bulkiness and perishability of planting materials; and
- use of traditional varietal mixtures, including local varieties.

2.4.2 Plant density

Plant density has a considerable influence on growth and development of RTCs and is closely correlated with the architecture of the vegetative parts that affect biomass partitioning. According to Lebot (2019), the average density for yam varies depending on planting methods (10,000 plants ha⁻¹

on mounds; 20,000 plants ha⁻¹ on ridges). In Ethiopia, the highest average total yield (49.85 t ha⁻¹) were obtained at 25,000 plants ha⁻¹ (Tsedalu et al., 2014). Ambe (1995) observed yield of 37 t ha⁻¹ when sweet potato was planted at 20,000 plants ha⁻¹.

For all RTCs, increasing plant densities above a threshold will increase the non-marketable yield of RTCs (Ambe, 1995; Lebot, 2019; Sadras et al., 2012). Orkwor et al. (1998) reported a recommended plant population of 10,000 plants ha⁻¹ for yam, but higher plant populations up to 20,000 plants ha⁻¹ are associated with increased tuber yield and reduced tuber size (Igwilu, 1994).

2.4.3 Fertiliser recommendations

Generally, RTCs can thrive under low soil fertility; however, nutrient deficiencies can cause a reduction in growth (Lebot, 2019). Cassava can deplete soil nutrients due to its high efficiency in nutrient absorption (Ezui et al., 2016). The recommendation for Nitrogen (N) fertilisers is between 30 and 90 kg N ha⁻¹ (Lebot, 2019). Sweet potato is more sensitive to Phosphorus (P) deficiency, which can reduce growth by 50% (Lebot, 2019). Improving water and soil N can increase sweet potato and taro yields; however, water availability has a stronger and more positive relationship than N with yield (Hartemink et al., 2000; Vidigal et al., 2016). According to Lebot (2019), nutrient requirements of taro have shown that when plants are fertilised with 100 kg N ha⁻¹, 50 kg P ha⁻¹ and 100 kg K ha⁻¹, they produce twice the root biomass of unfertilised taro.

2.4.4 Climate and site requirements

Research on water use of RTCs is scarce in comparison to legume and cereal crops. Unlike cereals and pulses, they are big plants that cannot be grown easily in pot experiments in greenhouses. It is therefore difficult to secure the controlled conditions necessary for reliable physiological studies. This has led to the scarcity of standard and credible values of crop water requirements, water productivity and water use efficiency of RTCs. Absence of key water use information and how this may affect nutritional quality of RTCs stem from the lack of adequate research. The lack of information on water use has also limited the extent to which these crops can be recommended for production in new areas from a water productivity and nutrition standpoint. If these crops are to form part of crop choices within South Africa, knowledge is required on crop water use, water productivity, nutrition and health benefits, as well as future production scenarios under projected climate change concerning water availability.

A systematic review was undertaken to quantify the amount of knowledge on a) crop water use and drought adaptation mechanisms, b) nutritional value, and c) tools and methods that can aid in improving data availability of RTCs within South Africa. This information is summarised in **Table 13-1** in **Section 13**. Optimising rainfed production and effectively utilising scarce water resources available for RTCs production in South Africa requires particular attention to rainfall requirements. Successfully cultivation of cassava requires an annual rainfall of between 1,000-3,000 mm, but it can tolerate lower rainfall if it is well distributed (Daryanto et al., 2016). Sweet potato grows well in areas receiving a well-distributed annual rainfall of 1,000-2,000 mm to achieve highest yield potential. Similar to cassava, sweet potato is also adapted to areas receiving less than 1,000 mm of rainfall; however, crop competition for resources should be managed (Gomes and Carr, 2001). Yam can grow in areas with as little as 500-700 mm of rainfall (e.g. in southern Madagascar), but yields are lower than when produced under higher rainfall conditions (Lebot, 2019). Well-distributed rainfall, or the irrigation equivalent of 1,500 mm during the total growth cycle is needed for high yields and commercial production (Lebot, 2019)

Aroids such as taro can be grown throughout the year provided there is sufficient rainfall and no frost (Lebot, 2019). Aroids are best adapted to high temperatures, moist environments with high humidity. According to Mabhaudhi et al. (2013a), rainfall of 200-300 mm month⁻¹ is ideal for optimum growth and production for taro provided evenly distributed rainfall. According to Mabhaudhi et al. (2013a), taro is perceived as one of the least water-efficient food crops (Uyeda et al., 2011), which has resulted in lack

of attention in not only breeding attempts, but crop water relations as highlighted in **Figure 2-2** (cf. **Section 2.3**).

Mabhaudhi and Modi (2015) observed a wide yield response in taro to different levels of water availability, suggesting that there is a need to optimise agronomy under water scarcity. Except for taro, RTCs are generally sensitive to water-logged conditions and require well-drained soils for maximum production. However, it is important to note the above-mentioned rainfall requirements do not indicate the amount of water required for their successful production.

2.5 NUTRIENT CONTENT

Nutritional information can be subdivided into three composition categories, namely (i) proximate (e.g. caloric energy and fat, protein and carbohydrate composition), (ii) mineral (both major and minor), and (iii) bioactive (e.g. antioxidants, phenols, flavonoids, saponins and carotenoids). The list of minerals, vitamins and compounds given in **Table 2-2** is not considered exhaustive as it does not list, for example, sulphur-containing amino acids such as methionine and cystine.

Table 2-2 List of nutritional constituents of root and tuber crops

Proximate	Mineral (mg kg ⁻¹)		Bioactive
	Major	Minor	
Energy (kcal)	Calcium (Ca)	Iron (Fe)	Vitamin A (IU)
Crude fat (%)	Magnesium (Mg)	Copper (Cu)	Vitamin C (mg)
Protein (%)	Potassium (K)	Selenium (Se)	Thiamine (mg)
Carbohydrates (%)	Zinc (Zn)	Nickel (Ni)	Riboflavin (mg)
Total sugars (% fresh weight)	Manganese (Mn)	Lead (Pb)	Niacin (mg)
Starch (g)	Phosphorus (P)	Sulphur (S)	Vitamin B-6 (mg)
Crude fibre (%)	Sodium (Na)	Boron (B)	Vitamin E (mg)
Dry matter (% fresh weight)	Copper (Cu)	Iodine (I)	Vitamin K (µg)
Moisture (%)	Sulphur (S)	Silicon (Si)	Total ascorbic acid (mg)
Ash (%)	Cobalt (Co)	Bromine (Br)	Folate (µg-DFE)
Nitrogen free extract (%)	Nitrogen (N)		Antioxidant activity (% LP)
			Phenols (mg/g)
			Flavonoids (mg)
			Saponins (%)
			Carotenoids (µg/100g)

2.5.1 Proximate composition

Proximate composition of foods includes moisture, ash, lipid, protein and carbohydrate contents (Kabuo et al., 2015). These food components may be of interest in the food industry for product development, quality control or regulatory purposes. Nutritionally, roots and tubers have great potential to provide economic sources of dietary energy in the form of carbohydrates (**Table 13-2** in **Section 13**). The energy from tubers is about one-third of that of an equivalent weight of rice or wheat due to the high moisture content of tubers (Chandrasekara and Kumar, 2016). However, high yields of roots and tubers give more energy per land unit per day compared to cereal grains. Overall yam contains a high amount of protein, fibre and crude fats when compared with the other RTCs. In general, the protein content of roots and tubers is low, except for yam. Despite RTCs having been domesticated in SSA, crops such as taro and tannia are not yet fully explored for their nutritional and health benefits (Chandrasekara and Kumar, 2016).

2.5.2 Mineral composition

The wide range in mineral elements that occur in RTCs is shown in **Table 13-3** (cf. **Section 13**). Minerals can generally be classified as

- significant minerals (or macronutrients) such as calcium (Ca), potassium (K), magnesium (Mg), sodium (Na), phosphorus (P), cobalt (Co), manganese (Mn), nitrogen (N), chlorine (Cl) and Zinc (Zn), as well as
- essential minor and trace minerals (or micronutrients) such as iron (Fe), copper (Cu), selenium (Se), Nickel (Ni), lead (Pb), sulphur (S), boron (B), iodine (I), silicon (Si), bromine (Br).

The importance of optimal mineral intake to maintain good health is widely recognised. RTCs are an important source of different dietary minerals. For instance, taro is deemed to have superior nutritional value over other major RTCs, especially in terms of protein digestibility and mineral composition (Fe, Ca, Mg and P) and is also a good source of Na and K (Lebot, 2019). Yellow yam exhibits the highest levels of minerals, except for P and Na (Omoruyi et al., 2007).

2.5.3 Bioactive compounds

The bioactive compounds and vitamins for RTCs are presented in **Table 13-4** in **Section 13**. RTCs contain numerous antioxidative, hypoglycaemic, hypocholesterolaemia, antimicrobial and immunomodulatory bioactive compounds. Several bioactive constituents such as phenolic compounds, saponins, bioactive proteins, glycoalkaloids and phytic acids are responsible for these health benefits. Orange flesh sweet potato contains high levels of vitamin A, B, C, E and K, all of which help with antimicrobial and immunomodulatory activities that assist in recovery from illness (Govender et al., 2019; Kruger et al., 2018). Yam contains some chemical constituents like good amounts of anti-oxidants and vitamin C, which play an essential role in anti-ageing and collagen formation. Yellow or orange varieties of sweet potato, yam, and cassava contain β -carotene, which is a pre-cursor to vitamin A, and thus can play a crucial role in alleviating vitamin A deficiency. Although vitamin A, iodine, and iron are classified as “the big three”, deficiencies of other micronutrients such as folate, zinc, vitamin B12 and vitamin D are also important (Chandrasekara and Kumar, 2016).

2.5.4 Anti-nutritional factors

Apart from cassava, which contains cyanogenic glucosides, cultivated varieties of most edible roots and tubers do not contain any serious toxins (Lebot, 2019). Three of the sugars which occur in plant tissues, namely raffinose, stachyose and verbascose, are not digested in the upper digestive tract and so, are fermented by colon bacteria to yield the flatus gases, hydrogen and carbon dioxide. For example, sweet potato contains raffinose (i.e. one of the sugars responsible for flatulence), where the level of raffinose depends on the cultivar (FAO, 1990). Generally, processing methods (e.g. drying, soaking or boiling) can be effective in reducing the amount of anti-nutritional factors available in tubers down to tolerable levels.

2.5.5 Linking nutrient content to water productivity

In pursuing food and nutrition security, the wide range of existing food production systems require different approaches to the sustainable utilisation of genetic diversity (Padulosi et al., 2013). Apart from adding variety to a diet, RTCs offer numerous desirable nutritional and health benefits. The recognition of their valuable nutrient content is becoming a key component towards their mainstreaming, especially in terms of improving dietary diversity. Dietary diversity plays a significant role in the attainment of sustainable agricultural practices and strategies to alleviate malnutrition.

There is a wide range in mineral contents reported for RTCs, as shown in the tables in **Section 13**. Similar to other crops, the mineral composition of RTCs is affected by genotype and stage of development, as well as environmental factors such as soil type, soil pH, soil organic matter content, fertilisation, water availability and weather conditions. In addition, sampling issues can also affect nutrient content. Therefore, it particularly important to study linkages between growing environments and nutrition. From a water availability standpoint, this can be achieved through quantification of nutritional water productivity.

Nutritional water productivity (NWP) is an emerging concept that combines information on the nutritional value of crops with crop water productivity. According to Renault and Wallender (2000), *NWP* (nutrition unit m⁻³) is calculated as:

$$NWP = NC \cdot \frac{Y}{ET} \quad \text{Equation 1}$$

where *NC* is the nutrient content (mg kg⁻¹ or g kg⁻¹) or caloric energy (MJ kg⁻¹ or kcal kg⁻¹) of food, *Y* is crop yield (dry kg ha⁻¹) and *ET* is crop evapotranspiration (m³ ha⁻¹). For this project, the preferred units of *NC* are dry g kg⁻¹ (cf. **Section 2.5.6**). The latter represents the amount of soil water a) lost by evaporation, and b) utilised for biomass accumulation via transpiration (Dong et al., 2018). Crop evapotranspiration accumulated over the growing season is referred to as crop water use. However, the ratio of *Y* to *ET* is referred to as crop water productivity (or *CWP* in dry kg m³ ha⁻¹) as follows:

$$CWP = \frac{Y}{ET} \quad \text{Equation 2}$$

where *ET* (or crop water use) is multiplied by 10 to convert depths (in mm) into volumes (in m³). This metric is useful in identifying crops that produce “more crop per drop”, i.e. crops that produce more yield and/or use less water and thus, are considered more water use efficient. In the literature, *CWP* is often (incorrectly) called water use efficiency (*WUE*), and thus these two terms are used interchangeably. Although both terms seek to address the notion of “more crop per drop” (Zhou et al., 2012), they are different, since *WUE* is defined as the ratio of biomass accumulation or yield to water applied, i.e. amount of rainfall and/or irrigation applied to the crop. Hence *WUE* does not account for unproductive losses, such as, inter alia, soil water evaporation, runoff or deep percolation.

When the above two equations are combined, *NWP* is therefore the product of nutrient/energy content per kg of edible portion (*C*) and *CWP*:

$$NWP = NC \cdot CWP \quad \text{Equation 3}$$

NWP combines crop nutrient content with *CWP*, which makes it a useful metric for evaluating agricultural impacts on food and nutrition security, especially under limited water availability (Nyathi et al., 2019b). The index provides a way of understanding the complex and dynamic interlinkages between a crop’s nutrient content and its water use, which should allow for holistic assessment of water, food and nutrition security (Chibarabada et al., 2017; Nyathi et al., 2019b). High *NWP* values indicate more nutrients for less water consumed by the crop. *NWP* is considered a useful metric that can help identify (and promote) crops that are nutrient dense and/or have low water use and thus, exhibit high *NWP*. For example, potato’s *NWP* is higher than that of cereals, producing 5,626 kcal m⁻³, compared to maize (3,856 kcal m⁻³), wheat (2,279 kcal m⁻³) and rice (1,989 kcal m⁻³) (Renault and Wallender, 2000). The quantification of *NWP* within agricultural systems is in its infancy, with Chibarabada et al. (2017) evaluating *NWP* for legumes (e.g. bambara nut and cowpea), whilst Nyathi et al. (2019b) considered African leafy vegetables (e.g. amaranth sweet potato).

2.5.6 Converting nutrition units

Data on food composition is expressed in a various ways depending on, inter alia, national conventions, practices of various institutions and journal requirements. Since nutritional data was aggregated from different sources for this project, it is necessary to convert units to standardise them, which allows for data comparison. Unit conversion is a common source of error, and thus FAO/INFOODS published guidelines in 2012 (FAO, 2012b). The denominator often causes the most confusion and ambiguity as composition data is reported as per:

- 100 g;
- edible and/or inedible portion; and
- total food, total lipid or total protein.

Some references fail to provide an unambiguous description of the dominator (e.g. per 100 g), thus limiting the usefulness of the nutrient composition data. FAO (2012b) also recommended that certain units should be avoided, such as parts per million (ppm), parts per billion (ppb) and percentages (%). Since metric units are preferred, measured nutritional composition was converted to g kg⁻¹ of edible portion (**Table 2-3**). However, edible portion must also differentiate between leaves and roots/tubers.

Table 2-3 Conversion factors for nutritional composition data (FAO, 2012b)

Units	Conversion to	
	mg kg ⁻¹	g kg ⁻¹
µg/100 g	x 10 ⁻²	x 10 ⁻⁵
mg/100 g	x 10 ¹	x 10 ⁻²
g/100 g	x 10 ⁴	x 10 ¹
%	x 10 ⁴	x 10 ¹
µg/kg	x 10 ⁻³	x 10 ⁻⁶
g/kg	x 10 ³	x 10 ⁰
ppm	x 10 ⁰	x 10 ⁻³
ppb	x 10 ³	x 10 ⁰

Since crop models such as AquaCrop output CWP in dry kg per m³ of evapotranspired water, it is important to convert all compositional data from fresh weight to dry matter. Scientific articles often report data per 100 g of dry matter, as it allows for direct comparisons without the influence of changing water content. Furthermore, scientific journals and laboratories should urge the publication of water contents for all data when expressed per dry matter, as it allows for the conversion to fresh weights if needed (FAO, 2012b). Water contents (*WC*) should be expressed in % and the following equation can be used to convert nutrient contents (*NC*) from a fresh weight (*NC_{FRE}*) to a dry weight (*NC_{DRY}*) basis:

$$NC_{DRY} = NC_{FRE} \times \frac{100}{100 - WC} = \frac{NC_{FRE}}{1 - WC/100} \quad \text{Equation 4}$$

A simpler method is to convert CWP from dry kg m⁻³ to fresh kg m⁻³ using a similar equation, i.e. divide the dry value by dry matter content expressed as a fraction, i.e. 1 – WC/100. Either method requires the moisture content of the leaves and root/tuber to be known.

2.6 RESEARCH AGENDA FOR UNDERUTILISED CROPS

Of the five underutilised RTCs, two (sweet potato and taro) have been prioritised for further research in terms of their existing potential and body of knowledge (Mabhaudhi et al., 2017a; Modi and Mabhaudhi, 2016). Within South Africa, sweet potato and taro have potential to contribute towards addressing national priorities such as the poverty-unemployment-inequality and water-food-nutrition-health nexus by creating new value chains in marginal areas. According to the strategy proposed by Mabhaudhi et

al. (2017a), there is need for investment in research, development and innovation. These investments should be targeted in a way that develops and promotes new value chains for the two prioritised RTCs. Human capacity development and knowledge management, including indigenous knowledge, should support such investments to ensure sustainability (Allemann et al., 2004; Duque and Villordon, 2019; Mabhaudhi et al., 2017a, 2017b). The strategy outlined by Mabhaudhi et al. (2017a) aligns with existing policies and provides new knowledge that can be used to inform new policies that either specifically target or include RTCs. For example, the national policy on Food and Nutrition Security (DAFF, 2014) recognises the role of underutilised crops for improving dietary diversity in South African households. The general inclusion of RTCs into existing production systems also addressed certain Sustainable Development Goals (SDGs) such as no poverty (SDG1), good health and well-being (SDG3), gender equality (SDG5), reduced inequality (SDG10) and responsible consumption (SDG12). In all this, the role of champions is critical as they are needed to drive the strategy at various levels. As a way forward, new research projects that target prioritised RTCs and address knowledge gaps need to be initiated.

2.7 SUMMARY & CONCLUSIONS

Based on the literature review, OFSP and taro were selected for field-based work for the following reasons:

- 1) OFSP and taro of the only RTCs that have been prioritised for further research in South Africa (cf. **Section 2.5.6**).
- 2) Availability of propagation material: Taro corm heads can be purchased from smallholder farmers in Swayimane (near Wartburg, KwaZulu-Natal). OFSP vines are available from the College of Agriculture at Cedara (near Merrivale, KwaZulu-Natal).
- 3) Taro is one of the most under-researched RTCs (**Figure 2-2**; cf. **Section 2.3**) and exhibits high water use, with a wide range, i.e. 1,750-2,500 mm (**Section 2.4.4**).
- 4) Taro has high nutritional value, especially in terms of protein digestibility and mineral composition (Fe, Ca, Mg and P) and is also a good source of Na (**Section 2.5.2**).
- 5) Although the water use of sweet potato and cassava are similar (700-1,500 mm), sweet potato provides more protein, fibre and carbohydrates. In addition, the mineral composition of sweet potato is superior to that of cassava, especially for Mg, K and P. More importantly, sweet potato can help address vitamin A deficiency in women and children in South Africa.

In addition, crop parameters for the AquaCrop model have been developed for (i) OFSP by Nyathi et al. (2016; local study) and by Rankine et al. (2015; international study), and (ii) taro by Mabhaudhi (2012), which were later modified by Mabhaudhi et al. (2014b; local study). This is a very important consideration since the crop modelling work presented in **Chapter 6** would not be possible without the crop parameter values. The parameterisation of AquaCrop for a new crop represents a complex process as described by Mabhaudhi (2012), where crop parameters for taro and bambara nut Mabhaudhi et al. (2014a) were developed from his PhD field work.

The literature review highlighted the scarcity of research on water use of RTCs in comparison to legume and cereal crops. Unlike cereals and pulses, RTCs are large plants that cannot be grown easily in greenhouse pot experiments. It is therefore difficult to secure the controlled conditions necessary for reliable physiological studies. This has led to the scarcity of standard and credible values of crop water requirements, water productivity and water use efficiency of RTCs. For this project, large field trials were conducted at Fountainhill Eco-estate (Wartburg, KwaZulu-Natal) with sufficient fetch to facilitate crop evapotranspiration measurements using two micrometeorological techniques, namely the eddy

covariance and surface renewal. Thereafter, OFSP and taro was grown in raised greenhouse beds (not pots) under two water treatments representing water stressed and unstressed conditions. The literature review was extended, with the focus on sweet potato and taro only, and results are presented in the next chapter.

3 OVERVIEW OF SWEET POTATO & TARO

The focused review on sweet potato and taro was undertaken by a postgraduate student (Mr Thando Mthembu) as part of his MSc degree. The sections that follow were summarised from his MSc dissertation (Mthembu, 2023) and provide additional information on the water use, yield, nutrient content and water productivity for both crops. Where appropriate, information gleaned from the initial literature review (previous chapter) was included here.

3.1 CLIMATE & SITE REQUIREMENTS

3.1.1 Sweet potato

Sweet potato (*Ipomoea batatas*) is well suited to subtropical and tropical growing conditions (Dladla et al., 2019), where average night-time temperatures range from 15-25°C (Masango, 2015). Although regions where annual rainfall ranges from 750-1,000 mm are most suited to sweet potato, 500 mm is acceptable, provided that all other conditions are optimal (Masango, 2015). An air temperature range from 21-29°C is considered optimum for sweet potato. The crop can tolerate average temperatures as low and high as 18 and 35°C, respectively (DAFF, 2011). The crop's ability to adapt easily to a wide range of ecologies suggests it has the potential to produce high yields (Motsa et al., 2015a). However, sweet potato can also be produced with low inputs under sub-optimal weather conditions and on marginal soils (Motsa et al., 2015a). According to Dladla et al. (2019), such growing conditions are associated with uneven rainfall distribution, high temperatures and high evapotranspiration rates. Sweet potato is well suited to loamy, sandy and clayey soil textures (Masango, 2015).

Sweet potato can grow to a height of approximately 1 m and takes between 4 to 5 months to reach physiological maturity (DAFF, 2011). Planting from mid-November to mid-December is considered ideal to ensure optimum production and the crop is usually harvested from April to May (DAFF, 2011). However, due to the crop's short season length, plantings in early January can also be considered. Rooting depth is typically 0.5 to 0.6 m (Masango, 2015). It is recommended that sweet potato is planted with an inter-row spacing of 0.9-1.06 m and between plant spacing of 0.3 m, which translates to a population of 31,447 to 37,037 plants ha⁻¹ (DAFF, 2011). Optimum spacing for sweet potato is 0.3 m between plants and 0.6 m between rows (55,278 plants ha⁻¹). However, row spacing can be decreased to 0.5 m (66,600 plants ha⁻¹) or increased to 0.9 m (~37,000 plants ha⁻¹).

Sweet potato is a short-cycle crops of three to four months in length (Dong et al., 2018). Their short growing cycle allows for flexible planting and harvesting times and also permits quick production of foods to augment "hunger months", i.e. a period of several months between sowing and harvest when people do not have food to satisfy their food requirements to meet their necessary caloric and nutritional needs (Allemann et al., 2004; Beletse et al., 2013).

Sweet potato is generally considered a drought tolerant crop, but the selection for appropriate genotypes for drought conditions remains a priority. Therefore, sweet potato (cassava and yam) produce more "yield per drop" than major cereal crops. The plant has several coping mechanisms, such as reducing leaf area with increasing water stress, as well as leaves that wilt permanently at a much lower water potential (-1.3 MPa) when compared to other crops (Ravi et al., 2014; Sunitha et al., 2013). This is because sweet potato leaves accumulate large quantities of proline (Saravanan and Ravi, 2012). In addition, the crop's leaf area decreases as water stress increases (Nedunchezhiyan et al., 2012).

However, mechanisms that allow for drought avoidance usually have a high yield penalty, i.e. water stress inhibits the growth of sweet potato. Water stress may delay tuber initiation, thus reducing the final yield. Water stress during tuber bulking can also lead to malformation of tubers. According to Önder

et al. (2015), water deficits of 20 to 40% under drip irrigation caused a crop yield decrease of 25 to 50%. Regarding genotype differences, there is a difference between white- and orange flesh tubers.

3.1.1.1 White flesh cultivars

In general, white flesh cultivars (e.g. A40) have a lower nutrient content than orange flesh cultivars. This typically translates to lower nutritional water productivity. Thus, white flesh sweet potato (WFSP) should not be grown, especially in rural communities where vitamin A deficiency is a known problem.

3.1.1.2 Orange flesh cultivars

Orange flesh sweet potato (OFSP) cultivars (e.g. A45 and 199062.1) are good sources of natural β -carotene (van Jaarsveld et al., 2006), is a precursor of vitamin A. The higher β -carotene gives the flesh its more orange colour, which explains why the vitamin A content of OFSP is considerably higher than that of WFSP. According to Labadarios et al. (2005), vitamin A deficiency in South Africa remains a health issue for growing children and teenage women. The consumption of boiled OFSP cultivars can therefore improve low vitamin levels (Low et al., 2017). These cultivars should therefore be promoted in developing countries (Wenhold et al., 2007). Masango (2015) recommended that the South African Medical Research Council and the Agricultural Research Council should promote the production of foods rich in natural β -carotene, such as OFSP.

3.1.2 Taro

Taro grows optimally in warm conditions where frost occurrence is minimal (Sibiya, 2015). It grows well in areas with (i) elevations ranging from 0-1,800 m, (ii) average temperatures range from 21-27°C, and (iii) annual rainfalls exceeding 800 mm (Modi and Mabhaudhi, 2016). Although tannia and taro possess similar growth habits, tannia is more drought tolerant and sensitive to waterlogging compared to taro. This is reflected in the crop water requirement differences of both these crops, where taro requires 250-500 mm more water.

Taro (*Colocasia esculenta*) can reach a height of 1-2 metres over a 6-8 month growing season (Miyasaka et al., 2003; Deo et al., 2009). Although taro takes 7 months (210 days) on average to mature, authors differ on how to define the different growth stages (Mabhaudhi, 2012). The root system is considered fibrous and grows mainly in the top metre of soil (Joubert and Allemann, 1998). According to DAFF (2010), a planting date from mid-November till December is recommended for taro to achieve optimum crop development. However, planting dates up to April can be viable in warmer areas. Mabhaudhi et al. (2023) also stated that the best planting time is between December and April, but plantings can be made any time during the year if moisture is adequate.

An inter-row spacing of 1.3 m and an intra-row spacing of 0.4 to 0.5 m is recommended to achieve a population of between 20,000 and 25,000 plants ha⁻¹. For small areas, the distance between rows and plants should be 1 m, i.e. 10,000 plants ha⁻¹ (DAFF, 2010). In KwaZulu-Natal, a common row spacing of 0.6 m is used, where the plants are also planted 0.6 m apart, resulting in a plant density of 27,778 plants ha⁻¹. According to Mabhaudhi et al. (2023), plant density should range between 6,000 and 10,000 plants ha⁻¹ for smallholder plots but should be increased to 15,000-20,000 plants ha⁻¹ for commercial cultivation.

Shange (2004) reported that taro can grow in well-drained, aerated soils, and soils that experience waterlogging for prolonged periods. However, to ensure maximum growth, the crop prefers sandy loam soils with good drainage and high organic matter content (Shange, 2004). The wide range in suitable soils and crop water requirements reported in **Section 2.4.4** (cf. **Chapter 2**) is primarily due to genotype

differences in water use and drought tolerance. There are two genotypes, namely upland and lowland taro, which are described next.

3.1.2.1 Upland taro

Upland taro (e.g. Umbumbulu landrace) generally has lower optimum crop water requirements and yield potential compared to lowland taro. Among the dasheen and eddoe types of taro, eddoe type is more tolerant to drought conditions since eddoes are hardier than the dasheens and can be grown in rainfed conditions in less fertile soils (Sunitha et al., 2013). Stomatal regulation plays a role in acclimation of taro water stress. The increase in stomata and leaf area between 4 and 6 months of crop growth indicates more transpiration loss from the crop canopy, which eventually increases water requirements during this period. Mabhaudhi et al. (2013b) showed that stomatal conductance was lower under low water availability. Stomatal closure is a drought avoidance mechanism (Ferreira-Silva et al., 2008; Otieno et al., 2012), which allows the crop to minimise transpiration. It is widely accepted as a major limitation to photosynthesis and biomass production under drought stress. However, mechanisms that allow for drought avoidance usually have a high yield penalty.

In contrast, have a greater degree of stomatal control and, thus, can minimise water loss via transpiration. Therefore, upland taro landraces exhibit higher water productivity compared to the lowland landrace (cf. **Section 3.2.2**). Hence, this landrace is better suited to water-scarce conditions (Uyeda et al., 2011; Mabhaudhi, 2012), where it can produce sufficient yields and, thus, can positively contribute to food security.

3.1.2.2 Lowland taro

Lowland taro (e.g. KwaNgwanase landrace) has a higher crop water requirement than upland taro, and thus some farmers grow the crop in waterlogged areas such as marshes and wetlands (Everson and Mengistu, 2011), particularly along the coastal regions of KwaZulu-Natal. Thus, lowland taro landraces are highly tolerant of waterlogging. The crop is also grown in the Limpopo and Mpumalanga provinces, including the Pondoland region of the Eastern Cape. Since lowland landraces are more sensitive to conditions of limited water availability, they should not be considered for low-input farming under rainfed conditions in South Africa. Yields and crop water productivity are generally lower for lowland taro when compared to upland taro (cf. **Section 3.2.2**).

However, Everson and Mengistu (2011) found that lowland taro grown in a *Cyperus latifolius* marsh where water availability is non-limiting to growth, did not necessarily produce high evapotranspiration rates. They calculated the crop coefficients (K_c) as the ratio of measured ET (using an eddy covariance system) and reference crop evapotranspiration (ET_0). Daily K_c values (4 in November 2009 and 6 in January 2010) varied between 0.46 and 0.81, suggesting that lowland taro was relatively conservative in terms of water use (Everson and Mengistu, 2011).

3.2 CROP WATER USE, YIELD & WATER PRODUCTIVITY

3.2.1 Sweet potato

Using the soil water balance method, Masango (2015) estimated the water use of rainfed and irrigated sweet potato. Four water treatments were considered as shown in **Table 3-1**. Crop evapotranspiration (ET) of the T_{T1W} treatment was 38% greater than that of the T_{DRY} treatment, yet there was only a 7.1% difference in yields. This is because crop growth and the degree of yield reduction resulting from water deficits depend on various factors, such as the timing and duration of the water deficit (FAO, 2002). Pandey et al. (2000) reported that CWP increases by improving yield or decreasing ET. From **Table 3-1**, CWP was highest under the T_{DRY} treatment and decreased with increasing irrigation. Under water

limited relative to optimum conditions (Motsa et al., 2015b), sweet potato can produce higher yields, and thus higher CWP, as shown in the table below.

Table 3-1 Yield and water balance components per treatment for sweet potato, from which crop water use (ET) and water productivity (CWP) were estimated (Masango, 2015)

Treatments	P (mm)	I (mm)	ΔS (mm)	ET (mm)	Yield (dry t ha ⁻¹)	CWP (kg m ⁻³)
T _{DRY}	301	50	-7	298	7.6	2.55
T _{O2W}		232	89	321	6.6	2.06
T _{O1W}		282	83	365	6.5	1.78
T _{T1W}		447	31	478	7.1	1.49

T_{DRY} = rainfed with supplemental irrigation; T_{O2W} = irrigated once every two weeks; T_{O1W} = irrigated once in a week; T_{T1W} = irrigated twice in one week; P = precipitation; I = irrigation; ΔS = change in soil water content

Dladla et al. (2019) studied the water use, yield and CWP of three cultivars of sweet potato under two different agronomic practices (flattened and peaked ridges) at two locations (Umbumbulu and Fountainhill in KwaZulu-Natal, South Africa). Total biomass production comprises the above-ground biomass and root yield and at Fountainhill, was 60-70% lower than at Umbumbulu (**Table 3-2**). Similarly, fresh root yield was higher at Umbumbulu (13.2 to 35.5 t ha⁻¹) than at Fountainhill (7.6 to 17.8 t ha⁻¹). Although yields were lower at Fountainhill, the HI was approximately 30 to 50% higher when compared to Umbumbulu. This suggests that at Umbumbulu, the crop produced greater above-ground biomass than root yield. This can be due to the environment at Umbumbulu favouring vine and leaf growth at the expense of root growth. However, it could also be due to tubers at Umbumbulu being harvested before the completion of tuber yield formation.

Dladla et al. (2019) calculated the water use of sweet potato as a residual of the soil water balance equation (**Table 3-2**). Plants at Fountainhill used approximately 50% more water than at Umbumbulu. The authors indicated that sweet potato at Fountainhill took longer to reach maturity, which may have contributed to its higher water use due to the longer crop cycle. The higher water use and lower sweet potato yield at Fountainhill resulted in lower CWP estimates (0.74 to 2.08 kg m⁻³) relative to Umbumbulu (2.17 to 6.67 kg m⁻³), as shown in **Table 3-2**. Dladla et al. (2019) stated that the results obtained at Umbumbulu were in the same range as those from previously conducted studies (e.g. Önder et al., 2015).

Table 3-2 Water use and yield components of three sweet potato cultivars (A40, A45 and 199062.1) under two ridge types (peaked and flattened) at Fountainhill (FH) and Umbumbulu (UM) (Dladla et al., 2019)

Site	Ridge type	Cultivar	Total biomass (t ha ⁻¹)	Fresh yield (t ha ⁻¹)	ET (mm)	CWP (kg m ⁻³)	HI (%)
FH	Peak	A40	24.7	17.8	911	1.95	72.1
		A45	21.5	16.0	1,042	1.54	74.4
		199062.1	20.7	13.7	660	2.08	66.2
FH	Flat	A40	11.6	9.0	992	0.91	77.6
		A45	12.3	7.6	944	0.81	61.8
		199062.1	13.1	8.0	1,077	0.74	61.1
UM	Peak	A40	77.3	35.5	532	6.67	45.9
		A45	60.1	22.5	548	4.11	37.4
		199062.1	69.9	31.1	558	5.57	44.5
UM	Flat	A40	61.3	22.9	655	3.50	37.4
		A45	44.0	13.2	609	2.17	30.0
		199062.1	56.6	22.4	615	3.64	39.6

Planting sweet potato on ridges maximises biomass production and yield, as ridging allows for root expansion and improved water conservation (**Table 3-2**). Thus, CWP values were lower for flattened ridges due to lower yields when compared to values for peaked ridges. In contrast, Bombik et al. (2013) reported that sweet potato biomass and yield favoured flattened ridges.

Table 3-3 shows the dry tuber yield, total biomass (above-ground biomass and root yield), ET and CWP of OFSP, which were obtained from open-field experiments conducted at Rooiland (Pretoria, South Africa) over two seasons (Nyathi, 2019). Measurements were obtained from six treatments as indicated in the table. As expected, dry tuber yield was:

- highest for the W1F1H1 treatment (i.e. no water and soil fertility stresses, as well as no leaf harvesting), and
- lowest for the W2F2H2 treatment, which combined water and soil fertility stresses with leaf harvesting.

ET values were lower during the first (2013/14) season relative to the second (2014/15) (**Table 3-3**), which could be attributed to the shorter growing period of 130 vs 150 days. CWP values ranged from 1.05 to 2.71 dry kg m⁻³ and 1.18 to 2.78 dry kg m⁻³ for the 2013/14 and 2014/15 seasons, respectively. The water-stressed with no leaf harvesting treatment (W2F2H1 and W2F1H1) resulted in the highest exhibited CWP of 2.71 and 2.78 dry kg m⁻³, respectively. This is supported by Motsa et al. (2015b), who noted that sweet potato could produce high yields, and thus higher CWP under water-stressed conditions. This shows that sweet potato has the potential to be grown by rural-poor households under low agricultural input where crops are mostly rainfed.

Table 3-3 Dry tuber yield, total biomass, ET and CWP of OFSP (Nyathi, 2019)

Season	Treatments	Total biomass (t ha ⁻¹)	Tuber yield (t ha ⁻¹)	ET (mm)	CWP (kg m ⁻³)
S1	W1F1H1	13.0	10.0	491	2.04
	W1F1H2	10.0	5.7	427	1.33
	W1F2H1	0.0	8.1	460	1.76
	W1F2H2	8.8	4.7	446	1.05
	Mean	10.5	7.1	456	1.56
	W2F1H1	8.2	5.8	244	2.38
	W2F1H2	8.7	5.8	257	2.26
	W2F2H1	7.1	5.9	218	2.71
	W2F2H2	7.4	4.4	231	1.90
	Mean	7.9	5.5	238	2.31
S2	W1F1H1	20.0	17.0	658	2.58
	W1F1H2	14.0	11.0	629	1.75
	W1F2H1	13.0	11.0	595	1.85
	W1F2H2	10.0	7.1	592	1.20
	Mean	14.3	11.5	619	1.85
	W2F1H1	15.0	13.0	467	2.78
	W2F1H2	14.0	11.0	462	2.38
	W2F2H1	8.2	6.5	447	1.45
	W2F2H2	7.7	5.2	439	1.18
	Mean	11.2	8.9	454	1.95

W1 = optimum irrigation; W2 = deficit irrigation; F1 = optimum fertiliser application; F2 = no fertiliser application; H1 = no leaf/vine harvesting; H2 = leaf/vine harvesting; S1 = 2013/14; S2 = 2014/15

Leaf harvesting can therefore cause substantial reductions in tuber yield production (Nyathi, 2019), possibly due to reduced crop photosynthesis. Although yields were lower due to leaf harvesting, it shows that sweet potato is a dual-purpose crop. The stressed treatment combinations with no leaf harvesting produced reasonable amounts of dry total biomass and tuber yield, thus illustrating the capability of OFSP to survive under water-stressed conditions.

3.2.2 Taro

Mabhaudhi (2012) investigated the ET and yield of two taro landraces grown over two seasons and found that yields declined with decreasing irrigation (**Table 3-4**). Compared to the fully irrigated treatment, tuber yield was 15% and 47% lower for the moderate and deficit treatments, respectively. Under conditions of limited water availability, corm mass (not corm number) is more important (Mabhaudhi, 2012). The reduction of yield due to limited water availability is caused by reductions in canopy growth and production of biomass (Badr et al., 2012), which was supported by the findings of Mabhaudhi (2012)

Upland taro (Umbumbulu landrace), which is more adapted to water-limited conditions, produced higher fresh yields than upland taro (KwaNgwanase landrace). Hence, the latter landrace was negatively affected by water-limited conditions, especially in the second season. Upland taro has good stomatal control, enabling it to minimise water loss through transpiration and thus, produces more biomass and yield than lowland taro (Mabhaudhi, 2012).

For CWP, differences were observed between both seasons with CWP increasing with decreasing irrigation level, especially in the second season. The upland and lowland taro landraces had an average CWP of 0.32 and 0.15 kg m⁻³, respectively. Hence, upland taro was approximately twice more water use efficient than the lowland landrace, which is supported by Uyeda et al. (2011). However, taro's CWP is relatively low when compared to measured values for tree crops such as avocados (1.2-1.6 kg m⁻³) and indigenous fruit trees (2.0-2.5 kg m⁻³).

Table 3-4 Yield, harvest index and CWP of two taro landraces grown under a rainshelter at three irrigation levels over two seasons (Mabhaudhi, 2012)

Season	Irrigation treatment	Land-race	Fresh yield (t ha ⁻¹)	Harvest index (%)	CWP (kg m ⁻³)
S1	Deficit	UM	6.10	87	0.15
		KW	4.32	86	0.11
	Moderate	UM	9.31	90	0.17
		KW	3.83	86	0.07
	Optimum	UM	9.00	85	0.12
		KW	4.23	57	0.06
S2	Deficit	UM	12.96	62	0.53
		KW	5.70	71	0.17
	Moderate	UM	22.32	74	0.49
		KW	10.70	82	0.22
	Optimum	UM	23.90	63	0.44
		KW	17.33	79	0.27

S1 = 2010/11; S2 = 2011/12; UM = Umbumbulu (upland taro); KW = KwaNgwanase (lowland taro)

3.3 NUTRITIONAL WATER PRODUCTIVITY

3.3.1 Sweet potato

Sweet potato is regarded as a drought-tolerant crop that can also supply substantial vitamin and mineral amounts (Leighton, 2008). Sweet potato provides adequate amounts of starch and protein and is nutrient-dense as the tubers and leaves also contain nearly all nutrients (both macro and micro), and substantial amounts of vitamin C (Mabhaudhi et al., 2019).

Masango (2015) investigated the response of OFSP tubers under four water treatments. From **Table 3-5**, OFSP grown mainly under rainfed conditions (with only supplemental irrigation; T_{DRY}) exhibited the highest nutritional water productivity (NWP) of 1,177 mg m⁻³ for β-c (β-carotene). This further highlights the water use efficiency and nutritious benefits of OFSP.

Table 3-5 Nutritional water productivity of β-carotene (NWP_{β-c}) for OFSP (Masango, 2015)

Treatment	NWP _{β-c} (mg m ⁻³)
T _{T1W}	656
T _{O1W}	718
T _{O2W}	796
T _{DRY}	1,177

T_{DRY} = mostly rainfed with supplemental irrigation; T_{O2W} = irrigated once every two weeks; T_{O1W} = irrigated once in a week; T_{T1W} = irrigated twice in one week; β-c = β-carotene

Mulovhedzi (2017) estimated the NWP for OFSP and WFSP under three water treatments (**Table 3-6**). For both OFSP and WFSP, the NWP for Fe, Zn and β-c was higher under rainfed vs optimum irrigation. Although both white and orange flesh sweet potato can contribute to alleviating malnutrition in term of Fe and Zn content, OFSP has a much higher β-c content than WFSP, especially under rainfed conditions. Thus, the cultivation of OFSP should be promoted, instead of WFSP.

Table 3-6 Nutritional water productivity (NWP) of orange and white flesh sweet potato under three water treatments (Mulovhedzi, 2017)

Cultivar	Treatments	NWP (mg m ⁻³)		
		Fe	Zn	β-c
OFSP	Optimum irrigation	14.5	7.0	95.9
	Supplemental irrigation	12.6	6.7	93.9
	Rainfed	11.7	6.4	108.5
WFSP	Optimum irrigation	16.5	7.6	11.4
	Supplemental irrigation	13.9	7.6	18.6
	Rainfed	19.0	12.0	22.2

Table 3-7 presents the nutrient content (NC) for Fe, Zn and β-c (β-carotene) of OFSP tubers expressed on a dry mass basis, as measured by Nyathi et al. (2019a) over two seasons. OFSP tubers are rich in β-c with mean values of 2,250 and 1,980 mg kg⁻¹ for the non-harvested (H1) and harvested (H2) leaves, respectively. Furthermore, β-c was higher under water stressed conditions, irrespective of leaf harvesting. For the water and soil fertility stress (W2F2) treatment, tuber contents of Fe and Zn were higher when leaves were not harvested compared to when they were harvested. This suggests that under low agricultural input, Fe and Zn content in OFSP tubers can be maximised, provided there is no leaf/vine harvesting. Nyathi et al. (2019a) noted that leaf/vine harvesting should not be considered for market-oriented farming due to the high potential of reduced yields and nutritional concentrations of Fe and Zn. In general, nutritional water productivity (NWP) for Fe, Zn and β-c was higher under deficit irrigation, compared to optimum irrigation. As expected, NWP was higher when the crop was fertilised,

compared to the non-fertilised treatment. Furthermore, NWP was higher when no leaves were harvested, compared to leaf harvesting.

Table 3-7 Nutrient content of OFSP tubers obtained for the 2013/14 and 2014/15 growing seasons (Nyathi et al., 2019a)

Treatments		Nutrient content (mg kg ⁻¹)						Nutritional water productivity (mg m ⁻³)		
		Tubers			Leaves			Tubers		
		Fe	Zn	β-c	Fe	Zn	β-c	Fe	Zn	β-c
H1	W1F1S1	39	17	2,350	n.d.	n.d.	n.d.	84	35	4,906
	W1F1S2	45	13	2,210	n.d.	n.d.	n.d.	116	33	5,675
	W1F2S1	51	14	1,850	n.d.	n.d.	n.d.	64	18	2,401
	W1F2S2	70	11	2,210	n.d.	n.d.	n.d.	135	23	4,665
	Mean	51	14	2,155				100	27	4,412
	W2F1S1	29	14	1,820	n.d.	n.d.	n.d.	99	46	6,119
	W2F1S2	87	12	2,480	n.d.	n.d.	n.d.	210	27	5,966
	W2F2S1	38	17	2,140	n.d.	n.d.	n.d.	107	45	3,838
	W2F2S2	112	13	2,930	n.d.	n.d.	n.d.	160	19	4,307
Mean	67	14	2,343	n.d.	n.d.	n.d.	144	34	5,058	
H2	W1F1S1	46	16	2,140	530	320	430	61	21	2,875
	W1F1S2	35	9	1,730	480	250	370	60	16	2,689
	W1F2S1	48	16	1,820	690	300	630	63	20	2,367
	W1F2S2	70	10	1,730	440	200	380	139	20	3,256
	Mean	50	13	1,855	535	268	453	81	19	2,797
	W2F1S1	43	13	2,030	450	310	440	80	24	5,893
	W2F1S2	62	10	2,180	480	260	480	99	15	3,336
	W2F2S1	27	14	1,930	450	300	470	55	28	3,724
	W2F2S2	38	11	2,290	460	260	480	47	13	2,712
Mean	43	12	2,108	460	283	468	70	20	3,916	

H1 = no leaf/vine harvesting; H2 = leaf/vine harvesting; W1 = optimum irrigation amount; W2 = deficit irrigation; F1 = optimum fertiliser application; F2 = no fertiliser application; S1 = 2013/14; S2 = 2014/15; β-c = β-carotene

Table 3-8 provides the NC of sweet potato cultivars grown under optimum and deficit conditions (Mabhaudhi et al., 2019). Mabhaudhi et al. (2019) reported that in some instances, the protein content of sweet potato cultivars increases with increasing water use, which was not the case of the 199062.1 cultivar. β-c was higher under the water deficit treatment for all cultivars, but this was not the case for all elements. This again highlights sweet potato's ability to produce higher amounts of β-c under water-limited conditions. The β-c content of the orange flesh cultivars (A45 and 199062.1) for both water treatments was considerably higher than that for the white flesh (A40) cultivar. Thus, the cultivation of OFSP cultivars should be promoted rather than white flesh cultivars. The β-carotene content of OFSP tubers shown in **Table 3-8** was substantially lower than that obtained by Nyathi (2019) (cf. **Table 3-7**), which cannot be explained (i.e. unlikely due to cultivar differences alone).

Mabhaudhi et al. (2019) also estimated the NWP of sweet potato (**Table 3-9**). For at least one of the cultivars, the change in NWP from deficit to optimum water treatment was statistically significant (Mabhaudhi et al., 2019). As expected, the NWP of β-c for OFSP (A45 and 199062.1) is much higher than for WFSP (A40). However, under optimum conditions the β-c content and NWP_{β-c} of the A45 cultivar is more than twice that of the 199062.1 cultivar. The most significant finding is that NWP was higher for all elements under water-limited conditions, compared to optimum conditions, regardless of the cultivar. This trend was also observed in all the above-mentioned studies (Masango, 2015; Mulovhedzi, 2017; Nyathi et al., 2019a), including a study by Lundqvist et al. (2021) in Ethiopia, which also showed that the NWP of minerals and vitamins was substantially higher under the stressed treatment, compared to the non-stressed water treatment.

These results show that sweet potato has the potential to produce a higher amount of nutrients per unit of water consumed under water-stressed conditions. Thus, this crop has the potential to sustain poor rural households located in marginal areas, as OFSP produces not only relatively high yields (Motsa et al., 2015b; Masango, 2015) but also a high amount of nutrients, whilst efficiently using water.

Table 3-8 Nutrient content of three sweet potato cultivars under two water treatments (Mabhaudhi et al., 2019)

Water treatment	Cultivar	Nutrient content							
		(g kg ⁻¹)		(mg kg ⁻¹)					
		Fat	Pro	Fe	Zn	β-c	Ca	Mg	Na
Optimum	A40	7.3	75.1	399	9.0	2	5.3	1.3	2.1
	A45	9.1	61.8	622	15.4	198	2.4	0.7	2.4
	199062.1	14.3	43.0	529	13.4	53	4.8	0.9	0.8
Deficit	A40	7.5	53.6	868	16.8	29	5.1	1.2	1.0
	A45	9.4	38.9	269	11.0	232	1.3	0.6	1.0
	199062.1	1.4	53.8	428	14.4	101	4.6	1.0	1.1

Pro = Protein; β-c = β-carotene

Table 3-9 Nutritional water productivity of three sweet potato cultivars under two water treatments (Mabhaudhi et al., 2019)

Water treatment	Cultivar	Nutritional water productivity							
		(g m ⁻³)		(mg m ⁻³)					
		Pro	Fat	Fe	Zn	β-c	Ca	Na	Mg
Optimum	A40	354	34	1,877	42	9	25.4	9.88	5.58
	A45	295	43	2,968	72	945	11.9	11.45	3.82
	199062.1	352	117	4,325	106	433	62.8	7.36	7.36
Deficit	A40	555	77	8,968	176	300	52.7	10.33	12.40
	A45	499	121	3,464	141	2,976	16.7	14.11	7.70
	199062.1	1,405	268	7,978	261	1,881	85.7	22.47	18.64

Pro = Protein; β-c = β-carotene

3.3.2 Taro

The high nutritional value of taro is one of the main reasons for promoting its commercial-scale production. Mabhaudhi et al. (2016a) stated that taro leaves are (i) high in minerals (e.g. Na, Zn and Fe) and vitamins (e.g. A, B and C), and (ii) suitable for human consumption. Vitamin B and C complexes (niacin, thiamine and riboflavin) found in taro leaves and corms are essential for a healthy diet. The starch contained in the corms is generally high (70-80% dry weight basis) and highly digestible (Mabhaudhi et al., 2023). Therefore, taro may be consumed as a source of carbohydrates and protein (11% dry weight basis) (Mabhaudhi et al., 2016a; 2023). Taro's high potassium-to-sodium ratio is recommended for people with high blood pressure (Modi and Mabhaudhi, 2016). Vitamins B (niacin, riboflavin and thiamine) and C are present in appreciable quantity in corms and leaves of taro (Mabhaudhi et al., 2023).

Table 3-10 provides the mineral composition of upland taro tubers (Umbumbulu landrace), which is higher under deficit irrigation, when compared to fully irrigated conditions (except for Cu). However, when NWP is considered, it is higher under water-stressed conditions for all elements (including Cu). This is the same trend observed for sweet potato (cf. **Section 3.3.1**) and supports the finding by Chivenge et al. (2015) that certain nutrient-dense RTCs can address nutrition insecurity issues in environments that are water scarce.

Table 3-10 Average nutritional content of taro tubers (UM landrace) under two water treatments (Shelembe, 2020)

Water treatment	Nutrient content (mg kg ⁻¹)				
	Na	Fe	Al	Mn	Cu
Optimum	229.91	45.77	39.48	6.19	4.59
Deficit	371.77	83.27	62.93	7.84	3.56
	Nutritional water productivity (mg m ⁻³)				
Optimum	1,487.33	269.29	255.87	39.33	29.79
Deficit	2,889.41	643.33	486.45	58.90	27.73

3.4 SUMMARY & CONCLUSIONS

The CWP metric measures how efficiently a plant utilises water and converts it into yield (Masango, 2015). Modi and Mabhaudhi (2020) stated that the main aim of crop production is to produce “more crop” while using water efficiently. It is crucial to improve water productivity within existing rainfed agricultural systems (Renault and Wallender, 2000). Compared to staple food crops such as maize and soybean, RTCs exhibit resilience under water stressed conditions and can produce higher yields using less water. Both sweet potato and taro are regarded as dual-purpose crops, as both their leaves and tubers can be consumed. Although sweet potato leaves can be harvested during the growing season, this reduces tuber yield (Islam, 2006; Nyathi, 2019).

Sweet potato is known for its lower water use under rainfed conditions (Masango, 2015), and thus is considered water use efficient with a moderate to high NWP (Masango, 2015; Mabhaudhi et al., 2019). Due to sweet potato’s drought tolerance (Motsa et al., 2015b), the crop can adapt to a wide range of agro-ecologies and thus, has the potential to produce high yields under water-stressed conditions (Motsa et al., 2015a). Masango (2015), Mulovhedzi (2017) and Mabhaudhi et al. (2019) reported that sweet potato exhibits high NC and CWP values, which translates to high NWP values under water limited relative to optimum conditions. This highlights the crop’s ability to respond well to soil water deficits. Furthermore, OFSP tubers and leaves exhibit substantially higher β -carotene levels than (i) WFSP tubers, and (ii) other indigenous RTCs (e.g. taro).

Taro landraces have a lower CWP compared to that of other RTCs, such as potato and sweet potato (Uyeda et al., 2011; Badr et al., 2012; Mabhaudhi, 2012). Taro yields are negatively affected by decreasing water application rates, due to lower biomass production. Hence, reducing the amount of applied irrigation did not substantially increase taro’s CWP (Mabhaudhi, 2012). Certain RTC landraces struggle under water-limited conditions due to a lack of defensive mechanisms that enable the crop to consume water while maintaining canopy expansion and biomass production efficiently (Badr et al., 2012). For example, upland taro landraces exhibit better stomatal control, and thus are more water use efficient when compared to lowland taro landraces.

From the literature review, more information exists for sweet potato when compared to taro. However, Nyathi (2019) highlighted the importance of future research assessing NWP across agro-ecologies. To address the knowledge gaps, field trials were conducted to measure the water use, yield and nutrient content of OFSP and taro under rainfed conditions, from which information on CWP and NWP was gleaned. The methodology and results pertaining to the field trials is presented in the next chapter.

4 MEASUREMENT OF WATER PRODUCTIVITY: SEASON 2

4.1 INTRODUCTION

Field trials were conducted in KwaZulu-Natal with sufficient fetch to facilitate crop evapotranspiration measurements using two micrometeorological techniques, namely the eddy covariance and surface renewal. In the first season (2020/21), animal damage was first observed on 11th January 2021. The initial damage caused by porcupine was then gap filled. However, bush pig attracted to the corm's sugar content caused significant damage over the next 10 days. A decision was taken in mid-February to discontinue the field trial due to (i) difficulty in obtaining additional material for further gap filling, and (ii) excessive weed growth. The latter was caused by high rainfall and hot temperatures experienced since planting and limitations in hiring casual workers from Swayimane for manual weeding. OFSP was not planted because a postgraduate student decided not to pursue his MSc study due to concerns related to the COVID-19 pandemic. In the second season (2021/22), crop water use, yield and nutrient content of OFSP and taro were measured at two trial sites at Fountainhill Eco-estate. A summary of the approach taken and main findings are presented next.

4.2 MATERIALS AND METHODS

4.2.1 Site description

Fountainhill Eco-estate (29°26'57"S; 30°32'41"E; elevation 851 m a.s.l.) is located about 32 km north-east of Pietermaritzburg along the R614 road to Wartburg in the uMshwathi Local Municipality of KwaZulu-Natal, South Africa. It represents an agro-ecological model that blends commercial agriculture (primarily sugarcane and avocado production) and conservation. Of the total 2,243 ha eco-estate, 780 ha is utilised for commercial agriculture, with the balance set aside for conservation of biodiversity in the Umgeni catchment (Musokwa et al., 2020). All revenues derived from commercial operations are invested in a trust fund to support the main goal of the eco-estate. Fountainhill offers the eco-estate and its facilities for research purposes and works closely with three universities (KwaZulu-Natal, Rhodes and Potchefstroom). A research symposium is held annually at the eco-estate to provide feedback on research undertaken on the farm, including topics of relevance to sustainable agriculture and conservation (source: Fountainhill [website](#)).

Fountainhill Estate is situated within the Moist Midland Mistbelt agro-ecological zone, with natural vegetation biomes being a mixture of Valley Thicket and Natal Central Bushveld Savanna (Low and Rebelo, 1996). Soil textures in the Wartburg region are mainly fertile loamy sand and sandy loam soils with medium to high drainage, which is ideal for agricultural crop production (Modi and Mabhaudhi, 2020). However, climate and soils across the eco-estate vary considerably. Soils range from 350 mm in depth with clay contents of 5% or less, to deep and heavy clays. More than 34% of the soils are extremely sandy with clay contents below 13%. High value crops are grown on deep, well-drained soils where annual rainfall exceeds 1,000 mm and where possible, clay contents are 18% or more. Cultivation is restricted to areas with adequate agricultural potential that receive on average at least 640 mm of rainfall per annum (source: Fountainhill [website](#)). Climate data was obtained from the South African Sugarcane Research Institute (SASRI) weather portal for an automatic weather station (AWS) located at Bruyns Hill and Fountainhill (**Table 4-1**).

Table 4-1 Climate data obtained from two automatic weather stations located at Bruyns Hill and Fountainhill

Location	Mean annual		Mean monthly temperature (°C)		Data range
	Rainfall (mm)	Temperature (°C)	Minimum	Maximum	
Bruyns Hill	568-1,094 (830)	17.9	11.8	24.0	Jan 2000 to Aug 2021
Fountainhill	603-853	17.5	10.2	24.8	Jan 2016 to Dec 2021

In July 2020, an initial site visit was conducted where the Project Team met with the Farm Manger to discuss the location of two suitable trial sites and the issue of potential threat of animals such as bush pig and porcupine. The Farm Manager mentioned that monkeys were likely to be the only nuisance affecting crop cultivation, adding that vehicle access gates must be kept closed to prevent larger animals from entering the trial sites.

Fountainhill is not ideally suited for the optimum growth of OFSP (Dladla et al., 2019) or taro. Hence, above-ground biomass and tuber yield are lower compared to more sub-tropical sites such as Umbumbulu. Since the project wanted to include the nearby Swayimane community to assist with establishing, weeding and harvesting the field trial, Fountainhill was chosen as the experimental site. Both OFSP and taro are grown by the subsistence and smallholder farmers within the Swayimane community, thus proving a source of material for the trials, especially for taro.

4.2.2 Planting material

OFSP and taro planting material were obtained from two locations in KwaZulu-Natal. The planting material is considered well suited to growing conditions at Fountainhill. For both crops, it was necessary to establish a nursery for propagating healthy planting material ahead of planting. This was important due to the large area of each trial. Based on the literature review, this project only considered one common cultivar of OFSP (199062.1). The orange flesh cultivar was selected due to its high β -carotene content, which is a precursor of vitamin A (Chivenge et al., 2015). In September 2021, approximately 100 vines were obtained from the horticultural greenhouse at the College of Agriculture in Cedara, KwaZulu-Natal, South Africa.

Corms of the Dumbe dumbe landrace were sourced from local smallholder farmers located in Swayimane, who were compensated for their produce. Dumbe dumbe is an upland (eddoe type) landrace characterised by a central corm and numerous edible side cornels (Lebot, 2019). In order to eliminate propagule size effects, corms were initially selected for uniform plant size (Singh et al., 1998). Propagules were treated with a bactericide and fungicide (Sporekill®) to prevent rotting during sprouting.

The vine cuttings (or slips) of OFSP and sprouted corms of taro were then propagated (i) at UKZN's research farm (Ukulinga), and (ii) in raised greenhouse beds located at UKZN in Pietermaritzburg (**Figure 4-1**). An automated drip irrigation system was programmed to deliver 10 mm of water daily. Although the propagation of planting material began two months prior to the target planting date, insufficient OFSP material was produced to only cover a 50 m by 50 m area (2500 m²) and not 6,400 m² as originally planned.

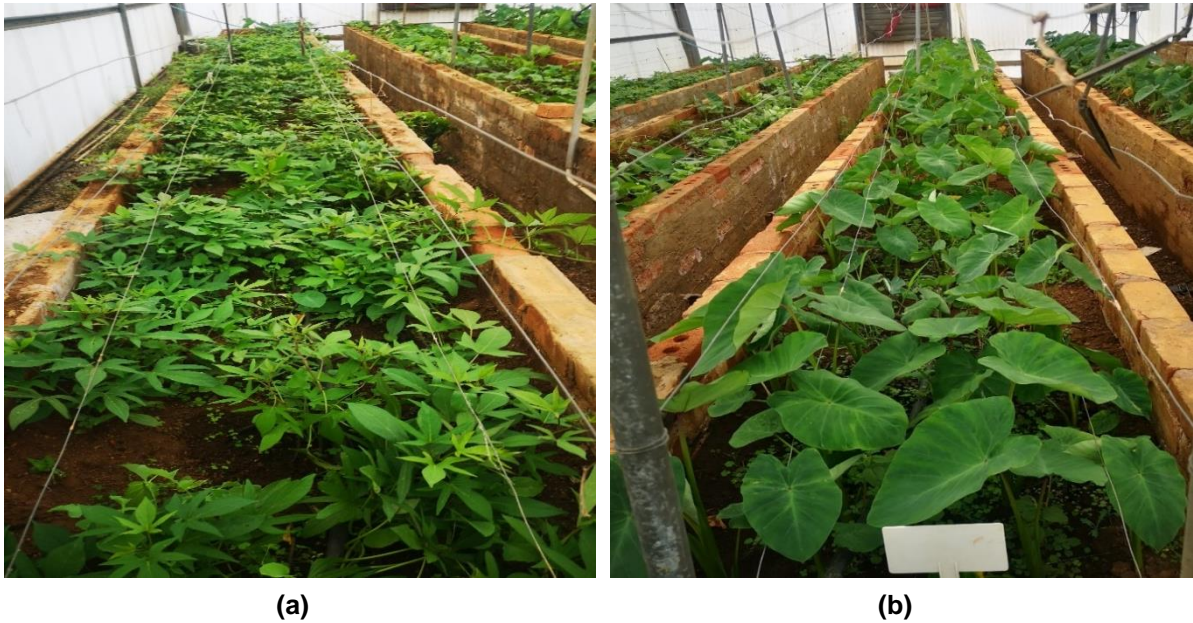


Figure 4-1 Propagation of (a) orange flesh OFSP (199062.1 cultivars) and (b) taro (Dumbe dumbe landrace) in raised greenhouse beds located at the University of KwaZulu-Natal in Pietermaritzburg

4.2.3 Experimental design

This rainfed study was conducted at two sites selected for field trials within the Fountainhill Eco-estate as shown in **Figure 4-2**. Trial site 1 was 9,750 m² (130 by 75 m) in size and was allocated to taro. Trial site 2 was approximately 130 by 50 m (6,500 m²), which was allocated to OFSP. Both trial sites provided sufficient fetch to accurately measure crop water use using two micrometeorological techniques described in **Section 4.2.5**.



Figure 4-2 Satellite-based image showing the location of the two trial sites at Fountainhill Eco-estate (source: Google Earth®)

4.2.4 Agronomic practices

Land preparation involving mechanical ploughing and disking of both trial sites was completed by Fountainhill staff in early November 2021, which was delayed by equipment breakdowns. This resulted in the trials being planted later than initially expected. Mechanical ploughing was necessary to ensure that weeds were removed prior to planting. However, the agronomic practices described next were completed mainly by two postgraduate students working on the project, together with staff from UKZN's Ukulinga research farm as well as casual workers from the local Swayimane community.

4.2.4.1 Planting

Planting of taro corms and OFSP vines was completed at site 1 and 2 on 18-19 November and 13-14 December 2021, respectively. Trial establishment involved 20 workers from the Swayimane community. Both trials were planted at a target density of 20,000 plants ha⁻¹ (1 m row spacing and 0.5 m plant spacing). Sweet potato vines were hand planted on ridges, whereas taro corms were individually sown at a depth of 0.15 m in furrows that were opened up mechanically. Trial establishment involved 20 casual workers from the Swayimane community.

4.2.4.2 Fencing

Although both trial sites were already fenced off, a second (inner) fence was installed at site 1 and strengthened with netting, to prevent further animal damage in the second season. At site 2, the fence was also reinforced with netting and secured with heavy logs to prevent animals destroying the growing roots. These tasks were completed with the assistance of staff from the UKZN's research farm. This was necessary after the Farm Manager eventually admitted that both trial sites are highly susceptible to animal damage, and thus are no longer used by the farm for sugarcane production.

4.2.4.3 Fertilisation

Based on the results of soil fertility tests (cf. **Section 4.2.6.2**), the required fertiliser application rates were calculated for both trial sites, including the number of fertiliser bags that needed to be purchased. An organic fertiliser called Gromor Accelerator® (30 g kg⁻¹ N, 15 g kg⁻¹ P and 15 g kg⁻¹ K) was applied at a rate of 5,333 and 3,333 kg ha⁻¹ to site 1 (taro) and site 2 (OFSP), respectively. The fertiliser application rate was calculated by accounting for the amount of pure Nitrogen (in kg ha⁻¹) recommended by Cedara (cf. **Section 4.3.2.1**), the pure Nitrogen content of the Gromor Accelerator® fertiliser and the trial site area. Fertiliser granules were applied 10 cm away from each transplanted vine or corm.

4.2.4.4 Pest and weed control

During sweet potato propagation, the crops were sprayed with Kemprin insecticide (a/l cypermethrin), diluted at a rate of 185 ml per 16 L of water. The same insecticide was sprayed halfway through the growing season at the experimental site at the same dilution rate.

Prior to planting and midway through the growing season, weed growth was controlled by spraying both trial sites with Gramoxone (pre-emergent herbicide) at a dilution rate of 200 ml per 16 L of water. However, high temperatures and frequent rainfall events that occurred after planting, resulted in rapid weed development. Due to the university being closed in the last week of December 2021, it was not possible to organise casual workers to assist with weeding. Hence, this task was delayed to the end of January 2022, which not only influenced initial crop growth but also delayed crop measurements to the 9th of February (57 DAP).

4.2.5 Instrumentation

Crop water use refers to the amount of soil water a) lost by evaporation, and b) utilised for biomass accumulation via transpiration. Various methods are used to measure crop water use, of which hydrological approaches (e.g. soil water balance and lysimetric measurements) are the most common. More recently, micro-meteorological techniques (e.g. eddy covariance and surface renewal) have also been used to assess crop water use. The soil water balance method was used to estimate crop water use, which was then compared to measurements obtained by the eddy covariance and surface renewal techniques, as explained next.

For the soil water balance method, runoff plots were only installed at trial site 1 as the gradient was deemed sufficient to produce overland flow. Weekly field visits were undertaken to measure runoff and crop growth, as well as to ensure that other instrumentation was working correctly. Daily rainfall measurements were obtained from the AWS located on the eco-estate. No irrigation was applied since the trials were rainfed. The CS650 soil moisture probe (Campbell Scientific Inc, Utah, USA) was used to directly measure volumetric soil water content. Three probes were installed at depths of 0.15, 0.30 and 0.60 m, considering the rooting depth of OFSP and taro seldom exceeds 0.60 m (Mabhaudhi, 2012; Masango, 2015; Mulovhedzi, 2017). Furthermore, a hard layer of sandstone was found below 60 cm, which prevented the installation of additional sensors to measure drainage beyond the effective rooting zone. Soil water content measurements were made every 15 to 30 minutes, then averaged to hourly and daily values and stored using a CR1000 data logger (Campbell Scientific, Utah, USA).

A lattice mast tower was setup at trial site 1 and 2 in June and August 2021, respectively (**Figure 4-3**). On each tower:

- an eddy covariance (EC) flux system was installed at 1.5 m (Campbell Scientific Inc., Logan, Utah, USA), which consisted of a three-dimensional sonic anemometer (Campbell Scientific Inc., Logan, Utah, USA) for measuring sonic temperature, wind speed and direction, as well as an infrared gas analyser (IRGA) (Campbell Scientific Inc., Logan, Utah, USA) for measuring atmospheric CO₂ concentrations (Nordbo et al., 2012);
- a surface renewal (SR) system was installed which consisted of two type-E fine wire thermocouples connected to two arms for measuring air temperature at high frequency above the canopy (1 m) and within the turbulent boundary layer (3 m) (Nagler et al., 2005; Nordbo et al., 2012).



Figure 4-3 Micrometeorological equipment installed at the (a) taro and (b) OFSP trial sites located within the Fountainhill Eco-estate

The EC and SR methods were connected to a CR3000 and CR1000 data logger (Campbell Scientific, Utah, USA), respectively. The high frequency (10 Hz) measurements of wind speed, wind direction, sonic temperature and air temperature (via thermocouples), together with 2- and 30-minute averages, were calculated and stored by the data loggers for further analysis. All instrumentation was powered by two 12V DC batteries secured in a strongbox near each lattice mast. Battery voltage was monitored weekly and batteries were changed once their voltage dropped below 12.2V DC. At trial site 2 (OFSP), a solar panel was installed to help recharge the batteries to minimise battery replacements.

Other relevant sensors required to complete the shortened energy balance equation were also installed. These included soil heat flux plates (HFP01-15) (Delft, Netherlands) at 8 cm, soil temperature averaging thermocouples (TCAV-L) (Campbell Scientific Inc., Utah, USA) at 2, 5 and 8 cm, a NR-LITE net radiometer (Kipp and Zonen, Delft, Netherlands) at 3 m and a Vaisala HMP45C-L temperature and relative humidity probe (Campbell Scientific Inc., Utah, USA) at 2 m. In addition, two DS-2 sonic anemometers (Decagon Devices, Washington, USA) were installed to measure wind speed and direction above the canopy (1 m) and within the turbulent boundary layer (2 m).

4.2.6 Data collection

At both sites, weekly measurements of crop growth (e.g. plant height, leaf number, leaf area index & biomass accumulation) and health/stress indicators (chlorophyll content index, stomatal conductance & leaf temperature) began on 9 February 2022 in four (1 m by 1 m) quadrants, each with four plants, i.e. 16 plants in total. Destructive sampling was also conducted every week for sweet potato, but every two weeks for taro.

4.2.6.1 Climate

Using data collected by the sensors attached to each lattice mast and buried in the ground, the Penman-Monteith method (**Equation 5**) was used to calculate hourly and daily reference evapotranspiration (ET_0 in mm d⁻¹) for a hypothetical grass surface (Allen et al., 1998). The equation requires daily net radiation (R_n in MJ m⁻² d⁻¹), air temperature (T in °C), wind speed (u_2 in m s⁻¹) and relative humidity (RH in %) measured at 2 m above the ground:

$$ET_0 = \frac{0.408\Delta(R_n - G) + \gamma \frac{900}{T + 273} u_2 (e_s - e_a)}{\Delta + \gamma(1 + 0.34u_2)} \quad \text{Equation 5}$$

For daily estimates of ET_0 , soil heat flux density (G in MJ m⁻² d⁻¹) is presumed to be zero. The saturated vapour pressure (e_s in kPa) is calculated from daily maximum and minimum air temperature, from which the actual vapour pressure in kPa (e_a) is estimated using relative humidity ($e_s \cdot RH/100$). The term ($e_s - e_a$) represents the vapour pressure deficit (kPa) and Δ is the slope of the vapour pressure curve (kPa °C⁻¹). The altitude of the site is required to estimate the atmospheric pressure in kPa, which is then used to determine the psychrometric “constant” (γ) in kPa °C⁻¹.

ET_0 was estimated using FAO’s ET_0 Calculator utility (version 3.2; FAO, 2012a), which is based on the FAO56 (Penman-Monteith) method described by Allen et. al. (1998). It is important to note that ET_0 was calculated from daily climate variables, which is slightly less accurate than daily totals derived from hourly-derived values, especially for the summer months (Kunz et al, 2020). However, it is generally accepted that the accuracy gained by using hourly data does not warrant the effort required. Although most crop simulation models can calculate ET_0 within the model, the preferred approach was to calculate this variable externally for error checking purposes. For example, it is unknown why ET_0 values calculated by the SWB crop model were lower than those calculated using ET_0 Calculator ($ET_{0_SWB} = 0.81 \cdot ET_{0_FAO} + 0.54$; $R^2 = 0.967$).

4.2.6.2 Soil fertility

During the first season, soil samples were taken for the top 15 cm from trial site 1 (August 2020) and site 2 (February 2021) for fertility analysis. The analysis was undertaken by the Cedara laboratory at the College of Agriculture (KwaZulu-Natal) using recognised techniques as described by Manson and Roberts (2001).

4.2.6.3 Soil depth and texture

Soil depth was randomly augured across both sites, which is at least 1.2 m deep, i.e. no layer restricting root development was found. Soil samples augured at three depths (0.15, 0.30 & 0.60 m) were taken at both trial sites, then sent to the College of Agriculture (Cedara, KwaZulu-Natal) to determine particle size distribution as described by Manson and Roberts (2001). Fractions of sand, silt and clay were also determined in the soil and water laboratory at UKZN using the hydrometer method. Soil texture was then determined using the USDA classification system adopted by South Africa's taxonomic soil classification system (SCWG, 1991).

4.2.6.4 Dry bulk density

Undisturbed soil cores taken at three depths were placed in an oven at 105°C for 24 hours, after which the dry soil mass was measured. The length and diameter of the soil core was measured to determine its volume. Thereafter, the dry bulk density was calculated, which was then used to estimate the porosity of the soil using standard equations.

4.2.6.5 Soil water content

Soil water content was determined from gravimetric samples taken infrequently, which were converted to volumetric content using the (i) measured dry bulk density measurements, and (ii) the density of water at 20°C. As noted in **Section 4.2.5**, soil water content was monitored at each site using CS650 probes installed at three depths.

Trial site 2 (OFSP) was visited on 20th December 2021 because the CS650 probes were providing intermittent measurements. The sensors and/or wiring were likely damaged when the lattice mast was moved the previous week. The replacement of these sensors was unfortunately delayed to 9th February 2022, after a set of unused CS616 probes were eventually sourced. These probes were then calibrated against gravimetric samples, which showed that they under-estimated soil water content by 6% (site 1) and 3% (site 2), and thus all measurements were adjusted accordingly.

4.2.6.6 Soil water retention

In the soil and water laboratory at UKZN, the soil water retention curve for each depth was obtained using the controlled outflow method using the detailed methodology described by Mokonoto (2018). The soil water retention curve is determined from observations of the amount of water (in mL) released in a certain amount of time at a given pressure (Adhanom et al., 2012; Marshall and Holmes, 1988). In essence, each soil core was initially saturated with water, then allowed to drain naturally to determine the soil water content at saturation. The sample was then desorbed of water at suction pressures ranging from 10 to 33 kPa to determine field capacity. Further readings were taken at increasing pressures, which were then used to determine soil water retention curves using the van Genuchten (1980) equation. From the soil water retention curves, volumetric water content (in %) at field capacity (FC) and permanent wilting point (PWP) were estimated using a pressure head of -10 and -1500 kPa, respectively.

4.2.6.7 Saturated hydraulic conductivity

Saturated hydraulic conductivity (K_{SAT}) represents the ease of water flow when a saturated soil is subjected to a hydraulic gradient. K_{SAT} typically decreases with increasing soil depth due to the presence of less organic matter and more clay (Karuku et al., 2012). At each trial site, K_{SAT} was measured using the constant-head permeameter method for each undisturbed core obtained at the three depths. This method involves applying Darcy's law to saturated soil cores (Klute, 1965).

4.2.6.8 Crop development

During the growing season, the following crop parameters were measured: (i) plant height, (ii) leaf number, (iii) leaf area index, (iv) biomass accumulation, and (vi) root/tuber formation. Measurements (and observations) were again undertaken using protocols developed by the Crop Science discipline at UKZN.

Plant height: Plant height refers to the distance from the soil surface to the tip of the youngest developing leaf (before floral initiation) or the growing panicle tip (post floral initiation). Plant height was measured every week using a tape measure.

Leaf number: Leaves that were fully unfolded, expanded and photosynthetically active (i.e. with at least a 50% green leaf area) were manually counted each week.

Leaf area index: Leaf area index (LAI) represents the ratio of one-sided leaf area per unit ground surface area occupied by the plant (LI-COR, 2010). A portable leaf area meter (model LAI-2200, LI-COR, 2010) was used to measure LAI. To ensure adequate light interception by the canopy, measurements were taken from above and below the crop canopy on sunny days.

Canopy cover: Canopy cover (CC in %) development was estimated from LAI measurements using the Beer-Lambert equation as follows:

$$CC = 100 \cdot (1 - e^{-k \cdot LAI}) \quad \text{Equation 6}$$

where k represents the light extinction coefficient. A value of 0.85 was used for OFSP (Masango, 2015). For taro, Bernardes et al. (2011) provided 15 measurements of k , which ranged from 0.44-0.91 (average of 0.68).

However, another preferred method of calculating CC uses LAI measurements to compute the diffuse non-intercepted radiation ($DIFN$). This method was not used in season 2 because the data card in the LAI meter was faulty. $DIFN$ values enable CC development to be calculated using the following equation as suggested by Mabhaudhi et al. (2014b):

$$CC = 100 \cdot (100 - DIFN) \quad \text{Equation 7}$$

Crop phenology:

Crop development was observed at various phenological stages over the growing season. These include the time from transplanting/sowing to:

- recovered plant,
- maximum rooting depth,
- maximum canopy cover,
- start of leaf senescence
- start of yield formation, and
- harvest maturity.

For example, when at least 10% of the crop foliage has senesced without the formation of any new foliage, then leaf senescence has occurred (Mabhaudhi et al., 2014b). Crop phenological stages were initially recorded in calendar days, which were then converted to growing-degree days (GDD). The same method used by the AquaCrop model was adopted, which is called “Method 3”. The latter was adapted from “Method 2”, that was initially developed by McMaster and Wilhem (1997).

Destructive sampling techniques were employed to measure above- and below-ground biomass production (fresh & dry weight basis). Randomly selected plants were removed from the field. The plants were weighed to determine fresh mass, then oven-dried at constant temperature (75°C) for 48 hours and re-weighed to obtain dry mass.

4.2.6.9 Crop health

Chlorophyll content index (CCI) and stomatal conductance (SC) were used as indicators of plant health. Measurements (and observations) were again undertaken using protocols developed by the Crop Science discipline at UKZN. For example, the adaxial (upper) surface of the second youngest, fully unfolded leaf was used for CCI measurements over the measurement period. Furthermore, SC was measured weekly between 12h00 and 13h30 on days with sufficient sunlight with minimal to no cloud cover.

4.2.6.10 Final biomass and yield

A total of 30 plants from two rows were harvested at the end of the season. Harvested plants were then separated into leaves, vines/stems and roots/tubers. Each component was weighed before and after being air/oven dried. Final accumulated biomass and root/tuber yield were measured, from which the harvest index was calculated, i.e. as the ratio of root/tuber yield to total biomass, then expressed as a percentage.

4.2.6.11 Crop water use

Daily crop water use was measured using the EC and SR methods (cf. **Section 4.2.5**). The SR method was calibrated against the method. The 30-minute averages of latent energy flux (λET in $W m^{-2}$) calculated by the data logger were multiplied by a factor 0.000734 to convert them into equivalent depths of crop evapotranspiration (ET in mm). This factor equals the number of seconds in 30 minutes (1800 s) divided by the latent heat of vapourisation λ ($2.454 \times 10^6 J kg^{-1}$). The half-hourly ET estimates were then summed for daylight hours (i.e. when R_n was positive) to obtain daily values. Seasonal crop water use was estimated by summing daily ET values from planting to physiological maturity.

From the daily measurements of crop ET and ET_o , daily crop coefficients were calculated, then averaged to monthly values. Monthly crop coefficients were determined for the fallow period prior to planting (from July/August to November/December) and after harvest (April/May to July/August), similar to the approach adopted by Kunz et al. (2020). Even though these K_c values were determined for non-standard conditions where plant water stress was not alleviated by irrigation, they were needed for the hydrological modelling component of this project (cf. **Chapter 7**).

4.2.6.12 Nutrient content

After the trials were harvested, OFSP and taro samples were peeled and sliced, then stored in a deep freeze at -20°C to preserve nutrient content. In June 2022, frozen material was oven-dried at 60°C (for 48 hours), then milled and ashed. The material was sent to a laboratory at the Institute for Commercial Forestry Research (ICFR) for analysis of nutrient content. The following elements were measured: B,

Ca, Cu, Fe, K, Mg, Mn, Mo, Na, P, and Zn. For Mo analysis, a standard was imported from the US. In addition, total C, N and S were also determined.

All OFSP and taro samples sent to the ICFR laboratory were scanned with a near-infrared (NIR) spectrometer to develop calibration models for each measured parameter. The advantage of this is that future samples do not require laboratory analysis, just a single NIR scan to obtain nutrient content. For example, Magwaza et al. (2016) used a pool of 104 sweet potato varieties to develop a NIR model to predict protein content in sweet potato. The results demonstrated that NIR can rapidly and accurately predict protein content and is cheaper than laboratory analysis.

β -carotene content was determined by the Horticultural laboratory at UKZN. Two fresh root/tuber samples were peeled, chopped into cubes and freeze-dried at -80°C for 96 hours. The samples were blended to form a powder, mixed with hexane, acetone and saturated NaCl, then vortexed and centrifuged to achieve phase separation. The top layer was extracted and filtered, then injected into a High-Performance Liquid Chromatography (HPLC) system. β -carotene content was then calculated from peak area generated from a standard calibration curve (Biehler et al., 2010; Biswas et al., 2011). The β -carotene was not undertaken for OFSP leaves (only roots) or taro.

4.2.6.13 Water productivity

Aim 5 of this project relates to improving knowledge of crop and nutritional water productivity of RTCs (cf. **Section 1.2**). These two metrics were calculated using the equations given in **Section 2.5.5**.

4.2.7 Crop modelling

A preliminary analysis was undertaken to determine the feasibility of using default crop parameters, with little to no adjustment, to estimate crop water productivity using two crop simulation models (CSMs). The methodology used is briefly described next. For more detail, the reader is referred to Mthembu (2023).

4.2.7.1 Model selection

For this exercise, the SWB and AquaCrop models were chosen, which are described in **Section 6.2.1** (cf. **Chapter 6**).

4.2.7.2 Model inputs

Climate data: Rainfall data was obtained from the AWS located at Fountainhill Eco-estate. Air temperature was measured site 2 with the EC method. ET_0 was calculated using net radiation, air temperature, relative humidity and wind speed from the EC method (cf. **Section 4.3.1**). Climate files required by both CSMs were developed using the daily rainfall, temperature (maximum and minimum) and ET_0 data measured over the growing season. The default ambient carbon dioxide (CO_2) concentrations packaged with the AquaCrop model for Mauna Loa (Hawaii) were used for the simulations.

Soil data: A detailed description of soil characteristics at each trial site was provided in **Section 4.3.2**. Based on field observations, roots did not extend beyond 0.6 m and thus, the soil profile depth was set to 60 cm. From experience, AquaCrop provides better simulations when using a single soil layer as opposed to two layers (i.e. A- and B-horizons). Hence, observations at each of the three depths (0.15, 0.30 & 0.60 m) were depth weighted to provide values for a single profile, as shown in **Table 16-7** (**Section 16.3**). Total available water is the difference between field capacity and permanent wilting point, expressed in mm per m of soil depth. Readily evaporable water was also estimated from field capacity and permanent wilting point as per the equation (2.23s – 4; p 2-266) provided by Raes et al.

(2018). The curve number was based on K_{SAT} values measured for the topsoil as recommended in the AquaCrop manual (Raes et al., 2018). The SWB model also requires the dry bulk density and a depth-weighted value of 1.7 was used. Two additional parameters required by the model are the drain factor and drainage rate, which were set to 0.7 and 70 mm d⁻¹, respectively. The initial soil water content of 44.2 mm was obtained from the volumetric water measurements provided by the CS650 soil moisture sensors.

Field management: For the field management options in AquaCrop, the non-limiting fertility option was selected since the trials were fertilised at the required rate (cf. **Section 4.2.4.3**). No mulch layer was considered to mimic field conditions. Factors that affect surface runoff were also not invoked, due to the flat terrain at the experimental site. Since the field trial was kept relatively weed-free from 57-118 DAP, the option to suppress canopy cover development due to the presence of weeds was not considered. An irrigation file was not created as the crop was grown under rainfed conditions.

4.2.7.3 Model parameters

AquaCrop: As explained in **Section 5.2.6.3**, the decision was made to use crop parameters derived by Rankine et al. (2015) and Beletse et al. (2013), but where possible, replace certain values obtained from the field work conducted in season 2.

SWB: The SWB model was calibrated and validated for OFSP (Resisto cultivar) by Masango (2015) using data from a field trial undertaken at Hatfield experimental farm (University of Pretoria, Gauteng) during the 2011/12 season.

Calibration: A minimal calibration was done following guidelines developed by Steduto et al. (2012), where certain parameters were fine-tuned, i.e. adjusted to values observed or measured in the second season. The list of 18 parameters published by Rankine et al. (2015), together with corresponding values from Beletse et al. (2013) and the parameter values that were adjusted using field observations from the season are presented in **Table 16-9** (cf. **Section 16.3**). For example, maximum canopy cover (CC_x in AquaCrop) is one of the important parameters to fine-tune (Steduto et al., 2012). Based on observations (cf. **Figure 4-24** in **Section 4.3.7.1**), a value of 92% was used for OFSP. The maximum rooting depth of 0.6 m was observed at physiological maturity after digging a trench between the rows. Most of the crop phenological parameters were initially observed in calendar days, which were then converted to growing-degree days as suggested by Raes (2016b) (cf. **Table 16-8** in **Section 16.3**). The maximum evapotranspiration of 7.1 mm was measured at 112 DAP by the EC method (Reddy, 2024). For the SWB model, a minimal calibration was also done where nine parameters were adjusted to better represent the 199062.1 cultivar grown at Fountainhill as shown in **Table 16-10** (cf. **Section 16.3**).

4.2.7.4 Model simulations

For both models, the planting date and plant density were set to the 14th of December 2021 and 20,000 plants ha⁻¹, respectively. This was done to mimic field conditions as described in **Section 4.2.4.1**. Crop water use and yield simulated by SWB and AquaCrop were used to calculate the crop water productivity. In addition, simulations of LAI (SWB), CC (AquaCrop), biomass accumulation, tuber yield and soil water content were compared to field measurements. The results are presented in **Section 4.3.7**.

4.2.7.5 Model evaluation

Four statistical measures were used to evaluate model performance, namely the (i) coefficient of determination (R^2), (ii) root mean square error (RMSE), (iii) Nash-Sutcliffe efficiency coefficient (NSE), and (iv) Willmott's index of agreement (d). The number of observations (n) was also provided to help with the interpretation of the statistics. Each statistical measure is explained in **Section 5.2.6.5**.

4.3 RESULTS AND DISCUSSION

This study focused on measuring the water use, yield and nutrient content of two prioritised RTCs, namely OFSP and taro. A field trial was conducted for each crop at the Fountainhill Eco-estate during the 2021/22 season. Results obtained from both trials are presented next.

4.3.1 Climate data

Daily climatic data was obtained from an [online data portal](#) developed and maintained by SASRI for an AWS located at Fountainhill Eco-estate (AWS-512; 29°27'02" S; 30°32'42" E; 853 m a.s.l.). Measurements began on 13 August 2015, and thus are not shown due to incomplete record. Annual means/totals of precipitation (P), incoming solar radiation (R_s), air temperature (T), relative humidity (RH), sunshine duration (SD), wind run (WR), reference grass evapotranspiration (ET_o) and A-pan evaporation (E_{PAN}) are shown in **Table 4-2**.

Table 4-2 Annual means/totals of climate variables measured by the AWS located at Fountainhill Eco-estate near Wartburg

YR	P (mm)	R_s (MJ m ⁻² d ⁻¹)	T _{MAX} (°C)	T _{MIN} (°C)	RH _{MAX} (%)	RH _{MIN} (%)	SD (h)	WR (km d ⁻¹)	ET _O (mm)	E _{PAN} (mm)
2016	700	15.1	24.7	10.5	80	53	5.6	125	3.1	3.6
2017	853	16.0	24.4	10.1	75	52	6.3	166	3.3	3.9
2018	682	15.7	24.5	9.9	80	53	5.8	201	3.5	4.1
2019	603	15.4	25.3	10.5	77	51	5.7	135	3.2	3.7
2020	757	16.1	24.9	9.9	77	51	6.2	118	3.2	3.8
2021	793	14.3	24.0	9.7	81	54	5.1	129	2.9	3.5
2022	977	14.2	24.2	10.2	81	58	5.0	100	2.8	3.3

Climate data representative of Fountainhill was also obtained from another nearby SASRI AWS situated at Bruyns Hill near Wartburg (AWS-455; 29°25'00" S; 30°41'00" E; elevation 990 m a.s.l.). This AWS is located approximately 14 km from the Fountainhill AWS. The Bruyns Hill station has a 22-year climate record from 1 January 2001 onwards (**Table 4-3**). A comparison of the 7-year averages (AVE1) from both stations indicates that Fountainhill receives less rainfall than Bruyns Hill (766 vs 996 mm), but conditions are drier (RH_{MAX} of 77 vs 89%) and windier at Fountainhill (139 vs 100 km d⁻¹), which means slightly higher reference evapotranspiration rates (3.1 vs 2.9 mm). In addition, missing data at Fountainhill can be infilled with values from Bruyns Hill after adjusting for the altitude difference between the two AWSs (853 vs 990 m a.s.l.).

Table 4-3 Annual means/totals of climate variables measured by the AWS located at Bruyns Hill near Wartburg

YR	P (mm)	R_s (MJ m ⁻² d ⁻¹)	T _{MAX} (°C)	T _{MIN} (°C)	RH _{MAX} (%)	RH _{MIN} (%)	SD (h)	WR (km d ⁻¹)	ET _O (mm)	E _{PAN} (mm)
2016	982	14.3	24.1	11.7	75	52	5.1	110	3.0	3.5
2017	1,095	14.4	23.9	11.5	95	42	5.2	96	2.8	3.3
2018	851	15.3	24.3	11.1	93	42	5.7	100	3.0	3.5
2019	835	14.9	24.8	11.6	79	50	5.5	103	2.9	3.5
2020	851	16.1	23.8	11.8	93	44	6.3	102	3.0	3.5
2021	1,098	15.3	23.1	11.6	95	46	5.8	95	2.7	3.2
2022	1,263	14.9	23.1	12.1	95	49	5.5	93	2.7	3.2
AVE1	996	15.0	23.9	11.6	89	46	5.6	100	2.9	3.4
AVE2	877	15.2	24.0	11.8	78	51	5.7	139	3.2	3.8

AVE1 = average from 2016 to 2022; AVE2 = average from 2001 to 2022

Installation of the EC and SR equipment began in June (at site 1) and August (at site 2) 2021 at Fountainhill. The micrometeorological systems were finally removed from the field on the 6 September 2022, after an entire year of ET data had been collected. The Fountainhill and Bruyns Hill stations only measure incoming solar radiation (R_s), and thus outgoing longwave radiation (R_L) is estimated. However, daily net radiation (R_N) measured by the EC method at the taro site was used to estimate ET_0 (cf. **Section 4.2.6.1**), since it is more accurate than R_N calculated from measured R_s and estimated R_L . Temperature, relative humidity and wind speed data measured by the EC methods were also used to calculate ET_0 , since the data better represented each trial site. ET_0 calculated from data measured at by the EC method at the taro site was compared to that obtained from the Fountainhill station, as shown in **Figure 4-4**. The graph shows the Fountainhill station under-estimated ET_0 when compared to the EC method, probably due to the Fountainhill station not being properly maintained as a result of the COVID-19 pandemic and associated lockdown periods. It also highlighted the importance of accurately calculating reference evapotranspiration for the trial sites. Based on this, it would have been better to install a tipping bucket rain gauge at the trial site.

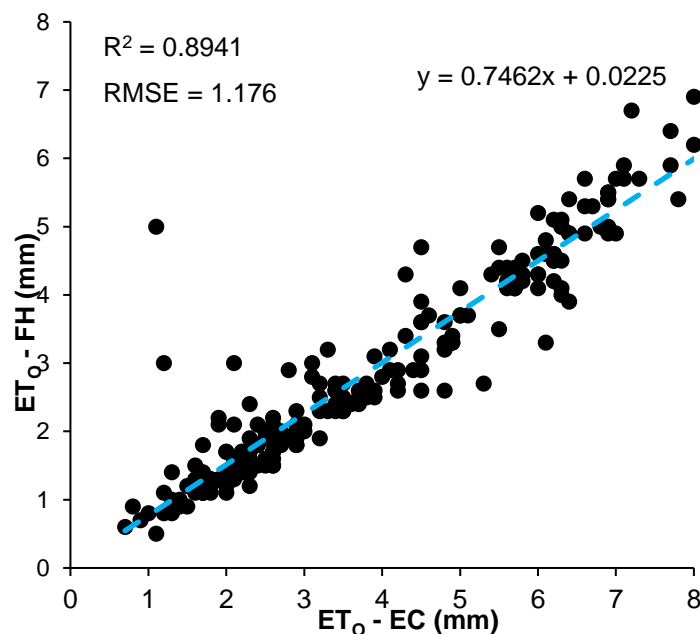


Figure 4-4 Reference evapotranspiration (ET_0) measured by the eddy covariance (EC) system compared to that obtained from the Fountainhill (FH) weather station

As shown in **Figure 4-5**, the daily average air temperature ranged from 7.6 to 28.2°C (coldest: -0.1°C; hottest: 35.3°C). Frost was likely on 199 and 215 DAP due to low minimum temperatures. Daily ET_0 ranged from 0.7 to 8.1 mm for the trial sites. ET_0 is higher during periods of no rainfall and also decreases during periods of low temperatures. Since rainfall was not measured at the trial sites, daily data was obtained from the Fountainhill AWS. There was no rainfall data for 28 February 2022, which was corrected to 0 mm when compared to data from the Bruyns Hill AWS. It is worth noting that an unusually large rainfall event of 86.6 mm occurred in the late afternoon on 14th April (148 DAP of taro). Similarly, on 26th May 2022 (188 DAP), another large event of 101.1 mm was recorded. Both events resulted in significant runoff events from the taro trial site. A total of 473 mm of rainfall fell over the OFSP growing period of 118 days, compared to 844 mm for the taro season (217 days). The hot and wet conditions experienced from 30-50 DAP resulted in excessive weed growth after planting. For the majority of the growing season, the maximum air temperature did not exceed 35°C and thus, did not negatively affect crop development and yield.

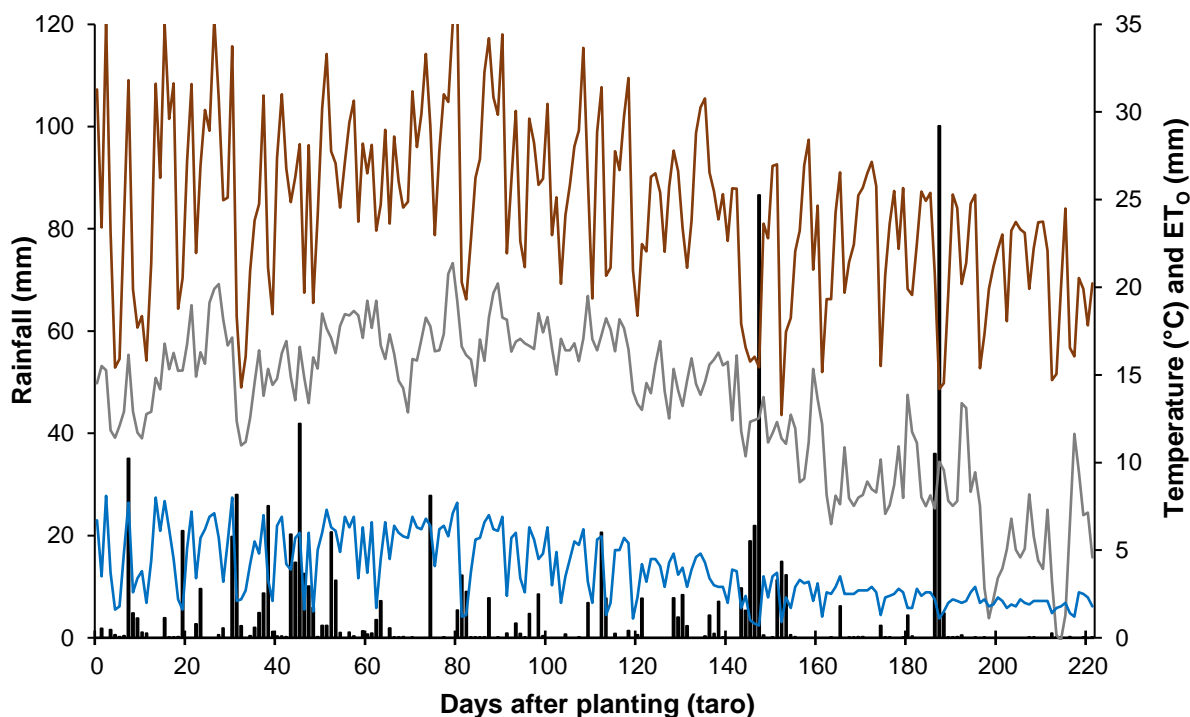


Figure 4-5 Variation in maximum (brown line) temperature, minimum (grey line) temperature, ET_0 (blue line) and rainfall (black bars) from 19 November 2021 (0 DAP) to 27 June 2022 (220 DAP) at Fountainhill Eco-estate

4.3.2 Soil properties

In the first season, soil samples were taken at three depths (0.15, 0.30 & 0.60 m) from both trial sites to determine soil fertility, texture and water content (gravimetric & volumetric). Furthermore, undisturbed soil cores were obtained from open pits to determine bulk density, soil water retention and saturated hydraulic conductivity. The results from the analyses are presented next.

4.3.2.1 Soil fertility

The soil fertility tests highlighted the acidity of the soil, which was not corrected with an application of lime. The results were used to determine appropriate fertiliser application rates at both trial sites (cf. **Section 4.2.4.3**). The low clay content at site 2 (OFSP) indicates the soil is sandier in texture. The results highlight the variability in soils across the Fountainhill Eco-estate, as mentioned in **Section 4.2.1**, and indicate the importance of detailed analyses to be done for each trial site.

Table 4-4 Chemical properties of soil samples taken at two trial sites at Fountainhill Eco-estate in the first season

Trial site	Soil fertility characteristics										
	Mg L ⁻¹								%		
	P	K	Ca	Mg	Zn	Mn	Cu	pH	Org. C	N	Clay
1	14.5	201.0	735.5	177.5	4.4	8.7	21.0	2.4	1.3	0.1	25.5
2	239.5	378.5	913.5	159.0	4.8	28.2	17.0	4.0	1.9	0.1	12.5

4.3.2.2 Soil texture

The soil textural analysis shown in **Table 4-5** for trial site 1 indicates that the top 0.3 m is dominated by sandy loam, which then transitions into a sandy clay loam at 0.6 m. This suggests that clay translocation

occurs at site 1, which involves the mechanical transfer (eluviation) of clay particles from the topsoil by percolating water and the redeposition of the clay particles in the subsoil (illuviation). For site 2, a loamy sand texture is dominant and there is no evidence of clay translocation. The fine silt fractions are similar for both sites and values relatively consistent (range 3-5%). The low clay and high sand content at site 2 explains why animals could easily burrow under the perimeter fence and netting to eat the OFSP.

Table 4-5 Soil particle size distribution and textural classes for three depths at each trial site

Trial site	Soil depth (m)	Particle size distribution (%)			Soil textural class
		Clay	Fine silt	Sand	
1	0.15	17	3	80	Sandy loam
	0.30	16	4	80	Sandy loam
	0.60	34	3	63	Sandy clay loam
2	0.15	8	5	87	Loamy sand
	0.30	8	4	88	Loamy sand
	0.60	7	4	89	Loamy sand

4.3.2.3 Soil water retention

Soil bulk density (ρ_b) and soil porosity (Φ) were calculated using standard equations. The soil water retention parameters (SAT, FC and PWP) and saturated hydraulic conductivity (K_{SAT}) were determined using the methods described in **Section 4.2.6.4** to **Section 4.2.6.7**, respectively. For FC, values obtained at a suction pressure of 10 kPa were used (not 33 kPa). Soil porosity (Φ) agrees favourably with saturation (SAT), especially for site 2, which validates the soil water retention parameters obtained from the outflow pressure method. From the results presented in **Table 4-6**, the bulk density values are slightly higher than expected, considering ideal bulk densities range from 1.1 to 1.6 g cm⁻³ for clayey and sandy textured soils, respectively. Bulk densities exceeding 1.4-1.7 g cm⁻³ may affect root growth and values above 1.5-1.8 g cm⁻³ will likely restrict root growth (USDA, 1999).

Table 4-6 Measurement of soil bulk density, soil water retention and soil hydraulic conductivity for trial sites 1 and 2

Soil property	Units	Site 1			Site 2		
		Sample depth (m)			Sample depth (m)		
		0.15	0.30	0.60	0.15	0.30	0.60
ρ_b	g cm ⁻³	1.7	1.7	1.7	1.5	1.8	1.8
Φ	% volume	32	38	36	40	32	32
SAT	% volume	35	38	40	40	31	32
FC	% volume	25	23	23	31	21	20
PWP	% volume	10	11	10	7	5	8
K_{SAT}	mm d ⁻¹	84	6	8	541	137	764

Bulk density, soil water retention parameters and saturated hydraulic conductivity were also calculated using the Soil-Plant-Air-Water (SPAW) utility (**Table 4-7**), which was developed by the United States Department of Agriculture (Saxton and Willey, 2009). This software utility is based on a set of pedo-transfer equations described by Saxton and Rawls (2006), which are updated versions of the original equations presented by Saxton et al. (1986). The input values required by SPAW are the particle size distribution (cf. **Table 4-5**) and organic matter content. The latter input was derived by multiplying the topsoil's organic carbon content (cf. **Table 4-4** in **Section 4.3.2.1**) by a factor of 1.724 (Howard, 1965). The default value in SPAW of 0.5% for soil organic carbon was used for the other two depths.

Furthermore, soil compaction, soil salinity and gravel content were not measured at Fountainhill and thus, default values in SPAW were used.

Table 4-7 Calculation of soil bulk density, soil water retention and soil hydraulic conductivity for trial sites 1 and 2 using the SPAW utility

Soil property	Units	Site 1			Site 2		
		Sample depth (m)			Sample depth (m)		
		0.15	0.30	0.60	0.15	0.30	0.60
ρ_b	g cm ⁻³	1.5	1.6	1.6	1.4	1.6	1.5
Φ	% volume	42	40	41	47	42	42
SAT	% volume	42	40	41	47	42	42
FC	% volume	18	16	30	13	10	9
PWP	% volume	12	10	21	8	5	4
K_{SAT}	mm d ⁻¹	757	770	67	2,055	1,859	2,073

A comparison of measured (**Table 4-6**) against calculated (**Table 4-7**) soil properties indicates the importance of measuring these values, especially when they are needed for the calibration and/or validation of crop simulation models. SPAW over-estimated SAT and FC compared to measured values. FC in the laboratory was determined at a suction pressure of 10 kPa, whereas SPAW is based on 33 kPa. However, the largest discrepancy occurred between measured and calculated K_{SAT} values, where measured values were much lower than calculated values. In addition, measured values were lower than the range 200-2000 mm d⁻¹ given by Raes et al. (2018) for group I (sandy) soils, especially at trial site 1.

4.3.3 Crop development

OFSP: At both trial sites, regular measurements of crop growth (plant height, leaf number, leaf area, & biomass accumulation) and stress (chlorophyll content index, stomatal conductance & leaf temperature) began on 9 February 2022 in four (1 m by 1 m) quadrants, each with four plants, i.e. 16 plants in total. Destructive sampling was also conducted every week for OFSP and every two weeks for taro. The OFSP and taro trial was harvested in April and June 2022, respectively. This section provides a summary of the climate, soils, crop growth, water use, yield and nutrient content data obtained from the field trials conducted at Fountainhill.

4.3.3.1 Plant height

OFSP: The crop reached its maximum height of 69 cm at 112 DAP (**Figure 4-6**), which equates to an average increase of approximately 4 cm per week. This height reached was taller than the maximum value of 0.5 m provided by Pereira et al. (2021b) (cf. **Table 16-13** in **Section 16.4**).

Taro: The crop reached its maximum height of 54 cm after 157 DAP (**Figure 4-9**), which is much shorter than the maximum value of 1.2 m suggested by Pereira et al. (2021b) (cf. **Table 16-13** in **Section 16.4**). However, plant growth was likely affected by weedy conditions up to 86 DAP. Plant measurements only began after the trials were weed free.

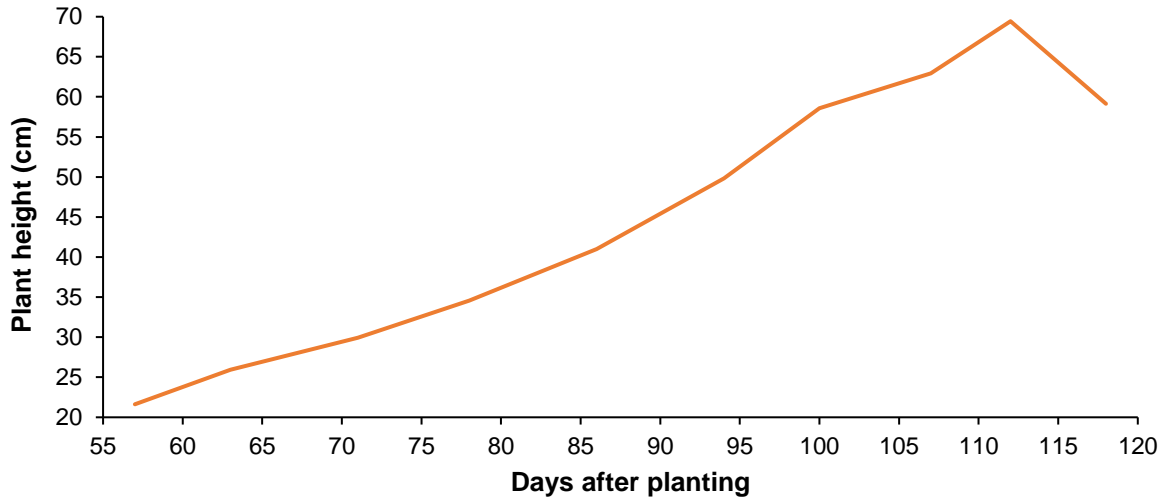


Figure 4-6 Plant height of OFSP grown under rainfed conditions over the 2021/22 growing season at Fountainhill (Mthembu, 2023)

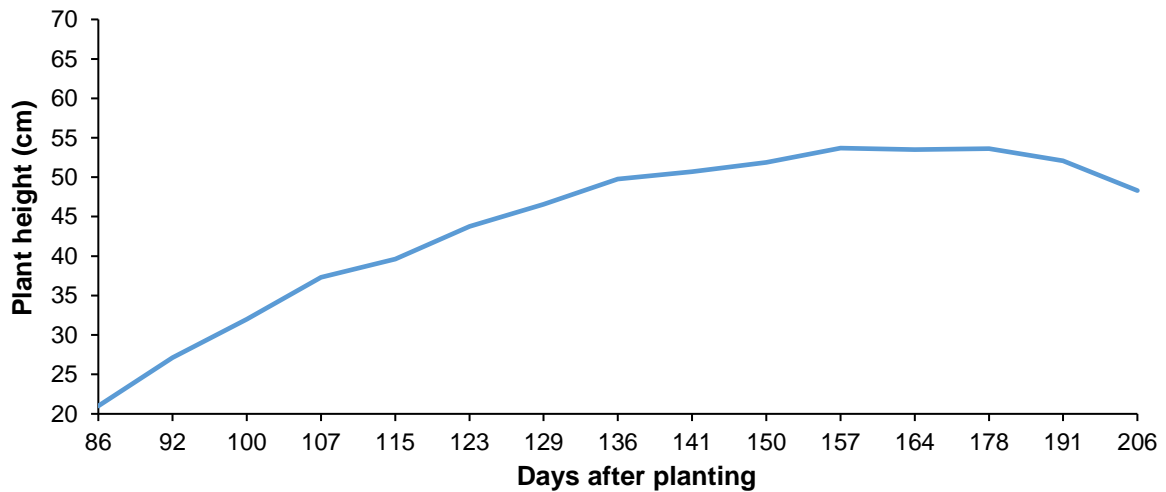


Figure 4-7 Plant height of taro grown under rainfed conditions over the 2021/22 growing season at Fountainhill (Reddy, 2024)

4.3.3.2 Leaf number

OFSP: From **Figure 4-8**, a similar trend was noted where leaf number (LN) steadily increased over the growing season until 112 DAP, after which it started to decline. From 57-112 DAP, LN increased on average by 9 every week, reaching a maximum value of 127. This value is substantially higher than that (~80) reported by Dladla (2017), who also grew sweet potato under peaked ridges at the same experimental site. The difference may have been due to the fertiliser application, which was not done by Dladla (2017). From 86 to 112 DAP, which represents the vegetative stage, LN increased from 80 to 127.

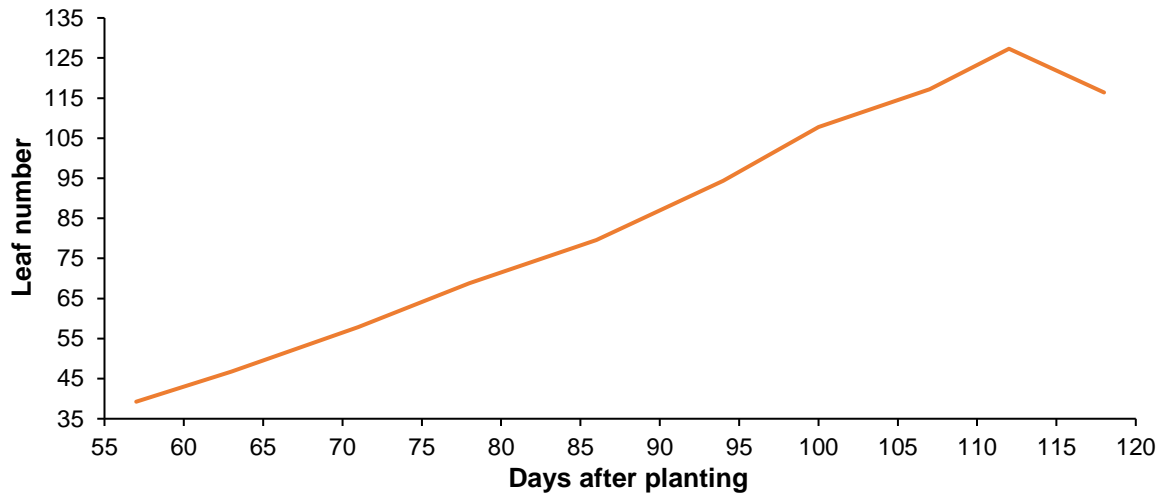


Figure 4-8 Leaf number of OFSP grown under rainfed conditions over the 2021/22 growing season at Fountainhill (Mthembu, 2023)

Taro: Average LN peaked at ~12 at 141 days after planting (Figure 4-9). However, the plants continued to grow as shown in Figure 4-9. When compared to OFSP (Figure 4-8), taro has far fewer leaves, which affects both leaf area and transpiration rates.

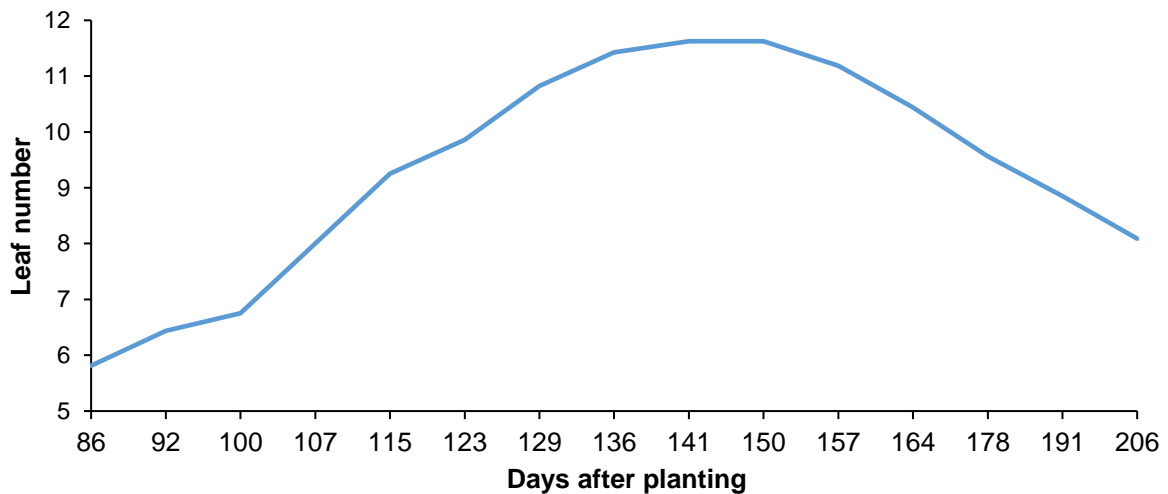


Figure 4-9 Leaf number of taro grown under rainfed conditions over the 2021/22 growing season at Fountainhill (Reddy)

4.3.3.3 Leaf area index

OFSP: The measured LAI trend for OFSP over the growing season is shown in Figure 4-10. LAI peaked at 3.02 m² m⁻² at 112 DAP. The measured LAI values were comparable to those reported by Nyathi et al. (2016), which ranged from 1.8 to 4 m² m⁻².

Taro: As shown in Figure 4-11, LAI peaked at 0.72 m m⁻² at 136 DAP when leaf number stopped increasing (Figure 4-9). The shape of the LAI cure is almost identical to the leaf number curve. Taro's LAI was much lower compared to OFSP (Figure 4-10), due to the lower number of leaves.

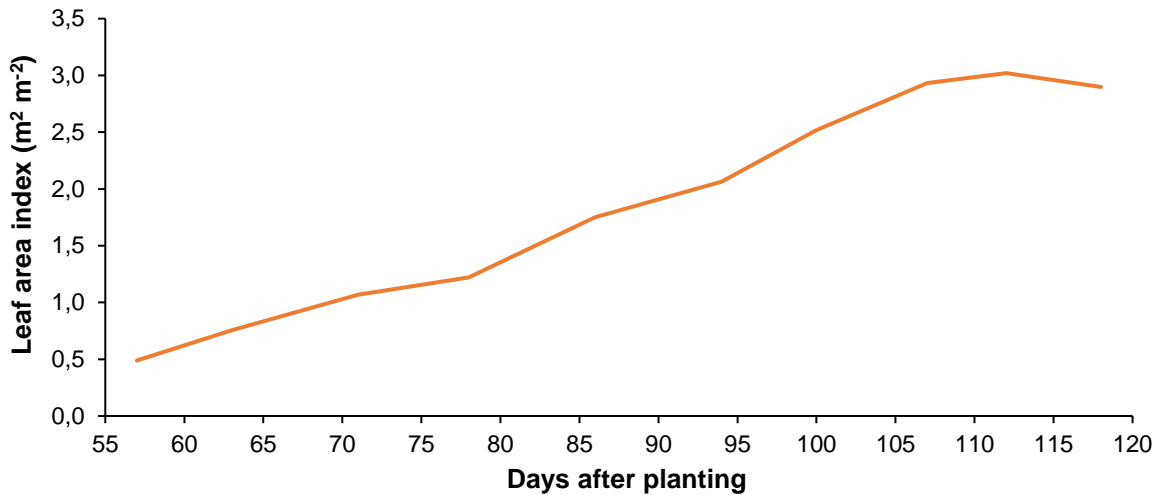


Figure 4-10 Leaf area index of OFSP grown under rainfed conditions over the 2021/22 growing season at Fountainhill (Mthembu, 2023)

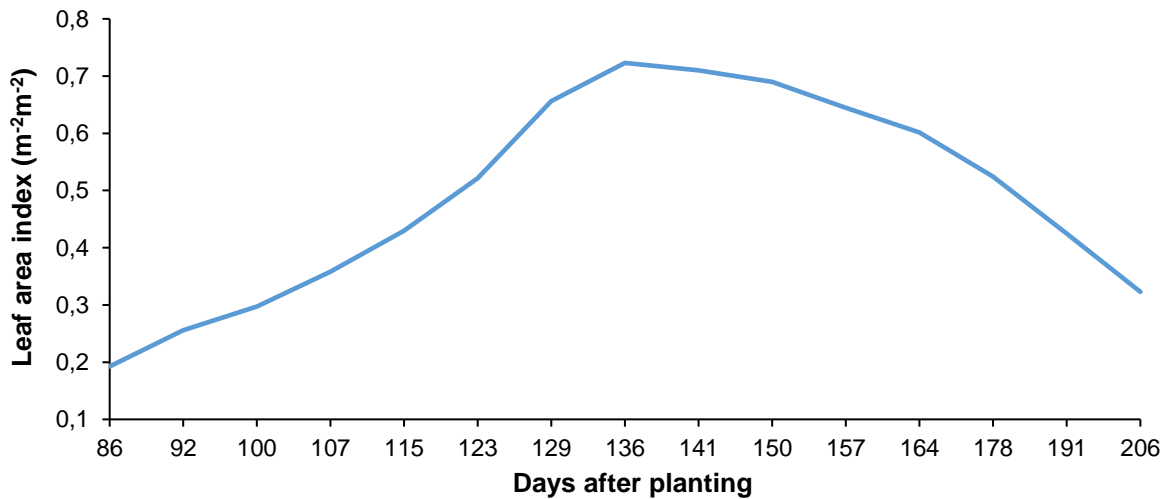


Figure 4-11 Leaf area index of taro grown under rainfed conditions over the 2021/22 growing season at Fountainhill (Reddy, 2024)

4.3.3.4 Canopy cover

OFSP: As noted in **Section 4.2.6.8**, canopy cover (CC) was estimated from LAI using the Beer-Lambert equation (**Figure 4-12**). An extinction coefficient of 0.85 (Masango, 2015) was used. As expected, CC followed a similar trend to LAI (cf. **Figure 4-10**). Maximum CC of 92.3% was reached at 112 DAP, which are both important parameters required by the AquaCrop model.

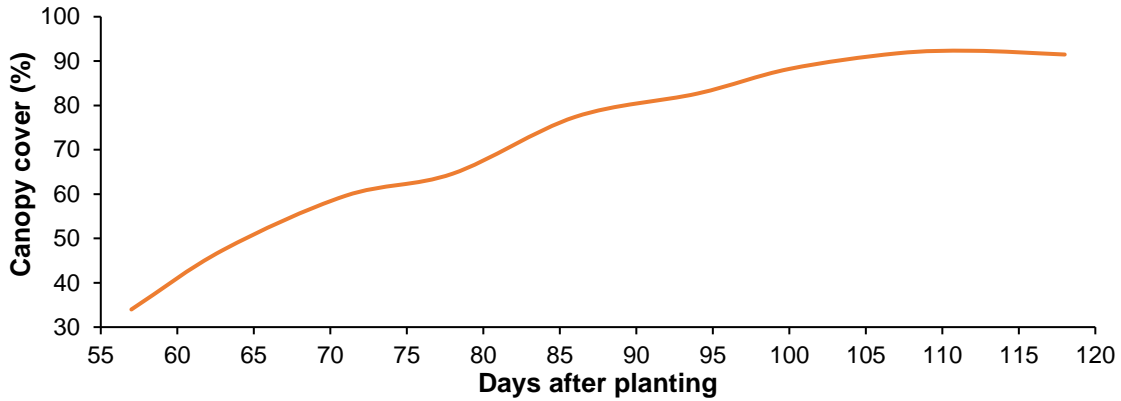


Figure 4-12 Estimated canopy cover of OFSP grown under rainfed conditions over the 2021/22 growing season at Fountainhill (Mthembu, 2023)

Taro: CC was estimated from LAI using the Beer-Lambert equation (**Figure 4-13**). An extinction coefficient (k) of 0.68 (Bernardes et al., 2011) was used. However, k was determined from the season 3 experiment (cf. **Section 5.3.7.2**), and thus was also used to estimate CC using a value of 0.81. Maximum values of 38.8 ($k = 0.68$) and 44.3% ($k = 0.81$) were reached at 136 DAP when LAI peaked at 0.72 (**Figure 4-11**).

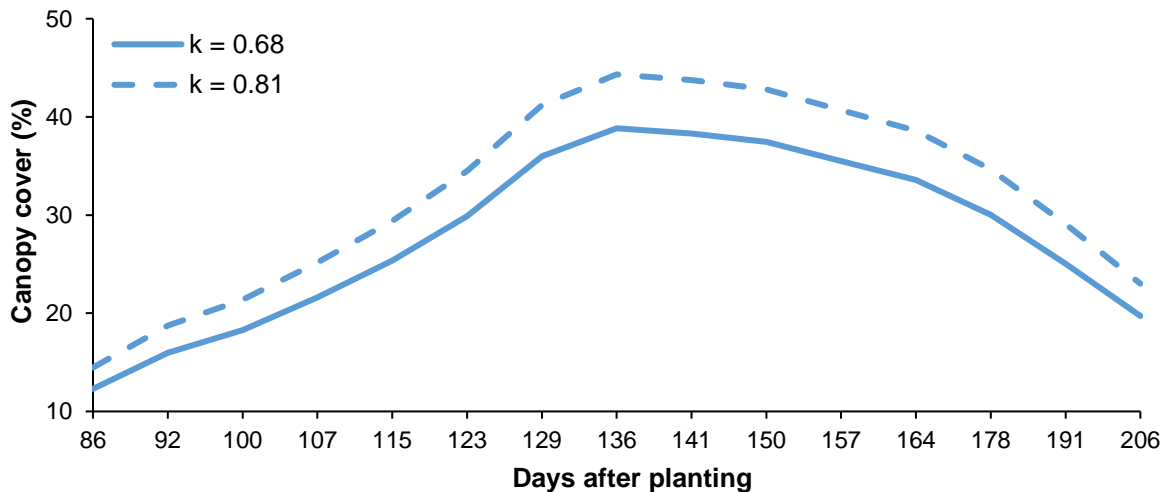


Figure 4-13 Estimated canopy cover of taro grown under rainfed conditions over the 2021/22 growing season at Fountainhill (Reddy, 2024)

4.3.3.5 Biomass accumulation

OFSP: The accumulation of fresh biomass, measured weekly over the growing season, is presented in **Figure 4-14**. The decline in fresh above-ground biomass (AGB) after 100 DAP marked the translocation of carbon assimilates from above- to below-ground development, which results in reduced AGB and increased tuber yield. This is similar to findings reported by Al-Jamal et al. (2001), Belehu (2003) and Masango (2015).

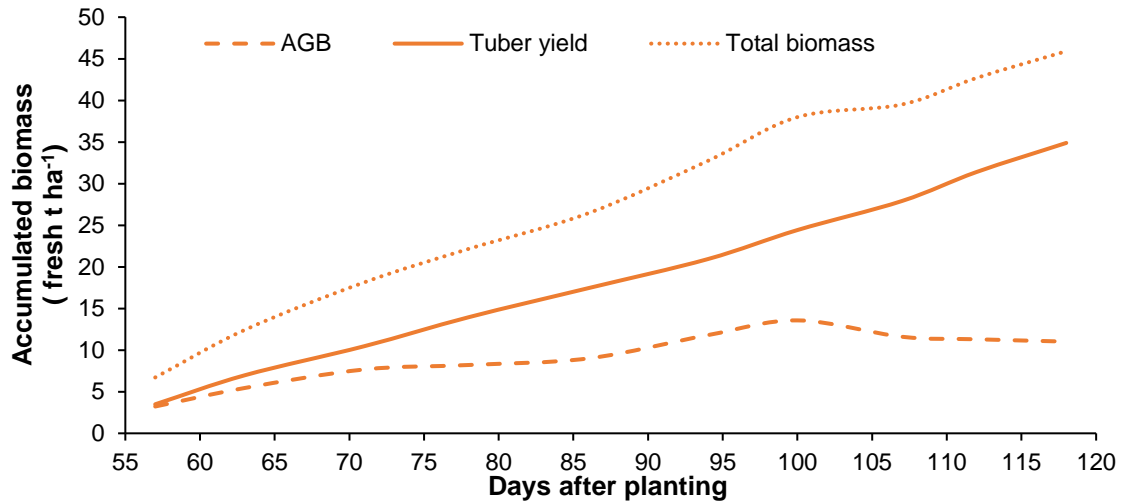


Figure 4-14 Fresh biomass accumulation of OFSP grown under rainfed conditions over the 2021/22 growing season at Fountainhill (Mthembu, 2023)

The difference between the fresh (**Figure 4-14**) and dry biomass accumulation (**Figure 4-15**) was substantial during the latter stages of the measurement period. During the initial stage of crop development, the fresh crop had a low water content therefore, a small amount of water was lost during the oven-drying process. However, as the crop grew, the roots and leaves accumulated larger amounts of water. Therefore, large differences between fresh and dry biomass accumulation were observed towards the end of the growing season. Masango (2015) found that over a growing season, the dry total biomass of sweet potato exhibits a sigmoidal curve, which was also observed here.

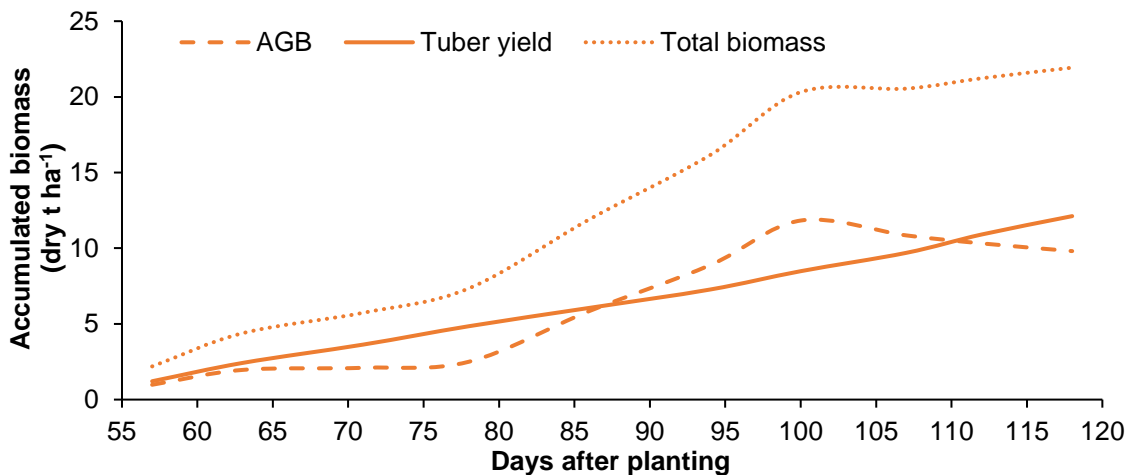


Figure 4-15 Dry biomass accumulation of OFSP grown under rainfed conditions over the 2021/22 growing season at Fountainhill (Mthembu, 2023)

Taro: The accumulation of fresh biomass, measured weekly over the growing season, is presented in **Figure 4-16**. No decline in fresh AGB was noted, which occurred for OFSP (**Figure 4-14**). Tuber formation began after 136 DAP and was completed ~30 days later. These two values are required as input parameters for the AquaCrop model, namely the (i) start of yield formation (line no. 56), and (ii) length of the harvest index buildup period (line no. 60).

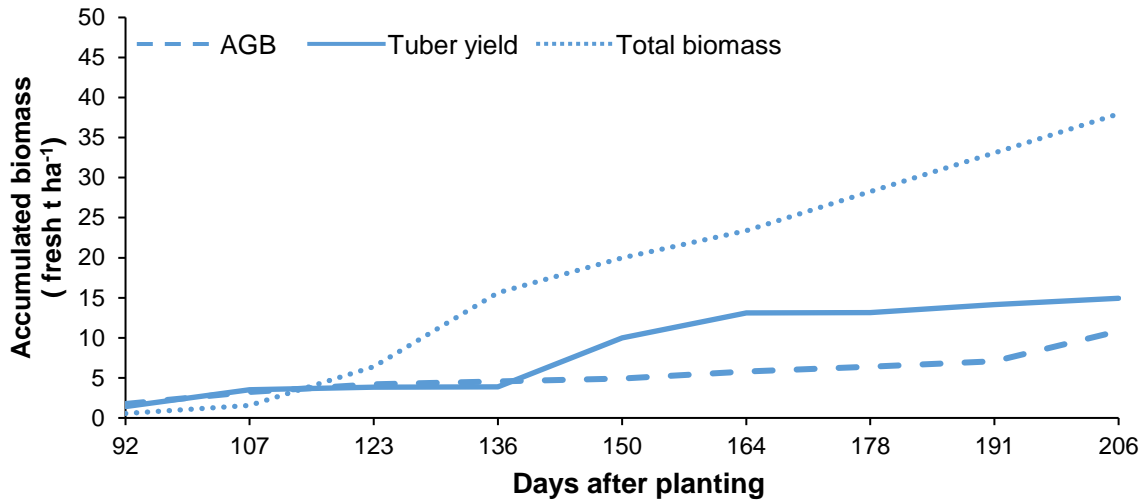


Figure 4-16 Fresh biomass accumulation of taro grown under rainfed conditions over the 2021/22 growing season at Fountainhill (Reddy, 2024)

Differences between fresh (**Figure 4-16**) and dry biomass accumulation (**Figure 4-17**) are due to the storage of water in the leaves, stems and tubers. Therefore, the tuber formation period is much clearer and shows a rapid growth phase from 136 to 150 DAP. The reason for the large decline in tuber mass from 150 to 178 DAP is unclear but may be related to a loss of starch or root mass.

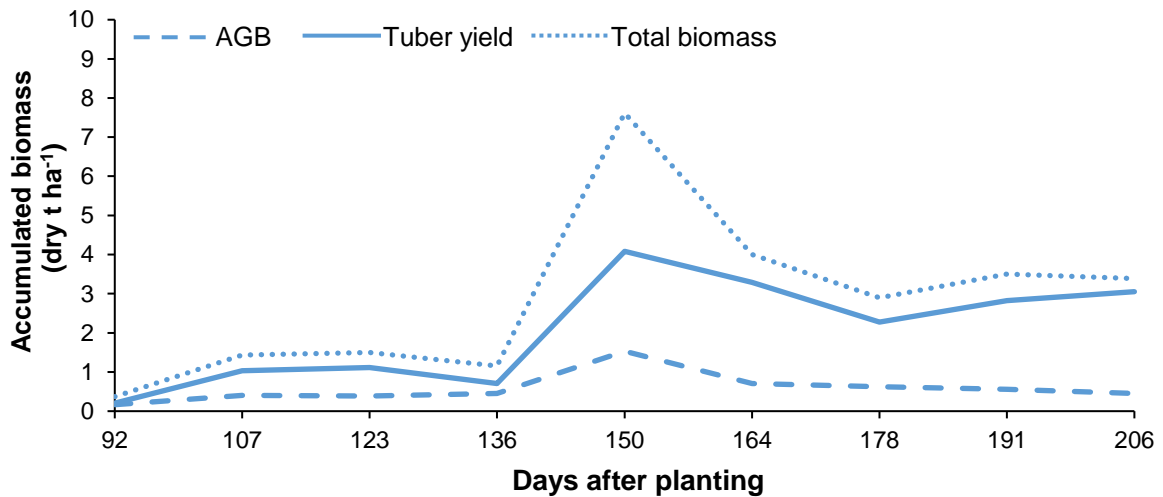


Figure 4-17 Dry biomass accumulation of taro grown under rainfed conditions over the 2021/22 growing season at Fountainhill (Reddy, 2024)

4.3.4 Crop health

4.3.4.1 Chlorophyll content index

The chlorophyll content index (CCI) was measured over the growing season as it can be used to indicate plant health and the plant's ability to capture photosynthetically active radiation (Devnarain et al., 2016). CCI can also indicate plant senescence and maturity, as it increases during plant development, then starts to decrease towards (or after) the maturity stage.

OFSP: CCI showed an increasing trend until 100 DAP, reaching a maximum value of 58.1% (**Figure 4-18**). The CCI trend was similar to that obtained by Dladla (2017) who obtained a maximum CCI value of approximately 65%. The slow decline in CCI towards the end of the season is due to the “stay-green” trait of OFSP, which is similar to other crops such as sorghum.

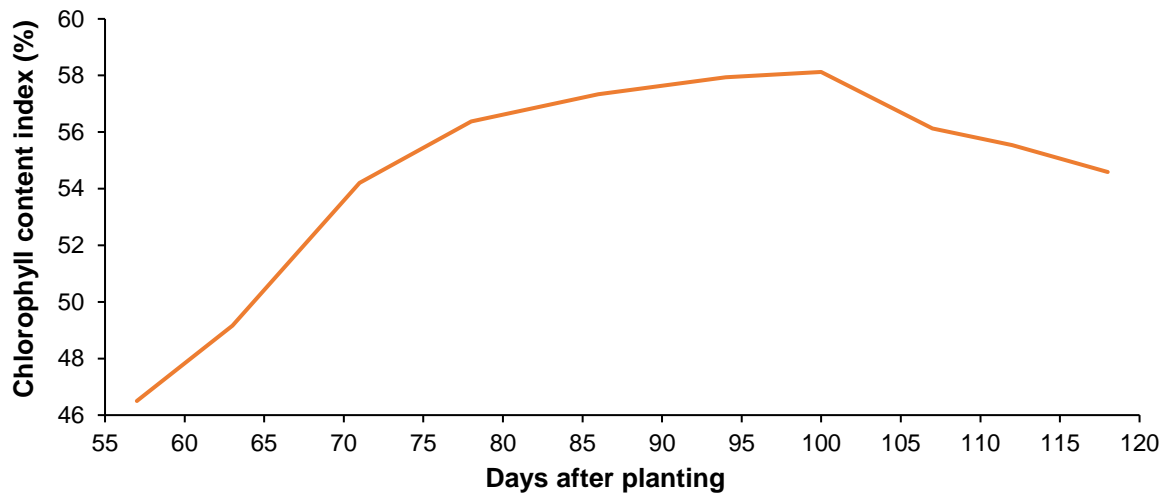


Figure 4-18 Chlorophyll content index of OFSP grown under rainfed conditions over the 2021/22 growing season at Fountainhill (Mthembu, 2023)

Taro: CCI peaked on 75.5% at 123 DAP, then decreased towards the end of the season, which may indicate the start of senescence (Figure 4-19). The decline was more apparent from 164 DAP and far more noticeable when compared to OFSP (Figure 4-18).

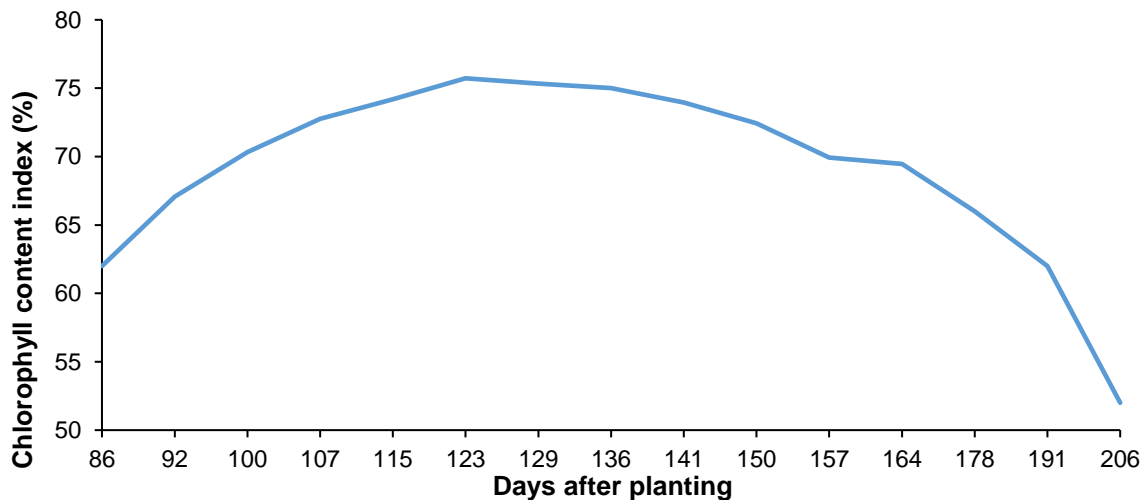


Figure 4-19 Chlorophyll content index of taro grown under rainfed conditions over the 2021/22 growing season at Fountainhill (Reddy, 2024)

4.3.4.2 Stomatal conductance

Stomatal conductance (SC) is the rate at which carbon dioxide (CO₂) and water vapour diffuses in and out of leaf stomata, respectively (Mabhaudhi, 2012). The opening and closing of stomata determine the rate of diffusion, and thus SC can be considered an important indicator of plant water stress (Cornic and Massacci, 1996). One of a crop's defence mechanisms to water stress is stomatal closure, which reduces the transpiration and photosynthetic rates and increases leaf temperature. These changes result in reduced plant growth. Higher transpiration rates increase the flow of CO₂ into plant leaves, thus implying more photosynthesis and increased plant growth.

OFSP: The relationship between stomatal conductance (SC) and leaf temperature (LT) is shown in Figure 4-20. After 70 DAP, LT declined steadily in response to ambient conditions, which gradually

cooled towards the end of the growing season (118 DAP). However, the highest SC of the season ($1,256 \text{ mmol m}^{-2} \text{ s}^{-1}$) was measured at 86 DAP. This was due to the warm and less humid conditions that resulted in high transpiration rates. Furthermore, 20.6 mm of rainfall occurred on day 83, and thus there was sufficient soil water that resulted in a high transpiration rate (i.e. high SC). The yellowing of leaves and stunted crop growth, which occurs due to crop water stress, was not observed during the growing season. The results also showed no evidence that water stress over a prolonged period occurred during the growing season, especially during critical stages of crop development. The tuber initiation and filling development stages are critical for tuber growth, and thus water stress should be avoided during these stages.

Taro: Leaf temperature peaked at 32.7°C at 115 DAP, then declined towards the end of the season in response to the cooling weather conditions (**Figure 4-21**). Low SC rates at 107, 141 and 206 DAP coincided with cool, cloudy and rainy conditions when ET_0 was 1.1, 0.8 and 1.4 mm, respectively. Similarly, SC peaked at 115 and 129 DAP during warm and sunny conditions when ET_0 exceeded 4 mm.

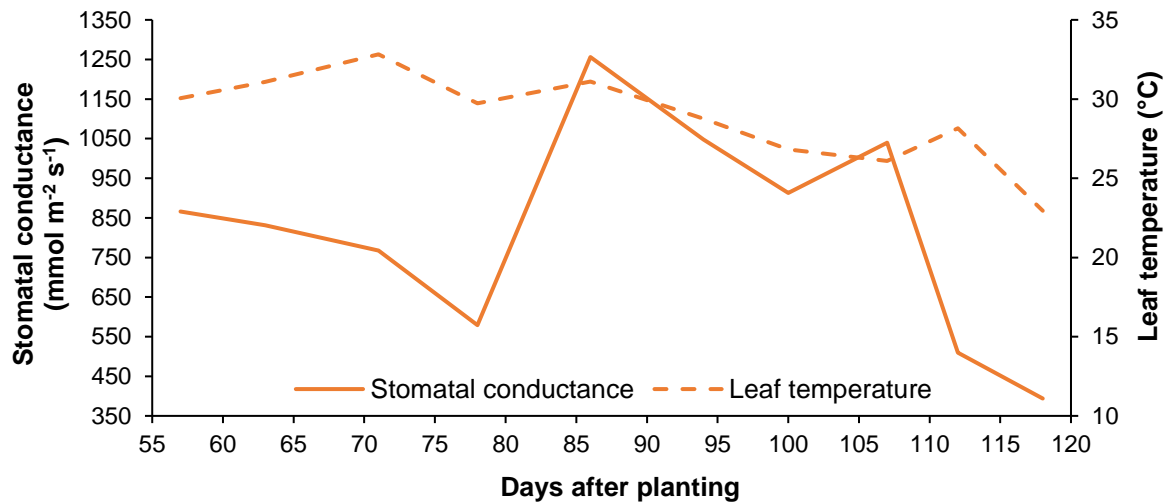


Figure 4-20 Stomatal conductance and leaf temperature of OFSP grown under rainfed conditions over the 2021/22 growing season at Fountainhill (Mthembu, 2023)

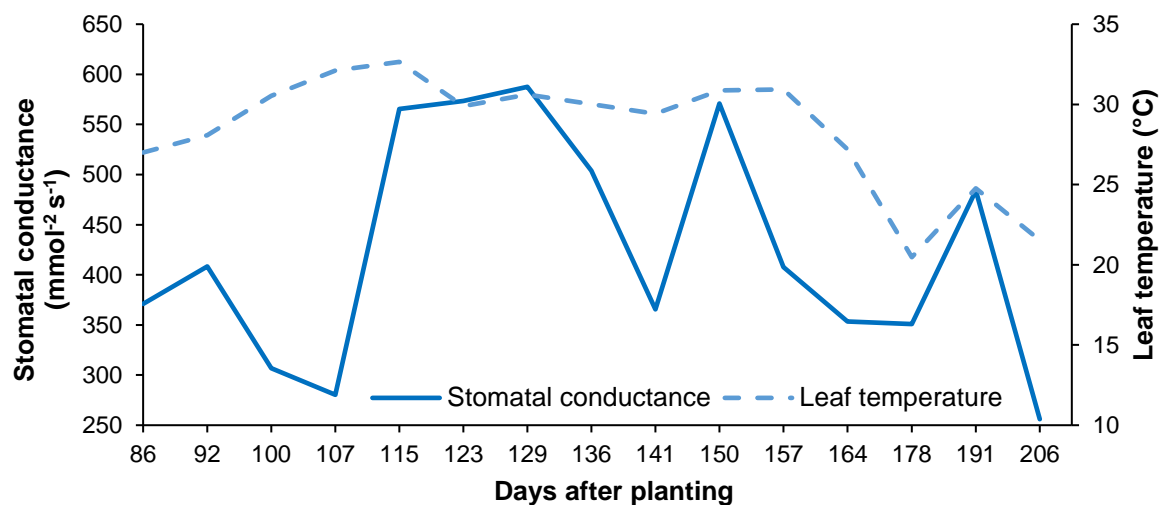


Figure 4-21 Stomatal conductance and leaf temperature of OFSP grown under rainfed conditions over the 2021/22 growing season at Fountainhill (Mthembu, 2023)

4.3.5 Crop water use and yield

4.3.5.1 Crop evapotranspiration

At both trial sites, the eddy covariance (EC) and surface renewal (SR) methods provided water use estimates for both crops. The EC method is considered the “gold” standard and provides the most reliable water use estimate. However, due to the cost and complexity of implementing this technique, cheaper alternatives such as SR are gaining popularity. Energy fluxes were calculated using two methods (direct & energy balance), which produced very similar results. Since the infrared gas analyser is more susceptible to moisture effects than the standard 3D ultrasonic anemometer, the latter instrument was preferred for EC measurements.

The classic SR method, referred to as SR-1, requires calibration against the EC method to obtain the so-called alpha factor. Hence, SR-1 will always provide similar results to those obtained from the EC method. In addition, sensible heat flux was also calculated using dissipation theory (SR-DT). An improved method called SR-2 does not need calibration against the EC method. Sensible heat is calculated using Monin-Obukhov similarity theory, which requires measurements of wind speed at canopy height (using a DS-2 sensor), LAI measurements and the height from the ground to the lowest leaf. However, Masanganise et al. (2022) recently showed that SR-DT was more accurate in estimating soybean ET compared to SR-2. Furthermore, SR-DT requires fewer input parameters and thus, is more robust and less expensive compared to SR-2. Hence, sensible heat flux was not estimated at site 1 for taro.

Results show that SR tends to under-estimate crop water use when compared to the EC method (**Table 4-8**). Sensible heat flux could not be calculated using dissipation theory (SR-DT) at site 2 due to the failure of the DS-2 sensor (suspected lightning damage). The high frequency measurements have shown that when the fine-wire thermocouple is cold or wet, sensible heat flux is over-estimated and thus, latent heat flux approaches zero, i.e. ET = 0 mm. This can occur (i) during and after rainfall events, and (ii) in the early morning after dew formation (i.e. when air temperature is below dew point temperature). The thermocouples also need to be kept free of spider webs and will under-estimate ET in dusty environments. However, when compared to EC, SR provides better estimates of soil water evaporation for bare soil conditions. Furthermore, the SR method is much cheaper and easier to install than the EC method.

Table 4-8 Comparison between observed crop water use (ET) for OFSP and taro grown under rainfed conditions at Fountainhill Eco-estate during the 2021/22 season

Method	Crop water use (ET in mm)	
	OFSP	Taro
EC	354.0	357.8
SR-DT	-	349.1
SR-1	322.2	330.4

From the daily measurements of crop ET and ET_o , daily crop coefficients were calculated, then averaged to monthly values for the fallow period prior to planting (Sep-Nov 2021) and after harvest (May-Aug 2022) as shown in **Table 4-9**. A 2nd order polynomial was fitted through the measured K_c values ($R^2 = 0.9825$) to predict values for Mar and April of 0.76 to 0.53, respectively. Even though these K_c values were determined over the fallow period for non-standard conditions, they were needed for the hydrological modelling component of this project (cf. **Chapter 7**). The K_c values obtained in this project were higher than those measured consecutively from May to October 2017 at Baynesfield (KwaZulu-Natal) by Masanganise (2019). One of the reasons for the difference in crop coefficients is due to the higher weed load at Fountainhill during the fallow period. At Baynesfield, far fewer weeds emerged after the maize crop was harvested, which is attributed to the regular use of herbicide

(Roundup) at this commercial farm. Hence, the fallow K_c values obtained in this project better reflect smallholder farming systems, where weeds are not regularly sprayed. For comparison, Mbangiwa (2018) determined crop coefficients at Baynesfield during a fallow period in summer.

Table 4-9 Monthly crop coefficients (K_c) estimated for the fallow period at Fountainhill and Baynesfield

¹ Site	Year	Dec	Jan	Feb	May	Jun	Jul	Aug	Sep	Oct	Nov	Source
FH	2021/22				0.38	0.26	0.20	0.27	0.29	0.44	0.62	Reddy (2024)
BF	2022				0.26	0.15	0.10	0.18	0.22	0.40		Masanganise (2019)
BF	2012/13	0.54	0.98	0.95						0.18	0.52	Mbangiwa (2018)

¹FH = Fountainhill; BF = Baynesfield

4.3.5.2 Final yields and harvest index

OFSP: From the beginning of March 2021, animals began burrowing under the perimeter fence, which was strengthened with netting and weighted down using heavy logs (**Figure 4-22a**). The animals therefore gained entry to trial site 2 to dig up and eat the OFSP roots (**Figure 4-22b**). The decision was therefore made to harvest the trial on 11 April (118 DAP), which was justified considering the severity of animal damage that occurred in the following week. The roots were completely destroyed by the animals by the second week after harvest.

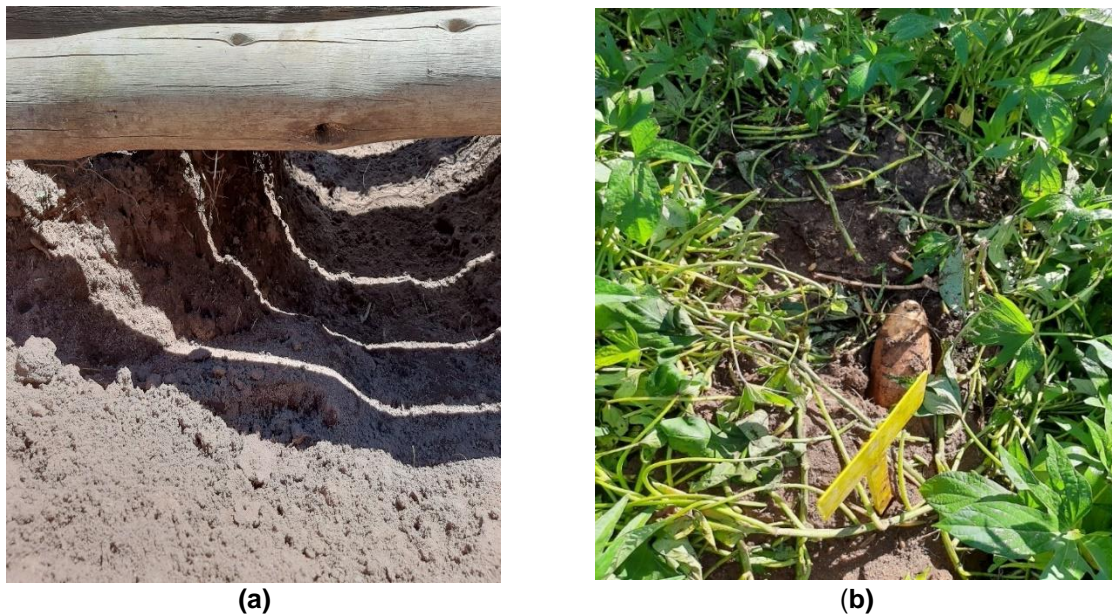


Figure 4-22 Evidence of animal entry (a) and damage (b) to OFSP roots grown at Fountainhill Eco-estate (trial site 2) during the 2021/22 season

A total of 15 plants were harvested from two representative rows, totalling 30 plants and 109 roots. Plants were separated into their separate components (leaves, vines & roots). Each component was weighed to obtain the fresh mass. Owing to the volume of harvested material, samples were then air-dried (not oven-dried) in a greenhouse over seven days to obtain dry mass. Harvested yields were then scaled up to a per hectare basis. The leaves, stems and vines contribute to the above-ground biomass, while the total biomass includes the above-ground biomass and the storage root yield. The fresh and dry storage root yield obtained at harvest was 34.89 and 12.12 t ha⁻¹, respectively. The fresh and dry above-ground biomass was 11.02 and 9.81 t ha⁻¹, respectively.

The fresh root yield is slightly higher than the range 7.6 to 32.2 t ha⁻¹ reported by Masango (2015), Mulovhedzi (2017) and Dladla et al. (2019). However, the dry tuber yield was substantially higher than values reported by Masango (2015) and Mulovhedzi (2017), which ranged from 6.5 to 7.6 t ha⁻¹ and 7.5 to 8.7 t ha⁻¹, respectively. The dry yield is within the 4.4 to 17 t ha⁻¹ range reported by Nyathi et al. (2019a).

From the results, a fresh:dry ratio of 2.88 and a harvest index (dry yield) of 55% were calculated. The fresh:dry ratio is required to convert dry yields simulated by crop models to fresh yields and is also important for the dried foods industry. This harvest index was within the ranges of 22-77% (Bhagsari and Doyle, 1990) and 37-81% (Bouwkamp and Hassam, 1988). In addition, the harvest index was comparable to values reported by Masango (2015), Mulovhedzi (2017) and Yeng et al. (2012), which ranged from 41-63%. Although sweet potato is mainly consumed fresh, it is important to conduct research on dry yield for the dried foods industry (Mulovhedzi, 2017), as well as for calculating fresh yields from dry yields simulated by crop models. However, for dual-purpose crops such as sweet potato, relatively high HI values are desirable since the leaves are edible.

Taro: The taro trial was weeded again in April and May 2022 and the trial was finally harvested on 24 June, as (i) dew formation in the early morning was resulting in leaf tip burn, and (ii) animals had begun to damage the outer rows of the trial. A total of 15 plants were harvested from two representative rows, totalling 30 plants. An allometric study was then undertaken, where the plants were separated into their separate components (leaves, stems, roots & tubers). Each component was weighed to obtain the fresh mass. The samples were then oven-dried for 48 hours at 60°C to obtain the dry mass of each component (**Figure 4-23**). Harvested yields were then scaled up to a per hectare basis.



Figure 4-23 Oven-drying of taro (a) leaves, stems and roots, and (b) corms that were harvested on 24 June 2022

The mass of fresh and dry material was used to calculate a final yield of 11.79 fresh t ha⁻¹ and 4.91 dry t ha⁻¹, respectively. Hence, the fresh to dry mass ratio is 2.40, which as mentioned previously, is required to convert dry yields simulated by the crop models to fresh yields.

4.3.6 Crop and nutritional water productivity

4.3.6.1 Nutrient content

OFSP: Measured nutrient content of OFSP is presented in **Table 14-1 (Section 14)**. Ca, Mg and Na levels were substantially higher than those reported by Mabhaudhi et al. (2019). Similarly, Fe and Zn levels were much higher than values obtained by Nyathi et al. (2019a). Foliar samples showed higher

values compared to the roots for almost all elements (cf. **Table 14-3** in **Section 14**). In particular, the leaves had much higher (10-30 times) contents for Ca, Mn, Mg and B

Taro: For taro tubers, measured mineral contents (**Table 14-2** in **Section 14**) were compared to values obtained by Shelembe (2020) for two water treatments, as shown in **Table 4-10**. The values for Ca and Mg obtained in this project are within the ranges provided by Shelembe (2020). However, Fe and Zn values were much higher, and Na is considerably lower.

Table 4-10 Comparison of nutrient content of taro tubers obtained in this project to those from Shelembe (2020) for two water treatments

Element	Nutrient content (mg kg ⁻¹)		
	Rainfed	Stressed	Unstressed
Ca	1,240	1,700	900
Cu	7	4	5
Fe	284	83	46
Mg	1,281	1,600	1,100
Na	29	372	230
Zn	137	90	91
Source	Table 14-2	Shelembe (2020)	

The variation in nutrient content is also evident from the data shown in **Section 14**, especially for the OFSP foliar samples. It is important to note that similar to other crops, nutrient composition of RTCs also varies across, inter alia, varieties, climatic conditions, water availability, other environmental conditions (e.g. soil type and properties) and harvesting methods (Uusiku et al., 2010). This makes it particularly important to study linkages between growing environments and nutrition and health. It also makes it difficult to compare nutrient contents from different studies. However, this project has added to the existing knowledge base on nutrient content of RTCs, as provided in **Section 3.3** (cf. **Chapter 3**).

Both crops were low in B and Cu, but especially Mo. African soils are typically deficient in B, Cu, Fe and Zn (Kihara et al., 2020). Therefore, when aiming to maximise micronutrient availability, foliar sprays consisting of these micronutrients should be applied regularly to the growing crop. Mo is tightly bound to clay particles, especially in acidic soils, and thus is not readily available for plant uptake. The soil pH at both sites was low especially at the taro site, which should have been corrected with agricultural lime to help increase the availability of applied N, P and K. including Mo.

Overall, the results confirm that both OFSP and taro are dual-purpose crops, where both the roots/tubers and leaves are edible and exhibit high nutritional value are . The results support the finding by Chivenge et al. (2015) that a RTCs are known to be nutrient-dense, and thus their consumption can (i) address nutrition insecurity issues, and (ii) help to alleviate malnutrition.

4.3.6.2 Crop water productivity

One of the main aims of this project is to improve the knowledge on the efficiency and productivity of water required for rainfed production of RTCs (cf. Aim 5 in **Section 1.2**). Crop water productivity (CWP; dry kg m⁻³) is defined as the attainable yield (dry kg ha⁻¹), relative to crop water use (i.e. ET in m³) accumulated from planting date to physiological maturity date. Crop water productivity increases by either improving yield or reducing ET (Pandey et al., 2000).

OFSP: From observations, a CWP of 3.42 dry kg m⁻³ was calculated from dry yield and water use obtained from the EC method. In comparison, Mulovhedzi (2017) and Masango (2015) provided CWP values of 2.18 and 2.55 kg m⁻³, respectively. Nyathi et al. (2019a) obtained CWP values ranging from

1.05 to 2.78 kg m⁻³ for irrigated (supplemental) and fully fertilised experiments for two seasons, where leaves were not harvested.

Taro: A CWP of 1.37 dry kg m⁻³ was calculated for taro, which is much lower than that for OFSP, due to taro's lower yield. A CWP of 3.29 fresh kg m⁻³ was estimated, which is much higher than the range of 0.06 to 0.53 fresh kg m⁻³ reported by Mabhaudhi (2012).

4.3.6.3 Nutritional water productivity

CWP (dry kg m⁻³), derived using water use measured by the EC method, was then multiplied by the measured nutrient content (in g kg⁻¹ of edible portion) to obtain nutritional water productivity (NWP; in g m⁻³). The NWP metric is most sensitive to NC since CWP is a constant value. Results are presented in **Table 14-4** (cf. **Section 14**) for OFSP (roots and leaves) and taro tubers. For OFSP, leaves exhibited higher NWP values than roots, especially for Ca, B, Fe, Mg, Mn and S. However, for 6 of the 11 elements, taro's NWP was lower than that of OFSP.

For taro, no comparison could be made with figures determined by Shelembe (2020) as fresh (not dry) yields were given and crop water use was based on the amount of irrigation applied in the two treatments (not actual crop ET) (cf. **Section 3.3.2**).

The NWP values obtained in this study for OFSP roots are much higher than other published values (e.g. Mabhaudhi et al., 2019; Nyathi et al., 2019b), especially for Ca, Fe, Mg, Na and Zn (cf. **Section 3.3.1**). Lunqvist et al. (2021) reported values that range from 1.885 to 2.945 g m⁻³. The NWP for β -carotene content in tubers (0.51 g m⁻³) was higher than values reported by Mulovhedzi (2017), which ranged from 0.09 to 0.11 g m⁻³ but was similar to the range of 0.43 to 1.88 g m⁻³ given by Mabhaudhi et al. (2019) for the same cultivar. OFSP is known for its high β -carotene content. Laurie et al. (2012) recommended that breeding programmes should aim to improve NWP in OFSP roots and leaves.

4.3.7 Crop modelling

For OFSP, the AquaCrop and SWB models were evaluated by comparing simulated and observed canopy cover (CC) development, leaf area index (LAI), above-ground biomass accumulation and storage root yield over the growing season. The model's ability to predict the final biomass, yield and crop water use under rainfed conditions was also evaluated. Model performance was evaluated using the following four statistics: (i) root mean square error (RMSE), (ii) Nash-Sutcliffe efficiency coefficient (NSE), and (iii) Willmott's index of agreement (DI), and (iv) the coefficient of determination (R²). Each statistic is described in more detail in **Section 5.2.6.5**.

4.3.7.1 Canopy cover

A problem with the data storage card in the LAI-2200 canopy analyser (LI-COR, USA) resulted in corrupted DIFN values. Hence, CC development could not be estimated from DIFN, and was therefore estimated using the Beer-Lambert equation. A light extinction coefficient (k) of 0.85 obtained from Masango (2015) was used in this study.

In AquaCrop, it is important to obtain good agreement between simulated and observed canopy cover (cf. **Section 5.2.6.4**). As shown in **Figure 4-24**, AquaCrop under-simulated initial CC development for OFSP, which resulted in a relatively high RMSE of 9.5%. A NSE of 0.765 indicates the model's ability to provide reasonable simulations of CC development, which is in contrast to the high Willmott's D-I and R² of 0.954 and 0.957, respectively.

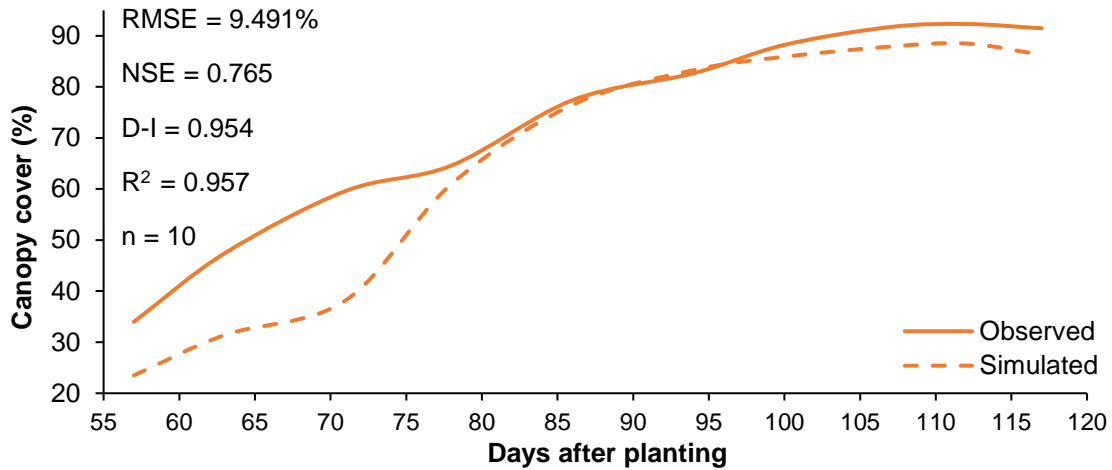


Figure 4-24 Comparison between simulated (AquaCrop) and observed canopy cover development for OFSP grown under rainfed conditions over the 2021/22 season at Fountainhill (after Mthembu, 2023)

Transpiration is directly related to CC, whereas soil water evaporation is proportional to the area of uncovered soil (i.e. $1 - CC$). Achieving high canopy cover is therefore important in reducing soil water evaporation losses and improving biomass production via maximising transpiration. As leaves grow, evaporation from the soil surface decreases (due to shading effects) and transpiration from leaf surfaces increases. Canopy coverage of about 70 to 80% for crops results in higher transpiration. The under-estimation of CC in the early- to mid-stages of development will result in higher simulation of soil water evaporation and reduced transpiration, thus resulting in lower biomass production (cf. **Section 4.3.7.3**).

4.3.7.2 Leaf area index

AquaCrop does not simulate leaf area index (only canopy cover development). Hence, a comparison of simulations against observations was only undertaken for the SWB model. A good correlation ($R^2 = 0.938$) between simulated and observed leaf area index (LAI) was obtained using the SWB model (**Figure 4-25**). The model slightly over-estimated LAI from 57-86 DAP. However, from 94-117 DAP, the model under-estimated LAI. peak LAI was not well simulated as indicated by the RMSE of $0.364 \text{ m}^2 \text{ m}^{-2}$. Overall, SWB's ability to simulate LAI was deemed very good.

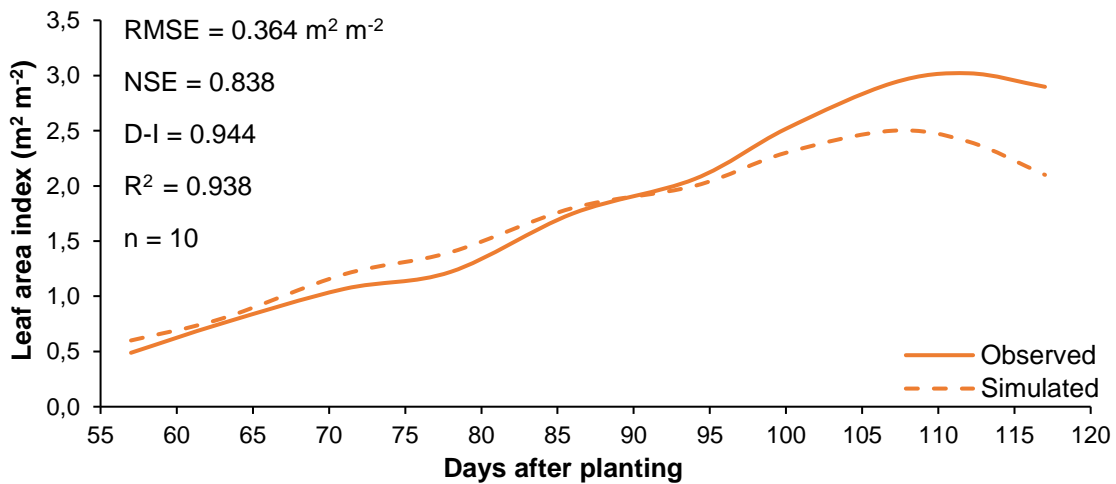


Figure 4-25 Comparison between simulated (SWB) and observed leaf area index for OFSP grown under rainfed conditions over the 2021/22 season at Fountainhill (after Mthembu, 2023)

4.3.7.3 Biomass accumulation

AquaCrop: Although the R^2 between simulated and observed above-ground biomass (AGB) accumulation was reasonable (0.614), the other statistical measures indicated that AquaCrop underestimated this variable for most of the growing season (**Figure 4-26**). Observations showed that leaf and vine biomass production increased rapidly after ~78 days and peaked at 100 DAP, then decreased after senescence.

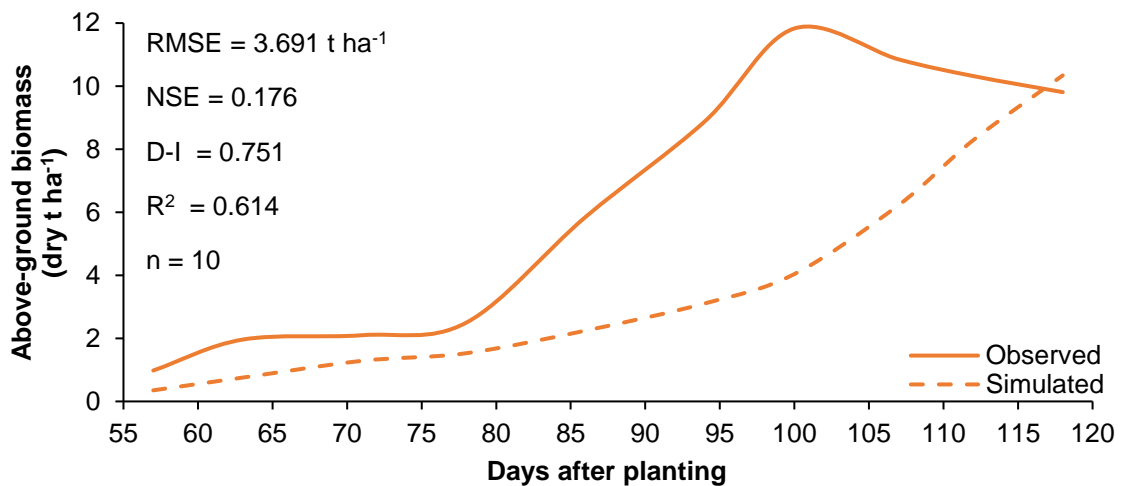


Figure 4-26 Comparison between simulated (AquaCrop) and observed dry above-ground biomass for OFSP grown under rainfed conditions over the 2021/22 season at Fountainhill (after Mthembu, 2023)

SWB: Similar results were obtained from the SWB model as shown in **Figure 4-27**, which also underestimated AGB accumulation. Masango (2015) also showed that AGB was under-simulated by the model. However, SWB (and AquaCrop) predicted the final biomass well.

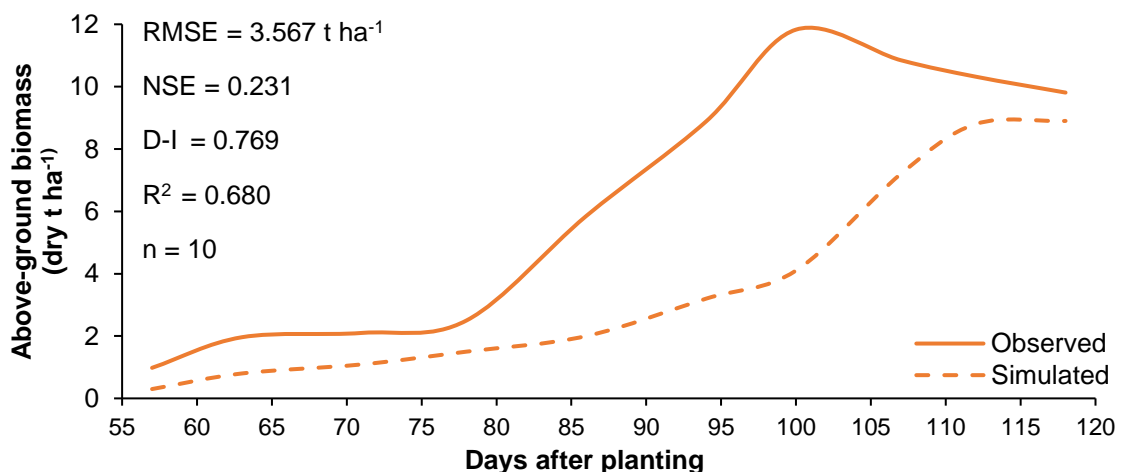


Figure 4-27 Comparison between simulated (SWB) and observed above-ground biomass for OFSP grown under rainfed conditions over the 2021/22 season at Fountainhill (after Mthembu, 2023)

4.3.7.4 Storage root yield

AquaCrop: Dry storage root yield was under-estimated by AquaCrop, despite the high R^2 and D-I values (**Figure 4-28**). The high RMSE (2.643 t ha^{-1}) and low NSE are likely due to the consistent under-estimation of root yield, especially during the mid-season growth stage. However, the simulation did improve slightly towards the end of the growing season.

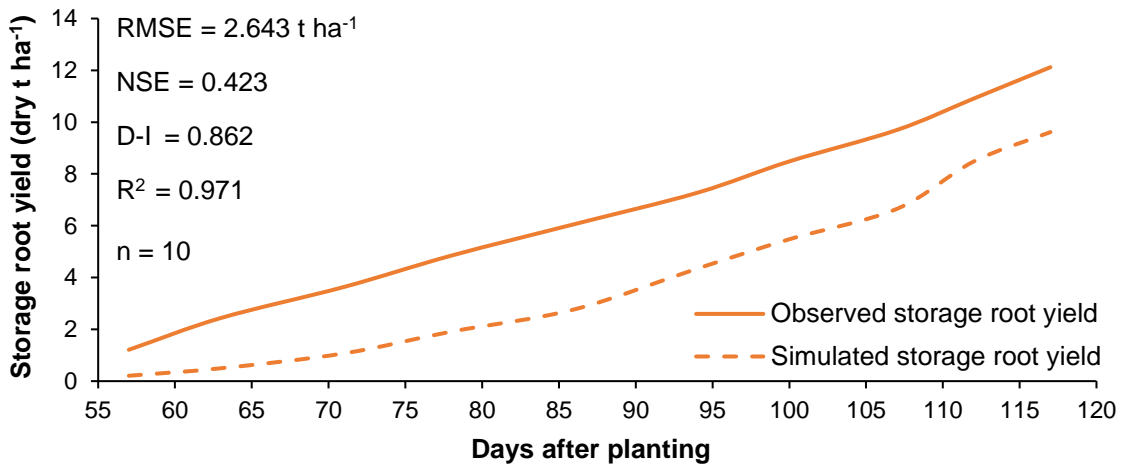


Figure 4-28 Comparison between simulated (AquaCrop model) and observed dry storage root yields for OFSP under rainfed conditions over the 2021/22 growing season (after Mthembu, 2023)

SWB: The high R^2 value of 0.964 between simulated and observed root yield again shows this statistical indicator can be misleading. The SWB model under-estimated root yield (**Figure 4-29**), which resulted in a high RMSE, negative NSE and low DI. A negative NSE indicates poor model performance (FAO, 2015; Zhong and Dutta, 2015). Annandale et al. (2005) stated that the SWB model was originally designed for predicting crop water use, and not for predicting crop yield. They added that various consultants reported they did not get sufficiently accurate yield and biomass simulations, which may explain the model's poor performance. AquaCrop provided a better simulation of root storage yield when compared to the SWB model.

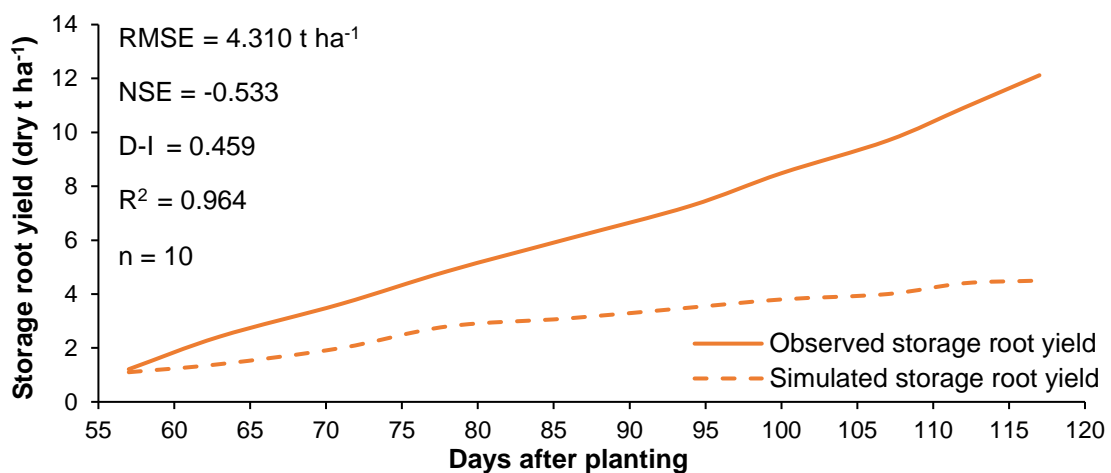


Figure 4-29 Comparison between simulated (SWB model) and observed dry storage root yields for OFSP under rainfed conditions over the 2021/22 season at Fountainhill (after Mthembu, 2023)

4.3.7.5 Final biomass and yield

The modelling results showed that the SWB model substantially under-estimated the observed dry yield of OFSP, despite the minimal calibration that was undertaken (cf. **Section 4.2.7.3**). This suggests that the model did not adequately account for the translocation of assimilates from the leaves, vines and stems to the roots as the crop approached maturity. This issue is further highlighted by the under-simulation of HI by the SWB model. AquaCrop also under-estimated the final root yield, but to a far lesser extent. The HI simulated by AquaCrop was 48%, which indicates an almost equal sharing of assimilates between above-ground biomass and root formation. Dry yields simulated by the models were converted to fresh yields using the fresh:dry ratio obtained from observations.

Table 4-11 Simulated versus observed data for final root yield, total biomass and harvest index for OFSP grown under rainfed conditions at Fountainhill

Method	Final root yield (kg ha ⁻¹)			Above-ground biomass (kg ha ⁻¹)	Harvest index (%)
	Fresh	Dry	Ratio	Dry	Dry
Observed	34,890	12,120	2.88	9,810	55
Simulated (AquaCrop)	27,693	9,620	2.88	10,340	48
Simulated (SWB)	12,954	4,500	2.88	8,900	34

4.3.7.6 Soil water content

Soil water content (SWC) was measured using CS616 probes installed on day 57 after planting, due to the failure of the CS650 probes. As shown in **Figure 4-30**, SWC water content was closer to permanent wilting point than field capacity throughout the season, due to the high drainage rate of the sandy soil found at trial site 2. However, this did not negatively effect on crop development, which suggests that OFSP can utilise soil water held at higher matric potentials than other crops.

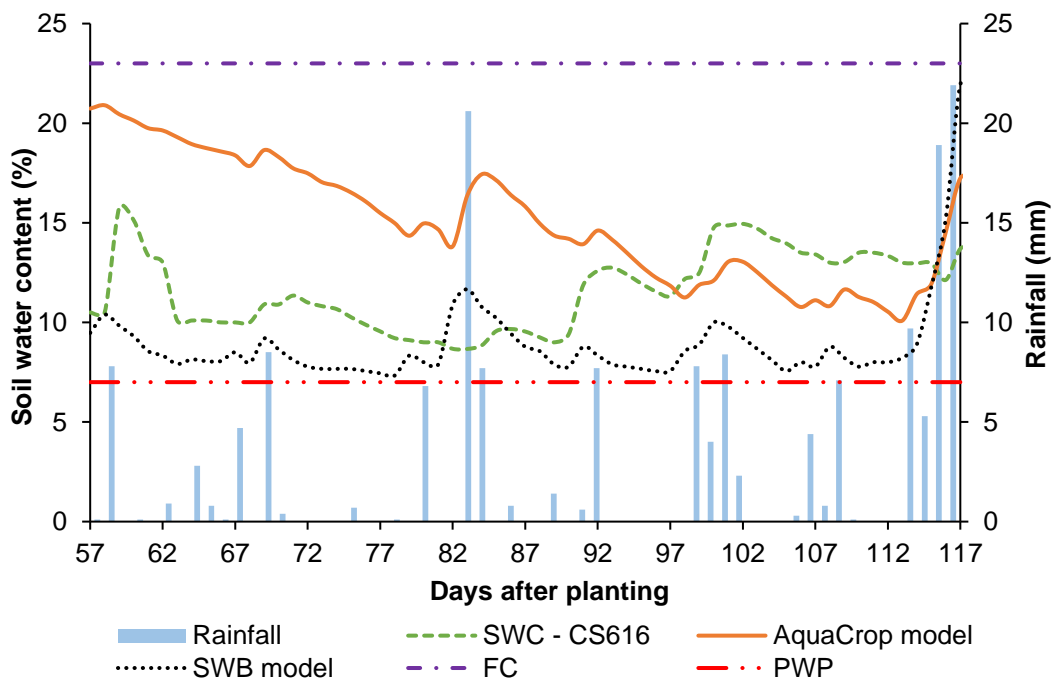


Figure 4-30 Comparison between profile water content measured by CS616 probes at Fountainhill and simulations by the SWB and AquaCrop model (after Mthembu, 2023)

According to Annandale et al. (2005), the SWB model is well suited to simulating crop water use and soil water content (SWC). Other studies also reported that AquaCrop is a valuable tool for simulating SWC (e.g. Pereira et al., 2015). However, neither model adequately estimated SWC when compared to measurements from the CS616 probes. For most of the measurement period, the AquaCrop model simulated a higher SWC relative to the SWB model (**Figure 4-30**). The SWB model's initial SWC was set at 18%, which was obtained from the CS650 probes at planting. For AquaCrop, the default option was used, which assumes the initial SWC is at FC (23%). This decision was due to AquaCrop's sensitivity to water stress at emergence (FAO, 2017).

4.3.7.7 Crop water use

Both models were used to estimate crop water use as ET accumulated over the growing season. When compared to the value of 354 mm measured by the EC method, both models over-estimated crop ET. Even though the site 2 was completely flat and the soil had a high sand content (loamy sand texture), both models simulated runoff. In AquaCrop, the coefficient of initial abstraction (I_a) was changed from 0.20 (version 4 or below; Raes et al., 2012) to 0.05 (version 5 or above; Raes et al., 2018), based on research by Woodward et al. (2003). Thus, version 5 or later generates more runoff than previous versions. The SWB model also uses a single value for I_a of 0.20, whereas ACRU requires monthly values (COIAM), with the default value being 0.20.

AquaCrop simulated no capillary rise due to the sandy soil texture, whereas the SWB model does not account for capillary rise. However, SWB calculates interception loss, but AquaCrop does not. Although both models simulated relatively similar ET, AquaCrop simulated much less transpiration compared to SWB. This is explained by the under-simulation of canopy cover development in the early- to mid-stages of development (cf. **Figure 4-24** in **Section 4.3.7.1**).

Table 4-12 Simulated (AquaCrop and SWB) vs measured ET for OFSP

Variable (mm)	Aqua-Crop	SWB
Precipitation (P)	472.9	472.9
Irrigation (I)		
Runoff (R)	46.9	65.4
Drainage (Dr)	97.3	64.2
Change in soil water content (ΔS)	31.9	8.3
Crop water use (ET)	376.7	388.4
Transpiration (T)	164.6	216.3
Soil water evaporation (E)	212.1	172.1

4.3.7.8 Crop water productivity

From observations, a CWP of 3.42 kg m⁻³ was calculated from dry yield and water use obtained from the EC method as shown in **Table 4-13**. CWP values of 2.55 and 1.16 were kg m⁻³ were calculated from the AquaCrop and SWB model simulations, respectively. The low CWP simulated by the SWB model was largely influenced by the low tuber yield. AquaCrop was able to better predict observed CWP when compared to the SWB model.

Table 4-13 Comparison between simulated and observed crop water productivity of OFSP grown under rainfed conditions

Method	Tuber yield (dry kg ha ⁻¹)	Water use (ET in m ³)	Crop water productivity (kg m ⁻³)
Measured	12,120	3,540	3.42
AquaCrop	9,620	3,767	2.55
SWB	4,500	3,884	1.16

4.3.7.9 Nutritional water productivity

NWP was estimated as the product of nutrient content and model-derived CWP. These values were then compared to observed NWP for each element. The results shown in **Table 4-14** highlight the importance of the models to adequately simulate yield and CWP. Hence, the minimal calibration of each model is vital for accurate simulations of CWP and NWP.

Table 4-14 Observed versus estimated NWP of OFSP for the 2021/22 season at Fountainhill

Element	NWP (g m ⁻³)		
	Observed	AquaCrop model	SWB model
K	79.59	59.38	26.93
P	11.56	8.62	3.91
Ca	4.69	3.50	1.59
Mg	3.46	2.58	1.17
β-c	0.68	0.50	0.23
Na	0.22	0.16	0.07
Fe	0.14	0.11	0.05
Zn	0.05	0.04	0.02
Mn	0.04	0.03	0.01
B	0.02	0.01	0.01
Cu	0.01	0.01	0.00
Mo	0.00	0.00	0.00

4.4 SUMMARY AND CONCLUSIONS

Based on the literature review presented in **Chapter 3**, one common cultivar of OFSP (199062.1) was selected for further study based on its high β-carotene content. Vines were obtained from the College of Agriculture in Cedara (KwaZulu-Natal). An upland (eddoe type) taro landrace called Dumbe dumbe was sourced from smallholder farmers in Swayimane. Vine cuttings of OFSP and sprouted taro corms were then propagated two months prior to the target planting date. Taro and OFSP were planted on 19 November and 14 December 2021 respectively, at a target density of 20,000 plants ha⁻¹ at two trial sites within the Fountainhill Eco-estate near Wartburg (KwaZulu-Natal). Both trials were initially affected by excessive weed growth, which was finally cleared on 9th February 2022. Prior to planting, a lattice mast was installed at each trial site and fitted with EC (e.g. 3D sonic anemometer) and SR (e.g. fine wire thermocouple) equipment to measure crop water use.

A total of 16 plants were randomly selected, which underwent regular measurements of plant height, leaf number, leaf area index, chlorophyll content index, leaf temperature and stomatal conductance. Leaf area index was then used to estimate canopy cover development using the Berr-Lamber equation.

Root/tuber formation and above-ground biomass accumulation were also determined from random destructive sampling. Phenological growth stages were also recorded as the time from transplanting/sowing to (i) recovered plant, (ii) maximum rooting depth, (iii) start of leaf senescence, (iv) start of yield formation, and (iv) physiological maturity. The final above-ground biomass and root/tuber yield was measured from 30 plants harvested 118 and 217 DAP for OFSP and taro, respectively.

Results showed that storage root development for OFSP starts early and continues throughout most of the season, whereas taro tubers form later in the season and develop rapidly. Taro's height, leaf number and LAI were all lower than expected, which may have been a consequence of weed competition. OFSP's leaf area is much higher than for taro, especially before and during the vegetative growth phase. This is due to OFSP's higher leaf number when compared to taro. This resulted in more canopy cover and greater shading of the soil surface, leading to less soil water evaporation. Hence, soil water evaporation is dominant for approximately two months after taro is planted, which highlights the need for proper weed maintenance before and after emergence. This helps to explain why both crops used a similar amount of water, despite the difference in crop cycle (118 vs 217 days).

Due to the threat of animal damage at Fountainhill, OFSP was harvested prematurely, and thus observed yields may be lower than what could have been achieved. Summarised results are presented in **Table 4-15** for both RTCs. Since the SR method was calibrated against EC, it will always produce similar results of crop water use. The EC method is considered the "gold" standard, and thus water productivity (crop and nutritional) calculations were based on EC estimates of crop water use. From the literature review, taro has a lower CWP when compared to OFSP. This was confirmed by results obtained in season 2, where taro's CWP was much lower than that for OFSP (1.37 vs 3.42 kg m⁻³), due mainly to the yield difference (4.91 vs 12.12 dry t ha⁻¹).

Table 4-15 Measured data for OFSP and taro grown in the second season (2021/22) at Fountainhill

Variable	Method	OFSP	Taro
Harvest index	Fresh	76	63
	Dry	55	76
Tuber yield (t ha ⁻¹)	Fresh	34.89	11.79
	Dry	12.12	4.91
Fresh/dry ratio		2.88	2.40
Water use (mm)	EC	354	358
	SR-DT	-	349
	SR-1	322	330
CWP (kg m ⁻³)	EC; Dry	3.42	1.37

Harvested tuber and foliar samples were analysed to determine nutrient content for the following minerals: β-c, B, Ca, Cu, Fe, K, Mg, Mn, Mo, Na, P and Zn. In addition, total C, N and S were also measured. Nutrient contents were then multiplied by CWP to estimate nutritional water productivity (NWP). OFSP leaves exhibited higher nutrient contents compared to the roots for almost all of the analysed minerals. Taro tubers contained more nutrients for most minerals (except K) when compared to OFSP storage roots. This highlights the dual-purpose nature of OFSP and taro, where both the roots/tubers and leaves are edible and exhibit high nutritional value.

For the modelling exercise, considerable effort was spent on creating reliable, error-free climate files for use in AquaCrop and SWB. The estimation of ET₀ should be undertaken accurately as possible, as was done in this project, especially if such data is used for (i) model calibration and/or validation, and for (ii) calculating of crop coefficients. Soil parameters required by both crop models (e.g. saturation, field capacity, permanent wilting point) were determined from laboratory measurements, which provided more accurate values compared to simulations by the SPAW model. Default (i.e. initial) crop parameters

for OFSP required by both crop models were sourced from the literature. Crop parameters were then fine-tuned (i.e. partially calibrated) to better represent local crop and growing conditions at trial site 2. The AquaCrop and SWB models were run to simulate CC, LAI, AGB and storage root yield of OFSP over the growing season. Since AquaCrop and SWB do not simulate LAI and CC respectively, model comparisons were done on biomass, storage root yield and soil water content. Although SWB performed slightly better when simulating biomass than AquaCrop, it substantially under-estimated storage root yield. This resulted in a large under-estimation of CWP by the SWB model when compared to AquaCrop. If CWP is under-estimated, then NWP will also be lower than observations. Based on the preliminary modelling results for OFSP, AquaCrop performed much better than SWB, and thus was selected to model the water use of both RTCs, as described in **Chapter 6**. Since the trials were rainfed (not irrigated), only a limited number of parameters could be adjusted. Hence, further work was required to improve AquaCrop simulations by adjusting other crop parameters, which is described in **Section 5.2.6**, with results presented in **Section 5.3.7**.

5 MEASUREMENT OF WATER PRODUCTIVITY: SEASON 3

5.1 INTRODUCTION

In the final season, research efforts continued to address Aim 2 (cf. **Section 1.2**), namely to measure the water use and yield of OFSP and taro. As noted in **Chapter 4**, various problems were experienced at Fountainhill in the previous two seasons, especially trials being damaged by animals. Furthermore, the budget allocated to field work had been exhausted, mainly due to the (i) cost of taro corms purchased from Swayimane smallholder farmers to establish trials with sufficient fetch for the EC and SR to accurately estimate crop ET, and (ii) travel expenses associated with weekly visits to/from Fountainhill Eco-estate. Hence, there was a need to reduce field work-related expenses. Four raised beds (two for each crop) located in the same greenhouse on the Agric campus in Pietermaritzburg were secured for exclusive use by this project. Results from the greenhouse experiment were used to finalise crop parameters for OFSP and taro, which were required by AquaCrop for the national-scale model runs. This work formed part of Mr Reddy's PhD study.

5.2 MATERIALS AND METHODS

5.2.1 Planting material

OFSP vines (199062.1 variety) were grown in other raised beds in the same greenhouse, from which cuttings (or slips) were propagated. This was important since no material was available from the horticultural greenhouse at the College of Agriculture in Cedara (KwaZulu-Natal). The sweet potato vines and leaves were also inspected for any disease and when identified, were discarded from the rest of the material.

An eddoe type taro landrace (Dumbe dumbe) was obtained from the Swayimane community at no cost. Material with a well-defined root system was stored in a cool, dark room to help slow down the physiological process of starch breakdown (i.e. remobilisation of assimilates), before being planted into the two beds. Corms that were smaller in size with no defined root structure or were decomposing were discarded to prevent the spread of diseases or contamination with other taro corms.

5.2.2 Experimental design

Four raised beds were used in the greenhouse (two for each RTC). Two beds were fully irrigated to meet 100% of crop water requirement (i.e. non-stressed treatment) and the other two received deficit irrigation (30% of crop water requirement).

5.2.3 Agronomic practices

5.2.3.1 Site preparation

The greenhouse tunnel beds were prepared prior to planting by hand ploughing with the help of Ukulinga staff. Hand hoes were used to manually remove weeds and for turning the soil to ensure a smooth seedbed.

5.2.3.2 Planting

The four raised beds in the greenhouse tunnel were planted on the 27th of October 2022. In each bed, two rows (0.60 m apart) were planted at a spacing of 0.30 m between plants, i.e. 55,556 plants ha⁻¹. Planting rows were opened using hand hoes and individual OFSP vines and taro corms were

transplanted/sown. Once the taro emerged, gaps that appeared between plants in each bed were filled using material planted in an adjacent bed (Figure 5-1).

Orange flesh sweet potato (199062.1 variety)



Taro (Dumbe dumbe landrace)



100% of CWR

30% of CWR

Figure 5-1 Sweet potato and taro grown under two water treatments (i.e. 30% and 100% of CWR)

5.2.3.3 Fertilisation

Prior to the commencement of the experiment, soil samples taken at 0.15 m and 0.40 m from each of the four beds were sent to the ICFR laboratory for soil fertility and textural analysis. Based on the soil fertility results, fertiliser application quantities for each bed were calculated. Gromor Accelerator (0.30 N: 0.15 P: 0.15 K) was applied to each of the four beds based on the soil fertility calculations. Gromor Accelerator was chosen due to its slow release of nutrients into the soil making it readily available for both crops during the growing period and is less harmful to the crops (i.e. prevents root and leaf burn). A further top dressing of fertiliser was not applied during the growing period.

5.2.3.4 Pest and weed control

Prior to planting, the beds were sprayed with a contact herbicide (Gramoxone) to control weeds. A dilution of 150 ml of herbicide per 16 L of water was used to spray each of the four beds. A period of approximately one week was allocated for spraying and settling prior to planting. When necessary, weeds were manually removed from the beds throughout the growing season.

Observations of white fly infestations and red spider mites were sprayed with Applaud insecticide. The taro beds were mostly affected by the spider mites. A dilution of 30 to 60 ml per 16 L of water of Applaud was used. Insects such as grasshoppers, ants and caterpillars were also observed. Kemprin insecticide was sprayed using a dilution of 32 ml per 16 L of water. Pest control was important to prevent a breakout in the greenhouse that could have affected adjoined experiments.

5.2.4 Instrumentation

For the partial calibration of AquaCrop to be successful, the following was required:

- measurements of net radiation, wind speed, air temperature and relative humidity (minimum & maximum) inside the greenhouse;
- calculation of the evaporating power of the atmosphere (ET_o) using the FAO56 (Penman-Monteith) method described by Allen et al. (1998);
- recordings of weekly irrigation volumes applied to each water treatment;
- measurements of physical soil characteristics in each bed; and
- observations of crop phenology and life cycle for each crop;

5.2.4.1 Climate

A battery-powered automatic weather station was installed inside the greenhouse. Daily reference evapotranspiration was calculated using FAO's ET_o Calculator utility (FAO, 2012a) using measurements of:

- solar radiation (CMP3 pyranometer; Kipp and Zonen, Delft, Netherlands),
- air temperature and relative humidity (Vaisala HMP60; Campbell Scientific Inc., Utah, USA), and
- wind speed (DS-2 ultrasonic anemometer; Decagon Devices, Washington, USA).

5.2.4.2 Irrigation system

Irrigation equipment was purchased from a local irrigation company and installed to facilitate both water treatments. The irrigation system included a 24V AC irrigation controller (Hunter X-core), two water meters, two solenoid valves, dipper lines, emitters, piping and connections. A pressure reducing valve was also purchased to reduce the incoming water pressure from 5 to 2 bars, which is required for drip irrigation systems.

5.2.4.3 Soil water content

Eight CS655 soil water probes (Campbell Scientific Inc., Utah, USA) were ordered from the supplier in late September 2022, yet were only delivered in mid-January 2023. Due to the delay in obtaining these probes, four CS650 and four CS616 probes were also installed at two depths (0.15 and 0.40 m). This facilitated a comparison of the different sensors manufactured by Campbell Scientific (CS). Despite the reported accuracy of the CS655 probes being $\pm 3\%$, they were calibrated according to the procedure outlined in the product manual (Campbell Scientific, 2021). Calibration is deemed important when dry bulk density exceeds 1.55 g cm^{-3} , which was not the case for the greenhouse beds.

5.2.5 Data collection

5.2.5.1 Climate and soil water content

The automatic weather station was connected to a CR1000 data logger (Campbell Scientific Inc., Utah, USA), together with the CS655 and CS616 probes. The CS650 probes were connected to a CR300 logger (Campbell Scientific Inc., Utah, USA). Both data loggers were installed in waterproof boxes and powered by two 12V DC 100 Ah batteries housed in a strong box. Weather variables were measured at 15-minute intervals, from which hourly and daily values were calculated and stored by the data logger. The data logger was linked to a data telemetry system so that current conditions could be easily monitored online (Figure 5-2).

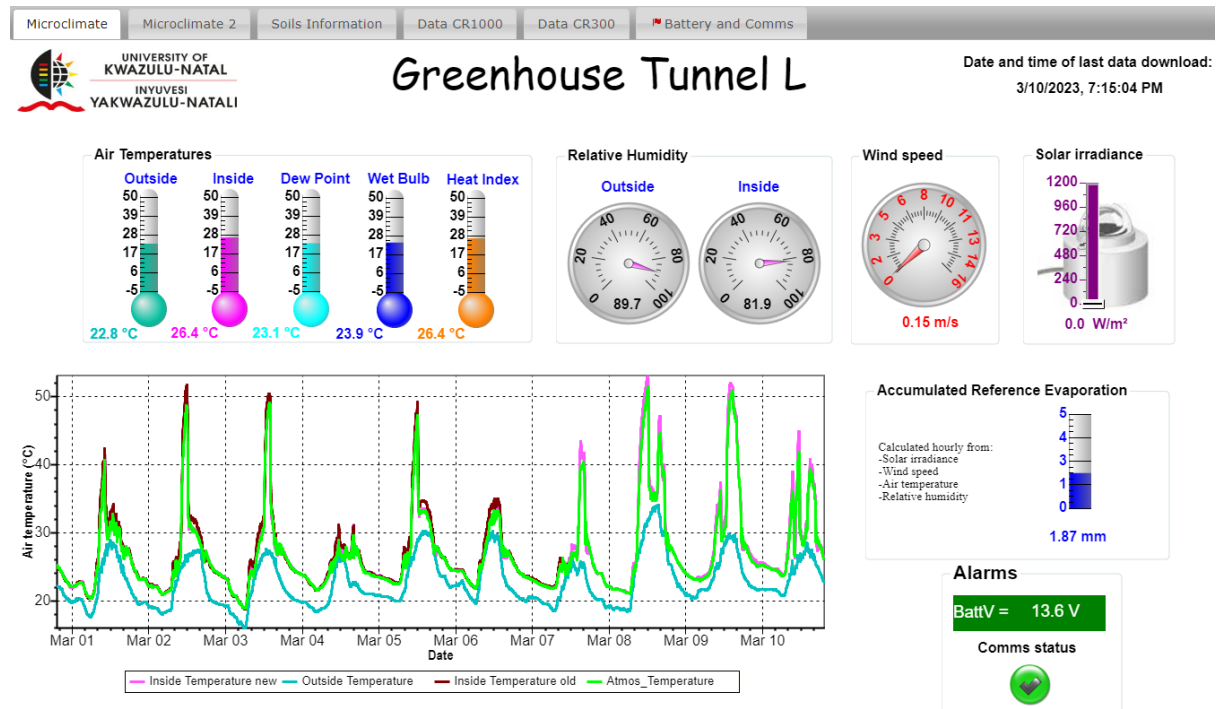


Figure 5-2 Web-based monitoring of weather conditions (insider and outside), soil water content and battery status in the greenhouse at UKZN over the 2022/23 growing season

5.2.5.2 Other soil properties

Prior to planting, a small pit was dug in each of the four soil beds to obtain undisturbed soil cores at a soil depth of 0.30 m soil to determine dry bulk density. The cores were dried in an oven for 24 hours at a constant temperature of 105°C, then weighed to determine mass of solids. The length and diameter of each core was measured to calculate the volume of soil, from which soil bulk density was calculated. The undisturbed soil cores were also used to determine soil water retention parameters such as saturation (SAT), field capacity (FC) and permanent wilting point (PWP) using the controlled outflow pressure method in the soil water laboratory at UKZN. Outputs from the outflow pressure apparatus were used to create soil water retention curves via the Van Genuchten equation. From these curves, volumetric water content (%) at FC was estimated at a pressure head of -10 and -33 kPa. Similarly, PWP was obtained at a pressure of -1500 kPa, respectively. Saturated hydraulic conductivity (K_{SAT}) was measured for each core using the constant head permeameter method.

5.2.5.3 Crop growth and yield

Initial canopy cover: Once the experiment was established, the mean leaf area was measured at 90% emergence and used to estimate the initial canopy size (cm² per plant). This variable was required by the AquaCrop model to estimate initial canopy cover (CC₀). Thereafter, the following measurements were made weekly throughout the growing season.

Canopy cover development: Leaf area index (LAI) was measured using a LAI-2200 plant canopy analyser (LI-COR Inc., Nebraska, USA), from which diffuse non-intercepted radiation (DIFN) was calculated. DIFN represents the fraction of sky not obscured by the plant's canopy (LAI-2200, 2010). Canopy cover (CC) development (in %) was then calculated as $100 \cdot (1 - \text{DIFN})$, as suggested by Mabhaudhi (2012). CC development was also estimated from measured LAI using the Beer-Lambert equation, which required a crop-specific parameter called the light extinction coefficient (k). This coefficient was measured for both crops using an AccuPAR model LP-80 ceptometer (Decagon Devices, Pullman, Washington, USA). Measurements of k were then compared to values sourced from available literature (cf. **Section 4.2.6.8**).

Plant height and leaf number: Plant height (from the base of the stem to the top of the canopy) and leaf number (fully formed leaves) were also measured.

Plant health: Chlorophyll content index (CCI) was measured weekly on dry, fully expanded and exposed leaves using a chlorophyll content meter (SPAD CCM-200 PLUS, Opti-Sciences, USA). Stomatal conductance (flux of carbon dioxide entering, or water vapour exiting, through the stomata of a leaf) was measured weekly (around midday) using a steady state leaf porometer (Model SC-1, Decagon Devices, USA). In addition, diurnal measurements were also made for sweet potato when the plant reached the end of the vegetative growth stage. No measurements were made for taro because the leaves were too thick for the instrument.

Phenological development: The time taken to reach each phenological stage was recorded in calendar days when 50% or more of the experimental plant population exhibited diagnostic signs of that particular growth stage. Measurements of CCI were used to help determine the onset of senescence. The depth of growing roots was also closely monitored from emergence until the maximum rooting depth was obtained. The time in calendar days to reach maximum rooting depth and maximum canopy cover (CC_x) was also recorded, which were required by AquaCrop as inputs.

Biomass accumulation: Using destructive sampling, biomass accumulation (or total dry matter) was determined by measuring the mass of a representative plant (with the roots removed prior to weighing).

5.2.5.4 Crop water requirement

Weather data (solar radiation, air temperature, relative humidity & wind speed) measured inside the greenhouse was used to calculate daily reference crop evapotranspiration (ET₀), from which maximum evapotranspiration (ET_c) was estimated via the single crop coefficient (K_c) approach. For both crops, a K_c value of 1.10 was used ((**Table 16-13**; cf. **Section 16.4**). Incremental increases in regular measurements of LAI for OFSP were used as a guide to increase K_c over the growing season, such that K_c increased from 0.20 (at planting) to 1.10 when LAI peaked at 3.0 m² m⁻². The irrigation depth to be applied when soil water content depleted by 40% of total available water (TAW) was calculated for each treatment, with the average being 12 mm (**Table 5-1**).

Table 5-1 Estimation of irrigation demand for each water treatment

% of CWR	Bed no.	FC (% vol)	PWP (% vol)	AWC (mm m ⁻¹)	ERD (m)	TAW (mm)	Allowable depletion	Irrigation depth (mm)
100	3 & 4	37.5	29.5	80	0.40	32	0.40	12.8
30	1 & 2	43.5	36.5	70	0.40	28	0.40	11.2

Daily ET_c values were accumulated daily and when the total reached 12 mm, this irrigation depth was then applied to both raised beds receiving 100% of crop water requirement (CWR). For the water deficit treatment, 30% of ET_c was accumulated daily, and thus intervals between irrigation events were longer. However, when extreme temperatures occurred in the greenhouse during regular load shedding and load reduction events (extraction fans stopped working), additional irrigation was applied to the crop to help ensure survival. Hence, the volume of irrigated water applied was recorded daily, which was then used to calculate the final irrigation depth applied to each treatment.

5.2.5.5 Nutrient content

As noted in **Section 4.2.6.12**, OFSP and taro samples (tubers & leaves) were sent to the Cedara laboratory (College of Agriculture, Cedara, KwaZulu-Natal) for nutrient analysis. In addition, samples were analysed by the Horticultural laboratory at UKZN to determine β -carotene content of OFSP. In comparison to the ICFR laboratory, the Cedara laboratory was unable to measure B or Mo but they did measure Al.

5.2.6 Crop modelling

5.2.6.1 Model selection

As noted in **Section 4.4**, AquaCrop was selected to model the water use and yield of OFSP and taro. However, further work was required to fine-tune the crop parameters to improve model simulations, especially for taro. This was done using data from season 3 as described next.

5.2.6.2 Model inputs

Raes et al. (2018) noted that before running the AquaCrop model, it is important the following is done correctly:

- Rainfall and air temperature (minimum, maximum and mean) data is measured at or nearby the experimental site.
- The evaporating power of the atmosphere (ET_o) is correctly determined using the FAO56 (Penman-Monteith) method described by Allen et al. (1998).
- Physical soil characteristics (e.g. soil depth, soil water retention and K_{SAT}) of the various soil horizons are well defined.
- Crop phenology and crop cycle are fine-tuned to the environment and the crop species.
- Field management practices that affect soil surface runoff, reduce soil water evaporation (mulches), and crop development and production (soil fertility) are specified correctly.

5.2.6.3 Model parameters

AquaCrop (version 6.0) can simulate the growth, productivity and water use of 15 herbaceous crops (Raes et al., 2018). However, model parameters for RTCs such as sweet potato and taro have not been provided by FAO. In order to run AquaCrop, initial crop parameters were sourced from the available literature, as described next.

The Water Research Commission (WRC) has funded research on underutilised indigenous crops, which has led to the development of AquaCrop parameter files for OFSP and taro. For example, WRC Project No. K5/2171 titled “Nutritional water productivity of traditional vegetable crops” (Nyathi et al., 2016) developed crop parameters for OFSP. Beletse et al. (2011; 2013) also developed crop parameters for OFSP (Isondlo cultivar) using experiments undertaken at the ARC’s rain shelter facility (Roodeplaat, Gauteng) across two seasons. Similarly, Rankine et al. (2015) used default AquaCrop parameters for potato (Raes et al., 2018), then developed calibrated values for OFSP for Jamaica. Pushpalatha et al. (2021) and Lamaro et al. (2023) also published calibrated parameter values for India and Ethiopia, respectively. For certain parameters, Lamaro et al. (2023) used the same values derived by Beletse et al. (2013).

WRC Project No. K5/1771 titled “Water use of drought tolerant crops” (Modi and Mabhaudhi, 2013) developed crop parameters for bambara nut and taro. The calibration and validation of bambara nut was published by Mabhaudhi et al. (2014a). For taro, crop parameters were initially developed by Mabhaudhi (2012), then published by Mabhaudhi et al. (2014b). The authors concluded that despite canopy cover being under-estimated for rainfed conditions, the model was able to simulate final biomass and yield reasonably well. However, further research was required to improve simulations under water deficit conditions. Thereafter, Mabhaudhi et al. (2016a) adjusted certain crop parameters for taro to further improve simulations under rainfed conditions, which were then used to model the impacts of climate change on taro production. These parameters were also used to model the impacts of climate change on taro production as part of WRC Project No. K5/2717 (Kunz and Mabhaudhi, 2023).

For each study mentioned above, four calibration (and validation) statistics were extracted for canopy cover (CC): (i) root mean square error (RMSE) or normalised RMSE (NRMSE), (ii) Nash-Sutcliffe efficiency coefficient (NSE), and (iii) Willmott’s index of agreement (DI), and (iv) the coefficient of determination (R^2). **Table 16-1** and **Table 16-2** (cf. **Section 16.1**) show the calibration and validation statistics extracted for canopy cover development. No calibration or validation statistics for OFSP were provided by Pushpalatha et al. (2021) and Lamaro et al. (2023). The studies were ranked using RMSE for CC. RMSE represents the average magnitude of the squared residual errors, with values ranging from 0 (excellent) to positive infinity (poor). Analysis of the residual error (i.e. the difference between model predictions and observations) can be used to detect systematic error (Moriassi et al., 2007). Based on the results, the locally developed crop parameters developed by Nyathi et al. (2016) and Mabhaudhi et al. (2014b) should provide the best simulations of crop water use and yield of OFSP and taro, respectively.

Unfortunately, this project was unable to obtain crop parameter files for OFSP from the primary authors (Dr Yacob Beletse and Dr Melvin Nyathi). This was deemed important since (i) not all parameter values are published, and (ii) values reported in journal papers often contain errors. For example, the parameter values published by Beletse et al. (2013) and Nyathi et al. (2016) as shown in **Table 16-3** (cf. **Section 16.2**). Likely errors in parameter values are highlighted in red in the tables. For example, the canopy growth/decline coefficients (increase/decrease per growing degree-day), which are important parameters describing canopy growth/decline, were much larger than expected. From 12 crop parameter files released with AquaCrop version 6, the canopy growth coefficient (CGC) ranges from 0.00500-0.01615, whereas the canopy decline coefficient (CDC) ranges from 0.00150-0.01000 (Raes et al, 2018). As shown in **Table 16-3** (cf. **Section 16.2**), CGC and CDC are deemed too high, and thus likely mistakes.

Parameter files were obtained from Rankine et al. (2015) and Pushpalatha et al. (2021) as shown in **Table 16-4** and **Table 16-5**, respectively (cf. **Section 16.3**). These latter parameter values were compared to those published by Lamaro et al. (2023), with likely errors again highlighted in red (**Table 16-5** in **Section 16.3**). Hence, the decision was made to use parameters derived by Rankine et al.

(2015) and where possible, derive crop parameters values from the field work conducted in season 2. For taro, parameter files were sourced from Prof. Tafadzwa Mabhaudhi (cf. **Table 16-6** in **Section 16.3**) and the latest version (2016) was used in this project, due to possible errors in CGC and CDC published by Mabhaudhi et al. (2014b).

5.2.6.4 Parameter fine-tuning

As noted above, crop parameters for both crops were obtained from the available literature, which were then partially calibrated using experimental observations from the greenhouse experiment. Hence, the default parameter values were fine-tuned to better represent local crop and growing conditions. The list of crop parameters provided by Steduto et al. (2012; Table 2 on p 44) that should be adjusted was used as a guide. This process highlights the importance of developing high quality data from well designed and executed experiments for the partial calibration of model parameters. No changes were made to parameters related to soil fertility or soil salinity stress. Some of the important parameters that were changed are described next.

Crop type and planting method (lines 4 & 5): For the crop type, option 3 was selected to reflect a root/tuber crop. For OFSP, the crop was transplanted (option 0), whereas taro was sown (option 1).

Base and upper temperature (lines 8 & 9): In AquaCrop, two crop parameters are required that specify temperature thresholds when crop development ceases, i.e. the base (T_{BSE}) and upper (T_{UPP}) thresholds. These values are used to calculate accumulated heat units across the growing season in growing degree-days.

Basal crop coefficient (line 35): The basal crop coefficient (K_{CB}) is an important input parameter that determines the maximum rate of transpiration under non-stressed growing conditions. Pereira et al. (2021a; 2021b) provided updated standard parameter values (e.g. K_C and K_{CB}) for those originally published by Allen et al. (1998). The authors also derived new values for new crops, including RTCs such as sweet potato and taro. Hence, K_{CB} was set to the values shown in **Table 16-13** (cf. **Section 16.3**).

Maximum effective rooting depth (line 38): The raised beds have a 40 cm soil profile, below which is a thin layer of gravel and plastic sheeting that prevents any drainage beyond the rooting zone, i.e. at a depth of 0.45-0.50 m.

Reference harvest index or HI_o (line 64): In AquaCrop, HI slowly increases from the start of root enlargement/tuber formation and should reach the reference value (HI_o) shortly before the physiological maturity date. HI_o was determined from measurements of final yield and biomass from the non-stressed treatment (cf. **Section 5.3.5.1**).

Canopy related factors: Since AquaCrop is a canopy-level model (cf. **Section 6.2.1.1**), simulated canopy cover must first be matched to observations. Hence, it is important for AquaCrop to accurately simulate canopy cover development, since it determines the rate of transpiration, which is then used to estimate biomass accumulation, from which crop yield is determined. As shown in **Figure 5-3**, AquaCrop requires seven important parameters that determine the shape of the green canopy development curve.

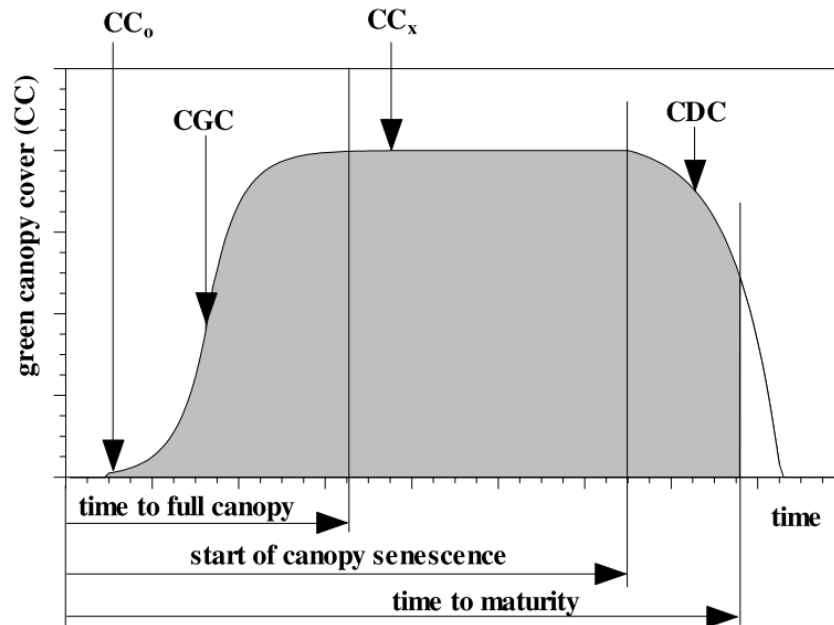


Figure 5-3 Parameters required by AquaCrop to simulate canopy cover development (Raes et al., 2012)

The seedling leaf area (in cm^2 ; line no. 43) is measured at emergence and together with plant density as inputs, is used by the model to compute initial canopy cover (CC_0). CC_0 is generally very small (e.g. $\sim 1\%$), and thus can only be slightly adjusted. Measurements of leaf area index (LAI; cf. **Section 5.3.3.3**) were used to compute diffuse non-intercepted radiation (DIFN), which represents the fraction of sky not obscured by the plant's canopy (LAI-2200, 2010). CC development (in %) was then calculated as $100 \cdot (1 - \text{DIFN})$, as suggested by Mabhaudhi (2012). Alternatively, CC can also be estimated from LAI using the Beer-Lambert equation. The canopy (or light) extinction coefficient was determined by finding the value that produced the smallest root mean square error (RMSE) between CC determined via the DIFN and Beer-Lambert methods.

From the CC curve, maximum canopy cover (CC_x in %; line 50) and the time to reach CC_x was determined as inputs required by AquaCrop. CC_x is typically reached at mid-season and ranges from 75 to 100% based on the crop type and plant density. The model then calculates the canopy growth coefficient (CGC; line 46), which is the percentage increase in CC per day or degree day) from inputs of CC_0 , CC_x and the time taken to reach CC_x (in calendar days). CGC is a conservative parameter and typically ranges from 0.03 to 0.40 (i.e. 3 to 40%) per day. Hence, this parameter cannot be increased above 0.40. AquaCrop also calculates the canopy decline coefficient (line no. 51) from observations of time to start of canopy senescence and physiological maturity.

Phenological growth stages: The model requires parameter values for certain phenological growth stages as shown in **Table 16-14** (cf. **Section 16.4**), which are observed in calendar days. These values are stored in the crop parameter file from line no. 53 to 57. The parameters related to phenological growth stages can be adjusted by ± 7 days since observations are typically done weekly or bi-weekly. Although flowering in RTCs is linked to photoperiod, it seldom occurs, especially for taro (Mabhaudhi, 2012).

The start of canopy senescence is defined as the time when green leaf area declines as a result of (i) yellowing of leaves (under optimal conditions with no water stress), or (ii) when significant senescence of lower leaves has begun. The time to start of senescence can be based on declining chlorophyll content (cf. **Section 5.3.4.1**). The time to reach maturity, which is closely linked to the time to canopy senescence, occurs when only $\sim 5\%$ of maximum green leaf area remains on the canopy. The

stabilisation of root/tuber growth was used to determine the physiological maturity date (cf. **Section 5.3.3.5**).

Crop determinacy linked with flowering: This important parameter indicates whether crop determinacy is linked with flowering or pod formation (line no. 58). Root and tubers are indeterminant crops, and thus crop determinacy is unlinked with flowering. Hence, the parameter value must be set to 0 to indicate the vegetative growth period stretches from sowing till canopy senescence (**Figure 5-4**). In other words, the canopy continues to develop (i.e. increase in plant height) after flowering has occurred.

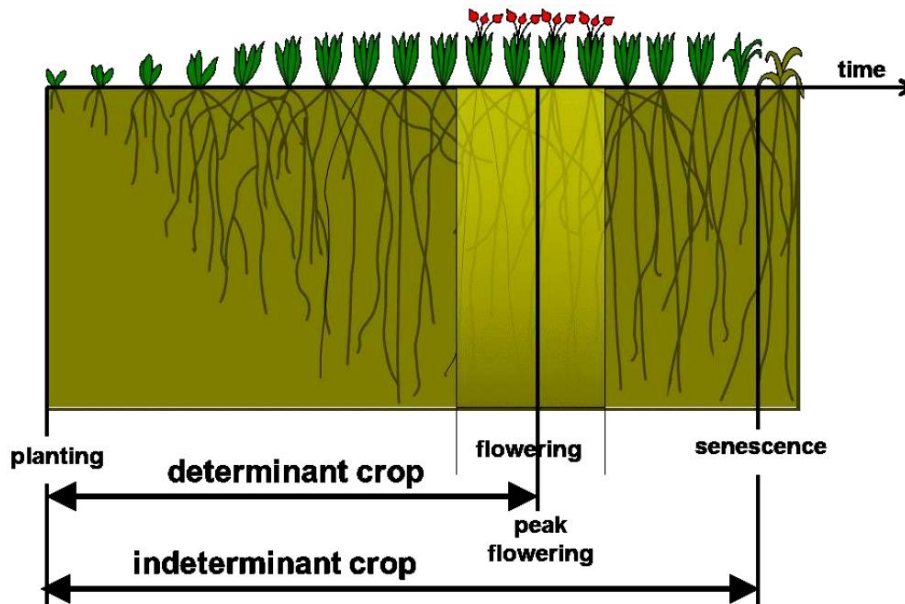


Figure 5-4 Period of potential vegetative growth for determinant and indeterminant crops (Raes, 2016a)

Root expansion: The model requires the minimum ($Z_{r_{min}}$; line no. 37) and maximum ($Z_{r_{max}}$; line no. 38) rooting depths, as well as the time required to reach $Z_{r_{max}}$ as inputs, which are then used to calculate the (i) root expansion rate (in cm day^{-1}), including the daily maximum root water extraction rate (m^3 of soil water per m^3 of soil) in the (ii) top, and (iii) bottom quarter of the root zone.

Conversion to growing degree-days: Running AquaCrop in growing degree-day (GDD) mode and not calendar day (CD) mode produces more reliable yield estimates, especially in cooler (i.e. higher altitude) areas. In GDD mode, the influence of cold temperature stress on phenology and canopy expansion are accounted for. For example, the model inhibits the conversion of transpiration into biomass at low temperatures (Steduto et al., 2012). Kunz et al. (2015a) noted that AquaCrop runs much slower in GDD compared to CD mode, considering a simulation of 49 consecutive seasons for soybean took 55.1 vs 1.2 seconds to complete.

Once the fine-tuning of certain parameter values is complete, parameter values related to phenological growth stages should be converted from CDs to GDDs, i.e. thermal time (**Table 16-14** in **Section 16.4**). These values in GDDs are stored in the crop parameter file on lines 69 to 74. This step is normally done in the model, which also converts the CGC and CDC parameters to represent the fraction of canopy cover growth and decline per degree-day (line no. 75 and 76). AquaCrop uses "Method 3" to calculate thermal time, which was adapted from "Method 2" developed McMaster and Wilhem (1997). The model does not adjust the minimum temperature when it drops below the base temperature, which is believed to better represent the damaging or inhibitory effects of cold temperatures on plant processes (Steduto et al., 2012), Growing degree-days (GDD) are calculated in AquaCrop as follows:

1. If the minimum air temperature (T_{MIN}) exceeds T_{UPP} , it is adjusted to T_{UPP} .
2. The maximum air temperature (T_{MAX}) is adjusted to fall in the range T_{BSE} to T_{UPP} .
3. T_{AVE} is then calculated from the adjusted T_{MAX} and T_{MIN} values and cannot be below T_{BSE} .
4. GDD are calculated as $T_{AVE} - T_{BSE}$ and accumulated over the growing period.

5.2.6.5 Model evaluation

Evaluation of model performance provides a quantitative estimate of the model's ability to reproduce an observed variable or to assess the impact of partially or fully calibrating the model (Krause et al., 2005). Several statistical indicators are used to evaluate model performance, each with its own strengths and weaknesses. Hence, an ensemble of different indicators should be used to sufficiently assess model performance (Willmott, 1984).

The deviation percentage (also known as the percentage error) was used to measure how well the model performed in predicting final biomass and yield. This statistic is defined as $100 \cdot (\text{simulated} - \text{measured}) / \text{measured}$ (Hsiao et al., 2009). According to Dua et al. (2014), deviations within $\pm 6\%$ are considered negligible. For the assessment of canopy cover simulation, the following four statistics were used: (i) normalised root mean square error, (ii) Nash-Sutcliffe efficiency coefficient, (iii) Willmott's index of agreement, and (iv) the coefficient of determination. Each statistic is discussed next in more detail.

Normalised root mean square error (NRMSE)

RMSE calculates the average magnitude of the squared residual errors, with values ranging from 0 (excellent) to positive infinity (poor). This statistical indicator does not distinguish between over- or under-estimation. Analysis of the residual error (i.e. the difference between model predictions and observations) can be used to detect systematic error (Moriassi et al., 2007). Since RMSE can be large depending on the units of the variable, NSE is often given with RMSE (Zhong and Dutta, 2015). Hence, a preferred statistic is the normalised root mean square error (or NRMSE), where RMSE is divided by the mean of observed values and expressed as a percentage. A simulation is considered excellent if NRMSE is smaller than 10%, and poor if larger than 30% (**Table 5-2**). NRMSE is easier to interpret as the range (and units) is always 0-100%.

Nash-Sutcliffe efficiency (NSE) coefficient

The NSE coefficient compares the relative magnitude of the residual variance [i.e. $(P - O)^2$] to the variance of the observations, i.e. $(O - \bar{O})^2$ (Nash and Sutcliffe, 1970). NSE indicates how well the plot of observed versus simulated data fits the 1:1 line (Moriassi et al., 2007), with a value of 1 indicating a perfect match between predictions and observations (**Table 5-2**). As NSE approaches zero, model predictions are as accurate as the observed data average (\bar{O}), whereas negative values indicate model predictions are worse than \bar{O} . Hence, NSE can be used to assess and quantitatively describe the accuracy between observed and simulated model outputs.

Willmott's index of agreement (D-I)

D-I was developed by Willmott (1981; 1982; 1984) and is a commonly used statistic to assess agreement between observed and predicted data. The value ranges between 0 (complete disagreement) and 1 (complete agreement) (**Table 5-2**). It represents the ratio of the sum of squared residual errors to the "potential error". The latter is defined as the sum of the squared absolute values of the differences between predicted values and the mean observed value and differences between the observed values to the mean observed value (Willmott, 1984).

Since D-I squares the residual variance between predicted (P) and observed (O) values [i.e. $(P - O)^2$], it is overly sensitive to extreme values or outliers (Moriassi et al., 2007). This is also true for NSE and RMSE. Furthermore, none of these three statistics (including R^2) can differentiate between over- and

under-estimation. For example, a model that systematically under- or over-estimates the observations can still have good statistical measures (Krause et al., 2005).

Coefficient of determination (R^2)

R^2 is defined as the square of the Pearson correlation coefficient (r). When the trend is linear, it indicates the proportion of variation in measured data that is explained by the model (Moriassi et al., 2007). Values range from 0 (poor) to 1 (excellent) and values above 0.5 are typically considered acceptable (Table 5-2). However, this statistical indicator can be misleading, since models can exhibit high R^2 values, yet consistently over- or under-estimate when compared to observations (Krause et al., 2005). The accuracy of the R^2 statistic is also sensitive to the sample size (n), i.e. small samples can exhibit high R^2 values (Mabhaudhi et al., 2014a). Hence, the sample size should also be given to help with the interpretation of each statistical measure. This highlights the importance of including other statistical indicators to test model robustness.

Table 5-2 Interpretation of commonly used statistical indicators of model performance (FAO, 2015)

Interpretation	NRMSE (%)	NSE	D-I	R^2	r
Very good	≤ 5	0.80 to 1.00	0.90-1.00	0.81-1.00	0.90-1.00
Good	6-15	0.60 to 0.79	0.80-0.89	0.64-0.80	0.80-0.89
Moderately good	16-25	0.40 to 0.59	0.65-0.79	0.49-0.63	0.70-0.79
Moderately poor	26-35	0.00 to 0.39	0.50-0.64	0.25-0.48	0.50-0.69
Poor	36-45	-10.00 to 0.00	0.25-0.49	0.00-0.24	0.00-0.49
Very poor	> 46	< -10.00	0.00-0.25		< 0.00

5.3 RESULTS AND DISCUSSION

5.3.1 Climate data

Climate measurements began on 13 October 2022 and the crop was planted on 27 October. Since taro was harvested on 04 June 2023, data is shown for the 220-day growing period. The monthly averages shown in Table 5-3 reflect growing conditions in the greenhouse where temperatures and relative humidity are typically elevated when compared to outside conditions. Wind speed was determined by the temperature-controlled extraction fans, and thus remained fairly constant. Solar radiation was lower than outside measurements was due to the opaque plastic roofing.

Table 5-3 Monthly means/totals of climate variables measured by the AWS located inside the greenhouse at UKZN

Month	CWR (mm)		R_s	T_{MAX}	T_{MIN}	RH_{MAX}	RH_{MIN}	u_2	ET_o
	100%	30%	($MJ\ m^{-2}\ d^{-1}$)	($^{\circ}C$)	($^{\circ}C$)	(%)	(%)	($m\ s^{-1}$)	(mm)
Nov 2022	19	8	8.80	32.0	17.4	90.92	39.92	0.14	2.2
Dec 2022	35	12	7.57	34.8	19.6	90.10	43.28	0.18	2.0
Jan 2023	68	25	10.32	40.5	20.6	87.29	32.94	0.20	2.7
Feb 2023	43	16	5.70	33.2	21.6	88.53	45.59	0.18	1.5
Mar 2023	77	30	9.05	37.1	20.8	88.20	37.73	0.20	2.2
Apr 2023	62	26	8.00	34.0	16.5	86.50	30.05	0.21	1.8
May 2023	43	18	5.28	31.7	14.3	90.11	34.29	0.23	1.3

From the above table, the hottest conditions were experienced in January 2023 but does not reflect the daily variation, especially in maximum temperatures. The latter peaked at $58.8^{\circ}C$ on 14 January 2023, followed by $58.1^{\circ}C$ and $56.0^{\circ}C$ on 20 and 17 January, respectively. In total, T_{MAX} exceeded $35^{\circ}C$ on 86 of the 220 days (Figure 5-5). These extreme temperatures occurred when the two extraction fans stopped working due to stage 6 load shedding. T_{MIN} peaked at $25.6^{\circ}C$ on 11 January 2023, and

gradually declined to 7°C on 27 May 2023. Minimum relative humidity is typically lowest on extremely hot days, with the lowest value (8.90%) recorded during the period of 12 to 16 January 2023 when T_{MAX} exceeded 50°C (**Figure 5-6**). RH_{MAX} remained relatively constant and peaked at 100% on 29 May 2023. Average daily wind speed was recorded using a DS-2 sonic anemometer, which was affected by load shedding events that caused the two extraction fans to stop working (**Figure 5-7**). The maximum value of 0.31 m s^{-1} occurred on 17 January 2023 when T_{MAX} reached 56.0 °C, and never dropped below 0.10 m s^{-1} . Although incoming solar radiation (R_s) peaked at 15.59 MJ m^{-2} on 09 January 2023 (**Figure 5-10**), this did not result in the highest ET_o value of 4.3 mm, which occurred on 14 January when T_{MAX} and RH_{MIN} was the highest and lowest, respectively. R_s was zero MJ m^{-2} on 12 December 2022, when T_{MAX} and T_{MIN} in the greenhouse were 21.8 and 21.5°C, respectively. This indicated cloudy conditions, which was confirmed when the same instrument (CMP3 pyranometer) recorded 6.11 MJ m^{-2} outside the greenhouse and T_{MAX} and T_{MIN} varied by only 5.2°C. **Figure 5-8** shows that ET_o is largely driven by R_s , which is confirmed in **Figure 5-9** since R_s explained 93.9% of the variation in ET_o , particularly for $ET_o < 1.5 \text{ mm}$. This highlights an important finding that for irrigation scheduling in greenhouses, R_s measurements are essential for accurate ET_o estimation.

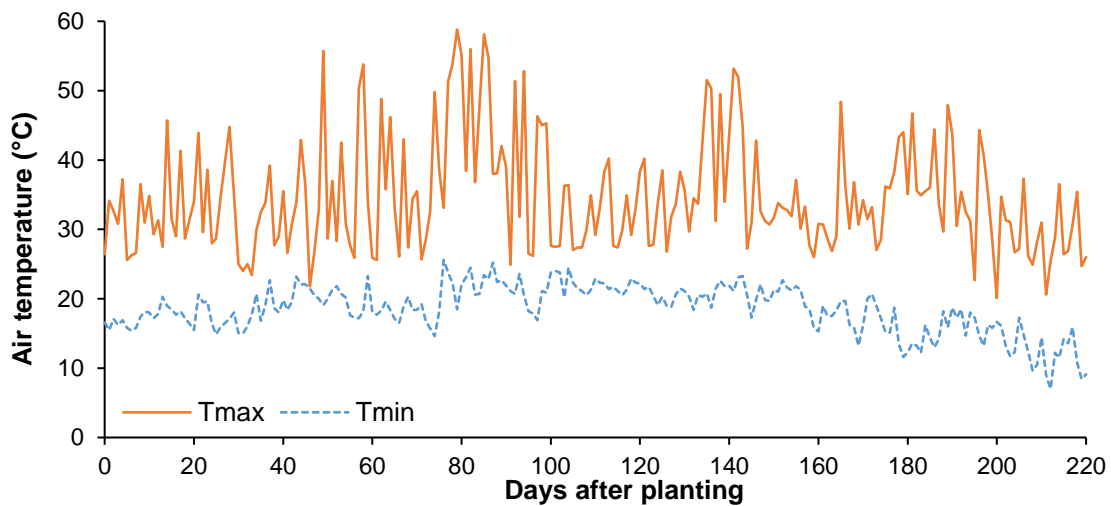


Figure 5-5 Variation in temperature (maximum & minimum) measured inside the greenhouse over the 220-day growing period in season 3

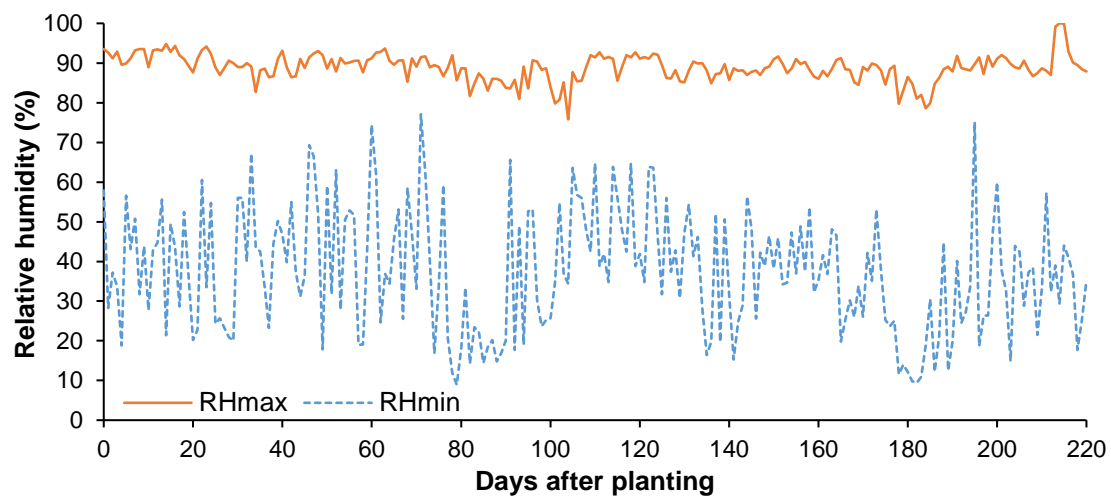


Figure 5-6 Variation in relative humidity (maximum & minimum) measured inside the greenhouse over the 220-day growing period in season 3

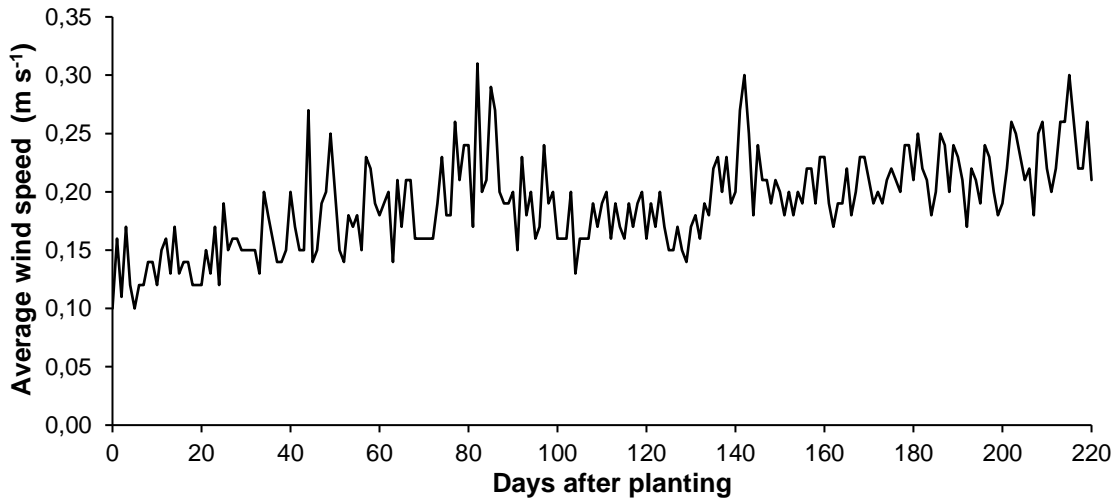


Figure 5-7 Variation in average wind speed measured inside the greenhouse over the 220-day growing period in season 3

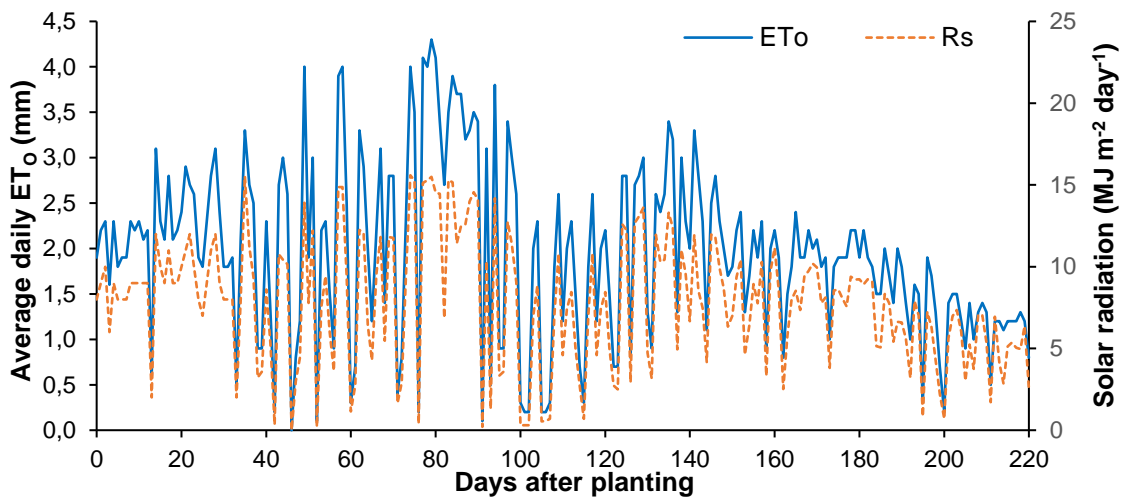


Figure 5-8 Variation in average daily ET_0 and incoming solar radiation measured inside the greenhouse over the 220-day growing period in season 3

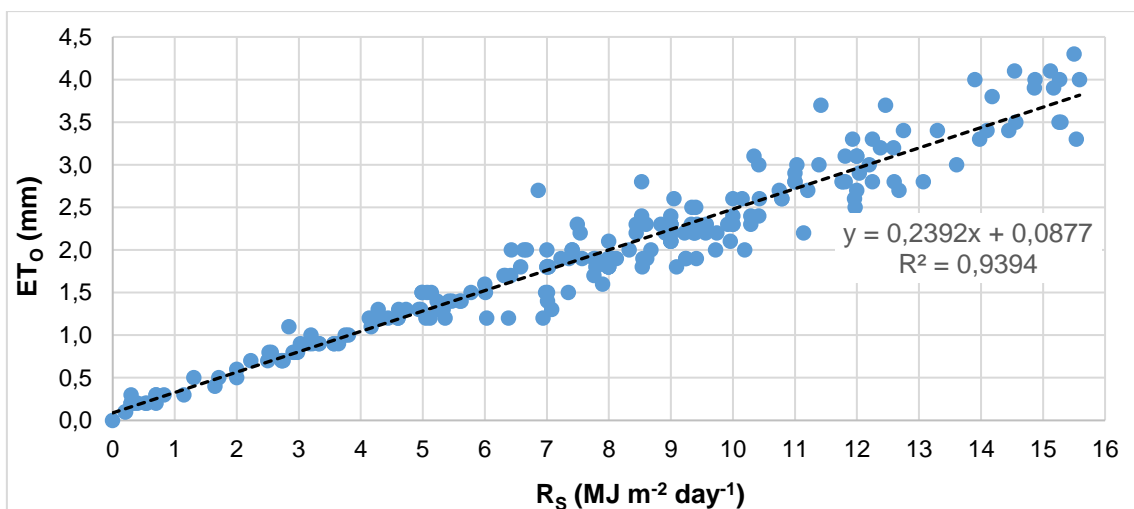


Figure 5-9 Variation in reference evaporation (ET_0) explained by incoming solar radiation (R_s) measured inside the greenhouse for season 3

As mentioned previously, crop growth in the greenhouse was affected by extreme temperatures recorded during frequent two-hour load shedding events (stage 5+) when the exhaust fans stop working (i.e. no generator backup). Extreme air temperatures were first experienced during the December 2022 period as shown in **Figure 5-10**, which highlights seven events where temperatures exceeded 40°C. Temperatures ranging from 40 to 55°C were typically recorded between 10 am and 2 pm (cf. **Figure 5-11**) when load shedding coincided with very hot conditions (i.e. outside air temperatures > 30°C).

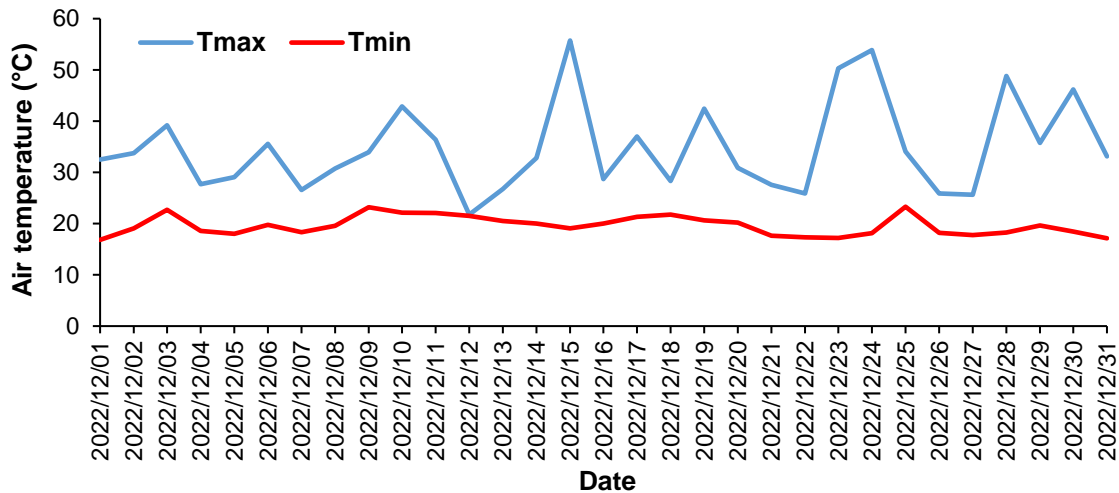


Figure 5-10 Daily air temperature measured inside a greenhouse during December 2022

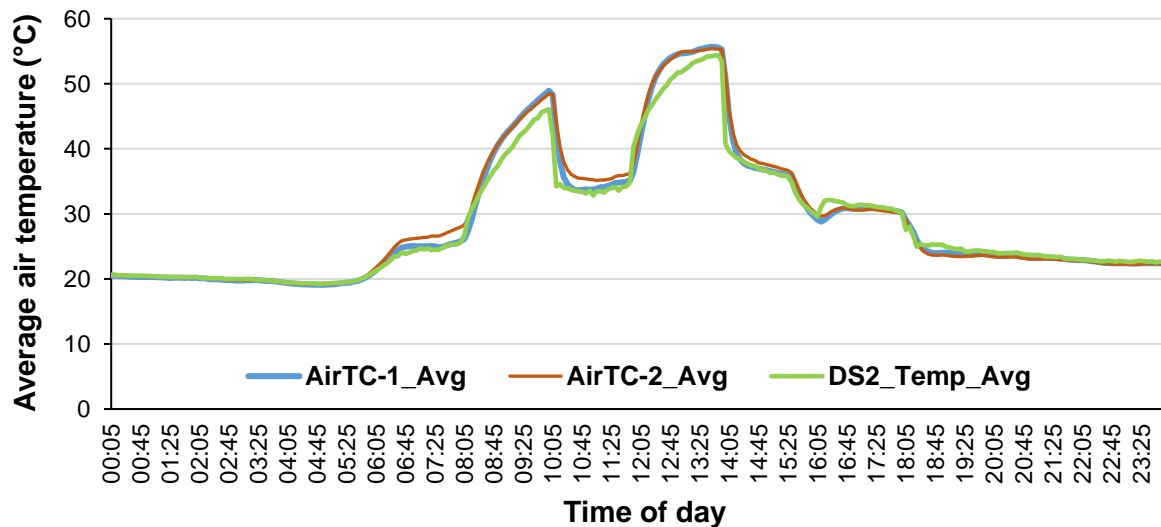


Figure 5-11 Half-hourly temperatures recorded on 15 December 2022 by three sensors inside a greenhouse at UKZN, where temperatures peaked during two load shedding events

The high temperatures experienced over most of the growing season resulted in severe leaf turgor loss for sweet potato (**Figure 5-12b**) and leaf curling for taro, i.e. leaf edges curl/roll inwards and die off to reduce leaf area and transpiration loss (**Figure 5-13b**). To prevent crop loss during the extreme conditions, attempts to spray the greenhouse roof with cold water made no difference to inside temperatures. Despite the extreme temperatures experienced over the growing season, both crops survived, which indicates their tolerance to heat stress. From observations, both sweet potato and taro tolerate temperatures up to 35°C, which therefore explains the physiological responses observed in **Figure 5-12** and **Figure 5-13** due to the extreme conditions (> 40°C).



Figure 5-12 (a) Healthy vs (b) heat-stressed leaves of OFSP during the 2022/23 season



Figure 5-13 (a) Healthy vs (b) heat-stressed leaves of taro during the 2022/23 season

Due to a municipal transformer fault that occurred on 07 March at 2 pm, which coincided with a UKZN generator failure, the Agric campus experienced both load reduction and load shedding up to 10 March 2023. Although the generator was repaired on 09 March, it kept overheating and shutting down. The following day (Friday), additional air vents were installed in the side of the generator to improve cooling. This was important considering load reduction occurred from 6:00 am to 11:30 am on Friday. The transformer was finally repair in the late evening. The power outages are clearly evident in **Figure 5-2** (cf. **Section 5.2.5.1**), which shows 10 extreme temperature conditions ($> 40^{\circ}\text{C}$) that occurred from 01 to 10 March.

5.3.2 Soil properties

5.3.2.1 Soil fertility

The laboratory results for soil fertility show high concentrations of macro- (i.e. P and K) and micro-nutrients (Ca and Mg) but low concentrations of nitrogen in the beds (**Table 5-4**). Hence, nitrogen fertiliser was added to the four beds. The range in pH values was favourable for both OFSP and taro cultivation, negating the need to add lime to the soil.

Table 5-4 Soil fertility results for topsoil samples from each of the four greenhouse beds

Treatment	N	Org. C	pH	Ca	P	K	Mg	Na
	%		KCL	mg kg ⁻¹				
1 - Taro - stressed	0.16	2.34	5.53	2,009.89	458.40	216.51	179.21	52.36
2 - OFSP - stressed	0.19	2.77	5.66	2,229.82	687.34	242.07	179.41	46.15
3 - Taro - unstressed	0.19	2.96	6.21	2,534.81	618.74	213.38	205.92	55.20
4 - OFSP - unstressed	0.18	2.51	6.15	2,324.78	497.54	237.43	201.01	58.67

5.3.2.2 Soil texture

Results obtained from the ICFR laboratory show that the top 0.15 m is dominated by a clay loam. Soil texture then transitions into a clay over the next 0.25 m (**Table 5-5**). Clay textured soils have higher water holding capacity compared to other soil textures, and thus provided favourable conditions for the cultivation of OFSP and taro.

Table 5-5 Soil particle size distribution and textural classes for the four beds at soil depths of 0.15 m and 0.40 m

Treatment	Coarse silt and sand		Fine silt		Clay		Soil textural class	
	0.15	0.40	0.15	0.40	0.15	0.40	0.15	0.40
1 - Taro - stressed	23.66	26.84	36.13	31.50	40.21	41.66	Clay	Clay
2 - OFSP - stressed	44.44	27.71	19.71	31.43	35.86	40.85	Clay Loam	Clay
3 - Taro - unstressed	36.83	22.82	26.21	38.74	36.96	38.44	Clay Loam	Clay Loam
4 - OFSP - unstressed	40.48	21.15	21.51	38.61	38.00	40.25	Clay Loam	Clay

5.3.2.3 Soil water retention

Soil water retention parameters such as saturation (SAT), field capacity (FC) and permanent wilting point (PWP), were determined from undisturbed cores taken at 0.30 m in each bed (**Table 5-6**). The values correlate well with the soil texture results shown in **Table 5-5**, since high clay content in the four beds results in higher soil water retention and dry bulk density. The latter values showed no evidence of soil compaction as expected. Estimates of saturation from dry bulk density agreed favourably with measured values as shown in the table below.

Table 5-6 Estimation of soil water retention results using the outflow pressure method

Treatment	Dry bulk density	Soil water retention					K _{SAT}
		SAT		FC		PWP	
	g cm ⁻³	Est.	0 kPa	10 kPa	33 kPa	1,500 kPa	mm day ⁻¹
1 - Taro - stressed	1.36	49	48	43	39	30	60.9
2 - OFSP - stressed	1.60	40	39	37	34	28	69.1
3 - Taro - unstressed	1.49	44	44	41	38	29	82.2
4 - OFSP - unstressed	1.52	43	43	40	37	30	70.1

Bulk density, soil water retention (SAT, FC & PWP) and saturated hydraulic conductivity (K_{SAT}) were also calculated using the SPAW utility (Saxton and Willey, 2009) as shown in **Table 5-7**. SPAW required the particle size distribution (cf. **Table 5-5**) and organic matter content. The latter input was derived by multiplying the topsoil's organic carbon content (cf. **Table 5-4**) by a factor of 1.724 (Howard, 1965). Estimated values for each bed were depth-weighted. A comparison of the results in **Table 5-6** and

Table 5-7 showed that SPAW under-estimated dry bulk density and PWP, yet over-estimated SAT and K_{SAT} . This highlights the importance of measuring these values, especially when they are needed for the calibration and/or validation of crop simulation models, as was noted in **Section 4.3.2.3**.

Table 5-7 Calculation of soil bulk density, soil water retention and soil hydraulic conductivity for the soil in each greenhouse bed using the SPAW utility

Treatment	Dry bulk density	Soil water retention			K_{SAT}
		SAT	FC	PWP	
	$g\ cm^{-3}$	0 kPa	33 kPa	1,500 kPa	$mm\ day^{-1}$
1 - Taro - stressed	1.30	51	39	25	99.3
2 - OFSP - stressed	1.32	50	38	25	111.6
3 - Taro - unstressed	1.27	52	38	24	162.5
4 - OFSP - unstressed	1.30	51	38	25	117.8

5.3.3 Crop development

5.3.3.1 Plant height

Plant height measured for OFSP and taro for both water treatments (i.e. 30% and 100% of CWR) is shown in **Figure 5-14**. As expected, plant heights for the unstressed water treatment for both crops are higher than the stressed treatment. The difference in plant height between the two treatments is more pronounced for taro when compared to OFSP. Optimum water conditions therefore result in a faster growth rate. In general, taro stems and leaves grow much taller than OFSP vines since vines branch out horizontally rather than vertically.

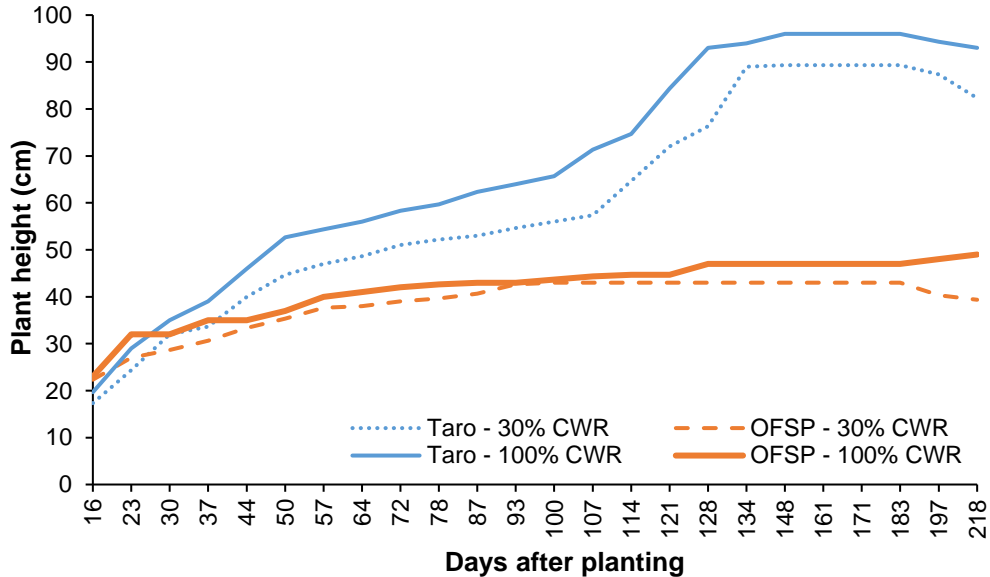


Figure 5-14 Measured plant height for OFSP and taro for both water treatments, i.e. 30% and 100% of crop water requirement (CWR)

5.3.3.2 Leaf number

Leaf number measured for OFSP and taro for both water treatments is shown in **Figure 5-15**. For the unstressed treatment, taro and sweet potato produced more leaves compared to the stressed treatment. The difference in leaf number due to water treatment is more pronounced for OFSP than taro. Nitrogen forms an essential nutrient in the promotion of leaf development and chlorophyll content.

However, this benefit is lost if the plants are water stressed. Since OFSP has far more leaves than taro, this will increase the leaf area index and transpiration rate, which in turn, should translate to higher biomass accumulation and root/tuber yield.

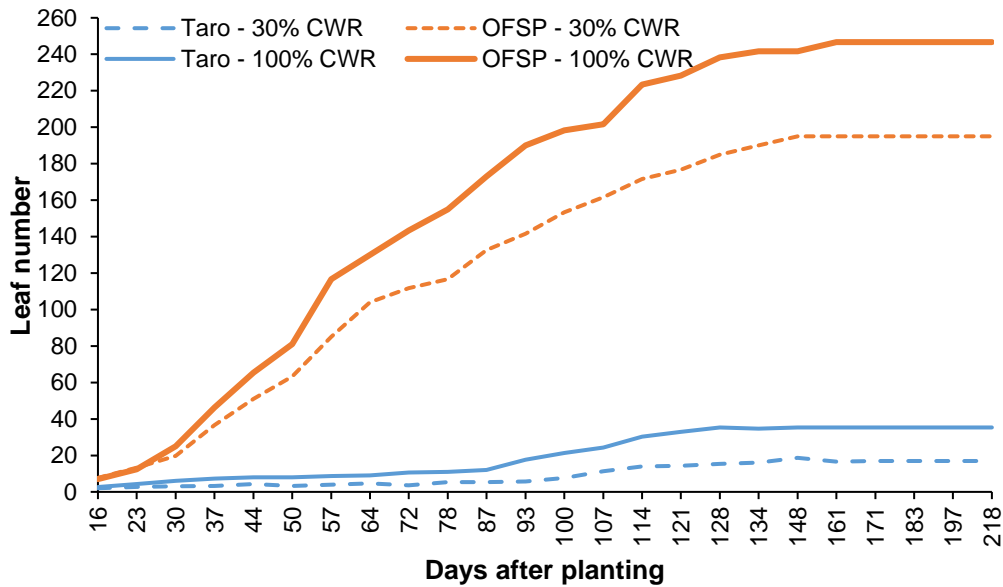


Figure 5-15 Measured leaf number for sweet potato and taro for both water treatments (i.e. 30% and 100% of CWR)

5.3.3.3 Leaf area index

When compared to OFSP, taro has much larger leaves but far fewer in number. Hence, due to the higher number of OFSP leaves compared to taro (**Figure 5-15**), OFSP will have a larger surface area for sunlight absorption and transpiration. This should result in higher photosynthetic rates and increased growth of OFSP compared to taro. As expected, leaf area index (LAI) is higher for OFSP than taro (**Figure 5-16**) and is highest for the unstressed treatment. Since LAI is higher for OFSP than taro, more of the ground area is shaded, which reduces solar radiation reaching the soil surface and results in lower soil temperature and soil water evaporation. Taro also has a longer growing season, and thus a slower growth rate, which means less surface shading and higher soil water evaporation rates (especially after establishment). For OFSP, the initial gain in LAI for the unstressed treatment was lost from at 87 DAP. This suggests that under water limiting conditions, sweet potato can still produce high leaf area, which is important for reducing soil water evaporation.

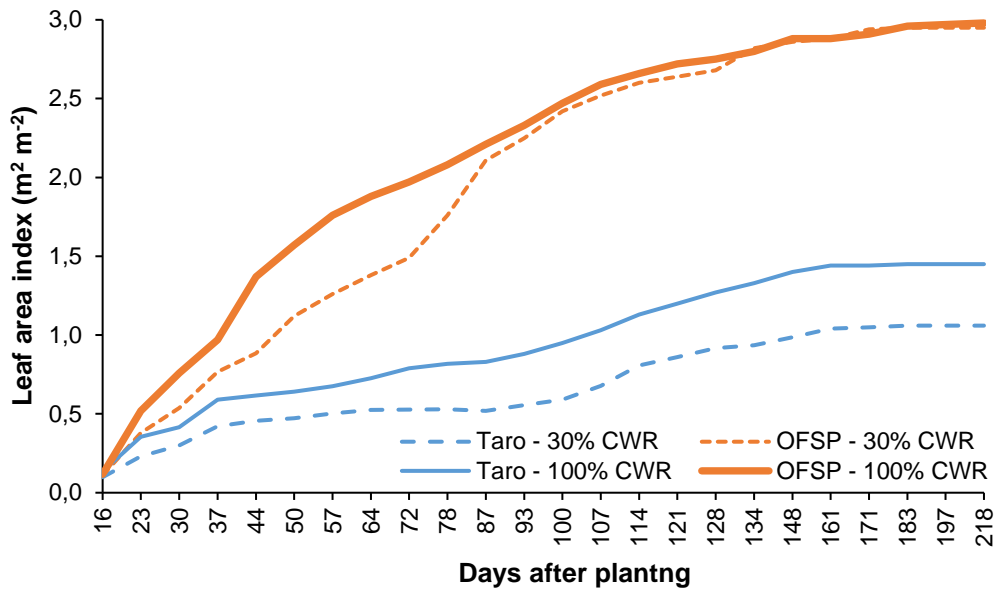


Figure 5-16 Measured leaf area index for OFSP and taro for both water treatments (30% and 100% of CWR)

5.3.3.4 Canopy cover

It is important to note that canopy cover (CC; **Figure 5-17**) is derived from LAI (cf. **Figure 5-16**) and thus, the two variables are directly proportional to one another. Hence, they follow similar trends with low values at planting, which peaked during the vegetative and tuber initiation stages for both treatments. The higher production of leaves and shorter growing season for OFSP resulted a higher canopy closure compared to taro. This is important with respect to crop ET since less unproductive water loss through soil water evaporation results in more water availability for crop development.

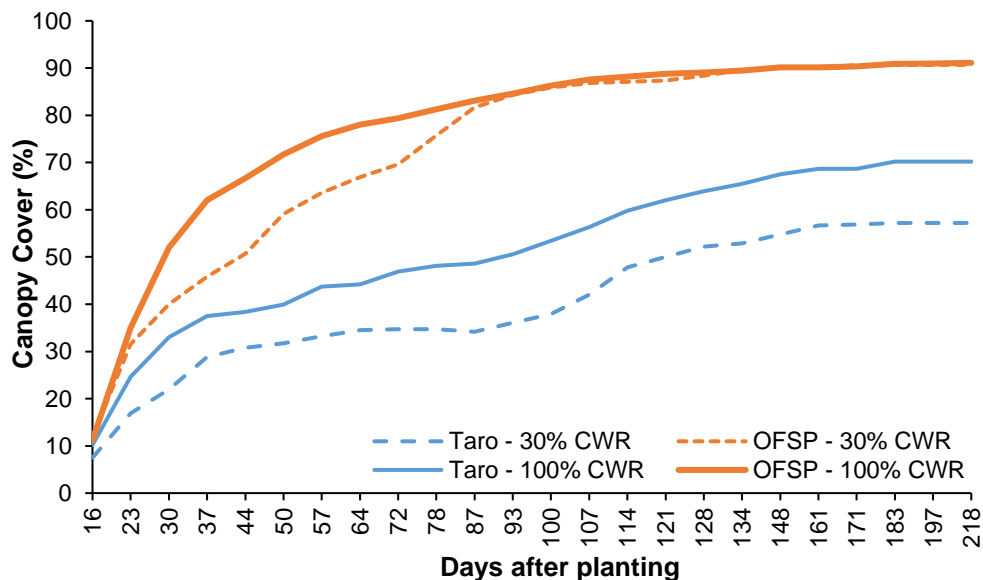


Figure 5-17 Estimated canopy cover for OFSP and taro for water both treatments (i.e. 30% and 100% of CWR)

5.3.3.5 Biomass accumulation

As expected, total fresh biomass production was lower for the stressed treatment (**Figure 5-18**) compared to the unstressed treatment (**Figure 5-19**) for OFSP and showed no signs of senescence. Root/tuber formation began after 65 DAP for both treatments and continued to grow until the crop was harvested. According to the literature, sweet potato has three distinct growth phases characterised by an (i) initial phase of rapid growth of adventitious roots (but slow vine growth), an (ii) intermediate phase of rapid vine growth, including leaf area increase and storage root initiation, and (iii) a final stage of storage root bulking (but no vine growth). This growth pattern is not apparent from the curves shown in the figures below. Furthermore, the translocation of photosynthates from leaves/vines to the storage roots as the crop approaches maturity is also not clear.

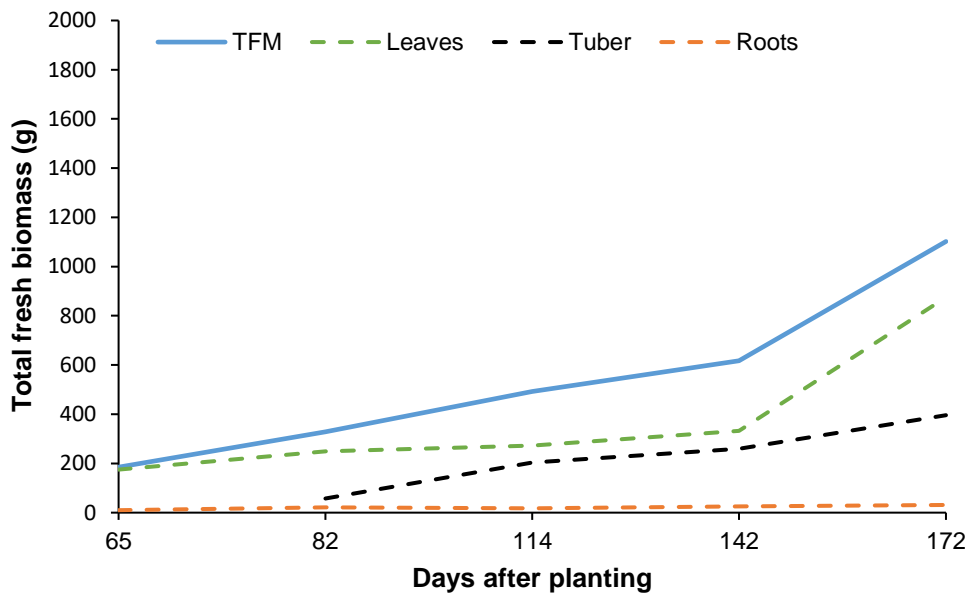


Figure 5-18 Total fresh biomass accumulation for OFSP (30% of CWR)

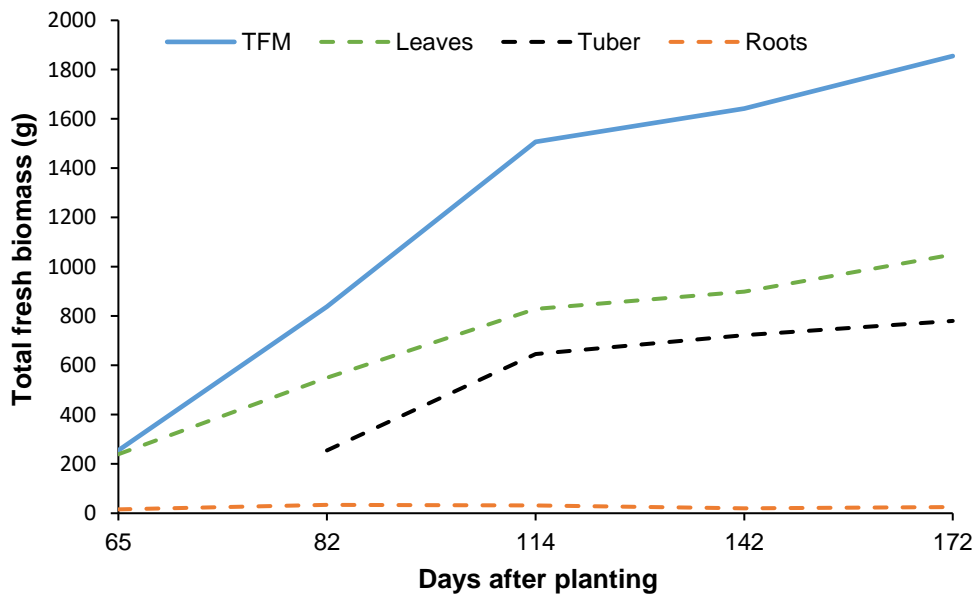


Figure 5-19 Total fresh biomass accumulation for OFSP (100% of CWR)

For taro, the total fresh biomass production peaked at 1,003 g for the stressed treatment ((**Figure 5-20**), compared to 1,266 g for the unstressed treatment (**Figure 5-21**). However, a reduction in biomass production was evident from 142 DAP. More importantly, tuber formation began much later in the season (172 DAP) compared to OFSP and again tubers continued to grow until the crop was harvested. Similar graphs for total dry biomass production are shown in **Section 15**.

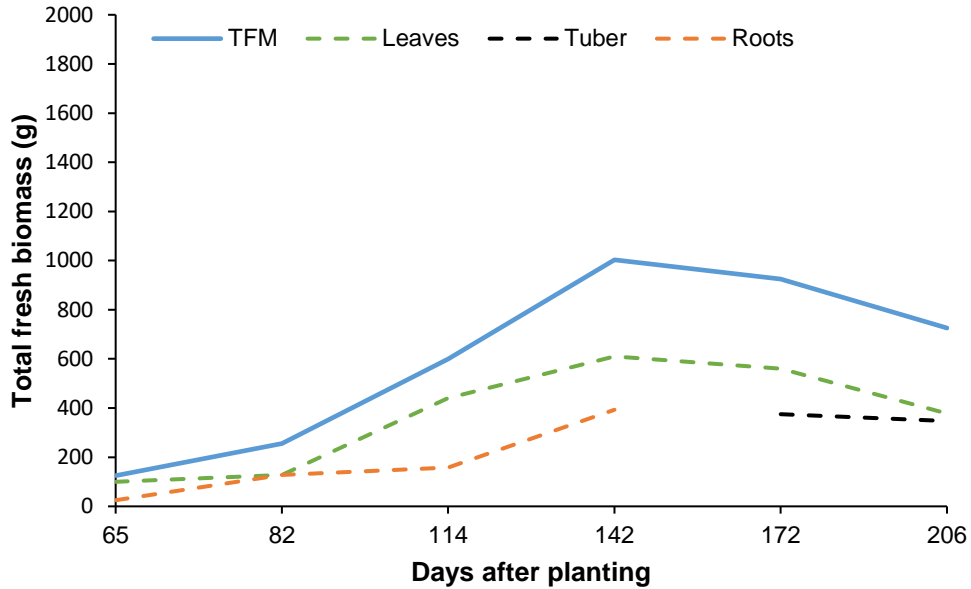


Figure 5-20 Total fresh biomass accumulation for taro (30% of CWR)

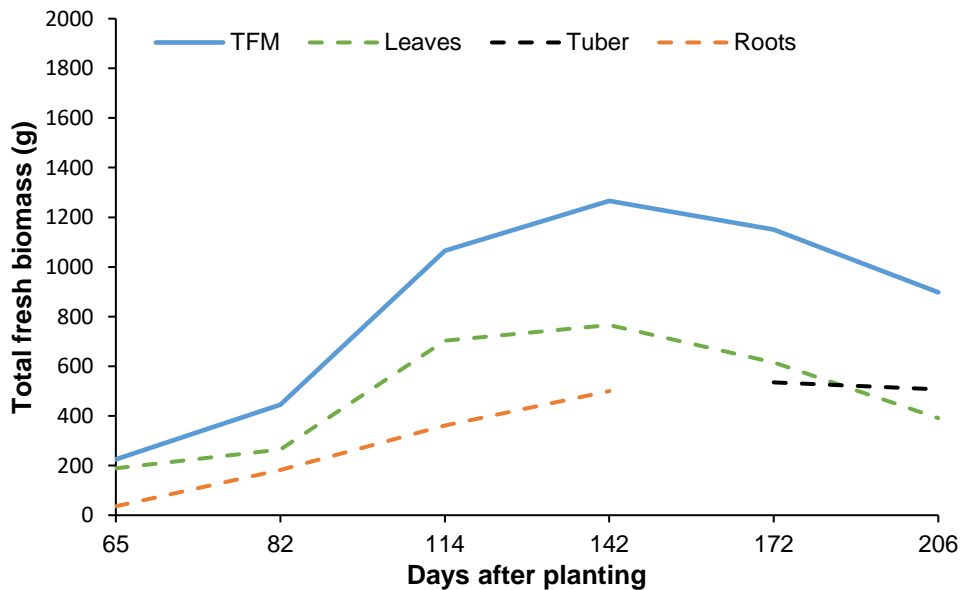


Figure 5-21 Total fresh biomass accumulation for taro (100% of CWR)

5.3.4 Crop health

5.3.4.1 Chlorophyll content index

Chlorophyll content index (CCI) was measured as an indicator of both plant health and its ability to capture photosynthetically active radiation (**Figure 5-22**). When compared to the stressed treatment, CCI was mostly higher for the unstressed treatment for both crops, which suggests healthier crops. CCI was lower for OFSP compared to the taro, which can be due to the rate of consumption of nitrogen

fertiliser applied to the beds. Nitrogen is an important nutrient for promoting leaf development and is a vital component of chlorophyll. OFSP is a vine crop that produces more leaves when compared to taro, and therefore can consume more nitrogen over the growing period. Combined with water limiting conditions, CCI for OFSP should be lower than compared to taro. The fact that taro could maintain chlorophyll content during stressed conditions indicates that its photosynthetic apparatus remained functional even under stressed conditions, which is an attractive adaptive mechanism. Towards the end of the season, CCI of OFSP decreased after 148 DAP, which was not expected due to its “stay-green” trait (Adugna and Tirfessa, 2014; Borrell et al., 2014; Klein and Jordan, 2014). Hence, senescence may have started between 134-148 DAP for both crops.

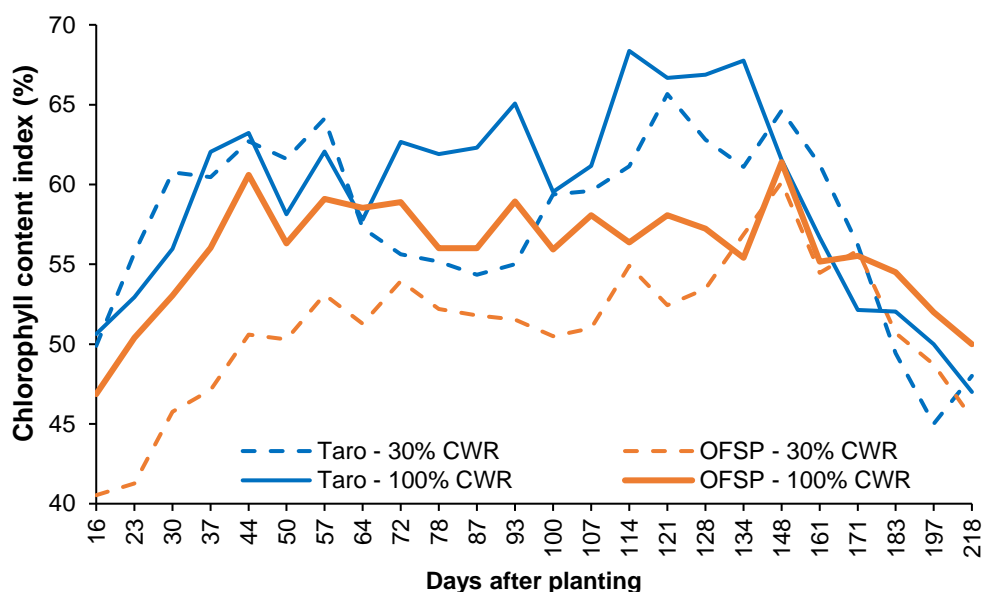


Figure 5-22 Measured chlorophyll content index for OFSP and taro for both water treatments (i.e. 30% and 100% of CWP)

5.3.4.2 Leaf temperature

Leaf temperature is an indicator of how actively a crop transpires during its growing season. The leaf temperature measured for OFSP and taro for both treatments (i.e. 30% and 100% of CWR) are shown in **Figure 5-23**. The leaf temperature for the unstressed treatment should be lower than the unstressed treatment, since actively transpiring leaves should be cooler than the ambient air. Since measurements were mostly taken on a Friday at around noon, the peaks in leaf temperature indicate when measurements coincided with load shedding from 12 pm to 02 pm. In general, OFSP leaves were hotter than taro leaves, but this does not necessarily indicate less transpiration. The highest leaf temperatures for OFSP (both treatments) on day 78 after planting coincided with the hottest T_{MAX} of 58.8°C recorded over the growing season (**Figure 5-5**; cf. **Section 5.3.1**). T_{MAX} exceeded 50°C from 77-80 DAP and 134-136 DAP, thus indicating a stressful environment for the crops.

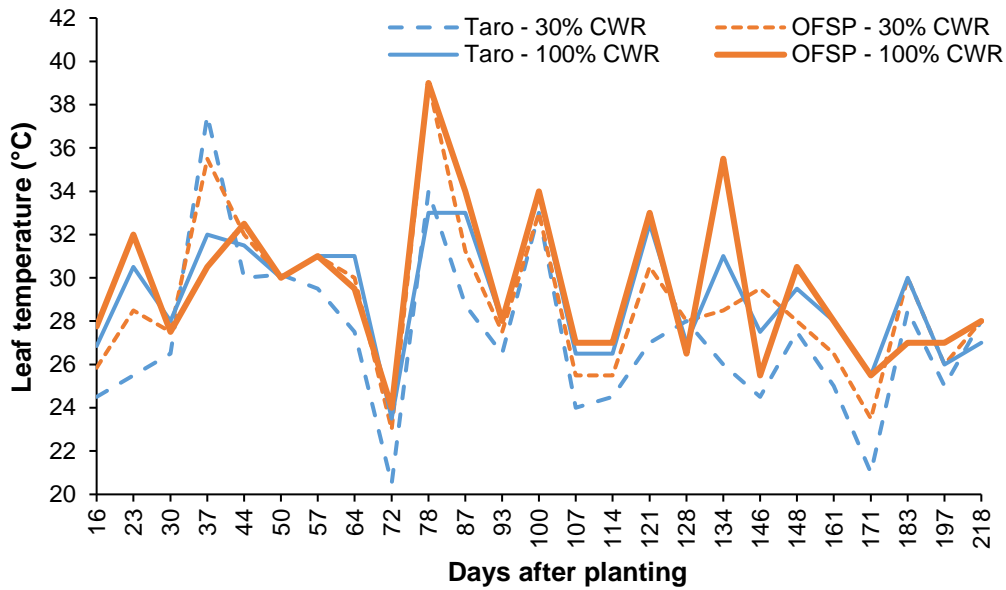


Figure 5-23 Measured leaf temperature for OFSP and taro for both water treatments (i.e. 30% and 100% of CWR)

5.3.4.3 Stomatal conductance

Stomatal conductance also indicates how actively a crop transpires during its growing season and is influenced by climatic conditions as well as other crop growth parameters (e.g. leaf number). An increase in leaf number will increase the number of stomata found on the leaves, thus influencing transpiration rates, which affects biomass accumulation as well as root/tuber yield. The stomatal conductance measured for OFSP and taro for both treatments (i.e. 30% and 100% of CWR) is shown in **Figure 5-24**. As expected for both crops, stomatal conductance is higher for the unstressed water treatment compared to the stressed treatment, especially when leaf temperature was highest (i.e. 78 and 134 DAP). Under both treatments, OFSP has higher stomatal conductance than taro. This is due to the greater leaf number, resulting in a larger surface area for absorption of solar radiation, and thus higher leaf temperature. The larger leaf surface area results in more stomatal openings, and thus higher stomatal conductance and transpiration rates.

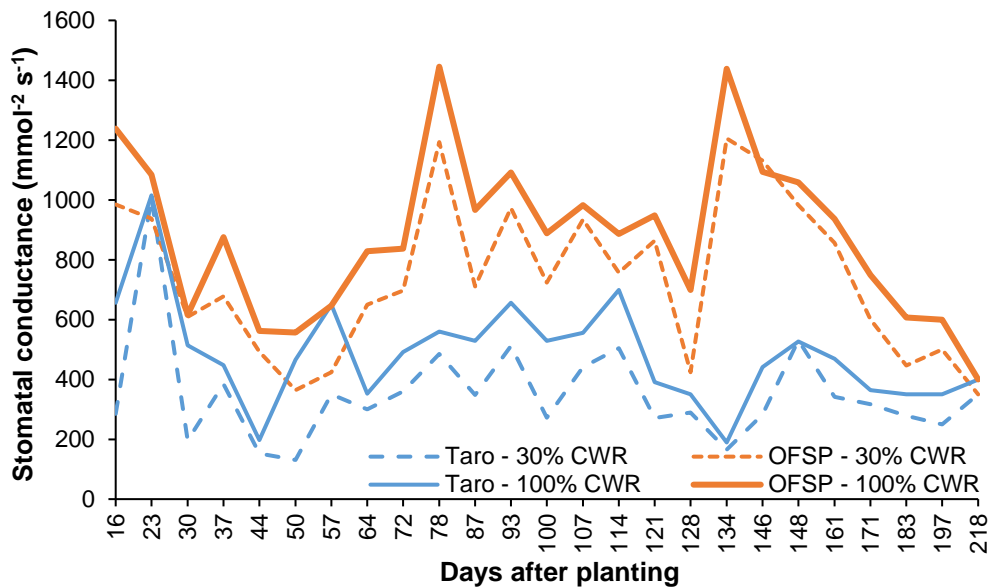


Figure 5-24 Measured stomatal conductance for OFSP and taro for both water treatments (i.e. 30% and 100% of CWR)

As shown in **Figure 5-23** and **Figure 5-24**, there is a direct relationship between leaf temperature and stomatal conductance, where an increase in leaf temperature results in higher stomatal conductance, and thus higher transpiration rates. This is often a result of higher solar radiation absorbed by leaf surfaces (**Figure 5-8**). On day 78 after planting, there is a significant increase in stomatal conductance for OFSP (both treatments) when compared to taro (**Figure 5-24**), which correlates well with higher leaf temperature (**Figure 5-23**), as well as higher solar radiation (**Figure 5-8**) and air temperature (**Figure 5-5**).

5.3.4.4 Diurnal leaf water potential

OFSP: Diurnal leaf water potential of OFSP was measured for both water treatments and indicates the amount of water in the leaves. As transpiration increases, leaf water potential decreases as water is lost from the leaves via the stomatal openings. Leaf water potential was highest before sunrise, then rapidly decreased after 7:00 am, reaching its lowest value at 1 pm (**Figure 5-25**). This was in response to the peak in stomatal conductance (and transpiration) at 11 am, which resulted in the highest rate of water loss from the leaves. At 1 pm, there was less water in leaves of stressed plants compared to unstressed plants, which meant lower transpiration and reduced stomatal conductance. Leaf water potential is therefore highly influenced by weather conditions and thus, increasing air temperature and net irradiance, and decreasing relative humidity (**Figure 5-27**) induce higher transpiration rates, leading to decreasing leaf water potential. From the literature (Ravi et al., 2014; Sunitha et al., 2013), sweet potato leaves wilt permanently at leaf water potentials of -1.3 MPa. However, a lower value of -1.4 MPa was measured at 1 pm.

Stomatal conductance peaked one hour before noon in response to maximum solar radiation, and as expected, was highest for the unstressed treatment (**Figure 5-26**). Reduced stomatal conductance results in closure of stomatal openings, and thus lower transpiration rates and higher leaf water potential. Lower transpiration can result in reduced growth, thus affecting the quantity and quality of biomass and final yield. Leaf water potential is therefore useful as it can be used to indicate plant water stress during the day.

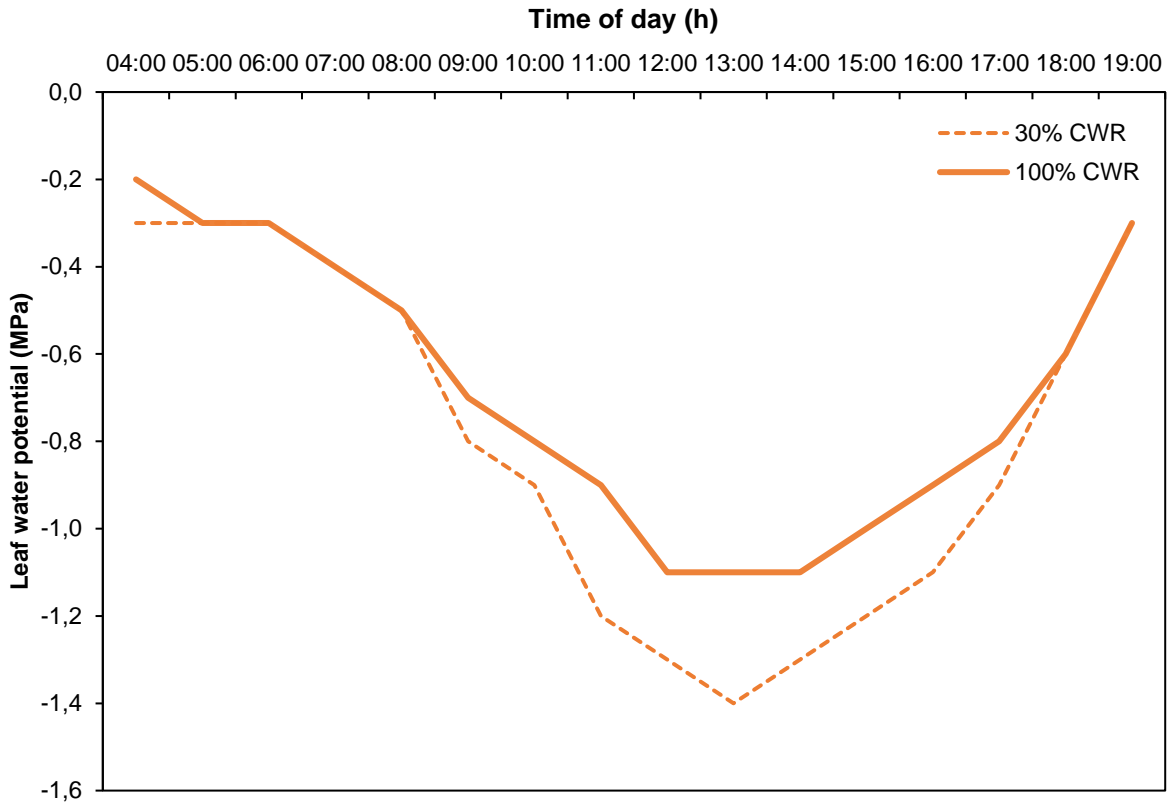


Figure 5-25 Measured diurnal leaf water potential for OFSP for both water treatments (i.e. 30% and 100% CWR)

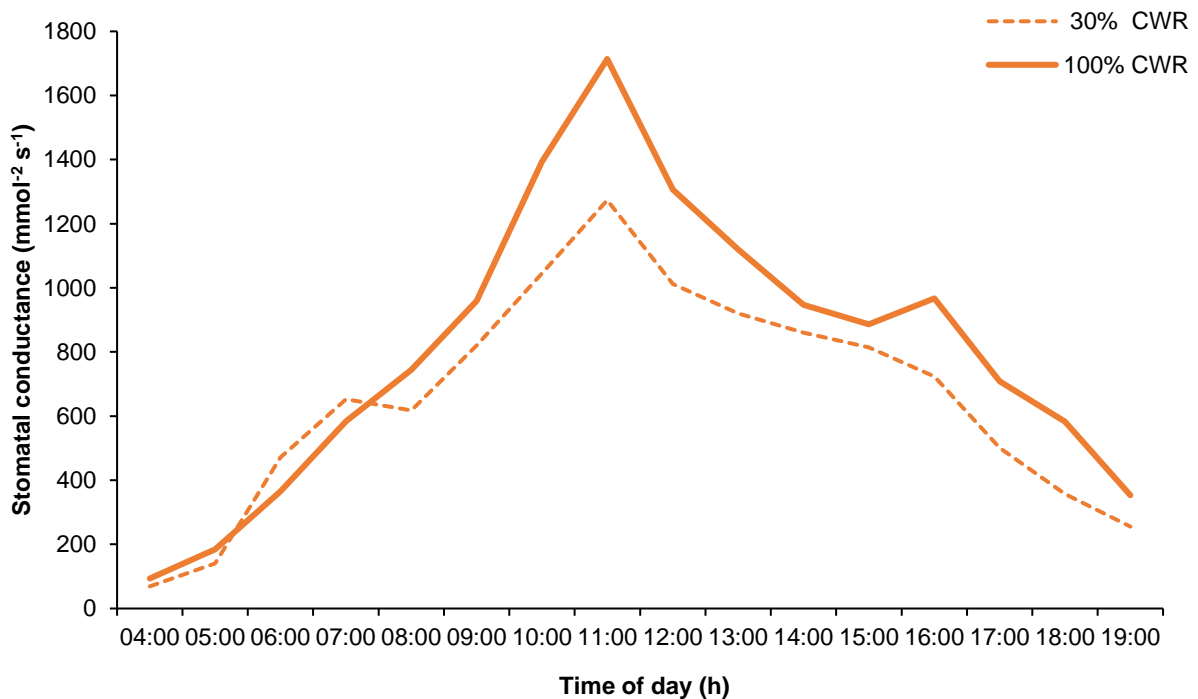


Figure 5-26 Measured stomatal conductance for OFSP for both water treatments (i.e. 30% and 100% of CWR)

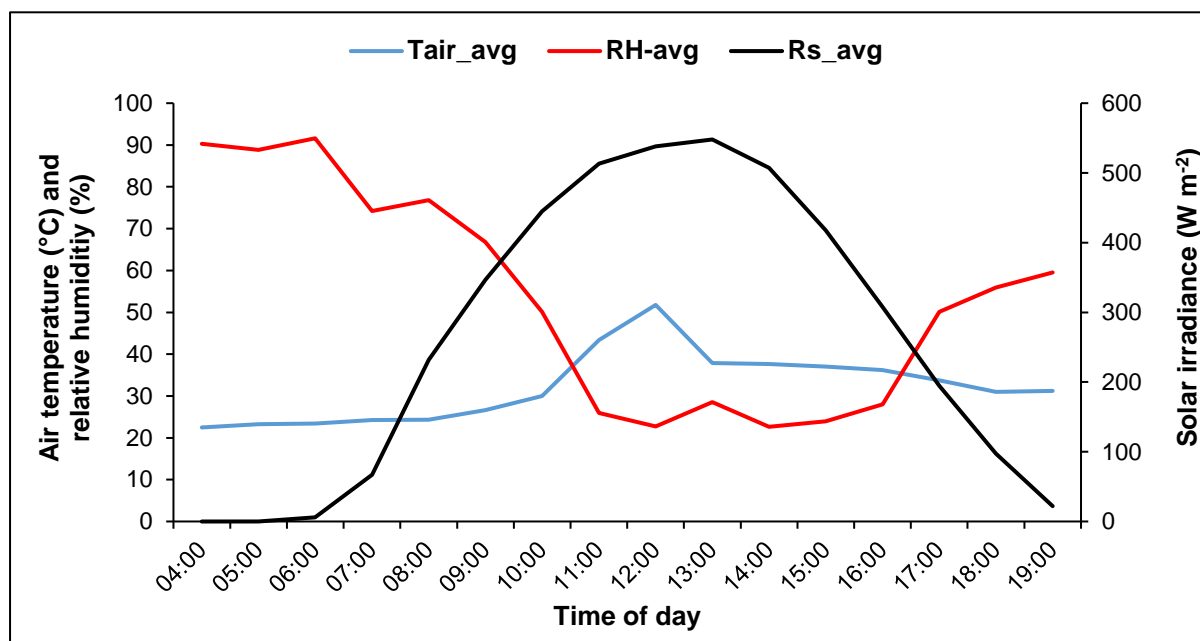


Figure 5-27 Diurnal weather conditions such as average air temperature (T_{air_avg}), average relative humidity (RH_avg) and net irradiance (R_n)

Taro: No measurements were made for taro because the leaves were too thick for the instrument.

5.3.5 Crop growth and yield

5.3.5.1 Final yields and harvest index

For sweet potato, determining the time to reach senescence was difficult since the storage roots continued to grow (**Figure 5-18** & **Figure 5-19**; cf. **Section 5.3.3.5**), especially if conditions are suitable (i.e. no soil water stress) as was the case in the greenhouse. Sweet potato also exhibits delayed leaf senescence when water stressed (i.e. “stay-green” trait). For taro, tillering at the end of the season can reduce the decline in LAI, thus making it harder to determine when senescence has started. For RTCs, dew formation or the first frost typically kills the leaves, thus determining the time to harvest. In addition, when roots/tubers begin to split due to continued growth, farmers typically harvest the crop to halt any further decline in crop quality. Both crops were finally harvested in May and June 2023 as shown in **Table 5-8**.

Table 5-8 Final biomass, yield and harvest index obtained at the end of season 3

Bed - crop - treatment	Harvest date	DAP	Harvest index (%)	Biomass (dry t ha ⁻¹)	Yield (dry t ha ⁻¹)
4 - OFSP - unstressed	2023/05/07	192	78.2	19.354	15.143
2 - OFSP - stressed	2023/05/13	198	72.3	16.948	12.250
3 - Taro - unstressed	2023/06/04	220	80.9	8.144	6.588
1 - Taro - stressed	2023/06/04	220	76.0	5.903	4.505

The maximum rooting depth measured at harvest for each crop and treatment is shown in **Table 5-9**. The unstressed (fully irrigated) treatment should have encouraged shallower roots, which was not the case for both crops. Furthermore, there was no correlation between the rooting depths and the clay contents shown in **Table 5-5** (cf. **Section 5.3.2.2**), except for the fine silt content at 0.40 m.

Table 5-9 Maximum rooting depths for OFSP and taro at the end of season 3

Bed - crop - treatment	Maximum rooting depth (m)
1 - Taro - stressed	0.34
2 - OFSP - stressed	0.35
3 - Taro - unstressed	0.38
4 - OFSP - unstressed	0.39

5.3.6 Nutrient content

The measured β -carotene content of OFSP storage roots is shown in **Table 5-10** and values for the stressed treatment (i.e. 30% of CWR) compare favourably with those obtained from season 2 (**Table 14-1**; cf. **Section 14.1**). In addition, lower β -carotene contents were obtained for the unstressed treatment (i.e. 100% of CWR), which is consistent with findings from other studies (e.g. Mabhaudhi et al., 2019; Nyathi et al., 2019a), as discussed in **Section 3.3.1**.

Table 5-10 β -carotene (β -c) content of OFSP storage roots grown in a greenhouse during the 2022/23 season

Rep	β -c content (g kg ⁻¹)	
	Unstressed	Stressed
1	0.101	0.206
2	0.101	0.205
3	0.101	0.206
Ave	0.101	0.206

The mineral composition of roots/tubers (and leaves) for both OFSP and taro is presented in **Table 14-5** and **Table 14-6** (cf. **Section 14.2**), respectively. K was again the most abundant element in both roots/tubers and leaves for both RTCs. Leaves exhibited higher nutrient contents compared to the roots/tubers for both crops for almost all of the analysed minerals, except for Na (OFSP), K (taro) and P (taro). Taro tubers contained more nutrients for most minerals (except K) when compared to OFSP storage roots. This highlights the dual-purpose nature of OFSP and taro, where both the roots/tubers and leaves are edible and exhibit high nutritional value. Thus, the consumption of both RTCs can help address hidden hunger, as well as improve household food security.

For OFSP storage roots, nutrient content was highest for the stressed treatment for Al, β -c, Fe, K, Mg, Mn, C and N but not for Ca, Cu, Na, P and Zn. Similarly, the stressed treatment resulted in higher nutrient content in taro tubers for Al, Fe, Mg, Mn, P, Zn, C, N and S, but not for Ca, Cu, K and Na. Compared to nutrient data from season 2 at Fountainhill, K, P, Zn and N content of OFSP tubers were much lower, whereas Fe and Na content were much higher. For taro, Mn and Na were lower, yet Zn was higher. As noted in **Section 2.5.5**, mineral composition of RTCs is affected by genotype and stage of development, as well as environmental factors such as soil type, soil pH, soil organic matter content, fertilisation, water availability and weather conditions.

5.3.7 Crop modelling

5.3.7.1 Model setup

In the model, the day after planting was set to 28 October 2022 and the plant density was set to 55,556 plants ha⁻¹ to match the greenhouse experiment (cf. **Section 5.2.3.2**). The simulation period was linked to the growing cycle, i.e. day one after sowing/transplanting to physiological maturity. The management

options were also set to reflect actual experimental conditions: (i) no fertility stress (i.e. fully fertilised), (ii) no weed stress (weed-free experiment), (ii) no salinity stress (municipal water used for irrigation), and (iv) no contours/buds (raised beds were flat). In addition, a management (.MAN) file was created with the option “practices preventing runoff are present”, and thus the model ignores the CN_{II} value. This sets the option “surface runoff affected or completely prevented by field surface practices” to 1. Finally, the initial soil water content was set to field capacity to match conditions in the greenhouse.

The volume of drip irrigation applied to each water treatment (stressed and unstressed) was determined after each irrigation application, which was then converted to depths. These depths were then used to create an irrigation (.IRR) file in AquaCrop. A rainfall (.PLU) file was created with zero daily values from 27 October 2022 to 04 June 2023. Maximum and minimum air temperature recorded inside the greenhouse were used to create an input temperature data (.TNX) file for AquaCrop. Similarly, daily ET_0 was estimated from measurements of solar radiation, relative humidity, air temperature and wind speed using FAO’s ET_0 Calculator utility (cf. **Section 4.2.6.1**). These values were then used to create the reference evapotranspiration data (.ET0) file required by AquaCrop.

Soil samples taken from the four raised beds in the greenhouse were analysed to determine soil fertility (at 0.15 m), soil texture (at 0.15 and 0.40 m), soil water retention and saturated hydraulic conductivity (at 0.30 m). From the results (cf. **Section 5.3.2**), an AquaCrop soil input (.SOL) file was created (cf. **Table 16-11** in **Section 16.4**) for a single soil layer (0.40 m deep). To further prevent AquaCrop generating runoff from the raised beds in the greenhouse, CN_{II} was set to 10, which equates to a K_{SAT} value approaching 3,000 mm day⁻¹.

5.3.7.2 Model calibration

The calibration procedure was outlined in **Section 5.2.6.4** and is similar to that followed by Mabhaudhi et al. (2014b). For each crop, the initial calibration involved matching observed CC to simulated CC using data from the unstressed treatment (i.e. 100% of CWR). Where possible, parameter values were set according to measurements and observations. Thereafter, data obtained from the stressed treatment was used to fine-tune the calibration of CC development, as well as to adjust stress factors related to canopy expansion, stomatal control and canopy senescence. Finally, the calibration was evaluated by comparing observed and simulated final biomass and yield. Model performance was evaluated using four statistical measures described in **Section 5.2.6.5**.

OFSP: Crop parameters developed by Rankine et al. (2015) were partially calibrated (i.e. fine-tuned) as follows:

- 1) The base temperature (line no. 8) was decreased from 15 to 10°C to match the value for taro. However, 8°C was most commonly used in the literature (e.g. Beletse et al., 2013; Lamaro et al., 2023; Pushpalatha et al., 2021).
- 2) The basal crop coefficient (K_{CB} ; line no. 35) was set to 1.05 as suggested by Pereira et al. (2021b; **Table 16-13**; cf. **Section 16.4**).
- 3) The maximum rooting depth (line no. 36) was reduced to 1.20 m. This value agrees with the range of 1.00-1.20 m provided by Pereira et al. (2021b; **Table 16-13**; cf. **Section 16.4**). However, the observed rooting depth at harvest was only 0.39 m.
- 4) Using the maximum allowed value for the soil surface covered by a transplanted crop (i.e. 50 cm²; line no. 43), together with the actual plant density of 55,556 plants ha⁻¹, the model calculated the initial canopy cover (CC_0) at 0.83%. This was larger than values of 0.42% and 0.63% obtained by Beletse et al. (2013) and Nyathi et al. (2016), respectively.

- 5) Measurements of LAI were used to estimate canopy cover (CC) development via the DIFN method. The maximum value (CC_x ; line no. 50) was set to 91%. Using an extinction coefficient of 0.80, the Beer-Lambert equation produced very similar CC values, with CC_x also being 91%.
- 6) Based on observations, the number of days for transplanted vines to recover (line no. 52) was set to six days.
- 7) The time to maximum rooting depth (line no. 53) was estimated at 93 days.
- 8) The start of senescence (line no. 54) was set to 150 days to replicate the “stay-green” trait of sweet potato. As shown by the CC development curves for both water treatments (**Figure 5-17**; cf. **Section 5.3.3.4**), CC did not decline as the crop approached physiological maturity. Sweet potato exhibits delayed leaf senescence when water stressed, which is referred to as the “stay-green” trait, i.e. the plant’s ability to retain greenness (no reduction in chlorophyll content) during tuber formation
- 9) Although tubers continued to grow from 142 to 172 DAP, the time to reach physiological maturity (line no. 55) was set to 160 days when CC development peaked (**Figure 5-17**; cf. **Section 5.3.3.4**). In addition, chlorophyll content index declined after 148 DAP (**Figure 5-22**; cf. **Section 5.3.4.1**).
- 10) The start of yield formation (line no. 56) was based on observations where root/tuber formation started sometime between 65 to 82 DAP and was adjusted to 68 days to improve the calibration (**Figure 5-18 & Figure 5-19**; cf. **Section 5.3.3.5**).
- 11) The length of the HI buildup period (line no. 60) was set to 92 days to finish at physiological maturity (i.e. $160 - 68 = 92$ days). This is based on evidence that showed roots/tubers continue to grow after 172 DAP.
- 12) The model calculated the CGC parameter (line no. 46), based on the time to reach maximum canopy cover (**Figure 5-17**; cf. **Section 5.3.3.4**). The value was then adjusted to 11.14% per day to improve the simulation of canopy over development.
- 13) The CDC parameter (line no. 51) was set to the lowest value of 3.0% to mimic little to no senescence due to the crop’s “stay-green” trait.
- 14) The normalised water productivity parameter (WP^*) was not changed (remained at 20 g m^{-2}), which represents the upper limit for C3 crops.
- 15) The harvest index was set to 78% based on final biomass and yield values of 19.354 and $15.143 \text{ dry t ha}^{-1}$ respectively, which were measured at harvest from the unstressed water treatment.

Once the partial calibration process was finalised using observations from the non-stressed water treatment, the stress coefficients affecting canopy expansion (line no. 11-13), stomatal control (line no. 14-15) and canopy senescence (line no. 16-17) were adjusted to achieve the best fit between simulations and observations for the 30% water treatment. For example, due to sweet potato’s “stay-green” trait, the upper threshold of the soil water depletion factor for canopy senescence (line. No. 16) was set to 0.80. This means early canopy senescence is extremely tolerant to water stress. The shape factor (line. No 17) was set to 3, which means the stress coefficient (K_s) declines slowly from 1 (no stress) to 0 (full stress) as the soil water content approaches permanent wilting point. Delayed leaf senescence facilitates continued photosynthesis even during water-stressed conditions, which can result in continued root/tuber growth and larger end-season yields when compared to other senescent

cultivars/landraces. A list of parameters that were fine-tuned for OFSP is given in **Table 16-15** (cf. **Section 16.4**).

Taro: As shown in **Table 16-16** (cf. **Section 16.4**), crop parameters developed by Mabhaudhi et al. (2016a) were partially calibrated (i.e. fine-tuned) as follows:

- 1) The basal crop coefficient (K_{CB} ; line no. 35) was set to 1.05 as suggested by Pereira et al. (2021b; **Table 16-13**; cf. **Section 16.4**).
- 2) The maximum rooting depth (line no. 36) was set to 0.40 m, based on observations at harvest of 0.38 m. This value agrees with the range of 0.30-0.40 m provided by Pereira et al. (2021b; **Table 16-13**; cf. **Section 16.4**), as well as observations of 0.30-0.45 m made by Mabhaudhi et al. (2014b).
- 3) Using the maximum allowed value for the soil surface covered by a transplanted crop (i.e. 25 cm²; line no. 43), together with the actual plant density of 55,556 plants ha⁻¹, the model calculated the initial canopy cover (CC_0) at 0.28%.
- 4) Measurements of LAI were used to estimate canopy cover (CC) development via the DIFN method. The maximum value (CC_x) was set to 70% (line no. 50). Using an extinction coefficient of 0.81 resulted in very similar CC values being calculated via the Beer-Lambert equation, with CC_x being 69%.
- 5) Based on observations, the number of days from sowing to emergence (line no. 52) was set to 14 days. Mabhaudhi (2012) noted that emergence can take up to 49 days. However, due to the warm conditions experienced in the greenhouse during the two weeks after planting, crop emergence was accelerated.
- 6) The time to maximum rooting depth (line no. 53) was estimated at 35 days.
- 7) The start of senescence (line no. 54) was set to 170 days since the CC development curve showed no decline at the end of the season (**Figure 5-17**; cf. **Section 5.3.3.4**). However, measurements of chlorophyll content index showed a decline between 134-148 DAP (**Figure 5-22**; cf. **Section 5.3.4.1**).
- 8) The length of the crop cycle (line no. 55) was set to 180 days when CC development peaked (cf. **Figure 5-17**; cf. **Section 5.3.3.4**). However, the crop was only harvested at 220 DAP to allow for additional time to observe a decline in CC, but this did not occur.
- 9) The start of yield formation (line no. 56) was set to 130 days based on observations where root/tuber formation only began after 142 DAP, but before 172 DAP (cf. **Figure 5-20** & **Figure 5-21**; cf. **Section 5.3.3.5**).
- 10) The length of the HI buildup period (line no. 60) was set to 50 days to finish at physiological maturity (i.e. 180 – 130 = 50 days).
- 11) Based on the time to reach maximum canopy cover (**Figure 5-17**; cf. **Section 5.3.3.4**), the model calculated the CGC parameter value (line no. 46). It was then adjusted to of 24.74% per day to improve the simulation of canopy over development.
- 12) The CDC parameter was again set to the lowest value of 3.0% to mimic no senescence of the canopy as shown in **Figure 5-17** (cf. **Section 5.3.3.4**). The same approach was used by Mabhaudhi et al. (2014b).

- 13) The normalised water productivity parameter (WP^*) was not changed (line no. 61), i.e. remained at 15 g m^{-2} , which represents the lower limit for C3 crops.
- 14) The harvest index was set to 80% (line no. 64) based on final biomass and yield values of 8.14 and $6.58 \text{ dry t ha}^{-1}$, respectively.
- 15) The possible increase in HI due to water stress before the start of yield formation (line no. 65) was decreased from 10% to 0% (i.e. no impact), as HI declined from 81 to 76% due to water stress.
- 16) Similarly, the coefficient describing a positive impact on HI due to restricted vegetative growth during yield formation (line no. 66) was decreased from 10 to 0 (i.e. no impact).
- 17) The coefficient describing a negative impact on HI due to stomatal closure during yield formation (line no. 67) was set to 10% to mimic the decline in observed HI from 81 to 76% caused by water stress.
- 18) Finally, the stress coefficients affecting canopy expansion (line no. 11-13), stomatal control (line no. 14-15) and canopy senescence (line no. 16-17) were adjusted to achieve the best fit between simulations and observations for the 30% water treatment.

It is important to note that the calibration of taro was very sensitive to the maximum rooting depth ($Z_{r_{\max}}$; line no. 38). Mabhaudhi et al. (2014b) stated that although observed $Z_{r_{\max}}$ ranged between 0.30-0.45 m, the parameter was set to 0.80 m, which provided better simulations for both irrigated and rainfed conditions. However, this was not the case in this project. When $Z_{r_{\max}}$ was increased to 0.8 m, AquaCrop grossly over-estimated CC development, biomass production and final yield for both water treatments. This may have been the reason why Mabhaudhi et al. (2016a) reduced $Z_{r_{\max}}$ to 0.30 m, as shown in **Table 16-6** (cf. **Section 16.2**). Hence, $Z_{r_{\max}}$ was set to 0.40 m to match observations, which concurs with values published by Mabhaudhi et al. (2014b) and Pereira et al. (2021b).

5.3.7.3 Canopy cover simulation

Unstressed water treatment: As shown in **Figure 5-3** (cf. **Section 5.2.6.4**), the rate at which CC initially develops in AquaCrop is determined by the CGC parameter (line no. 46) and is typically concave-shaped, whereas CC decline is typically convex-shaped. However, for the unstressed water treatment, initial CC development followed a convex shape (i.e. very fast development), especially for OFSP (**Figure 5-17**; cf. **Section 5.3.3.4**), likely due to extremely high temperatures ($\sim 55^\circ\text{C}$) experienced in the greenhouse during frequent load shedding and load reduction events. When the soil surface area covered by an individual seedling (line no. 43) was set to measured values, AquaCrop grossly underestimated initial canopy development, which resulted in lower final biomass and yield values when compared to observations. Rankine et al. (2015) also noted that AquaCrop underestimated CC development for both irrigated and rainfed treatments for approximately 66 DAP. To correct this, the parameter was set to the maximum allowable value ($25 \text{ \& } 50 \text{ cm}^2$ for a sown and transplanted crop, respectively). This resulted in the initial CC development curve being convex shaped, which provided a better match to observations (**Figure 5-28**), especially for OFSP (unstressed treatment). However, the disadvantage is AquaCrop's tendency to then over-estimate the final biomass and yield when compared to measurements.

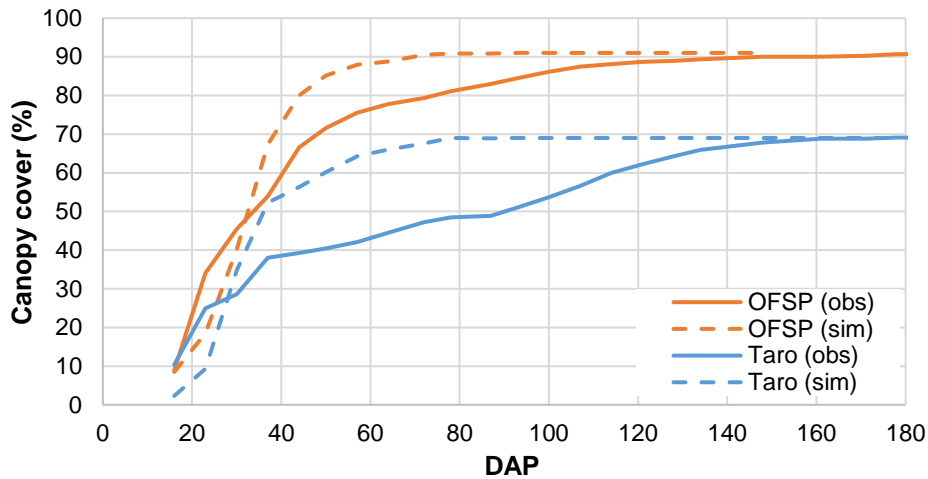


Figure 5-28 Comparison of simulated against observed canopy cover development for OFSP and taro (unstressed water treatment)

Stressed water treatment

For the stressed water treatment, AquaCrop again over-estimated initial CC development during the vegetative growth stage, especially for OFSP (**Figure 5-29**), which also resulted in over-simulation of biomass production and final yield. This was due to the high values used for the soil surface covered by a sown/transplanted crop (line no. 43). In contrast, AquaCrop produced a very good simulation for taro’s CC development, as shown in **Figure 5-29**.

As both crops approached physiological maturity, CC decline due to senescence was not apparent, especially for OFSP due to its “stay-green” trait. Mabhaudhi et al. (2014b) stated that unless frost occurs and kills off the foliage, taro’s canopy is maintained through winter as a perennial crop. Hence, if weather conditions are favourable, roots/tubers continue to grow until they start to split open, and thus should be harvested immediately to avoid further deterioration on product quality. It is therefore difficult to determine when the RTC has reached physiological maturity. These issues, together with the initial rapid development of CC may help to explain why calibration of RTCs in AquaCrop is difficult, as highlighted by Rankine et al. (2015).

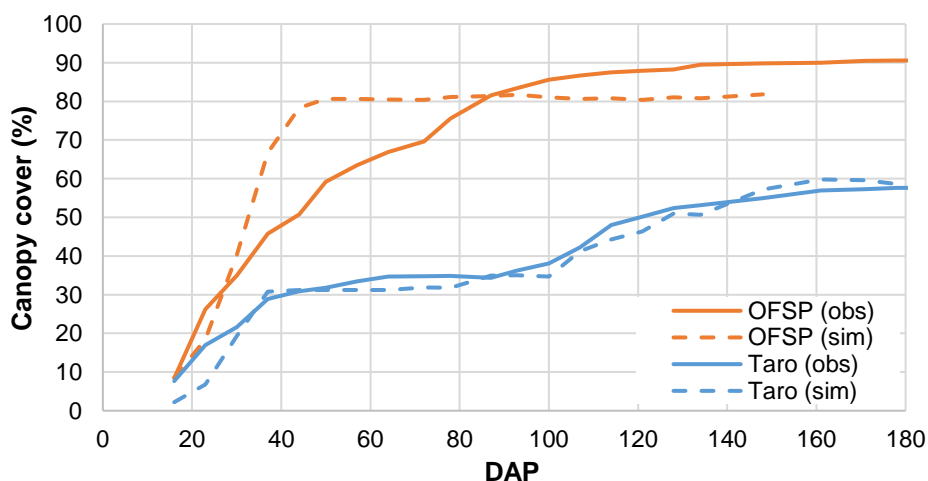


Figure 5-29 Comparison of simulated against observed canopy cover development for OFSP and taro (stressed water treatment)

Model evaluation: Using the guidelines provided in **Table 5-2** (cf. **Section 5.2.6.5**), the calibration of CC for OFSP is considered “good” (NRMSE) to “very good” (NSE, D-I, R^2 & r) for the unstressed treatment, whereas for the stressed treatment, the calibration is deemed “moderately good” to “very good” (**Table 5-11**). In comparison, Nyathi et al. (2016) obtained values of 12.10% and 0.77 for RMSE and R^2 (irrigated treatment), respectively (cf. **Table 16-1** in **Section 16.1**). In contrast, Rankine et al. (2015) obtained lower RMSE values across two seasons when simulating CC development under rainfed conditions (4.48-9.42%) but higher RMSE values for the irrigated treatment (10.86-25.20%). However, statistics were derived from only 3-5 measurements of CC between 50-150 DAP, compared to statistics derived from 19 measurements in this project.

Table 5-11 Calibration statistics for canopy cover development for OFSP and taro under two water treatments

RTC	Water treatment	RMSE (%)	NRMSE (%)	NSE	D-I	R^2	r	n
OFSP	Unstressed	8.8	12.1	0.83	0.96	0.92	0.96	19
	Stressed	12.0	17.8	0.74	0.93	0.76	0.87	
Taro	Unstressed	14.0	27.8	0.19	0.84	0.71	0.84	22
	Stressed	3.4	8.6	0.94	0.99	0.98	0.99	

Similarly, taro’s calibration of the stressed treatment is also deemed “good” to “very good”, whereas for the unstressed treatment, it ranged from “moderately poor” to “good” (**Table 5-11**). The calibration of taro for unstressed conditions undertaken by Mabhaudhi et al. (2014b) achieved RMSE, D-I and R^2 values of 2.38%, 0.92 and 0.79, respectively. However, the statistics were developed from 8 measurements of CC between 100-200 DAP, whereas in this project, 22 measurements from 16-178 DAP were used. However, when tested against rainfed trial data, Mabhaudhi et al. (2014b) stated that CC development was poorly simulated, with RMSE, D-I and R^2 values of 20.17%, 0.65 and 0.02, respectively. The authors highlighted the model’s limitation to effectively capture taro growth under water deficit conditions, which was not the case in this project.

Simulation of final biomass and yield: As shown in **Table 5-12**, AquaCrop successfully simulated the final biomass and yield of both RTCs for the water stressed treatment since deviations were within $\pm 6\%$ (cf. **Section 5.2.6.5**). This outcome is in contrast with other studies (e.g. Heng et al., 2009; Hsiao et al., 2009; Patel et al., 2011), which showed AquaCrop’s inability to accurately simulate water stressed conditions.

For OFSP, the model over-estimated the final biomass and root yield for the unstressed treatment by 26.8 and 23.8% respectively (**Table 5-12**). In comparison, Rankine et al. (2015) reported larger deviations ranging from -70.7 to -19.5% and -76.0% to 8.7% for final (total) biomass and root yield of sweet potato, respectively. For unstressed taro, AquaCrop grossly over-estimated the final biomass and yield by 89.7% and 83.3%, respectively (**Table 5-12**).

Table 5-12 Comparison of observed final biomass, yield and harvest index of OFSP and taro to AquaCrop simulations for both water treatments

RTC	Water treatment	Harvest index (%)		Biomass (dry t ha ⁻¹)		Yield (dry t ha ⁻¹)		Deviation (%)	
		Obs	Sim	Obs	Sim	Obs	Sim	Bio-mass	Yield
OFSP	Unstressed	78.2	76.4	19.35	24.54	15.14	18.75	26.8	23.8
	Stressed	72.3	76.4	16.95	15.95	12.25	12.18	-5.9	-0.6
Taro	Unstressed	80.9	78.1	8.14	15.46	6.59	12.07	89.7	83.3
	Stressed	76.3	69.5	5.90	6.19	4.51	4.31	4.9	-4.4

In total, 20 and 22 parameters were adjusted to improve the simulation of OFSP and taro, respectively. This is similar to the 21 parameters adjusted by Mabhaudhi (2012) when calibrating AquaCrop for bambara nut and taro. Overall, the calibration for both crops can be considered good, especially for the water stressed treatments, given that the model was simulating two landraces. Calibrating AquaCrop for OFSP was much easier than for taro. Rankine et al. (2015) stated that parameterising AquaCrop for RTCs is more difficult than for other crop types. According to Raes et al. (2018), potato represents one of the least reliable parameterisations in AquaCrop when compared to other crops such as maize and soybean.

Various reasons for AquaCrop's poor performance for RTCs such as potato and sweet potato are as follows: Several studies (e.g. Lebot, 2019) reported that the water requirements of sweet potato are site- and time-specific, which therefore makes parameterisation difficult. Furthermore, the crop is sensitive to over-irrigation. For example, yield data used by Rankine et al. (2015) to parameterise AquaCrop had higher values for rainfed compared to irrigated conditions. Hence, a short period of water stress appeared to stimulate root development of sweet potato. Lebot (2019) also reported that over-irrigation in Taiwan reduced storage root yields, which may be due to reduced aeration.

Rankine et al. (2015) found that irrigation improved the uniformity of storage roots, which led to better AquaCrop yield predictions. They also showed that AquaCrop does not adequately simulate water-stressed conditions. They reported a very low yield (2.6 t ha^{-1}) due to sweet potato's failure to form storage roots since the rainfed trial received about half the amount of water of the irrigated treatment (11 t ha^{-1}). However, AquaCrop simulated a yield of 7.3 t ha^{-1} for both water treatments. Other studies have also reported AquaCrop's inability to adequately simulate conditions of high water stress (e.g. Heng et al., 2009). Hence, AquaCrop may struggle to accurately predict yields for rainfed conditions, since observed yields are more variable.

5.3.7.4 Model validation

A validation was undertaken by testing AquaCrop's ability to predict CC development, as well as final biomass and yield measured at Fountainhill in season 2. As shown in **Table 5-13**, AquaCrop predicted OFSP's final biomass well (0.81% deviation) but over-estimated the final yield by 39.3%. This is due to the large difference between observed and simulated HI (i.e. 55.3 vs 76.4%). If the HI_0 parameter (line no. 64) is changed from 78 to 55%, the simulated yield becomes $12.23 \text{ dry t ha}^{-1}$, which represents a 0.87% deviation. However, HI varies from 22-81% in the literature (cf. **Section 4.3.5.2**). In contrast, Pushpalatha et al. (2021) obtained excellent agreement between observed and simulated yields for cassava and sweet potato, with percentage differences ranging from 0.08 to 5%. However, the authors used a relatively high HI_0 of 85%, which is similar to 90% used by Beletse et al. (2013).

Table 5-13 Comparison of observed final biomass, yield and harvest index of OFSP and taro at Fountainhill in season 2 to AquaCrop simulations under rainfed conditions

RTC	Water treatment	Harvest index (%)		Biomass (dry t ha^{-1})		Yield (dry t ha^{-1})		Deviation (%)	
		Obs	Sim	Obs	Sim	Obs	Sim	Bio-mass	Yield
OFSP	Rainfed	55.3	76.4	21.93	22.11	12.12	16.88	0.81	39.30
Taro	Rainfed	86.4	77.9	5.68	14.38	4.91	11.21	153.22	128.21

However, AquaCrop grossly over-estimated taro's final biomass and yield by 153.2 and 128.2%, respectively. The model failed to adequately simulate the very slow CC development observed under rainfed conditions in season 2. CC development was over-simulated by the model, due to the high CGC parameter of 27.4% (line no. 46) (**Figure 5-30**). CC peaked at 44% on 136 DAP), whereas the model simulated 69% (58 DAP). This outcome was expected, based on CC_x (line no. 50) and CGC (line no.

46) parameter values of 69% and 24.736% per day, respectively (cf. **Table 16-16** in **Section 16.4**). Mabhaudhi et al. (2014b) also obtained a poor simulation of CC under rainfed conditions, with RMSE, D-I and R^2 values of 20.17%, 0.645 and 0.018, respectively. In contrast, AquaCrop simulated a final CC of 91% (line no. 50) for OFSP, which agreed favourably with the measured value of 90%. This explains why AquaCrop was more successful in simulating OFSP than taro. Further testing of both crop parameter files is therefore required for rainfed conditions.

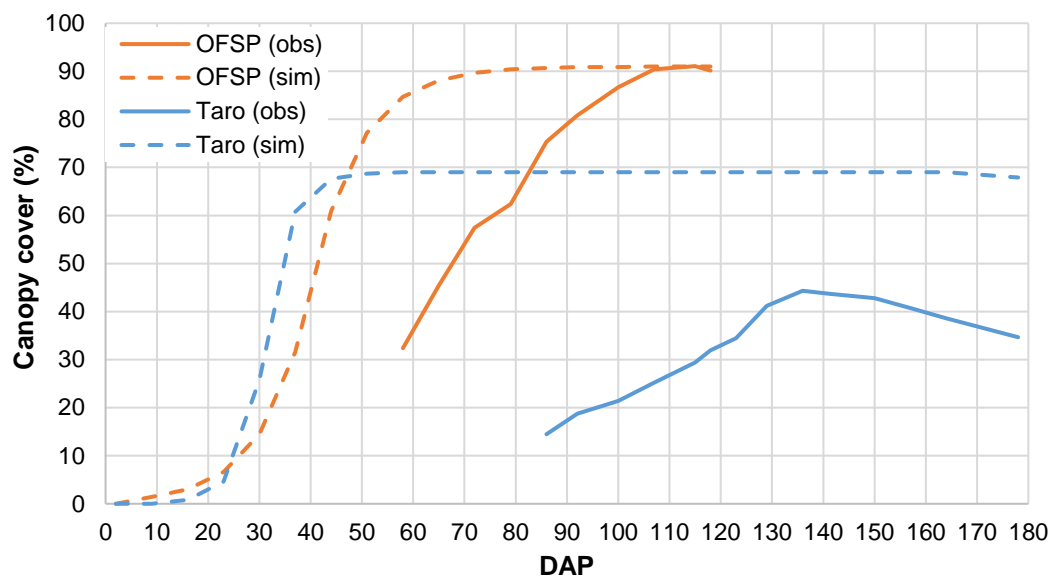


Figure 5-30 Comparison of observed and simulated canopy cover development for OFSP and taro under rainfed conditions in season 2

5.3.7.5 Conversion to GDDs

AquaCrop was then used to convert the phenological growth stages and canopy growth/decline coefficients to thermal time. Extremely warm conditions were experienced in the greenhouse over the growing season, especially during frequent load shedding and load reduction events between December 2022 and March 2023. This resulted in a rapid accumulation of growing degree-days (GDDs), with the total length of OFSP's crop cycle being 2,533 GDDs. This value is almost double the 1,294 GDDs derived by Rankine et al. (2015) for sweet potato grown in in a tropical climate (Jamaica). Since AquaCrop is run in GDD mode for the national-scale simulations, the high value is likely to affect the yield simulations and in particular the land suitability assessments. For taro, the crop cycle increased from 2,580 (Mabhaudhi et al., 2016a) to 2,824 GDDs. The crop parameter files in GDD format were then used to perform the national-scale simulations, with results presented in the next chapter.

5.4 SUMMARY AND CONCLUSIONS

A greenhouse experiment was conducted at UKZN in season 3 due to the need to reduce field work-related expenses and the problems experienced at Fountainhill regarding animals damaging the trials. The same OFSP cultivar (199062.1) and taro landrace (Dumbe dumbe) studied in season 2 were planted in two adjacent beds that received 100% of crop water requirement (CWR). Similarly, each crop was planted in another two beds and subjected to water stress, i.e. irrigated to 30% of CWR.

The two crops were planted on the same date (27 October 2022) and plant density (55,556 plants ha⁻¹). Prior to planting, the four raised beds were fully fertilised, where recommended application rates for each crop were based on soil fertility measurements. The raised beds were kept weed-free throughout

the growing season. Pesticides were used to control outbreaks of insects, especially red spider mites that favoured the taro plants. These measures were necessary to maximise crop growth.

From measured soil texture, the topsoil (0.15 m) is dominated by a clay loam that transitioned to clay at lower depths (0.40 m). Soil water retention was measured for each bed, then compared to estimates derived from textural data using the SPAW model. The results highlight the importance of measuring soil properties, especially when used for modelling purposes.

An automatic weather station was installed inside the greenhouse to accurately estimate ET_o , from which maximum crop evapotranspiration was determined using the single crop coefficient approach. Results showed that 94% of the variation in ET_o was explained by solar radiation, thus highlighting the importance of measuring the latter variable inside greenhouses for accurate irrigation scheduling. Soil water sensors monitored water content at two depths (0.15 and 0.40 m).

Regular measurements of plant height, leaf number, leaf area index, chlorophyll content index, leaf temperature and stomatal conductance were conducted over the growing season. Leaf area index was then used to estimate canopy cover development. Root/tuber formation and above-ground biomass accumulation were also determined from random destructive sampling from 65-172 DAP. Final (total) biomass and root/tuber yield was determined after OFSP and taro were harvested on 198 and 220 DAP, respectively.

Results showed that OFSP has a much higher leaf number compared to taro, which translates to higher leaf area and canopy cover. From LAI measurement, maximum canopy cover was estimated 91 and 69% for OFSP and taro, respectively. Although leaf number was higher for the unstressed treatment as expected, leaf area was the same from 87 DAP for OFSP. Chlorophyll content was higher for taro than OFSP. Due to the larger leaf area, stomatal conductance for OFSP was higher than for taro, which means higher transpiration rates. Diurnal measurements for OFSP from 4 am to 7 pm showed that reduced stomatal conductance results in closure of stomatal openings, and thus lower transpiration rates and higher leaf water potential.

For both water treatments, final (total) biomass ranged from 16.95-19.35 and 5.90-8.14 dry t ha⁻¹ for OFSP and taro, respectively. Similarly, storage root/tuber yields ranged from 12.25-15.14 and 4.51-6.59 dry t ha⁻¹ for OFSP and taro, respectively. This resulted in harvest index value of 72-78 and 76-81% for OFSP and taro, respectively. The yields for the water stressed treatment were similar to those obtained from season 2 of 12.12 and 4.91 dry t ha⁻¹ for OFSP and taro, respectively,

Harvested root/tuber and leaf samples were analysed to determine nutrient contents for 13 minerals, as well as β -c. OFSP leaves exhibited higher nutrient values compared to the storage roots for all of the analysed minerals, except for Na. The results were similar to those obtained from samples taken during season 2. Similarly, taro leaves were more nutritious than tubers for all minerals except K and P. Furthermore, taro tubers contained more nutrients for most minerals (except Ca and Na) when compared to OFSP storage roots. This again highlights the dual-purpose nature of OFSP and taro, where both the roots/tubers and leaves are edible and exhibit high nutritional value. Results also showed that nutrient contents were higher for stressed OFSP and taro, compared to unstressed plants. This trend has been reported in other studies (cf. **Section 3.3**) and highlights the suitability of growing both crops in marginal areas.

From the preliminary modelling results obtained from season 2, further work was required to improve AquaCrop simulations of yield. Hence, default (i.e. initial) AquaCrop parameters for OFSP and taro were sourced from the literature, then fine-tuned (i.e. partially calibrated) using growth and yield data measured in the greenhouse during season 3. Considerable effort was spent on creating reliable, error-free climate files for use in AquaCrop, especially for ET_o estimates. Soil water retention parameters

required by AquaCrop (e.g. saturation, field capacity, permanent wilting point) were determined from laboratory measurements, which provided more accurate values compared to SPAW simulations. AquaCrop was calibrated to simulate CC, biomass production and root/tuber yield. Calibration results showed AquaCrop's ability to successfully simulate the final biomass and yield of both RTCs for the water stressed treatment. However, the model over-estimated the final biomass and root/tuber yield for the unstressed treatment, especially for taro. The calibration was then tested against observations from season 2, which again showed an over-estimation of taro's yield.

6 MODELLING OF CROP WATER PRODUCTIVITY

6.1 INTRODUCTION

As noted in **Section 1.3**, phase 3 of this project represented the crop modelling component. Crop modelling is the simulation of crop development using numerically integrating processes (Sinclair and Seligman, 1996). Crop models are important as they can be used as tools for decision making, yield forecasting and for assessing climate change impacts (Mabhaudhi, 2012). However, the modelling of water use and yield of RTCs has not been given the same attention as that given to conventional crops. In South Africa, taro has been modelled using the AquaCrop model (Mabhaudhi, 2012; Mabhaudhi et al., 2014b; Mabhaudhi et al., 2016a) and sweet potato was modelled using the SWB model (e.g. Masango, 2015; Mthembu, 2023).

A preliminary analysis was undertaken to determine the feasibility of using default crop parameters, with little to no adjustment, to estimate crop water productivity of OFSP using the AquaCrop and SWB models. The methodology was presented in **Section 4.2.7** and the results given in **Section 4.3.7** (cf. **Chapter 4**). The SWB model was evaluated, despite not being able to run at a national scale in “batch mode”, as reported by Kunz et al. (2015b). Since AquaCrop simulated crop water productivity more accurately than the SWB model, AquaCrop model was therefore selected to meet the aims of this project. The model can be run at a national scale using climate and soils data currently available for each of the 5,838 homogeneous response zones. The altitude range across each zone is much smaller compared to the quaternaries, and thus variation in climate and soils is far less. Hence, each zone is considered relatively homogeneous in response. AquaCrop is well suited to estimating yield in areas where crop growth is mostly water and/or temperature limited. The model has also been used in various other WRC-funded projects to assess crop yield and water productivity of underutilised crops. This chapter therefore provides a description of the AquaCrop model, and the methodology used to model the yield and water use of OFSP and taro across the entire country, including Lesotho and eSwatini.

6.2 METHODOLOGY

6.2.1 Model description

6.2.1.1 AquaCrop

AquaCrop (Raes et al., 2009; Steduto et al., 2009; Steduto et al., 2012) was developed by the Food and Agricultural Organisation (FAO) and designed to simulate yield response of several crops to water availability. The model has a water-driven growth engine (Steduto et al., 2009) and thus, is particularly suited to simulating yield response to water availability, i.e. simulating yields where water is a key limiting factor in crop production. Hence, AquaCrop is a simplified interpretation of the effects of water stress on crop productivity. Although the model is simple, it emphasises the fundamental processes involved in crop productivity and response to water deficits, both from a physiological and an agronomic perspective (Steduto et al., 2009). Features that distinguishes AquaCrop from other crop models include the:

- normalised water productivity parameter,
- use of canopy cover instead of leaf area index for biomass production, and
- effects of water and temperature stress on biomass production and crop yield.

Version 6 was released in March 2017 (Raes et al., 2018), which has been successfully parameterised to simulate the daily growth, productivity and water use of 16 herbaceous crops. Although version 7 was released in August 2022 with new crop parameters for cassava (Wellens et al., 2022) and alfalfa (Raes et al., 2023), version 6 was used in this project. The structural components of the model are

shown schematically in **Figure 6-1**, which shows the model requires daily rainfall, minimum and maximum temperature as well as reference crop evapotranspiration (ET_0) as climatic input data. ET_0 is determined using the FAO56 (or Penman-Monteith) method described by Allen et al. (1998). The basic concepts and fundamental calculation procedures are briefly described next.

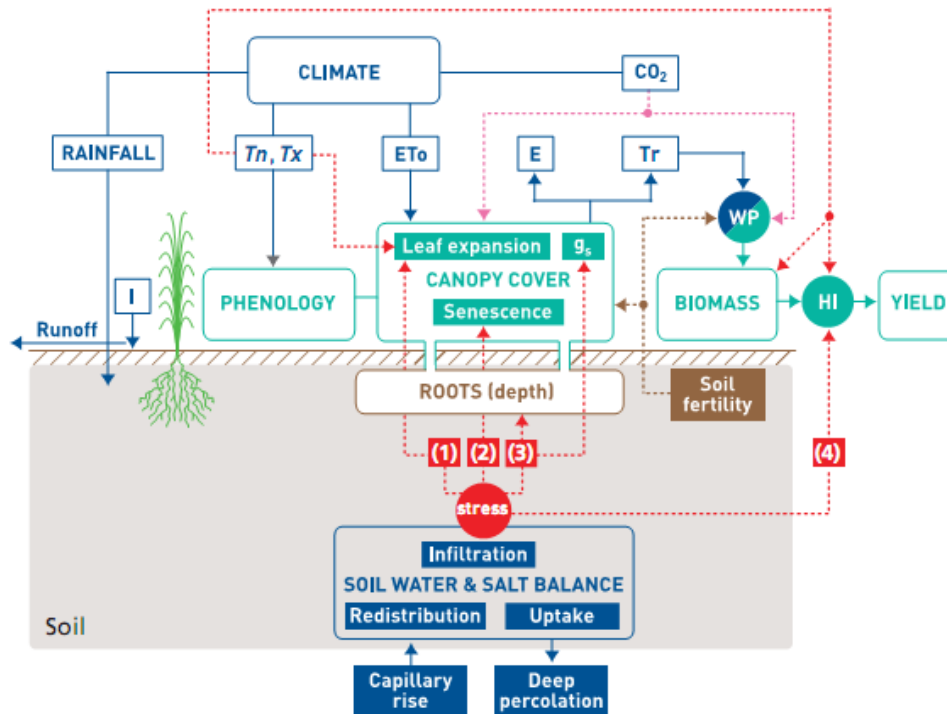


Figure 6-1 The structural components of AquaCrop, including stress responses and the functional linkages between them (Steduto et al., 2012)

AquaCrop simulates crop yield in four sequential steps. Firstly, canopy cover development is simulated, in particular leaf and root expansion. Temperature (i.e. thermal time) governs both canopy cover development and pollination success. Canopy cover development affects, inter alia, the rate of crop evapotranspiration. Secondly, the model calculates transpiration (Tr) and soil water evaporation (E) separately using the dual crop coefficient method. This approach is especially useful during periods of incomplete ground cover when E is high (e.g. as for taro). Since crop evapotranspiration is affected by soil water content, the model also simulates the following processes using a soil water balance approach: (i) runoff via the SCS-based method, (ii) infiltration into the topsoil, (iii) drainage out of the root zone (i.e. deep percolation), and (iv) capillary rise.

Thirdly, transpiration (Tr in mm) is used to estimate biomass production (B in $g\ m^{-2}$) via the biomass water productivity parameter (WP in $g\ m^{-2}\ mm^{-1}$). This crop-specific input parameter represents the amount of above-ground dry matter (g) produced per unit land area (m^2), per unit of water transpired (mm). WP varies with crop physiology and is higher for C4 (30-35 $g\ m^{-2}$) than C3 crops (15-20 $g\ m^{-2}$). To improve the model's robustness and applicability across different climates, both Tr and WP are normalised by ET_0 . WP is also normalised by ambient CO_2 levels, which is then called WP^* . Hence, WP is expected to increase over time due to anthropogenic increases in ambient CO_2 concentration. WP is therefore an important parameter in AquaCrop that behaves conservatively and is not affected by water stress, i.e. remains virtually constant over a wide range of environments (Steduto et al., 2009).

In the fourth step, Yield (Y in $g\ m^{-2}$), which is the harvestable portion of the biomass, is calculated using the harvest index. The model requires a reference harvest index as an input parameter, which is adjusted on a day-by-day basis over the yield formation period. This approach also enhances the

robustness of the model. No other partitioning among the various plant organs occurs, thus avoiding the complexity of partitioning processes that are the most difficult to model (Steduto et al., 2009).

AquaCrop version 6 onwards can model the influence of weed growth on crop production. Weeds reduce the crop's canopy cover and therefore, crop transpiration and crop production are reduced. In addition, weeds affect the soil water balance and may affect the timing and magnitude of soil water stress experienced during the season, which could indirectly affect crop development and production. In AquaCrop, weeds also suppress soil water evaporation and increase transpiration (crop + weed). Hence, the modelling of weeds in AquaCrop reduces crop yield and increases total evapotranspiration, which results in reduced crop water productivity.

It is important to note that for version 6 of the model, the cold stress coefficient is now applied to the basal crop coefficient (K_{CB}), which is obtained from the crop parameter file. In previous versions of AquaCrop, this temperature stress coefficient was applied to biomass water productivity. This means that crop transpiration during cold periods will be less and thus, biomass production is also lower. Reduced transpiration also results in a wetter root zone and lower water stress later in the season.

6.2.1.2 Other crop models

As noted in **Sections 4.2.7** and **4.3.7**, the SWB model was used to simulate OFSP by Masango (2015) and as part of this project, by Mthembu (2023). The SWB model is a mechanistic, real-time, soil water balance model, which was originally developed by Annandale et al. (1999) as an irrigation scheduling tool. However, SWB is also a field-scale crop growth model that has been developed for a number of crops (Jovanovic and Annandale, 1999; Jovanovic et al., 1999). The model's "scenario generator" allows multiple crop and irrigation scenarios to be easily configured. Jovanovic and Annandale (2000) developed a newer version of the model (SWBPro), which was used in this project. The model has been applied widely in South Africa to estimate crop water use and for irrigation scheduling (e.g. Annandale et al., 2002). However, problems were experienced in obtaining the latest model version from the Department of [Plant and Soil Sciences](#) (University of Pretoria) and the software developer's [website](#). Hence, an older version (no. 19.05.2010) of the model was run. Although challenges were also experienced in running SWB on a Windows 10/11 computer, various workarounds were found to get the model to run. This may explain why the model is no longer available for download.

Other crop simulation models that have been successfully used to estimate the water use and yield or RTCs include: (i) Agricultural Production Systems Simulator (APSIM; Keating et al., 2003), (ii) Decision Support System for Agrotechnology (DSSAT; Jones et al., 1998), and (iii) Light Interception and Utilisation (LINTUL; Kooman and Haverkort, 1995). For a brief description of each of these models, the reader is referred to Mthembu (2023). Although two other sweet potato models (MADHURAM and SPOTCOMS) have been developed, their application is limited. In contrast, many crop models have been developed for both potato and cassava (Raymundo et al., 2014).

6.2.2 Model inputs

6.2.2.1 Homogeneous response zones

AquaCrop (and ACRU) were run at a national scale using the 5,838 relatively homogeneous regions. In the past, these regions were referred to as quinary sub-catchments, as they were derived by dividing each of the 1,946 quaternary catchments into three sub-catchments of similar altitude, i.e. $1,946 * 3 = 5,838$. Since the altitudinal range across each sub-catchment is relatively small, the spatial variation in climate and soils is also deemed minimal, and thus are considered relatively homogeneous. For this project, they are referred to as homogeneous response zones (HRZs), to avoid confusion with recent updates. Since the quaternary boundaries were updated in 2018, new zones of similar altitude were developed, which are now referred to as altitude zones. This is necessary since each quaternary was

also subdivided into hydrological sub-catchments, which are true quaternaries that represent a 5th level sub-division of the primary catchment. The process of running AquaCrop for each HRZ has been fully automated, where a national model run takes less than 3 hours to complete (cf. **Section 6.2.4**).

6.2.2.2 Climate data

Kunz et al. (2020) significantly improved the rainfall and temperature data originally developed for each HRZ as follows:

- The driver rainfall station for 11 quaternary catchments (i.e. 33 HRZs) was changed to improve the representation of the rainfall in those catchments.
- The SAWS ID numbers of each of the driver rainfall stations was checked, which resulted in 317 corrections. For each of the 1,240 driver stations, rainfall data was then re-extracted from the Lynch (2004) database and compared to the original climate files and no errors were found. However, for very few occurrences where the daily value had not been patched by Lynch (2004), these were simply set to 0 mm.
- A total of 13 extreme rainfall events (> 400 mm) were found. Of these, four values were appropriately corrected when compared to rainfall data from neighbouring gauges.

Daily temperature deemed representative of each HRZ was revised by Kunz et al. (2020), which is now based on observed data, thus replacing values originally derived from the gridded temperature database developed by Schulze and Maharaj (2004). A temperature station was selected for the driver rain gauge assigned to each HRZ. Thereafter, a lapse rate adjustment was undertaken to account for the altitude difference between the temperature station and the average value for each HRZ. Using the FAO56 version of the Penman-Monteith equation (Allen et al., 1998), daily reference evapotranspiration (ET_0 in mm) for each HRZ was then calculated from mainly temperature data, assuming a daily default value of 2 m s^{-1} .

A new climate file was generated for each HRZ in ACRU-composite format, which contains daily data from 1950 to 1999. This was done by combining the extracted daily rainfall data (and quality codes) with the lapse rate-adjusted temperatures (and quality codes) and the estimated ET_0 data. Each climate file was called "*obstmp_xxxx.txt*", where *xxxx* represents the unique HRZ identifier (*sub_cat*) that ranges from 0,001 to 5,838. The reader is referred to Kunz et al. (2020) for a full description of the improvements made and error checking that was undertaken.

Finally, the revised climate files in ACRU format were then converted to the format required by AquaCrop using a utility developed in Fortran. The model requires a climate (.CLI) file, which contains the names of the daily rainfall (.PLU), air temperature (.TNX), reference evaporation (.ETo) and atmospheric CO₂ (.CO2) files. The format of the .PLU, .TNX and .ETo files are almost identical, with five header lines that provide station details, but more importantly, the start date of the climate record, followed by the daily time series data (Raes et al., 2018). The Fortran utility four climate files per HRZ, i.e. 23,352 individual files totalling 5.41 GB. Monthly adjustment factors were applied to the rainfall data from each driver station to improve its representativeness of the HRZ.

6.2.2.3 Soil properties

Soil water retention: SAT, FC and PWP for each soil horizon were derived for up to five terrain units within each of the 7,082 land types across South Africa (Clulow et al., 2023b). Hence, soil properties are now available for 27,473 terrain unit polygons, which were used to provide area-weighted values for each of the 5,838 HRZs. The improved soil properties for South Africa were then merged with previous values for Lesotho and eSwatini using other soil databases, since land type data does not

exist for these two neighbouring countries (SIRI, 1987). Hence, improved values for PWP, FC and SAT were obtained for both soil horizons in each HRZ.

Soil depth: From the terrain unit polygons, the area-weighted depth of the A- and B-horizons was derived for each HRZ. It is important to note that the maximum soil depth recorded for each land type was 1.2 m, i.e. standard soil auger depth (SIRI, 1987). As shown in **Figure 6-2**, the topsoil ranges from 0.1-0.3 m in depth in 80.7% of all HRZs. Since the total soil depth is 1.2 m, the maximum subsoil depth is 0.9 m, with 84.3% of all HRZs less than 0.4 m (**Figure 6-3**). However, the total soil depth is below 0.3 m in 30.4% of all HRZs, which is considered too shallow for RTC production. In 50% of all HRZs, the total depth ranges from 0.3-0.6 m (**Figure 6-4**). The remaining 19.6% of all HRZs have a total depth exceeding 0.6 m.

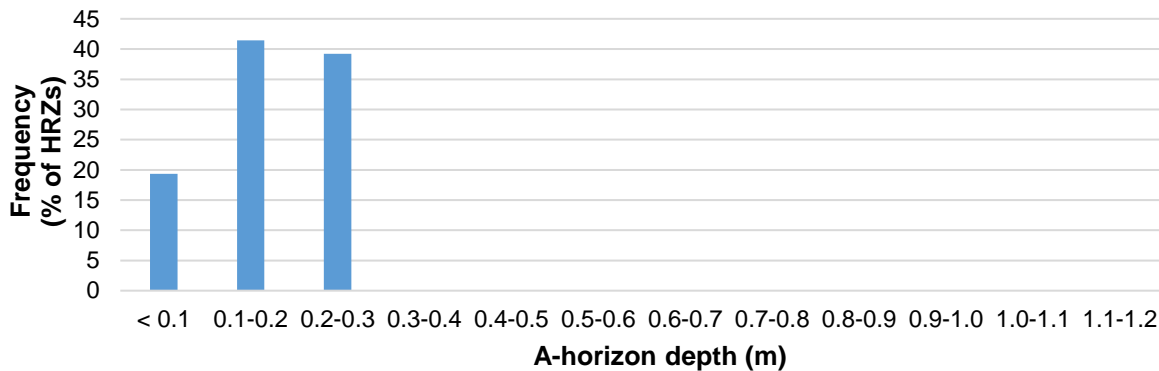


Figure 6-2 Depth of the A-horizon determined from the terrain unit soil polygons for all HRZs

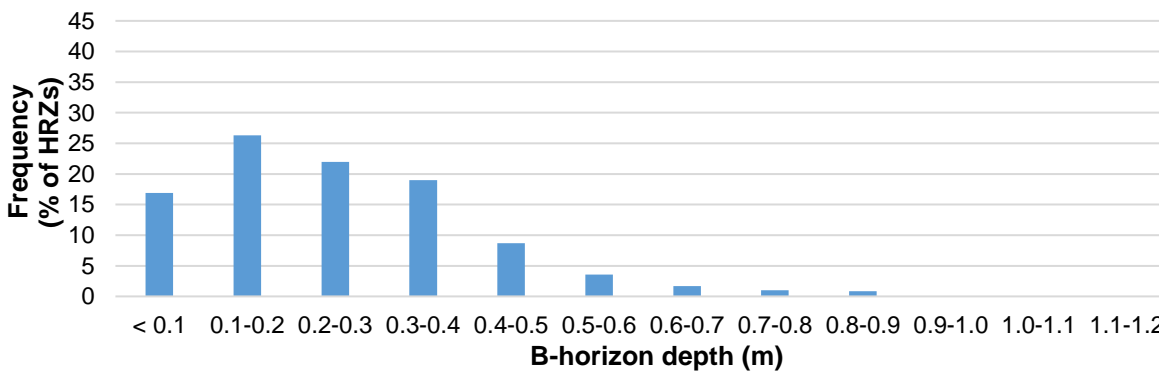


Figure 6-3 Depth of the B-horizon determined from the terrain unit soil polygons for all HRZs

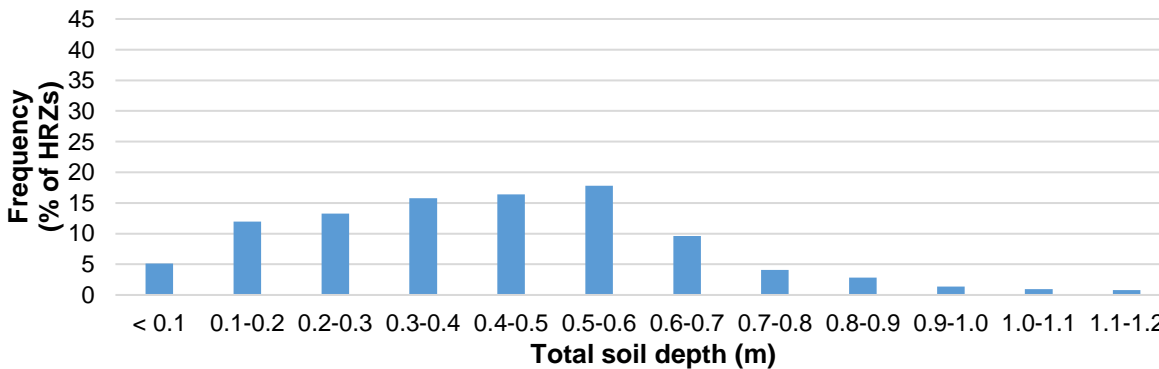


Figure 6-4 Total soil depth determined from the terrain unit soil polygons for all HRZs

Total available water: TAW (mm) represents the total amount of water in the soil profile that is available to plants. It is calculated as the product of effective root depth (ERD in m) and plant available water

(PAW in mm m^{-1}). The latter is also commonly referred to as available water capacity (AWC in mm m^{-1}) and is the amount of soil water held between field capacity and permanent wilting point, i.e. $\text{PAW} = \text{AWC} = \text{FC} - \text{PWP}$. TAW reflects the changes in FC, PWP and soil depth of each horizon between the previous (TAW_{OLD}) and revised (TAW_{NEW}) soils properties for each HRZ. As shown in **Figure 6-5**, TAW_{NEW} is 82.3% of TAW_{OLD} , and thus $\text{TAW}_{\text{NEW}} < \text{TAW}_{\text{OLD}}$. This will likely result in reduced yields simulated by AquaCrop.

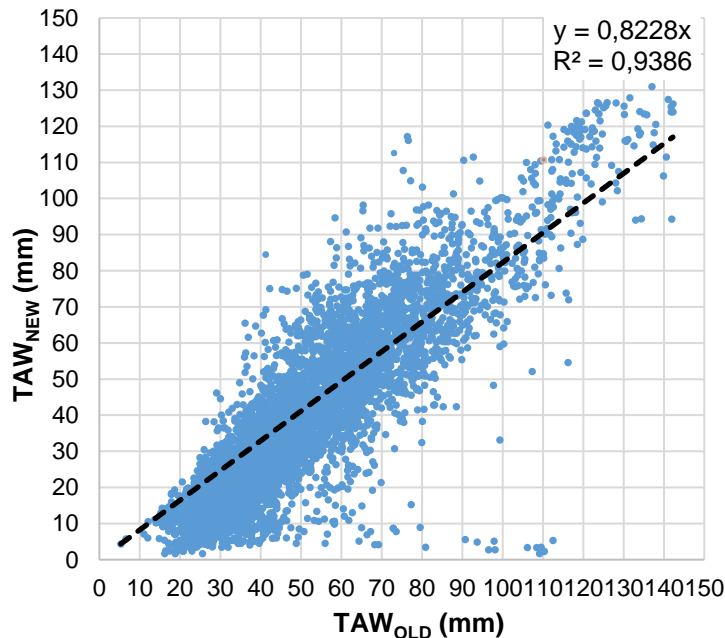


Figure 6-5 Comparison of total available water between the previous (TAW_{OLD}) and revised (TAW_{NEW}) soil properties for each HRZ

$\text{TAW}_{\text{NEW}} - \text{TAW}_{\text{OLD}}$ is therefore negative for 88.1% of all HRZs (**Figure 6-6**). The majority (70.9%) of these differences range from 0 to -20 mm. The difference is zero for 387 HRZs located in Lesotho and eSwatini since the soil properties in these HRZs was not updated. The largest difference of -107.9 mm occurred in zone no. 3,214, where TAW decreased from 110.3 to 2.4 mm, due to the large decrease in soil depth from 1.08 to 0.03 m. Similarly, the largest increase in TAW was 43.2 mm in zone no. 162 (i.e. from 41.2 to 84.5 mm), due to the lower soil water retention values, particularly for PWP for the B-horizon.

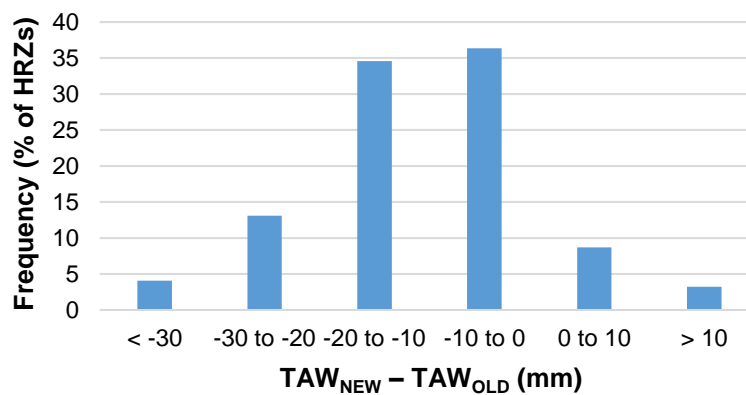


Figure 6-6 Differences in total available water (TAW) between the revised (TAW_{NEW}) and previous (TAW_{OLD}) soil properties for each HRZ

Readily evaporable water: REW expresses the maximum amount of water (mm) that can be extracted during stage I evaporation from a 4 cm soil surface layer. An equation provided by Raes et al. (2018) was used to derive REW (in mm) from the A-horizon's soil water content at FC and PWP (in vol %).

Saturated hydraulic conductivity: K_{SAT} represents the speed that soil water moves downward through the saturated pore spaces in soil. A pedo-transfer function developed by Saxton and Rawls (2006) was used to estimate K_{SAT} from soil water retention parameters (SAT, FC & PWP in vol %) for each soil horizon, as detailed by Kunz et al. (2020; cf. Equation 13). Values range of 35 to 3,000 mm day⁻¹ depending on soil texture (Raes et al., 2018).

Curve number: AquaCrop also requires the curve number (CN_{II}) for antecedent moisture class II (AMC II), i.e. a soil water content halfway between field capacity and permanent wilting point. CN_{II} was determined from estimated K_{SAT} for the topsoil. For example, if $K_{SAT} \leq 35$ mm d⁻¹, then CN_{II} is 77 for hydrological soil group D in good condition (Table 2.14d; p 2-165; Raes et al., 2018). This represents the highest runoff potential for soils with a high silt and clay content, which conduct water slowly through the soil profile, i.e. more runoff production due to reduced infiltration. At run time, the model adjusts CN_{II} based on the calculated wetness of the topsoil layer to a depth of 0.3 m (**Figure 6-7**).

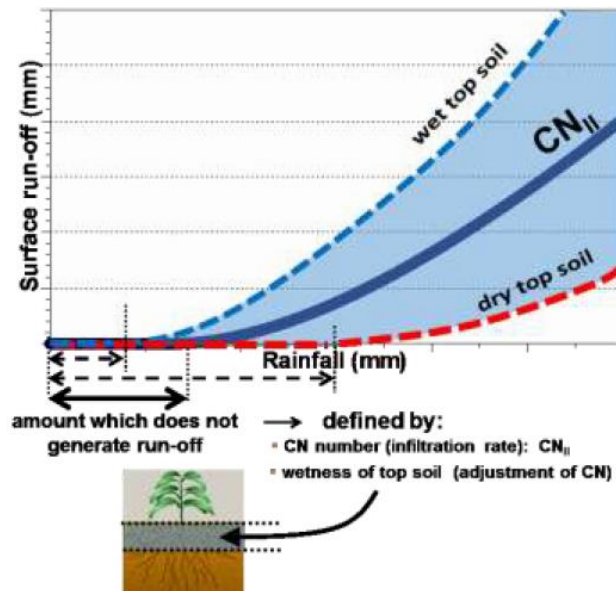


Figure 6-7 The rainfall-runoff relationship as a function of the topsoil wetness (RAES, 2016a)

One-layer vs two-layer soils: Although soil properties were derived for both the A- and B-horizons for each HRZ, the decision was made to depth weight the soil water retention parameters (SAT, FC & PWP) and K_{SAT} to create a one-layer soil profile. However, REW and CN_{II} were calculated from the soil properties for the A-horizon. This was done because AquaCrop more accurately simulated final yield using a single soil layer as opposed to two layers (i.e. topsoil & subsoil), as noted in **Section 4.2.7.2**. The impact of this decision on simulated yield is shown in **Section 6.3.1.3**.

6.2.2.4 Planting date and density

Under rainfed conditions, rainfall variability is an important determinant of crop yield. Thus, selecting a suitable planting date is important to ensure that critical growth stages do not coincide with dry spells. Based on an analysis of 50 years of rainfall and temperature data available for each HRZ (cf. **Section 6.2.2.2**), **Figure 6-8** shows the first planting date:

- could not be determined for 26.2% of all HRZs, thus indicating their unsuitability for crop production,
- occurs in either November or December for most (68.8%) of the HRZs, and
- occurs in October or January for a few (5.1%) HRZs.

Since the crop model was used to derive monthly crop coefficients (K_c) for unstressed growing conditions, the planting day was set to the beginning of the month (not mid-month) so that the initial K_c value was averaged from 30 days of crop water use simulations (not 15 days). Hence, the 1st of November and 1st of December were selected as the two planting dates used in this project, which is the same approach adopted by Kunz et al. (2020).

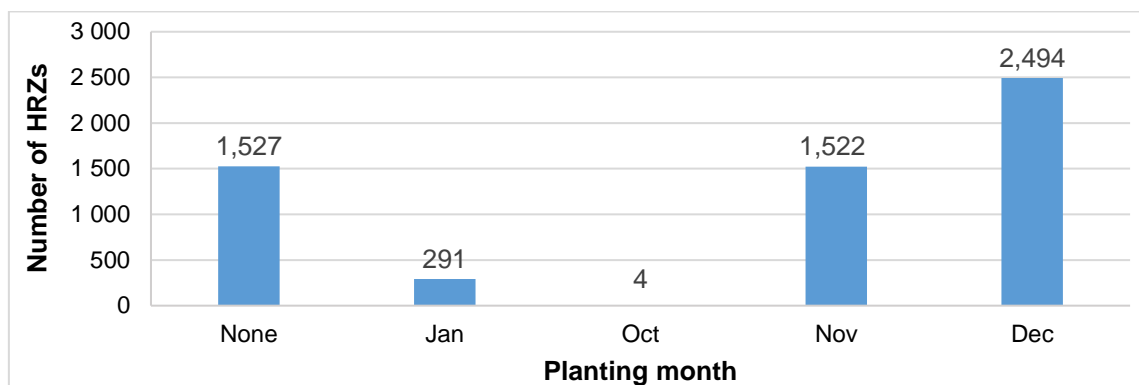


Figure 6-8 Histogram of the average planting month determined from 50 years of climate record for each of the 5,838 altitude zones (Kunz et al., 2020)

For each crop, two plant densities were used that represent smallholder and commercial farming environments, e.g. 10,000 and 27,000 plants ha⁻¹ for taro, respectively (cf. **Section 3.1.2**). For sweet potato, DAFF (2011) recommended plant densities ranging from 31,447 to 37,037 plants ha⁻¹ (**Section 3.1.1**), whereas Beletse et al. (2013) used 41,447 plants ha⁻¹. However, international modelling studies on sweet potato used values of 55,556 (Amaro et al., 2023), 83,000 (Pushpalatha et al., 2021) and 90,000 (Rankine et al., 2015) plants ha⁻¹ for Ethiopia, India and Jamaica, respectively. Therefore, plant densities of 31,447 and 55,556 plants ha⁻¹ were used to represent smallholder and commercial farming environments, respectively. Ideally, a third plant density should be considered for each crop, but this represents additional four national model runs for AquaCrop (and ACRU).

6.2.2.5 Management options

For the national scale runs, the management file for AquaCrop was setup to reflect the following: (i) no soil fertility stress, (ii) no contours or soil bunds to reduce runoff, and (iii) no weed stress. Since crop coefficients should be obtained under standard (i.e. non-stressed) growing conditions, AquaCrop has a useful feature to estimate a crop's irrigation water requirements, where irrigation water is added to the soil profile to artificially relieve crop water stress. Hence, irrigation was invoked in AquaCrop to relieve plant stress, which was assumed to occur when the soil water content dropped below 60% of readily evaporable water (cf. **Table 7-3** in **Section 7.2.3.2**).

6.2.3 Model parameters

The field trials conducted at Fountainhill in the second season were under rainfed conditions (cf. **Chapter 4**). Furthermore, the trials were initially affected by weed growth up to 82 and 57 DAP for OFSP and taro, respectively. Such growing conditions may have affected the attainable biomass production and root/tuber yield. Since growing conditions were not considered optimum in terms of minimal water stress, only a limited number of crop parameters could be adjusted. Despite the few

adjustments made, AquaCrop under-estimated the final yield of OFSP and taro by 21% (cf. **Section 4.3.7.5**) and 64% (results not shown), respectively. Mabhaudhi (2012) stated that further work was required to improve taro simulations for rainfed conditions. Furthermore, **Table 16-6** (cf. **Section 16.2**) highlights likely errors in parameter values obtained from the literature. Hence, there was a need to improve the calibration for both RTCs.

Using measurements of crop growth and yield from season 3, additional model parameters for OFSP and taro were fine-tuned as described in **Section 5.2.6**. These modified parameters provided better estimates of biomass and yield for both crops, as shown in **Section 5.3.7**, especially for OFSP. For the stressed water treatment, AquaCrop accurately simulated the final yield of OFSP and taro, with deviations of -0.6 and -4.4%, respectively. This represents a valuable contribution by this project. However, the model over-estimated the yield for unstressed conditions, especially for taro. Overall, additional work is needed to refine the calibration of OFSP and taro and to further test the model for rainfed conditions. This requires high-quality datasets from other locations and crop seasons than those used in this project. This is particularly important for RTCs since large variations exist between landraces. Crop parameters shown in **Table 16-14** to **Table 16-16** (cf. **Section 16.4**) were used for the national scale model runs.

6.2.4 Minimising computational expense

Running AquaCrop at a national scale for 5,838 HRZs, each with 50 years of dally climate data and representative soil data, is computationally expensive. This ability was first developed in 2015, where a national run took up to 16 days to complete, and a summary of the methodology is provided in **Section 17.1**. Since then, additional improvements were made in 2019, and again in 2023 for this project. This effort has been worthwhile considering a national model run now takes under three hours to complete. A detailed and technical description is provided in **Section 17.2** (2019 improvements) and **Section 17.3** (2023 improvements) to assist other researchers and modellers to improve model performance and to benefit from the experience gained over the past nine years. It is important to note that this work, which is considered innovative, was only possible due to funding received from the WRC.

6.2.5 Modelling approach

AquaCrop was then run at the national scale using climate and soils data currently available for each of the 5,838 HRZs (homogeneous response zones; also referred to as altitude zones and previously called quinary catchments). For both rainfed and irrigated conditions, model runs were undertaken for:

- two RTCs (OFSP and taro);
- two planting dates (1st of November and 1st of December);
- two plant densities representing smallholder
 - (i.e. 31,447 and 10,000 plants ha⁻¹ for OFSP and taro respectively); and
- commercial farming environments
 - (i.e. 55,556 and 27,778 plants ha⁻¹ for OFSP and taro respectively).

The above modelling scenarios were required to meet Aim 3 (cf. **Section 1.2**), i.e. to model the water use and yield of selected RTCs. AquaCrop output was then used to meet the following project aims:

- Aim 4: develop land suitability maps for each RTC (cf. **Chapter 8**);
- Aim 5: map the spatial variability in crop yield, crop cycle and water productivity (CWP and NWP; this chapter); and
- Aim 6: derive monthly crop coefficients for each HRZ as input for the ACRU model (cf. **Chapter 7**).

Kunz et al. (2015b) developed a utility to calculate statistics for most of AquaCrop's (version 4) output variables. The utility was used to extract simulated output for each of the 49 simulated seasons (1950/51 to 1998/99). It then calculated the following 19 statistics for each output variable: mean, variance, standard deviation, coefficient of variation, skewness, kurtosis, minimum, maximum, sum and number of seasons, as well as 10th to 90th percentiles. This stats utility was modified by Kunz et al. (2020) to include new variables outputted by version 6 of AquaCrop. Recently, the utility was thoroughly checked by comparing results with those calculated in MS Excel for each output variable.

For the irrigated runs, the utility also calculated monthly crop water use (ET_c in mm) as the sum of transpiration (Tr) and soil water evaporation (E), i.e. crop evapotranspiration accumulated over the growing season for unstressed conditions. From this, monthly crop (or water use) coefficients (K_c) were calculated as the ratio of crop ET_c to ET_o . The values obtained for each season were then averaged to obtain long-term monthly crop coefficients, where a unique set of values was calculated for each HRZ. This procedure has been fully automated to minimise computational expense.

6.3 RESULTS AND DISCUSSION

Output from the national-scale AquaCrop model runs facilitated the mapping of simulated crop yield, crop cycle, CWP and NWP for OFSP and taro. Four maps were produced per crop since the model was run for two planting dates, each with two plant densities. The maps clearly highlight the spatial variability of these metrics, especially due to changes in planting date and plant density. Areas in light grey identify HRZs where the statistic is zero, i.e. average (AVE) or coefficient of variation (CV). These are highlighted separately for better interpretation of maps. For example, a zero CV in crop yield indicates all seasonal yields were identical, which only occurs when they are all zero. Furthermore, areas in white identify HRZs where no statistics were produced. This occurs when three or less seasons were simulated by the model (i.e. too few data points), which is discussed next in more detail.

The HRZs coloured white are simply too cold for crop production. In these areas, the crop cycle is typically longer than 365 days in all 49 seasons, resulting in average yields that are either 0 t ha⁻¹ or very low (< 0.1 t ha⁻¹). As explained in **Section 17.3.5**, the model is no longer run for these zones to improve performance, and thus the average yield is set to -999 to indicate no (i.e. missing) value. This value was used (and not zero) so that these zones can be distinguished from those with a very small average yield that rounds to 0 t ha⁻¹. This decision not only resulted in better model run times, but also prevented seasonal yield averages from being skewed by zero values. This new approach therefore eliminates average yields close to 0 t ha⁻¹ since the yield is set to -999. Furthermore, it prevents the coefficient of variation in seasonal yield from being 0%, which as explained in **Section 6.3.1.2**, is misleading.

6.3.1 Yield

6.3.1.1 Average yield

Yield estimates are in dry tons per hectare (dry t ha⁻¹) and were derived using AquaCrop for each of the 5,838 HRZs (or altitude zones). The model was run in GDD mode to simulate the effects of temperature on crop production. The mean yield was calculated from up to 49 seasonal estimates (1950/51-1998/99). Dry yields can be converted to fresh yields using the dry:fresh ratios derived from observations in season 2 (cf. **Section 4.4**) and season 3 (**Section 5.4**). The accuracy of yield estimates is largely dependent on the success of the calibration. The partial calibration procedure is described in **Section 6.2.3** but more details can be found in **Section 5.3.7**.

All four maps produced for each crop highlight the suitability of the eastern seaboard for rainfed crop production, which is not surprising since the same areas currently produce commercial timber and sugarcane, which have higher rainfall requirements than most crops. Although an average yield was simulated for each HRZ, the entire zone may not be suitable for crop production due to current land uses, which is discussed further in **Section 8.4.3**. Furthermore, each altitude zone is considered a homogeneous response zone, which does not consider microclimatic effects. In general, the higher plant density produced higher yields, particularly in areas with sufficient rainfall, i.e. along the eastern seaboard of South Africa and eSwatini. However, such increases are only visible when the mean seasonal yield crosses a mapping range.

The two planting dates were derived by Kunz et al. (2020) from an analysis of historical climate data from 1950-1999. However, weather is known to vary between seasons, which affects the selection of planting dates. Hence, it is acknowledged that planting dates should be determined using climate forecasts, rather than using historical data. Access to seasonal weather forecasts is recommended so that farmers can select appropriate planting dates. Despite this, the maps show the impact of planting date on attainable yields, thus highlighting the month that produced the higher yield.

The spatial extent of the maps was largely influenced by two factors. Firstly, the model is no longer run for HRZs where the climate is deemed too cold for economically viable crop production. These zones were identified using crop cycle, which typically exceeds 365 days. Since both RTCs are frost sensitive, the first severe frost is likely to kill the leaves, and thus the crop should be harvested. This decision not only reduces model run time, but also prevents many zero (or very small) seasonal yields from being simulated, which tend to skew the mean statistics. These zones are marked as unsuitable on the maps and not coloured (i.e. appear white). These cold HRZs are clearly identified in red in **Figure 8-5** and **Figure 8-6** (cf. **Section 8.4.1**). Secondly, the extremely warm conditions experienced in the greenhouse during frequent load shedding and load reduction events during season 3 resulted in a rapid accumulation of heat units (in GDD). Hence, the thermal time to reach physiological maturity was higher than expected, especially for OFSP. This resulted in the simulation of zero or very low yields in the cooler interior regions of the country.

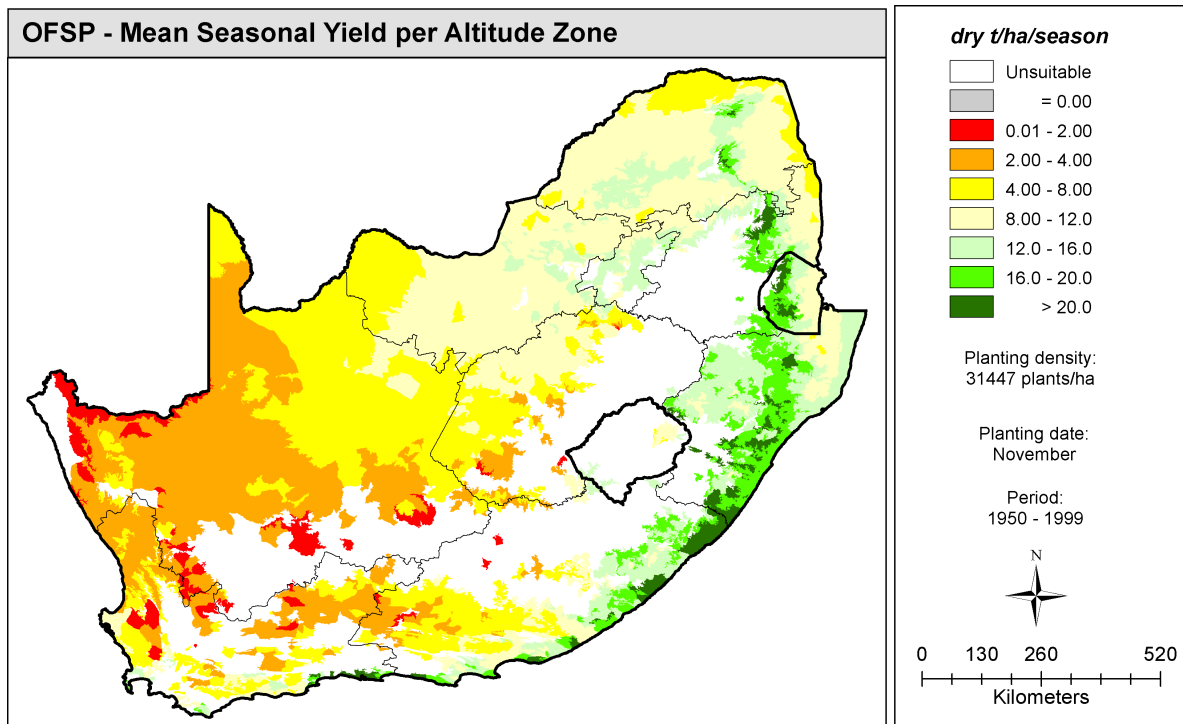
The four maps for each RTC represent rainfed conditions where attainable yield is not affected by weed growth, soil fertility, soil salinity or pests and diseases. Hence, actual yields will be lower, especially in low-input farming systems. A comparison of the four maps is useful for assessing the impact of (i) November vs December plantings, and (ii) low vs high plant densities. For the lower density scenario, it may have been better to model fertility and weed stress. According to Nyathi et al. (2016), sweet potato is ideally suited for two diverse farming systems practised in South Africa, namely (i) low external input agriculture that encourages use of on-farm inputs, and (ii) high input agriculture, which promotes the use of off-farm resources such as irrigation, fertiliser and pesticides (Daberkow and Katherine, 1988). Nyathi et al. (2016) ran AquaCrop for three different locations for both low (water-stressed; no fertiliser) and high (irrigated; fertilised) inputs. Results showed potential yield increases for OFSP of 173-309% (**Table 6-1**). Nyathi et al. (2016) encouraged all stakeholders to use AquaCrop for decision making, and also for identifying suitable locations where crops can grow optimally.

Table 6-1 Simulations of OFSP yield at three locations under low and high input agriculture (Nyathi et al., 2016)

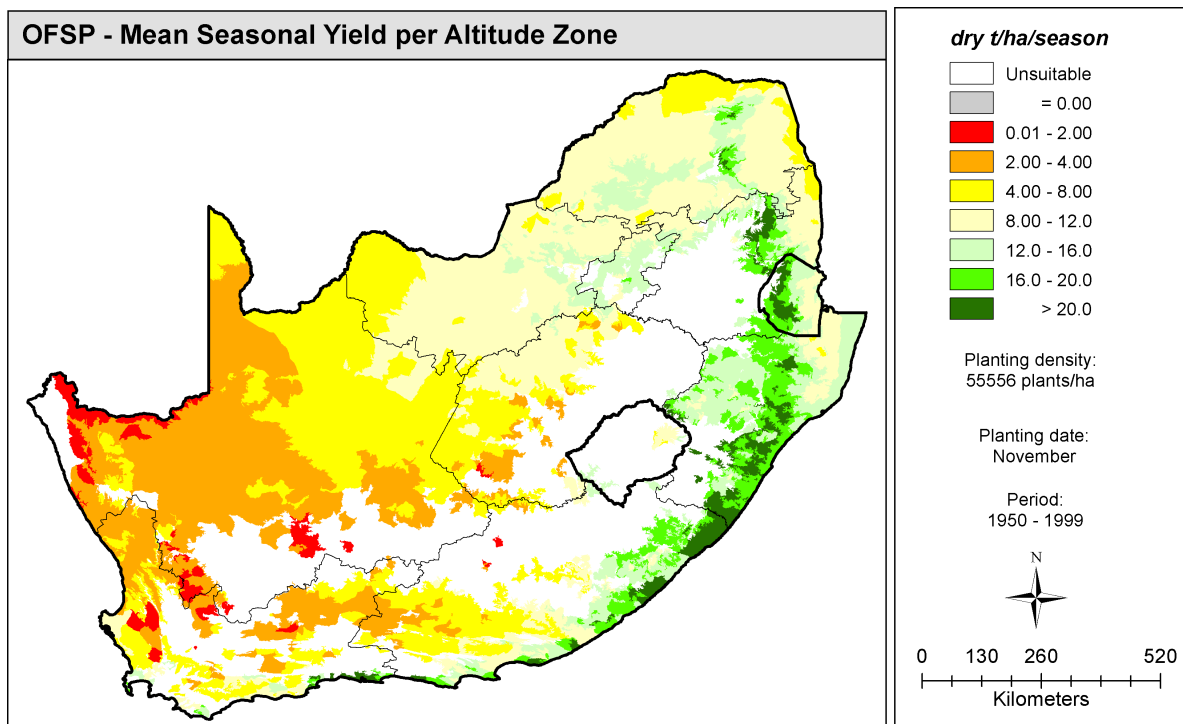
Characteristic	Dzindi	Tugela Ferry	Dingleydale
Province	Limpopo	KwaZulu-Natal	Mpumalanga
Latitude (S)	23°01'	28°44'	24°41'
Longitude (E)	30°26'	30°27'	31°10'
Rainfall (mm)	< 500	700	600
Altitude (m)	712	699	478
Yield (t ha ⁻¹)			
- low input	3.0	2.6	3.2
- optimum	10.5	7.1	13.1
- increase (%)	250	173	309

OFSP: **Figure 6-9** to **Figure 6-10** show average OFSP yields for two plant densities (i.e. 31,447 and 55,556 plants ha⁻¹) and two planting dates (1st of November and 1st of December). These maps, which were produced for the first time in this project, highlight the potential of OFSP production in the country, especially since the crop produces larger yields compared to taro. A comparison of the maps indicates larger yield changes due to the planting date rather than plant density. Irrespective of the plant density, there is a general decrease in yield due to the later planting (December), most notably along the eastern seaboard.

Taro: **Figure 6-11** to **Figure 6-12** show average taro yields for two plant densities (i.e. 10,000 and 27,778 plants ha⁻¹) and the same two planting dates. Owing to the longer crop cycle of 180 days (vs 160 days for OFSP), cooler areas (at higher altitudes) in the interior of the country are less suited to taro production. Taro yields are higher along the eastern seaboard when planted in December, especially at the higher density. However, the Limpopo province is better suited to a November planting.

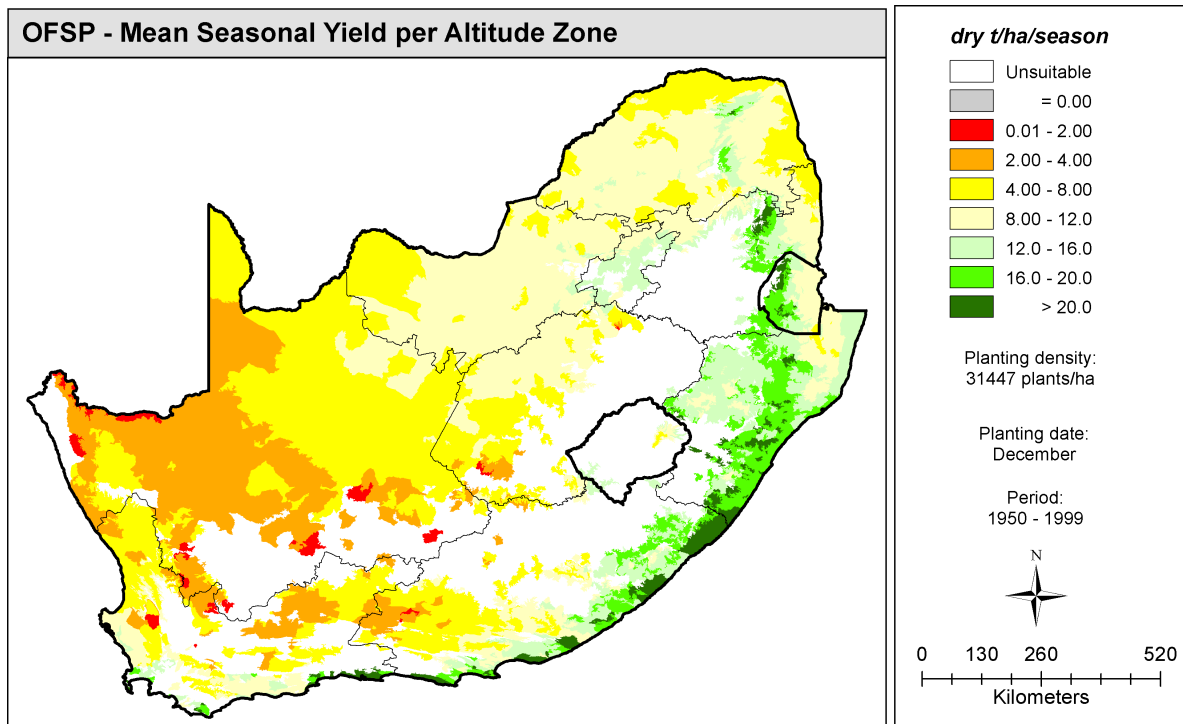


(a)

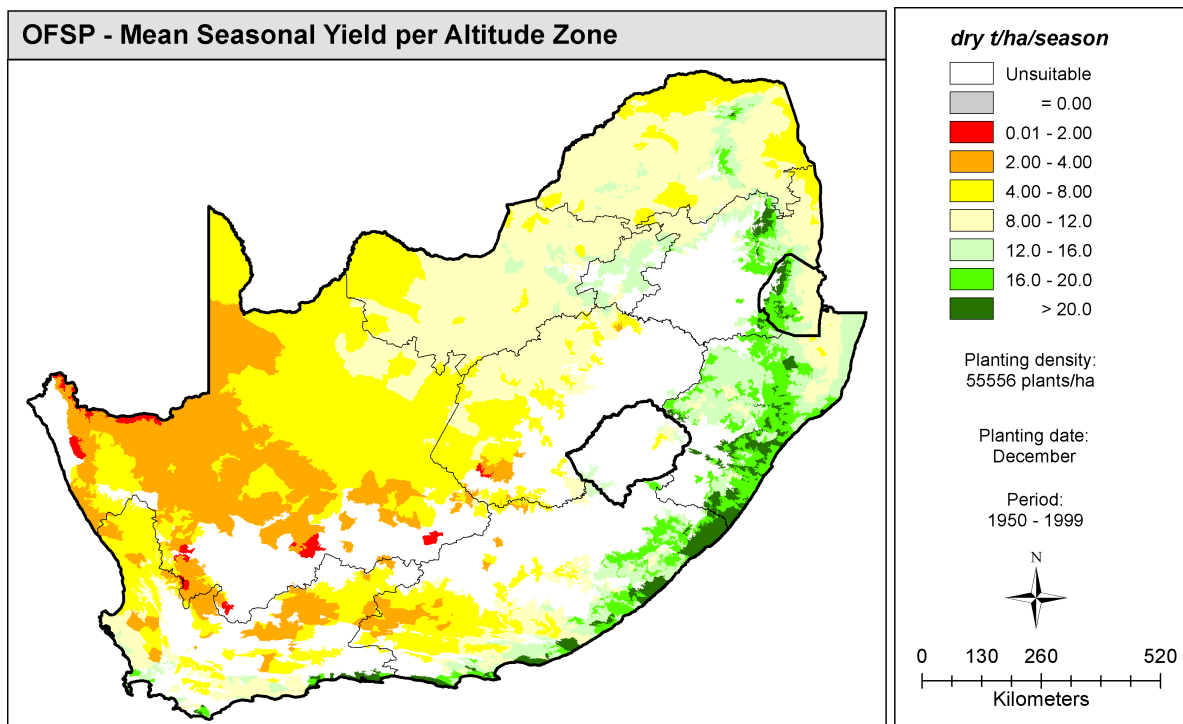


(b)

Figure 6-9 Averaged seasonal yield for OFSP planted in November at a density of (a) 31,447 and (b) 55,556 plants ha⁻¹

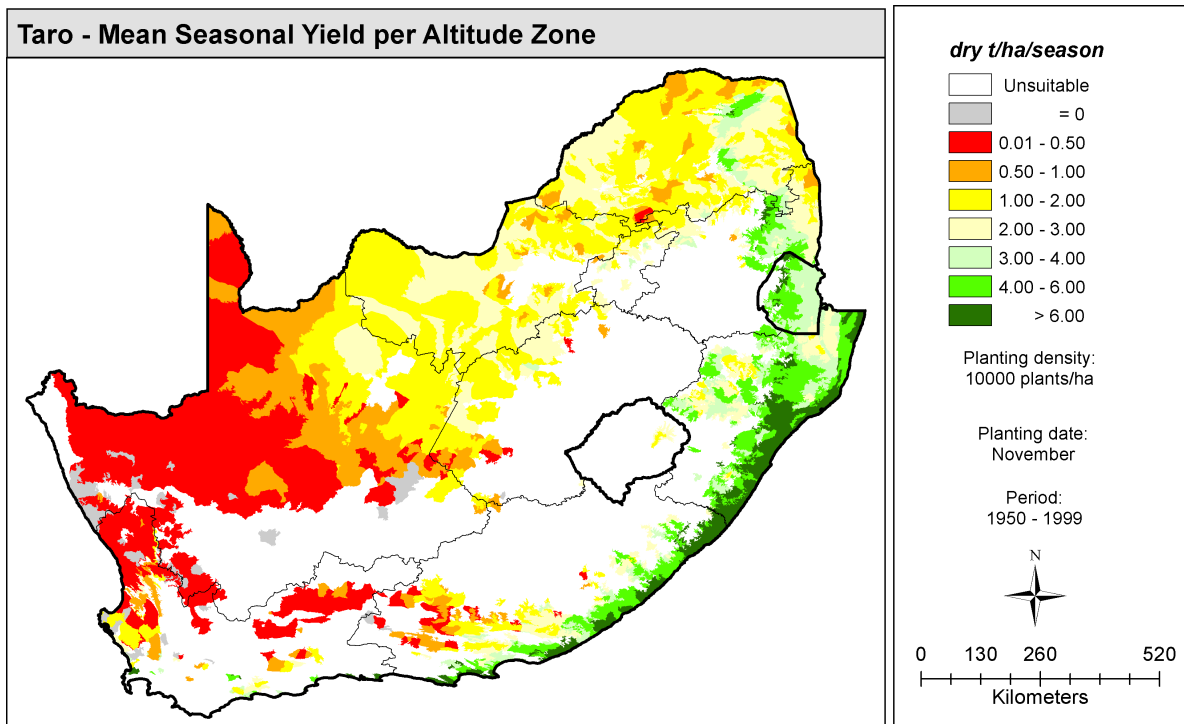


(a)

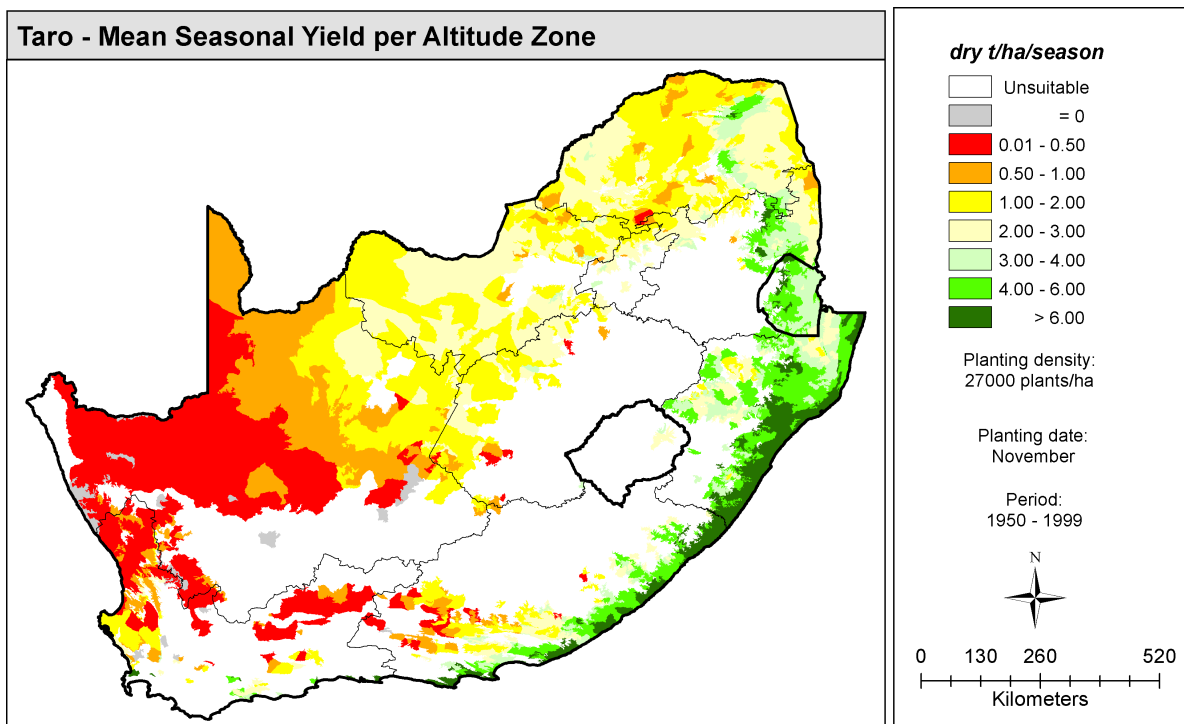


(b)

Figure 6-10 Averaged seasonal yield for OFSP planted in December at a density of (a) 31,447 and (b) 55,556 plants ha⁻¹

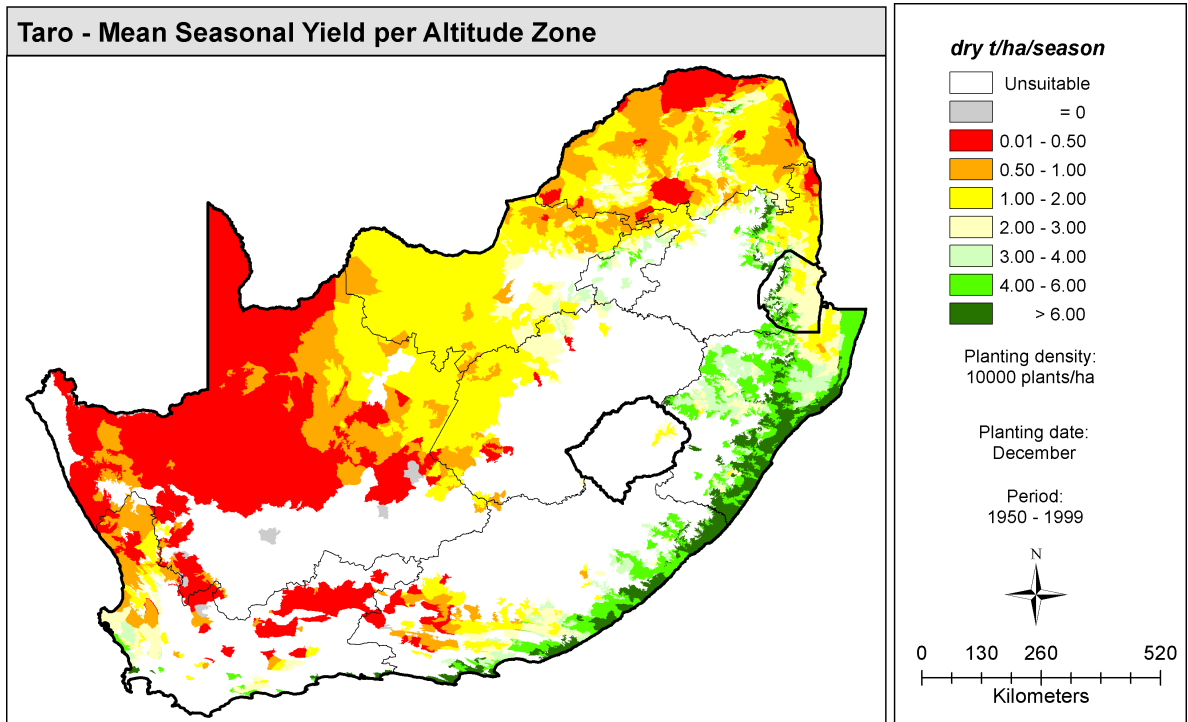


(a)

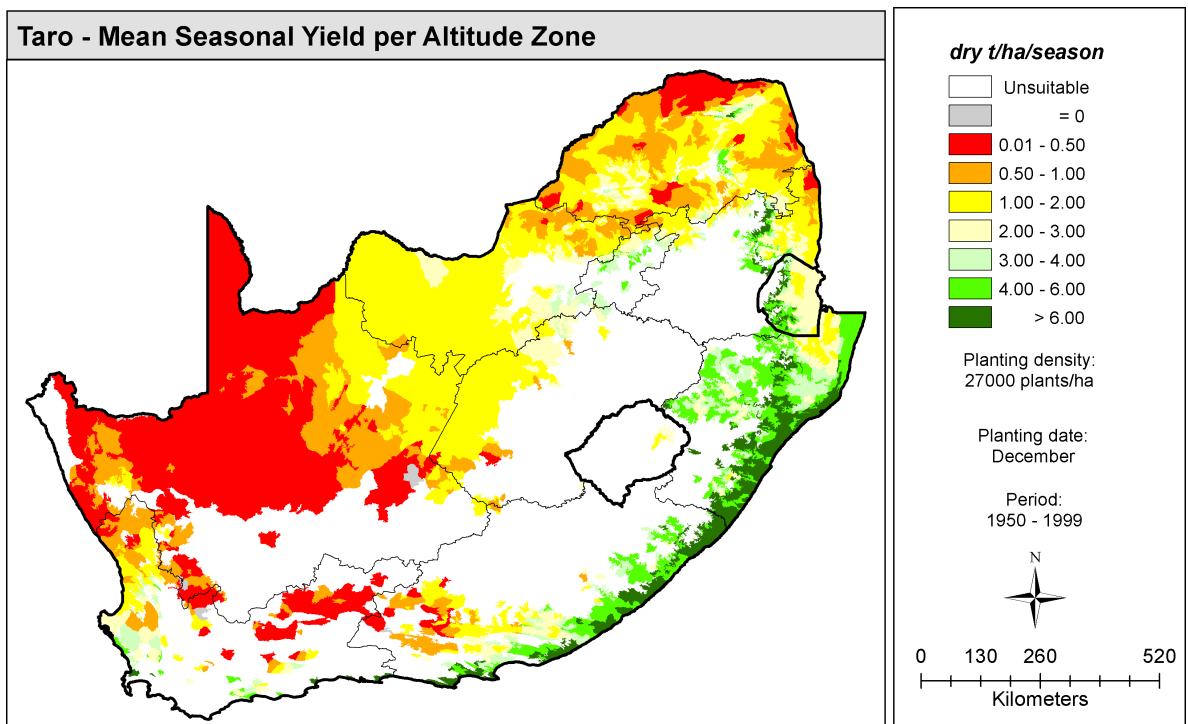


(b)

Figure 6-11 Averaged seasonal yield for taro planted in November at a density of (a) 10,000 and (b) 27,000 plants ha⁻¹



(a)



(b)

Figure 6-12 Averaged seasonal yield for taro planted in December at a density of (a) 10,000 and (b) 27,000 plants ha⁻¹

6.3.1.2 Coefficient of variation

The simple yield models developed by Smith (2006) only provide one yield estimate using long-term (i.e. annual) climate data, whereas AquaCrop provides up to 49 seasonal yields from 1950/51 to 1998/99. From this, the inter-seasonal variation in crop yield (Y_{CV}) can be determined, which represents a major advantage of using AquaCrop. This useful statistic describes how the yield varies over the 49 consecutive seasons. However, it is important to fully understand the impact of zero yields on this statistic.

The model typically simulates a zero yield when the crop fails to germinate or dies early in a particular season, due to the seasonal climate being too cold or too dry. Furthermore, if the crop cycle is beyond 365 days (i.e. season's climate is too cold), the model is no longer run (i.e. no yield estimate) and the yield is marked as missing, i.e. -999 (cf. **Section 17.3.5**). Hence, the number of simulated seasons will be less than 49. If the total number of simulated seasons is three or less, then no statistics (e.g. Y_{AVE} , Y_{CV} , etc.) are calculated since there are too few data points, i.e. Y_{CV} is set to -999. Such areas are deemed unsuitable for crop production and are coloured white on the maps. This prevents instances of Y_{CV} being 0% (i.e. identical yield values of 0 t ha⁻¹).

Table 6-2 provides a clearer understanding of how Y_{CV} is affected by the number of seasons with zero yields, relative to the total number of simulated seasons. Y_{CV} is 0% when all simulated seasons have zero yield and reaches a maximum value of 700% when 48 of the 49 seasons have a zero yield. A Y_{CV} value of 0% can therefore be misleading, especially when Y_{CV} is mapped in classes, since < 5% identifies zones that are highly suited to crop production (due to low yield variability), yet it includes zones where all simulated yields are zero (i.e. zones too cold for crop production). Hence, it is best to map Y_{CV} of 0% separately (coloured grey on the maps), thus highlighting all zones also deemed unsuitable for crop production. Hence $Y_{CV} > 0\%$ should then be used to classify highly suitable cropping areas. As highlighted in **Table 6-2**, if most of the simulated seasons have zero yield values, this results in high Y_{CV} values.

Table 6-2 Effect of zero yields on the coefficient of variation in seasonal yield (Y_{CV})

Y_{CV} (%)	No. of zero yields	Total no. of seasons
0	n	n
245	5	6
265	6	7
400	15	16
412	16	17
436	18	19
469	21	22
480	22	23
500	24	25
600	35	36
671	44	45
678	45	46
686	46	47
693	47	48
700	48	49

As shown in **Figure 6-13** for taro planted in November at a density of 10,000 plant ha⁻¹, low Y_{CV} is associated with high average yields, which is expected. Average yields exceeding 10 dry t ha⁻¹ (17 in total) exhibited Y_{CV} values ranging from 14.8 to 45.1%. For $Y_{CV} > 150\%$, average yields were below 1.46 dry t ha⁻¹. Average yields below 0.35 dry t ha⁻¹ typically exhibit high Y_{CV} values exceeding 134%. From **Table 6-2**, a Y_{CV} of 700% indicates the average was calculated from only one non-zero yield. This was the case for 12 HRZs, where the average yield ranged from 0.00 to 0.10 dry t ha⁻¹. Y_{CV} was 0% for a total of 40 zones where the average yield was zero dry t ha⁻¹.

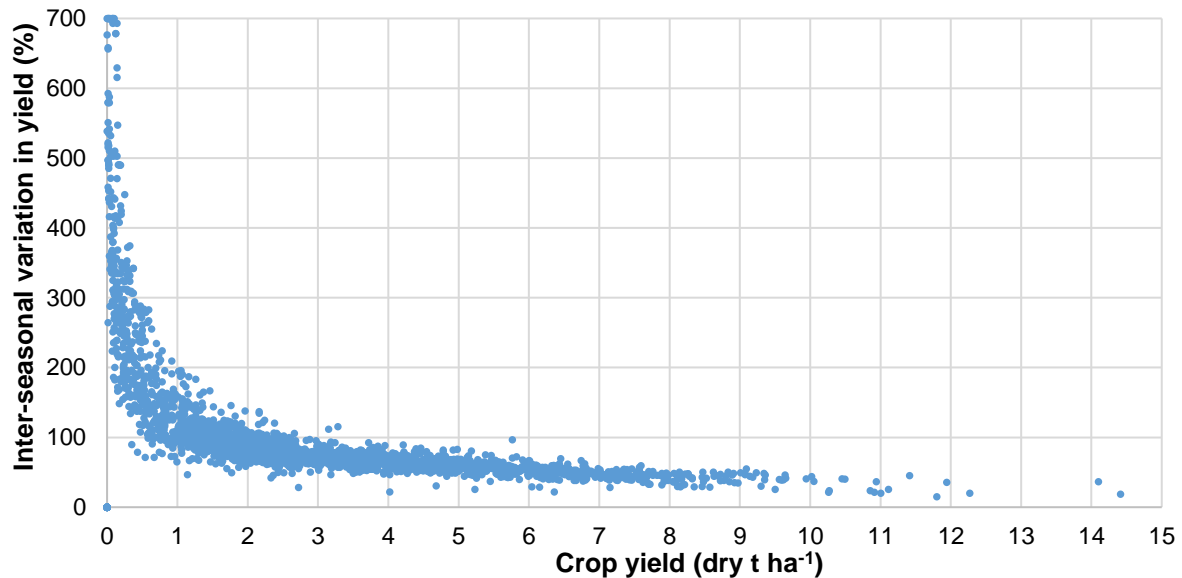
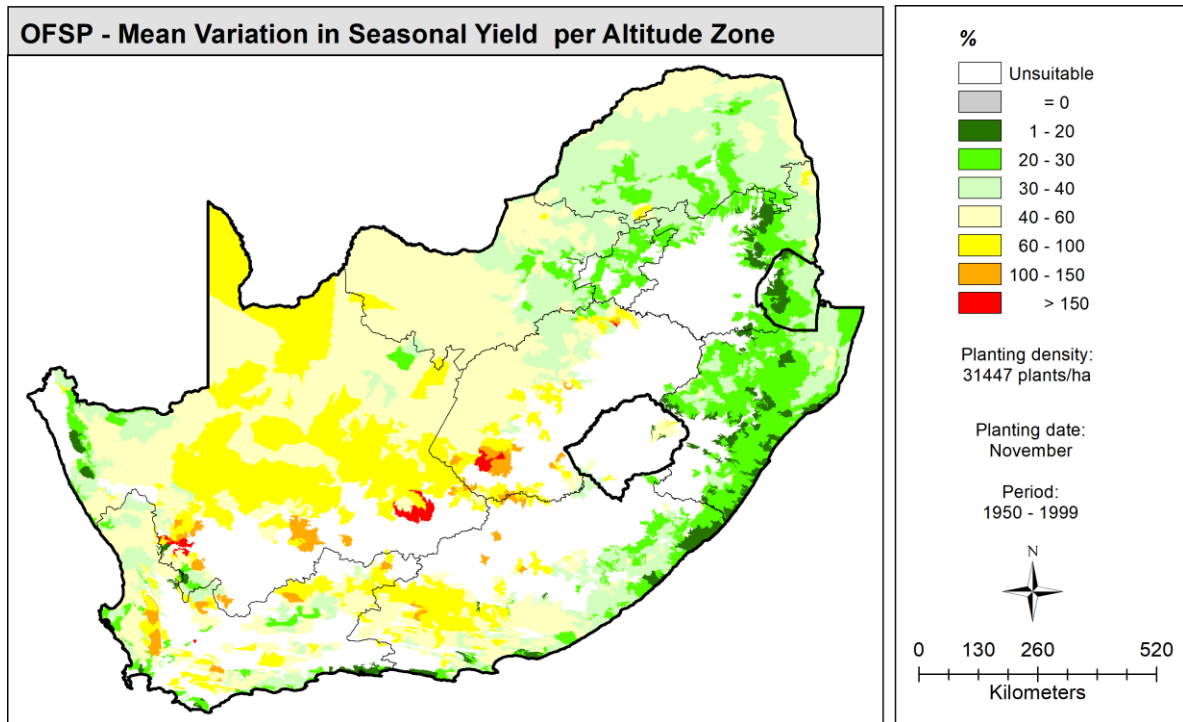


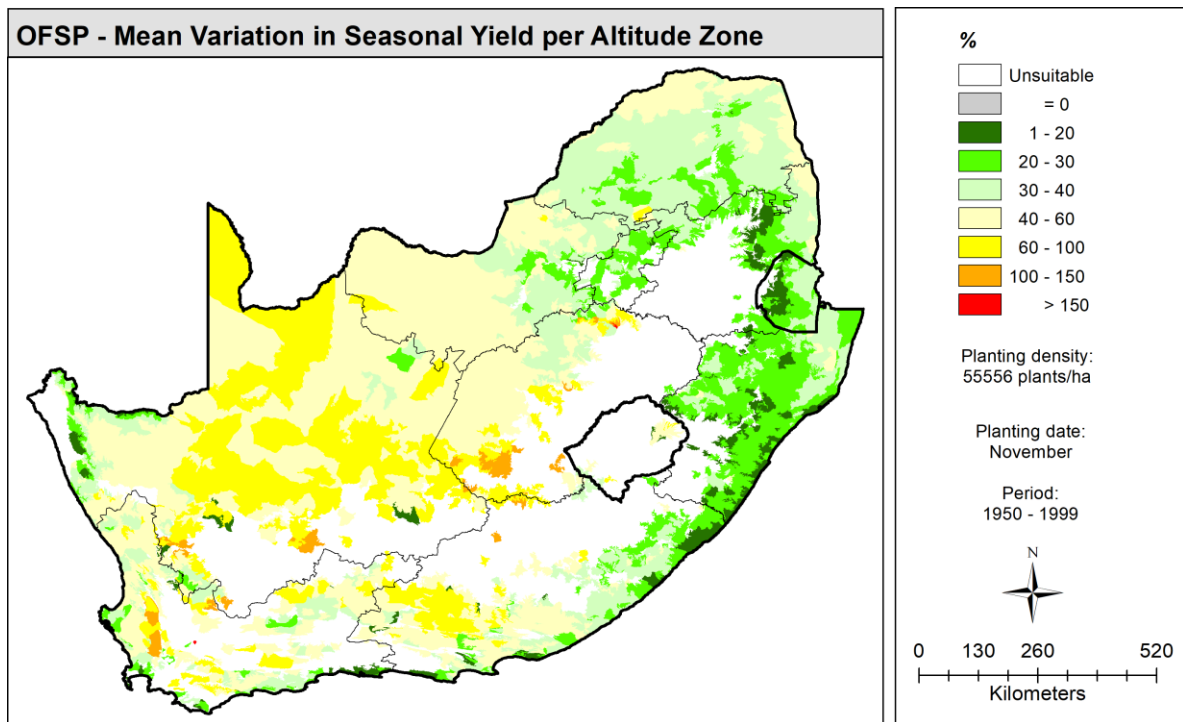
Figure 6-13 Relationship between non-zero seasonal yield averages for taro and the inter-seasonal variability in yield across 2,452 HRZs, as simulated by the AquaCrop model

OFSP: As noted above, high Y_{CV} is typically associated with low yields, and thus crop cultivation in these areas should be avoided. Such zones are typically located in the drier western parts of the country that are associated with erratic (i.e. more variable) monthly rainfall. As expected, Y_{CV} is lower along the eastern seaboard of the country where rainfall is sufficient to support not only rainfed crop cultivation, but commercial timber and sugarcane production. More zones had a low Y_{CV} (1-20%) for the November planting, in particular along the coast of KwaZulu-Natal (**Figure 6-14**) and are best suited to crop production.

Taro: As shown in **Figure 6-16** and **Figure 6-17**, Y_{CV} for taro is higher than for OFSP, particularly for a December planting. This indicates taro yields are more variable across the 49 seasons compared to OFSP, especially in the Limpopo province. It is important that the average yield and Y_{CV} maps are interpreted together, which will help explain why yields are lower in certain regions where Y_{CV} is higher. There are more zones with Y_{CV} of 0% (coloured grey on the maps), which are much easier to identify compared to the OFSP maps. The November planting at the lower density produced more zero Y_{CV} values in the Northern Cape province. This highlights the importance of mapping HRZs where Y_{CV} is 0%, so that these zones are not classified as highly suitable (i.e. $Y_{CV} < 20\%$).

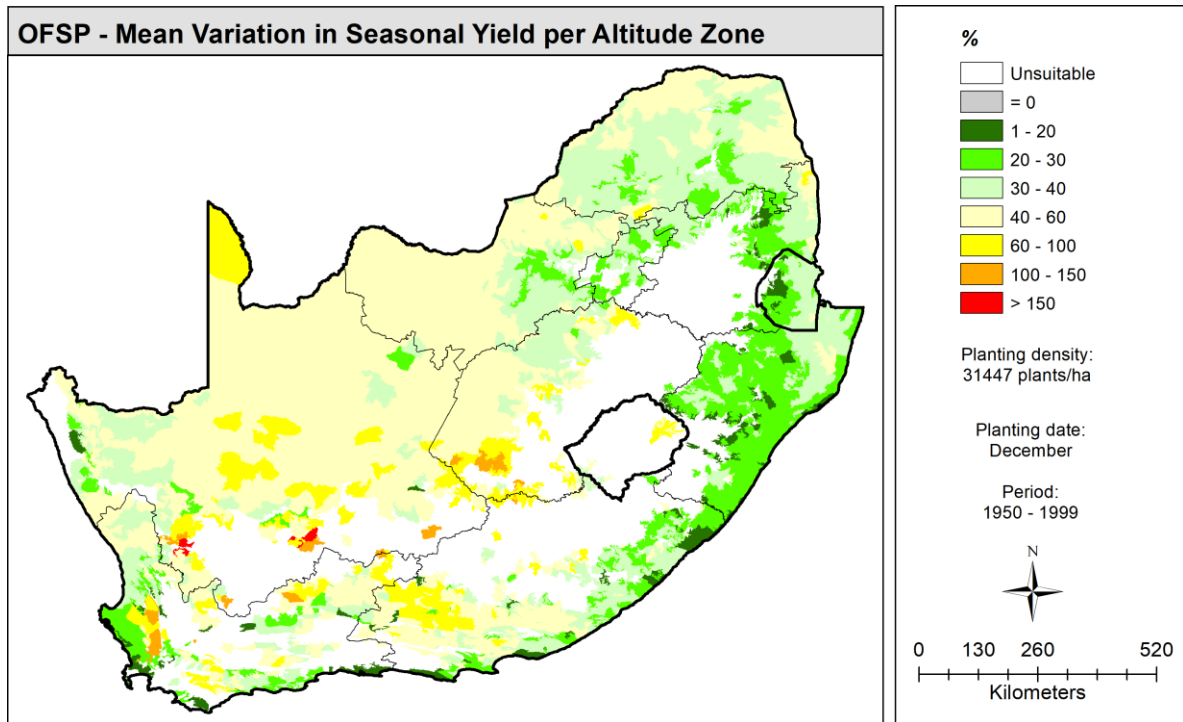


(a)

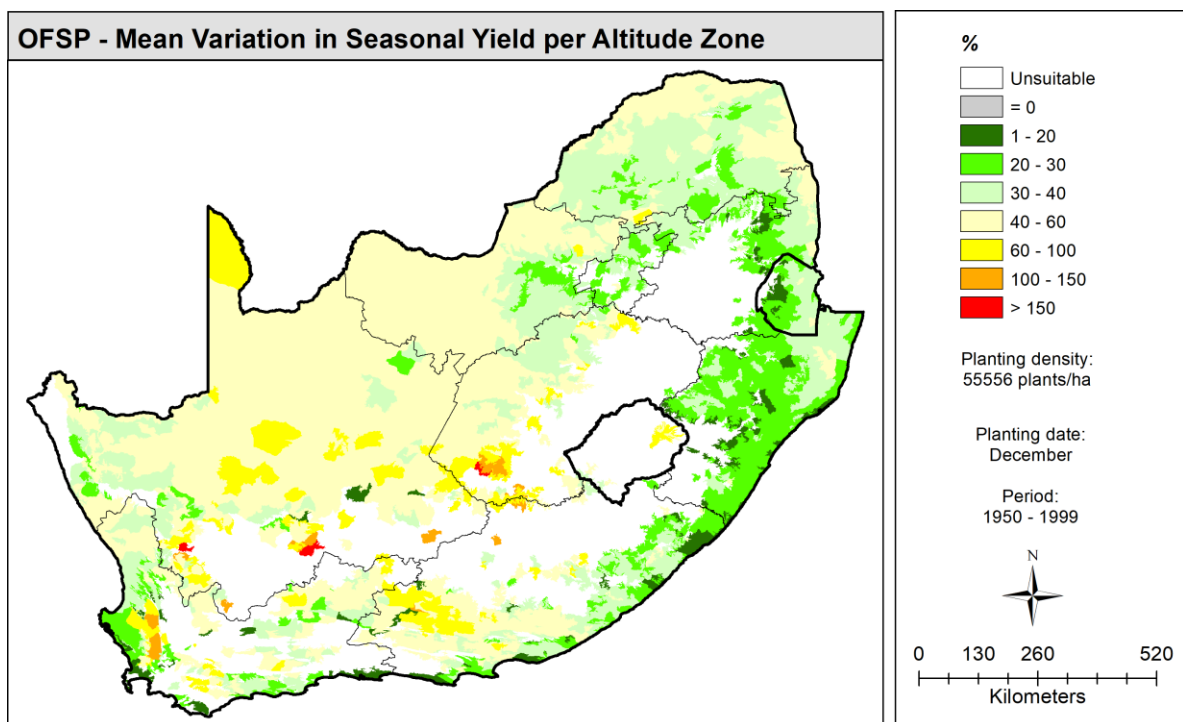


(b)

Figure 6-14 Inter-seasonal variation in yield for OFSP planted in November at a density of (a) 31,447 and (b) 55,556 plants ha⁻¹

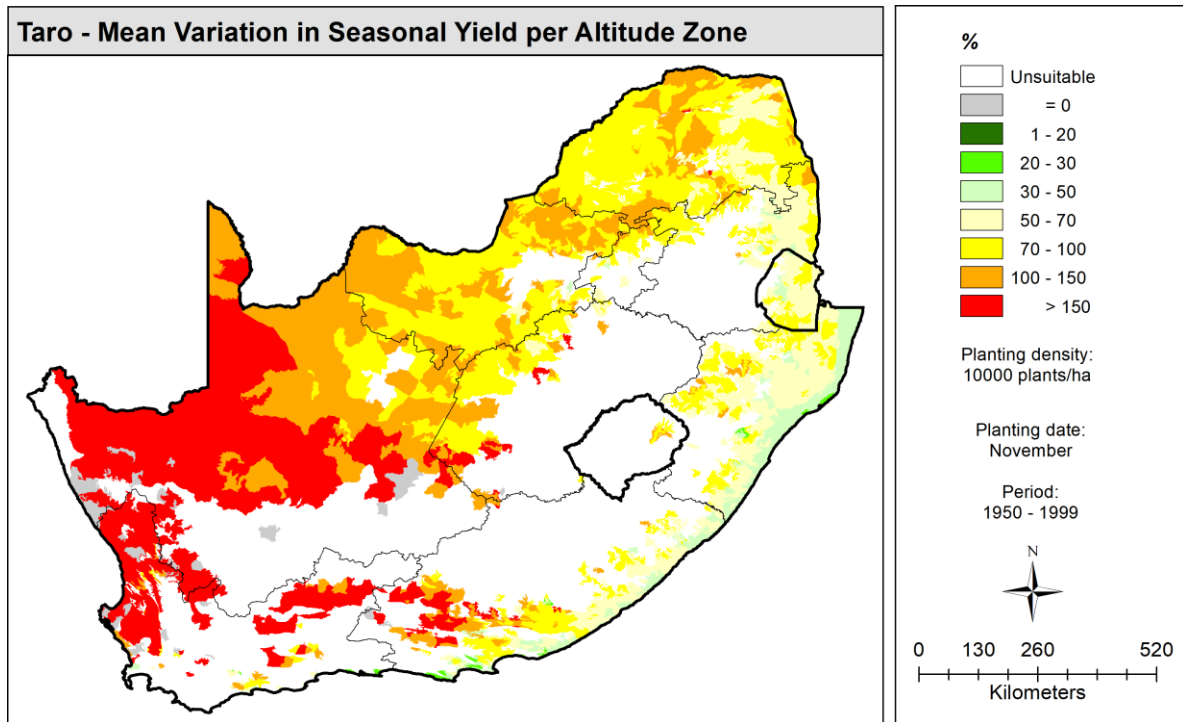


(a)

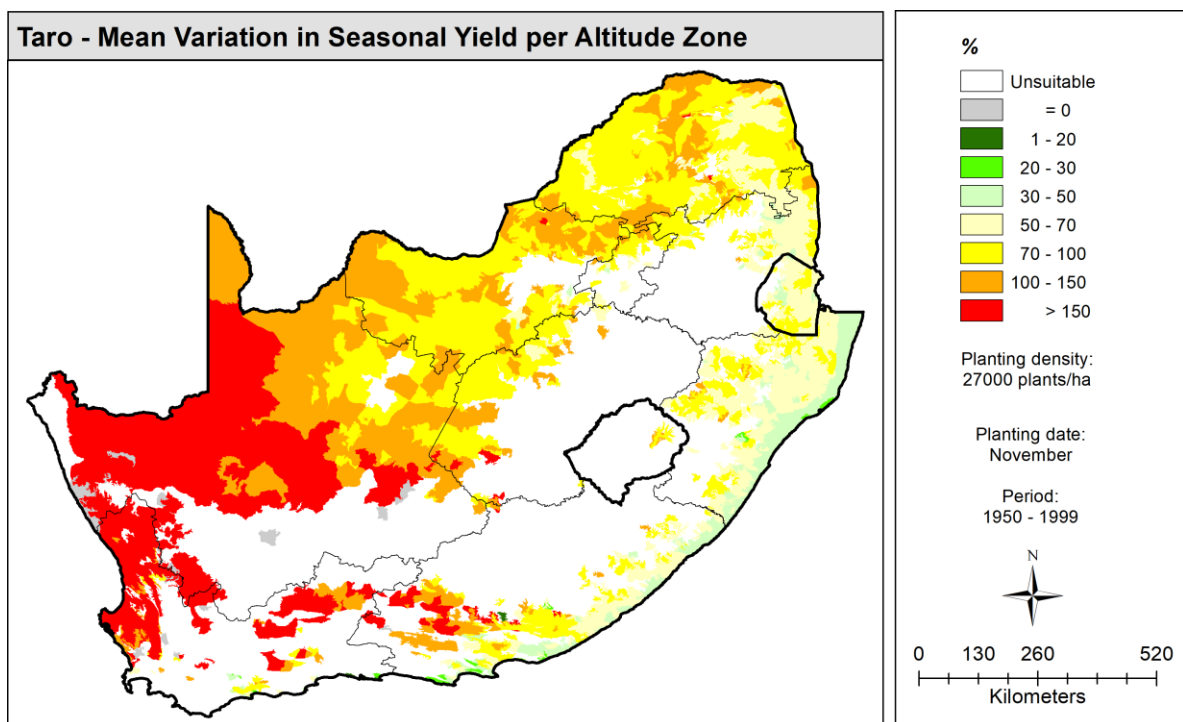


(b)

Figure 6-15 Inter-seasonal variation in yield for OFSP planted in December at a density of (a) 31,447 and (b) 55,556 plants ha⁻¹

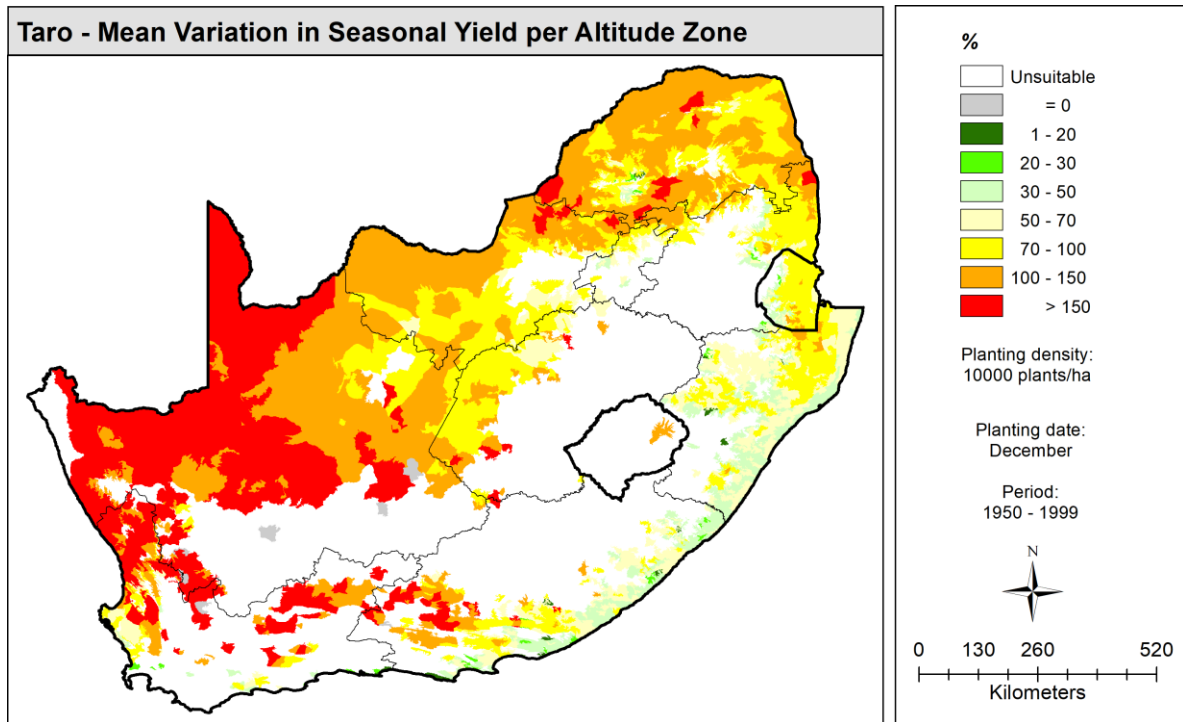


(a)

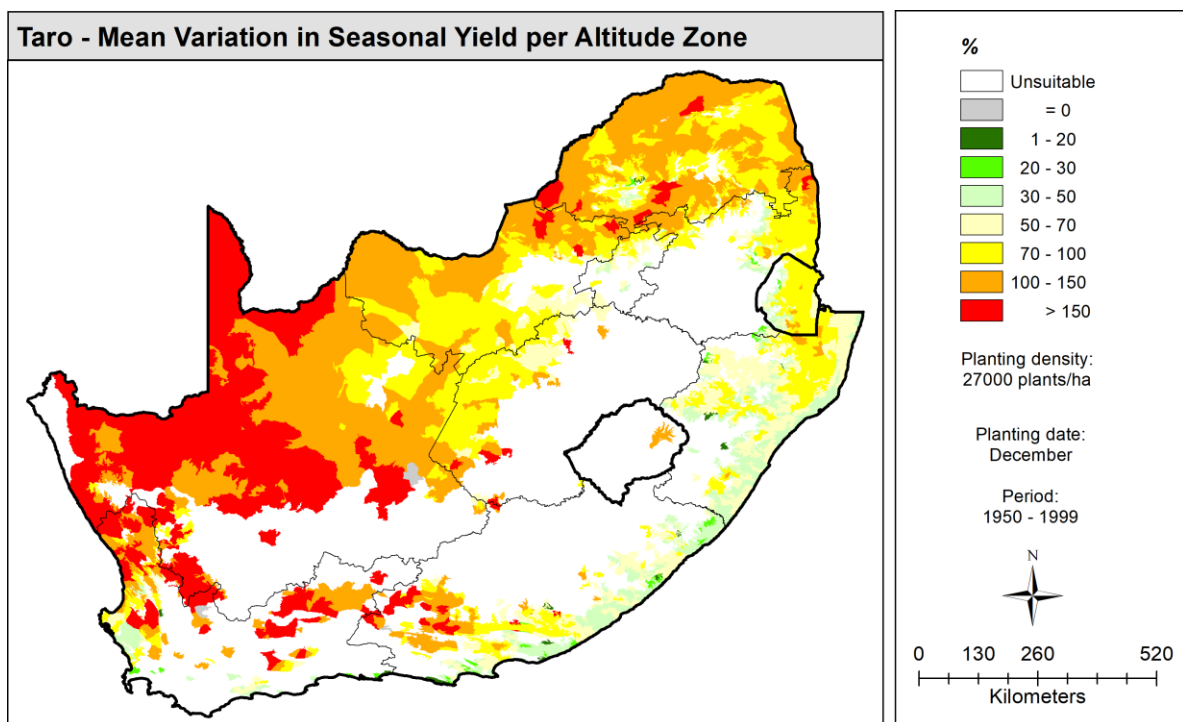


(b)

Figure 6-16 Inter-seasonal variation in yield for taro planted in November at a density of (a) 10,000 and (b) 27,000 plants ha⁻¹



(a)



(b)

Figure 6-17 Inter-seasonal variation in yield for taro planted in December at a density of (a) 10,000 and (b) 27,000 plants ha⁻¹

6.3.1.3 Impact of revised soil data

Using the same (i) taro parameter file, (ii) planting date (15th November), and (iii) plant density (20,000 plants ha⁻¹) used by Mabhaudhi et al. (2016a) and Kunz and Mabhaudhi (2023), AquaCrop was run with the previous (i.e. old) and revised (i.e. new) soil properties. Average yields (Y in dry t ha⁻¹) were then compared and as shown in **Figure 6-18**, Y_{NEW} is 93.9% of Y_{OLD} , i.e. $Y_{NEW} < Y_{OLD}$. This is expected since $TAW_{NEW} < TAW_{OLD}$ (cf. **Section 6.2.2.3**).

However, $Y_{NEW} - Y_{OLD}$ is negative for 51.7% of all HRZs (**Figure 6-19**). The majority (83.1%) of the differences range from -0.25 and 0.25 dry t ha⁻¹. The yields were identical for 1,033 HRZs, of which 387 HRZs have the same soils in Lesotho and eSwatini (i.e. not updated). The largest difference of -3.05 dry t ha⁻¹ occurred in zone no. 4,630, where the average yield decreased from 4.66 to 1.61 dry t ha⁻¹, due to a decrease in TAW of 33.9 mm. Similarly, the largest increase in average yield was 3.33 dry t ha⁻¹ in zone no. 3,326 (i.e. from 1.89 to 5.22 dry t ha⁻¹), yet TAW was almost identical (100.1 vs 100.2 mm). This illustrates that changes in TAW do not always explain yield differences.

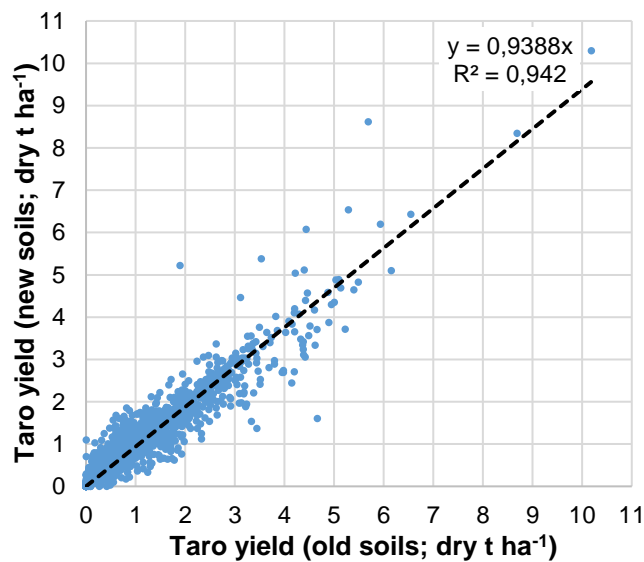


Figure 6-18 Comparison of taro yields simulated using the previous (Y_{OLD}) and revised (Y_{NEW}) soil properties for each HRZ

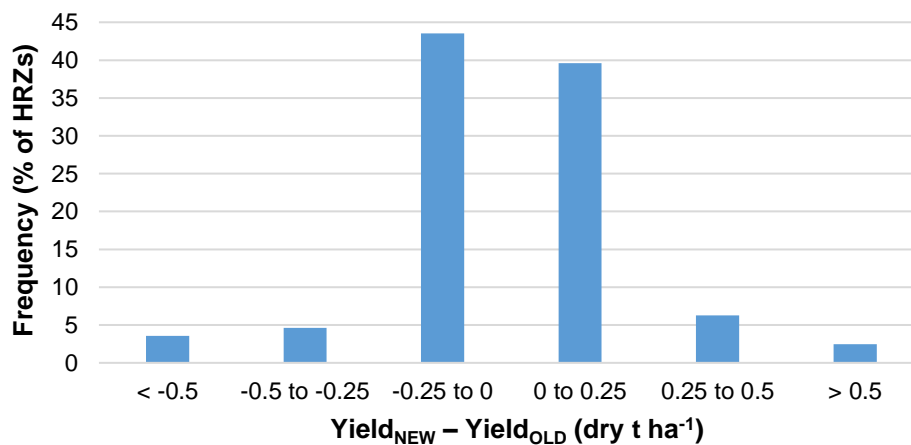


Figure 6-19 Differences in taro yields simulated using the revised (Y_{NEW}) and previous (Y_{OLD}) soil properties for each HRZ

The decision to run AquaCrop with a single-layer soil profile (cf. **Section 6.2.2.3**) for the first time impacted simulated taro yields as shown in **Figure 6-20**. Yields were simulated in 3,231 HRZs, with the remaining 2,607 zones being mostly too cold (and too dry) for taro production. On average, yields increased by 11.1% due to the change from two-layer to one-layer soils for all HRZs. Hence, as shown in **Figure 6-21**, the difference in yield obtained from a one-layer soil vs a two-layer soil ($\text{Yield}_{\text{LAY1}} - \text{Yield}_{\text{LAY2}}$) is positive for 59.1% of the 3,231 HRZs. The largest yield increase of 1.20 dry t ha⁻¹ occurred in zone no. 4,711, where the yield changed from 1.90 to 3.10 dry t ha⁻¹. The majority (85.3%) of the differences range from -0.25 and 0.25 dry t ha⁻¹, and thus are considered relatively small. The yields were identical in 1,058 HRZs, of which 387 HRZs have the same soils in Lesotho and eSwatini (i.e. not updated). However, all data points below the 1:1 trendline (solid black line) indicate yield decreases, with the largest being 2.55 dry t ha⁻¹ in zone no. 3,375, where the yield declined from 4.83 to 2.28 dry t ha⁻¹. In a few zones, yields up to 1.4 dry t ha⁻¹ decreased to zero dry t ha⁻¹. It is also worth noting that a single-layer soil profile provided no speed improvement in terms of the total model run time.

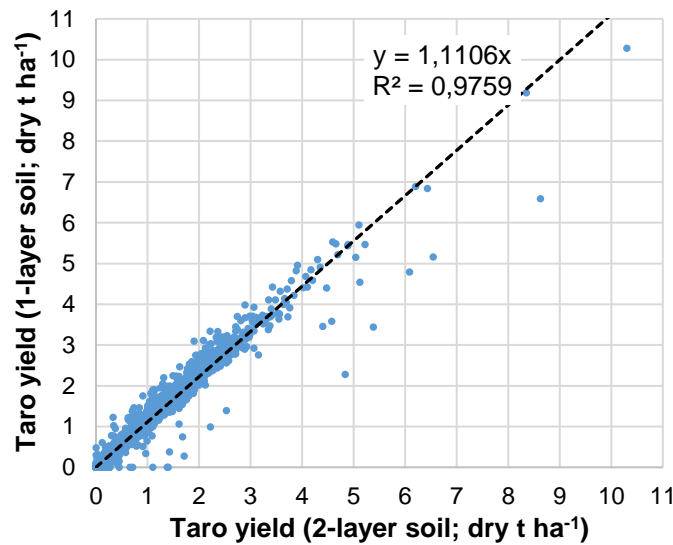


Figure 6-20 Comparison of taro yields simulated using the revised soils for two-layer vs one-layer soil profiles

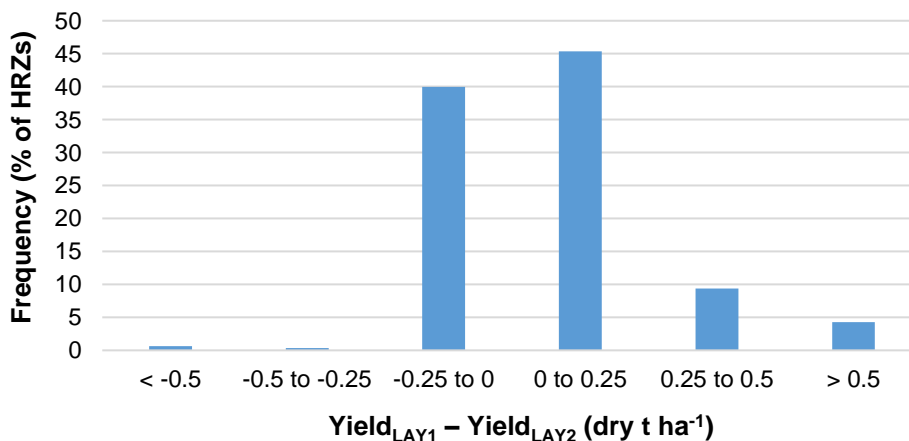


Figure 6-21 Differences in taro yields simulated using the revised soils for one-layer vs two-layer soil profile in each HRZ

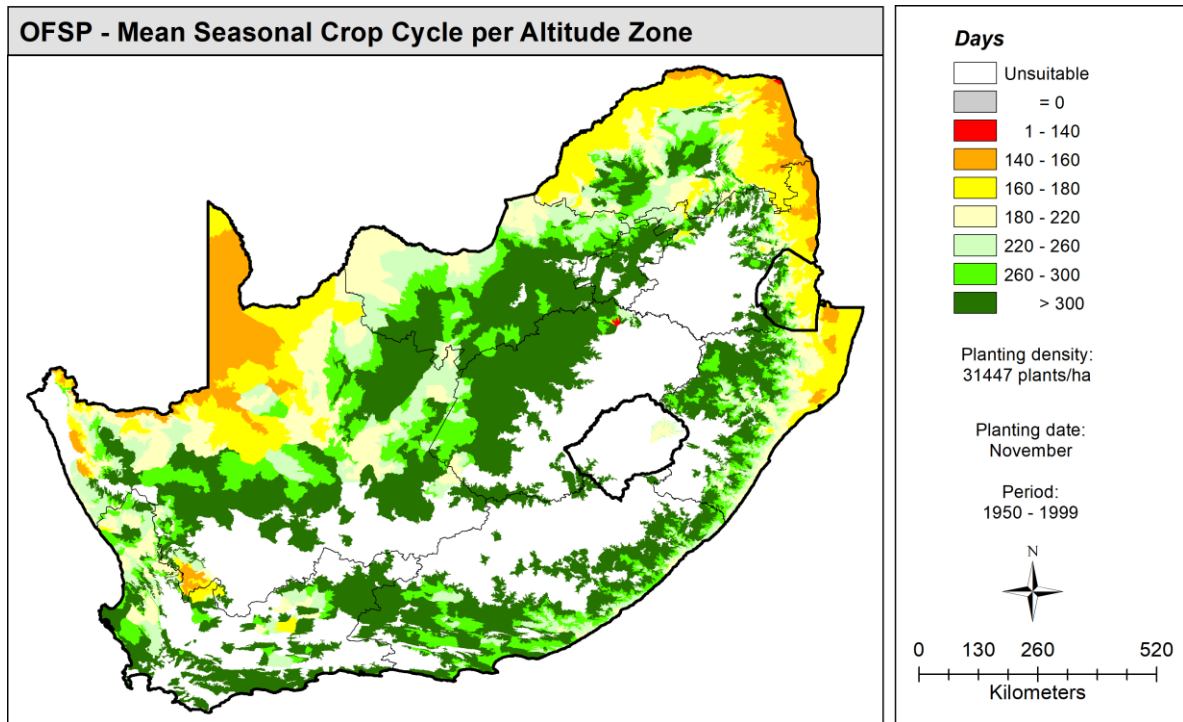
6.3.2 Crop cycle

AquaCrop defines the length of the crop cycle from the number of days after emergence to when the yield peaks, i.e. physiological maturity. It is different to the growing season length, which is the number of days from planting to physiological maturity. Hence, the crop cycle is always shorter than the season length. Maps of crop cycle are useful as they help identify areas too cold for crop production (shown in white on the maps) and in which HRZs a crop will reach physiologically maturity faster than in others. As mentioned before, the crop model is no longer run if the crop cycle exceeds 365 days. If this occurs in 46 of the 49 seasons, the average statistic is not generated and the zone is marked as unsuitable for crop production (i.e. -999). Such HRZs are coloured white on the maps, which are mostly located in the country's interior in the higher altitude or mountainous areas.

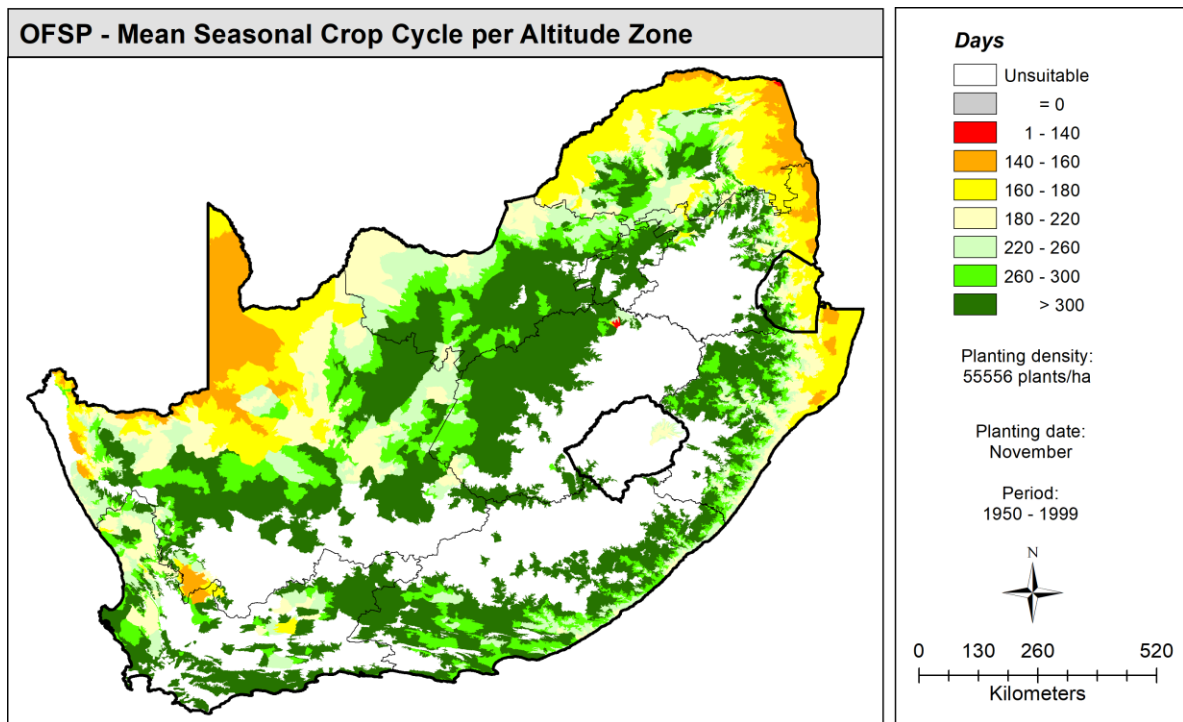
Zones with long crop cycles (300-365 days) are coloured green on the maps and typically are adjacent to the colder (white) HRZs. It is clear from the maps that crop cycle shortens towards the warmer, lower altitude (i.e. coastal) areas, with certain parts of the Limpopo (northern & eastern), Mpumalanga (eastern) and KwaZulu-Natal (northern-eastern) provinces exhibiting the shortest crop cycles. For both RTCs, crop cycles were longer when planted in December as a longer season is required to accumulate sufficient heat units to reach physiological maturity.

OFSP: As expected, plant density had little to no impact on crop cycle when compared to the planting date. For the December planting of OFSP, the maps are identical (**Figure 6-23**). OFSP planted in November at either density (31,447 or 56,667 plants ha⁻¹) had similar crop cycles. Large variations in crop cycle (due to plant density) may indicate that a zone is not well suited to crop production, and thus yields will be low with high variation between seasons.

Taro: For taro, more differences in crop cycle were noted, particularly in the drier western parts of the country. However, taro production is unlikely viable in these areas due to the low attainable yields (cf. **Section 6.3.1.1**) and high Y_{CV} values (cf. **Section 6.3.1.2**). There are more unsuitable areas for taro when compared to OFSP due to the longer thermal time required to reach physiological maturity (2,822 vs 2,533 GDDs; cf. **Table 16-14** in **Section 16.4**). Taro can take up to 49 days to emerge (Mabhaudhi, 2012), and thus is unlikely to fully mature within 100 days. The crop can take up to 300 days to mature (Mugiyo et al., 2021b).

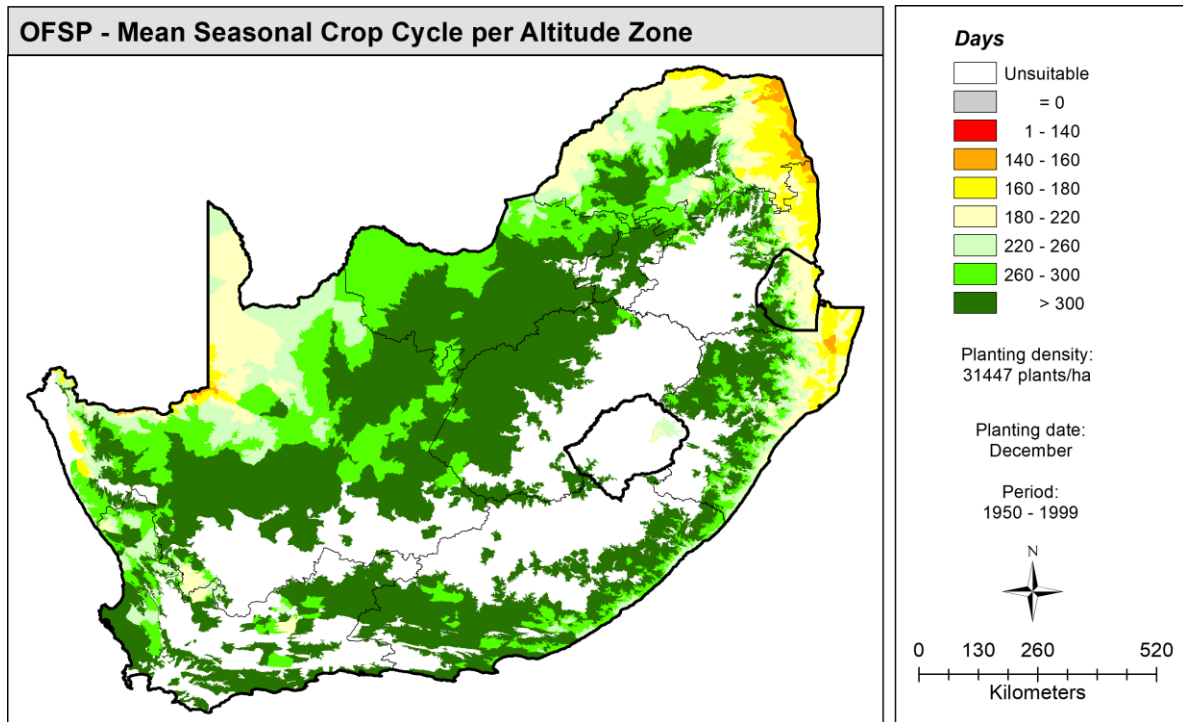


(a)

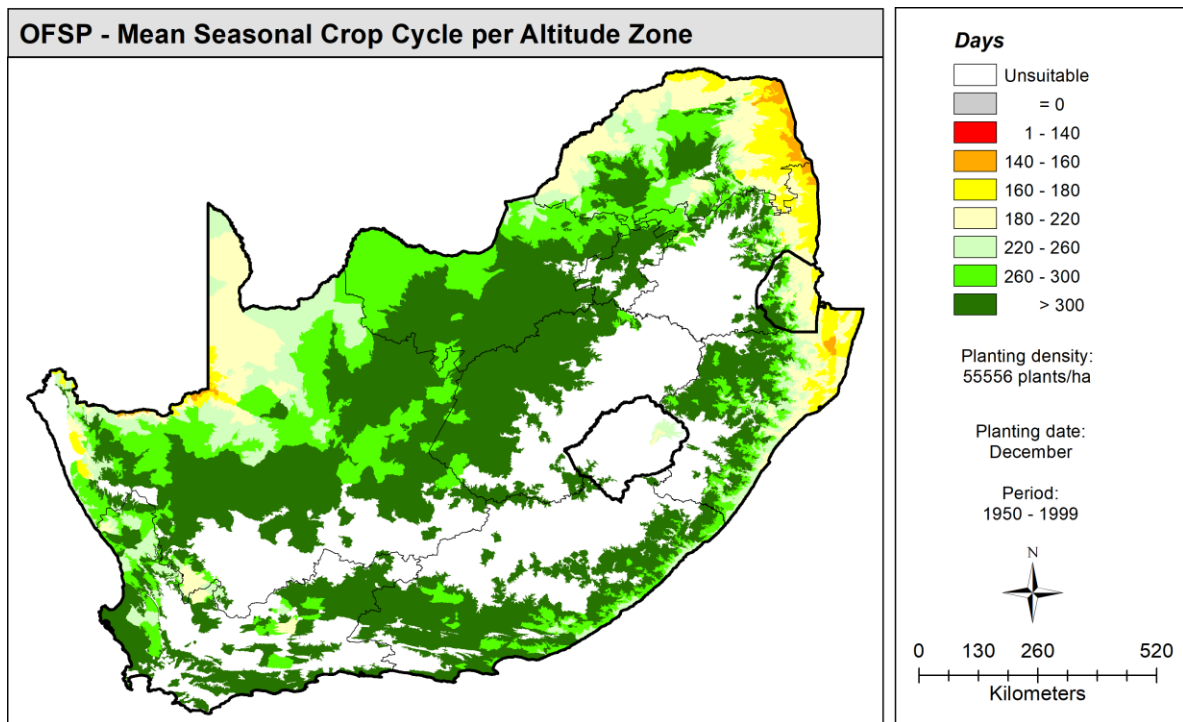


(b)

Figure 6-22 Averaged crop cycle for OFSP planted in November at a density of (a) 31,447 and (b) 55,556 plants ha⁻¹

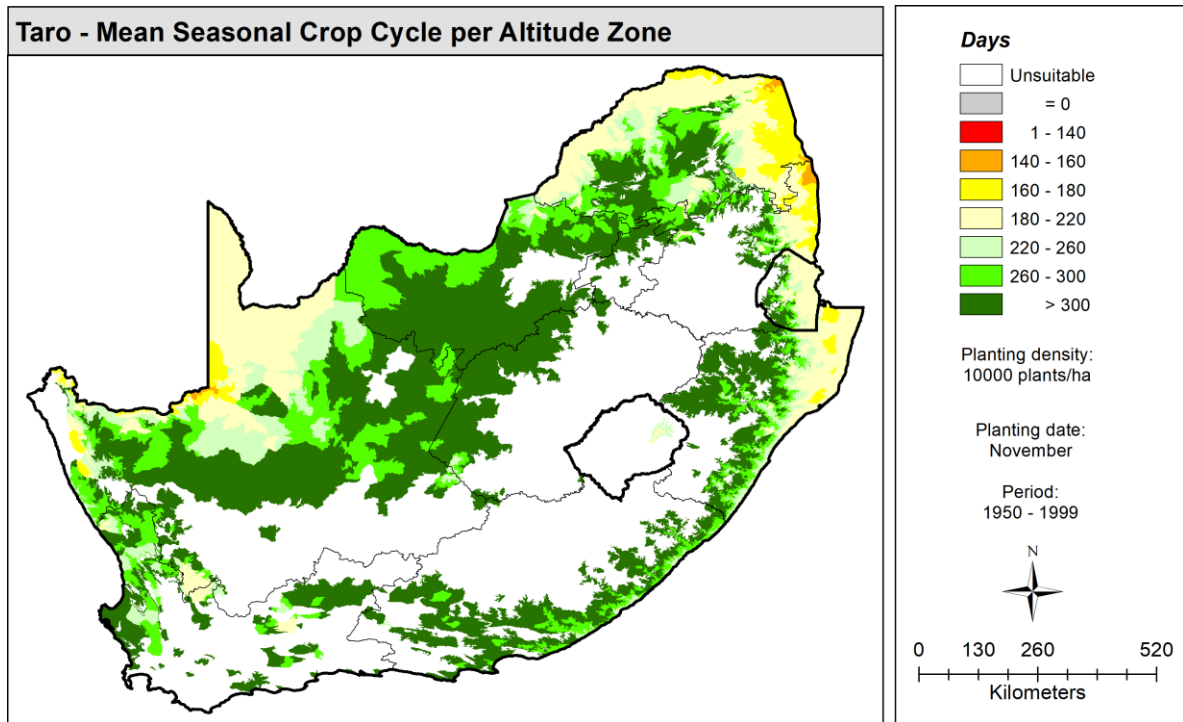


(a)

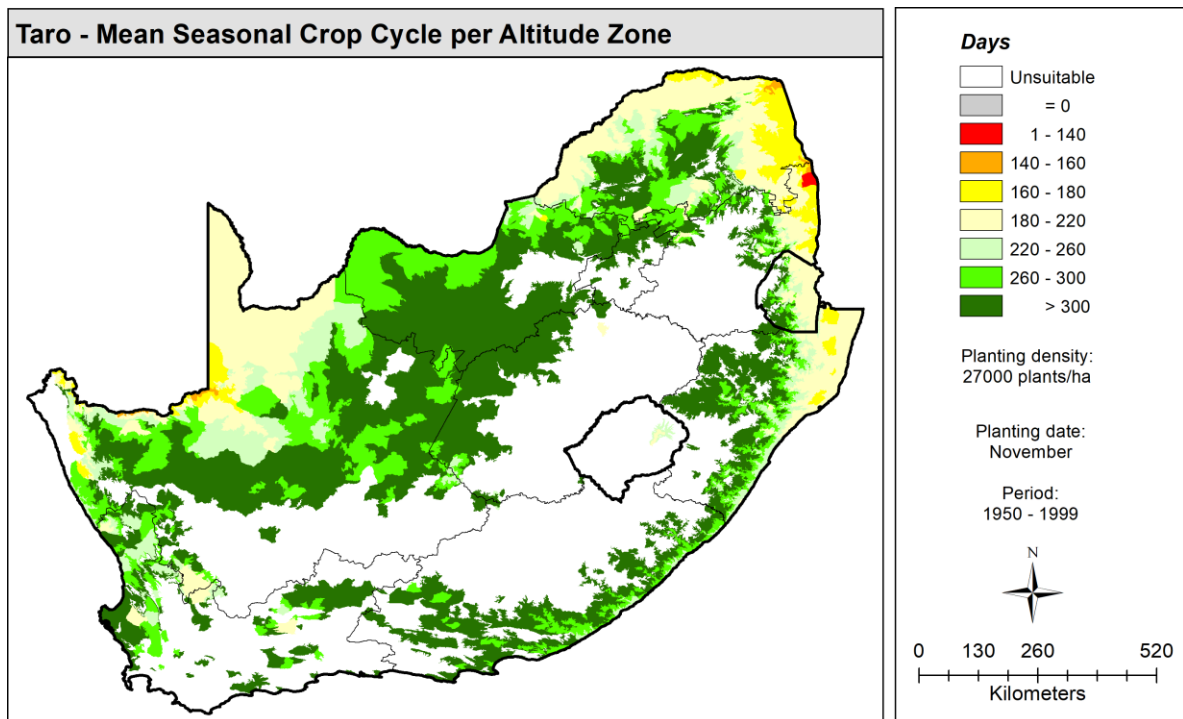


(b)

Figure 6-23 Averaged crop cycle for OFSP planted in December at a density of (a) 31,447 and (b) 55,556 plants ha⁻¹

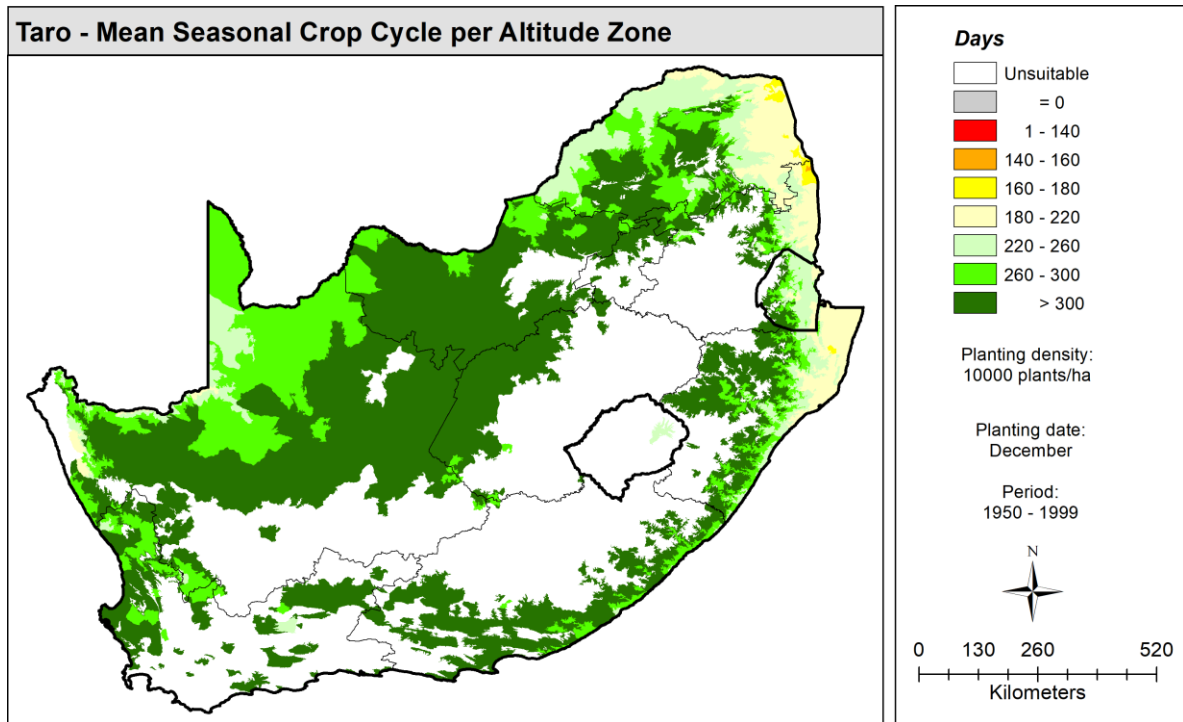


(a)

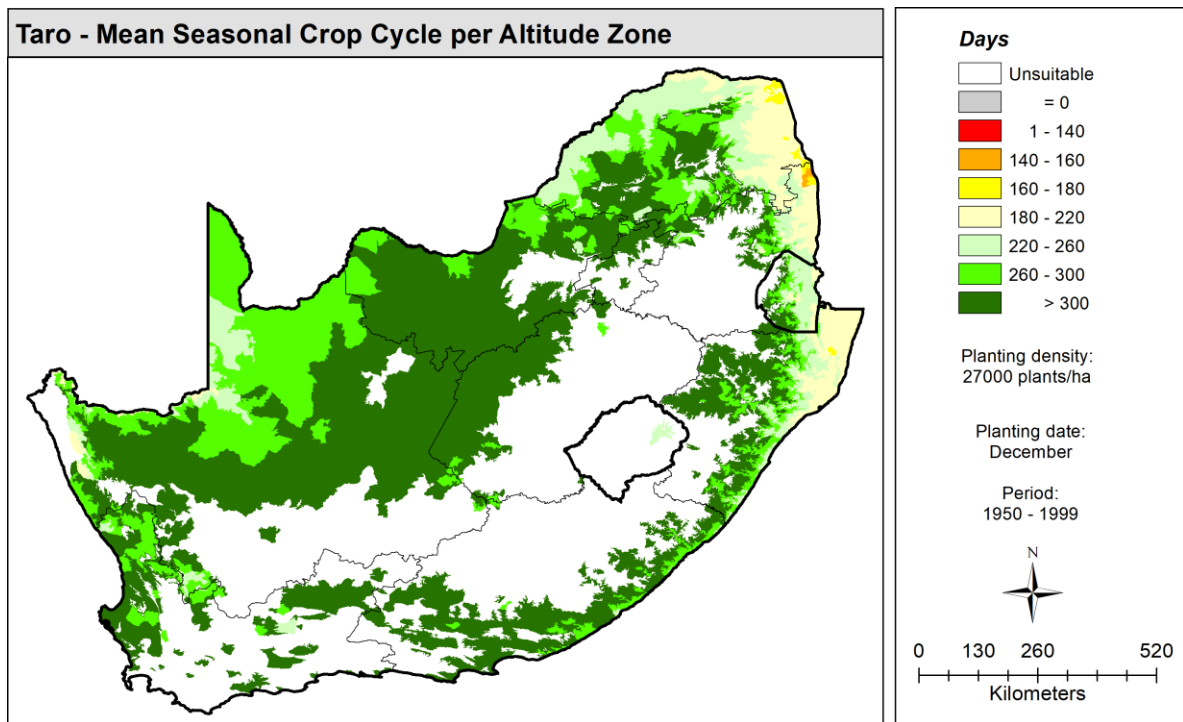


(b)

Figure 6-24 Averaged crop cycle for taro planted in November at a density of (a) 10,000 and (b) 27,000 plants ha⁻¹



(a)



(b)

Figure 6-25 Averaged crop cycle for taro planted in December at a density of (a) 10,000 and (b) 27,000 plants ha⁻¹

6.3.3 Risk of crop failure

Kunz and Mabhaudhi (2023) calculated the risk of crop failure (RCF) as the ratio of the number of zero yields, to the total number of seasons (i.e. 49), which is expressed as a percentage. For HRZ no. 1,509, the model simulated 19 seasons of zero yield. For the other 30 seasons, the model “crashed” with a “division-by-zero” error, and thus no model output was produced. This typically occurs when the climate is too cold for viable crop production. Hence, RCF was calculated as 38.8% (i.e. $100 \times 19/49$).

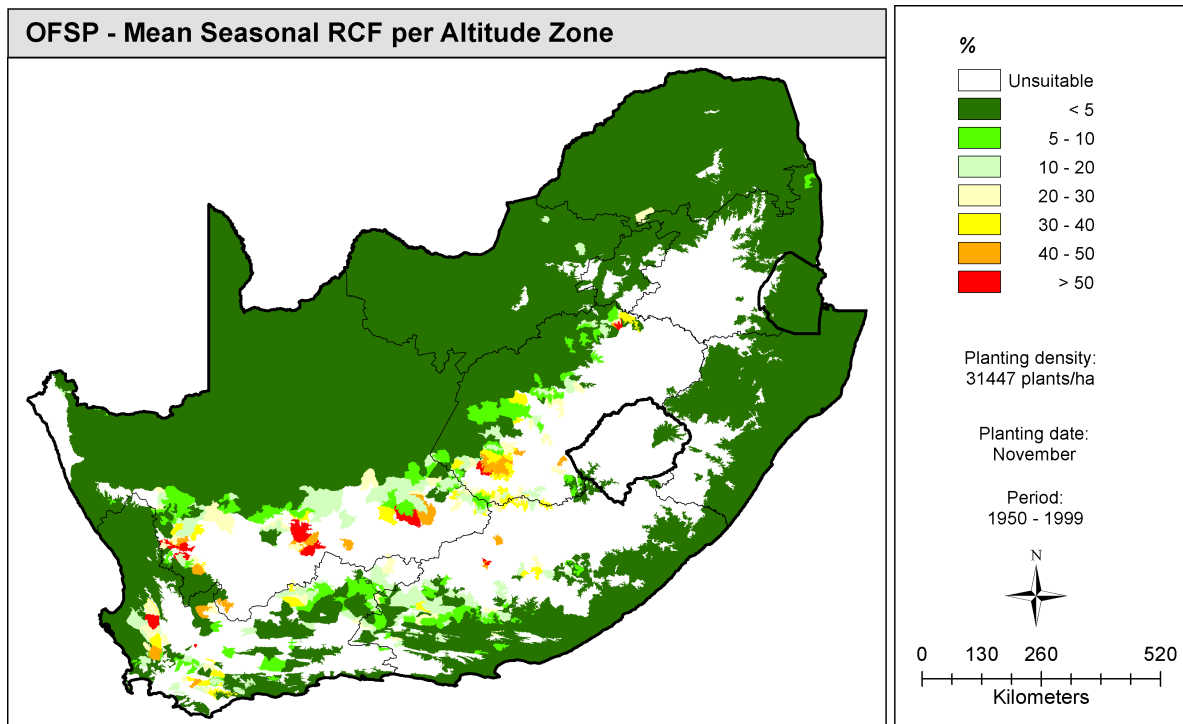
For this project, RCF was defined as the number of zero yields divided by the number of simulated seasons. Hence, for zone no. 1,509, RCF is 100% (i.e. $100 \times 19/19$), which is more than double the value obtained by Kunz and Mabhaudhi (2023). In other words, when the model “crashed”, the yield should be assumed zero for all 30 seasons. Therefore, there are 49 zero yields (19 + 30) out of 49 simulations, which gives a RCF of 100%.

However, crop failure can also be defined as a 10% or more decline in yield compared to the mean yield, i.e. a 10% negative deviation from the mean (Caparas et al., 2021). Instead of using means, some studies adopted deviations from a trendline of yield vs time. The use of these definitions of crop failure should be investigated in future studies.

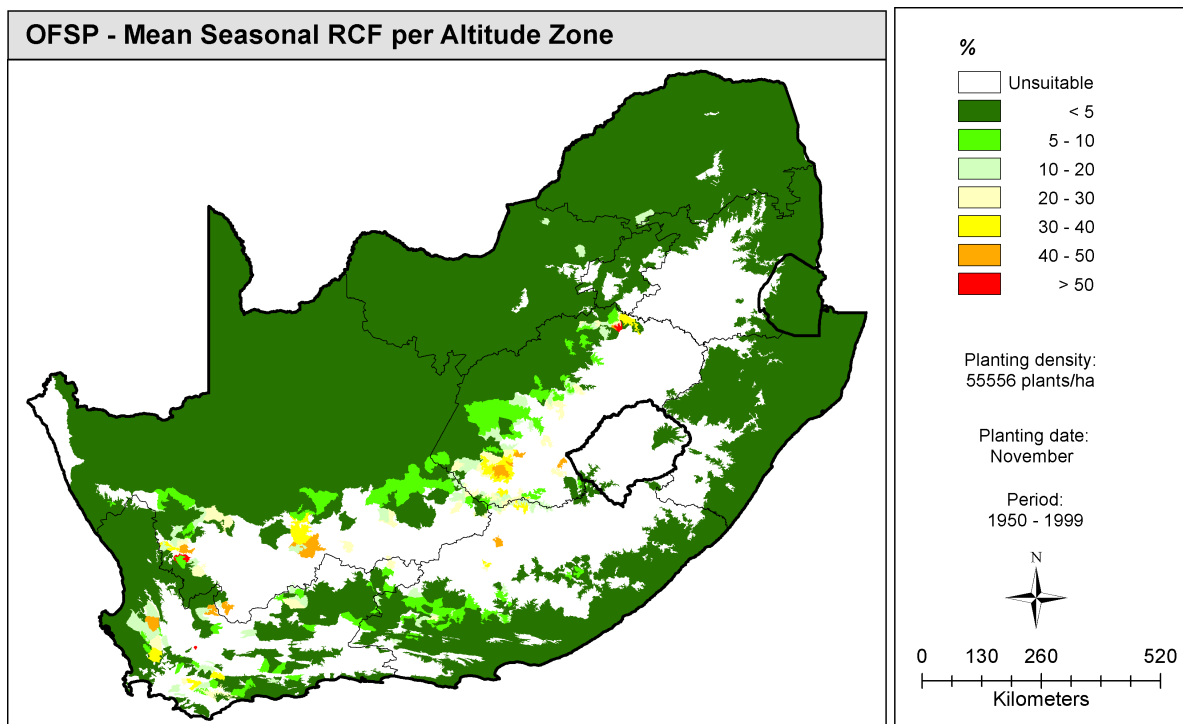
Maps showing the spatial variability in RCF were produced for OFSP and taro. They clearly highly areas in the country where crop production is not viable, mostly due to cold temperatures (coloured white on the maps) and/or erratic rainfall (coloured red on the maps). If RCF is 50% it indicates the model simulated a zero yield (i.e. crop failure) every second season. Such areas are not deemed unsuitable for crop production, especially for subsistence farmers.

OFSP: The RCF for OFSP is relatively low, For the majority of HRZs, the RCF for OFSP was low, i.e. < 5%, which indicates the model simulated a zero yield across 20 seasons (on average). However, RCF increases for HRZs located adjacent to cold areas (coloured white). In the Free State, a December planting was associated with lower crop failure risk (**Figure 6-27**). The maps show low RCF for the Northern Cape province, which indicates very few zero yields were simulated across the 49 seasons. As mentioned previously, maps should not be interpreted “in isolation”, as the yield and Y_{CV} maps show the western parts of the country are not suited to rainfed crop production.

Taro: The RCF is higher to taro compared to OFSP, especially in the Limpopo and North West provinces. In these provinces, a December planting (Figure 6-29) was associated with higher risk compared to November (**Figure 6-28**). As expected, the drier Northern and Western Cape provinces are associated with high risk of crop failure.

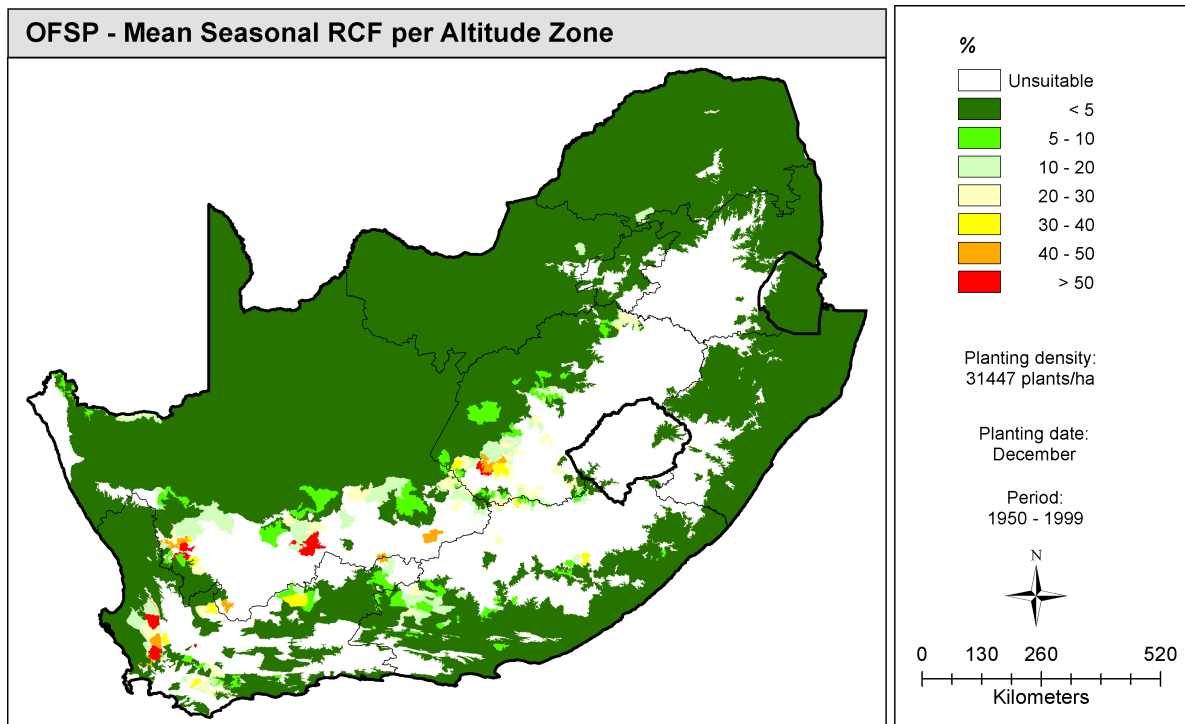


(a)

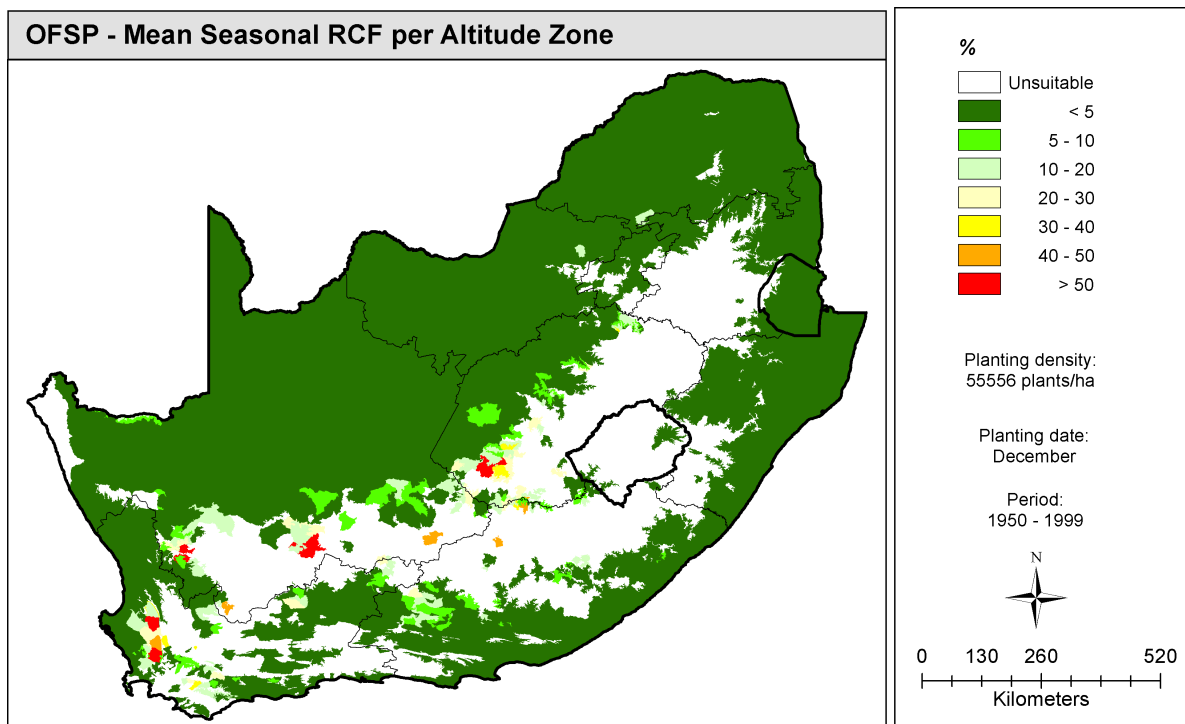


(b)

Figure 6-26 Risk of failure for OFSP planted in November at a density of (a) 31,447 and (b) 55,556 plants ha⁻¹

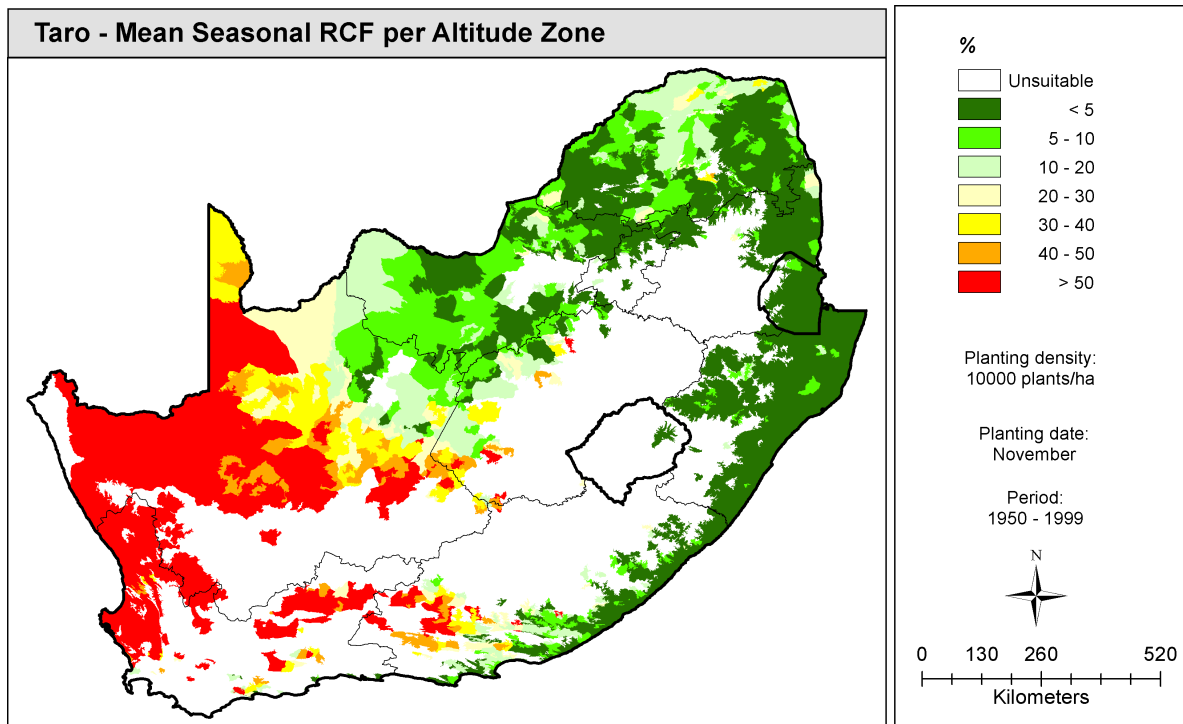


(a)

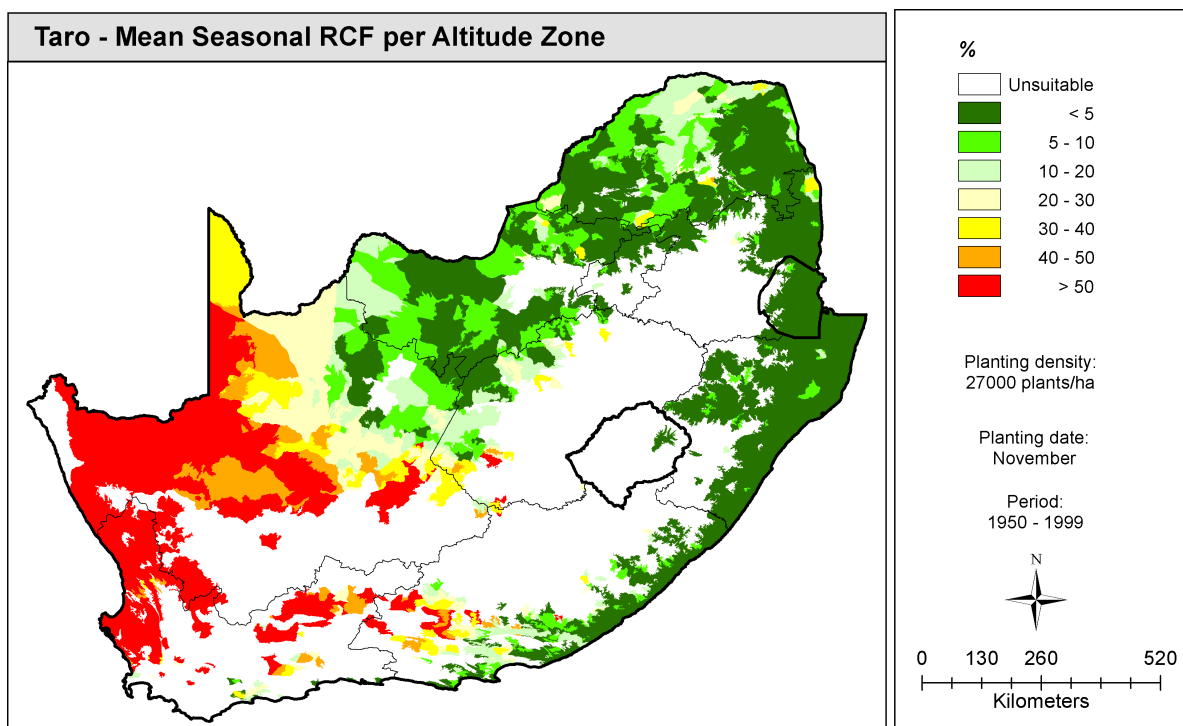


(b)

Figure 6-27 Risk of failure for OFSP planted in December at a density of (a) 31,447 and (b) 55,556 plants ha⁻¹

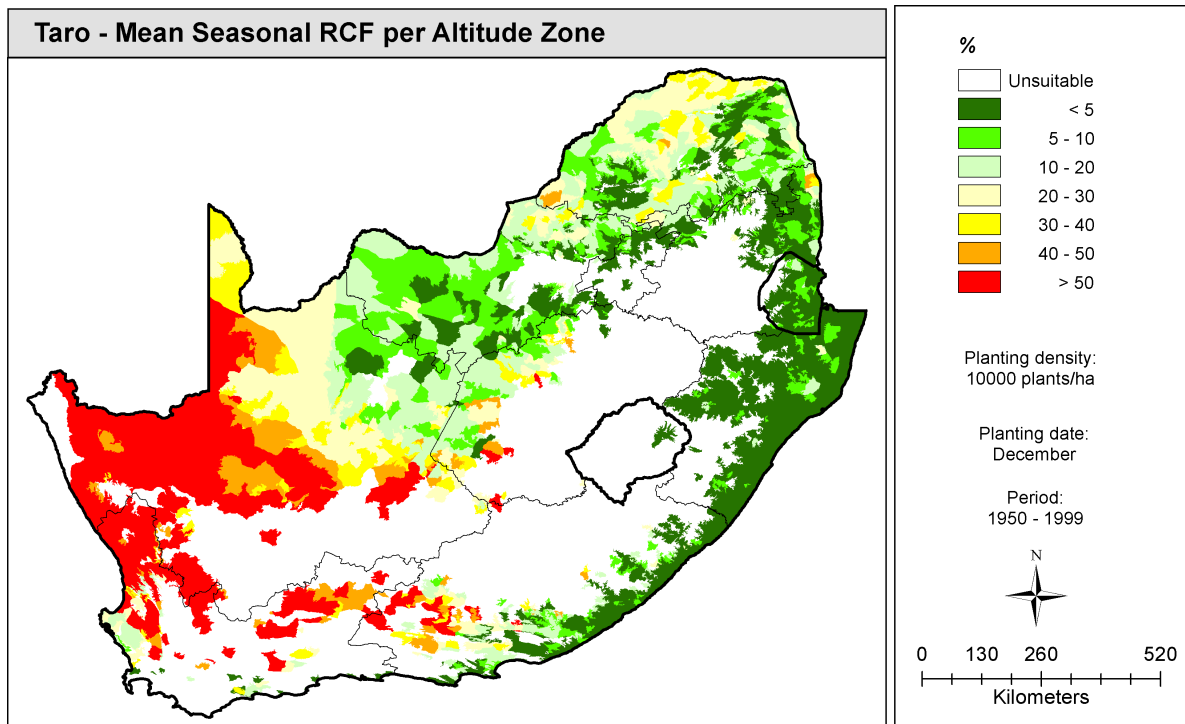


(a)

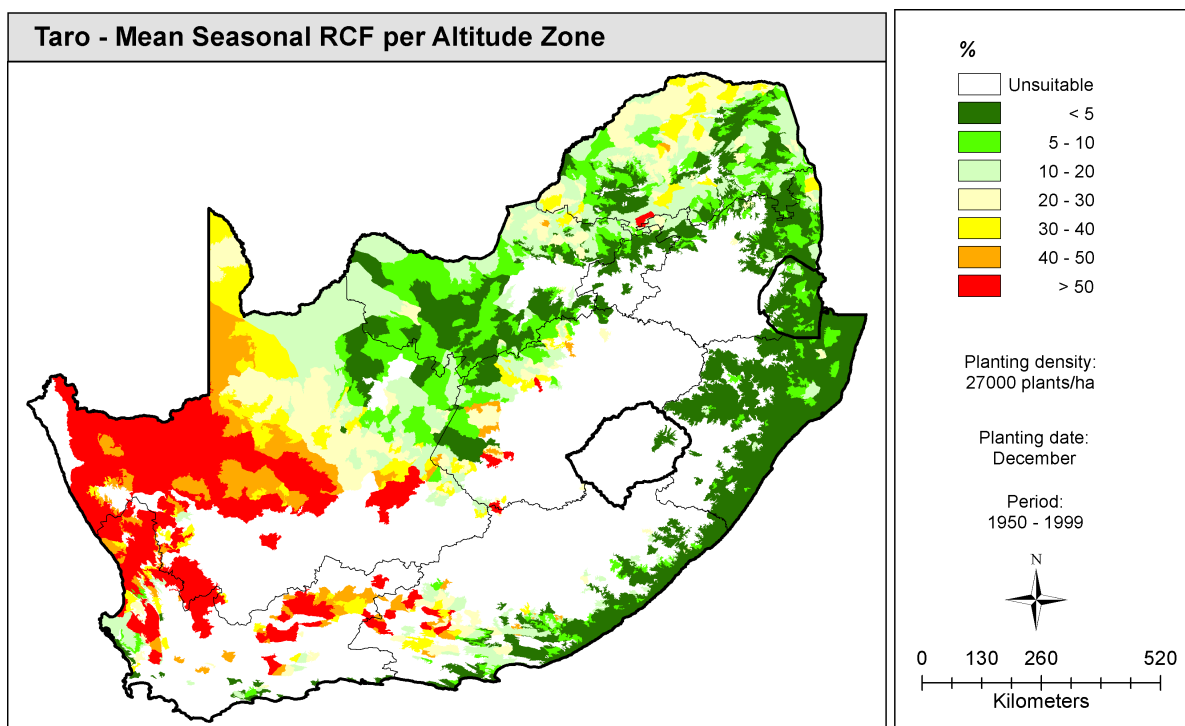


(b)

Figure 6-28 Risk of failure for taro planted in November at a density of (a) 10,000 and (b) 27,000 plants ha⁻¹



(a)



(b)

Figure 6-29 Risk of failure for taro planted in December at a density of (a) 10,000 and (b) 27,000 plants ha⁻¹

6.3.4 Crop water productivity

6.3.4.1 Average CWP

Aim 5 of this project is to improve the knowledge on the productivity of water required for the rainfed production of RTCs (cf. **Section 1.2**). Crop water productivity (CWP) is the attainable yield (in dry kg ha⁻¹), relative to crop water use (i.e. actual evapotranspiration in m⁻³) accumulated from planting to physiological maturity. Hence, the CWP metric is sensitive to crop yield, which is influenced by crop management. This metric can also be used as an indicator to assess the performance of a system and to identify the environments in which (or management strategies by which) the yield per unit water can be maximised (Raes et al., 2018). CWP measures the trade-off between carbon gain and water loss of agricultural ecosystems and understanding its dynamics and controlling factors is essential for predicting ecosystem responses to environmental variability

Underutilised crops can exhibit higher CWP when stressed in comparison to non-stressed conditions. CWP is most useful for determining if crops are grown in optimum environments as opposed to those produced in sub-optimum areas. AquaCrop is designed to improve water productivity of rainfed and irrigated crops by helping to identify constraints to crop production. The model can also help to develop strategies to maximise crop water productivity, especially under water-deficit growing conditions. Hence, the model was used to estimate the CWP of OFSP and taro at a national scale. However, root and tubers are indeterminate crops, which continue to form new leaves after initiation of tuber formation. Hence, AquaCrop will struggle to accurately simulate crop evapotranspiration of indeterminate crops, since the model will reduce transpiration towards the end of the season. This is especially true for OFSP that exhibits the “stay-green” trait. Hence, the model is likely to under-estimate measured crop water use, and thus over-estimate CWP.

The seasonally averaged CWP under rainfed conditions was determined for each planting date and density scenario, i.e. four maps per crop. Estimates of averaged CWP (in dry kg m⁻³) were derived using AquaCrop for up to 49 seasons. The maps follow similar trends to the yield maps, which highlights the sensitivity of this metric to yield input. Areas in white indicate HRZs not suited to crop production, i.e. too cold for crop production. When the CWP is zero dry kg m⁻³, this indicates the average yield estimate was also zero dry kg ha⁻¹ (shown in light grey).

It is important to note that CWP maps can be misinterpreted. A relatively high CWP can occur when crop evapotranspiration is low. It is therefore recommended that the CWP maps are interpreted in conjunction with the yield and crop cycle maps. Various ways to increase CWP of underutilised crops include:

- modifying crop eco-physiology (e.g. intercropping),
- harvesting of rain water and conserving soil water,
- improving agronomic practices,
- planting more drought-tolerant varieties/landraces, and
- using decision support tools (e.g. remote sensing, gene mapping and climate modelling) for better decision making.

The CWP maps highlight the same trend of higher CWP along the eastern seaboard, compared to the western regions. The maps show that large parts of the country’s interior region, especially towards the western areas, are too cold and/or too dry for rainfed crop production, and thus yield and CWP are very low. In general, high yield is associated with high CWP. The maps show that both crops are most water use efficient along the coastal regions of KwaZulu-Natal and the Eastern Cape, including the adjacent interior. In these areas, the model simulated the highest yields, which resulted in high CWP. Hence, RTC production by smallholder farmers should be promoted in these areas where the crop is most water use efficient.

Due to the drought tolerance of RTCs, they have the potential to use water more efficiently when compared to other food crops (Hadebe et al., 2017). This can be assessed by comparing CWP values of different crops. For example, the maps show that CWP of taro is much less than for OFSP, as observed in Season 2 (1.37 vs 3.42 dry kg m⁻³). This is due to the lower yields simulated for taro, when compared to OFSP. However, the comparison of measured and simulated CWP values is not advised. Furthermore, the comparison of CWP values derived from fresh yields will be higher than those from dry yields.

OFSP: Maps of seasonally averaged CWP for OFSP representing two planting dates and two plant densities are shown in **Figure 6-30** to **Figure 6-31**. Unsuitable areas (shown as white) indicate no CWP was calculated, since these HRZs are considered too cold for viable crop production, and thus the model was not run. As expected, CWP improves at higher density due to increased yields. Furthermore, CWP is lower in November (**Figure 6-30**) when compared to December (**Figure 6-31**).

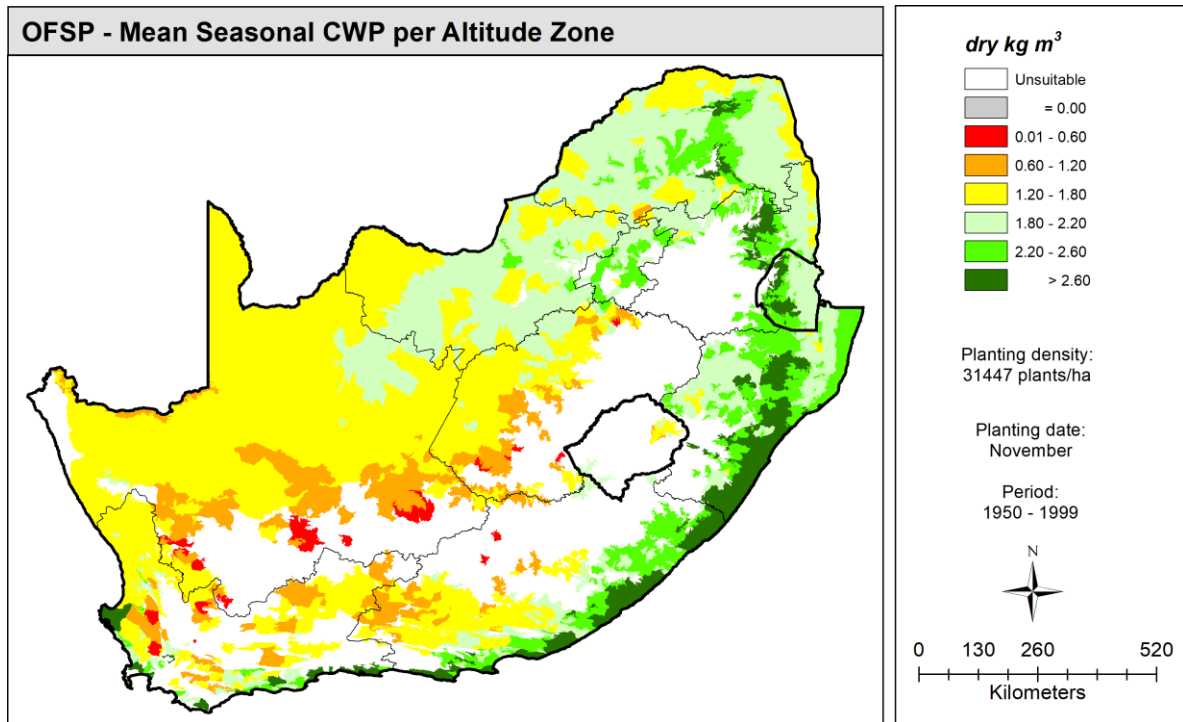
Taro: CWP improves when the crop is planted in November in the Limpopo and North West provinces. However, CWP is higher for the December planting along the coastal regions of KwaZulu-Natal and the Eastern Cape.

6.3.4.2 Coefficient of variation

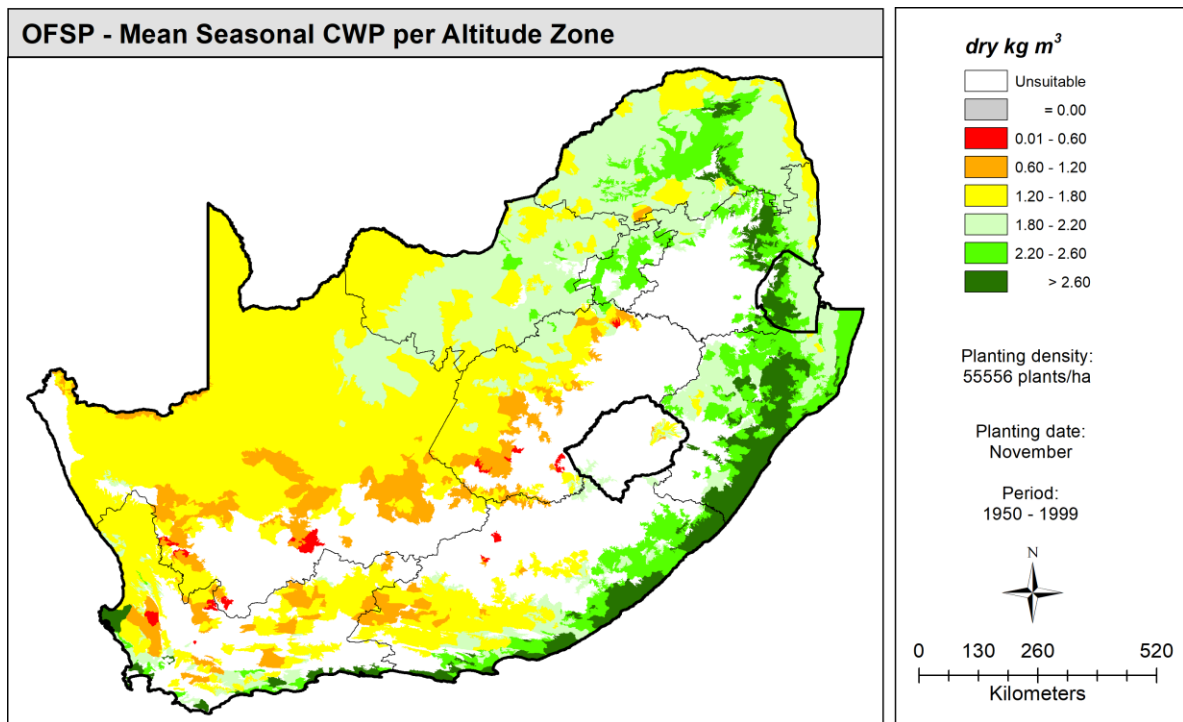
Maps of inter-seasonal variation in crop water productivity (CWP_{CV}) were also produced for both RTCs and are presented in **Section 18**. As expected, CWP_{CV} is lower along the eastern seaboard of the country where rainfall is sufficient to support rainfed crop cultivation.

OFSP: In general, CWP_{CV} for OFSP is lower for the December planting (**Figure 6-31**) when compared to November (**Figure 6-30**). However, Y_{CV} was lower for the November planting, in particular along the coast of KwaZulu-Natal (**Figure 6-14**), as noted in **Section 6.3.1.2**.

Taro: As shown in **Figure 6-32** and **Figure 6-33**, CWP_{CV} for taro is higher than for OFSP, particularly for a December planting. CWP_{CV} also declines when taro is planted in December, particularly in parts of the Limpopo and North West (north-eastern) provinces, Mpumalanga (eastern) and KwaZulu-Natal (north-eastern). This indicates taro yields are more variable across the 49 seasons compared to OFSP, especially in the Limpopo province.

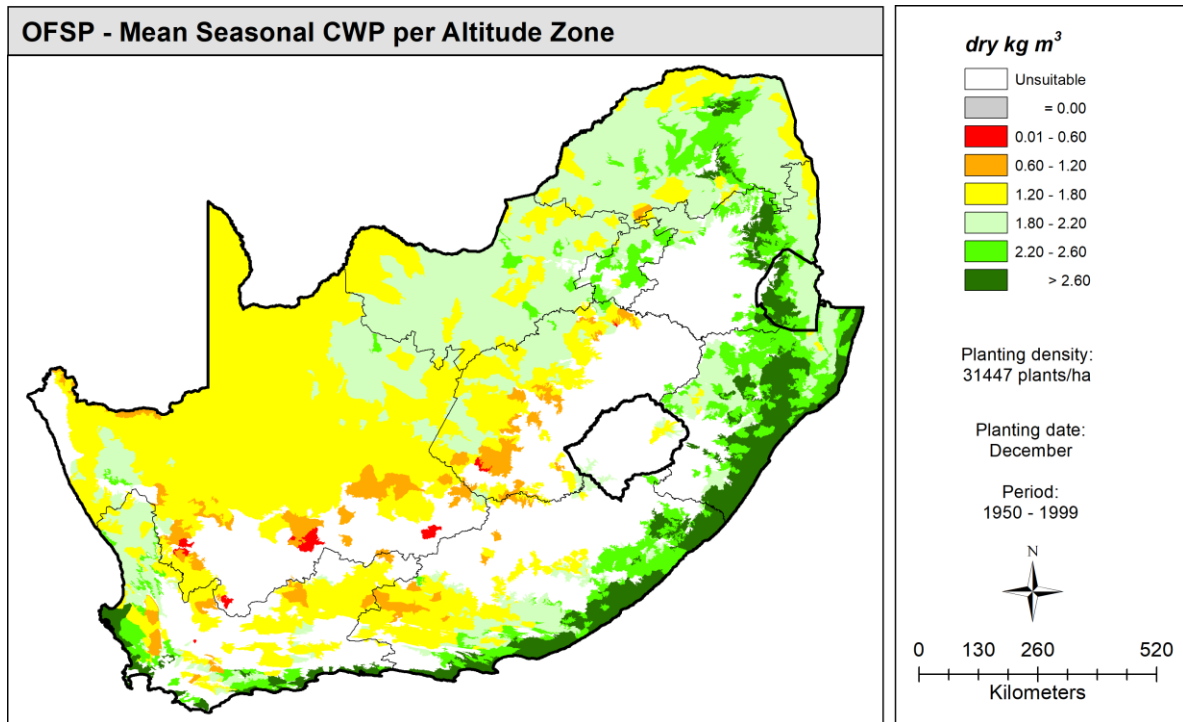


(a)

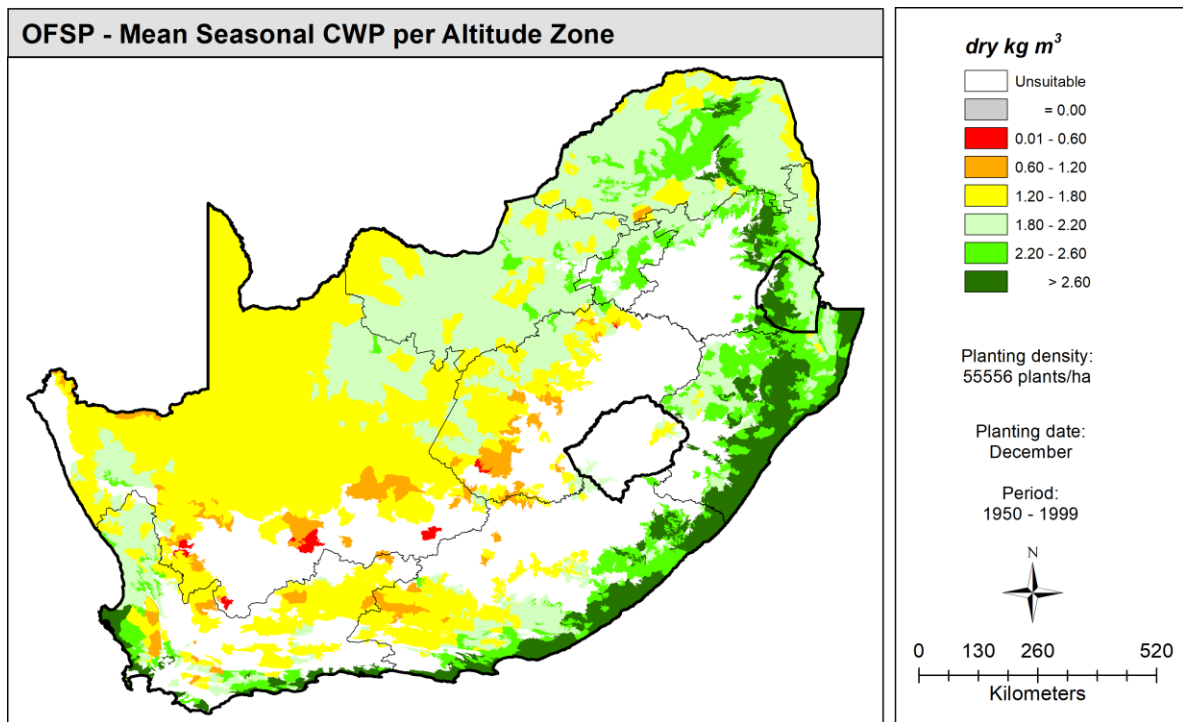


(b)

Figure 6-30 Averaged seasonal CWP for OFSP planted in November at a density of (a) 31,447 and (b) 55,556 plants ha⁻¹

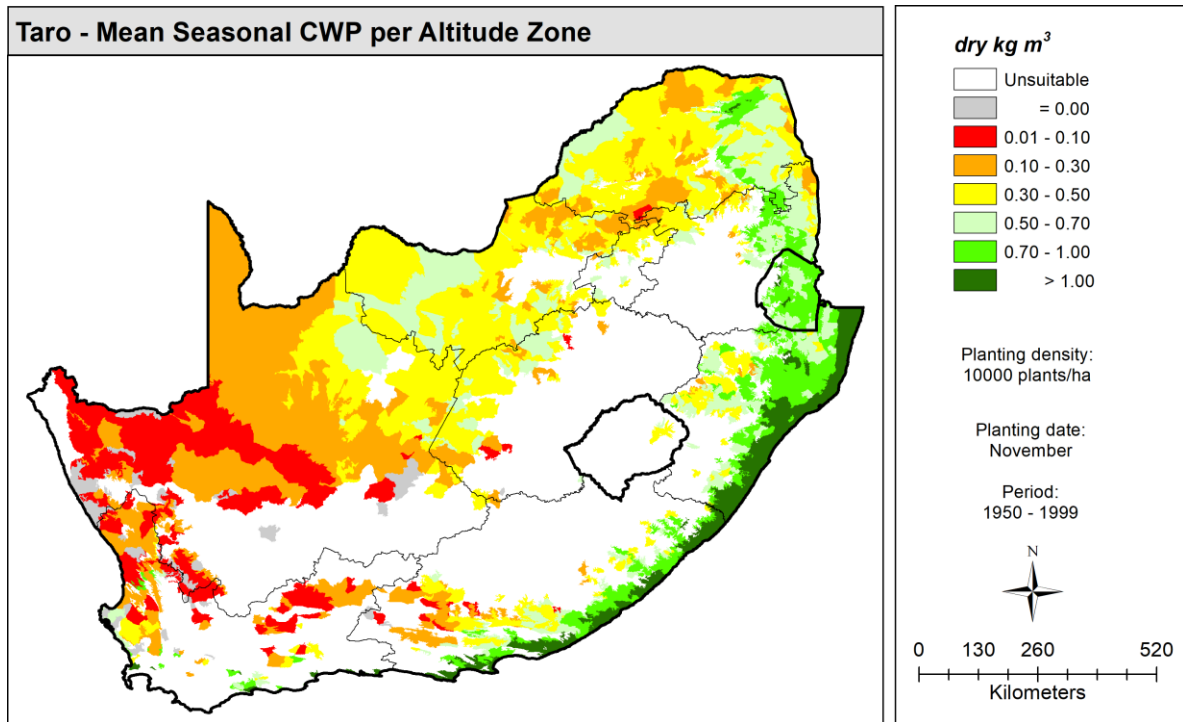


(a)

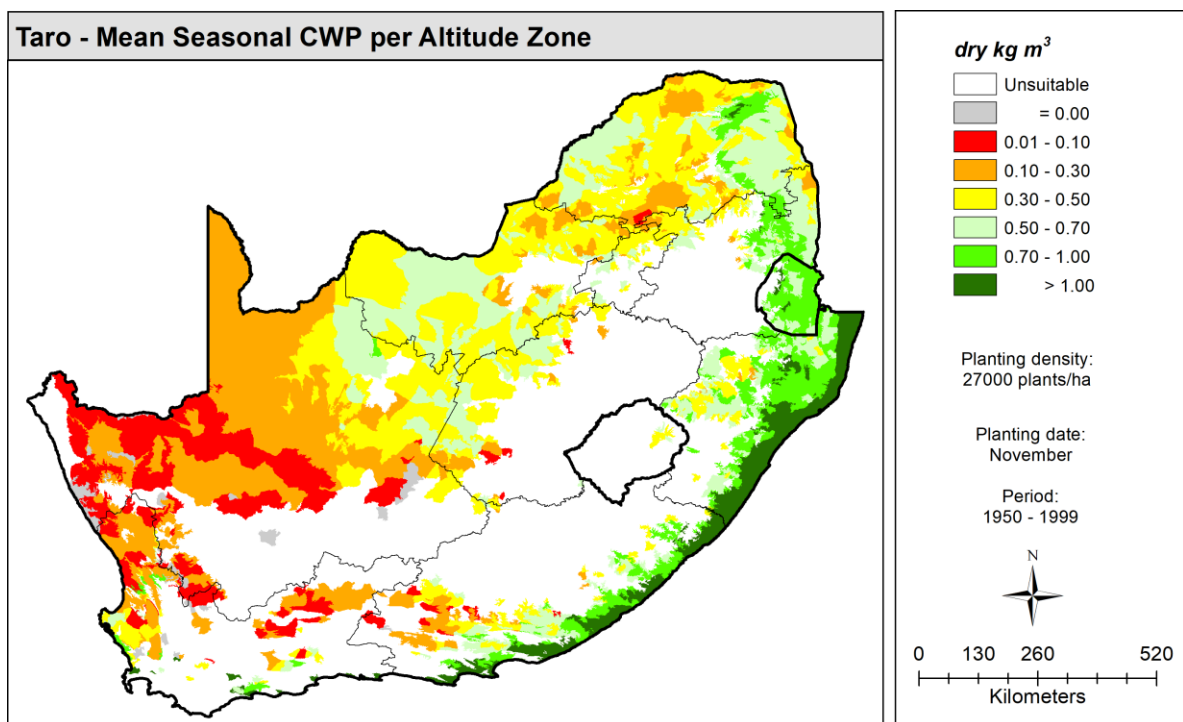


(b)

Figure 6-31 Averaged seasonal CWP for OFSP planted in December at a density of (a) 31,447 and (b) 55,556 plants ha⁻¹

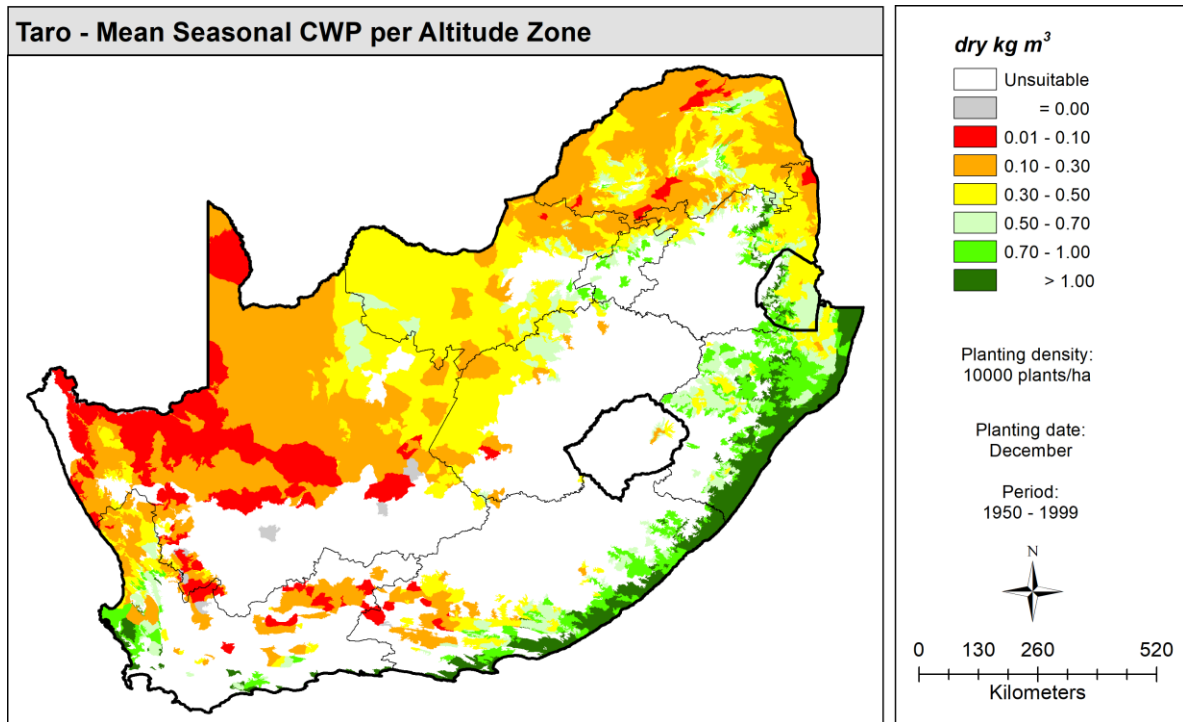


(a)

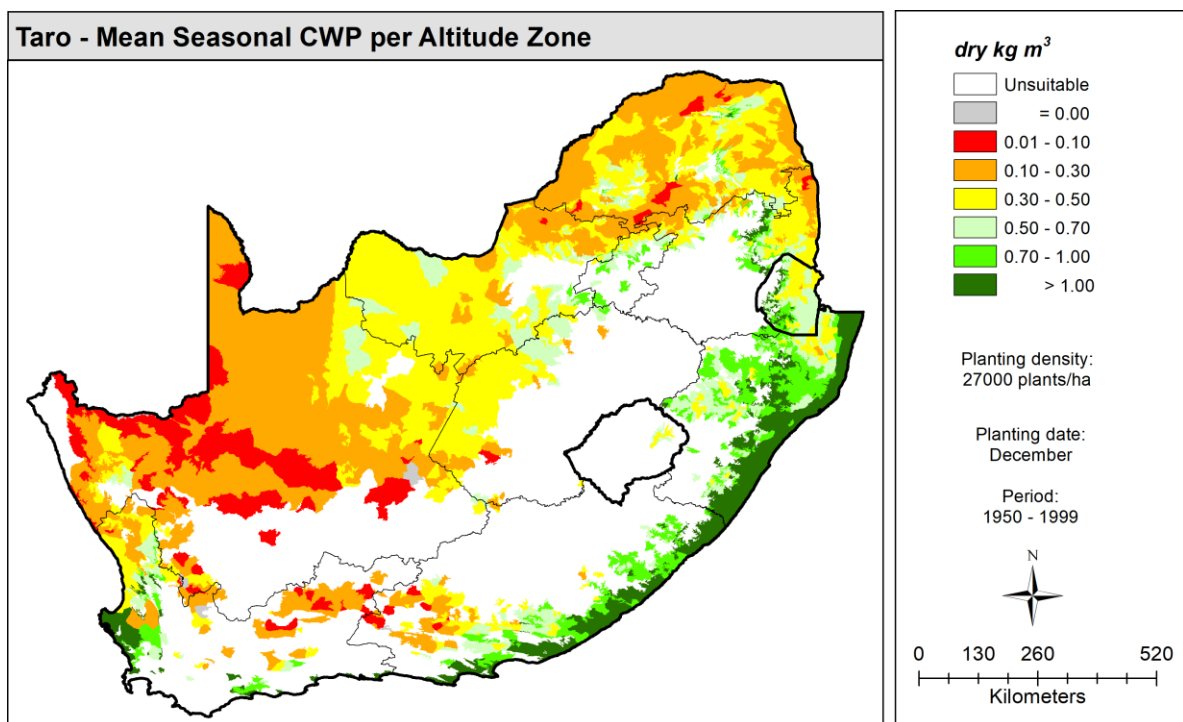


(b)

Figure 6-32 Averaged seasonal CWP for taro planted in November at a density of (a) 10,000 and (b) 27,000 plants ha⁻¹



(a)



(b)

Figure 6-33 Averaged seasonal CWP for taro planted in December at a density of 27,778 plants ha⁻¹

Figure 6-34 shows the map of taro CWP derived by Kunz and Mabhaudhi (2023). CWP estimates are much lower when compared to those shown in **Figure 6-32b**. Hence, the maps shown above supersede previous taro maps developed by Mabhaudhi et al. (2016a) and Kunz and Mabhaudhi (2023), since the following was significantly improved in this project: (i) crop parameters, (ii) climate and soil input data, and (iii) methodology for running AquaCrop. The improvements help to explain

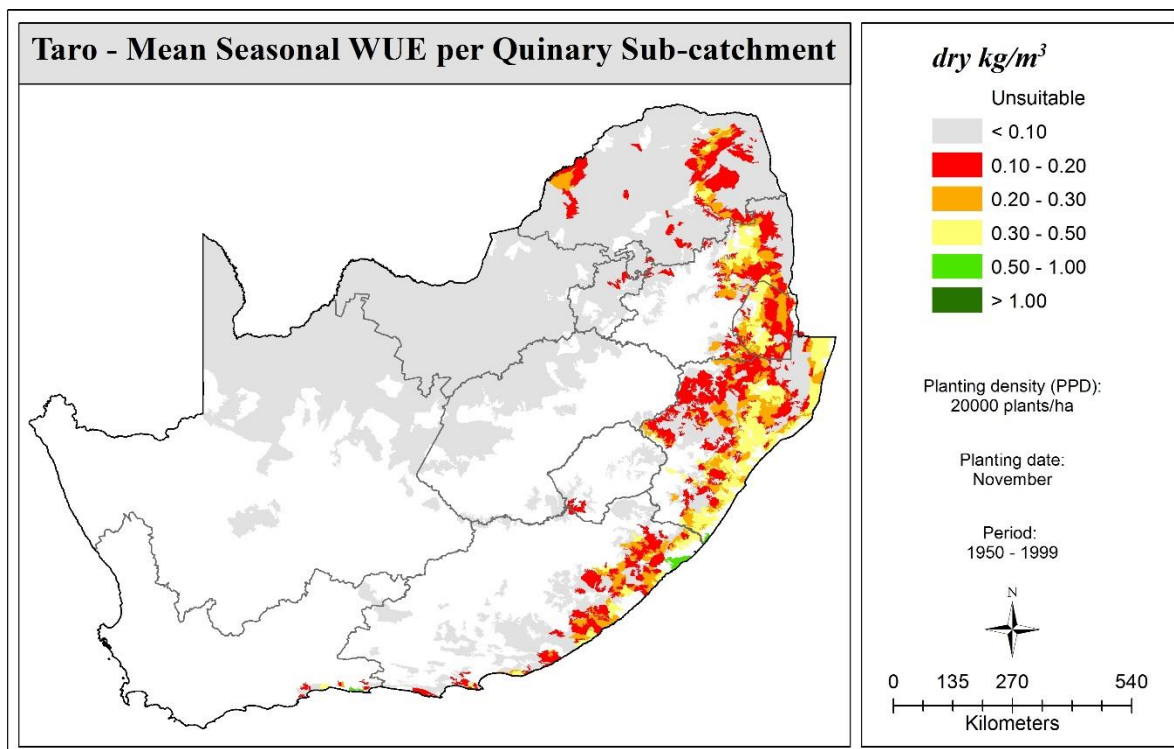
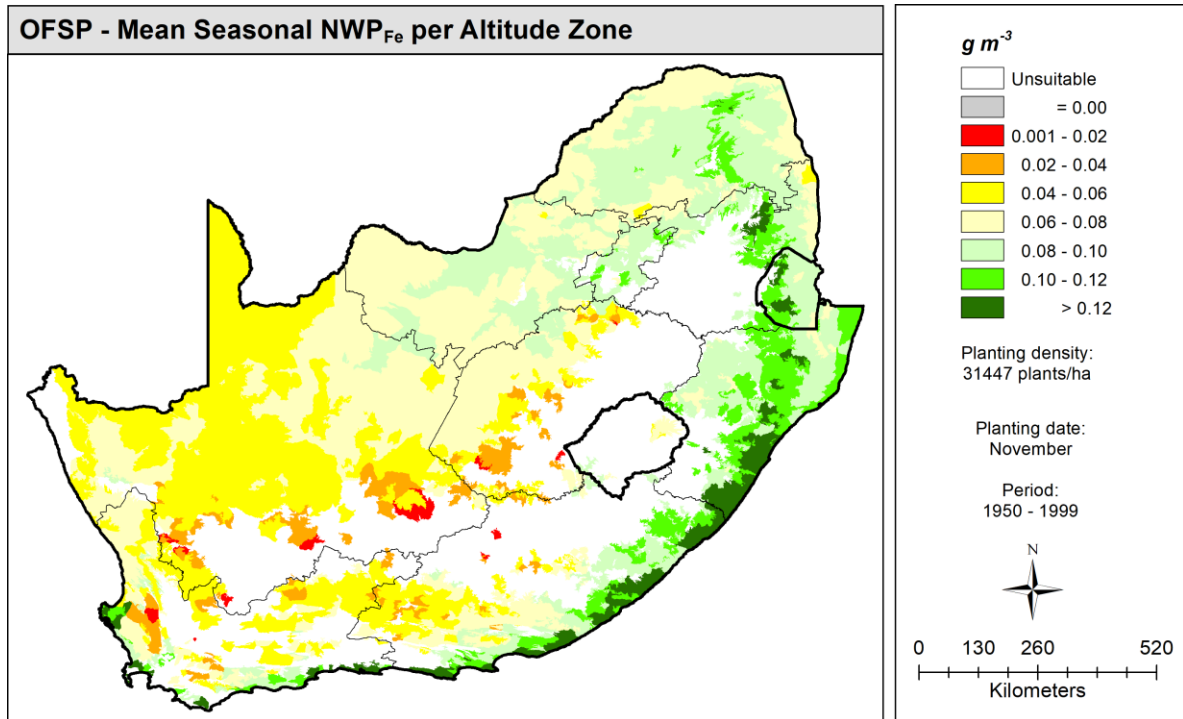


Figure 6-34 Seasonal crop water productivity (average of 49 seasons) for taro per quinary sub-catchment as simulated by AquaCrop (Kunz and Mabhaudhi, 2023)

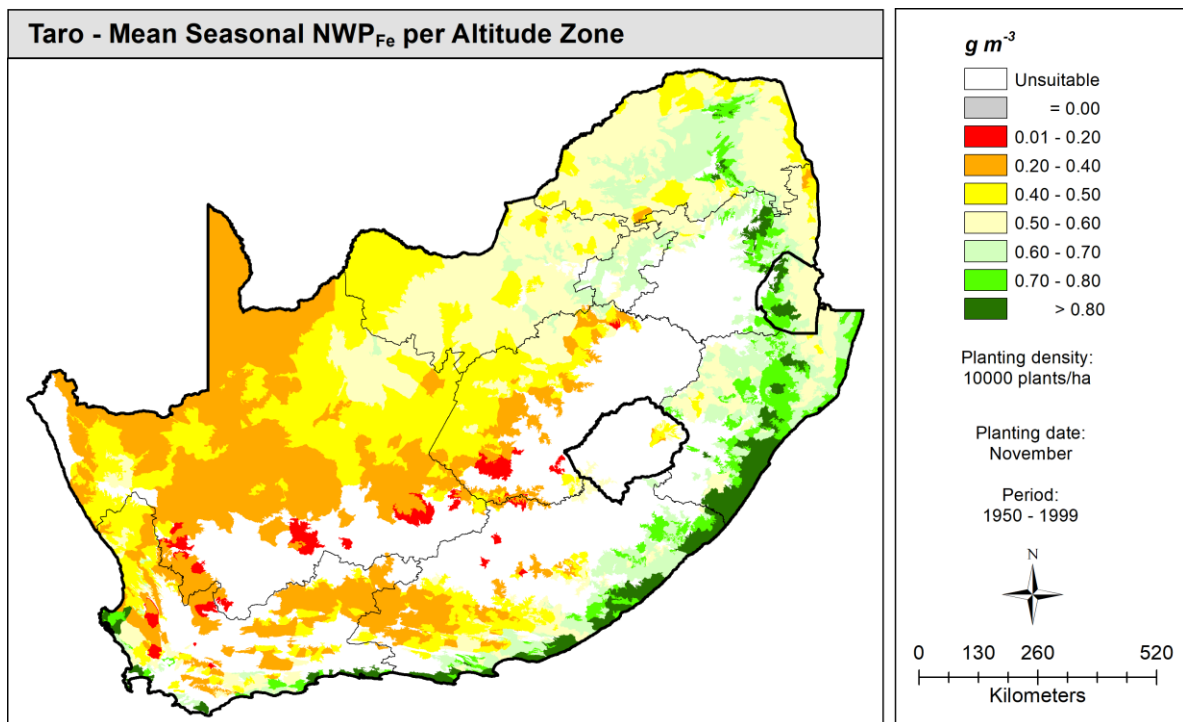
6.3.5 Nutritional water productivity

CWP (dry kg m^{-3}) was multiplied by the measured nutrient content (in g kg^{-1} of edible portion) to obtain nutritional water productivity (NWP; in g m^{-3}). Nutrient content of storage roots/tubers and leaves was measured by the ICFR laboratory (cf. **Table 14-1** and **Table 14-2**; cf. **Section 14.1**). NWP combines information of nutritional value with that of crop water productivity. The result is an index or metric that includes nutritional value-based output per unit of water consumed during crop growth. This concept is important in addressing food security issues, especially in arid and semi-arid regions where malnutrition remains high. Maps of NWP for both RTCs were produced for two important minerals, namely Fe and K. Maps of $\text{NWP}_{\beta\text{-c}}$ and NWP_{Zn} were also developed for OFSP and taro, respectively.

The NWP maps were produced using CWP values for OFSP and taro planted in November at a lower density, which represents smallholder farms. Hence, the spatial distribution in NWP matches that for CWP, i.e. HRZs with high yield will exhibit high CWP and thus NWP. From **Figure 6-35**, it is clear that NWP_{Fe} for taro tubers is higher than for OFSP storage roots, despite taro's lower CWP (cf. **Figure 6-32** in **Section 6.3.4.1**). From the tables shown in **Section 14.1**, K is by far the most abundant mineral element in OFSP storage roots and taro tubers. The K content and CWP of OFSP storage roots is higher than that for taro tubers, and thus NWP_{K} for OFSP is greater (**Figure 6-36**).

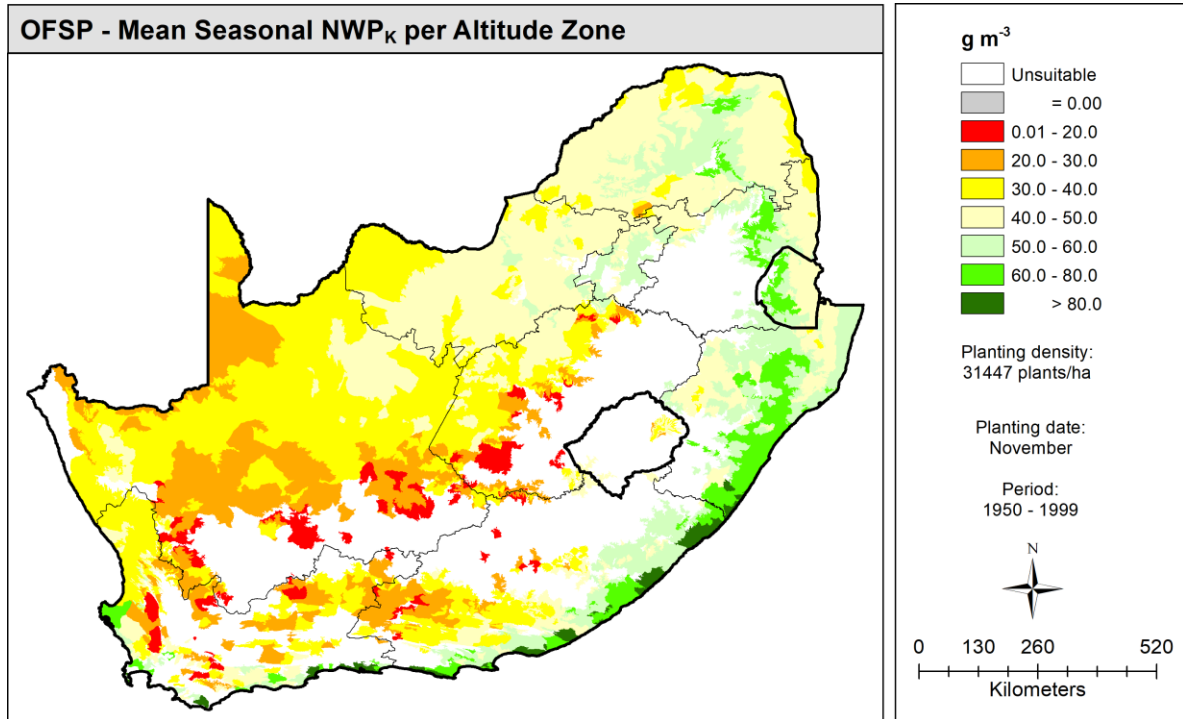


(a)

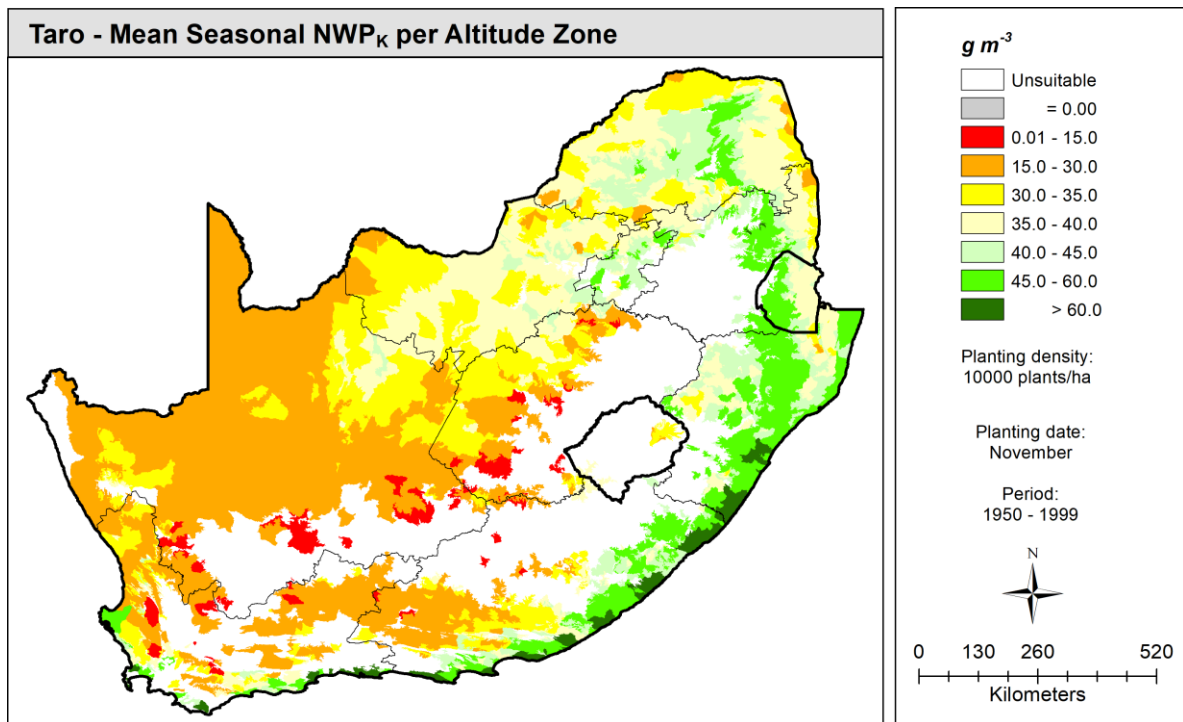


(b)

Figure 6-35 NWP_{Fe} for (a) OFSP and (b) taro planted in November at the lower density



(a)



(b)

Figure 6-36 NWP_K for (a) OFSP and (b) taro planted in November at the lower density

OFSP storage roots contain β -c, which is a precursor to vitamin A. Hence, the consumption of OFSP can address vitamin A deficiency among women and children in South Africa. **Figure 6-37** shows that OFSP grown along the coastal regions of the Eastern Cape province should produce the highest content of β -c per unit of water consumed. Hence, $NWP_{\beta-c}$ is at least double that for the majority of the Limpopo and North West provinces.

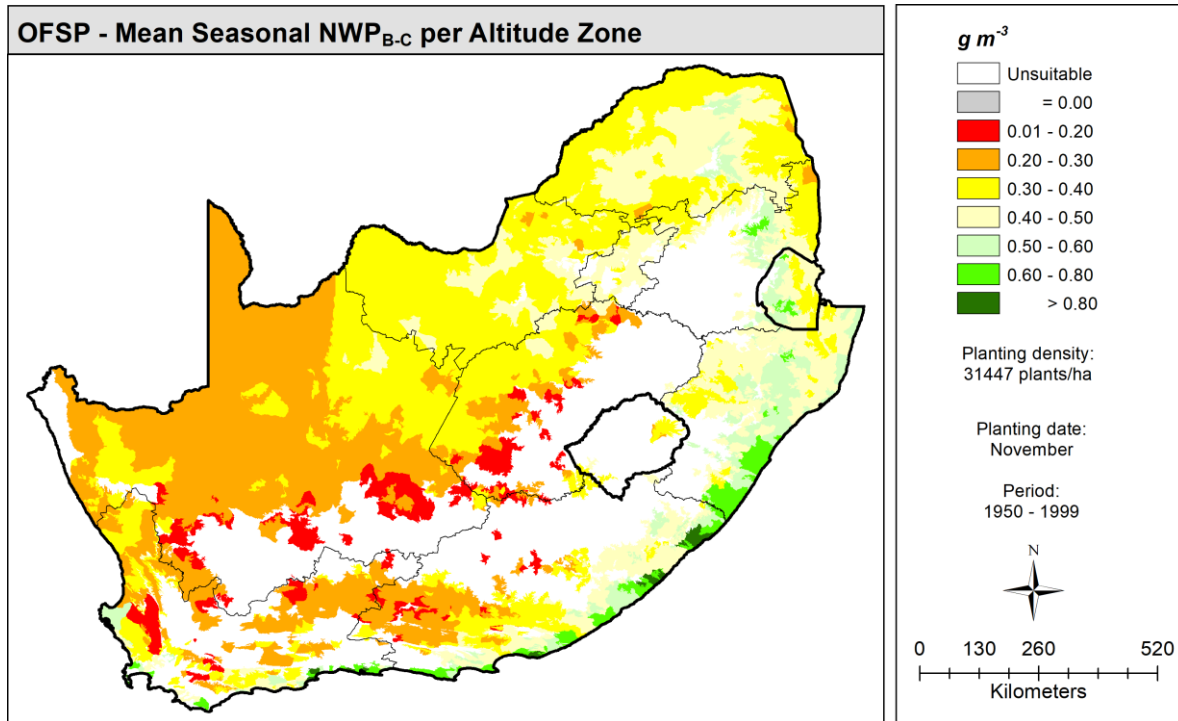


Figure 6-37 $NWP_{\beta-c}$ for OFSP planted in November at a density of 31,447 plants ha^{-1}

Zn deficiency is recognised as a global public health challenge (Stein, 2010), which can be addressed by promoting the consumption of taro. Taro tubers contain about 137 mg of Zn per dry kg of tuber (**Table 14-2**; cf. **Section 14.1**), compared to 14 mg per dry kg of OFSP storage root. Hence, taro tubers are a good source of this vital nutrient, which is important for boosting human immune systems. Taro can therefore address hidden hunger among vulnerable communities located in KwaZulu-Natal and the Eastern Cape, especially along the coast and adjacent interior. However, Gerrano et al. (2021) evaluated the mineral composition of 14 taro accessions (13 from KwaZulu-Natal) and showed that mineral content varied significantly ($p < 0.05$) among the genotypes (**Table 13-5** in **Section 13.1**).

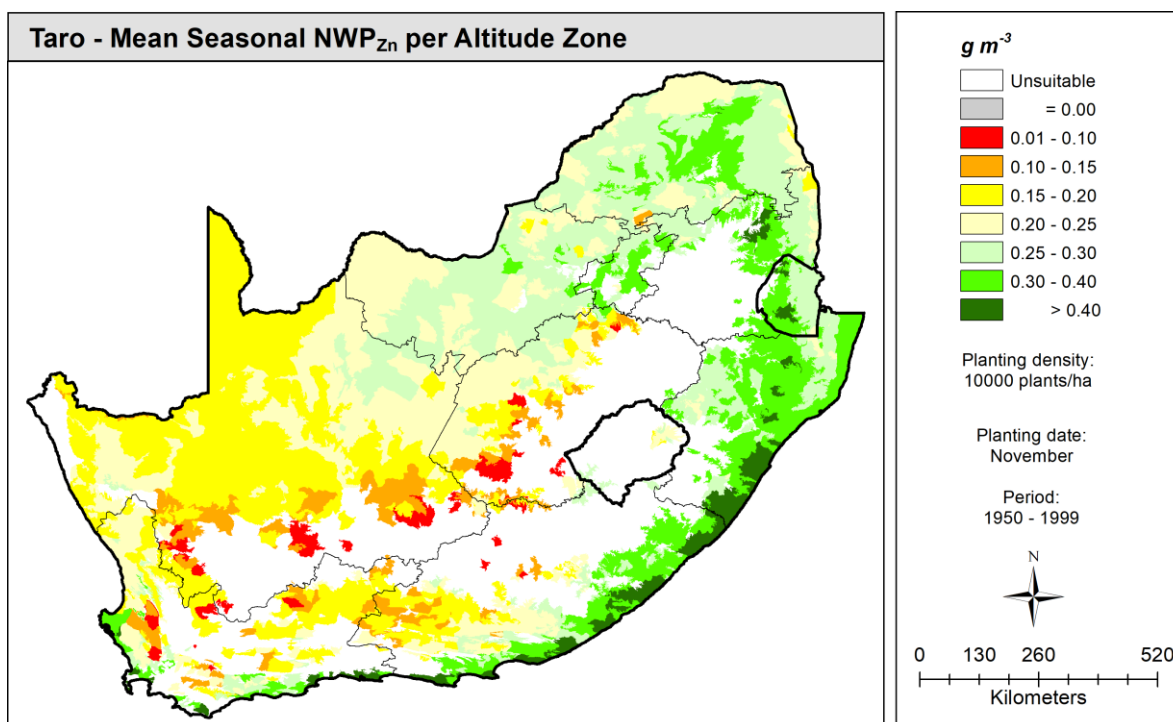


Figure 6-38 NWP_{Zn} for taro planted in November at a density of 10,000 plants ha⁻¹

6.4 SUMMARY AND CONCLUSIONS

Limited information exists on how water stress, temperature and soil type affect the yield of OFSP and taro across South Africa. Conducting experiments in different agro-ecological zones can be time consuming and costly (Nyathi et al., 2016). When calibrated and validated with data from well-designed experiments, crop models can help lower the overall costs of field experiments with regards to time and space (Mabhaudhi, 2012). Although such models can provide reasonable estimates of crop productivity, they are not a substitute for field experiments.

To meet the objectives of this project, a large number of AquaCrop simulations were undertaken. This was made possible since crop parameters already existed for both RTCs, which were then fine-tuned using data from season 3 as described in **Section 5.2.6**. These modified parameters provided better estimates of biomass and yield for both crops, as shown in **Section 5.3.7**, especially for water stress conditions. This represents a valuable outcome of this project.

Since a national model run is computationally expensive, considerable effort was spent on reducing model run time. A detailed and technical description of the speed improvements was provided in this report (cf. **Section 17**) so that other researchers and modellers can benefit from experiences gained over the past nine years. It is important to note that this work, which is considered innovative, was only possible due to funding received from the WRC. The significant speed improvements achieved to date allow for other modelling scenarios to be considered, e.g. multiple planting dates and plant densities.

AquaCrop was run at a national scale for all 5,838 HRZs, regardless of whether or not the zone is deemed suitable for rainfed crop production. This was done so that model output could be used to identify suitable crop production areas (cf. **Chapter 8**). For each HRZ, the model was run with 50 years of daily input climate data, which produced 49 consecutive seasons of simulated data. Model runs were completed for both rainfed and irrigated conditions, where the latter was used to derive crop coefficients for non-stressed growing conditions. The crop coefficients were required as input by the ACRU hydrological model to assess the potential impact of rainfed crop production on downstream water availability (cf. **Chapter 7**). AquaCrop was run for two plant densities representing small- and large-

scale production systems, each with two planting dates (01 November and 01 December). Since the modelling was undertaken for two RTCs, this equates to over 4.57 million seasonal simulations.

From the modelled results, national scale maps of attainable yield were produced for OFSP and taro, including maps on inter-seasonal variation in yield. In addition, maps showing the length of the crop cycle and potential risk of crop failure were also produced. Maps showing spatial variation in CWP and NWP were also produced, including inter-seasonal variation in CWP. The maps for OFSP were produced for the first time by the project. They provide valuable information for planning purposes, especially in areas where no (or insufficient) data exists on crop growth. The yield maps clearly highlight low and high potential production areas for OFSP and taro. They identify large parts of the country's interior region, especially towards the western areas, which are too cold and/or too dry for crop cultivation under rainfed conditions. The following are important trends that were identified:

- In general, higher plant density produces more crop yield (as expected).
- Planting date has a larger impact on crop yield than plant population.
- Yields are higher when OFSP is planted in November than December.
- Taro yields are higher along the eastern seaboard if planted in December,
- Taro yields are higher in the Limpopo province when planted in November.
- OFSP's CWP is higher than that for taro, due to higher storage root yields for OFSP.
- Y_{CV} is lower when OFSP is planted in November, especially along the coastal region of KwaZulu-Natal.
- Y_{CV} for taro is higher than for OFSP, particularly for a December planting.
- As expected, plant density had little to no impact on crop cycle compared to planting date, especially for OFSP.
- When compared to OFSP, less areas are suited to taro production.
- Colder regions are better suited to OFSP production than taro.
- The risk of failure for OFSP is relatively low compared to taro.
- For taro, a December planting is associated with a higher risk of crop failure.
- CWP improves at higher density due to increased yields.
- CWP is lower for OFSP planted in November when compared to December.
- CWP improves when taro is planted in November in the Limpopo and North West provinces. However, CWP is higher for the December planting along the coastal regions of KwaZulu-Natal and the Eastern Cape.
- CWP_{CV} for OFSP and taro is lower for the December planting compared to November.
- CWP_{CV} for taro is higher than that for OFSP, particularly for a December planting.
- $NWP_{TARO} > NWP_{OFSP}$ for Fe.
- $NWP_{TARO} < NWP_{OFSP}$ for K.
- For β -C, NWP_{OFSP} is highest along the coastal region of the Eastern Cape.
- For Zn, NWP_{TARO} is highest along the coastal region of KwaZulu-Natal and the Eastern Cape.

Although model output can be used to support decision-making, it should not be used to derive recommendations for best management (Debaeke and Aboudrare, 2004). Making decisions or drawing conclusions using only one variable (e.g. crop water productivity), whilst ignoring other variables (e.g. yield or crop cycle), must be avoided. The maps provided in this chapter help to identify areas in the country with high yield and productivity potential. The maps will prove useful to both small- and large-scale farmers, as they provide information on crop choice and expected yields for specific planting dates and plant densities. It is envisaged that the knowledge gained in this project will help promote the production of root and tuber crops, particularly in rural communities, thus resulting in poverty alleviation as well as the expansion of agricultural production. The maps showing the spatial variation in OFSP yield and NWP were produced for the first time by this project.

7 HYDROLOGICAL IMPACTS OF CROP PRODUCTION

7.1 INTRODUCTION

Agricultural expansion, facilitated by increased production of root and tuber food crops (RTCs), will result in land use changes, which may have a negative impact on available water resources, even if crops are rainfed. Therefore, one of the main outcomes of this project was to model the hydrological impact of RTC production on downstream water availability (cf. Aim 6 in **Section 1.2**).

Schulze (2023) produced a comprehensive report highlighting local and international verification studies that have been undertaken regarding ACRU. Results showed that ACRU can adequately simulate changes in runoff that may result from land use changes over time. ACRU was run for the first time in 2009 to assess land use change and climate change impacts on hydrological response. Since then, ACRU has been used extensively in many other WRC-funded projects to assess the impact of land use change on hydrological response. For example, the model was run in 2022 to assess the stream flow reduction potential of 15 commercial forestry species/hybrids/clones as part of WRC Project No. K5/2791 using model inputs obtained from field work (Clulow et al., 2023a) and remote sensing (Clulow et al., 2023b). ACRU has also been used to quantify the stream flow reduction potential of bamboo (Everson et al., 2021), sorghum and soybean (Kunz et al., 2020) and other crops such as sugarcane and sugarbeet (Kunz et al., 2015c).

7.2 METHODOLOGY

7.2.1 Model description

ACRU is an integrated hydrological model that has been frequently used to assess the impacts of land use change and climate change on the following:

- daily storm flows, base flows and total runoff,
- accumulated daily stream flows from all upstream catchments,
- peak discharge, sediment yields and recharge to groundwater, and
- daily soil water content and evapotranspiration.

ACRU operates on a daily time step, which is important since flow regimes and sediment yield are highly correlated with individual rainfall events (Schulze, 1995). The model is sensitive to changes in land cover, land use and land management that impact runoff response. ACRU is a physical model where processes are represented explicitly with initial and boundary conditions. It is also a conceptual model where important processes are coupled (**Figure 7-1**), and thus is considered a physical-conceptual model of intermediate complexity. Total evaporation from a vegetated surface consists of both soil surface evaporation (E) and transpiration (Tr), which is governed by rooting distributions. These two processes were modelled separately for improved simulation accuracy. During periods of sustained plant stress, when the soil water content of both the upper and lower soil horizons falls below 40% of plant available water (for example), transpiration losses are reduced in proportion to the level of plant stress. When plant available water increases above this threshold in either soil horizon, plant stress is relieved and evaporative loss recovers to the optimum value, at a rate dependent on the air temperature. In ACRU, runoff response variables are used to govern the portion of storm flow exiting a catchment on a particular day (as quick flow), as well as the portion of base flow originating from the groundwater store, which contributes to runoff generation (Schulze, 1995). For a more detailed description of ACRU, the reader is referred to Schulze (2023; cf. Chapter 4).

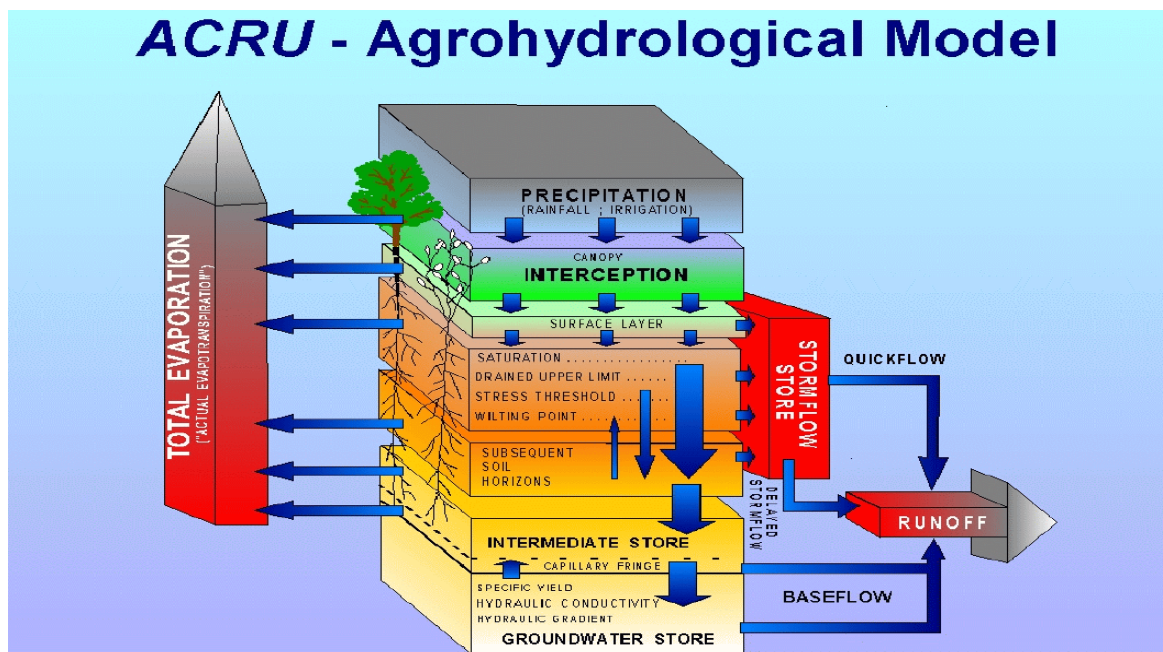


Figure 7-1 Structure of the ACRU agro-hydrological modelling system (Schulze, 1995)

7.2.2 Model inputs

A brief description of the climate and soil data available for each of the 5,838 HRZs was provided in **Sections 6.2.2.2** and **6.2.2.3**, respectively. Since ACRU requires A-pan equivalent reference evaporation, FAO56 E_{To} was adjusted using the method developed by Kunz et al. (2015b). This adjustment was based on a modified version of the PenPan equation, which was successfully applied in Australia to estimate A-pan equivalent evaporation. The adjustments suggest that A-pan equivalent evaporation exceeds FAO56 reference evapotranspiration by a factor ranging from 17 (for summer) to 51% (for winter) for southern Africa. The reader is referred to Kunz et al. (2015b) for more detail on the PenPan method.

Two other ACRU parameters, namely ABRESP and BFRESP, were also derived for each HRZ. These represent the fraction of “saturated” soil water that is redistributed each day from the topsoil into the subsoil horizon, and from the subsoil horizon into the intermediate/groundwater store. They were also determined for each terrain unit per land type (cf. **Section 6.2.2.3**), from which area-weighted values were then calculated for each HRZ.

7.2.3 Land cover parameters

ACRU requires seven key parameters to model the water use of the vegetation layer (**Table 7-1**). These variables are required to consider four processes, namely canopy interception loss, evaporation from the canopy (of transpired and intercepted water), evaporation of water from the soil surface and soil water extraction by plant roots (to quantify transpiration). In the context of assessing stream flow reduction potential, water use of the vegetation layer is defined as the difference in runoff generated by the land cover (e.g. crop) to that generated by natural vegetation. Thus, to determine the hydrological impact of land use change to OFSP and taro production, it is necessary to first define the baseline vegetation against which water use comparisons are made.

Table 7-1 Key variables (monthly values) in ACRU that account for land cover/use (Smithers and Schulze, 1995)

Parameter	Definition
<i>CAY</i>	A monthly consumptive water use (or “crop”) coefficient, which reflects the ratio of water use by vegetation under conditions of freely available soil water to the evaporation from a reference surface (e.g. A-pan equivalent).
<i>ELAIM</i>	Monthly LAI values. Can be used to calculate monthly interception losses and/or to determine the crop’s consumptive water use.
<i>VEGINT</i>	Monthly interception loss values, which can change during a plant’s annual growth cycle. They estimate the magnitude of rainfall that is intercepted by the plant’s canopy on a rainy day.
<i>ROOTA</i>	The fraction of plant roots that are active in extracting soil moisture from the A-horizon in a given month. This fraction is linked to root growth patterns during a year and periods of senescence brought on, for example, by a lack of soil moisture or by frost.
<i>COLON</i>	Extent of colonisation of plant roots in the B-horizon. Determines the amount of water that may be extracted by the plant from the B-horizon. Hence, this variable reflects the extent to which the subsoil is “colonised” by roots. Total evaporation from the B-horizon is suppressed by the fraction <i>COLON</i> /100. Default in ACRU: 100%.
<i>PCSUCO</i>	The fraction (expressed as a percentage) of the soil surface covered by a mulch or litter layer. This layer suppresses soil water evaporation. However, 20% of the soil water evaporation still takes place with 100% cover. Default in ACRU: 0%.
<i>CONST</i>	Fraction of plant available water at which plant stress sets in. The plant’s physiological characteristics determine the onset of wilting in response to drier soil conditions.
<i>FOREST</i>	Specifies whether evaporation from a wet canopy occurs at potential rate (for short vegetation) or at an enhanced rate (if more than 50% of the catchment is forestry).

7.2.3.1 Baseline land cover

Prior to 2019, the Department of Water and Sanitation (DWS) supported and accepted the use of “natural vegetation” as depicted by the Acocks (1988) veld type map as a reasonable standard or reference land cover against which impacts of land use change were assessed. However, DWS has recently adopted the vegetation clusters derived by Toucher et al. (2020) as the new baseline. The 2012 vegetation map produced by the South African National Botanical Institute (SANBI) identified 435 vegetation types, which were simplified into 121 hydrologically relevant vegetation groupings called clusters. For each cluster, Toucher et al. (2020) derived appropriate values for the seven parameters shown in **Table 7-1**. For example, remotely sensed leaf area index (*ELAIM*) for each vegetation cluster was used to derive monthly crop coefficients (*CAY*). Monthly LAI values were also used to estimate monthly interception loss (*VEGINT*) using the von Hoyningen-Huene (1983) equation. This new baseline has already been used in two projects (Clulow et al., 2023b; Kunz et al., 2020).

7.2.3.2 Root and tuber crops

CAY

Monthly crop coefficients (K_c) are an important ACRU model input that is used to estimate water use of the vegetation layer. Sensitivity analyses conducted by Angus (1989) and Toucher et al. (2020) showed that ACRU is highly sensitive to changes in *CAY* and slightly sensitive to changes in both *ROOTA* and *VEGINT*. For this reason, it is therefore important to accurately determine representative *CAY* values for OFSP and taro for use in ACRU.

The methodology to derive representative *CAY* values for each HRZ involved running AquaCrop for non-stressed conditions to determine maximum crop evapotranspiration (ET_c), from which *CAY* was calculated as the ratio of ET_c to reference evapotranspiration (ET_o). Hence, a unique set of monthly *CAY* values were calculated for each HRZ, which is more robust than using one set of values derived from field work for all HRZs. This approach was first used in WRC Project K5/2491 (Kunz et al., 2020),

which assessed, inter alia, the hydrological impact on runoff generation that may result from a land use change from natural vegetation to sorghum and soybean cultivation.

The decision to set the planting date to the 01 November and 01 December (not day 15) was important, since ET_c values were summed over 30 (or 31) days, and thus CAY calculated for the first month was considered more accurate since CAY estimated from 15 days of data is typically higher. For each HRZ, the average crop cycle simulated by AquaCrop in days was divided by 30 to determine the crop cycle length in months, which varied from 4 to 12 months for OFSP and 5 to 12 months for taro. The maximum length of 12 months was expected as the crop cycle was restricted to a maximum of 365 days.

AquaCrop is no longer run for cold seasons where the crop cycle exceeds 365 days (cf. **Section 17.3.5**). This decision was made to reduce model run time. Furthermore, if three or less seasons (out of 49) are simulated, averaged seasonal ET_c cannot be calculated (i.e. too few data points). When this occurs, the crop coefficient is set to -999 to indicate no data, i.e. missing value. For zones where no ET_c was simulated for any month, K_c was therefore not calculated. Since these HRZs are unsuitable for crop production, CAY was set to monthly values derived for natural vegetation by Toucher et al. (2020). This was done so that differences in runoff generation that may result from a land use change from natural vegetation to crop production was zero (i.e. no stream flow reduction potential).

Since taro takes up to 300 days (or 10 months) to mature (Mugiyo et al., 2021b), crop cycles of 11-12 months are considered too long. Furthermore, taro is frost sensitive (cf. **Table 13-1** in **Section 13.1**) so is unlikely to survive the cold winter months, especially June to August. Hence, the decision was made to reduce the maximum crop cycle to 10 months for taro (and 7 months for OFSP). For months with no AquaCrop-derived CAY values (e.g. from April/May to October), crop coefficients for the fallow period were used, which were derived from measured ET for weedy conditions at Fountainhill over season 2 (cf. **Section 4.3.5.1**).

The smallest and largest CAY values calculated from AquaCrop output for each month across all 5,838 HRZs is shown in **Table 7-2**. It is important to note that ET_c simulated by AquaCrop is limited by the basal crop coefficient (K_{CB}) input parameter, which was set to 1.05 for both crops (**Table 16-13**; cf. **Section 16.4**). The values highlight the potential of each RTC to utilise approximately the same amount of water as the reference crop (hypothetical short, green grass).

Table 7-2 Minimum and maximum monthly crop coefficients for OFSP and taro across all 5,838 HRZs

RTC	Planting date/ density	Stat	Nov	Dec	Jan	Feb	Mar	Apr	May	Jun	Jul	Aug	Sep
OFSP	01 Nov/ 31,447	Min	0.26	0.20	0.20	0.20	0.31	0.31	0.23				
		Max	0.95	1.01	1.00	0.95	0.86	0.73	0.64				
	01 Dec/ 31,447	Min		0.28	0.20	0.20	0.31	0.31	0.23	0.20			
		Max		1.01	1.00	0.95	0.86	0.74	0.67	0.60			
	01 Nov/ 55,556	Min	0.28	0.20	0.20	0.20	0.31	0.31	0.23				
		Max	0.95	1.01	1.00	0.95	0.86	0.73	0.64				
	01 Dec/ 55,556	Min		0.31	0.20	0.20	0.31	0.31	0.23	0.20			
		Max		1.01	1.00	0.95	0.86	0.74	0.66	0.59			
Taro	01 Nov/ 10,000	Min	0.20	0.20	0.20	0.20	0.31	0.31	0.26	0.20	0.20	0.20	
		Max	0.95	1.01	1.00	0.95	0.86	0.74	0.78	0.63	0.68	0.58	
	01 Dec/ 10,000	Min		0.20	0.20	0.20	0.31	0.31	0.26	0.20	0.20	0.20	0.20
		Max		1.01	1.00	0.95	0.86	0.74	0.78	0.64	0.68	0.62	0.67
	01 Nov/ 27,000	Min	0.20	0.20	0.20	0.20	0.31	0.31	0.26	0.20	0.20	0.20	
		Max	0.95	1.01	1.00	0.95	0.86	0.74	0.78	0.63	0.68	0.58	
	01 Dec/ 27,000	Min		0.21	0.20	0.20	0.31	0.31	0.26	0.20	0.20	0.20	0.20
		Max		1.01	1.00	0.95	0.86	0.74	0.78	0.63	0.68	0.61	0.67

Everson and Mengistu (2011) reported daily K_C values ranging from 0.46-0.81 (average of 0.60) for lowland taro grown in the Mbongolwane wetland catchment in KwaZulu-Natal. These values are relatively low considering taro was planted on raised beds cleared of sedge (*Cyperus latifolius*) and furrows were created to increase water flow (i.e. relatively unstressed conditions). However, values were only calculated for 4 and 6 days in November 2009 and January 2010, respectively.

ACRU requires monthly K_C values calculated using the A-pan as the reference evaporation (E_{PAN}). Since monthly K_C values for OFSP and taro are based on FAO56 reference evapotranspiration (E_{ETO}), they were adjusted using monthly pan coefficients (E_{PAN}/E_{ETO}). The latter ratios were calculated by Kunz et al. (2015b) for each HRZ and range from 1.16 to 0.51. They are always greater than unity (i.e. 1) since $E_{PAN} > E_{ETO}$, especially during the winter months. Hence, crop coefficients for OFSP, taro and the fallow period (K_{C_ETO}) were multiplied by the inverse of monthly pan coefficients for each HRZ to determine pan adjusted crop coefficients (K_{C_PAN}) as follows:

$$K_{C_PAN} = K_{C_ETO} * \frac{E_{ETO}}{E_{PAN}} = \frac{ET_{CRP}}{E_{ETO}} * \frac{E_{ETO}}{E_{PAN}} = \frac{ET_{CRP}}{E_{PAN}} \quad \text{Equation 8}$$

In summary, the following procedure was followed to determine the A-pan equivalent crop coefficients for each RTC, which were required as input by ACRU:

- AquaCrop was run with an option to relieve water stress by artificially applying a minimum amount of irrigation water.
- Monthly ET_C (maximum evapotranspiration) was calculated for each season and then averaged.
- Similarly, average ET_O (reference evapotranspiration) was calculated and used to determine monthly K_C values.
- Crop coefficients (K_{C_ETO}) were then adjusted to A-pan equivalent values (K_{C_PAN}) using the pan coefficient (E_{PAN}/E_{ETO}).
- Any adjusted value below 0.20 was set to this value, which represents the minimum soil water evaporation that can occur from a bare soil.
- The average crop cycle was used to determine the end-season month (e.g. May/June and August/September for OFSP and taro, respectively), beyond which K_C values were set to values determined for the fallow period at Fountainhill during season 2.
- Zones with 12 missing crop coefficients were not considered suitable for crop production, and thus missing values were replaced with A-pan equivalent crop coefficients for natural vegetation.

VEGINT

For OFSP and taro, monthly canopy interception values required as input by ACRU were estimated using the von Hoyningen-Huene (1983) equation, which uses LAI and gross rainfall (P_g in mm) to estimate daily interception loss (I_C in mm) as follows:

$$I_C = 0.30 + 0.27P_g + 0.13LAI - 0.013P_g^2 + 0.0285P_g \cdot LAI - 0.007LAI^2 \quad \text{Equation 9}$$

This equation was also used to estimate $VEGINT$ for the 121 vegetation types representing baseline land cover, i.e. natural vegetation (cf. **Section 7.2.3.1**). Weekly LAI measurements for the non-stressed water treatment in season 3 were used to calculate I_C . A software utility was developed by Kunz et al. (2020) to estimate daily interception loss from 1950 to 1999, from which long-term monthly averages were calculated for each of the 5,838 HRZs, then used as input for ACRU for each modelling scenario.

ROOTA

ROOTA represents the fraction of plant roots that are active in extracting soil water from the A-horizon. From the literature, Kunz et al. (2020) found that 60-80% of the fine-root volume for most crops is found in the top 20 cm of soil. Similarly, the majority of crop roots occur in the upper 30 cm of the soil profile. Based on this, the depth of the A-horizon (*DEPAHO*) was used to set *ROOTA* to:

- 0.70 if $DEPAHO \leq 20$ cm,
- 0.85 if $0.20 < DEPAHO \leq 25$ cm, and
- 1.00 if $DEPAHO > 25$ cm.

When *ROOTA* is set to 1, it indicates that evapotranspiration mainly takes place from the A-horizon. Toucher et al. (2020) noted that setting *ROOTA* to 1 resulted in large increases in simulated stream flow and greater increases in simulated base flow. For the fallow period, *ROOTA* was set to 0.70 since the roots of weeds would tend to extract soil water from the likely wetter B-horizon since the A-horizon would be dried out by the crop roots during the crop growing season.

COLON

In ACRU, it is assumed that the topsoil is 100% colonised by roots, i.e. roots can extract all available soil water in the A-horizon. *COLON* therefore reflects the extent to which the subsoil is colonised by roots. When *ROOTA* is set to 1 (e.g. during the fallow period), *COLON* is ignored in ACRU, but should be set to 0. However, *COLON* was set to 100% due to reflect weedy conditions during the fallow period. *ROOTA* was used to set *COLON* to:

- 70% if *ROOTA* is 1.00,
- 85% if *ROOTA* is 0.85, and
- 100% if *ROOTA* is 0.70.

PCSUCO

The percentage of the soil surface covered by mulch, litter and stones (*PCSUCO*) is used in ACRU to suppress soil water evaporation. For the baseline, Toucher et al. (2020) estimated monthly *PCSUCO* values from *CAY*. Since it is important to maintain weed-free conditions for up to 7-8 weeks after planting, *PCSUCO* was set to 0% for the first two months. In addition, OFSP and taro do not shed dead leaves, and thus there was no litter layer build-up at the end of the season. Hence, *PCSUCO* was set to 0% for the crop growing season. For the fallow period, *PCSUCO* was set to 33.3% based on observations of prolific weed growth at site 1 during the second season.

CONST

CONST represents the onset of plant water stress. For the baseline, the default value of 0.40 was used for all vegetation types. Allen et al. (1998: 163-165) provided values for the depletion fraction (p) for a range of crops including root and tubers (**Table 7-3**), which represents the fraction of plant available water that can be depleted before moisture stress occurs. Pereira et al. (2021a; 2021b) provided updated K_C , K_{CB} and p value for numerous crops, including RTCs such as cassava, sweet potato and taro. Since *CONST* is equivalent to $1 - p$, a value of 0.60 was used for both crops, which indicates they are less drought tolerant. For the altitude zones where the crop cannot grow, *CONST* was set to the default value of 40% to mimic the natural vegetation setting.

FOREST

For both crops, *FOREST* was set to zero (i.e. no enhanced wet canopy evaporation).

Table 7-3 Values of the depletion fraction (ρ) provided by Allen et al. (1998) and Pereira et al. (2021a; 2021b)

Root and tuber crops	Allen et al. (1998)	Pereira et al. (2021a; 2021b)
Beets	0.50	0.45
Cassava (year 1)	0.35	0.50
Cassava (year 2)	0.40	0.50
Potato	0.35	0.40
Sweet potato	0.65	0.40
Parsnip	0.40	0.40
Taro		0.40
Turnip	0.50	0.50
Sugarbeet	0.55	0.55

7.2.4 Rainfall:runoff parameters

Key parameters and variables that influence runoff generation in ACRU are shown in **Table 7-4**. Sensitivity analyses (e.g. Angus, 1989; Toucher et al., 2020) indicate that ACRU is most sensitive to changes in rainfall input (*CORPPT*) and highly sensitive to changes in certain soil-related parameters (e.g. *SMDDEP*). The monthly rainfall (*CORPPT*) and pan evaporation (*CORPAN*) adjustment factors were developed by Kunz et al. (2020) and Kunz et al. (2015b), respectively. The effective rooting depth (*EFRDEP*) is assumed to be the total soil depth, i.e. the sum of the A-horizon (*DEPAHO*) and the B-horizon (*DEPBHO*) depths in each HRZ.

The remaining four parameters in **Table 7-4** are difficult to measure and thus, values were obtained from previous studies involving ACRU that best represent the scale of the HRZs. For example, Kunz et al. (2020) set *SMDDEP* to the thickness of the topsoil as suggested by Smithers and Schulze (1995). The catchment's storm flow response fraction (*QFRESP*) was set to a value of 0.30 as used in previous studies (e.g. Warburton et al., 2010; Schulze, 2011; Kunz et al., 2020; Everson et al., 2021; Clulow et al., 2023b).

Table 7-4 Key parameters and variables in ACRU that influence rainfall:runoff response

Variable	Definition	Value	Source
<i>CORPPT</i>	Monthly precipitation adjustment factors (e.g. to account for differences in monthly rainfall between the selected driver station and spatially averaged estimates for the subcatchment)	12 monthly values unique to each altitude zone	Kunz et al. (2020)
<i>CORPAN</i>	Monthly A-pan adjustment factors (e.g. to adjust Penman-Monteith evaporation estimates to A-pan equivalent evaporation)	12 monthly values unique to each altitude zone	Kunz et al. (2015b)
<i>EFRDEP</i>	Effective soil depth for colonisation by plant roots	<i>DEPAHO</i> + <i>DEPBHO</i>	Clulow et al. (2023b)
<i>SMDDEP</i>	Effective soil depth from which storm flow generation takes place	<i>DEPAHO</i>	Clulow et al. (2023b)
<i>QFRESP</i>	Storm flow response fraction for the catchment	0.30	Clulow et al. (2023b)
<i>COFRU</i>	Base flow recession constant	0.009	Clulow et al. (2023b)
<i>COIAM</i>	Coefficient of initial abstraction that accounts for vegetation, soil surface and climate influences on storm flow generation	0.15-0.35	Kunz et al. (2020)

Similarly, the base flow recession constant (*COFRU*) was set to 0.009 (or 0.9%) as was used by Clulow et al. (2023b). In ACRU, the coefficient of initial abstraction (*COIAM*) varies month-to-month according to changes in rainfall intensity and vegetation growth (Schulze 1995). *COIAM* typically varies from 0.15 to 0.35 (default of 0.20) and unique monthly values were determined for each HRZ by Kunz et al. (2020), based on rainfall seasonality and distance from the coastline. The parameter values shown in **Table 7-4** were used for both the baseline simulation, as well as for each crop modelling scenario.

7.2.5 Minimising computational expense

For previous WRC-funded projects (e.g. Everson et al., 2021; Kunz et al., 2015c; Kunz et al., 2020; Clulow et al., 2023b; Schütte et al., 2023), significant improvements were made to the model to reduce run time, thus minimising computational expense. In 2015, a national run took approximately 8.5 hours to complete, which was reduced to 51 minutes in 2020 (Kunz et al., 2020). In 2023, the model run time was further reduced to 40 minutes (Clulow et al., 2023b). It is important to note that this work, which is considered innovative, was only possible due to funding received from the WRC.

7.2.6 Modelling approach

As noted previously (cf. **Section 7.1**), ACRU has been extensively used to assess stream flow reduction potential that could result from various land use changes (e.g. Clulow et al., 2023b; Everson et al., 2021; Kunz et al., 2020). For this project, ACRU was run at the national scale to estimate runoff response for all 5,838 HRZs, regardless of whether sweet potato or taro can successfully be grown in the zone.

7.2.6.1 Estimation of runoff

The approach followed was similar to that used in previous SFRA studies and was as follows:

- For each HRZ, daily climate data and soil information was obtained from existing databases described by Kunz et al. (2020) and Clulow et al. (2023b) respectively, then used as input to ACRU (cf. **Section 6.2.2**).
- The ACRU model was run to simulate mean monthly and annual runoff (MAR) response for:
 - baseline conditions (MAR_{BASE}), i.e. the runoff produced from a land cover of natural vegetation, and
 - each root and tuber crop (MAR_{CROP}), assuming a 100% change in land cover.
- For the baseline, ACRU input parameters derived by Toucher et al. (2020) for each vegetation cluster (cf. **Section 7.2.3.1**) were used to represent natural vegetation.
- For taro and sweet potato, the parameter values given in **Section 7.2.3.2** were used.

7.2.6.2 SFRA assessment

In the context of assessing stream flow reduction potential, crop water use is defined as the reduction in MAR that may result from a land use change from the baseline (base) to crop cultivation (crop), i.e. $MAR_{BASE} - MAR_{CROP}$. Although this reduction can be expressed in absolute (i.e. mm) terms, it is more appropriate to consider runoff differences in relative (i.e. %) terms. Hence, the simulated reduction in MAR is expressed as a percentage change relative to the baseline, i.e. $MAR_{REDN} = 100 \cdot (MAR_{BASE} - MAR_{CROP}) / MAR_{BASE}$. If the relative impact on runoff exceeds 10%, the proposed land use change may be declared as a SFRA (Jewitt et al., 2009b).

7.3 RESULTS AND DISCUSSION

The purpose of the national ACRU model runs was to (i) quantify the stream flow reduction potential of RTC production on available water resources in South Africa, and (ii) assess the feasibility of declaring a specific RTC as a Stream Flow Reduction Activity (SFRA). ACRU was used to estimate the mean annual runoff (MAR) produced from a land cover of OFSP or taro (MAR_{CROP}), as well as that from the

baseline (MAR_{BASE}), i.e. natural vegetation. Crop “water use” is defined as the difference in mean annual runoff from these two land covers, i.e. $MAR_{DIFF} = MAR_{BASE} - MAR_{CROP}$.

7.3.1 Crop water use

For the two planting dates and plant densities, the absolute reduction in MAR resulting from a proposed land use change from natural vegetation to OFSP cultivation (i.e. MAR_{DIFF}) ranged from -117 to 62 mm (**Table 7-5**). Relatively similar differences in runoff were simulated for taro (**Table 7-5**). When this reduction is positive, more runoff is produced from natural vegetation than from the crop (i.e. $MAR_{BASE} > MAR_{CROP}$). This means the crop uses more water than natural vegetation ($ET_{CROP} > ET_{BASE}$), which occurred in a maximum of 1,058 and 781 HRZs for OFSP and taro, respectively. Hence, OFSP may have a greater impact on catchment water resources than taro, which is linked to the longer crop cycle.

The potential reduction in annual runoff appears more sensitive to planting date, rather than plant density. For OFSP, a November planting is likely to result in a larger reduction in runoff compared to a December planting. In contrast, a positive reduction on MAR occurred in more zones for a December planting, as shown in **Table 7-5**. As expected, the higher plant density resulted in a larger impact on annual runoff.

Table 7-5 Absolute reduction in mean annual runoff resulting from a proposed land use change from natural vegetation to OFSP production

RTC	Planting date (month)	Plant density (plants ha ⁻¹)	MAR_{DIFF} (mm)	$MAR_{BASE} > MAR_{CROP}$ (number of HRZs)
OFSP	11	31,447	-117 to 62	1,035
	11	55,556	-116 to 62	1,058
	12	31,447	-102 to 55	926
	12	55,556	-102 to 55	964
Taro	11	10,000	-113 to 55	692
	11	27,778	-112 to 55	711
	12	10,000	-101 to 54	754
	12	27,778	-101 to 54	781

The crop coefficients calculated from AquaCrop output assume weed-free conditions throughout the crop cycle. Experience has shown that for smallholder farmers planting up to a hectare of taro, manual weeding is not a viable option due to the cost of required labour. Hence, crop ET during the growing season may be greater than that simulated by AquaCrop. However, the crop coefficients for the fallow period represent weedy conditions, not bare soil.

7.3.2 Reduction in annual runoff

For the above two worst case scenarios, it is important to assess whether MAR_{REDN} exceeds 10% relative to natural vegetation and if so, the crop may need to be considered by the Department of Water and Sanitation for declaration as a potential SFRA. As shown in **Figure 7-2**, runoff production from OFSP and taro is very similar to that from natural vegetation (i.e. $-2 < MAR_{REDN} \leq +2\%$) in 56.8% and 68.1% of all HRZs, respectively. For the majority of these zones, the climate is too cold for crop production. Hence, the ACRU parameters were not altered and therefore reflect natural vegetation conditions. Thus, the relative reduction in runoff is zero.

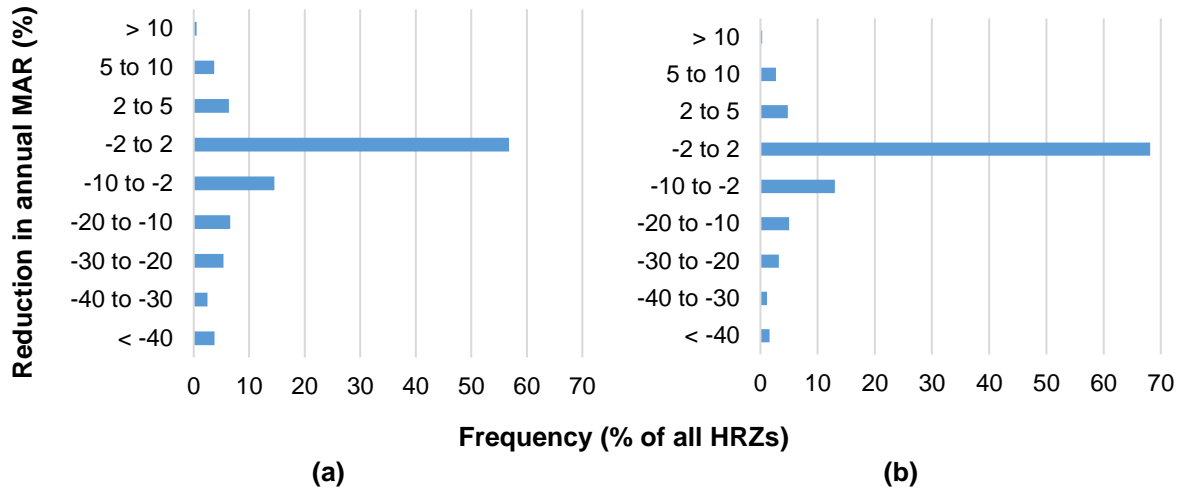


Figure 7-2 Histograms of the percentage reduction in mean annual runoff (MAR) per HRZ that may result from a change in land use from natural vegetation to (a) OFSP and (b) taro cultivation

However, MAR_{REDN} exceeds the 10% threshold suggested by Jewitt et al. (2009b) in some HRZs, which is of more concern. The largest reduction of 18% was simulated in zone no. 5,432 for OFSP planted in November at the higher density, due to a reduction in annual runoff of 55.88 mm relative to the baseline (310.83 to 254.95 mm). As shown in **Table 7-6**, MAR_{REDN} exceeding 10% occurred most often in (i) 30 HRZs when OFSP was planted in November at a plant density of 55,556 plants ha^{-1} , and (ii) 19 zones for taro planted in December at a plant density of 10,000 or 27,778 plants ha^{-1} . Hence a December planting of OFSP and a November planting of taro may have less impact on downstream water users.

Table 7-6 Relative reduction in mean annual runoff resulting from a proposed land use change from natural vegetation to OFSP production

RTC	Planting date (month)	Plant density (plants ha^{-1})	Maximum MAR_{REDN} (%)	$MAR_{REDN} > 10\%$ (number of HRZs)
OFSP	11	31,447	18	28
	11	55,556	18	30
	12	31,447	14	14
	12	55,556	15	16
Taro	11	10,000	17	13
	11	27,778	17	13
	12	10,000	16	19
	12	27,778	16	19

For these two worst case scenarios, maps were produced that show where these zones are located for OFSP (**Figure 7-3**) and taro (**Figure 7-4**). HRZs where $MAR_{REDN} > 10\%$ are mostly situated along the eastern seaboard in the Mpumalanga, KwaZulu-Natal and Eastern Cape provinces. Some of the highlighted zones are located within protected areas large scale crop production is prohibited. Furthermore, the relative reductions assume a 100% change in land cover from natural vegetation to crop cultivation in each HRZ, which is unrealistic. When assessing SFRA potential, this needs to be considered. Taro can take up to ~49 days to emerge. During this time, soil water evaporation is dominant (not transpiration), and thus crop ET is likely to be lower than for other conventional crops or natural vegetation types. A layer of mulch may help to reduce unproductive water losses, further decreasing crop ET.

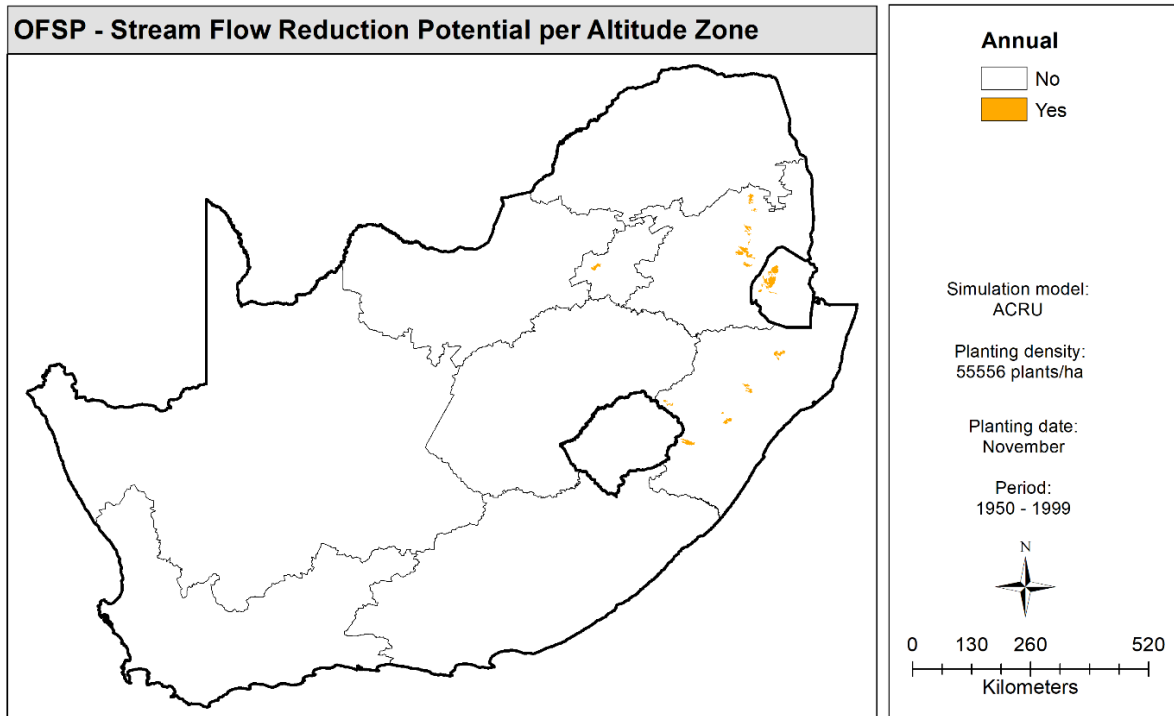


Figure 7-3 Location of HRZs where the reduction in mean annual runoff exceeds 10% that may occur due to a land cover change from natural vegetation to OFSP cultivation

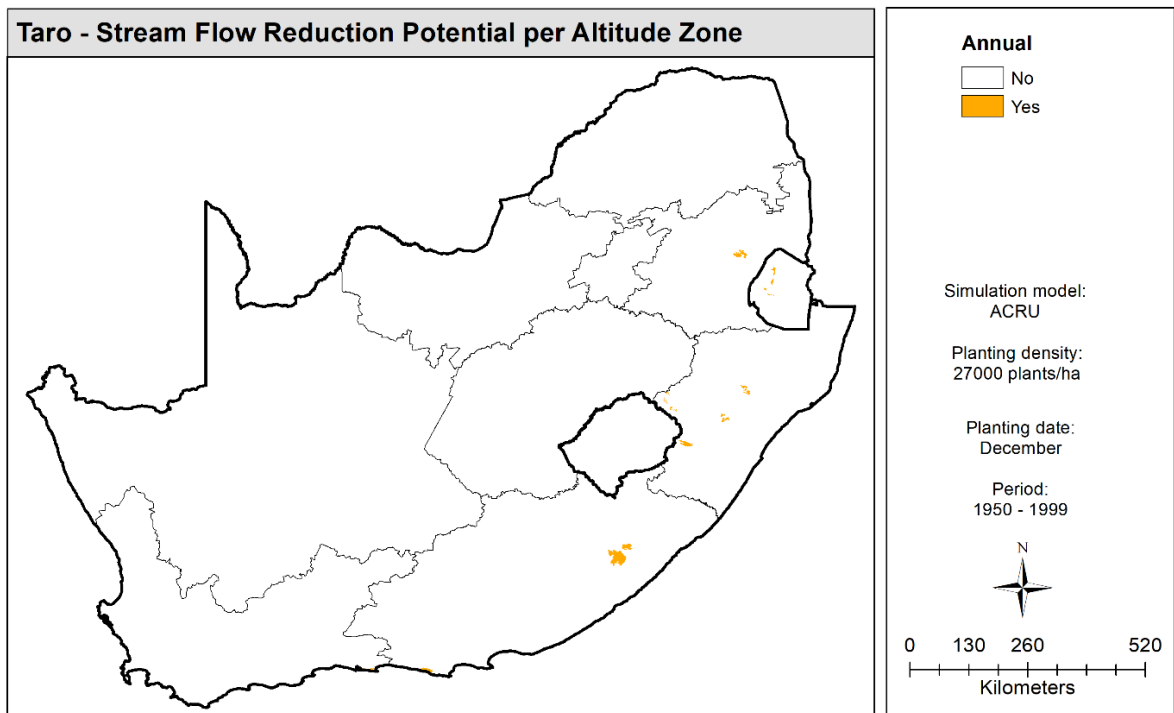


Figure 7-4 Location of HRZs where the reduction in mean annual runoff exceeds 10% that may occur due to a land cover change from natural vegetation to taro cultivation

Everson et al. (2021) also used ACRU to assess the SFRA potential of two bamboo species (*B. balcooa* and *B. bema*) using crop coefficients (K_c) obtained from ET measurements in KwaZulu-Natal and Eastern Cape under rainfed conditions. K_c values for *B. balcooa* in KwaZulu-Natal were higher than those for the Eastern Cape, re-iterating the site-specific nature of crop water use. Hence, modelling

was done by applying both sets of monthly K_C values to all HRZs. Crop coefficients for KZN produced a greater impact on runoff generation than those for the Eastern Cape. This is expected since higher K_C values result in greater evapotranspiration and hence reduced runoff, especially in the summer months. In total, crop coefficients for KwaZulu-Natal resulted in a reduction in MAR of 10% or more in 32 zones, compared to only 18 for the Eastern Cape K_C values. However, it is important to note that the runoff results simulated by ACRU for bamboo were based on K_C values derived from experiments that were rainfed. Thus, the crop coefficients do not represent standard, non-stressed conditions, which are required to estimate maximum crop evapotranspiration and water use.

The approach used by Everson et al. (2021) also assumed that K_C values from the two experimental sites were applicable to all other HRZs deemed suitable for crop production. The authors concluded that this assumption represented a weakness in the methodology, which should be addressed in future studies. In response, Kunz et al. (2020) decided to model the water use of sorghum and soybean using AquaCrop, from which a unique set of monthly crop coefficients for unstressed (i.e. irrigated) growing conditions was obtained for each HRZ. Their results, which were also based on two planting dates and two plant densities, showed that with the exception of only a few altitude zones, the cultivation either crop is likely to significantly affect the quantity of water available to downstream users. For this project, the same methodology was used where standard K_C values were derived from AquaCrop simulations. Similar results were also obtained in that OFSP and taro cultivation is highly unlikely to significant impact downstream water availability.

7.3.3 Impact on low flows

Scott and Smith (1997) highlighted the fact that stream flow reductions during the low flow period may be proportionately greater than for annual flows. Hence, a similar analysis was undertaken for mean monthly flows accumulated over the driest quartile (i.e. 3 months with the lowest runoff response) for OFSP and taro, which were then compared to baseline values. If the percentage difference (relative to the baseline) exceeds 25%, then the reduction is considered significant, as recommended by Jewitt et al. (2009b; cf. Figure 4.1). The potential reduction in low flows appears more sensitive to planting date compared to plant density. For both crops, a December planting is likely to result in a larger reduction in winter runoff compared to a November planting (**Table 7-7**).

Table 7-7 Relative reduction during the low flow period (LFP) resulting from a proposed land use change from natural vegetation to OFSP production

RTC	Planting date (month)	Plant density (plants ha ⁻¹)	Maximum LFP _{REDN} (%)	LFP _{REDN} > 25% (number of HRZs)
OFSP	11	31,447	83	55
	11	55,556	83	55
	12	31,447	89	68
	12	55,556	89	70
Taro	11	10,000	89	57
	11	27,778	89	58
	12	10,000	89	72
	12	27,778	90	73

For the above two worst case scenarios, runoff production during the winter months from OFSP and taro is very similar to that from natural vegetation (i.e. $-2 < MAR_{REDN} \leq +2\%$) in 48.9% and 61.1% of all HRZs, respectively. For the majority of these zones (3,290 in total), the climate is too cold for crop production, and thus there is no reduction in runoff as ACRU parameters were not altered (**Figure 7-5**). Of more concern are reductions in low flows that exceed 25% for OFSP and taro, which may occur in 70 to 73 zones, respectively. The largest reduction of 90% was simulated in zone number 2,249 for taro planted in December at the higher density, due to a reduction in low flow runoff of 0.43 mm relative to

the baseline (0.48 mm). The reduction in runoff during the low flow period only ranged from 0.01 to 3.20 mm, which highlights the problem of small absolute values resulting in large changes when expressed in relative (i.e. %) terms. The largest reduction in low flow runoff of 3.89 mm occurred in zone number 4,293.

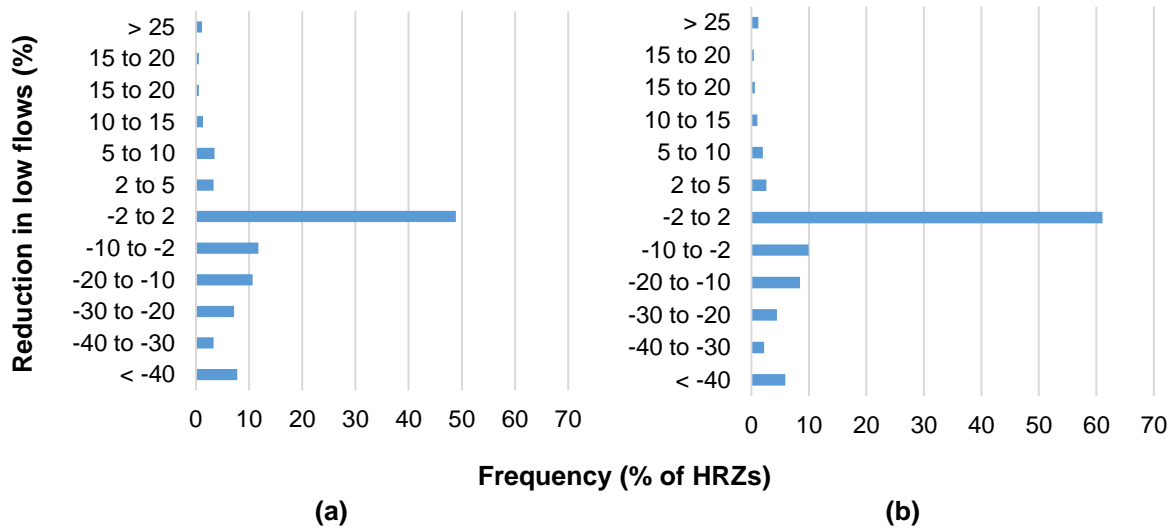


Figure 7-5 Histogram of the percentage reduction in low flows per HRZ that may result from a change in land use from natural vegetation to (a) OFSP and (b) taro cultivation

It is again important to consider where these changes may occur, as shown in **Figure 7-7** and **Figure 7-7** for the above two worst case scenarios. Rainfed crop production is not viable in the drier western parts of the country and potential impacts on downstream water availability in neighbouring eSwatini are also of less concern. Hence, OFSP and taro production are unlikely to impact downstream water availability during the low flow period. Runoff in the winter months was mostly affected by the relatively high crop coefficients representing weedy conditions. Hence, to further reduce any potentially negative impact on downstream water availability, farmers are encouraged to keep their fields weed free during the fallow period.

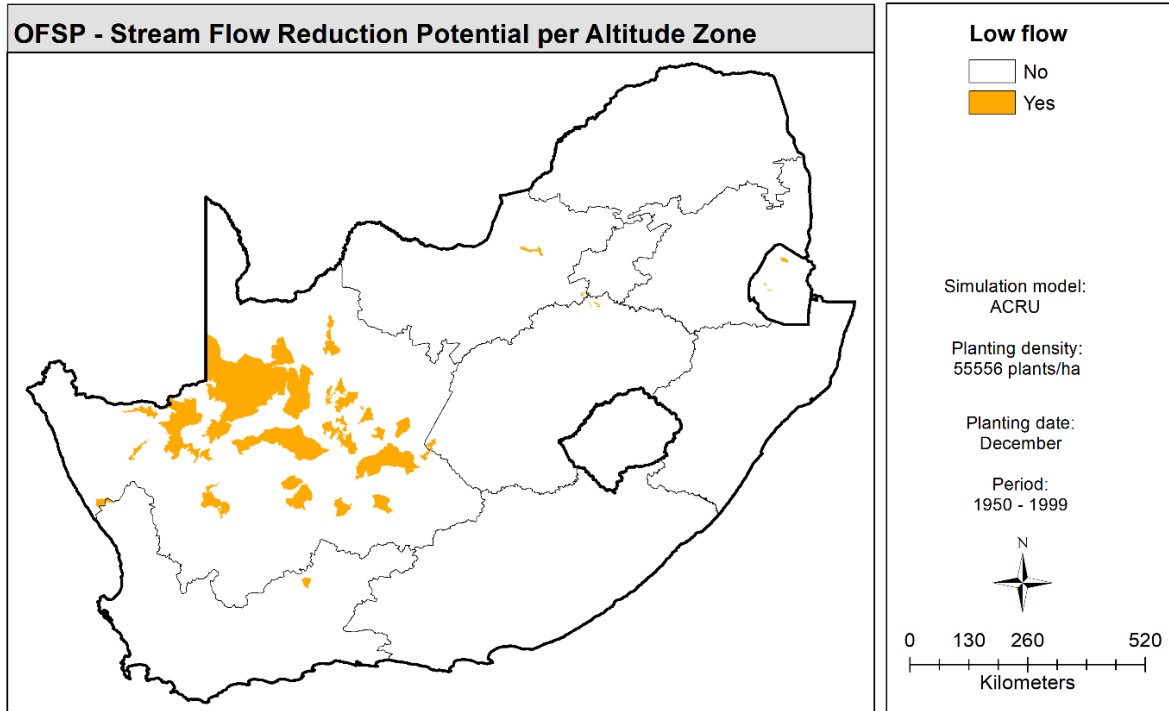


Figure 7-6 Location of HRZs where the reduction in runoff during the low flow period exceeds 25% that may occur due to a land cover change from natural vegetation to OFSP planted in December a the higher density

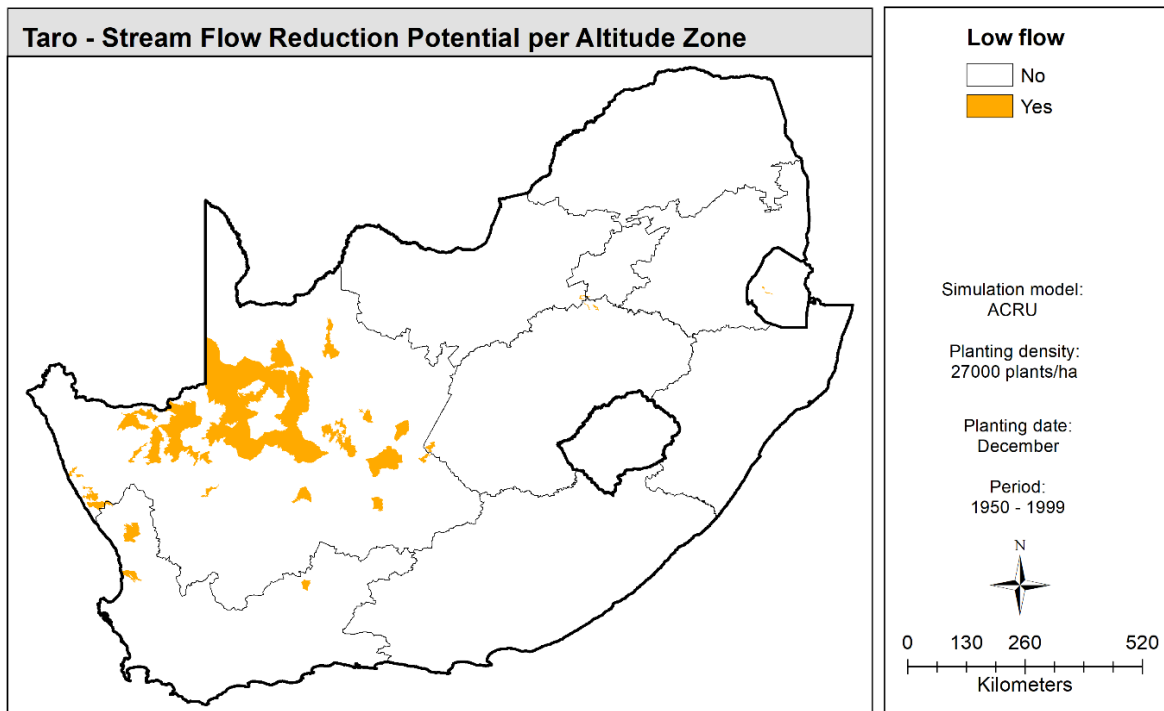


Figure 7-7 Location of HRZs where the reduction in runoff during the low flow period exceeds 25% that may occur due to a land cover change from natural vegetation to taro planted in December a the higher density

7.4 SUMMARY AND CONCLUSIONS

Agricultural expansion, facilitated by increased production of indigenous root and tuber crops, will result in land use changes that may have a negative impact on available water resources, even if crops are rainfed. Hence, one of the main aims of this project was to model the hydrological impact of RTC production on downstream water availability. The ACRU hydrological model was selected since it has been used extensively in many other WRC-funded projects to assess the impact of land use change on hydrological response. ACRU was run at a national scale using climate and soil data currently available for each of the 5,838 HRZs. The purpose of these national model runs was to (i) quantify the stream flow reduction potential of RTC production on available water resources in South Africa, and (ii) assess the feasibility of declaring a specific RTC as a Stream Flow Reduction Activity (SFRA).

ACRU is particularly sensitive to inputs of monthly crop coefficients, and thus representative values for each HRZ were simulated using AquaCrop for unstressed (i.e. irrigated) growing conditions. This approach was first adopted by Kunz et al. (2020) for assessing stream flow reduction potential of sorghum and soybean. It is considered more robust than assuming that crop coefficients obtained at one location (e.g. experimental site) over one or two seasons, are representative of all other regions where the crop can be grown. Crop coefficients for the fallow period were derived from water use measurements in season 2 using the eddy covariance method. During the fallow period, weed growth was not controlled, which typifies a smallholder farming environment. Other parameters required by the model to assess runoff production from OFSP and taro are described in this chapter (e.g. interception loss of the vegetation layer in ACRU).

Runoff production is assessed relative to that generated from natural vegetation. ACRU parameters for natural vegetation were determined as part of a previous WRC-funded project (Toucher et al., 2020). The stream flow reduction potential is calculated as the percentage difference in mean annual runoff (MAR) generated from the cropped surface (MAR_{CROP}), relative to baseline conditions (MAR_{BASE}), i.e. natural vegetation. Crop “water use” is defined as the difference in mean annual runoff, i.e. $MAR_{DIFF} = MAR_{BASE} - MAR_{CROP}$. This difference is then expressed as a percentage relative to MAR_{BASE} . If it exceeds 10%, then the Department of Water and Sanitation may declare the crop as a SFRA. This approach assumes a 100% change in land cover from natural vegetation to crop cultivation, which is unlikely to be the case.

Based on the modelled results of RTC water use, OFSP and taro are unlikely to significantly reduce runoff production when compared to natural vegetation, since (i) a significant reduction only may only occur in a relatively small number of HRZs (≤ 30 of 5,838), (ii) the results assume a 100% land use change, and (iii) the potential reduction can be offset by the water “gain” (when $MAR_{CROP} > MAR_{BASE}$) in other neighbouring catchments. Similarly, the impact on low flows (driest 3 months of the year) also showed that OFSP and taro are unlikely to significant impact downstream water availability during the drier rainfall season. Overall, rainfed production of these two RTCs does not appear to negatively impact downstream water availability to any great extent, and thus are therefore unlikely to be considered for declaration as a potential SFRA by the Department of Water and Sanitation. Hence, the government is unlikely to limit (i.e. restrict) the spatial extent of RTC cultivation in order to minimise possible negative impacts on local and regional water resources.

8 MAPPING OF LAND SUITABILITY

8.1 INTRODUCTION

In order to increase the production of OFSP and taro in South Africa, it is important to know where these crops can be successfully cultivated. Farmers typically obtain this knowledge from existing land suitability maps. Land evaluation measures the potential of land for alternative land uses, whereas land suitability is defined as the suitability of a particular area for a specified land use (Collins et al., 2001). Hence, land suitability classification is defined as a process of grouping specific regions according to their suitability (FAO, 1976). Most land suitability studies use the FAO (1976) approach, which classifies land according to order and class. The orders are defined as suitable (S) and not suitable (N) and the classes provide further detail regarding the level of suitability. For example, S1 is highly suitable, S2 is moderately suitable, S3 is marginally suitable. Similarly, N1 is currently not suitable and N2 is permanently not suitable.

Land suitability mapping is an important component in agricultural development as it provides farmers with an idea of what crops can best be grown in a particular area. In other words, they provide farmers with additional crop choices to plant. Land suitability maps are needed to help identify areas best suited to sustainable RTC production, especially in the North West, Limpopo, KwaZulu-Natal and Eastern Cape provinces, where most of the rural poor reside. The maps will help promote the expansion of RTC production by smallholder (and emerging) farmers in traditional farming environments. The increased production of RTCs will reduce the level of poverty in rural areas by creating new jobs and allowing smallholder farmers to participate in food value chains. It is also envisaged that national and household food security will improve due to increased cultivation of nutrient-dense RTCs. The mainstreaming of RTC production will also facilitate agricultural diversification (Modi and Mabhaudhi, 2016).

Phase 4 of this project involved the analysis and interpretation of crop model output to identify areas deemed suitable for the production of OFSP and taro (Aim 4). This chapter provides (i) an overview of different techniques used to create land suitability maps, (ii) a description of the approach taken in this project, and (iii) the results (i.e. maps) that were obtained for OFSP and taro. It represents a summary of the work undertaken by Lake (2022).

8.2 REVIEW OF MAPPING TECHNIQUES

Based on a review of relevant literature, different methods have been used to develop land suitability maps, which have been classified as either (i) traditional, or (ii) modern methods (Akpoti et al., 2019). The traditional (and simpler) methods are based on overlays of rainfall, temperature and soils criteria (e.g. Holl et al., 2007). The modern (more complex) methods are based on the analytical hierarchy process (e.g. Mugiyu et al., 2021b). Other methods used for suitability mapping involve machine learning techniques, such as those based on the MaxEnt model (e.g. Mugiyu et al., 2022). All these methods adopt different approaches for mapping land suitability and utilise different criteria (i.e. variables), thresholds (i.e. cut-offs) and weightings. However, a common aspect of all methods is they utilise climatic, edaphic, topographic and/or socio-economic data as input criteria. A more detailed discussion of each of these studies is presented in **Section 19**.

Crop simulation models are regarded as one of the most reliable methods of determining land suitability in terms of specific crop requirements (Mugiyu et al., 2021a). They are mathematical models that describe crop growth as a function of climatic, edaphic and management conditions. Simple empirical models (e.g. EcoCrop) have also been used for suitability assessments for crops that lack sufficient data. As noted in **Section 19.3**, process-based crop models (e.g. AquaCrop and DSSAT), which can simulate important physiological processes, have been used to validate land suitability maps developed

using other methods. However, there is no evidence to date that simulated output from AquaCrop has specifically been used to map areas deemed suitable for production of underutilised crops. Hence, this unique approach was used to map suitable production areas for OFSP and taro. It is important to note that the approach is strongly dependent on how well the model has been calibrated and validated for each crop.

8.3 METHODOLOGY

From AquaCrop simulations undertaken for each of the 5,838 HRZs (cf. **Chapter 6**), a comprehensive dataset of seasonal yield, crop cycle and crop water productivity (CWP) was developed for OFSP and taro. Maps showing the spatial variability in these three model outputs highlight HRZs that exhibit the most potential for RTC production (cf. **Section 6.3**). A three-tier approach, similar to that undertaken by Holl et al. (2007; cf. **Section 19.1.1**), was used to identify zones best suited to the cultivation of each RTC as follows:

- Tier 1 – identifying areas deemed unsuitable for crop growth, which required the (i) selection of specific criteria (e.g. CWP), and (ii) development of specific thresholds (e.g. $CWP < 0.10 \text{ kg m}^{-3}$) to eliminate areas considered unsuitable for crop production.
- Tier 2 – classifying the remaining suitable areas from marginal (S3: low productivity) to highly suitable (S1: high productivity), based on the productivity capacity of each altitude zone. Output from AquaCrop was again used to identify low to high production areas.
- Tier 3 – eliminating areas where crop production is not possible based on existing land use data to create more realistic land suitability maps. For example, permanently (N2; e.g. urban areas) and currently (N1; e.g. forest plantations) were identified and eliminated as possible crop production areas (Lake, 2022).

8.3.1 Elimination of unsuitable area

8.3.1.1 Selection of elimination criteria

A list of the main variables simulated by AquaCrop is provided in **Table 8-1**, which were considered for mapping land suitability for crop production. For example, the stress factors represent the percentage of the crop cycle when (i) cold temperature stress reduces transpiration (TmpStr), or when water stress (ii) reduces leaf expansion (ExpStr), or (iii) induces stomatal closure (StoStr).

Table 8-1 Variables simulated by FAO's AquaCrop model (Raes et al., 2018)

AquaCrop variable	Description
E	Soil water evaporation (mm)
E/Ex	Ratio of actual to maximum soil water evaporation (%)
Tr	Total transpiration of crop and weeds (mm)
Tr/Tx	Ratio of actual to maximum transpiration (%)
Cycle	Crop cycle (days)
TmpStr	Temperature stress (%)
ExpStr	Leaf expansion stress (%)
StoStr	Stomatal stress (%)
B	Above-ground biomass accumulation (dry t ha^{-1})
Brelative	Ratio of actual to maximum biomass accumulation (%)
HI	Harvest index (%)
Y	Yield (dry t ha^{-1})
CWP	Crop water productivity for yield part (dry kg m^{-3})

AquaCrop is not run for altitude zones that are too cold for crop production. Hence, no output is produced for 3,307 zones and are flagged as -999 (i.e. no/missing data). Furthermore, altitude zones deemed too dry for rainfed production were eliminated using mean annual precipitation, with a threshold of below 400 mm (Brouwer and Heibloem, 1986). When the stress variables were tested, they eliminated altitude zones along the eastern seaboard that are deemed suitable for crop production. Hence, these variables were not used to exclude zones with high water and/or temperature stress. Tests were also conducted to determine if collinearity exists between AquaCrop output variables. For example, stomatal stress and leaf expansion stress are correlated (R^2 of 0.973 in **Figure 8-1**), as both variables are indicative of water stress.

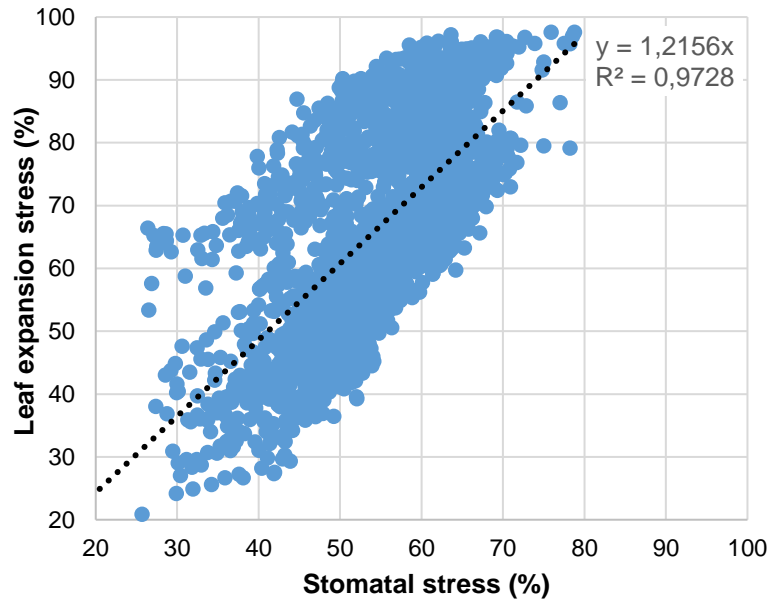


Figure 8-1 Relationship between AquaCrop simulations of stomatal stress and leaf expansion stress for taro

After a lengthy iterative process, only two variables (CWP and the number of simulated seasons) were selected. The latter variable represents the number of seasons that AquaCrop produced yield and ranges from 0 to 49. Altitude zones with 48 or 49 seasonal values are deemed more suited to crop growth than zones with less than 20 yield simulations. The use of a non-zero yield threshold to exclude HRZs considered unsuitable for crop production is problematic because this cut-off value is different for subsistence, smallholder and commercial farmers. Since yield is also strongly correlated to CWP (R^2 of 0.968 in **Figure 8-2**), the latter variable was used instead. The relationship also implies that the evapotranspiration of taro accumulated over the crop cycle is on average 5,170 m³ (or 517 mm). For each criterion, two statistics were considered, namely the seasonal mean and inter-seasonal variation. For example, a large variation in inter-seasonal CWP indicates that the climate is too variable and thus, is unsuitable for crop production.

It is important to note that the relationship between CWP and yield varies with each crop. For example, a non-linear relationship exists for both rainfed and irrigated maize crops in Morocco as shown in **Figure 8-3**. The red line is the 90th percentile of water productivity, which can be used to represent the upper limit of water productivity.

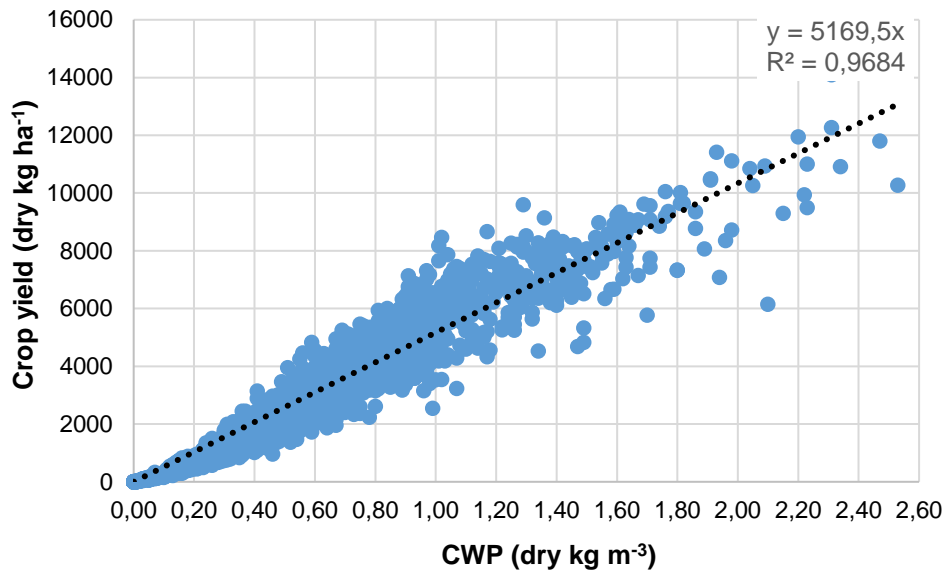


Figure 8-2 Relationship between yield and crop water productivity (CWP) for taro (1st November at 10,000 plants ha⁻¹), based on AquaCrop simulations

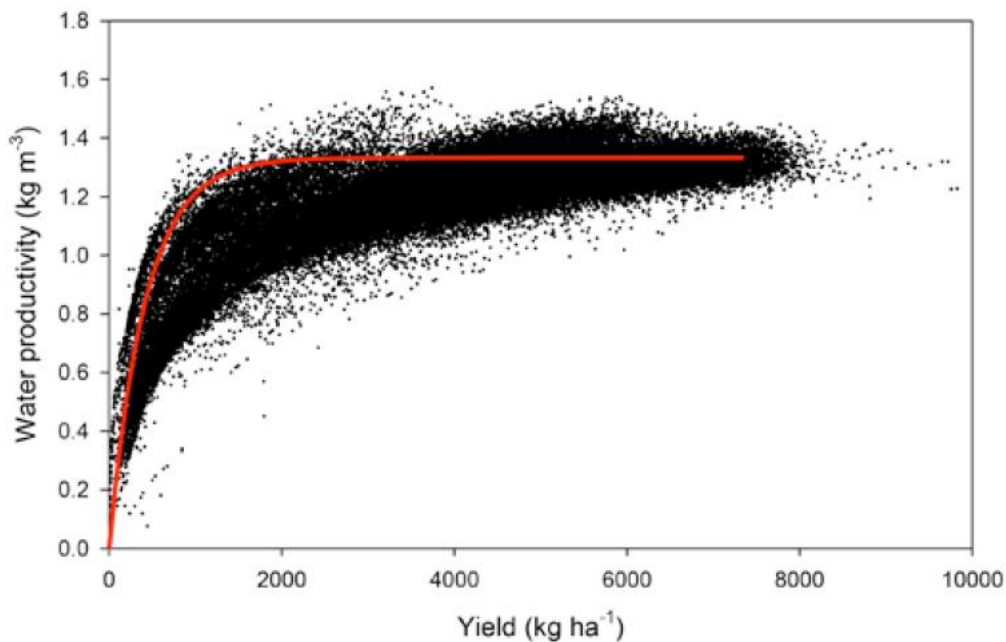


Figure 8-3 Relationship between water productivity and crop yield of maize produced from October 2010 to September 2011 in Morocco (Goudriaan and Bastiaanssen, 2013)

8.3.1.2 Determination of criteria thresholds

Where possible, thresholds (i.e. cut-off values) for each variable were obtained from the literature. If thresholds were not found, an iterative procedure was used to determine values that produced acceptable results. Threshold values determined for each RTC are given in **Section 8.4.1**.

8.3.2 Classification of suitable areas

As noted in **Section 6.3.4.1**, CWP is most useful for determining if crops are grown in optimum environments as opposed to those produced in sub-optimum areas. Hence, CWP (not yield) was used to classify the remaining HRZs into three suitability classes. For the remaining zones, the mean CWP

and standard deviation values were 0.38 and 0.20 kg m⁻³, respectively. Initially, the decision was made to classify zones with CWP values within one standard deviation of the mean as moderate (i.e. $0.18 < \text{CWP} \leq 0.58$ dry kg m⁻³). Thus, 68.3% of the remaining zones would be classified as moderate, assuming a normal distribution of CWP values (**Figure 8-4**). However, most (not approximately two-thirds as expected) of the zones were classified as moderate, and thus the decision was made to use half the standard deviation.

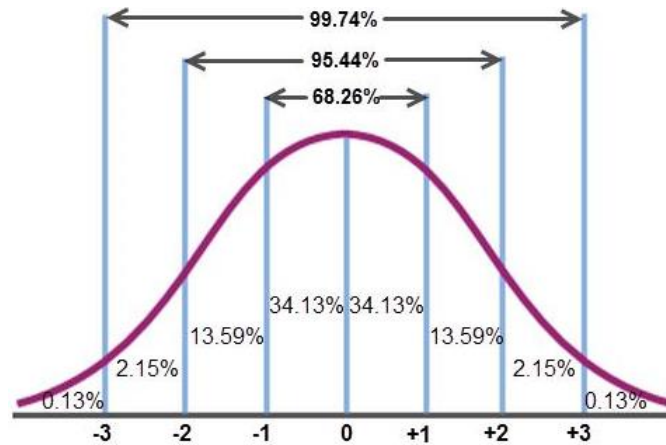


Figure 8-4 Typical bell-shape curve showing a normal distribution of values within three standard deviations (± 3) of the mean (0) (source: Google image)

8.3.3 Consideration of current land use

Khomo (2014) identified unsuitable crop production areas using land cover data from 2009 (cf. **Figure 20-1** in **Section 20**), which was applied to create a more representative (i.e. realistic) land suitability map for soybean. In this project, a similar approach was followed that utilised land cover data from 2018. Land uses that are currently (N1) and permanently (N2) unsuitable for crop production were identified (cf. **Figure 20-2** in **Section 20**). Final land suitability maps were then produced by eliminating these “no-go” areas from the suitable areas.

8.3.4 Production in subsistence farming areas

The 2018 national land cover map (1 km² resolution) that identified subsistence farmlands was also obtained from SAEON’s [data portal](#). If farmlands covered more than 30% of each 1 km² grid cell (or pixel), it was assumed the entire pixel had the same land use. The raster layer was reclassified as 0 (no subsistence farms) and 1 (subsistence farms), then used to determine the spatial extent of subsistence farming areas that are deemed suitable for OFSP and taro production.

8.4 RESULTS AND DISCUSSION

8.4.1 Elimination of unsuitable areas

Table 8-2 and **Table 8-3** provide a summary of the final criteria used for both OFSP and taro respectively, as well as the threshold values and the percentage of HRZs zones eliminated by applying each criterion individually. For both crops, cold temperatures eliminated the most HRZs. For example, 2,501 of 5,838 (42.8%) zones were eliminated for OFSP planted in November, compared to 2,486 (43.6%) for a December planting. Owing to taro’s longer growing season and higher growing-degree day requirements, more zones were identified as being too cold for viable production (3,284-3,307 or 56.3-56.6%). As noted in **Section 17.3.5**, AquaCrop is no longer run for these zones since they are considered too cold for viable crop production. Such HRZs have a very long crop cycle (i.e. exceeding 365 days), and thus are considered economically unviable. Simulated yields are typically zero or very

low (e.g. $< 0.1 \text{ t ha}^{-1}$), further highlighting the zone is too cold for crop production. This decision not to run the model for these zones prevents the seasonal yield average from being skewed by zero (or very small) values, since the yield is now set to -999 (not zero), which means unsuitable for crop production. Of the remaining 3,337 zones (5,838-2,501), 833 zones (or 25%) are considered too dry for rainfed crop production, and thus were also eliminated.

Table 8-2 Criteria and thresholds used to eliminate HRZs deemed unsuitable for OFSP production

Reasoning	Criterion & threshold	Number of HRZs eliminated			
		01 Nov 31,447	01 Nov 55,556	01 Dec 31,447	01 Dec 55,556
Too cold	Crop cycle > 365 days	2,501	2,501	2,486	2,486
Too dry	MAP < 400 mm	833	833	843	843
Too risky	Yield simulations < 20	458	458	480	480
Too variable	$CWP_{CV} > 100\%$	28	22	15	12
Too inefficient	$CWP_{AVE} < 0.60 \text{ kg m}^{-3}$	28	17	09	08

Table 8-3 Criteria and thresholds used to eliminate HRZs deemed unsuitable for taro production

Reasoning	Criterion & threshold	Number of HRZs eliminated			
		01 Nov 10,000	01 Nov 27,000	01 Dec 10,000	01 Dec 27,000
Too cold	Crop cycle > 365 days	3,307	3,307	3,284	3,284
Too dry	MAP < 400 mm	601	601	618	618
Too risky	Yield simulations < 20	461	461	498	498
Too variable	$CWP_{CV} > 150\%$	326	318	279	230
Too inefficient	$CWP_{AVE} < 0.10 \text{ kg m}^{-3}$	222	180	141	105

If the model simulated less than 20 of the maximum 49 seasons, these zones were also considered unsuitable for RTC production and therefore eliminated. This means the model was not run for 30 or more seasons, which typically occurs when the crop cycle exceeds the 365 day threshold. For OFSP, a relatively small number of zones were also eliminated if (i) the variability in inter-seasonal CWP (CWP_{CV}) exceeded 100%, and (ii) the seasonal average CWP (CWP_{AVE}) was below $0.60 \text{ dry kg m}^{-3}$. For taro, a CWP_{CV} threshold of more than 150% was used to eliminate 230-326 zones (depending on the modelling scenario), followed by CWP_{AVE} below $0.10 \text{ dry kg m}^{-3}$, which eliminated between 105-222 zones. This threshold equates to an average yield of $\sim 0.517 \text{ t ha}^{-1}$ (cf. **Figure 8-2** in **Section 8.3.1.1**).

Of the total 5,838 HRZs, 3,694 and 4,266 zones did not satisfy the selected criteria for OFSP and taro respectively, and thus were eliminated. These zones appear white in **Figure 8-5** (OFSP) and **Figure 8-6** (taro). Therefore, the remaining 2,144 and 1,572 HRZs are considered suitable for OFSP (coloured green in **Figure 8-5**) and taro (coloured green **Figure 8-6**) production, respectively. This represents 36.7 and 26.9% of the remaining zones for OFSP and taro, respectively. The totally unsuitable zones (coloured red in the maps below) are deemed too cold for crop production (crop cycle > 365 days, as explained previously).

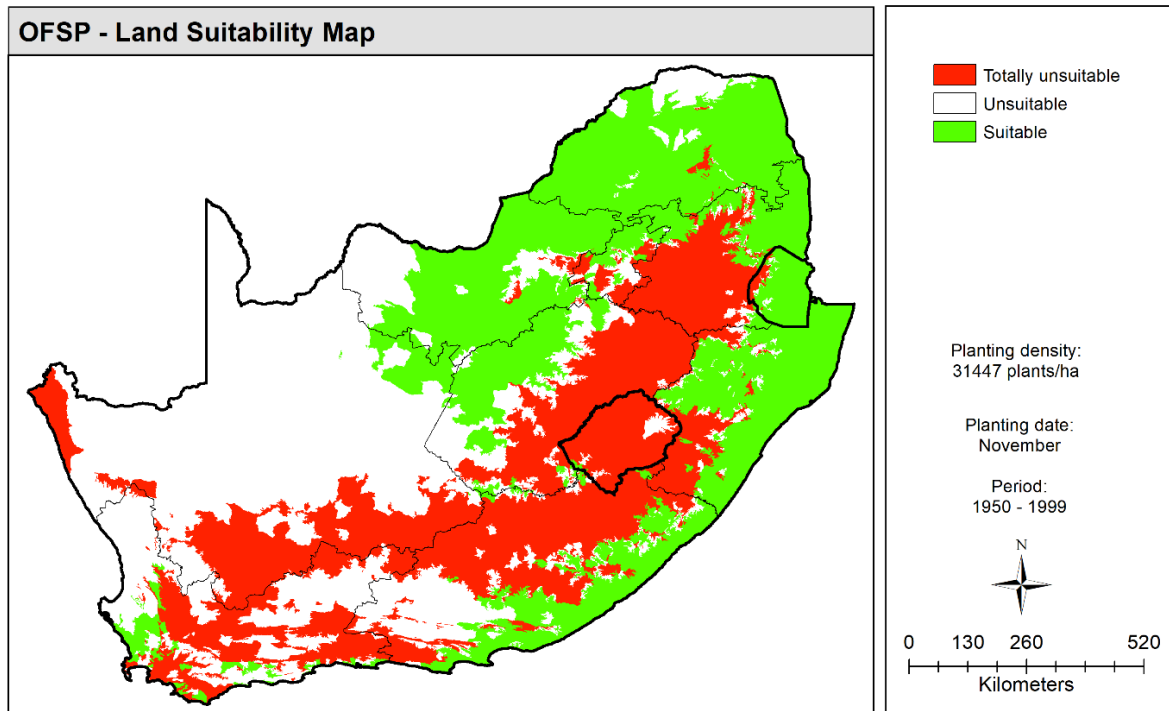


Figure 8-5 Suitable areas for rainfed production of OFSP planted in November at a density of 31,447 plants ha⁻¹

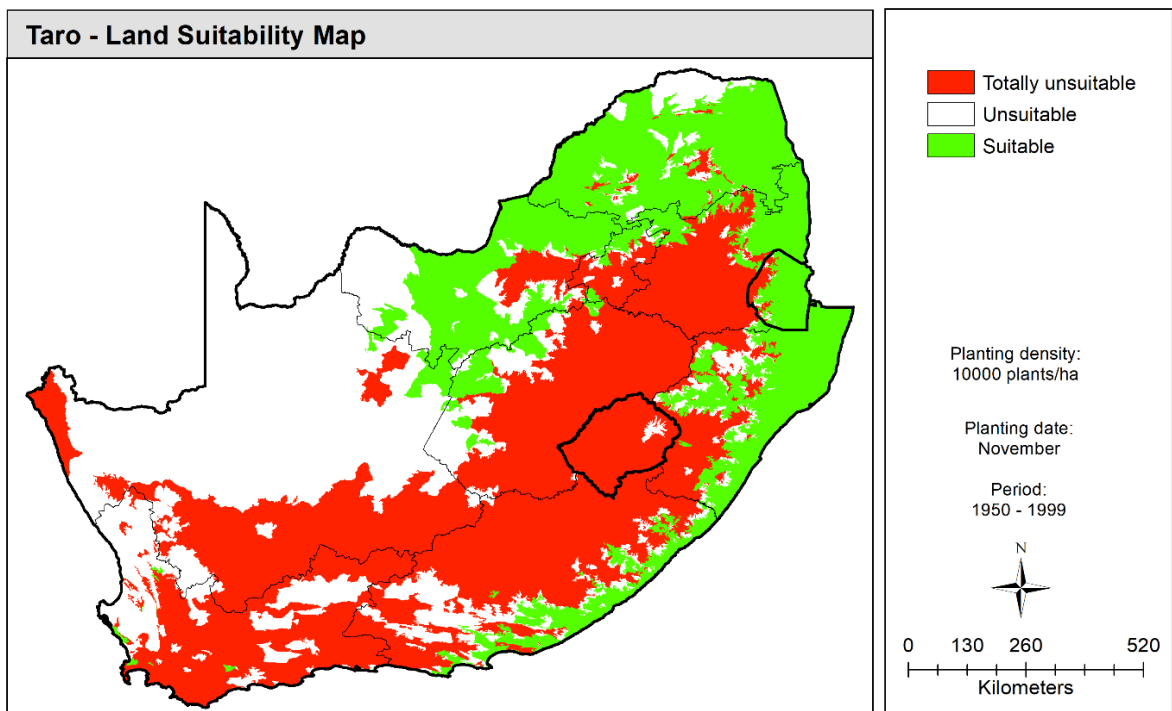


Figure 8-6 Suitable areas for rainfed production of taro planted in November at a density of 10,000 plants ha⁻¹

8.4.2 Classification of suitable areas

Since yield and CWP are highly correlated (**Section 8.3.1.1**), CWP was chosen to classify the suitable growing areas from low to high productivity. The normalisation of yield with water use (i.e. CWP) allows

for a better comparison of crops (i.e. OFSP vs taro). This metric represents the crop’s efficiency in using water to produce yield, which is a better illustration of land suitability than compared to using only yield. HRZs with a CWP value within half a standard deviation of the mean were classified as moderately suitable for crop production. The ranges in CWP provided in **Table 8-4** were used to classify zones as marginally, moderately and highly suited to RTC production.

Table 8-4 Thresholds of crop water productivity used to classify HRZs as marginally, moderately and highly suited to RTC production

Crop	Crop water productivity (dry kg m ⁻³)		
	Marginal (S3)	Moderate (S2)	High (S1)
OFSP	≤ 2.04	2.04-2.57	> 2.57
Taro	≤ 0.56	0.56-0.91	> 0.91

For a November planting at the lower density, 34.4% (OFSP) and 37.2% (taro) of the HRZs were classified as S3. Similarly, 42.7% (OFSP) and 39.7% (taro) of the HRZs were classified as S2. Hence, the remaining 22.9% (OFSP) and 23.2% (taro) were classified as highly suitable (S1), as shown in **Figure 8-7** and **Figure 8-8**, respectively.

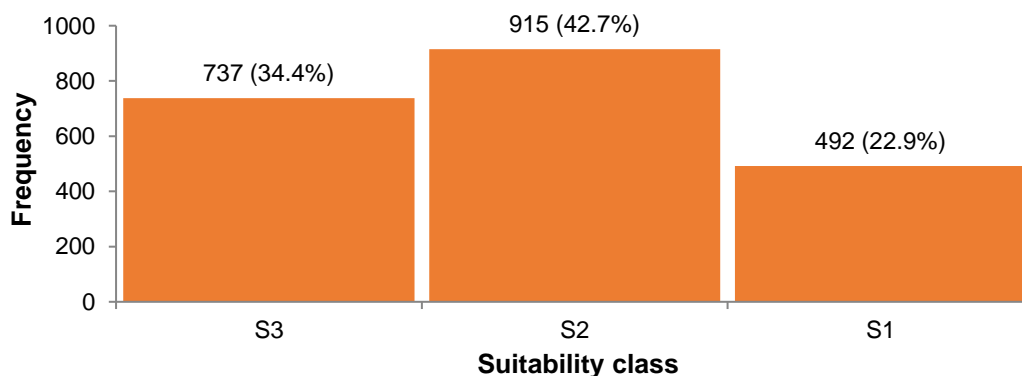


Figure 8-7 Histogram showing suitability classes for OFSP planted in November at a density of 31,447 plants ha⁻¹, based on AquaCrop simulations of crop water productivity

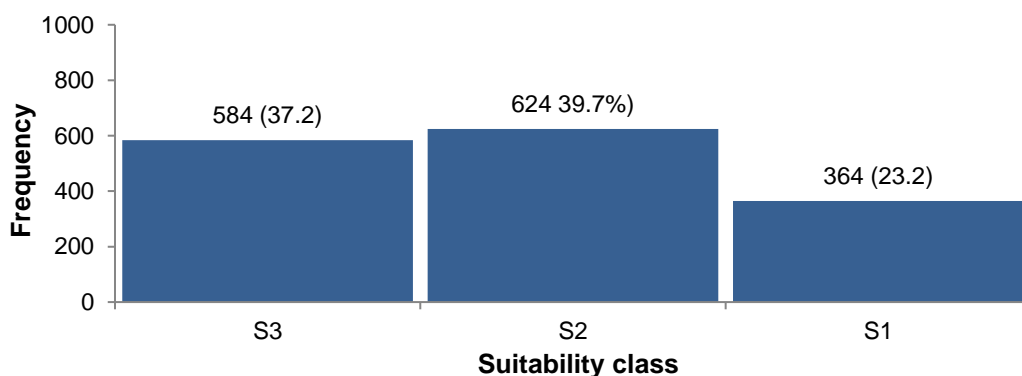


Figure 8-8 Histogram showing suitability classes for taro planted in November at a density of 10,000 plants ha⁻¹, based on AquaCrop simulations of crop water productivity

Figure 8-9 and **Figure 8-10** highlight the spatial distribution of potential OFSP and taro production areas, respectively. The maps indicate that the coastal regions of KwaZulu-Natal and the Eastern Cape are deemed most suitable for RTC production. Large parts of the Limpopo and North West provinces are considered marginally suitable to RTC production. Owing to the high GGD requirements to reach physiological maturity (cf. discussed further in **Section 8.4.4**), the central and western regions of

Mpumalanga produced low and highly variable yields, which were therefore eliminated. It is also clear that OFSP has greater potential for cultivation when compared to taro.

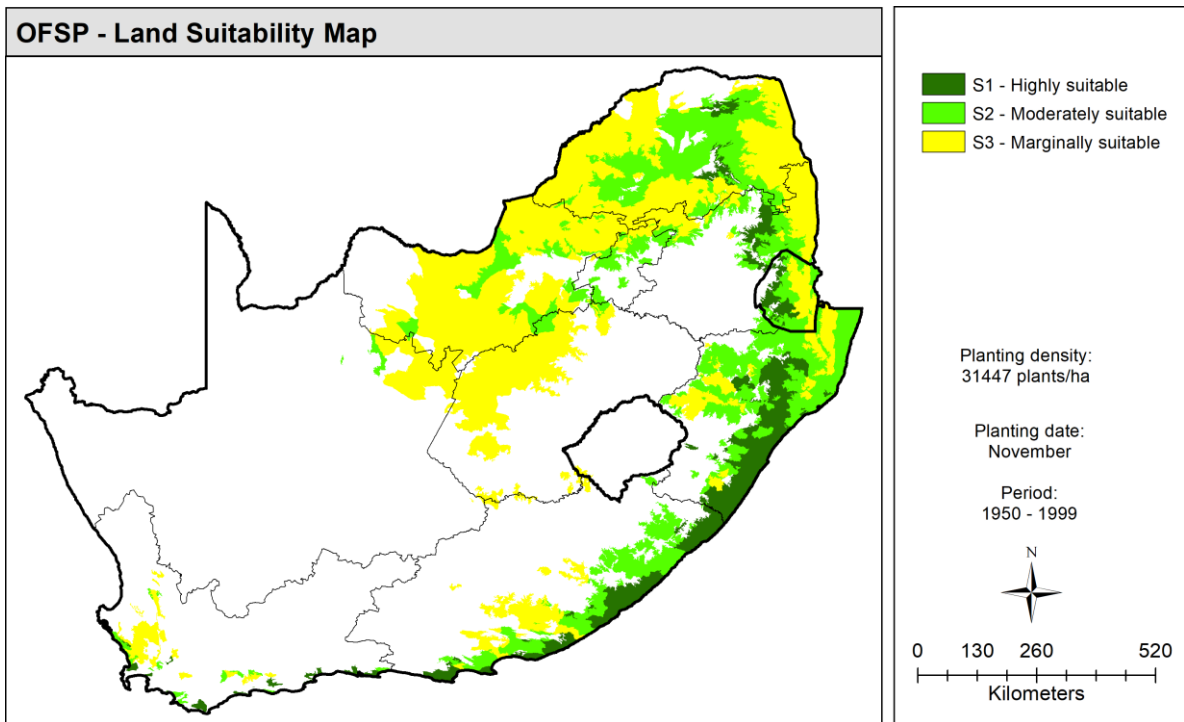


Figure 8-9 Land suitability classification for rainfed production of OFSP planted in November at a density of 31,447 plants ha⁻¹

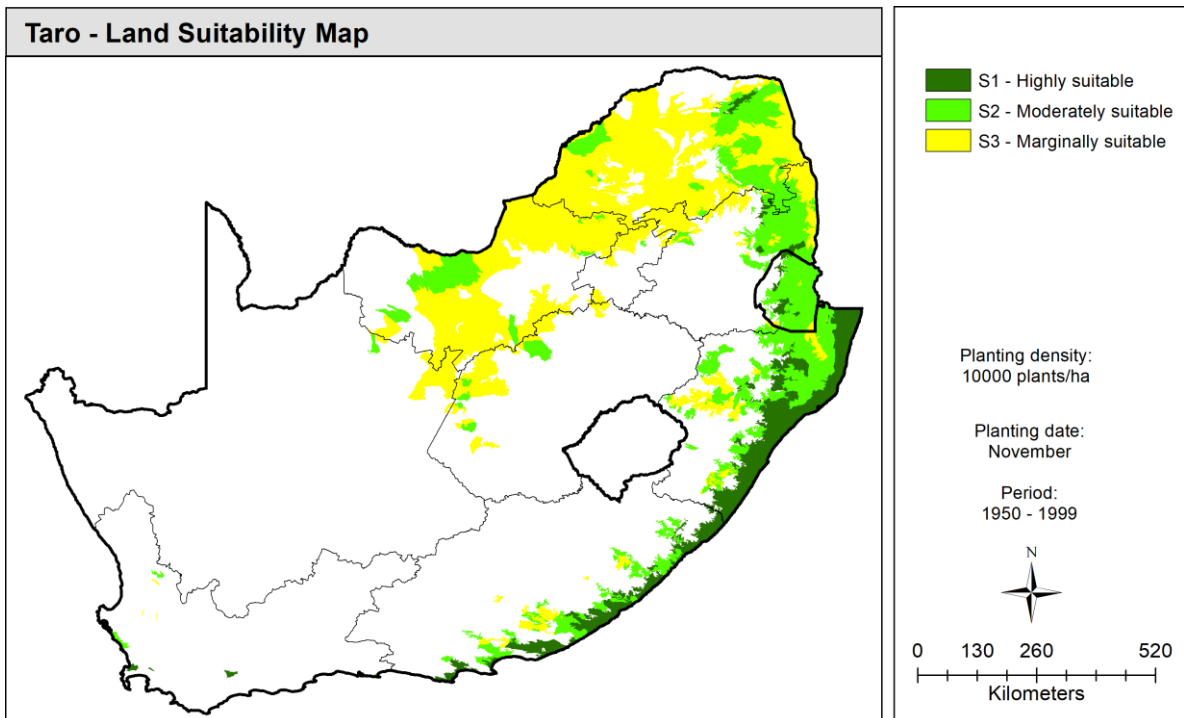


Figure 8-10 Land suitability classification for rainfed production of taro planted in November at a density of 10,000 plants ha⁻¹

8.4.3 Consideration of current land use

The consideration of current land use resulted in a 19 and 22% reduction in areas deemed suitable for OFSP (**Table 8-5**) and taro (**Table 8-6**) production, respectively. In general, more marginal areas (S3) are lost to existing land use compared to highly suitable (S1) areas. This is especially true for the eastern parts of the Limpopo province. The results highlight the importance of accounting for current land use when assessing land suitability, as it avoids over-estimating land area deemed suitable for crop production, and thus helps to produce more realistic maps. The suitable areas identified in eSwatini will be over-estimated, since the 2018 national land cover dataset only covers South Africa.

Table 8-5 Reduction in suitability areas for OFSP after consideration of land use

Class	Consideration of land use	01 Nov 31,447	01 Nov 55,556	01 Dec 31,447	01 Dec 55,556
S3	Before (km ²)	212,235	214,093	217,707	218,151
	After (km ²)	174,745	176,777	178,843	179,501
	Reduction (km ²)	37,490	37,316	38,864	38,650
	Reduction (%)	9.8	9.7	10.1	10.1
S2	Before (km ²)	126,958	124,837	119,290	119,994
	After (km ²)	102,402	100,064	98,056	98,257
	Reduction (km ²)	24,556	24,773	21,234	21,737
	Reduction (%)	6.4	6.5	5.5	5.7
S1	Before (km ²)	44,258	44,609	48,071	47,011
	After (km ²)	32,537	32,919	34,355	33,572
	Reduction (km ²)	11,721	11,690	13,716	13,439
	Reduction (%)	3.1	3.0	3.6	3.5
Total	Before (km ²)	383,451	383,539	385,068	385,156
	After (km ²)	309,684	309,760	311,254	311,330
	Reduction (km²)	73,767	73,779	73,814	73,826
	Reduction (%)	19.2	19.2	19.2	19.2

Table 8-6 Reduction in suitability areas for taro after consideration of land use

Class	Consideration of land use	01 Nov 10,000	01 Nov 10,000	01 Dec 27,000	01 Dec 27,000
S3	Before (km ²)	159,064	157,267	166,960	167,810
	After (km ²)	129,496	128,429	130,176	130,793
	Reduction (km ²)	29,568	28,838	36,784	37,017
	Reduction (%)	10.3	10.1	12.9	12.9
S2	Before (km ²)	88,402	90,870	73,000	70,928
	After (km ²)	67,594	69,246	60,953	59,204
	Reduction (km ²)	20,808	21,624	12,047	11,724
	Reduction (%)	7.3	7.5	4.1	4.1
S1	Before (km ²)	38,613	38,805	43,275	44,497
	After (km ²)	26,685	26,889	30,575	31,707
	Reduction (km ²)	11,928	11,916	12,700	12,790
	Reduction (%)	4.2	4.2	4.4	4.5
Total	Before (km ²)	286,079	286,942	283,235	283,235
	After (km ²)	223,775	224,564	221,704	221,704
	Reduction (km²)	62,304	62,378	61,531	61,531
	Reduction (%)	21.8	21.8	21.4	21.4

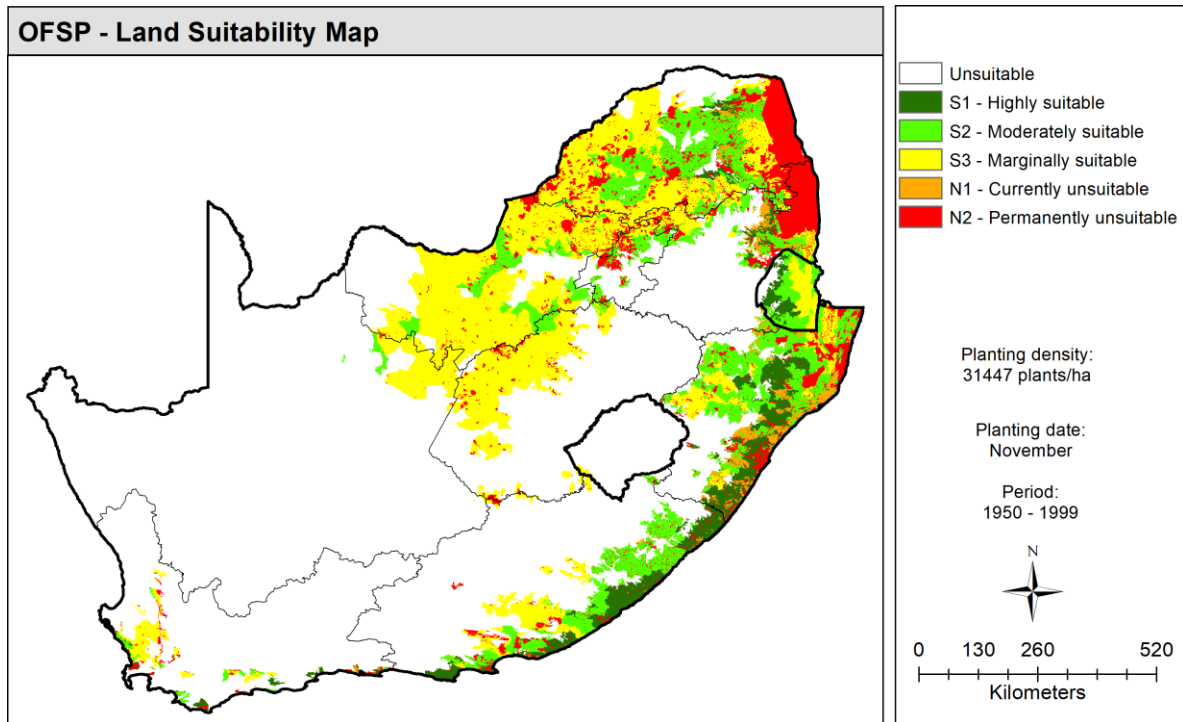
8.4.4 Final land suitability maps

Figure 8-11 to **Figure 8-14** show the spatial distribution of suitability classes for rainfed production of OFSP and taro, combined with the land use data that identifies the N1 and N2 regions. For both crops, maps were produced for each of the four modelling scenarios, i.e. two planting dates (01 November & 01 December) and two plant densities (representing smallholder vs commercial farming environments). Although the spatial extent of the four maps are very similar for each crop, they show that planting date had a larger influence on land suitability than plant density. Maps showing land suitability for OFSP production have been developed for the first time in this project, as well as the development of maps for specific planting dates and plant densities.

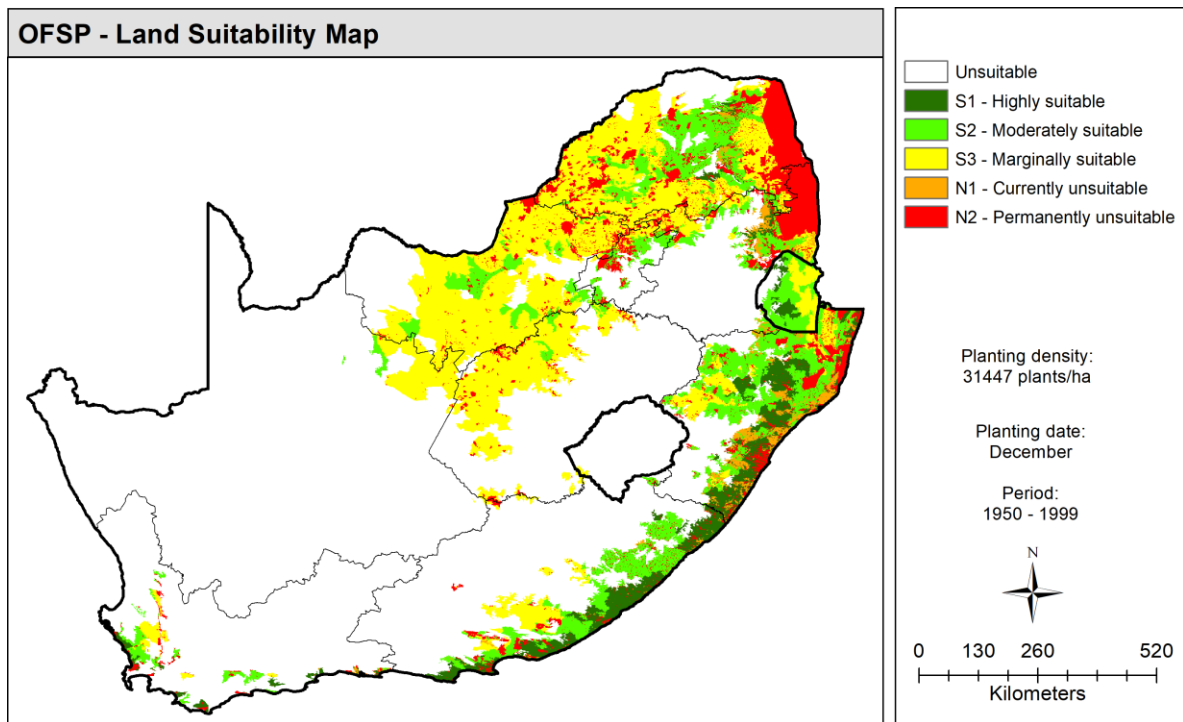
For both RTCs, a December planting produces more highly suitable (S1) areas along the east coast of KwaZulu-Natal and the Eastern Cape provinces. However, some areas change from S2 to S3 suitability. The maps clearly identify the coastal region of the Eastern Cape as being highly suited to RTC production. Therefore, RTC cultivation should be encouraged in this region, which exhibits higher crop water productivity as simulated by AquaCrop.

A comparison of **Figure 8-13** and **Figure 8-14** with the map produced by Mugiyo et al. (2021b) (cf. **Figure 19-5** in **Section 19.2.2.1**) shows some agreement in land suitability for the central parts of the Limpopo, North West and KwaZulu-Natal provinces. However, large differences in land suitability are evident in the Mpumalanga, Free State and Western Cape provinces, including the interior of the Eastern Cape. As mentioned previously, extreme temperatures ($> 55^{\circ}\text{C}$) were recorded in the greenhouse (season 3) between December 2022 and March 2023 when the extraction fans stopped working during frequent two-hourly load shedding and load reduction events. This resulted in the rapid accumulation of heat units, and thus high GGD requirements to reach physiological maturity. Hence, AquaCrop simulated low yield and CWP values in the cooler interior parts of the country due to insufficient heat units, thus resulting in their elimination as potential RTC production areas. Hence, the land suitability maps likely under-estimate the actual area that may support cultivation of both RTCs. Although taro production is possible during the summer months in the Western Cape, irrigation is necessary since it is a winter rainfall region. However, some HRZs in the western parts of the province may produce taro planted in December, as simulated by AquaCrop.

The land suitability map developed by Mugiyo et al. (2021b) identified only a few highly suitable areas for taro production (in KwaZulu-Natal and the Eastern Cape). Most land suitability studies utilise long-term monthly and annual means of climate variables (e.g. rainfall and temperature). This approach does not consider inter-seasonal climate variability and as such, the impact of climatic extremes (especially droughts) are not considered. However, AquaCrop runs at a daily time step, which considers the impact of dry spells on crop growth and final yield. Furthermore, the model is run for 49 consecutive seasons, from which valuable statistics related to inter-seasonal variation were calculated. For example, **Section 8.4.1** identified cold temperatures as having the largest impact on eliminating unsuitable areas. Many HRZs (2,501-3,284 of 5,838) were excluded because all 49 seasons had crop cycles exceeding 365 days, whereas other zones only had a few seasons with long crop cycles. This highlights the importance of considering inter-seasonal climate variability in land suitability studies, not only long-term means of monthly/annual rainfall and temperature.

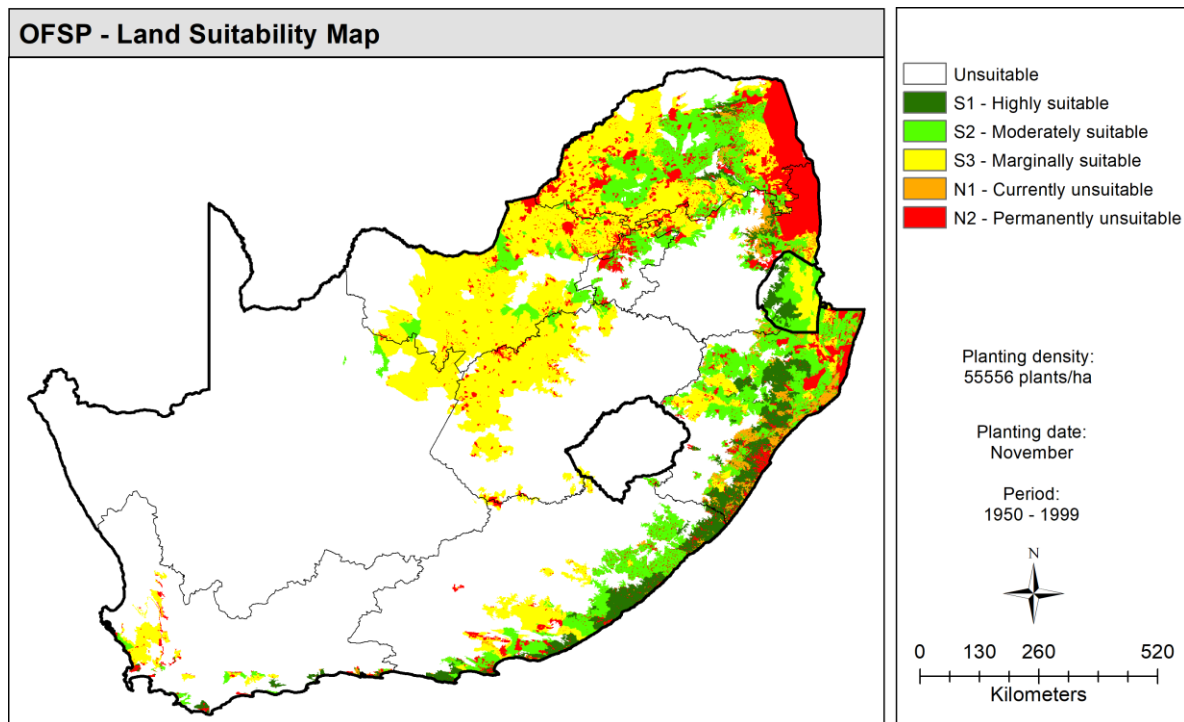


(a)

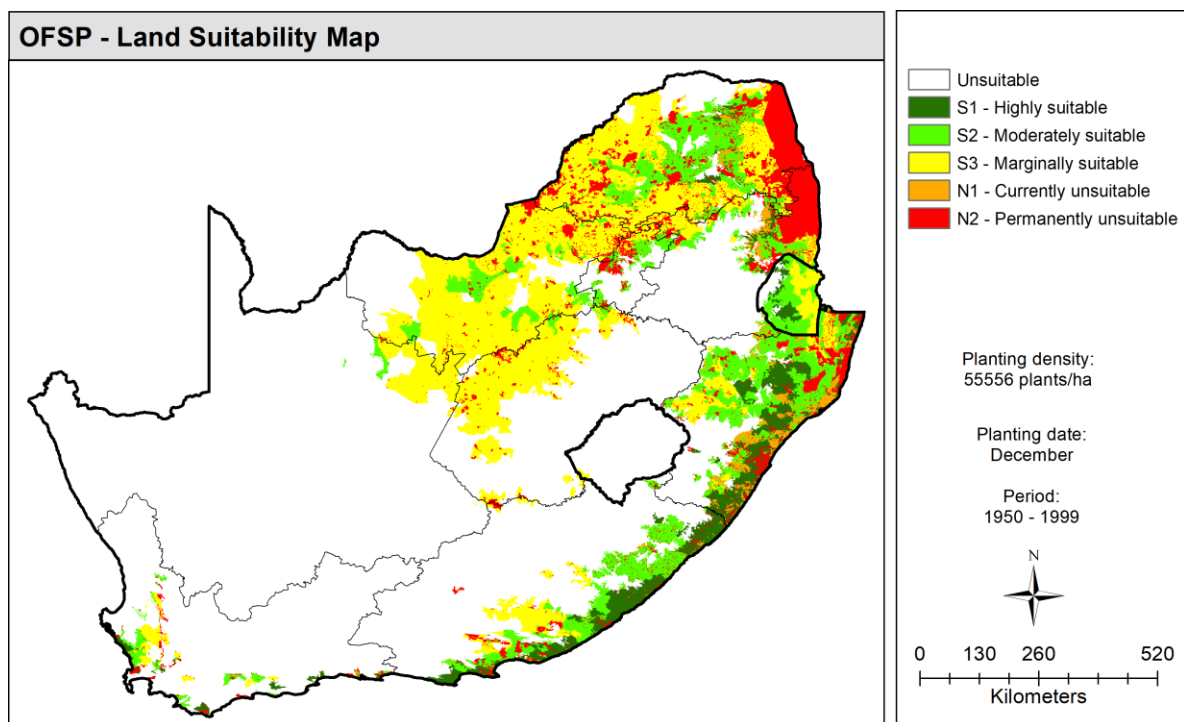


(b)

Figure 8-11 Final land suitability map for rainfed production of OFSP planted in (a) November and (b) December at a density of 31,447 plants ha⁻¹

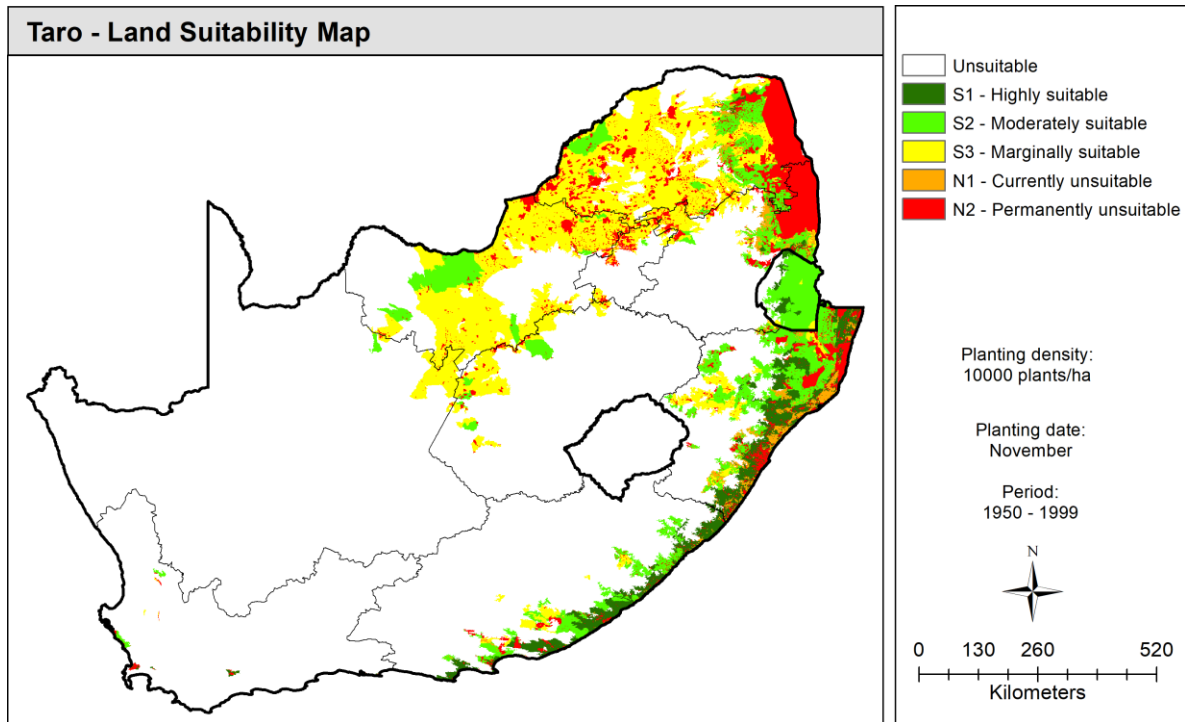


(a)

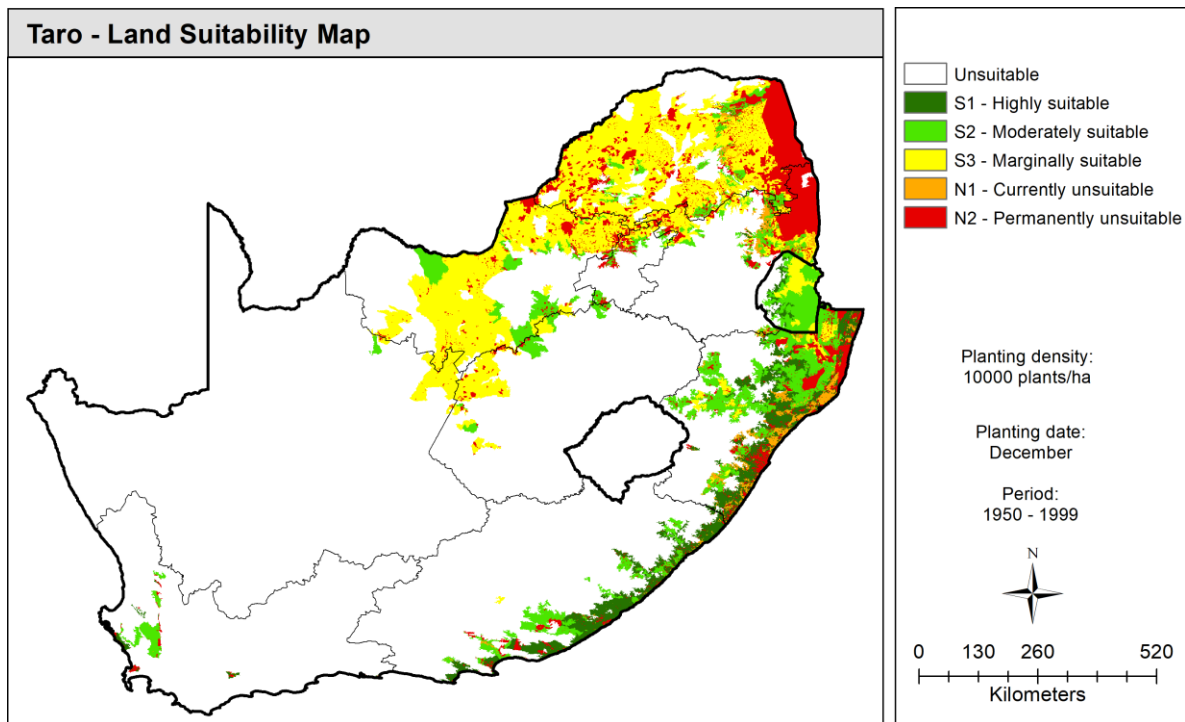


(b)

Figure 8-12 Final land suitability map for rainfed production of OFSP planted in (a) November and (b) December at a density of 55,556 plants ha⁻¹

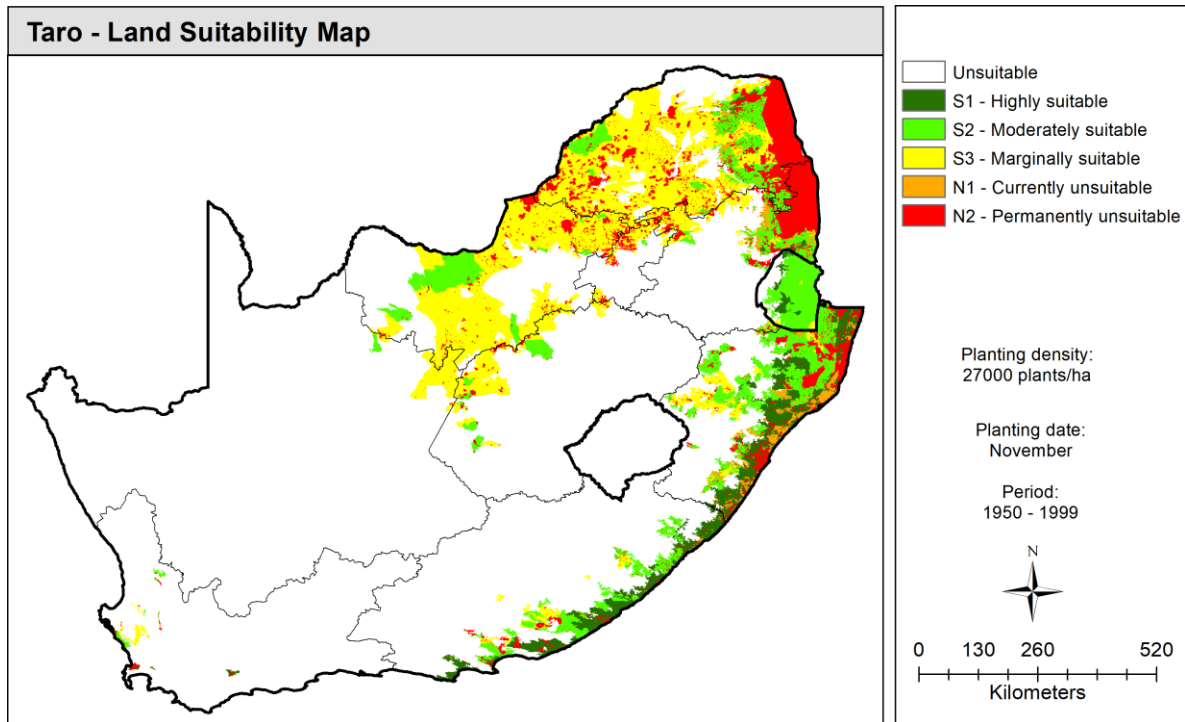


(a)

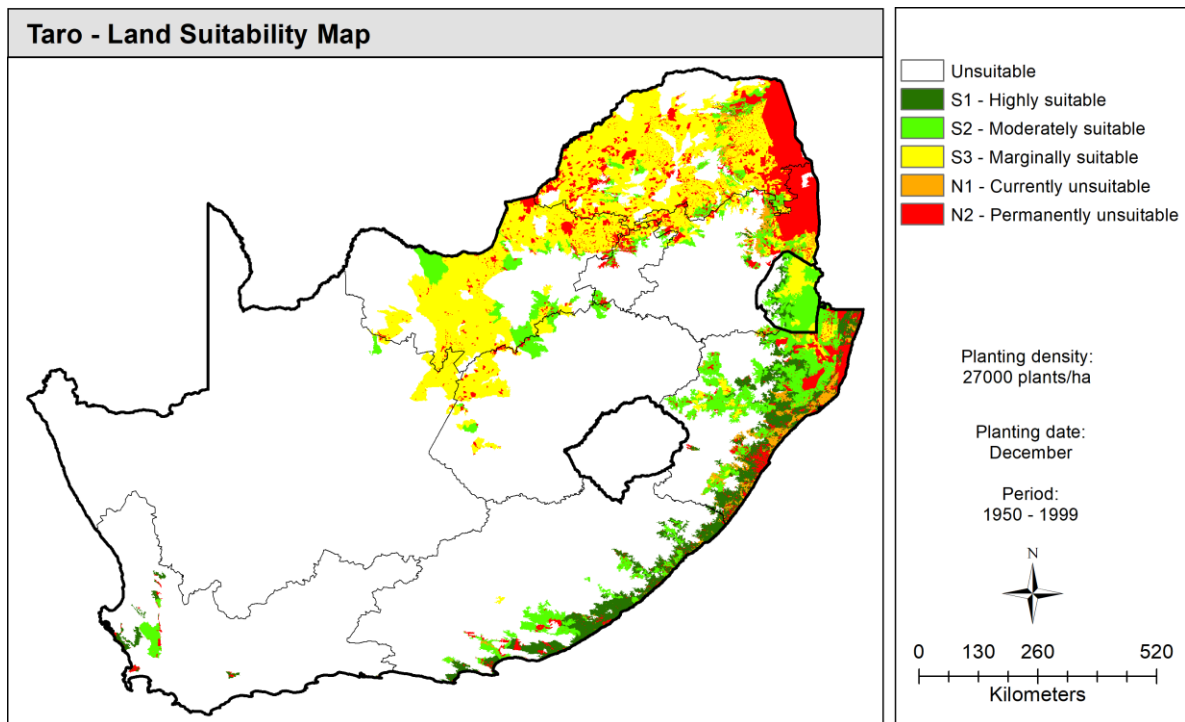


(b)

Figure 8-13 Final land suitability map for rainfed production of taro planted in (a) November and (b) December at a density of 10,000 plants ha⁻¹



(a)



(b)

Figure 8-14 Final land suitability map for rainfed production of taro planted in (a) November and (b) December at a density of 27,000 plants ha⁻¹

8.4.5 Production in subsistence farming areas

Expanding the production of underutilised indigenous crops has the potential to improve food security and reduce poverty. The suitable production areas shown in **Figure 8-11** and **Figure 8-12** for OFSP, including **Figure 8-13** and **Figure 8-14** for taro, were compared to subsistence farming areas identified from the NLC (2018) dataset. The results show that ~17,580 km² (68%) and ~12,739 km² (49%) of the total subsistence farmland of 25,690 km² is suitable for OFSP and taro production, respectively. For OFSP, the majority of the areas are classified as moderately suitable, compared to marginally suitable for taro (**Table 8-7**).

Table 8-7 Suitable OFSP and taro production areas located within existing subsistence farming areas

Suitability class	Suitable area km ² (%)			
	OFSP (31,447 plants ha ⁻¹)		Taro (10,000 plants ha ⁻¹)	
	November	December	November	December
Marginal (S3)	5,891 (22.9)	6,287 (24.5)	6,588 (25.6)	6,742 (26.2)
Moderate (S2)	9,125 (35.5)	8,231 (32.0)	4,022 (15.7)	3,119 (12.1)
High (S1)	2,688 (10.5)	2,938 (11.4)	2,214 (8.6)	2,793 (10.9)
Unsuitable (N1)	7,986 (31.1)	8,234 (32.1)	12,866 (50.1)	13,036 (50.7)
Total	25,690 (100)	25,690 (100)	25,690 (100)	25,690 (100)

More subsistence farming areas are suited to a November planting for both RTCs ((**Table 8-7**). Hence, **Figure 8-15** and **Figure 8-16** show the location of suitable production areas within existing subsistence farming areas for OFSP and taro, respectively. It is therefore recommended that RTC production, in particular OFSP, is promoted mainly along the coastal (and adjacent inland) regions of the KwaZulu-Natal and northern Eastern Cape provinces. This information may help policy makers to target specific areas where OFSP and taro can be produced under rainfed conditions by subsistence (and smallholder) farmers.

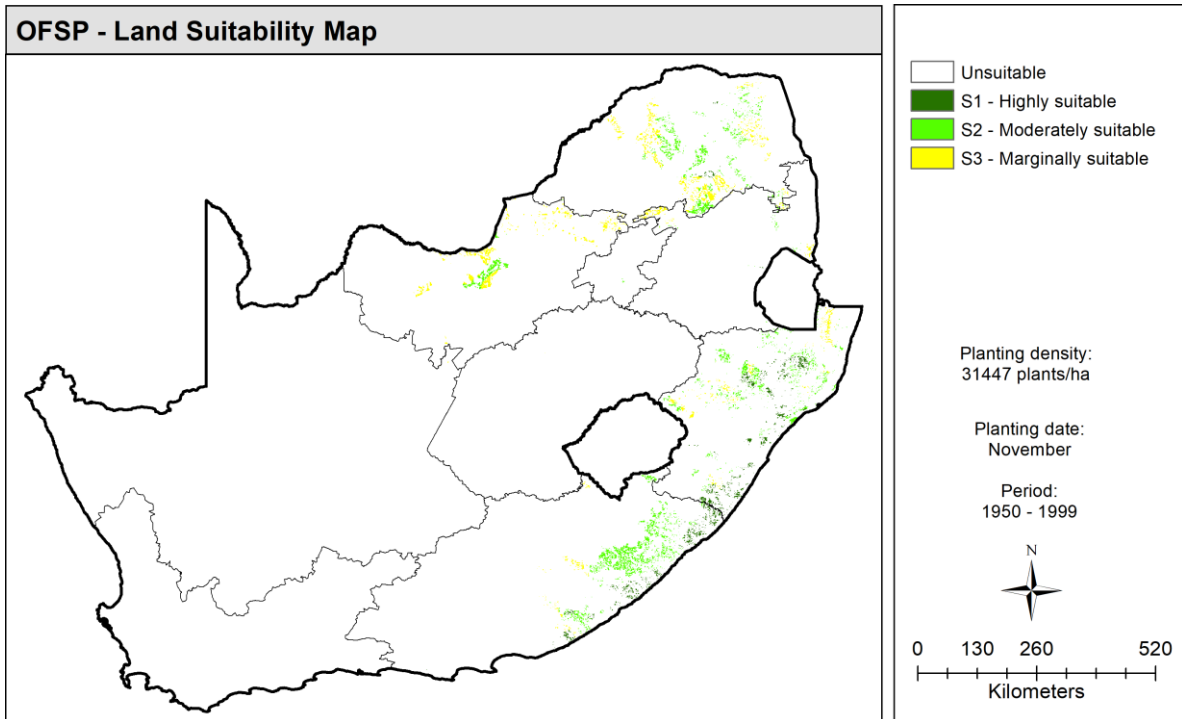


Figure 8-15 Suitable production areas located within existing subsistence farming areas for OFSP planted in November

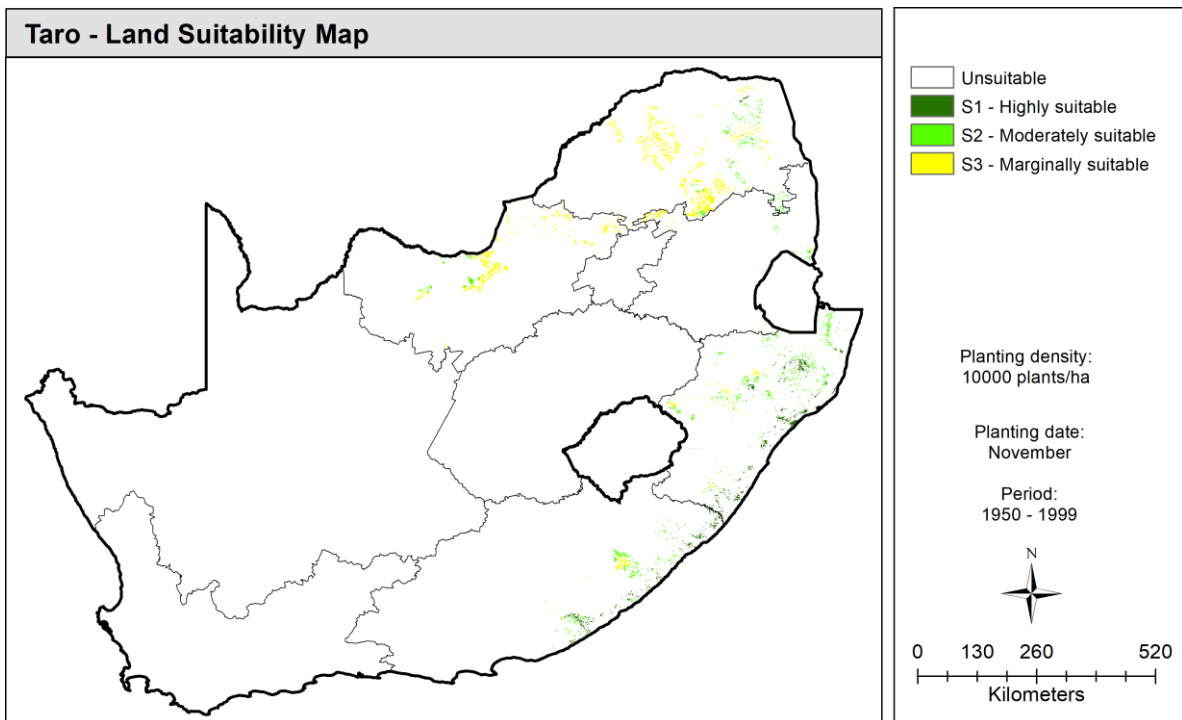


Figure 8-16 Suitable production areas located within existing subsistence farming areas for taro planted in November

8.5 SUMMARY AND CONCLUSIONS

The land suitability maps produced in this project identify areas that are deemed suitable for OFSP and taro production, and thus provide both smallholder and commercial farmers with alternative crop

choices. For both RTCs, simulated output from AquaCrop (four modelling scenarios) was used to identify potential cultivation areas using a three-tier approach. Firstly, certain variables were identified that showed potential to eliminate unsuitable crop production areas (e.g. number of seasonal simulations & crop water productivity). Other AquaCrop variables (e.g. yield & stomatal stress) were also considered but not used. The model is not run for seasons where the season length exceeds 365 days, which indicates the climate is too cold for economically viable crop production. In many instances, all 49 seasons are too cold, and thus the HRZ is considered totally unsuitable for crop production. Mean annual rainfall was also used to eliminate zones deemed too dry for crop production, especially in the western parts of the country.

Thereafter, thresholds were developed and applied, which resulted in the elimination of 3,694 and 4,266 HRZs deemed unsuitable for OFSP and taro production, respectively. The remaining 2,144 (OFSP) and 1,572 (taro) zones were then classified as low, moderate and high suitability (i.e. production potential) using crop water productivity. The final step involved the elimination of physically and currently unsuitable areas for crop production using existing land cover data. For example, urban and protected areas were classified as totally unsuitable, whereas commercial forestry plantations and sugarcane were considered currently unsuitable. This approach helped to obtain more realistic maps of areas that can be planted to each RTC as they eliminated 19% (OFSP) and 22% (taro) of suitable areas. Four land suitability maps were produced for each crop, which showed that planting date has more impact on land suitability than plant density. The maps also show that more areas of the country are suited to OFSP production than taro. Approximately 68% and 49% of existing subsistence farming areas are suited to OFSP and taro cultivation respectively, especially for a November planting. Hence, OFSP exhibits greater potential for uptake by more smallholder farmers and has a shorter growing season when compared to taro.

However, the thermal time required to reach physiological maturity was strongly influenced by the extreme temperatures experienced in the greenhouse during season 3 (cf. **Chapter 5**) that resulted from frequent load shedding events experienced during the growing season. Hence, some HRZs, particularly in the cooler interior regions of the Mpumalanga, KwaZulu-Natal and Eastern Cape provinces, have been excluded as potentially suitable production areas. Thus, the land suitability maps likely under-estimate land suitability for both crops.

The methodology used in this project to (i) identify land parcels (HRZs) deemed suitable for RTC cultivation, and (ii) classify production potential is unique, considering it has not been done before. The outcome of this novel approach is, however, dependent on the reliability of the simulated AquaCrop output, which is largely determined by the success of calibration and validation of crop parameters for both crops. Furthermore, maps showing land suitability for OFSP are also unique as none currently exist for southern Africa. Maps for specific planting dates and densities were also developed for the first time.

9 GENERAL CONCLUSIONS, RECOMMENDATIONS & FUTURE RESEARCH

9.1 SUMMARY OF APPROACH

9.1.1 Literature review

A mixed-method review of available literature was undertaken, which combined both quantitative and qualitative research/outcomes. Where applicable, the emphasis was placed on literature from South Africa, with some comparisons to regional literature. The review focused on five RTCs, namely sweet potato, cassava, taro, tannia and yam. The search was web-based and designed to cover both academic and grey literature. The main advantage of this was that it included the research undertaken in WRC-funded projects. Thereafter, a systematic review was completed to quantify the amount of knowledge on a) crop water use, b) drought adaptation mechanisms, c) water productivity, and d) nutritional value. Four databases (Google Scholar, Scopus, ScienceDirect & Web of Science) were used to search for peer-reviewed literature from 2000-2020 (cf. **Chapter 2**). Of the five RTCs considered in the review, two have been prioritised for further research in South Africa. Hence, the review was extended from 2020 onwards, with the focus on OFSP and taro only (cf. **Chapter 3**).

9.1.2 Experimental work

9.1.2.1 Season 1: Field trials

In the first season (2020/21), a taro trial was planted on 09 December with assistance provided by members from the nearby Swayimane community. Despite the trial area being fenced off, animal damage was first observed on 11th January 2021. In mid-February, the trial was discontinued due to (i) difficulty in obtaining additional material for further gap filling, and (ii) excessive weed growth caused by high rainfall and hot temperatures.

9.1.2.2 Season 2: Field trials

Installation of the EC and SR methods at Fountainhill was completed in August 2021 to measure evapotranspiration during the three months prior to planting. Similar ET measurements were undertaken over four months post-harvest from which monthly crop coefficients were estimated for the fallow period. The micrometeorological systems were finally removed in September 2022, after an entire year of ET data had been collected.

Taro corms and OFSP vines were planted on 19 November and 14 December 2021, respectively. Both trials were planted at a target density of 20,000 plants ha⁻¹ (1 m row spacing and 0.5 m plant spacing). Crop growth measurements were delayed until all weeds had been removed from both trial sites and faulty soil water probes had been replaced on 9th February. The OFSP and taro trials were harvested on 11 April (118 DAP) and on 24 June (217 DAP). A total of 15 plants were harvested from two representative rows, totalling 30 plants. Harvested material was separated into separate components (leaves, stems & roots/tubers). Each component was weighed to obtain the fresh mass. The samples were then dried to obtain the dry mass of each component. Harvested yields were then scaled up to a per hectare basis.

Crop water productivity (CWP in kg m⁻³) was determined as the ratio of dry yield (kg ha⁻¹) to crop water use (m³). CWP was estimated using crop ET measured using EC, since this method is considered the “gold” standard (i.e. more accurate than the SR method). CWP values were then multiplied by the

nutrient content in g kg^{-1}) to obtain nutritional water productivity (NWP in g m^{-3}). Nutrient content of roots/tubers and leaves was measured by the ICFR laboratory.

9.1.2.3 Season 3: Greenhouse experiment

A greenhouse experiment was conducted at UKZN in the third season. Two raised beds were planted to OFSP and taro that received deficit irrigation (30% of crop water requirement or CWP). Two adjacent beds were also planted and were fully irrigated (100% of CWP). The four beds were planted on the 27th of October 2022 at a plant density of 55,556 plants ha^{-1} . The beds were fertilised at recommended rates based on the soil fertility analysis and were kept weed-free throughout the growing season. Appropriate pesticides were utilised to prevent outbreaks, especially red spider mites that affected taro plants.

An automatic weather station was installed inside the greenhouse to measure net radiation air temperature, relative humidity and wind speed, from which daily reference evapotranspiration (ET_0) was calculated. Probes were installed at two depths in each bed to continually monitor soil water content. Prior to planting, Soil texture was determined at two depths in each bed. Furthermore, undisturbed soil cores were taken to obtain laboratory measurements of soil water retention, which were then compared to estimates from the SPAW model. An irrigation system was also installed to facilitate each water treatment. CWR was calculated using the single crop coefficient approach. Irrigation volumes were recorded weekly.

Over the growing season, the following variables were measured to assess crop development: plant height, leaf number, leaf area index, biomass accumulation and root/tuber formation. After the harvest of each crop, total biomass and root/tuber yield was determined from both fresh and dry material. Crop measurements were then used fine-tune existing AquaCrop parameters obtained from the literature. The adjusted parameters were then tested by comparing simulations against observations from the second season.

9.1.3 Crop and hydrological modelling

AquaCrop and ACRU were both run at a national scale using climate and soils data currently available for each of the 5,838 relatively homogeneous response zones (HRZs). These zones are also called altitude zones and were previously referred to as quinary sub-catchments. The models were run for all 5,838 HRZs, regardless of whether each zone is deemed suitable for rainfed crop production. This approach was followed so that AquaCrop output could be used to identify areas best suited to the cultivation of OFSP and taro.

The process of running both AquaCrop and ACRU for each HRZ has been fully automated to minimise computational expense. The automation procedure has continually been improved since 2014 to further improve model performance, and efforts are still ongoing. It facilitated the simulation for 49 consecutive seasons (1950/51 to 1998/99) using daily climate data as input, from which long-term means and other useful statistics (e.g. inter-seasonal variability) were generated. As noted previously, AquaCrop was partially calibrated for both RTCs using measurements from season 3.

AquaCrop simulated crop water use and yield for both unstressed (i.e. irrigated) and rainfed conditions. The latter runs facilitated the mapping of simulated crop yield, crop cycle, CWP and NWP for OFSP and taro. Averaged crop ET simulated for unstressed conditions was then used to derive monthly crop coefficients as input for ACRU. One of the main outcomes of this project was to model the hydrological impact of RTC production on downstream water availability. ACRU has been used extensively in many other WRC-funded projects to assess the impact of land use change on hydrological response. For example, the model was run in 2022 to assess the stream flow reduction potential of 15 commercial forestry species/hybrids. ACRU is particularly sensitive to inputs of monthly crop coefficients, which

explains why representative values for each HRZ were simulated using AquaCrop for unstressed (i.e. irrigated) growing conditions. Other parameters required by the model to assess runoff production from OFSP and taro are provided in the report.

Mean annual runoff produced from crop land (MAR_{CROP}) was assessed relative to the runoff generated from a baseline land cover (MAR_{BASE}), i.e. natural vegetation. ACRU parameters for natural vegetation were determined as part of a previous WRC-funded project. The stream flow reduction potential was calculated as the percentage difference in mean annual runoff ($MAR_{BASE} - MAR_{CROP}$) relative to baseline conditions. If this percentage exceeds 10%, then the Department of Water and Sanitation may declare the crop as a stream flow reduction activity.

9.1.4 Land suitability mapping

Simulated output from AquaCrop was used to identify potential cultivation areas for OFSP and taro using a three-tier approach. Firstly, certain output variables (e.g. CWP & crop cycle) were used to eliminate areas considered unsuitable for crop production. Secondly, the remaining areas were classified as low (S3), moderate (S2) and high (S1) production potential using CWP estimates. Thirdly, areas deemed (i) permanently (N2; e.g. urban & protected areas), and (ii) currently (N1; e.g. commercial forestry & sugarcane growing areas) were also eliminated. Consideration of existing land use helped to obtain a more realistic suitability map identifying areas that can be planted to each RTC. The approach, which uses model simulations to identify potential growing areas, is considered innovative as it was done for the first time in South Africa, especially for underutilised crops.

9.2 SUMMARY OF MAIN FINDINGS

9.2.1 Literature review

Growing crops that are considered nutrient-dense and water use efficient can positively contribute towards alleviating malnutrition and reduce the impact of agricultural production on the county's limited water resources. Root and tubers are considered versatile crops that have much potential in marginal communities as they can contribute to both food and nutrition security, as well as rural development. The literature review considered five RTCs, namely cassava, sweet potato, taro, tannia and yam. Although these crops belong to different botanical families, they share common traits. For example, they all store protein and carbohydrates (e.g. starch) in underground "reservoirs", which are bulky and perishable. In addition, RTCs are vegetatively propagated. However, an understanding of the developmental physiology of these crops, an essential prerequisite for improving their performance (as well as for developing and improving crop models), is poorly documented. Information is also fragmented and indigenous knowledge has not been effectively captured.

Within South Africa, the potential of underutilised indigenous crops remains largely untapped, which needs to be urgently addressed. A targeted research agenda was developed to help unlock the potential of 13 identified crops. Hence, these crops have been prioritised for further research in South Africa, two of which are RTCs. Within South Africa, OFSP and taro have potential to contribute towards addressing national priorities linked to addressing poverty, unemployment and inequality. However, this is strongly dependent on the creation of new value chains, particularly in marginal areas. To facilitate this goal, there is need for investment in research, development and innovation pertaining to RTCs. These investments should therefore target the development and promotion of new value chains that output sustainable products for the two prioritised RTCs. Human capacity development and knowledge management, including indigenous knowledge, should support such investments to ensure sustainability. Furthermore, the inclusion of RTCs into existing production systems also addresses various Sustainable Development Goals, such as zero poverty and hunger.

Unlike cereals and pulses, RTCs are relatively large plants that are not easily grown in greenhouse pots. It is therefore difficult to secure the controlled conditions necessary for reliable physiological studies. Furthermore, credible measurements of crop water using accepted micrometeorological techniques (e.g. eddy covariance) require sufficient fetch. Experience gained in this project highlighted certain challenges (e.g. cost and effort) in establishing large trials from propagated material.

Crop models for RTCs have also not received the same attention in model development, improvement and testing when compared to models for grain crops. Crop physiological knowledge, detailed field experimental data and agronomic research are rare for RTCs, especially for sweet potato, taro, tannia and yam. The lack of modelling initiatives for these crops poses as a serious gap for their mainstreaming into existing production systems within South Africa. In order to address these shortcomings, this project successfully contributed to the existing knowledge base for OFSP and taro. The literature review identified existing knowledge gaps, which helped to focus the field work undertaken by this project, as described next.

9.2.2 Experimental work

To address existing knowledge gaps around crop water use, two micrometeorological techniques (eddy covariance & surface renewal) were used to measure evapotranspiration. Field trials were conducted at Fountainhill Eco-state in KwaZulu-Natal with sufficient fetch to facilitate these measurements.

9.2.2.1 Season 2: Field trials

Water productivity (crop and nutritional) calculations were based on EC measurements of crop water use since this method is considered the “gold” standard. However, due to the cost and complexity of implementing this technique, cheaper alternatives such as SR are gaining popularity. Although the SR method was calibrated against the EC method, it under-estimated crop water use (e.g. 354 vs 322 mm for OFSP and 358 vs 330 mm for taro). Hence, both crops used similar amounts of water under rainfed conditions, despite taro’s longer growing season compared to OFSP (217 vs 118 days). This was expected since taro’s water use is largely dominated by soil water evaporation for the first two months after planting. Taro’s CWP was lower than that for sweet potato (1.37 vs 3.42 kg m⁻³), due to the lower yield (4.91 vs 12.12 dry t ha⁻¹), since water use was similar. The fresh to dry mass ratio obtained from the field work was 2.88 and 2.40 for OFSP and taro, respectively. These ratios are required for converting dry yields simulated by crop models to fresh yields. For most mineral elements, the nutrient content of OFSP leaves is higher than the content in storage roots.

From the preliminary crop modelling results, OFSP yield was under-simulated, especially by the SWB model. Hence, simulated crop water productivity was much lower than observed. Although the SWB model accounts for interception loss, AquaCrop does not consider this process. Since the SWB model cannot be run at a national-scale, AquaCrop was selected to perform the national scale model runs. However, further work was required to improve the calibration of the model for both RTCs.

9.2.2.2 Season 3: Greenhouse experiment

Extreme temperatures exceeding 55°C were experienced in the greenhouse when extraction fans stopped working due to load shedding. Despite this major challenge, both crops survived, which is clear evidence of their heat tolerance. Results were similar to those obtained in season 2, in that OFSP’s leaf number is much higher, which translated to higher LAI and more biomass production. For both crops, stomatal conductance (and transpiration) is largely governed by the evaporation power of the atmosphere, and soil water availability. Taro has a longer growing season compared to OFSP, and thus a slower growth rate, which means less surface shading and higher soil water evaporation rates. Therefore, unproductive water losses are higher for taro than OFSP, which highlights the need to keep

taro plantings weed free for two months after planting. For OFSP, the initial gain in LAI for the unstressed treatment was lost midway through the growth cycle. This suggests that under water limiting conditions, sweet potato can still produce high leaf area, which is important for reducing soil water evaporation, and maintaining biomass production. For most mineral elements, the nutrient content of OFSP and taro leaves is higher than the content in storage roots/tubers. Furthermore, nutrients contents were higher when the crops were water stressed.

Another important outcome from season 3 was to improve AquaCrop's ability to adequately predict yield of OFSP and taro. Hence, measurements and observations from the unstressed treatment were used to fine-tune existing parameter values available for both RTCs. Thereafter, adjustments were made to stress related parameters to improve model performance using data from the stressed treatment. These modified parameters provided better estimates of biomass and yield for both crops under water - stressed conditions, especially for OFSP. This achievement, which represents a valuable contribution by this project, was important for the modelling work described next.

9.2.3 Crop modelling

The AquaCrop model was run to estimate crop cycle, crop yield and water use, from which crop water productivity was calculated. For each crop, the model was run for two planting dates, each with two plant densities. Hence, for each variable, four maps were made that highlight the spatial variability across the rainfed crop production regions of South Africa. The maps show that yield and CWP for OFSP are higher than for taro. Planting date influenced crop yield more so than plant density. Although yields are higher when OFSP is planted in November than in December, yet CWP is lower. Yield and CWP are higher when taro is planted in (i) November in the Limpopo province, and (iii) December along the eastern seaboard.

Inter-seasonal variation in taro yield is higher than for OFSP, particularly for a December planting. For OFSP, inter-seasonal yield variability is lower when planted in November. However, inter-seasonal variability in CWP is lower when both crops are planted in December. Inter-seasonal variability in CWP is higher for taro than for OFSP. When compared to taro, more areas are suited to OFSP production since colder areas are better suited to OFSP production. The risk of failure for taro is higher compared to OFSP, especially for a December planting. Planting at a higher density improves CWP due to increased yields. Taro is more water efficient at producing Fe than OFSP, whereas the opposite is true for K production. OFSP is efficient at producing β -c along the coastal region of the Eastern Cape.

The maps help to identify areas in the country with high yield and productivity potential. Both RTCs should be grown along the coastal regions (and adjacent interior) of KwaZulu-Natal and the Eastern Cape. The maps will prove useful to both small- and large-scale farmers, as they provide information on crop choice and expected yields for specific planting dates and plant densities. It is envisaged that the knowledge gained in this project will help promote the production of OFSP and taro, particularly in rural communities, thus resulting in poverty alleviation as well as the expansion of agricultural production.

9.2.4 Hydrological modelling

The transparent approach adopted in this project to assess stream flow reduction potential for OFSP and taro was similar to that used for commercial forest plantations. The main difference was the development of monthly crop coefficients required as input for the ACRU model, which were derived from AquaCrop simulations of crop ET instead of using non-standard values obtained from field measurements under rainfed conditions.

When this reduction is positive, more runoff is produced from natural vegetation than from the crop (i.e. $MAR_{BASE} > MAR_{CROP}$). This means the crop could use more water than natural vegetation ($ET_{CROP} >$

ET_{BASE}), which occurred in up to 1,058 and 781 HRZs for OFSP and taro, respectively. Hence, OFSP may have a greater impact on catchment water resources than taro. Although crop coefficients were higher for taro compared to OFSP, up to 19 (taro) and 30 (OFSP) HRZs exhibited reductions in MAR exceeding 10% ,relative to natural vegetation. The reduction in annual runoff is more sensitive to planting date, rather than plant density. A December planting of OFSP and a November planting of taro may have less impact on downstream water users. Based on the results, rainfed production of OFSP and taro does not appear to negatively impact downstream water availability to any great extent. Therefore, these crops are unlikely to be declared as a SFRA by the Department of Water and Sanitation.

9.2.5 Land suitability mapping

Most of the highly suitable (S1) areas for both RTCS are located along the coastal regions (and adjacent interior) of KwaZulu-Natal and the Eastern Cape. This is due to the higher rainfall and warmer temperatures experienced along the coastal areas, compared to inland regions. The majority of Limpopo is marginally suited (S3) to taro production, with more areas being moderately suited to OFSP production. More areas are suited to OFSP production compared to taro, due to its shorter season length, especially in the interior regions of KwaZulu-Natal and the Eastern Cape.

The land suitability maps will provide farmers with additional crop choices to plant, thus facilitating agricultural diversification. The knowledge gained in this project should help to promote the expansion of RTC production, to be grown mostly by smallholder farmers in traditional farming environments. Agricultural expansion, facilitated by increased RTC production, will help to revive farming in rural communities, as well as encourage and motivate emerging farmers. Hence, production of RTCs should reduce the level of poverty in rural areas by creating new jobs and allowing smallholder farmers to participate in RTC food value chains. It is also envisaged that national and household food security will improve due to increased cultivation of nutrient-dense RTCs.

9.3 LIMITATIONS AND ASSUMPTIONS

The results presented in **Chapters 6** and **7**, including the land suitability maps in **Chapter 8**, are strongly dependent on the reliability of the AquaCrop and ACRU simulations. The model simulations are based on a number of assumptions, which may affect their accuracy as described next.

9.3.1 Fallow period crop coefficients

A single set of crop coefficients representing the fallow period was determined at Fountainhill in one season only. These values were then used to represent the fallow period in all other HRZs, which is not considered ideal. The monthly values were adjusted from FAO56 to A-pan equivalent crop coefficients, which produced a different set of values for each zone. However, the crop coefficients were not derived under standard conditions (i.e. unstressed) as described by Pereira et al. (2021a; 2021b), nor were they adjusted to represent a sub-humid climate with a minimum relative humidity of 45% and a wind speed at 2 m of 2 m s^{-1} . In other words, when local climatic conditions deviate from these standard values, observed crop coefficients need to be adjusted to become standard values, which are then considered transferable to other locations. This adjustment was not made because the height of the weeds was not measured during the fallow period.

9.3.2 Nutritional water productivity

NWP is the product of CWP and nutrient content. Although unique CWP were simulated for each HRZ, the same β -carotene value measured in a single season at one location was used to present all HRZs. However, the range in nutrient contents reported in the literature for OFSP and taro highlights their site-

specific nature. Nutritional value of RTCs is affected by, inter alia, the cultivar/landrace, climatic conditions and water availability, which highlights the need to study linkages between growing environments and nutrition.

9.3.3 Initial soil water content

For the national model runs, the initial soil water content was set to field capacity, which is AquaCrop's default option, but may be unrealistic for rainfed conditions. This assumption was made because in AquaCrop version 4, germination was particularly sensitive to initial soil water content. When the latter was set to 50% of plant available water, it resulted in failed germination and crop failure (i.e. zero yield). However, this issue was addressed in version 6 by assuming that sufficient reserves are available in the seed for leaf expansion to occur at the maximum rate just after germination.

9.3.4 Crop evapotranspiration

The two field trials conducted in season 2 were affected by excessive weed growth, which was only cleared on 57 and 82 DAP for OFSP and taro, respectively. Hence, weed competition may have resulted in taro's water use being over-estimated, especially before the crop emerged. Furthermore, crop yields were likely to be negatively impacted.

Root and tubers are indeterminate crops, which continue to form new leaves after initiation of tuber formation. Hence, AquaCrop will struggle to accurately simulate crop evapotranspiration of indeterminate crops, since the model will reduce transpiration towards the end of the season. This is especially true for OFSP that exhibits the "stay-green" trait. Hence, the model is likely to under-estimate actual crop water use, resulting in (i) over-estimation of CWP, and (ii) under-estimation of derived crop coefficients.

9.3.5 Increasing climate variability

Since the climate database for each HRZ ends in 1999, it does not adequately reflect the climate variability from 2000 onwards, when anthropogenically induced changes in extreme climatological events have occurred. For example, 2023 was the hottest year on record, as was 2022 previously, which was warmer than 2021, and so on. Hence, inter-seasonal variability likely increased over the past two decades, and thus has been under-simulated by AquaCrop and ACRU in this project.

9.3.6 Model calibration

The thermal time required to reach physiological maturity was strongly influenced by the extreme temperatures experienced in the greenhouse during season 3. Hence, some HRZs particularly in the cooler interior regions of the Mpumalanga, KwaZulu-Natal and Eastern Cape provinces have been excluded as potentially suitable production areas. Thus, the land suitability maps likely under-estimate land suitability for both crops.

Model accuracy is largely dependent on the outcome of the calibration of model parameters that was undertaken for both models and for both RTCs. For RTCs, fine-tuning of crop parameters is necessary to account for variability in cultivars and landraces. In principle, physically based models do not require extensive calibration, as their input parameters describe the physical characteristics of the field/catchment. However, all simulation models suffer from scale-related issues in that parameters derived at the point scale are considered representative of a larger area, which is discussed next.

9.3.7 Regional upscaling

The modelling approach adopted in this project assumes that measurements and simulations made at a point scale are representative of a larger area that is considered relatively homogeneous. In other words, the simulations represent the entire HRZ, without consideration of, for example micro-climatic effects. For the land suitability mapping, the entire zone may be classified as unsuitable for crop production, whereas parts may be suitable. Similarly, a suitable zone may contain areas unsuitable to crop production due to water logging (e.g. riparian areas).

9.4 REVISITING THE PROJECT AIMS

The main objective of this project was to quantify the yield, water use and nutrient content of selected root and tuber crops (RTCs) currently being grown in South Africa, where little or conflicting information currently exists. Each specific aim was achieved as follows:

- 1) Information on water use, yield and nutrient content was gleaned from the available literature from 2000 to 2020. The literature review considered five RTCs, namely cassava, sweet potato, taro, tannia and yam (**Chapter 2**). Since two of these crops have been prioritised for further research in South Africa, a more detailed review was undertaken for sweet potato and taro (**Chapter 3**).
- 2) Knowledge gaps were addressed through field work conducted over three seasons, where the water use, yield and nutrient content of OFSP and taro were measured (cf. **Chapters 4** and **5**). This was particularly important for taro, since a wide range of water use values were found in the literature.
- 3) The water use and yield of OFSP was initially simulated using the AquaCrop and SWB crop models. Results highlighted AquaCrop's ability to adequately estimate crop water productivity compared to the SWB model (**Chapter 4**). Experiments conducted in season 3 were specifically designed to collect data for partially calibrating AquaCrop for both OFSP and taro (**Chapter 5**).
- 4) AquaCrop simulations were used to identify suitable crop production areas across different agro-ecological zones (**Chapter 8**). This new approach was novel and can be adapted to develop land suitability maps for other underutilised crops assuming crop parameters exist.
- 5) Both the experimental and modelling work (**Chapters 4 to 6**) improved existing knowledge of the CWP and NWP of OFSP and taro. Measurements of crop water use for taro were similar to OFSP, despite a difference in crop cycle of almost 100 days. AquaCrop was run at a national scale for all 5,838 HRZs, from which maps of yield, CWP and crop cycle were produced. These maps highlight zones where both crops could achieve high yields, and thus exhibit high CWP and NWP. Multiple model runs were undertaken for both rainfed and irrigated conditions, each with two planting dates and two plant densities.
- 6) To assess the hydrological impact of crop production on downstream water availability, a unique set of monthly crop coefficients was determined for each HRZ using AquaCrop simulations of crop ET for unstressed growing conditions. These K_c values were required by the ACRU model, which was also run for all HRZs, to estimate the runoff generated from a land cover of OFSP and taro. Runoff values were then compared to those obtained from natural vegetation using a standardised and accepted methodology.

- 7) This final project report represents the final aim, i.e. a synthesis of all information generated by this project, which could be used to help promote the sustainable production of indigenous root and tuber food crops.

Hence, all of the project's aims were successfully met, except for one season of field work that produced no results. Unfortunately, the taro trial planted in the first season was abandoned after being severely affected by weed growth and animal damage. The sweet potato trial was not planted because the MSc student decided to deregister due to concerns related to the COVID-19 pandemic. Hence, it is important to note that challenges experienced in the first season were mostly related to the COVID-19 pandemic. Attempts to address these challenges were also hampered by the pandemic, which caused inefficiencies and restricted access to the work place. The second season of field work produced results, despite weed problems and the continued threat of animal damage at the Fountainhill Eco-estate. Similarly, the third season provided a valuable dataset for model calibration, despite the extreme temperatures experienced in the greenhouse during regular load shedding events.

Despite the above-mentioned challenges related to field work, the following outcomes were achieved for the first time in this project: (i) the water use of OFSP and taro was measured accurately using two micrometeorological techniques; (ii) more representative climate and soil datasets were used as input for AquaCrop and ACRU; (iii) AquaCrop was run with a single-layer (not a two-layer) soil profile; (iv) improved parameter values for OFSP and taro were developed; (v) the automation procedure was revised to run AquaCrop and ACRU more efficiently at the national scale; (vi) OFSP was modelled and mapped at the national scale using AquaCrop; (vii) maps of NWP were developed for both RTCs; (viii) risk of crop failure was mapped for both crops; (ix) land suitability maps were produced from AquaCrop output using a novel approach; and (x) the hydrological impact of OFSP and taro production on downstream water availability was assessed. These outcomes further improved the validity of model simulations, and thus the taro simulations presented in this report supersede those developed by Mabhaudhi et al. (2016a) and Kunz and Mabhaudhi (2023), which tended to under-estimate taro's yield.

9.5 RECOMMENDATIONS AND FUTURE RESEARCH

The various approaches developed and implemented in this study are by no means considered "exhaustive". Although much effort was spent on producing simulated output that is considered reliable and error-free, the following suggestions would further improve the accuracy of results. These suggestions pertain to the four main research thrusts: (i) measuring crop water use and yield, (ii) crop modelling, (iii) hydrological modelling, and (iv) land suitability mapping.

9.5.1 Measuring crop water use and yield

The field work represented only one season (2021/22) at a single location (Fountainhill). This effort should be replicated for multiple seasons and across different agro-ecologies. Although the EC method is considered the "gold" standard for measuring crop water use, it requires specialised skills to implement correctly and is also expensive. A new surface renewal method (called SR2) is highly recommended for crop water use measurement since there is no need for calibration against the EC method. The classic SR method (called SR1) used in this project requires calibration to derive the alpha coefficient. The SR methods (SR1 and SR2) should replace the soil water balance technique commonly used to estimate crop water use. The latter method tends to over-estimate crop evapotranspiration, due mainly to assumptions that runoff, drainage and/or capillary rise are considered negligible.

When the soil water balance method is used, runoff should be measured weekly using runoff plots, thus avoiding incorrect assumptions that it is negligible. Although drainage is difficult to measure, it should be estimated using appropriate techniques (e.g. Darcy-Buckingham equation or HYDRUS model).

Furthermore, the soil water balance approach does not consider the evaporation of intercepted water, which is accounted for by the EC and SR methods.

Since AquaCrop is a canopy-level model, it is important that the model simulates this variable well. Canopy cover is typically derived from measurements of LAI (via the DIFN or Beer-Lambert equations). Another approach to be explored in the future involves the derivation of CC development from regular drone flights. The images can be analysed to determine canopy cover development and relative coverage of weeds, which are both parameters required by AquaCrop.

The CWP and NWP of other root and tuber crops should be measured and compared to values for OFSP and taro. For example, the drought tolerance and nutritional value of yams needs further investigation, especially since yam is a good source of both protein and carbohydrates.

9.5.2 Crop modelling

9.5.2.1 Extended climate record

Rainfall data is a major source of uncertainty in simulation modelling, particularly in arid and semi-arid regions. A statistical rule-of-thumb states that uncertainty decreases with an increase in the number of observations. In other words, longer climate records can result in more reliable modelling. Since the climate data for each HRZ ends in 1999, it does not reflect the anthropogenically induced changes in extreme climatological events that have occurred from 2000 onwards. Therefore, it is vitally important that the climate database for the HRZs is extended beyond 2000 by at least 20 years. However, this task is made difficult by the ongoing closure of climate stations by custodians.

9.5.2.2 Model calibration and testing

The lack of available crop parameters for sweet potato, taro, tannia and yam represents a serious knowledge gap that will prevent their mainstreaming into existing production systems. Although this project contributed towards improving parameter values for two RTCs, additional model calibration and testing is needed for all RTCs. Studies have shown that model accuracy depends more on input data quality, rather than on the model itself. Models need to be (i) calibrated across different agro-climatic zones; and (ii) thoroughly tested to evaluate their responses to increasing rainfall variability (water stress), rising CO₂ levels, warming temperatures (heat stress) and combinations of these. Such extensive model improvement and testing requires high quality datasets obtained from well-designed and executed field experiments. Developing high quality datasets for model calibration and testing requires a coordinated international effort and long-term commitment to funding this work.

9.5.2.3 Additional modelling scenarios

Results from this project showed that planting date had a greater impact on simulated yield than plant density. Owing to time constraints, only two planting dates were considered (November and December). Using a variable planting date approach for each HRZ is not recommended. Instead, the model should be run for another two planting dates, namely October and January. This will provide a better understanding of crop response to planting date. In addition, modelling the impact of fertility and/or weed stress is recommended, as yield estimates may be more realistic for low input farming systems.

9.5.2.4 Initial soil water content

In the future, the new “hot start” option in AquaCrop should be investigated where the simulated soil water content at the end of a previous season can be taken as the initial conditions for the following

season. This option should replace the current approach where the soil water content is assumed to be at field capacity at the start of the season. In addition, national AquaCrop runs should be performed where the initial soil water content is set to 50% of plant available water (not field capacity) to assess the impact of this setting on crop yield. This will help determine AquaCrop's sensitivity to initial soil moisture levels.

9.5.2.5 Runoff curve number

For this project, CN_{II} was derived from K_{SAT} for the topsoil as suggested in the AquaCrop user manual. However, published tables of CNs already exist for South Africa. In addition, another WRC-funded project is investigating different methods for estimating CNs, one of which involves the use of ACRU to simulate runoff for different vegetation types (including crops). These options should be investigated in the future to derive a representative CN_{II} value for each HRZ for use in AquaCrop.

9.5.2.6 Risk of crop failure

For this project, RCF was defined as the number of zero yields divided by the number of simulated seasons. However, crop failure can also be defined as a 10% or more decline in yield compared to the mean yield, i.e. a -10% deviation from the mean. Instead of using means, other studies adopted deviations from a trendline of yield vs time. The use of these definitions of crop failure should therefore be investigated in future studies.

9.5.2.7 Impact of vine harvesting

Research aimed at enhancing the available knowledge on vine harvesting is needed to better understand its impact on sweet potato yield across different agro-ecologies. Furthermore, AquaCrop cannot account for vine harvesting, which results in a sudden decline in canopy cover and biomass accumulation. The model developers should be encouraged to modify AquaCrop to simulate the effects of reduced leaf area index and canopy cover on final biomass and yield at physiological maturity.

9.5.2.8 Maximum season length

Since crops like OFSP and taro are frost sensitive, the first frost date should be determined from daily minimum temperatures. If the physiological maturity date extends beyond the first frost date, the crop cycle should be shortened accordingly. This approach is better than limiting the maximum crop cycle to a set value (e.g. 365 days) and would provide more accurate yield estimates in each season.

9.5.3 Land suitability mapping

9.5.3.1 Elimination criteria

Break-even yields: Enterprise budgets could be developed (on a per-hectare basis) for both smallholder and commercial farmers to determine the profitability of RTC production. This approach would provide the break-even yield for OFSP and taro, which could then be applied to eliminate zones where crop production is economically unviable.

Criteria weighting: The elimination criteria were applied sequentially to remove unsuitable altitude zones, where the order in which they were applied was not important. Furthermore, this approach assumes each criterion is of similar importance, i.e. equal weighting. Alternatively, a multi-criteria decision approach could be adopted, where scores are assigned to each elimination criterion. For example, zones with a CWP of below $0.10 \text{ dry kg m}^{-3}$ (for example) are assigned a score of 1, compared to four for areas above $0.40 \text{ dry kg m}^{-3}$. The scores for each criterion are then weighted accordingly,

depending on its perceived importance to overall land suitability. The weighted scores for each criterion are then summed and finally, expressed as a percentage of the maximum score. The final score could then be used to eliminate unsuitable zones. A similar multi-criteria decision approach could also be used to rank the remaining zones from low to high productivity potential. One disadvantage of this approach is the issue of applying discrete thresholds to continuous datasets. For example, a final score of 60-80% is categorised as moderately suitable, whereas 81% is considered high suitable.

9.5.4 Additional performance improvements

9.5.4.1 Climate files

At present, AquaCrop runs progressively slower for each consecutive season. The reason for this is the model sequentially reads the climate file from the beginning for each seasonal simulation. As a workaround, the climate files were “trimmed” to a width of 12 characters to facilitate the rapid extraction of a single season of data using a method known as “direct access” in Fortran. This method can extract any portion of data from the climate file in the amount of time. However, it would be more efficient to alter AquaCrop’s code to rather read in the entire climate file once, or to use the same direct access method. This would significantly improve AquaCrop’s performance.

9.5.4.2 Failed national runs

The ability to “hot start” a failed national run should be developed. Load shedding poses a serious problem since all modelled output is stored in RAM and is only moved to permanent disk storage once the entire run is completed, i.e. after the statistics have been generated, then extracted and all output is compressed. A utility needs to be developed to determine when a power failure has occurred, which then copies the model output from RAM to hard drive, before the PC is shut down by the UPS. Another utility is then required to determine which model runs still need to be completed and to spread the load across multiple CPU threads.

9.5.4.3 WSL version 2 issues

WSL version 2 seems to struggle with running parallel tasks when compared to version 1, which represents one major disadvantage of WSL 2. It is hoped that Microsoft will address and fix this issue in the near future. As an interim solution, WSL 1 was used in this project for the required AquaCrop runs. Alternatively, the automation code that runs AquaCrop for all HRZs and for each season should be ported from Unix to Python, which could significantly improve overall model performance.

9.5.5 Development of seed systems

RTCs can be vegetatively propagated, which is an advantage for small-scale, low-income farmers who cannot afford to buy seed. However, their genotype remains fixed, thus making them more vulnerable to the build-up of viruses and other pathogens. Although the availability of clean, certified and quality seed would help to eliminate these issues, there are no organised seed systems in South Africa for sweet potato or aroids such as taro. Consequently, value chains to remain rudimentary. Currently available biotechnology tools, together with conventional crop genetics and breeding activities, can be used to improve the performance of RTCs. Several institutions in Africa are currently working on genetically enhancing RTCs. Hence, continued investments in breeding research is key to develop sustainable value chains for RTCs.

9.5.6 Development of agronomic guidelines

Although RTCs have become adapted to marginal farming areas within South Africa, poor crop establishment, low yield, poor storage and susceptibility to pests and diseases remain issues that need

addressing. The lack of agronomic information may restrict the promotion of RTCs, particularly within commercial farming systems. Generating site-specific information regarding plant densities, planting dates, water requirements, weed control, pest and disease control and harvest techniques is essential for upscaling production of RTCs. This is especially important considering that the efficient use of limited resources such as water can be enhanced through best agronomic practices. Therefore, further research is required on the various agronomic aspects of RTCs within the context of South Africa.

REFERENCES

- ACOCKS JPH (1988) *Veld types of southern Africa*. Botanical Survey of South Africa Memoirs 57, Botanical Research Institute, Pretoria, South Africa.
- ADHANOM GT, STIRZAKER RJ, LORENTZ SA, ANNANDALE JG, STEYN JM (2012) Comparison of methods for determining unsaturated hydraulic conductivity in the wet range to evaluate the sensitivity of wetting front detectors. *Water SA* **38** 67-75.
- ADUGNA A, TIRFESSA A (2014) Response of stay-green quantitative trait locus (QTL) introgression sorghum lines to post-anthesis drought stress. *African Journal of Biotechnology* **13** 4492-4500.
- AKPOTI K, KABO-BAH AT, ZWART SJ (2019) Agricultural land suitability analysis: State-of-the-art and outlooks for integration of climate change analysis. *Agricultural Systems* **173** 172-208.
- AL-JAMAL M, BALL S, SAMMIS T (2001) Comparison of sprinkler, trickle and furrow irrigation efficiencies for onion production. *Agricultural Water Management* **46** 253-266.
- ALLEMANN J, LAURIE SM, THIART S, VORSTER HJ (2004) Sustainable production of root and tuber crops (potato, sweet potato, indigenous potato, cassava) in southern Africa. *South African Journal of Botany* **70** 60-66.
- ALLEN RG, PEREIRA LS, RAES D and SMITH M (1998) *Crop evapotranspiration – guidelines for computing crop water requirements*. Irrigation and Drainage Paper No. 56, Chapter 6, Food and Agricultural Organisation, Rome, Italy. <https://www.fao.org/3/X0490E/x0490e00.htm>
- ALMEKINDERS CJM, WALSH S, JACOBSON KS, ANDRADE-PIEDRA JL, MCEWAN MA, DE HAAN S, KUMAR L, STAVER C (2019) Why interventions in the seed systems of roots, tubers and bananas crops do not reach their full potential. *Food Security* **11** 23-42.
- AMBE JT (1995) Effect of plant population density of sweet potato (*Ipomoea batatas* (L.) LAM) on weed incidence and severity in Cameroon. *International Journal of Pest Management* **41** (1) 27-30.
- ANGUS GR (1989) Sensitivity of ACRU model input. In: *ACRU: Background: Concepts and theory*, Schulze RE. WRC Report No. 154/1/89, Water Research Commission, Pretoria, South Africa.
- ANNANDALE JG, BENADÉ N, JOVANOVIĆ NZ, STEYN M, DU SAUTOY N (1999) *Facilitating irrigation scheduling by means of the soil water balance model*. WRC Report No. 753/1/99, Water Research Commission, Pretoria, RSA.
- ANNANDALE JG, JOVANOVIĆ NZ, STEYN JM, SOUNDY P, BACKEBERG GR (2002) *Technology transfer of the Soil Water Balance (SWB) model for irrigation scheduling*. Workshop organised by FAO-ICID, 24th July 2002, Montreal, Canada. 23 pp.
- ANNANDALE J, STEYN J, BENADÉ N, JOVANOVIĆ N, SOUNDY P (2005) *Technology transfer of the Soil Water Balance (SWB) model as a user friendly irrigation scheduling tool*, WRC Report No. TT 251/05, Water Research Commission, Pretoria, South Africa.
- BADR M, EL-TOHAMY W, ZAGHLOUL A (2012) Yield and water use efficiency of potato grown under different irrigation and nitrogen levels in an arid region. *Agricultural Water Management* **110** 9-15.

BELEHU T (2003) *Agronomical and physiological factors affecting growth, development and yield of sweet potato in Ethiopia*. Unpublished PhD thesis, Plant production and Soil Science, School of Natural and Agricultural Sciences, University of Pretoria, Pretoria, South Africa.

BELEHU T, HAMMES PS, ROBERTSE PJ (2004) The origin and structure of adventitious roots in sweet potato (*Ipomoea batatas*). *Australian Journal of Botany* **52 (4)** 551-558.

BELETSE YG, LAURIE R, DU PLOOY CP, LAURIE SM, VAN DEN BERG A (2013) Simulating the yield response of orange fleshed sweet potato 'Isondlo' to water stress using the FAO AquaCrop model. *ISHS Acta Horticulturae* **1007** 935-941.

BELETSE YG, LAURIE R, DU PLOOY CP, VAN DEN BERG A, LAURIE S (2011) Calibration and validation of AquaCrop model for orange fleshed sweet potatoes. In: *Capacity development for farm management strategies to improve crop water productivity using AquaCrop: lessons learned*, Ardakanian R, Walter T. UNW-DPC Publication Series, Knowledge No. 7, Bonn, Germany.

BERNARDES C, DA SILVA MARTINS CA, LOPES FS, DA ROCHA MJR, XAVIER, TMT (2011) Leaf area, leaf area index and light extinction coefficient for taro culture. *Enciclopédia Biosfera, Centro Científico Conhecer – Goiânia* **7 (12)** 1-9.

BHAGSARI AS, DOYLE AA (1990) Relationship of photosynthesis and harvest index to sweet potato yield. *Journal American Society of Horticultural Science* **115** 288-293.

BIEHLER E, MAYER F, HOFFMANN L, KRAUSE E, BOHN T (2010) Comparison of three spectrophotometric methods for carotenoid determination in frequently consumed fruits and vegetables. *Journal of Food Science* **75** 55-61.

BISWAS AK, SAHOO J, CHATLI MK (2011) A simple UV-Vis spectrophotometric method for determination of β -carotene content in raw carrot, sweet potato and supplemented chicken meat nuggets. *LWT-Food Science and Technology* **44** 1809-1813.

BOMBIK A, RYMUZA K, STOPA D (2013) Potato yield depending on ridge shape and harvest time Part II. The yield of tuber fractions. *Acta Scientiarum Polonorum Agricultura* **12 (4)** 70-90.

BORRELL AK, MULLET JE, GEORGE-JAEGGLI B, VAN OOSTEROM E J, HAMMER GL, KLEIN PE, JORDAN DR (2014) Drought adaptation of stay-green sorghum is associated with canopy development, leaf anatomy, root growth, and water uptake. *Journal of Experimental Botany* **65** 6251-6263.

BOUWKAMP JC, HASSAM MHM (1988) Source-sink relationship in sweet potato. *Journal American Society of Horticultural Science* **11** 627-629.

BRADSHAW J (2010) *Root and tuber crops*. Springer New York, New York, USA.

BROUWER C, HEIBLOEM M (1986) *Irrigation water management: Irrigation water needs – Training manual no. 3*. Food and Agricultural Organisation, Rome, Italy.

<https://www.fao.org/3/s2022e/s2022e01.htm>

CAPARAS M, ZOBEL Z, CASTANHO ADA, SCHWALM CR (2021) Increasing risks of crop failure and water scarcity in global breadbaskets by 2030. *Environmental Research Letters* **16 (10)** 104013.

CHANDRASEKARA A, KUMAR JT (2016) Roots and tuber crops as functional food: A review on phytochemical constituents and their potential health benefits. *International Journal of Food Science* 3631647.

CHIBARABADA TP, MODI AT, MABHAUDHI T (2017) Nutrient content and nutritional water productivity of selected grain legumes in response to production environment. *International Journal of Environmental Research and Public Health* **14 (11)** 1300.

CHIVENGE P, MABHAUDHI T, MODI ATA, MAFONGOYA P (2015) The potential role of neglected and underutilised crop species as future crops under water scarce conditions in sub-Saharan Africa. *International Journal of Environmental Research and Public Health* **12 (6)** 5685-5711.

CHOU JR (2013) A weighted linear combination ranking technique for multi-criteria decision analysis. *South African Journal of Economic and Management Sciences* **16 (5)** 28-41.

COLLINS MG, STEINER FR, RUSHMAN MJ (2001) Land-use suitability analysis in the United States: historical development and promising technological achievements. *Environmental Management* **28 (5)** 611-621.

CORNIC G, MASSACCI A (1996) Leaf photosynthesis under drought stress. In: *Photosynthesis and the Environment*, 347-366, Springer, Dordrecht, Netherlands.

CLULOW A, KAPTEIN N, EVERSON CS, GERMISHUIZEN I, KUNZ RP, GOKOOL S, TOUCHER ML (2023a) *The expansion of knowledge on evapotranspiration and stream flow reduction of different clones/hybrids to improve the water use estimation of SFRA species (i.e. Pinus, Eucalyptus, and wattle species): improved water use estimation of SFRA species – Volume 1: Improved water use estimation of SFRA species*. WRC Report No. TT 898/1/22, Water Research Commission, Pretoria, South Africa. 167 pp.

CLULOW AD, KUNZ RP, GOKOOL S, TOUCHER ML, SCHÜTTE S, SCHULZE RE, HORAN R, EVERSON CE, THORNTON-DIBB SLC, HORAN MJC, KAPEIN N, CLARK DJ, GERMISHUIZEN I (2023b) *The expansion of knowledge on evapotranspiration and stream flow reduction of different clones/hybrids to improve the water use estimation of SFRA species (i.e. Pinus, Eucalyptus, and wattle species): improved water use estimation of SFRA species – Volume 2: SFRA assessment utility*. WRC Report No. TT 898/2/22, Water Research Commission, Pretoria, South Africa. 212 pp.

DABERKOW SG, KATHERINE HR (1998) Low input agriculture: trends, goals, and prospects for input use. *American Journal of Agricultural economics* **70 (5)** 1159-1166.

DAFF (DEPARTMENT OF AGRICULTURE, FORESTRY AND FISHERIES) (2010) *Production guidelines: amadumbe*. DAFF, Pretoria, South Africa.
https://www.dalrrd.gov.za/phocadownloadpap/Brochures_and_Production_Guidelines/Brochure%20Amadumbe%202010.pdf

DAFF (DEPARTMENT OF AGRICULTURE, FORESTRY AND FISHERIES) (2011) *Production guidelines: sweet potato*. DAFF, Pretoria, South Africa.
https://www.dalrrd.gov.za/phocadownloadpap/Brochures_and_Production_Guidelines/Brochure%20Sweet%20potato.pdf

DAFF (DEPARTMENT OF AGRICULTURE, FORESTRY AND FISHERIES) (2014) *National Policy on Food and Nutrition Security*, DAFF, Pretoria, South Africa.
<https://www.gov.za/documents/national-policy-food-and-nutrition-security-south-africa>.

DARYANTO S, WANG L, JACINTHE P-A (2016) Drought effects on root and tuber production: A meta-analysis. *Agricultural Water Management* **176** 122-131.

DEBAEKE P, ABOUDRARE A (2004) Adaptation of crop management to water-limited environments. *European Journal of Agronomy* **21 (4)** 433-446.

DEO PC, TYAGI AP, TAYLOR M, BECKER DK, HARDING RM (2009) Improving taro (*Colocasia esculenta* var. *esculenta*) production using biotechnological approaches. *South Pacific Journal of Natural Science* **27 (1)** 6-13.

DEVNARAIN N, CRAMPTON BG, CHIKWAMBA R, BECKER JV, O'KENNEDY MM (2016) Physiological responses of selected African sorghum landraces to progressive water stress and re-watering. *South African Journal of Botany* **103** 61-69.

DLADLA LNT (2017) *Nutritional and water productivity of sweet potato*. Unpublished MSc thesis, Crop Science, School of Agricultural, Earth and Environmental Sciences, University of KwaZulu-Natal, Pietermaritzburg, South Africa.

DLADLA L, MODI A, MABHAUDHI T, CHIBARABADA T (2019) Yield, water use, and water use efficiency of sweet potato under different environments. In: *XXX International Horticultural Congress IHC2018: International Symposium on Water and Nutrient Relations and Management of 1253*. *Acta Horticulturae* **1253** 287-294.

DONG B, LIU H, WANG Y, QIAO Y, ZHANG M, YANG H, JIN L, LIU M (2018) Physio-ecological regulating mechanisms for highly efficient water use of crops. *Chinese Journal of Eco-Agriculture* **26** 1465-1475.

DU PLESSIS J (2003) *Maize production*. Department of Agriculture, Forestry and Fisheries, Pretoria, South Africa.

<https://www.dalrrd.gov.za/index.php/publications/16-brochures-and-production-guidelines?download=1638:maize-production&start=20>

DUA VK, GOVINDAKRISHNAN PM, SINGH BP (2014) Calibration of WOFOST model for potato in India. *Potato Journal* **41 (2)** 105-112.

DUQUE LO, VILLORDON A (2019) Root branching and nutrient efficiency: Status and way forward in root and tuber crops. *Frontier in Plant Science* **10** 1-8.

ESTES LD, BRADLEY BA, BEUKES H, HOLE DG, LAU M, OPPENHEIMER MG, SCHULZE R, TADROSS MA, TURNER WR (2013) Comparing mechanistic and empirical model projections of crop suitability and productivity: implications for ecological forecasting. *Global Ecology and Biogeography* **22** 1007-1018.

EVERSON C, MENGISTU M (2011) *The impact of madumbe (Colocasia esculenta) cultivation on the evaporation of a Cyperus latifolius marsh in KwaZulu-Natal*. WRC Report No. KV 260/10, Water Research Commission, Pretoria, South Africa.

EVERSON CS, GUMEDE MP, EVERSON TM, CLULOW AD, KUNZ RP (2021) *Quantification of the evapotranspiration and stream flow reduction caused by bamboo species on water resources in South Africa*. WRC Report No. TT/19, Water Research Commission, Pretoria, South Africa.

EZUI KS, FRANKE AC, MANDO A, AHIABOR BDK, TETTEH FM, SOGBEDJI J, JANSSEN BH, GILLER KE (2016) Fertiliser requirements for balanced nutrition of cassava across eight locations in West Africa. *Field Crops Research* **185** 69-78.

FABER M, SCHWABE C AND DRIMIE S (2009) Dietary diversity in relation to other household food security indicators. *International Journal of Food Safety, Nutrition, and Public Health* **2(1)** 1-15.

FAO (FOOD AND AGRICULTURE ORGANISATION) (1976) *A framework for land evaluation*. Soils Bulletin No. 32, FAO, Rome, Italy.

<https://www.fao.org/3/x5310e/x5310e00.htm>

FAO (FOOD AND AGRICULTURAL ORGANISATION) (1990) *Roots, tubers, plantains and bananas in human nutrition*. Food and Nutrition Series No. 24, FAO, Rome, Italy.

<https://www.fao.org/3/t0207e/T0207E00.htm>

FAO (FOOD AND AGRICULTURE ORGANISATION) (2002) *Deficit irrigation practices*. FAO, Rome, Italy.

<https://www.fao.org/3/y3655e/y3655e.pdf>

FAO (FOOD AND AGRICULTURAL ORGANISATION) (2012a) *ETo Calculator: Version 3.2*. FAO, Rome, Italy.

<https://www.fao.org/land-water/databases-and-software/en/>

FAO (FOOD AND AGRICULTURE ORGANISATION) (2012b) *FAO/INFOODS Guidelines for converting units, denominators and expressions, version 1.0*, FAO, Rome, Italy.

<http://www.fao.org/3/i3089e/i3089e.pdf>

FAO (FOOD AND AGRICULTURAL ORGANISATION) (2015) *AquaCrop new features and updates – Version 5.0*. FAO, Rome, Italy.

<http://www.fao.org/3/a-bc087e.pdf>

FAO (FOOD AND AGRICULTURAL ORGANISATION) (2017) *AquaCrop update and new features – Version 6.0*. FAO, Rome, Italy.

<http://www.fao.org/3/a-i7179e.pdf>

FAOSTAT (FOOD AND AGRICULTURE ORGANISATION STATISTICS) (2013) *Food and agriculture statistics per country*, FAO, Rome, Italy. <http://faostat3.fao.org/>

FAOSTAT (FOOD AND AGRICULTURE ORGANISATION STATISTICS) (2019) *Production: crops*, FAO, Rome, Italy. <https://www.fao.org/faostat/en/#home>

FERREIRA-SILVA SL, SILVEIRA JAG, VOIGT EL, SOARES LSP, VIEGAS RA (2008) Changes in physiological indicators associated with salt tolerance in two contrasting cashew rootstocks. *Brazilian Journal of Plant Physiology* **20 (1)** 51-59.

GERRANO AS, MATHEW I, SHAYANOWAKO AIT, AMOO S, MELLEM JJ, JANSEN VAN RENSBURG W, BAIRUA MW, VENTER SL (2021) Variation in mineral element composition of landrace taro (*Colocasia esculenta*) corms grown under dryland farming system in South Africa. *Heliyon* **7** e06727.

GOMES F, CARR MKV (2001) Effects of water availability and vine harvesting frequency on the productivity of sweet potato in Southern Mozambique. *Experimental Agriculture* **37 (4)** 223-537.

GOUDRIAAN R, BASTIAANSEN WGM (2013) Land and water productivity in the Doukkala irrigation scheme, Morocco. Internal Report to FAO Land and Water Division, Wageningen, Netherlands. 89 pp.

GOVENDER L, PILLAY K, SIWELA M, MODI AT, MABHAUDHI T (2019) Improving the Dietary Vitamin A Content of Rural Communities in South Africa by Replacing Non-Biofortified White Maize and Sweet Potato with Biofortified Maize and Sweet Potato in Traditional Dishes. *Nutrients* **11 (6)** 1-18.

HADEBE ST, MODI AT and MABHAUDHI T (2017) Calibration and testing of AquaCrop for selected sorghum genotypes. *Water SA* **43 (2)** 209-221.

HARTEMINK AE, JOHNSTON M, O'SULLIVAN JN, POLOMA S (2000) Nitrogen use efficiency of taro and sweet potato in the humid lowlands of Papua New Guinea. *Agricultural, Ecosystem and Environment* **79 (2-3)** 271-280.

HENG LK, HSIAO TC, EVETT S, HOWELL T, STEDUTO P (2009) Validating the FAO AquaCrop model for irrigated and water deficient field maize. *Agronomy Journal* **101 (3)** 488-498.

HOFFMAN AL, KEMANIAN AR, FOREST CE (2018) Analysis of climate signals in the crop yield record of sub-Saharan Africa. *Global Change Biology* **24** 143-157.

HOLL MA, GUSH MB, HALLOWES J, VERSFELD DB (2007) *Jatropha curcas in South Africa: An Assessment of its Water Use and Bio-Physical Potential*. WRC Report No. 1497/1/07, Water Research Commission, Pretoria, South Africa.

HOWARD PJA (1965) *The carbon-organic matter factor in various soil types*. *Oikos* **15 (2)** 229-236.

HSIAO TC, HENG LK (2011) *Using AquaCrop model*. Paper presented at: Joint ICTP-IAEA Conference on Coping with Climate Change and Variability in Agriculture through Minimizing Soil Evaporation Wastage and Enhancing More Crops per Drop. 9-13 May 2011, Trieste, Italy.

HSIAO TC, LEE H, STEDUTO P, BASILIO R-L, RAES D, FERERES E (2009) AquaCrop – The FAO crop model to simulate yield response to water: III. Parameterization and testing for maize. *Agronomy Journal* **101 (3)** 448-459.

IBSA F, GIRMA B, KASSA G, GEBREMEDHIN W (2013) Micropropagation Protocol for Mass Production of Released Potato Varieties. In: Seed Potato Tuber Production and Dissemination: Experiences, challenges and prospects, WOLDEGIORGIS G, SCHULZ S, BERIHUN B, 101-108. Ethiopian Institute of Agricultural research Institute (ARARI), Bahir Dar, Ethiopia.

IGWILO N (1984) *Comparison between the yield and growth patterns of yams grown from minisetts and normal seed yams*. Paper presented at the 20th Annual Conference of the Agricultural Society of Nigeria, 19-24 August 1984, University of Science and Technology, Port Harcourt, Rivers State, Nigeria.

ISLAM S (2006) Sweetpotato (*Ipomoea batatas* L.) leaf: its potential effect on human health and nutrition. *Journal of Food Science* **71 (2)** 13-121.

JEWITT GPW, KUNZ RP, WEN HW, VAN ROOYEN AM (2009a) *Scoping study on water use of crops/trees for biofuels in South Africa*. WRC Report No. 1772/1/09, Water Research Commission, Pretoria, South Africa.

JEWITT GPW, LORENTZ SA, GUSH MB, THORNTON-DIBB S, KONGO V, WILES L, BLIGHT J, STUART-HILL SI, VERSFELD D, TOMLINSON K (2009b) *Methods and guidelines for the licensing of*

SFRAs with particular reference to low flows. WRC Report No. 1428/1/09, Water Research Commission, Pretoria, South Africa.

JONES MR (2018) *Fast DSSAT simulations with low-performance computers*. South African Sugarcane Research Institute, Mt. Edgecombe, South Africa.

JONES JW, TSUJI GY, HOOGENBOOM G, HUNT LA, THORNTON PK, WILKENS PW, IMAMURA DT, BOWEN WT, SINGH U (1998) Decision support system for agrotechnology transfer: DSSAT v3. In: *Understanding options for agricultural production*, TSUJI GY, HOOGENBOOM G, THORNTON PK, 157-177. Springer, Dordrecht, Netherlands.

JOUBERT FJ, ALLEMANN L (1998) Madumbe. KwaZulu-Natal Department of Agriculture, Cedara College of Agriculture, KwaZulu-Natal, South Africa.

Horticultural Production Guidelines. JOVANOVIC NZ and ANNANDALE JG (1999) An FAO type crop factor modification to SWB for inclusion of crops with limited data: Examples for vegetable crops. *Water SA* **25** (2) 181-189.

JOVANOVIC NZ and ANNANDALE JG (2000) Calibration and validation of the SWB model for sunflower (*Helianthus annuus* L.). *South African Journal of Plant and Soil* **17** (3) 117-123.

JOVANOVIC NZ, ANNANDALE JG and MHLAULI NC (1999) Field water balance and SWB parameters determination of six winter vegetable species. *Water SA* **25** (2) 191-196.

KABUO NO, DIALOKE SA, OMEIRE GC, BEDI EN, PETER-IKECHUKWU AI, IREKPITA TE (2015) Comparison of proximate composition of some cultivars of chickpea (*Cicer arietinum* L.) cultivated in Owerri, Imo State, Nigeria. *Food Science and Quality Management* **37** 103-110.

KAHINDA JM, LILLIE ESB, TAIGBENU AE, TAUTE M, BOROTO RJ (2008) Developing suitability maps for rainwater harvesting in South Africa. *Physics and Chemistry of the Earth, Parts A/B/C* **33** (8-13) 788-799.

KARUKU GN, GACHENE CKK, KARANJA N, CORNELIS W, VERPLANCKE H, KIRONCHI G (2012) Soil hydraulic properties of a nitisol in Kabete, Kenya. *Tropical and Subtropical Agroecosystems* **15** 595-609.

KEATING BA, CARBERRY PS, HAMMER GL, PROBERT ME, ROBERTSON MJ, HOLZWORTH D, SMITH CJ (2003) An overview of APSIM, a model designed for farming systems simulation. *European Journal of Agronomy* **18** (3-4) 267-288.

KENNEDY G, RANERI J, STOIAN D, ATTWOOD S, BURGOS G, CEBALLOS H, EKESA B, JOHNSON V, LOW JW, TALSMA EF (2019) Roots, tubers and bananas: Contributions to food security. In: *Encyclopedia of Food Security and Sustainability*, FERRANTI P, ANDERSON JR, BERRY EM, 231-256. Elsevier.

KENYON L, ANANDAJAYASEKERAM P, OCHIENG C (2006) *A synthesis/lesson-learning study of the research carried out on root and tuber crops commissioned through the DFID RNRRS research programmes between 1995 and 2005*. Study commissioned by the Crop Protection Programme (CPP) of the UK Department for International Development (DFID; R1182).

https://www.researchgate.net/publication/216088436_A_synthesis_lesson-learning_study_of_the_research_carried_out_on_root_and_tuber_crops_commissioned_through_the_DFID_RNRRS_research_programmes_between_1995_and_2005

KHALID F, ULLAH S, REHMAN F, HADI R, KHAN N, IBRAHIM F, KHAN T, AZIZ F, FERAZ DA, NADEEM SG, HUSSAIN M (2021) Identification of suitable sites for *Jatropha curcas* L. bioenergy plantation using the AquaCrop model. *Forests* **12** (12) 1772.

KHOMO T (2014) *Spatial assessment of optimum and sub-optimum growing areas for selected biofuel feedstocks in South Africa*. Unpublished MSc dissertation. School of Agricultural, Earth and Environmental Sciences, College of Agriculture, Engineering and Science, University of KwaZulu-Natal, South Africa.

KIHARA J, BOLO P, KINYUA M, RURINDA J, PIIKKI K (2020) Micronutrient deficiencies in African soils and the human nutritional nexus: opportunities with staple crops. *Environmental Geochemistry and Health* **42** 3015-3033.

KLEIN PE, JORDAN DR (2014) Drought adaptation of stay-green sorghum is associated with canopy development, leaf anatomy, root growth, and water uptake. *Journal of Experimental Botany* **65** 6251-6263.

KLUTE A (1965) Laboratory measurement of hydraulic conductivity of saturated soil. In: *Methods of soil analysis, Part 1 – Physical and mineralogical Properties, including statistics of measurement and sampling volume 9*, Chapter 13, 210-221, American Society of Agronomy, Inc., USA.

KOOMAN PL, HAVERKORT AJ (1995) Modelling development and growth of the potato crop influenced by temperature and daylength: LINTUL-POTATO. In: *Potato ecology and modelling of crops under conditions limiting growth*, 41-59. Springer, Dordrecht, Netherlands.

KRAUSE P, BOYLE DP, BÄSE F (2005) Advances in geosciences comparison of different efficiency criteria for hydrological model assessment. *Advances in Geosciences* **5** 89-97.

KRUGER J, BREYNEART A, PIETERS L, HERMANS N (2018) Vegetable relishes, high in β -carotene, increase the iron, zinc and β -carotene nutritive values from cereal porridges. *International Journal of Food Science and Nutrition* **69** (3) 291-297.

KUNZ RP (2004) *Daily rainfall data extraction utility user manual version 1.4*. Institute for Commercial Forestry Research (ICFR), Pietermaritzburg, South Africa.

KUNZ R, MABHAUDHI T (2023) *Climate change atlas for rainfed production of selected underutilised crops: Volume 2*. WRC Report No. 2717/2/23, Water Research Commission, Pretoria, South Africa.

KUNZ RP, MENGISTU MG, STEYN JM, DOIDGE IA, GUSH MB, DU TOIT ES, DAVIS NS, JEWITT GPW, EVERSON CS (2015a) *Assessment of biofuel feedstock production in South Africa: Synthesis report on estimating water use efficiency of biofuel crops, Volume 1*. WRC Report No. 1874/1/15, Water Research Commission, Pretoria, South Africa.

KUNZ RP, MENGISTU MG, STEYN JM, DOIDGE IA, GUSH MB, DU TOIT ES, DAVIS NS, JEWITT GPW, EVERSON CS (2015b) *Assessment of biofuel feedstock production in South Africa: Technical report on the field-based measurement, modelling and mapping of water use of biofuel crops, Volume 2*. WRC Report No. 1874/2/15, Water Research Commission, Pretoria, South Africa.

KUNZ RP, DAVIS NS, THORNTON-DIBB SLC, STEYN JM, DU TOIT ES, JEWITT GPW (2015c) *Assessment of biofuel feedstock production in South Africa: Atlas of water use and yield of biofuel crops*

in suitable growing areas, Volume 3. WRC Report No. TT 652/15, Water Research Commission, Pretoria, South Africa.

KUNZ R, MASANGANISE J, REDDY K, MABHAUDHI T, LEMBEDE L, NAIKEN V, FERRER S (2020) *Water use and yield of soybean and grain sorghum for biofuel production.* WRC Report No. 2491/1/20, Water Research Commission, Pretoria, South Africa.

LABADARIOS D, MOODIE I, VAN RENSBURG A (2005) *Selected micronutrient status: vitamin A.* NFCS-FB Report No. 2007. National Food Consumption Survey: Fortification, Stellenbosch, South Africa.

LAHIFF E, COUSINS B (2005) Smallholder agriculture and land reform in South Africa. Institute of Development Studies (IDS) Bulletin **36 (2)** 127-131.

LAI-2200 (2010) *Instruction manual.* Publication No. 984-10633, LI-COR Biosciences, Lincoln, NE, USA.

LAKE SV (2022) *A novel approach for mapping areas suitable for rainfed production of taro.* Unpublished Honours HYDR730 project report. Centre for Water Resources Research, School of Agricultural, Earth and Environmental Sciences, University of KwaZulu-Natal, Pietermaritzburg, South Africa.

LAMARO GP, TSEHAYE Y, GIRMA A, RUBANGAKENE D (2023) The impact of future climate on orange-fleshed sweet potato production in arid areas of Northern Ethiopia. A case study in Afar region. *Heliyon* **9 (7)** e17288.

LAURIE SM (2010) *Agronomic performance, consumer acceptability and nutrient content of new sweet potato varieties in South Africa.* Unpublished PhD thesis, Plant sciences, School of Natural and Agricultural Sciences, University of the Free State, Bloemfontein, South Africa.

LAURIE SM, FABER M, VAN JAARVELD PJ, LAURIE RN, DU PLOOY CP, MODISANE PC (2012) β -carotene yield and productivity of orange-fleshed sweet potato (*Ipomoea batatas* L. Lam.) as influenced by irrigation and fertilizer application treatments. *Scientia Horticulturae* **142** 180-184.

LAURIE R, LAURIE SM, DU PLOOY CP, FINNIE JF, VAN STADEN J (2015) Yield of drought-stressed sweet potato in relation to canopy cover, stem length and stomatal conductance. *Journal of Agricultural Science* **7 (1)** 201-214.

LEBOT V (2019) *Tropical root and tuber crops: Cassava, sweet potato, yams and aroids.* 2nd Edition, Crop Science in Horticulture, CAB International, Wallingford, UK. 800 pp.

LEIGHTON CS (2008) *Nutrient and sensory quality of orange-fleshed sweet potato.* MSc dissertation, Consumer Science, School of Agricultural and Food Sciences, University of Pretoria, Pretoria, South Africa.

LEMOALLE J (2008) *Water productivity of aquatic systems.* Final report for the project: Improved fisheries productivity and management in tropical reservoirs, CP-PN34. Colombo, Sri Lanka: Challenge Program on Water and Food and Penang, Malaysia: the WorldFish Center. 32 p.
http://www.worldfishcenter.org/resource_centre/Wpfisheries_final_report.pdf

LOW AB, REBELO AG (1996) *Vegetation of South Africa, Lesotho and Swaziland.* Department of Environmental Affairs and Tourism (DEAT), Pretoria, RSA.
<http://www.ngo.grida.no/soesa/nsoer/Data/vegrsa/vegstart.htm>

LOW JW, MWANGA RO, ANDRADE M, CAREY E, BALL AM (2017) Tackling vitamin A deficiency with biofortified sweetpotato in sub-Saharan Africa. *Global Food Security* **14** 23-30.

LUNDQVIST J, MALMQUIST L, DIAS P, BARRON J, WAKEYO M (2021) *Water productivity, the yield gap, and nutrition: The case of Ethiopia*. Food & Agriculture Organisation (FAO) Land and Water Discussion Paper No. 17. Food and Agriculture Organisation, Rome, Italy.

LYNCH SD (2004) *Development of a raster database of annual, monthly and daily rainfall for southern Africa*. WRC Report No. 1156/1/04, Water Research Commission, Pretoria, South Africa.

MABHAUDHI T (2012) *Drought tolerance and water-use of selected South African landraces of taro (Colocasia esculenta L. Schott) and bambara groundnut (Vigna 202grohydrolog L. Verdc)*. Unpublished PhD thesis. Crop Science discipline, School of Agricultural, Earth and Environmental Sciences, University of KwaZulu-Natal, Pietermaritzburg, South Africa.

MABHAUDHI T, MODI AT (2015) Drought tolerance of selected South African taro (*Colocasia esculenta L. Schott*) landraces. *Experimental Agriculture* **51 (3)** 451-466.

MABHAUDHI T, MODI AT, BELETSE YG (2013a) Growth response of selected taro [*Colocasia esculenta (L.) Schott*] landraces to water stress. *Acta Horticulturae* **979** 327-334.

MABHAUDHI T, MODI AT, BELETSE, YG (2013b) Response of taro (*Colocasia esculenta L. Schott*) landraces to varying water regimes under a rain shelter. *Agricultural and Forest Meteorology* **121** 102-112.

MABHAUDHI T, MODI AT, BELETSE YG (2014a) Parameterization and testing of AquaCrop for a South African bambara groundnut landrace. *Agronomy Journal* **106 (1)** 243-251.

MABHAUDHI T, MODI A, BELETSE Y (2014b) Parameterisation and evaluation of the FAO-AquaCrop model for a South African taro (*Colocasia esculenta L. Schott*) landrace. *Agricultural and Forest Meteorology* **192-193** 132-139.

MABHAUDHI T, KUNZ RP, SCHULZE RE (2016a) Taro (*Amadumbe*) in South Africa and climate change. In: *Handbook for farmers, officials and other stakeholders on adaptation to climate change in the agriculture sector within South Africa*, Schulze RE. Section C: Crops in South Africa and climate change, Chapter C6.

MABHAUDHI, T, KUNZ RP, SCHULZE RE (2016b) Bambara Groundnut in South Africa and climate change. In: *Handbook for farmers, officials and other stakeholders on adaptation to climate change in the agriculture sector within South Africa*, Schulze RE. Section C: Crops in South Africa and climate change, Chapter C7.

MABHAUDHI T, CHIMONYO VGP, CHIBARABADA TP, MODI AT (2017a) Developing a roadmap for improving neglected and underutilized crops: a case study of South Africa. *Frontiers of Plant Science* **8** 2143.

MABHAUDHI T, CHIMONYO VGP, MODI AT (2017b) Status of underutilised crops in South Africa: Opportunities for developing research capacity. *Sustainability* **9** 1569.

MABHAUDHI T, KUNZ RP, SCHULZE RE (2018) *Farm sector case study: Taro (Amadumbe) and climate change*. In: *Climate change: A KwaZulu-Natal agricultural perspective*, SCHULZE RE, Chapter

13, 76-79. Developed for and published by the uMngeni Resilience Project. School of Agricultural, Earth and Environmental Sciences College of Agriculture, Engineering and Science, University of KwaZulu-Natal, Pietermaritzburg, South Africa.

MABHAUDHI T, CHIBARABADA T, MODI A (2019) Nutritional water productivity of selected sweet potato cultivars (*Ipomoea batatas* L.). *Acta Horticulturae* **1253** 295-302.

MABHAUDHI T, CHIMONYO VGP, KUNZ RP, MODI AT (2023) *Developing a guideline for rainfed production of underutilised indigenous crops and estimating green water use of indigenous crops based on available models within selected bio-climatic regions of South Africa: Volume 1*. WRC Report No. 2717/1/23, Water Research Commission, Pretoria, South Africa.

MAGWAZA LS, NAIDOO SIM, LAURIE SM, LAING MD, SHIMELIS H (2016) Development of NIRS models for rapid quantification of protein content in sweetpotato [*Ipomoea batatas* (L.) LAM.]. *LWT – Food Science and Technology* **72** 63-70.

MANSON AD, ROBERTS VG (2001) *Analytical methods used by the Soil Fertility and Analytical Services Section*. KwaZulu-Natal Department of Agriculture and Environmental Affairs. KZN AGRI-Report No. N/A/2001/04.

MARSHALL JJ, HOLMES JW (1998) *Soil physics second edition*. Press Syndicate of the University of Cambridge, New York, USA.

MASANGANISE J (2019) *Evapotranspiration of soybean and grain sorghum in a semi-arid climate*. PhD thesis, School of Agricultural, Earth and Environmental Sciences, College of Agriculture, Engineering and Science, University of KwaZulu-Natal, Pietermaritzburg, South Africa.

MASANGANISE J, KUNZ R, CLULOW AD, MABHAUDHI T, SAVAGE MJ (2022) Evapotranspiration estimates of soybean using surface renewal: Comparison with crop coefficient approach. *Physics and Chemistry of the Earth* **128** 103244.

MASANGO S (2015) *Water use efficiency of orange-fleshed sweetpotato (Ipomoea batatas L. Lam.)*. MSc dissertation, Plant production and Soil Science, School of Natural and Agricultural Sciences, University of Pretoria, Pretoria, South Africa.

MBANGIWA NC (2018) *Evapotranspiration over dryland maize and soybean using micrometeorological methods, modelling and remote sensing*. PhD thesis, School of Agricultural, Earth and Environmental Sciences, College of Agriculture, Engineering and Science, University of KwaZulu-Natal, Pietermaritzburg, South Africa.

MCMASTER GS, WILHELM WW (1997) Growing degree-days: one equation, two interpretations. *Agricultural and Forestry Meteorology* **87 (4)** 291-300.

MIYASAKA SC, OGOSHI RM, TSUJI GY, KODANI LS (2003) Site and planting date effects on taro growth: Comparison with aroid model predictions. *Agronomy Journal* **95 (3)** 545-557.

MODI AT, MABHAUDHI T (2013) *Water use and drought tolerance of selected traditional and indigenous crops*. WRC Report No. 1771/1/13, Water Research Commission, Pretoria, South Africa.

MODI AT, MABHAUDHI T (2016) *Developing a research agenda for promoting underutilised, indigenous and traditional crops*. WRC Report No. KV 362/16, Water Research Commission, Pretoria, South Africa.

MODI AT, MABHAUDHI T (2020) *Water use of crops and nutritional water productivity for food production, nutrition and health in rural communities in KwaZulu-Natal*. WRC Report No. 2493/1/20, Water Research Commission, Pretoria, South Africa.

MOKONOTO O (2018) *Assessing climate change impacts on productivity of sugarbeet and sugarcane using AquaCrop*. Unpublished MSc thesis, Hydrology and Crop Science, School of Agricultural, Earth and Environmental Sciences, University of KwaZulu-Natal, Pietermaritzburg, RSA.

MOLLE F, BERKOFF J (2007) *Irrigation water pricing: The gap between theory and practice*. CAB International, Wallingford, UK. 261 pp.

MORIASI DN, ARNOLD JG, LIEW MWV, BINGNER RL, HARMEL RD, VEITH TL (2007) Model evaluation guidelines for systematic quantification of accuracy in watershed simulations. *Transactions of the ASABE* **50** 885-900.

MOTSA NM, MODI AT, MABHAUDHI T (2015a) Sweet potato (*Ipomoea batatas* L.) as a drought tolerant and food security crop. *South African Journal of Science* **111** (11-12) 1-8.

MOTSA NM, MODI AT, MABHAUDHI T (2015b) Sweet potato response to low-input agriculture and varying environments of KwaZulu-Natal, South Africa: implications for food security strategies. *Acta Agriculturae Scandinavica, Section B – Soil and Plant Science* **65** (4) 329-340.

MTHEMBU T (2023) *Assessing the water productivity of sweet potato (Ipomoea batatas (L.) Lam.)*. Unpublished MSc dissertation. Centre for Water Resources Research, School of Agricultural, Earth and Environmental Sciences, University of KwaZulu-Natal, Pietermaritzburg, South Africa. 119 pp.

MUFUNGIZI AA, MUSAKWA W, GUMBO T (2020) A land suitability analysis of the Vhembe district, South Africa, The case of maize and sorghum. *The International Archives of the Photogrammetry, Remote Sensing and Spatial Information Sciences XLIII-B3-2020* 1023-1020.

MUGIYO H, CHIMONYO VGP, SIBANDA M, KUNZ R, MASEMOLA CR, MODI AT, MABHAUDHI T (2021a) Evaluation of land suitability methods with reference to neglected and underutilised crop species: A scoping review. *Land* **10** (2) 125.

MUGIYO H, CHIMONYO VGP, SIBANDA M, KUNZ R, NHAMO L, MASEMOLA CR, DALIN C, Modi AT, Mabhaudhi T (2021b) Multi-criteria suitability analysis for neglected and underutilised crop species in South Africa. *PLoS ONE* **16** (1) e0244734.

MUGIYO H, CHIMONYO VGP, KUNZ R, SIBANDA M, NHAMO L, MASEMOLA R, MODI AT, MABHAUDHI T (2022) Mapping the spatial distribution of underutilised crop species under climate change using the MaxEnt model: A case of KwaZulu-Natal, South Africa. *Climate Services* **28** 100330.

MULOVHEDZI N (2017) *Quantifying water use and nutritional water productivity of two sweet potato (Ipomoea batatas) cultivars grown in South Africa*. MSc dissertation, Plant production and Soil Science, School of Natural and Agricultural Sciences, University of Pretoria, Pretoria, South Africa.

MUSOKWA M, MAKHUBEDU T, MCCOSH J, SHEZI Z (2020) *Water Use of agroforestry systems for food and forage production*. WRC Report No. TT 827/20, Water Research Commission, Pretoria, South Africa.

NAGLER PL, SCOTT RL, WESTENBURG C, CLEVERLY JR, GLENN EP, HUETE AR (2005) Evapotranspiration on western US Rivers estimated using the enhanced vegetation index from MODIS and data from eddy covariance and Bowen ration flux towers. *Remote Sensing Environment* **97** 337-351.

NASH JE, SUTCLIFFE JV (1970) River flow forecasting through conceptual models Part I – A discussion of principles. *Journal of Hydrology* **10 (3)** 282-290.

NEDUNCHEZHIAN M, BYJU G, JATA SK (2012) Sweet Potato Agronomy. In: Nedunchezhiyan M, Byju G (Eds) *Sweet Potato*. Fruit, Vegetable and Cereal Science and Biotechnology **6 (1)** 1-10.

NORDBO A, JÄRVI L, VESALA T (2012) Revised eddy covariance flux calculation methodologies – effect on urban energy balance. *Tellus B: Chemical and Physical Meteorology* **64 (1)** 18184.

NYATHI MK (2019) *Assessment of nutritional water productivity and improvement strategies for traditional vegetables in South Africa*. PhD thesis, Wageningen School of Social Sciences (WASS), Wageningen University, Wageningen, Netherlands.

NYATHI MK, ANNANDALE JG, BELETSE YG, BEUKES DJ, DU PLOOY CP, PRETORIUS B, VAN HALSEMA GE (2016) *Nutritional water productivity of traditional vegetable crops*. WRC Research Report No. 2171/1/16, Water Research Commission, Pretoria, South Africa.

NYATHI MK, DU PLOOY CP, VAN HALSEMA GE, STOMPH TJ, ANNANDALE JG, STRUIK PC (2019a) The dual-purpose use of orange-fleshed sweet potato (*Ipomoea batatas* var. Bophelo) for improved nutritional food security. *Agricultural Water Management* **217** 23-37.

NYATHI MK, MABHAUDHI T, VAN HALSEMA GE, ANNANDALE JG, STRUIK PC (2019b) Benchmarking nutritional water productivity of twenty vegetables – A review. *Agricultural Water Management* **221** 248-259.

OLANREWAJU OO, OLUFAYO AA, OGUNTUNDE PG AND ILEMOBADE AA (2009) Water use efficiency of *Manihot Esculenta* Crantz under drip irrigation system in South Western Nigeria *European Journal of Agriculture* **7 (24)** 576-587.

OMORUYI F, DILWORTH L, ASEMOTA H (2007) Anti-nutritional factors, zinc, iron and calcium in some Caribbean tuber crops and the effect of boiling or roasting. *Nutrition and Food Science* **37 (1)** 8-15.

ÖNDER D, ÖNDER S, ÇALIŞKAN ME, ÇALIŞKAN S (2015) Influence of different irrigation methods and irrigation levels on water use efficiency, yield, and yield attributes of sweet potatoes. *Fresenius Environmental Bulletin* **24 (10a)** 3398-3403.

ORKWOR GC, ASIEDU R EKANAYAKE IJ (1998) *Food yams: Advances in research*. IITA and NRCRI, Nigeria. 249 pp.

OTIENO D, KREYLING J, PURCELL A, HEROLD N, GRANT K, TENHUNEN J, BEIERKUHNLIN C, JENTSCH A (2012) Drought responses of *Arrhenatherum elatius* grown in plant assemblages of varying species richness. *Acta Oecologica* **39** 11-17.

PADULOSI S, THOMPSON J, RUDEBJER P (2013) *Fighting poverty, hunger and malnutrition with neglected and underutilized species: needs, challenges and the way forward: Neglected and Underutilized Species*, BioDiversity International, Rome, Italy.

[https://cgspace.cgiar.org/bitstream/handle/10568/68927/Fighting%20poverty,%20hunger%20and%20malnutrition%20with%20neglected%20and%20underutilized%20species%20\(NUS\)_1671.pdf](https://cgspace.cgiar.org/bitstream/handle/10568/68927/Fighting%20poverty,%20hunger%20and%20malnutrition%20with%20neglected%20and%20underutilized%20species%20(NUS)_1671.pdf)

PALAO LK, NAZIRI D, BALANZA JG, CAMPILAN DM (2019) *Transformational adaptation of key root and tuber crops in Asia: Species distribution modelling for assessing crop suitability in response to climate change*. Final report, FOODSTART+ project, Lima, Peru. International Potato Center. 34 pp.

PANDEY R, MARANVILLE J, CHETIMA M (2000) Deficit irrigation and nitrogen effects on maize in a Sahelian environment: II. Shoot growth, nitrogen uptake and water extraction. *Agricultural Water Management* **46 (1)** 15-27.

PATEL N, KUMAR P, SINGH N (2011) Performance evaluation of AquaCrop in simulating potato yield under varying water availability conditions. Indian Agricultural Research Institute, New Delhi, India.

PEREIRA LS, ALLEN RG, SMITH M, RAES D (2015) Crop evapotranspiration estimation with FAO56: Past and future. *Agricultural Water Management* **147** 4-20.

PEREIRA LS, PAREDES P, HUNSAKER DJ, LÓPEZ-URREA R, MOHAMMADI SHAD Z (2021a) Standard single and basal crop coefficients for field crops. Updates and advances to the FAO56 crop water requirements method. *Agricultural Water Management* **243** 106466.

PEREIRA LS, PAREDES P, LÓPEZ-URREA R, HUNSAKER DJ, MOTA M, MOHAMMADI SHAD Z (2021b) Standard single and basal crop coefficients for vegetable crops, an update of FAO56 crop water requirements approach. *Agricultural Water Management* **243** 106196.

PHILLIPS SJ, DUDIK M (2008) Modeling of species distributions with Maxent: new extensions and a comprehensive evaluation. *Ecography* **31** 161-175.

PHILLIPS SJ, ANDERSON RP, SCHAPIRE RE (2006) Maximum entropy 206grohydro of species geographic distributions. *Ecological Modelling* **190 (3-4)** 231-259.

PUSHPALATHA R, SUNITHA S, SANTHOSH MITHRA VS, GANGADHARAN B (2021) Modelling the yield, water requirement, and water productivity of major tropical tuber crops using FAO-AquaCrop – A study over the main growing areas of India. *Journal of Tropical Agriculture* **59 (2)** 155-161.

PIKE A, SCHULZE RE (1995) *AUTOSOIL Version 3: A soils decision support system for South African soils*. Department of Agricultural Engineering, University of Natal, Pietermaritzburg, South Africa.

RAES D (2016a) *Book I: Understanding AquaCrop*. FAO, Rome, Italy. Updated in August 2023. <https://www.fao.org/3/cc2380en/cc2380en.pdf>

RAES D (2016b) *Book II: Running AquaCrop*. FAO, Rome, Italy. Updated in August 2023. <https://www.fao.org/3/i6052en/i6052en.pdf>

RAES D, STEDUTO P, HSIAO TC, FERERES E (2009) AquaCrop – the FAO crop model to simulate yield response to water: II. Main algorithms and software description. *Agronomy Journal* **101 (3)** 438-447.

RAES D, STEDUTO P, HSIAO TC, FERERES E (2012) *AquaCrop Version 4.0 reference manual*. Food and Agricultural Organisation, Rome, Italy. https://www.fao.org/fileadmin/user_upload/faowater/docs/AquaCropV40OutlineAndSymbols.pdf

RAES D, STEDUTO P, HSIAO TC and FERERES E (2018) *Reference manual AquaCrop (Version 6.0-6.1)*. Food and Agriculture Organisation, Rome, Italy.

<http://www.fao.org/3/BR248E/br248e.pdf>

RANKINE DR, COHEN JE, TAYLOR MA, COY AD, SIMPSON LA, STEPHENSON T, LAWRENCE JL (2015) Parameterizing the FAO AquaCrop model for rainfed and irrigated field-grown sweet potato. *Agronomy Journal* **107 (1)** 375-387.

RAVI V, CHAKRABARTI SK, MAKESHKUMAR T, SARAVANAN R (2014) Molecular regulation of storage root formation and development in sweet potato. In: *Horticultural Reviews*, WARRINGTON IJ, 157-207. John Wiley & Sons, Hoboken, New Jersey.

RAY RC (2015) Post harvest handling, processing and value addition of elephant foot yam – An overview. *International Journal of Innovative Horticulture* **4 (1)** 1-10.

RAY RC, SIVAKUMAR PS (2009) Traditional and novel fermented foods and beverages from tropical root and tuber crops: review. *International Journal Food Science and Technology* **44 (6)** 1073-1087.

RAYMUNDO R, ASSENG S, CAMMARANO D, QUIROZ R (2014) Potato, sweet potato, and yam models for climate change: A review. *Field Crops Research* **166** 173-185.

REDDY KCT (2024) *Evapotranspiration of rainfed taro and sweet potato in KwaZulu-Natal*. Unpublished PhD thesis. Centre for Water Resources Research, School of Agricultural, Earth and Environmental Sciences, College of Agriculture, Engineering and Science, University of KwaZulu-Natal, South Africa. In preparation.

RENAULT D, WALLENDER WW (2000) Nutritional water productivity and diets. *Agricultural Water Management* **45 (3)** 275-296.

SAATY TL (2008) Decision making with the analytic hierarchy process. *International Journal of Services Sciences* **1 (1)** 83-98.

SADRAS VO, GRASSINI P, STEDUTO P (2012) *Status of water use efficiency of main crops*. SOLAW Background Thematic Report – TR07, FAO, Rome, Italy. 41 pp.

http://www.fao.org/fileadmin/templates/solaw/files/thematic_reports/TR_07_web.pdf

SANGINGA N, MBABU A (2015) Root and tuber crops (cassava, yam, potato and sweet potato). In: *Feeding Africa*, 21-23 October 2015, Dakar, Senegal. 29 pp.

https://www.afdb.org/fileadmin/uploads/afdb/Documents/Events/DakAgri2015/Root_and_Tuber_Crops_Cassava_Yam_Potato_and_Sweet_Potato_.pdf

SARAVANAN R, RAVI V (2012) Fruit, vegetable and cereal science and biotechnology crop physiology of sweet potato. *Fruit, Vegetable and Cereal Science and Biotechnology* **6 (1)** 17-29.

SAXTON KE, RAWLS WJ (2006) Soil water characteristic estimates by texture and organic matter for hydrologic solutions. *Soil Science Society of America Journal* **70 (5)** 1569-1578.

SAXTON KE, RAWLS WJ, ROMBERGER JS, PAPENDICK RI (1986) Estimating generalized soil-water characteristics from texture. *Soil Science Society American Journal* **50** 1031-1036.

SAXTON KE, WILLEY PH (2009) The SPAW model for agricultural field and pond hydrologic simulation. United States Department of Agriculture, Pullman, USA.

<https://irrigationtoolbox.com/NEH/UserGuides/SPAW%20User%20Guide.pdf>

SCHULZE RE (1995) *Hydrology and 208grohydrology: A text to accompany the ACRU 3.00 agrohydrological modelling system*. WRC Report No. TT 69/9/95, Water Research Commission, Pretoria, South Africa.

SCHULZE RE (2011) Methods 3: Modelling impacts of climate change on the hydrological system: Model requirements, selection of the ACRU model, its attributes and computations of major state variables and outputs. In: *Methodological approaches to assessing eco-hydrological responses to climate change in South Africa*, SCHULZE RE, HEWITSON BC, BARICHIEVY KR, TADROSS M, KUNZ RP, HORAN MJC and LUMSDEN TG, Chapter 8, 75-88. WRC Report 1562/1/10, Water Research Commission, Pretoria, South Africa.

SCHULZE RE (Ed) (2023) *A national assessment of potential climate change impacts on the hydrological yield of different hydro-climatic zones of South Africa: Report 3 – South African and international verification studies of the ACRU daily time-step model across a range of processes, applications and spatial scales*. WRC Report No. 2833/3/22, Water Research Commission, Pretoria, South Africa.

SCHULZE RE, HORAN MJC (2007) Soils: Hydrological attributes. In: *South African Atlas of Climatology and Agrohydrology*, SCHULZE RE, Section 4.2. WRC Report No. 1489/1/06, Water Research Commission, Pretoria, South Africa.

SCHULZE R, HORAN M (2011) *Methods 1: Delineation of South Africa, Lesotho and Swaziland into quinary catchments*. In: *Methodological approaches to assessing eco-hydrological responses to climate change in South Africa*, SCHULZE R, HEWITSON B, BARICHIEVY K, TADROSS M, KUNZ R, HORAN M, LUMSDEN T. WRC Report No. 1562/1/10, Chapter 6, 55-62, Water Research Commission, Pretoria, South Africa.

SCHULZE RE, MAHARAJ M (2004) *Development of a database of gridded daily temperatures for southern Africa*. WRC Report No. 156/2/04, Water Research Commission, Pretoria, South Africa.

SCHULZE RE, HORAN MJC, KUNZ RP, LUMSDEN TG, KNOESEN DM (2011) *Methods 2: Development of the southern African quinary catchments database*. In: *Methodological approaches to assessing eco-hydrological responses to climate change in South Africa*, SCHULZE RE, HEWITSON BC, BARICHIEVY KR, TADROSS M, KUNZ RP, HORAN MJC, LUMSDEN TG, Chapter 7, 63-74. WRC Report No. 1562/1/10, Water Research Commission, Pretoria, South Africa.

SCHÜTTE S, SCHULZE RE, CLARK DJ (Eds) (2023) *A national assessment of potential climate change impacts on the hydrological yield of different hydro-climatic zones of South Africa: Report 1 – methodology and results*. WRC Report No. 2833/1/22, Water Research Commission, Pretoria, South Africa.

SCOTT DF, SMITH RE (1997) Preliminary empirical models to predict reductions in annual and low flows resulting from afforestation. *Water SA* **23 (2)** 135-140.

SCWG (SOIL CLASSIFICATION WORKING GROUP) (1991) *Soil Classification – Taxonomic System for South Africa*. Soil Classification Working Group. Department of Agricultural Development, Pretoria, South Africa.

SHANGE LP (2004) *Taro [Colocasia esculenta (L.) Schott] production by small-scale farmers in KwaZulu-Natal: farmer practices and performance of propagule types under wetland and dryland*

conditions. MSc thesis, Crop Science, School of Agricultural, Earth and Environmental Sciences, University of KwaZulu-Natal, Pietermaritzburg, South Africa.

SHELEMBE SC (2020) *Water use and nutritional water productivity of taro (Colocasia esculenta L.Schott) Landraces*. Unpublished MSc dissertation, Crop Science, School of Agricultural, Earth and Environmental Sciences, College of Agriculture, Engineering and Science, University of KwaZulu-Natal, Pietermaritzburg, South Africa.

SHIH SF, SNYDER GH (1984) Evapotranspiration and water use efficiency of taro. *American Society of Agricultural Engineers* **27 (6)** 1745-1748.

SIBIYA SG (2015) *Planting density effect on growth and yield of taro (Colocasia esculenta) landraces*. MSc dissertation, Crop Science, School of Agricultural, Earth and Environmental Sciences, University of KwaZulu-Natal, Pietermaritzburg, South Africa.

SINCLAIR TR, SELIGMAN NG (1996) Crop modelling: From infancy to maturity. *Agronomy Journal* **88** 694-704.

SINGH U, MATTHEWS RB, GRIFFIN TS, RITCHIE JT, HUNT LA, GOENAGA R (1998) Modeling growth and development of root and tuber crops. In: *Understanding options for agricultural production*, TSUJI GY, HOOGENBOOM G, THORNTON P, Systems Approaches for Sustainable Agricultural Development, Volume 7. Springer, Dordrecht, Netherlands.

Smith B (2006) *The farming handbook*. University of KwaZulu-Natal Press. Pietermaritzburg, South Africa.

SMITHERS JC and SCHULZE RE (1995) *ACRU agrohydrological modelling system: User manual Version 3.00*. WRC Report TT 70/95, Water Research Commission, Pretoria, South Africa.

SIRI (SOIL AND IRRIGATION RESEARCH INSTITUTE) (1987) *Land type series. Memoirs on the Agricultural Natural Resources of South Africa*. Soil and Irrigation Research Institute, Department of Agriculture and Water Supply, Pretoria, South Africa.

STEDUTO P, HSIAO TC, RAES D, FERERES E (2009) AquaCrop – the FAO crop model to simulate yield response to water: I. Concepts and underlying principles. *Agronomy Journal* **101 (3)** 426-437.

STEDUTO P, HSIAO TC, FERERES E, RAES D (2012) *Crop yield response to water*. Irrigation and Drainage Paper No. 66, Food and Agriculture Organization, Rome, Italy.

STEIN AJ (2010) Global impacts of human mineral malnutrition. *Plant and Soil* **335** 133-154.

SUNITHA S, RAVI V, GEORGE J, SUJA G (2013) Aroids and Water Relations: An Overview. *Journal of Root Crops* **39 (1)** 1-10.

TAGHIZADEH-MEHRJARDI R, NABIOLLAHI K, RASOLI L, KERRY R, SCHOLTEN T (2020) Land suitability assessment and agricultural production sustainability using machine learning models. *Agronomy* **10 (4)** 573-593.

TEGG RS, CORKREY R, HERDINA H, MCKAY AC, DE BOER RF, WIECHEL TJ (2015) Modeling pathogen DNA content and visual disease assessment in seed tubers to inform disease in potato progeny root, stolon, and tubers. *Plant Disease* **99 (1)** 50-57.

THOMAS-SHARMA S, ABDURAHMAN A, ALI S, ANDRADE-PIEDRA JL, BAO S, CHARKOWSKI AO, CROOK D, KADIAN M, KROMANN P, STRUIK PC, TORRANCE L, GARRETT KA, FORBES GA (2016) Seed degeneration in potato: the need for an integrated seed health strategy to mitigate the problem in developing countries. *Plant Pathology* **65** (1) 3-16.

TOUCHER ML, RAMJEAWON M, MCNAMARA MA, ROUGET M, BULCOCK H, KUNZ RP, MOONSAMY J, MENGISTU M, NAIDOO T, VATHER T (2020) *Resetting the baseline land cover against which stream flow reduction activities and the hydrological impacts of land use change are assessed*. Draft report for WRC Project No. K5/2437, Water Research Commission, Pretoria, South Africa.

TSEDALU M, TEFAYE B, GOA Y (2014) Effect of type of planting material and population density on corm yield and yield components of taro (*Colocasia Esculenta* L.). *Journal of Biology, Agriculture and Healthcare* **4** (17) 124-138.

USDA (UNITED STATES DEPARTMENT OF AGRICULTURE) (1999) *Soil quality test kit guide*. USDA Soil Quality Institute, Washington, DC, USA.

UUSIKU NP, OELOFSE A, DUODU KG, BESTER MJ, FABER M (2010) Nutritional value of leafy vegetables of sub-Saharan Africa and their potential contribution to human health: A review. *Journal of Food Composition and Analysis* **23** 499-509.

UYEDA J, RADOVICH T, SUGANO J, FARES A, PAULL R (2011) Effect of irrigation regime on yield and quality of three varieties of taro (*Colocasia esculenta*). *Hanaï'Ai/The Food Provider* **1** (1) 1-8.

VAN AVERBEKE W, KHOSA TB (2007) The contribution of smallholder agriculture to the nutrition of rural households in a semi-arid environment in South Africa. *Water SA* **33** (3) 413-418.

VAN GENUCHTEN MT (1980) A closed-form equation for predicting the hydraulic conductivity of unsaturated soils. *Soil Science Society of America Journal* **44** 892-898.

VAN JAARVELD P, MARAIS DW, HARMSE E, NESTEL P, RODRIGUEZ-AMAYA D (2006) Retention of β -carotene in boiled, mashed orange-fleshed sweet potato. *Journal of Food Composition and Analysis* **19** 321-329.

VIDIGAL SM, DE CARVALHO LOPES IP, PUIATTI M, SEDIYAMA MAN, DE FREITAS RIBEIRO MR (2016) Yield performance of taro (*Colocasia esculenta* L.) cultivated with topdressing nitrogen rates at the Zona da Mata region of Minas Gerais. *Soil Science and Plant Production* **63** (6) 887-892.

VON HOYNINGEN-HUENE J (1983) Die Interzeption des Niederschlages in landwirtschaftlichen Pflanzenbeständen. Deutscher Verband für Wasserwirtschaft und Kulturbau. *Schriften* **57** 1-66. Verlag Paul Parey, Hamburg Germany.

WAONGO M, LAUX P, KUNSTMANN H (2015) Adaptation to climate change: The impacts of optimized planting dates on attainable maize yields under rainfed conditions in Burkina Faso. *Agricultural and Forest Meteorology* **205** 23-29.

WARBURTON ML, SCHULZE RE and JEWITT GPW (2010) Confirmation of ACRU model results for applications in land use and climate change studies. *Hydrology and Earth System Sciences* **14** 2399-2414.

WEERARATHNE LVY, MARAMBE B, CHAUHAN BS (2017) Intercropping as an effective component of integrated weed management in tropical root and tuber crops: A review. *Crop Protection* **95** 89-100.

WENHOLD FAM, FABER M, VAN AVERBEKE W, OELOFSE A, VAN JAARVELD P, VAN RENSBURG WS, VAN HEERDEN I, SLABBERT R (2007) Linking smallholder agriculture and water to household food security and nutrition. *Water SA* **33 (3)** 327-336.

WEZEL A, SOBOKSA G, MCCLELLAND S, DELESPESE F, BOISSAU A (2015) The blurred boundaries of ecological, sustainable, and agroecological intensification: a review. *Agronomy for Sustainable Development* **35** 1283-1295.

WILLMOTT CJ (1981) On the validation of models. *Physical Geography* **2 (2)** 184-194.

WILLMOTT CJ (1982) Some comments on the evaluation of model performance. *Bulletin American Meteorological Society* **63** 1309-1313.

WILLMOTT CJ (1984) On the evaluation of model performance in physical geography. In: Gaile GL, Willmott CJ, Reidel D (Eds), *Spatial Statistics and Models*, Boston, US. 443-460.

WIMALASIRI EM, JAHANSHIRI E, PEREGO A, AZAM-ALI SN (2022) A novel crop shortlisting method for sustainable agricultural diversification across Italy. *Agronomy* **12 (7)**.

WOODWARD D, HAWKINS R, JIANG R, HJELMFELT A, MULLEM J, QUAN Q (2003) *Runoff curve number method: examination of the initial abstraction ratio*. World Water and Environmental Resources Congress, 1-10.

YENG S, AGYARKO K, DAPAAH H, ADOMAKO W, ASARE E (2012) Growth and yield of sweet potato (*Ipomoea batatas* L.) as influenced by integrated application of chicken manure and inorganic fertilizer. *African Journal of Agricultural Research* **7** 5387-5395.

ZHONG X, DUTTA U (2015) Engaging Nash-Sutcliffe efficiency and model efficiency factor indicators in selecting and validating effective light rail system operation and maintenance cost models. *Journal of Traffic and Transportation Engineering* **3** 255-265.

ZHOU Y, LAMBRIDES CJ, KEARNS R, YE C, FUKAI S (2012) Water use, water use efficiency and drought resistance among warm-season turfgrasses in shallow soil profiles. *Functional Plant Biology* **39 (2)** 116-125.

10 APPENDIX A

10.1 DATA STORAGE

The project has generated high-frequency temperature and wind speed data collected at Fountainhill Eco-estate over the period from August 2021 to August 2022. The data was analysed to estimate the evapotranspiration from a (i) 0.56 ha plot of taro, as well as fallow conditions (before and after harvesting), and (ii) 0.25 ha field of OFSP. In addition, the project generated ~2GB and ~80 GB of compressed model output pertaining to the AquaCrop and ACRU simulations, respectively. Data exists for eight national runs performed using AquaCrop and ACRU, i.e. two crops x two planting dates x two plant densities x two water treatments (rainfed & irrigated). The automation of the national model runs required the development of ~8,600 and ~10,000 lines of code (written in UNIX and Fortran) for AquaCrop and ACRU, respectively. In addition, ~1,400 lines of code were written to convert the climate input files from ACRU format to that required by AquaCrop. All raw, processed and modelled data is stored and archived on a fileserver located in the ICS Server Room on the University of KwaZulu-Natal's main campus in Pietermaritzburg.

Contact person: Richard Kunz (kunzr@ukzn.ac.za).

11 APPENDIX B

11.1 CAPACITY BUILDING

Three levels of capacity building are important to the WRC, namely postgraduate, institutional and community-based capacity building. Thus, each level is discussed separately in this section.

11.1.1 Postgraduate capacity building

Budget was allocated to support two full-time students (one MSc and one PhD) and a part-time post-doctorate student. In addition, Hydrology Honours students also contributed to the project on an annual basis. Details regarding the postgraduate students who benefitted from and contributed to this project are given in **Table 11-1**. As of December 2023, two Honours students and one MSc student have graduated. The part-time PhD student, who is currently in his 5th year, will strive to complete his degree in 2024 (expected graduation in April 2025).

Table 11-1 Individual capacity building: Postgraduate students

Name	Gender	Race	Degree	Discipline	Notes
Dr Vimbayi Chimonyo	Female	Black	Post-doc	Crop Science	Registered in 2018
Mr Thando Mthembu	Male	Black	BSc (Hons)	Hydrology	Registered in 2020 Degree awarded in 2021
Mr Kyle Reddy	Male	Indian	PhD	Hydrology	Registered in 2020
Mr Thando Mthembu	Male	Black	MSc	Hydrology	Registered in 2021 Degree awarded in 2023
Mr Simon Lake	Male	White	BSc (Hons)	Hydrology	Registered in 2022 Degree awarded in 2023

11.1.1.1 Honours degree candidates

Mr Mthembu: This student was responsible for developing an irrigation file in AquaCrop to alleviate crop water stress. He conducted simulations of water use and yield of taro under rainfed and irrigated conditions at Ukulinga (UKZN's research farm) across 49 consecutive seasons. Results showed that Ukulinga is not ideally suited to rainfed taro production, considering the large difference in yield obtained under rainfed and irrigated conditions.

Title: Assessing the water use and yield of taro and sweet potato

Abstract: With the impacts of climate change and increased climate variability on agricultural productivity becoming more certain, the ability to produce sufficient crop yields whilst simultaneously conserving as much water resources as possible is thus, imperative. In water-stressed countries like South Africa, the reliable quantification of crop evapotranspiration and yield is important for improved water resources management across a wide range of farming environments. As a result, hydrology and crop science researchers are shifting their primary focus from well-studied legume and grain crops to neglected and underutilised crops, including root and tuber crops (RTCs).

Taro (*Colocasia esculenta* L. Schott) and sweet potato (*Ipomoea batatas* L.) still remain underutilised RTCs in South Africa, despite their potential as being nutrient-dense, high yielding and water use efficient crops, as reported in local literature. It is therefore important to further investigate whether the water use of these two RTCs will hinder their production at the commercial scale. This study attempted to contribute towards the limited research pertaining to the water use and yield of taro and sweet potato. This desktop study used FAO's AquaCrop model to simulate the water use and yield of taro under

rained and irrigated conditions at Ukulinga across 49 seasons. Crop parameters were only available for taro at the time of this study and hence, sweet potato was not modelled as was initially planned.

There is a direct relationship between crop evapotranspiration rate (ET) and yield. Under dryland conditions, taro consumed on average 500 mm of water, which negatively impacted the average yield of 1.15 t ha⁻¹. This highlighted the importance of determining the crop's net supplemental irrigation requirement of 671 mm, which resulted in twice as much water being consumed, but a substantial increase in yield (23.78 t ha⁻¹). Crop water productivity (CWP) improves by increasing yield and/or decreasing water use. From water stressed to irrigated conditions, taro's CWP increased by 852% from 0.23 to 2.19 kg m⁻³. The nutritional water productivity (NWP) was higher for all nutrients (Al, B, Cu, Mn, Na and Zn) assessed in this study under irrigated conditions, relative to rainfed agriculture. This study showed that without supplemental irrigation, Ukulinga and other similar agro-ecologies are not considered suitable for production of taro. Future research should aim at assessing the impact of planting date on the yield, ET, CWP and NWP of RTCs, in order further enhance the limited knowledge on underutilised RTCs in South Africa.

Mr Lake: This student was responsible for developing a methodology that uses selected output from the AquaCrop model to identify areas deemed suitable for the rainfed production of taro. The work was then extended to include sweet potato and is presented in **Chapter 7** of this report.

Title: A novel approach for mapping areas suitable for rainfed production of taro

Abstract: South Africa is a water scarce region, and thus there is a growing need to cultivate more water use efficient crops under rainfed conditions. Taro is a neglected and underutilised Crop (NUC) that is considered more drought resistant and water use efficient than conventional crops. This nutrient-dense NUC also has the potential to improve food security and alleviate poverty, particularly at the smallholder farming scale. This study aimed to develop a land suitability map for taro cultivation under rainfed conditions in South Africa and eSwatini (southern Africa). The map was developed using simulated output data from a crop yield model (AquaCrop) and is considered a novel approach. Taro was selected so that the land suitability map could be compared to other maps recently developed for this NUC. Using a geographic information system, certain output variables from AquaCrop (e.g. crop water productivity, crop cycle and inter-seasonal variability of yield) were analysed, as well as planting date, risk of crop failure and national land cover data, to develop the land suitability map. The results indicated that of southern Africa's total land area, only 0.66% is highly suited to taro cultivation, compared to 1.75% and 1.63% that is considered moderately and marginally suitable, respectively. In addition, 1.66% of potentially suitable areas in South Africa cannot be used for taro production based on existing land cover and land use. Risk of crop failure had the greatest impact on land suitability. However, the selection of criteria thresholds used to eliminate unsuitable taro production areas was made difficult by the lack of research focus on NUCs. The land suitability can help guide policy makers to target specific regions in South Africa for promoting increased production of taro under rainfed conditions.

11.1.1.2 Master's degree candidates

Mr Mthembu: This student was responsible for establishing and monitoring of the sweet potato trial at Fountainhill Eco-estate during the second season (2021/22). The results from his MSc dissertation are presented in **Chapter 4** of this report.

Title: Assessing the water productivity of sweet potato (*Ipomoea batatas* (L.) Lam.)

Abstract: In water-stressed countries like South Africa, the reliable quantification of actual crop evapotranspiration (ET_A) and yield across a wide range of environments is important for improved agricultural water management. In addition, researchers are shifting their primary focus from well-studied major crops to neglected and underutilised crops. Orange flesh sweet potato (*Ipomoea batatas*

(L. Lam.) remains an underutilised root and tuber crop (RTC) in South Africa, despite its potential as being nutrient-dense, high yielding and water use efficient, as reported in local literature. When compared to conventional crops, knowledge is limited on the water use and yield of RTCs under rainfed and precision agricultural production in South Africa. It is therefore important to further investigate whether the water use of orange flesh sweet potato (OFSP) will hinder its production at the commercial scale. This study attempted to contribute towards the limited research on the crop water productivity (CWP) of OFSP. A rainfed field trial with optimum fertilisation was conducted at Fountainhill Eco-estate (KwaZulu-Natal, South Africa) to estimate seasonal ET, yield and CWP. The soil water balance method was used to determine ET accumulated over the growing season from 14 December 2021 to 11 April 2022. Total ET for OFSP was estimated at 468.13 mm, which was used to calculate fresh and dry CWP values of 7.45 and 2.59 kg m⁻³, based on final fresh and dry tuber yields of 34.89 and 12.12 t ha⁻¹, respectively. Harvested tuber and above-ground biomass samples were sent to a laboratory to analyse nutrient content (NC). The nutritional water productivity (NWP) was determined as the product of CWP and NC, highlighting the potential of OFSP to alleviate malnutrition, especially if grown in rural communities. Field observations were used to partially calibrate the Soil Water Balance (SWB) and AquaCrop models. These models were used to simulate ET, yield and biomass accumulation, from which CWP and NWP were calculated. Compared to observations, AquaCrop provided a better estimate of CWP (2.55 kg m⁻³) relative to the SWB model (1.16 kg m⁻³). However, AquaCrop simulated higher soil water content relative to measurements from volumetric soil water content sensors. This study showed that under suitable management practices, OFSP has the potential to be grown commercially, since the crop can produce high yields and nutrient contents under rainfed agricultural production. However, to improve production, future studies need to conduct research to improve tuber yield and biomass accumulation. Furthermore, the AquaCrop and SWB models should be calibrated and validated across different agro-ecological zones in South Africa.

11.1.1.3 Doctoral candidate

Mr Reddy: This student was responsible for establishing and monitoring of the taro trial at Fountainhill Eco-estate during the first (2020/21) and second (2021/22) seasons. The results from his PhD dissertation are presented in **Chapter 4** of this report. In the third season (2022/23), the student established and monitored an experiment conducted in raised greenhouse beds at UKZN. Both sweet potato and taro were grown under two water treatments, namely water stressed and unstressed conditions. Results of this experiment are reported in **Chapter 5**. The student also developed improved crop parameter values for both crops, which were then used to simulate water use and yield across the country (cf. **Chapter 6**).

Title: Quantifying water use and nutritional water productivity of taro and sweet potato

Abstract: Root and tuber crops (RTCs) such as cassava, sweet potato, taro and yams are important food crops for direct human consumption in Africa. RTCs play an important role in world food security due to their high nutritional value when compared to other crops. However, with global freshwater resources declining, there is increased pressure on agriculture to produce more food using less water. Despite emerging interest in RTCs due to their high nutritional value and their resilience to climate extremes, a paucity of information describing their agronomic requirements, production guidelines, water use and yield has hindered their widespread adoption by farmers in South Africa. The aim of this study was to quantify the water use, yield and nutrient content of sweet potato and taro. From the results, crop and nutritional water productivity were estimated. Research trials were conducted at Fountainhill Estate (KwaZulu-Natal, South Africa), where two micrometeorological techniques (eddy covariance and surface renewal) were setup to measure crop water use. From measurements of crop development over the growing season, certain crop parameters were calibrated for use in FAO's AquaCrop model. The model can be run for up to 5,838 homogeneous response zones in the country,

each driven with 50 years of daily climate data, to produce national-scale maps of crop yield, including crop and nutritional water productivity. The crop model can also be used to derive crop coefficients, which are required as input into the ACRU hydrological model to estimate the impact of RTC production on downstream water availability. Overall, reliable research focusing on the agronomy, water productivity and nutritional value of different RTCs will help to successfully promote their production by both emerging and commercial farmers, which would help particularly in rural areas in addressing food security, unemployment and inequality.

11.1.1.4 Post-doctorate candidate

Dr Chimonyo: This student was largely responsible for completing the first Deliverable report on 30th September 2020. The literature review was used to identify existing knowledge gaps, which guided the field-based research that focused on sweet potato and taro.

Title: Deliverable 01: State of the art literature review on root and tuber crops

Abstract: The project's first aim was to review production systems, water use, yield, nutritional and health benefits of indigenous root and tuber crops currently in production. From April to September 2020, a comprehensive literature review was conducted to meet this objective. The review cited over 180 references and was completed on 30 September 2020. It explored the current status of root and tuber crops (RTCs) in sub-Saharan Africa (SSA) and South Africa (SA) by focusing on their value chain (i.e. from production to consumption). It also provided an overview of production, post-harvest handling and processing, and marketing of RTCs in South Africa. The concepts of biotechnology, crop genetics and breeding, agronomy and agro-processing were deliberated as drivers to promote sustainable value chains for RTCs. Challenges and opportunities for mainstreaming RTCs into existing cropping systems within SA were also discussed. Since RTCs are promoted as alternative crop choices for risk mitigation against drought, information on water use, water productivity and drought tolerance was gleaned from the available literature. The review also considered aspects of health, nutritional benefits, nutritional content and nutritional water productivity of these crops. The role of crop simulation modelling was evaluated as a potential tool for providing additional information for RTCs. Of the five underutilised RTCs considered in the review, two (sweet potato and taro) have been identified as priority crops in terms of their existing potential and body of knowledge, as well as the availability of crop parameters to facilitate crop modelling.

11.1.2 Institutional capacity building

Postgraduate students benefit from various courses offered by the University of KwaZulu-Natal, which are designed to help them complete their degrees. Training is provided free of charge on using the Microsoft Office (MS) suite of products (MS Word, MS Excel, MS PowerPoint, etc.), as well as bibliographic managers (e.g. Endnote, RefWorks). Training on how to efficiently utilise the library is also provided. All postgraduate students working on this project were encouraged to attend the training sessions. In addition, the following more specialised courses were attended by researchers and students working on this project.

2020: In September 2020, Mr Reddy was selected to participate in the PhD Teacher Training Programme, which formed part of the UCDP PhD Capacity and Talent Development Project. The programme was designed to develop and capacitate individuals to enter academic careers. Mr Reddy participated in various online workshops to acquire teaching and learning skills, e.g. lecture delivery, classroom management and assessment.

2021: As part of the PhD Teacher Training Programme, Mr Reddy attended additional online workshops to (i) learn how to critically assess course modules, and (ii) how to recommend changes to the hydrology

curriculum. Mr Reddy also attended a two-hour SPSS workshop on basic statistical procedures, which was organised by the CAES Teaching and Learning Office.

2022: As part of the PhD Teacher Training Programme, Mr Reddy had to complete 100 hours of teaching before the end of his PhD. Mr Reddy has been exposed to the online teaching platform used by UKZN (i.e. Moodle). He has used Moodle to send three evaporation practicals, which he setup, to 2nd Hydrology and 3rd year Agricultural Engineering students. The students upload their completed practical assignments to Moodle, thus allowing Mr Reddy to download and mark them. Mr Reddy also helped to setup and mark the practical exam. Mr Mthembu also assisted with the evaporation practicals, as well as other practicals involving 3rd year undergraduate students.

Mr Kunz attended a workshop held on 23 September titled “Potential of African indigenous crops as future crops to combat climate change – celebrating African heritage”. The aim of the workshop was to promote sustainable production practices of indigenous crops and identify opportunities along the value chain for different role players, in order to create market demand. Various opportunities and challenges related to promoting the production of indigenous crops were highlighted. For example, seed availability and supply, market access (and penetration) and the need for production guidelines to be translated into African languages were some of identified barriers. Smallholder farmers will need to make use of herbicides and simple farm implements to reduce labour costs and improve profitability. “Bakkie” trading should be encouraged to target informal markets, as well as finding simple solutions to store and transport fresh produce (e.g. under refrigeration).

2023: Both Mr Reddy and Mr Mthembu again assisted with the evaporation practicals for 2nd year hydrology and 3rd agricultural engineering students, as well as other practicals involving 3rd year undergraduate students. Both students also assisted with invigilation of 2nd and 3rd year hydrology tests and exams.

11.1.3 Community-based capacity building

The project wanted the nearby Swayimane community (near Wartburg, KwaZulu-Natal) to participate in the research trials conducted at Fountainhill from planting through to harvesting. In this way, they were exposed to best management practices for underutilised crops production through action research and learning. The youths would then be allowed to harvest and market the produce after the research data has been collected. Taro corms were purchased from smallholder farmers in Swayimane for both seasons (2020/21 & 2021/22). Trial establishment in 2020/21 and 2021/22 involved 10 and 20 individuals from Swayimane, respectively. Community members were compensated for assisting with regular manual weeding of the trial sites.

At harvest, once leaf and tuber samples were obtained for research purposes (yield and nutrient content determination), the intention was to donate the roots and tubers to the Swayimane community and Ukulinga staff who worked on the trials. This was meant to demonstrate and strengthen community beneficiation from participatory action research. However, roots and tubers at both sites (in particular site 2) was completely destroyed by animals within a two-week period post-harvest.

12 APPENDIX C

12.1 TECHNOLOGY TRANSFER

Disseminating results from this project and engaging with stakeholders at conferences and workshops is important to increase awareness of this research project. Presentations that were made are listed below in chronological order.

12.1.1 Presentations

2021

Kunz R (2021) *Water use of indigenous root and tuber crops*. WRC Dialogue on “A Decade of Research on Water Use of Underutilized Indigenous and Traditional Crops”, 10:30-10:45, 24 February, online via Zoom.

Kunz R (2021) *Water use of indigenous root and tuber crops*. World Food Day dialogue on “Our actions are our future – Better production, better nutrition, a better environment and a better life”, 12:00-12:30, 15 October, online via Zoom.

Reddy K (2021) *Quantifying water use and nutritional water productivity of taro (Colocasia esculenta) and sweet potato (Ipomoea batatas)*. 5th Fountainhill Estate Research Symposium, 11:25-11:45, 21 October, Fountainhill Estate, KwaZulu-Natal.

2022

Mthembu T (2022) *Assessing the water productivity of sweet potato*. South African Hydrological Society (SAHS) Symposium, 11:00-11:15, 11 October, 26° South Hotel, Muldersdrift, Gauteng.

Reddy K (2022) *Quantifying the water use and nutritional water productivity of sweet potato*. South African Hydrological Society (SAHS) Symposium, 11:15-11:30, 11 October, 26° South Hotel, Muldersdrift, Gauteng.

Mthembu T (2022) *Assessing the water productivity of sweet potato*. Postgraduate Research and Innovation Symposium (PRIS, UKZN), 11:40-12:00, 08 December, online via Zoom. Awarded a cash prize for the 2nd best oral presentation within the SAEES.

Reddy K (2022) *Quantifying the water use and nutritional water productivity of sweet potato*. Postgraduate Research and Innovation Symposium (PRIS, UKZN), 14:00-14:20, 08 December, online via Zoom. Awarded a cash prize for the 3rd best oral presentation within the SAEES.

2023

Mthembu T (2022) *Assessing the water productivity of orange-fleshed sweet potato to optimise water resources management*. 7th Fountainhill Estate Research Symposium, 11:20-11:40, 19 October, Fountainhill Estate, KwaZulu-Natal.

2024

Kunz R (2024) *Developing a national database for underutilised crops*. Crop modelling workshop titled “Using crop models in research and assessing climate change impacts at various scales” held in Ghana from 19-23 February, 11:30-12:30, 21 February, online lecture via MS Teams.

12.1.2 Popular articles

The following published articles mentioned this project:

Kunz R (2021) *Water use of indigenous root and tuber crops*. Annual Report to the CWRR Board 2020-2021, Section 8.5, 43-44. Centre for Water Resources Research (CWRR), UKZN.

Kunz R (2022) *New CWRR Project: Water use of indigenous root and tuber crops*. Centre for Water Resources Research (CWRR), Online Newsletter Issue 2, 31 July 2020. Available [online](#).

Cuénod C (2023) *Passion for Research Stirred in Master's Graduate*. UKZNDabaOnline, Online Newsletter Volume 11 Issue 14, 04 May 2023. Available [online](#).

Cuénod C (2023) *Summa Cum Laude Graduate Finds Forte in Hydrology Research*. UKZNDabaOnline, Online Newsletter Volume 11 Issue 14, 04 May 2023. Available [online](#).

12.1.3 Papers

The following papers are currently being prepared for publication:

Reddy K, Clulow A, Kunz R, Mabhaudhi T (2024) *The potential of surface renewal for determining sensible heat flux of taro and sweet potato*.

Reddy K, Clulow A, Kunz R, Mabhaudhi T (2024) *Estimation of taro and sweet potato evapotranspiration using the surface renewal and eddy covariance*.

Reddy K, Kunz R, Mabhaudhi T (2025) *Calibration and evaluation of AquaCrop for sweet potato and taro under water deficit conditions*.

13 APPENDIX D

13.1 SUMMARY OF LITERATURE REVIEW FINDINGS

Table 13-1 Growth criteria, expected yields, crop water requirements and crop water productivity of selected root and tuber crops

Description	Sweet potato	Cassava	Taro	Tannia	Yam
Growing period (days)	90-150	300-600	180-240	180-240	180-240
Photoperiod	Day-neutral				
Temperature range (optimal temperature)	15-35 (24)	25-29	21-27	23-29	25-30
Relative drought tolerance	Very high	Moderate	Low	Very low	High
Frost tolerance	Very low	Very low	Low	Low	Low
Stage most susceptible to water stress	Vegetative root formation	Vegetative root formation	Tuber bulking	Vegetative tuber formation	Vegetative tuber formation
Water logging tolerance	Low	Low	High	Low	Medium
Expected yields (t ha ⁻¹)	4-10	11-21	4-24	30	
Crop water requirements (mm)	700-1,500	700-1,500	1,750-2,500	1,400-2,000	1,000-1,500
K _c (Ini; Dev; Mid; Late)	0.5; - ;1.15; 0.65	0.3; 0.8-1.10; 0.3-0.5; 1.0-1.5		1.05; - ; 1.15; 1.1	
Water productivity (kg m ⁻³)		1.00	0.12-0.44		1.00
Water use efficiency (kg mm ⁻¹)	65-95	19.2-23.6	0.53-0.71		23-55

Sources: Bradshaw (2010); Kennedy et al. (2019); Lebot (2019); Pereira et al., (2015); Mabhaudhi et al. (2014b); Lemoalle, 2008; Shih and Snyder (1984)

Table 13-2 Proximate composition of five root and tuber crops

Proximate analysis	Sweet potato	Cassava	Taro	Tannia	Yam
Moisture (%)	62.20-69.42	66.96	6.54-68.10		6.79-92.01
Dry matter (% fresh weight)	20-35	30-40	15-25	28.8-30	20-40
Starch (g)	18-28	27-37	15-25	15-25	20-25
Energy (kcal)	86 -170	130-160	276-352	270-373	118-358
Total sugars (% fresh weight)	1.5-5.0	0.5-5.5			0.5-2.0
Protein (%)	1.6-4.8	0.5-2.0	0.3-7.8	2.4-6.2	1.0-13.4
Crude fibre (%)	3.00-3.68	1.11-1.80	0.60-3.01	1.48-5.74	2.31-7.48
Crude fat (%)	0.10-0.42	0.30	0.11-0.77	0.47-1.26	0.2-1.30
Carbohydrates (%)	20.10-90.17	30.63-38.10	13.00-86.11	62.91-81.39	27.90-84.07
Ash (%)	2.04-2.11	1.05	0.60-7.78	2.23-5.50	1.76-6.36
Nitrogen free extract (%)				82.82-86.44	71.64-79.79

Sources: Bradshaw (2010); Chandrasekara and Kumar (2016); Kennedy et al. (2019); Ray (2015); Sanginga and Mbabu (2015)

Table 13-3 Mineral composition for five root and tuber crops

Minerals (mg kg ⁻¹)	Sweet potato	Cassava	Taro	Tannia	Yam
Zinc	0.01-8.42		1.65-2.63	1.64-2.06	0.03-6.66
Iron	0.48-3.26	1.70	2.95-12.85	3.96-13.50	11.48-66.32
Manganese	1.52-4.94		0.72-1.91	0.64-1.91	2.10-9.40
Calcium	30-48	16-33	3-132	3-11	17-748
Magnesium	25-111	8-21	25-415	25-84	21-656
Potassium	337-1242	271	227-340		816-1,624
Phosphorus	47-159	27-38	73-340		55-166
Sodium	3-55	14	82-1,521		6-168
Copper	0.72-7.52		1.04		2.46-14.56
Sulphur	11.98-24.00				

Sources: Bradshaw (2010); Chandrasekara and Kumar (2016); Kennedy et al. (2019); Ray (2015); Sanginga and Mbabu (2015)

Table 13-4 Vitamin and bioactive composition in selected root and tuber crops

Vitamins (per kg)	Sweet potato	Cassava	Taro	Tannia	Yam
Vitamin A (IU)	14187	13			138
Vitamin C (mg)	2.4	20.6	14.3		17.1
Thiamine (mg)	0.08	0.09	0.03-0.18		0.11
Riboflavin (mg)	0.06	0.05	0.02-0.04		0.03
Niacin (mg)	0.56	0.85	0.91		0.55
Vitamin B-6 (mg)	0.209	0.088			0.293
Vitamin E (mg)	0.26	0.19			0.35
Vitamin K (µg)	1.8	1.9			2.3
Total ascorbic acid (mg)	2.40	20.60			17.10
Folate (µg-DFE)	11	27	18		23
Phenols (mg)		2.1-120	34.83		1.21-1.91
Flavonoids (mg)	165		28.56	150-410	0.61-1.38
Saponins (%)		1.74-4.73	0.67-1.42	0.62-0.72	1.03-2.71

Sources: Bradshaw (2010); Chandrasekara and Kumar (2016); Kennedy et al. (2019); Ray (2015); Sanginga and Mbabu (2015)

Table 13-5 Variation in mineral content of 14 taro accessions from mostly KwaZulu-Natal (Gerrano et al., 2021)

Mineral element	Mineral element content (g kg⁻¹)		
	Minimum	Mean	Maximum
Mn	0.001	0.004	0.007
Zn	0.002	0.007	0.022
Fe	0.022	0.033	0.045
Na	0.087	0.132	0.206
Mg	0.199	0.246	0.320
P	0.219	0.314	0.425
Ca	0.285	0.359	0.463
K	1.080	1.451	1.761

14 APPENDIX E

14.1 MEASURED NUTRIENT CONTENTS FROM SEASON 2

Table 14-1 Nutrient content of OFSP storage roots grown at Fountainhill during the 2021/22 season (Mthembu, 2023)

Rep	Nutrient content (g kg ⁻¹)															
	Al	β-c	B	Ca	Cu	Fe	K	Mg	Mn	Mo*	Na	P	Zn	Total C	Total N	Total S
1	n.d.	0.200	0.006	1.359	0.003	0.044	23.66	1.018	0.012	0.0001	0.063	3.443	0.015	433.9	13.8	0.95
2	n.d.	0.200	0.005	1.391	0.003	0.045	23.90	1.021	0.012	0.0001	0.062	3.402	0.015	417.7	13.3	0.63
3	n.d.	0.190	0.005	1.362	0.003	0.038	22.18	0.991	0.011	0.0003	0.064	3.283	0.013	422.2	13.5	0.91
Ave	n.d.	0.200	0.006	1.370	0.003	0.042	23.25	1.010	0.011	0.0002	0.063	3.376	0.014	424.6	13.5	0.80

Table 14-2 Nutrient content of taro tubers grown at Fountainhill during the 2021/22 season (Reddy, 2024)

Rep	Nutrient content (g kg ⁻¹)															
	Al	β-c	B	Ca	Cu	Fe	K	Mg	Mn	Mo*	Na	P	Zn	Total C	Total N	Total S
1	n.d.	n.d.	0.005	1.237	0.007	0.253	18.86	1.280	0.104	0.0006	0.031	3.929	0.135	431.8	15.8	1.13
2	n.d.	n.d.	0.005	1.224	0.007	0.283	19.21	1.289	0.099	0.0008	0.028	3.966	0.139	432.5	15.7	1.14
3	n.d.	n.d.	0.005	1.258	0.007	0.316	19.28	1.275	0.100	0.0008	0.028	4.052	0.136	432.2	15.8	1.24
Ave	n.d.	n.d.	0.005	1.240	0.007	0.284	19.12	1.281	0.101	0.0007	0.029	3.982	0.137	432.2	15.8	1.20

Rep = replications; Ave = average; β-c = beta-carotene; n.d. = no data; *Level of quantification: 0.03

Table 14-3 Nutrient content of OFSP leaves grown at Fountainhill during the 2021/22 season (Mthembu, 2023)

Rep	Nutrient content (g kg ⁻¹)															
	Al	β-c	B	Ca	Cu	Fe	K	Mg	Mn	Mo*	Na	P	Zn	Total C	Total N	Total S
1	n.d.	n.d.	0.080	43.85	0.006	0.260	21.91	10.71	0.110	0.0006	0.070	3.740	0.010	409.5	34.0	3.10
2	n.d.	n.d.	0.070	47.19	0.004	0.260	22.98	12.31	0.180	0.0001	0.070	2.610	0.010	398.7	34.1	3.00
3	n.d.	n.d.	0.050	34.27	0.004	0.230	26.04	10.26	0.320	0.0001	0.070	3.170	0.030	408.0	43.0	3.00
4	n.d.	n.d.	0.070	40.39	0.004	0.200	20.86	10.83	0.140	0.0011	0.070	3.330	0.010	404.4	34.3	2.90
5	n.d.	n.d.	0.050	35.92	0.004	0.170	25.27	9.97	0.340	0.0004	0.070	2.800	0.020	411.8	42.0	3.50
Ave	n.d.	n.d.	0.060	40.33	0.004	0.230	23.41	10.82	0.220	0.0005	0.070	3.130	0.020	406.5	37.5	3.10

Rep = replications; Ave = average; β-c = beta-carotene; n.d. = no data; *Level of quantification: 0.03

Table 14-4 Nutritional water productivity of OFSP (roots and leaves) and taro tubers (Reddy, 2024)

Crop	Nutritional water productivity (dry g m ⁻³)															
	Al	β-c	B	Ca	Cu	Fe	K	Mg	Mn	Mo*	Na	P	Zn	Total C	Total N	Total S
OFSP root	n.d.	0.68	0.02	4.69	0.01	0.14	79.59	3.46	0.04	0.00	0.22	11.56	0.05	1,453.63	46.22	2.74
OFSP leaf	n.d.	n.d.	0.21	138.07	0.00	0.79	80.14	37.04	0.75	0.00	0.24	10.72	0.07	1,391.67	128.38	10.61
Taro tuber	n.d.	n.d.	0.01	1.70	0.01	0.39	26.23	1.76	0.14	0.00	0.04	5.46	0.19	593.10	21.68	1.65
Taro leaf	n.d.	n.d.	n.d.	n.d.	n.d.	n.d.	n.d.	n.d.	n.d.	n.d.	n.d.	n.d.	n.d.	n.d.	n.d.	n.d.

14.2 MEASURED NUTRIENT CONTENTS FROM SEASON 3

Table 14-5 Nutrient content of OFSP storage roots grown in a greenhouse during the 2022/23 season

Crop part	% of CWR	Nutrient content (g kg ⁻¹)															
		Al	β-c	B	Ca	Cu	Fe	K	Mg	Mn	Mo	Na	P	Zn	Total C	Total N	Total S
root	100	0.174	0.101	n.d.	1.20	0.003	0.179	11.10	0.600	0.006	n.d.	0.567	1.900	0.008	431.5	4.7	0.7
	30	0.248	0.206	n.d.	1.20	0.003	0.284	11.30	0.700	0.015	n.d.	0.526	1.800	0.006	451.4	5.1	0.7
leaf	100	1.284	n.d.	n.d.	15.10	0.006	1.379	18.00	5.800	0.101	n.d.	0.350	2.100	0.041	466.7	31.2	3.7
	30	0.622	n.d.	n.d.	16.40	0.010	0.680	32.70	7.100	0.130	n.d.	0.413	2.400	0.027	454.4	31.8	4.1

Table 14-6 Nutrient content of taro tubers grown in a greenhouse during the 2022/23 season

Crop part	% of CWR	Nutrient content (g kg ⁻¹)															
		Al	β-c	B	Ca	Cu	Fe	K	Mg	Mn	Mo	Na	P	Zn	Total C	Total N	Total S
root	100	0.329	n.d.	n.d.	0.90	0.005	0.354	22.30	1.000	0.010	n.d.	0.294	3.100	0.029	441.4	10.5	0.9
	30	0.464	n.d.	n.d.	0.90	0.004	0.503	21.00	1.100	0.015	n.d.	0.278	3.300	0.038	443.8	14.3	1.1
leaf	100	1.168	n.d.	n.d.	37.00	0.005	1.323	17.60	2.500	0.090	n.d.	0.546	2.000	0.042	447.9	12.6	1.2
	30	1.721	n.d.	n.d.	35.60	0.006	2.068	16.90	3.200	0.129	n.d.	0.689	2.100	0.052	447.8	18.9	1.5

β-c = beta-carotene; n.d. = no data

15 APPENDIX F

15.1 Dry biomass accumulation for OFSP

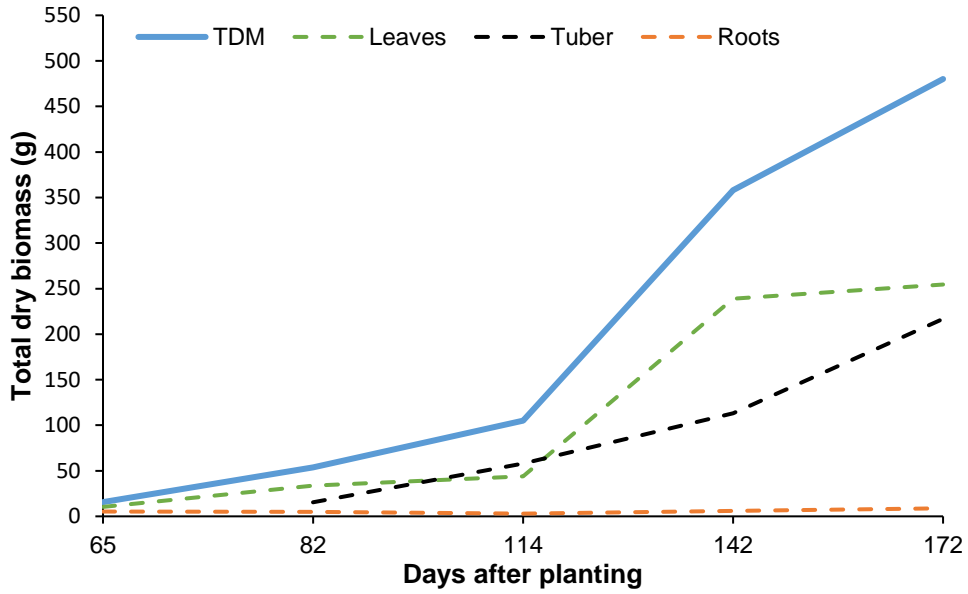


Figure 15-1 Total dry biomass accumulation for OFSP (30% of CWR)

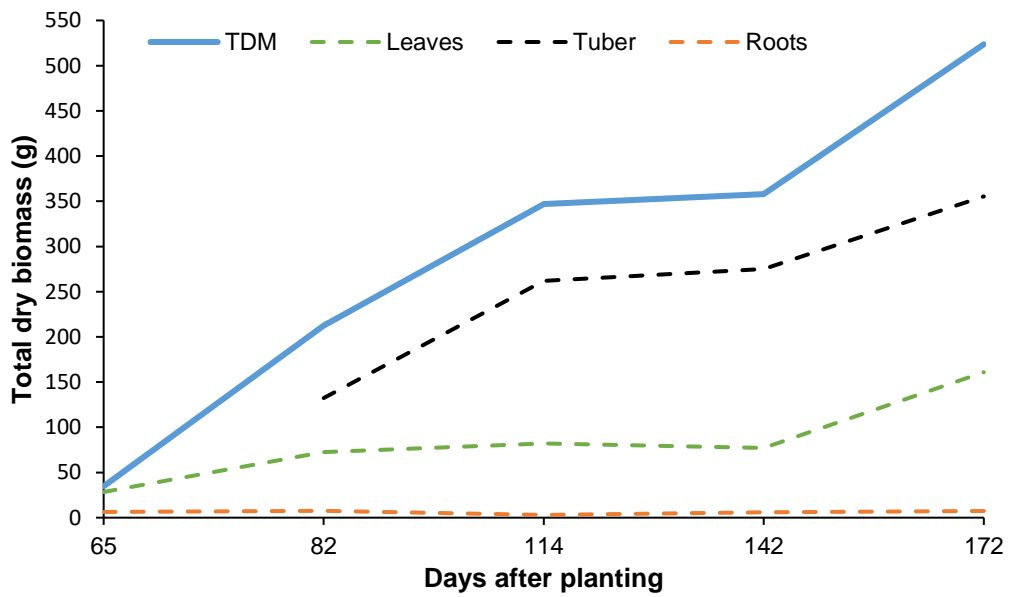


Figure 15-2 Total dry biomass accumulation for OFSP (30% of CWR)

15.2 Dry biomass accumulation for taro

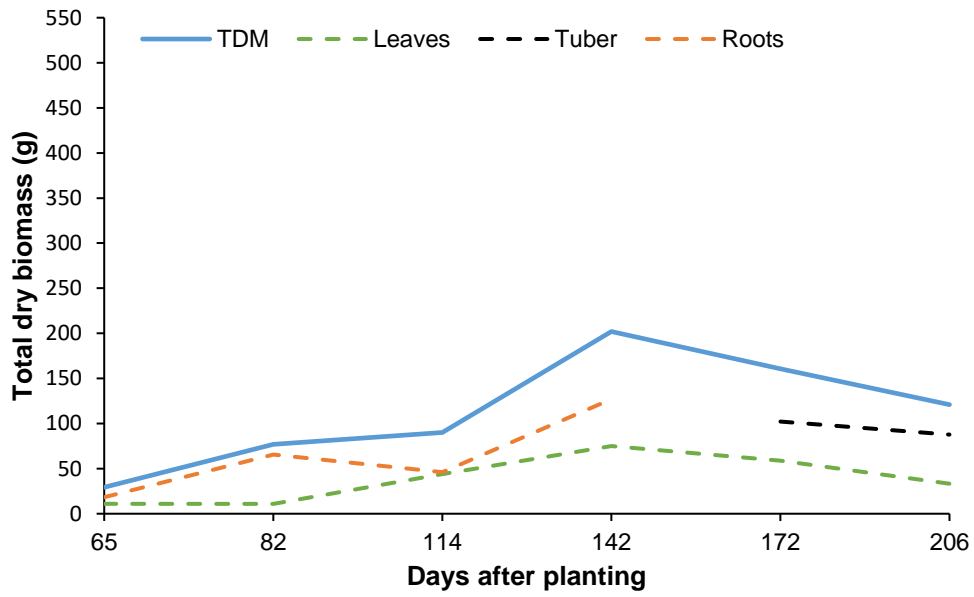


Figure 15-3 Total dry biomass accumulation for taro (30% of CWR)

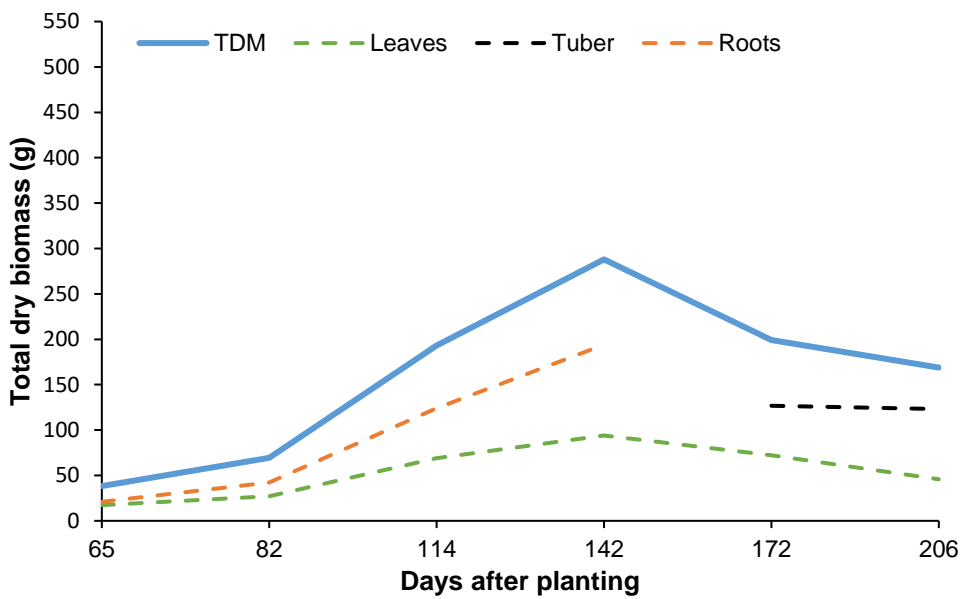


Figure 15-4 Total dry biomass accumulation for taro (100% of CWR)

16 APPENDIX G

16.1 CALIBRATION & VALIDATION STATISTICS

Table 16-1 AquaCrop calibration statistics for sweet potato and taro

Crop	Treatment	Cultivar/ Landrace	Trial type & location	CC (n)	Canopy cover CC (%)				Source
					RMSE	NSE	D-I	R ²	
Taro	Irrigated	Umbumbulu landrace	Field trial Ukulinga	8	2.38		0.92	0.79	Mabhaudhi et al. (2014b)
Sweet potato	Irrigated	Orange-flesh (Bophelo)	Rain shelter Roodeplaat	15	12.10			0.77	Nyathi et al. (2016)
Sweet potato	Irrigated	Orange-flesh (Isondlo)	Rain shelter Roodeplaat	4				0.92	Beletse et al. (2013)
Sweet potato	2012 irrigated rainfed	Ganja Uplifta Yellow Belly	Devon, Jamaica Devon, Jamaica	3	25.20	-0.59			Rankine et al. (2015)
	2013 irrigated rainfed				9.42	0.76			
					10.86	0.86			Rankine et al. (2015)
					4.48	0.97			

Table 16-2 AquaCrop validation statistics for sweet potato and taro

Crop	Treatment	Cultivar/ Landrace	Trial type & location	CC (n)	Canopy cover CC (%)				Source
					RMSE	NSE	D-I	R ²	
Taro	Irrigated	Umbumbulu landrace	Field trial Ukulinga	8	1.85		0.99	0.84	Mabhaudhi et al. (2014b)
	Rainfed				20.17		0.65	0.02	
Sweet potato	Irrigated	Orange-flesh (Bophelo)	Rain shelter Roodeplaat	15	4.98			0.99	Nyathi et al. (2016)
Sweet potato	Irrigated	Orange-flesh (Isondlo)	Rain shelter Roodeplaat	4					Beletse et al. (2013)
Sweet potato	2013 irrigated rainfed	Ganja Uplifta Yellow Belly	Ebony Park, Jamaica	5	17.25	0.29			Rankine et al. (2015)
					16.06	0.67			

16.2 DEFAULT AQUACROP PARAMETERS

Table 16-3 AquaCrop parameters for sweet potato derived by Nyathi et al. (2016) and Beletse et al. (2013)

*No.	Crop parameter	Beletse et al. (2013)	Nyathi et al. (2016)
04	Crop type	root/tuber (3)	root/tuber (3)
05	Crop is	transplanted	transplanted
06	Base temperature for no crop development (°C)	8	10
09	Cut-off temperature for no crop development (°C)	35	35
11	Soil water depletion factors for:		
12	Canopy expansion (upper threshold)		0.20
14	Canopy expansion (lower threshold)		0.55
14	Stomatal control		
16	Canopy senescence		0.65
13	Shape factor for:		
15	Water stress coefficient for canopy expansion	2.0	1.5
17	Water stress coefficient for stomatal control	2.0	0
39	Water stress coefficient for canopy senescence	2.0	0
39	Describing root zone expansion	15	0
35	Crop transpiration coefficient (K_{CB})	1.50	
36	Decline in K_{CB} due to ageing (% day ⁻¹)	0.15	
29	Minimum GDs required for full crop transpiration	8	
37	Minimum effective rooting depth (m)	0.25	0.30
38	Maximum effective rooting depth (m)	1.00	2.00
40	Maximum root water extraction in:		
41	Top quarter of root zone		
41	Bottom quarter of root zone		
46	Canopy growth coefficient: fraction per		
75	calendar day		
75	growing degree-day	1.15500	1.43600
51	Canopy decline coefficient: fraction per		
76	calendar day		
76	growing degree-day	0.14300	0.35500
43	Seedling leaf area (cm ²)		
50	Maximum canopy cover (CC_x)	1.00	0.98
50	Time to reach CC_x (GDD)		592
69	Growing degree-days from planting to:		
70	Emergence/recovered transplant		
70	Maximum rooting depth	677	1,885
71	Start of senescence	1,274	1,708
72	Maturity (length of crop cycle)	1,967	2,053
73	Start of yield formation/initiation		
74	Length of the flowering stage:		
74	Growing degree-days		
77	Building up of Harvest Index		
77	During yield formation (GDD)	261	
61	Normalised water productivity WP^* (g m ⁻²)	20.0	16.0
62	WP^* during yield formation (as a percentage of WP^*)		
64	Reference harvest index (percentage)	90	50
65	Increase (percentage) of harvest index:		
68	due to water stress before start of yield formation	0	
68	allowable maximum	5	

*Denotes line number in AquaCrop parameter file (version 6; March 2017)

red: denotes likely errors in parameter values

Table 16-4 AquaCrop parameters for sweet potato derived by Rankine et al. (2015) and compared to default parameter values for potato (Raes et al., 2018)

*No.	Crop parameter	Sweet potato Rankine et al. (2015)	Potato Raes et al. (2018)
04	Crop type	root/tuber (3)	root/tuber (3)
05	Crop is	transplanted	transplanted
06	Base temperature for no crop development (°C)	15	02
09	Cut-off temperature for no crop development (°C)	35	26
	Soil water depletion factors for:		
11	Canopy expansion (upper threshold)	0.26	0.20
12	Canopy expansion (lower threshold)	0.66	0.60
14	Stomatal control	0.65	0.60
16	Canopy senescence	0.69	0.70
	Shape factor for:		
13	Water stress coefficient for canopy expansion	3.3	3.0
15	Water stress coefficient for stomatal control	3.4	3.0
17	Water stress coefficient for canopy senescence	2.7	3.0
39	Describing root zone expansion	15	15
35	Crop transpiration coefficient (K_{CB})	1.10	1.10
36	Decline in K_{CB} due to ageing (% day ⁻¹)	0.15	0.15
29	Minimum GDs required for full crop transpiration	15.0	7.0
37	Minimum effective rooting depth (m)	0.30	0.30
38	Maximum effective rooting depth (m)	1.60	1.50
	Maximum root water extraction in:		
40	Top quarter of root zone	0.015	0.048
41	Bottom quarter of root zone	0.004	0.012
	Canopy growth coefficient: fraction per		
46	calendar day	0.13420	0.26994
75	growing degree-day	0.00966	0.01615
	Canopy decline coefficient: fraction per		
51	calendar day	0.09529	0.02781
76	growing degree-day	0.00798	0.00200
43	Seedling leaf area (cm ²)	-	15.0
50	Maximum canopy cover (CC_x) Time to reach CC_x (GDD)	0.94	0.92
	Growing degree-days from planting to:		
69	Emergence/recovered transplant	77	200
70	Maximum rooting depth	772	1,079
71	Start of senescence	1,091	894
72	Maturity (length of crop cycle)	1,294	1,276
73	Start of yield formation/initiation	415	550
	Length of the flowering stage:		
74	Growing degree-days	0	0
77	Building up of Harvest Index During yield formation (GDD)	872	700
61	Normalised water productivity WP^* (g m ⁻²)	20.0	18.0
62	WP^* during yield formation (as a percentage of WP^*)	92	100
64	Reference harvest index (percentage)	55	75
	Increase (percentage) of harvest index:		
65	due to water stress before start of yield formation	8	2
68	allowable maximum	9	5

*Denotes line number in AquaCrop parameter file (version 6; March 2017)

red: denotes likely errors in parameter values

Table 16-5 AquaCrop parameters for sweet potato derived by Pushpalatha et al. (2021) and Lamaro et al. (2023)

*No.	Crop parameter	Pushpalatha et al. (2021)	Lamaro et al. (2023)
04	Crop type	root/tuber (3)	
05	Crop is	transplanted	
06	Base temperature for no crop development (°C)	08	08
09	Cut-off temperature for no crop development (°C)	30	38
11	Soil water depletion factors for:		
12	Canopy expansion (upper threshold)	0.25	
14	Canopy expansion (lower threshold)	0.75	
16	Stomatal control	0.75	
16	Canopy senescence	0.75	
13	Shape factor for:		
15	Water stress coefficient for canopy expansion	2.0	2.0
17	Water stress coefficient for stomatal control	2.0	2.0
39	Water stress coefficient for canopy senescence	2.0	2.0
35	Describing root zone expansion	15	
35	Crop transpiration coefficient (K_{CB})	1.15	1.00
36	Decline in K_{CB} due to ageing (% day ⁻¹)	0.025	0.15
29	Minimum GDs required for full crop transpiration	08	08
37	Minimum effective rooting depth (m)	0.25	0.25
38	Maximum effective rooting depth (m)	1.00	1.50
40	Maximum root water extraction in:		
41	Top quarter of root zone	0.024	
41	Bottom quarter of root zone	0.006	
46	Canopy growth coefficient: fraction per calendar day	0.4200	
75	growing degree-day	-	0.2223
51	Canopy decline coefficient: fraction per calendar day	0.1430	
76	growing degree-day	-	0.1410
43	Seedling leaf area (cm ²)	15.0	
50	Maximum canopy cover (CC_x)	0.95	1.00
	Time to reach CC_x (GDD)		
69	Calendar days/Growing degree-days from planting to:	<i>CDs</i>	<i>GDDs</i>
70	Emergence/recovered transplant	6	-
71	Maximum rooting depth	40	658
72	Start of senescence	70	-
73	Maturity (length of crop cycle)	90	1,340
73	Start of yield formation/initiation	30	1,930
74	Length of the flowering stage:	<i>CDs</i>	<i>GDDs</i>
	Calendar days/Growing degree-days	-	-
77	Building up of Harvest Index		
	During yield formation (GDD)	-	997
61	Normalised water productivity WP^* (g m ⁻²)	20.0	20.0
62	WP^* during yield formation (as a percentage of WP^*)	100	
64	Reference harvest index (percentage)	85	90
65	Increase (percentage) of harvest index:		
68	due to water stress before start of yield formation	10	
	allowable maximum	30	5

*Denotes line number in AquaCrop parameter file (version 6; March 2017)

red: denotes likely errors in parameter values

Table 16-6 AquaCrop parameters for taro derived by Mabhaudhi (2012), then modified by Mabhaudhi et al. (2014b) and Mabhaudhi et al. (2016a)

*No.	Crop parameter	Mabhaudhi (2012)	Mabhaudhi et al. (2014b)	Mabhaudhi et al. (2016a)
04	Crop type	root/tuber (3)	root/tuber (3)	root/tuber (3)
05	Crop is	sown	sown	sown
08	Base temperature for no crop development (°C)	10	10	10
09	Cut-off temperature for no crop development (°C)	30	35	35
10	Crop cycle length (GDD)		2,406	2,580
	Soil water depletion factors for:			
11	Canopy expansion (upper threshold)	0.25	0.10	0.10
12	Canopy expansion (lower threshold)	0.55	0.45	0.45
14	Stomatal control	0.50	0.45	0.45
16	Canopy senescence	0.85	0.45	0.45
	Shape factor for:			
13	Water stress coefficient for canopy expansion	3	3	3
15	Water stress coefficient for stomatal control	3	3	3
17	Water stress coefficient for canopy senescence	3	3	3
39	Describing root zone expansion	15	1.5	15
35	Crop transpiration coefficient (K_{CB})	1.05	1.10	1.15
36	Decline in K_{CB} due to ageing (% day ⁻¹)	0.15		0.15
29	Minimum GDs required for full crop transpiration	11.1		-
37	Minimum effective rooting depth (m)	0.30	0.10	0.10
38	Maximum effective rooting depth (m)	1.00	0.80	0.30
	Maximum root water extraction in:			
40	Top quarter of root zone	0.024		0.080
41	Bottom quarter of root zone	0.006		0.020
46	Canopy growth coefficient: fraction per calendar day	0.05554		0.07730
75	growing degree-day		0.69800	0.007330
51	Canopy decline coefficient: fraction per calendar day	0.13671		0.03000
76	growing degree-day		0.57700	0.00300
43	Seedling leaf area (cm ²)	5	25	25
50	Maximum canopy cover (CC_x)	0.85	0.85	0.78
	Time to reach CC_x (GDD)			-
	Growing degree-days from planting to:	<i>CDs</i>	<i>GDDs</i>	<i>GDDs</i>
69	Emergence/recovered transplant	49	460	420
70	Maximum rooting depth	83	1,557	1,400
71	Start of senescence	210	2,115	1,990
72	Maturity (length of crop cycle)	130	2,406	2,580
73	Start of yield formation/initiation	126	1,512	1,370
	Length of the flowering stage:			
74	Growing degree-days	0		0
	Building up of Harvest Index	<i>CDs</i>	<i>GDDs</i>	<i>GGDs</i>
77	During yield formation	4	861	1,100
61	Normalised water productivity WP^* (g m ⁻²)	17.0	15.0	15.0
62	WP^* during yield formation (as a percentage of WP^*)	100		100
64	Reference Harvest Index (percentage)	50	80	83
	Increase (percentage) of harvest index:			
66	due to water stress before start of yield formation	10		10
68	allowable maximum	15		15

*Denotes line number in AquaCrop parameter file (version 6; March 2017)

red: denotes likely errors in parameter values

16.3 MODEL INPUTS AND PARAMETERS: SEASON 2

Table 16-7 Soil parameters for site 1 (taro) and site 2 (OFSP) at Fountainhill

Soil parameters	Units	Site 1	Site 2
Soil texture		Sandy loam Sandy clay loam	Loamy sand
Soil profile depth	m	0.6	0.6
Curve number (based on K_{SAT} of topsoil)		72	61
Saturated hydraulic conductivity (K_{SAT}) range	mm d ⁻¹	6-84	137-764
K_{SAT} (depth weighted)		26.5	551.5
K_{SAT} of topsoil	mm d ⁻¹	84	541
Saturation	% volume	38.3	33.8
Field capacity	% volume	23.5	23.0
Permanent wilting point	% volume	10.3	7.0
Available water capacity	mm m ⁻¹	133	160
Readily evaporable water	mm	7	8

Table 16-8 Conversion of phenological growth stages observed in calendar day (CD) format for OFSP and taro, then converted to growing degree-day (GDD) format

Phenological period	OFSP		Taro	
	CD	GDD	CD	GDD
From transplanting to recovered transplant	16	181	35	345
From transplanting to maximum rooting depth	64	874	150	1,408
From transplanting to start of senescence	114	1,524	157	1,661
From transplanting to physiological maturity	117	1,549	222	1,967
From transplanting to start of yield formation	80	1,096	136	1,617

Table 16-9 List of important crop parameters used to run the AquaCrop model for sweet potato, with partially calibrated values highlighted in bold

No.	Crop parameter	Beletse et al. (2013)	Rankine et al. (2015)	This project
08	Base temperature (°C)	08	15	08
09	Cut-off temperature (°C)	35	35	37
35	Crop transpiration coefficient (K_{CB})	1.5	1.1	1.0
37	Minimum rooting depth Z_{MIN} (m)	0.25	0.30	0.25
38	Maximum rooting depth Z_{MAX} (m)	1.00	1.60	0.60
75	Canopy growth coefficient (CGC in GD)	1.15500	0.00966	
76	Canopy decline coefficient (CDC in GD)	0.14300	0.00798	
50	Maximum canopy cover (CC_x)	1.0	0.94	0.92
69	Time to emergence/recovered transplant (GDD)	-	77	181
70	Time to maximum rooting depth (GDD)	677	772	874
71	Time to start senescence (GDD)	1,274	1,091	1,524
72	Time to maturity (GDD)	1,967	1,294	1,549
77	Building up of HI during yield formation (GDD)	261	872	122
61	Normalised water productivity (g m ⁻²)	20	20	
64	Reference harvest index (%)	90	55	55
65	Increase (%) of HI due to: Water stress before yield formation	0	8	0
68	Allowable maximum increase (%) of specified HI	5	9	

red: denotes likely errors in parameter values

Table 16-10 Orange flesh sweet potato crop parameters derived by Masango (2015) for SWB, together with partially calibrated values used in this project

Crop parameter	Masango (2015)	This project
Canopy radiation extinction coefficient (0-1)	0.85	
Corrected dry matter-water ratio (Pa)	6.5	
Radiation conversion efficiency (kg MJ ⁻¹)	0.00121	
Base temperature (°C)	8	
Temperature for optimum growth (°C)	28	
Cut-off temperature (°C)	38	37
Degree-days to emergence (GDD)	25	181
Degree-days to flowering day degrees (GDD)	650	650
Degree-days to maturity (GDD)	1,950	1,549
Day degrees for transition period (GDD)	480	480
Degree-days to leaf senescence (GDD)	1,650	1,524
Maximum crop height (m)	0.6	0.69
Maximum root depth (m)	1.5	0.6
Fraction of total dry matter translocated to roots (0-1)	0.45	
Canopy interception storage (mm)	1	
Leaf water potential at the maximum transpiration (kPa)	-1,500	
Maximum transpiration (mm d ⁻¹)	8	7.1
Specific leaf area (m ² kg ⁻¹)	9.8	
Leaf-stem partition parameter (m ² kg ⁻¹)	1	
Total dry matter at emergence (m ² kg ⁻¹)	0.03	
Root fraction (0-1)	0.15	
Root growth rate (m ² kg ^{0.5})	3.5	
Stress index (0-1)	0.9	
Depletion allowed (%)	40	

16.4 MODEL INPUTS AND PARAMETERS: SEASON 3**Table 16-11 Soil parameters for the raised beds in the greenhouse at UKZN**

Soil parameters	Units	Stressed	Unstressed
Soil texture		Clay	Clay Loam
Soil profile depth	m	0.40	0.40
Curve number (based on K _{SAT} of profile)		72	72
Saturated hydraulic conductivity (K _{SAT})	mm d ⁻¹	65.0	76.7
K _{SAT} of topsoil	mm d ⁻¹	-	-
Saturation	% volume	43.5	43.5
Field capacity	% volume	36.5	37.5
Permanent wilting point	% volume	29.0	29.5
Available water capacity	mm m ⁻¹	75	80
Readily evaporable water	mm	9	9

Table 16-12 Base (T_{BSE}) and cut-off (T_{UPP}) temperatures when crop development ceases

Crop	T_{BSE} (°C)	T_{UPP} (°C)	Source
Sweet potato	08	35	Beletse et al. (2013)
	15	35	Rankine et al. (2015)
	10	35	Nyathi et al. (2016)
	08	30	Pushpalatha et al. (2021)
	08	38	Lamaro et al. (2023)
Taro	10	35	Mabhaudhi et al. (2014b)

Table 16-13 Updated standard crop parameters provided by Pereira et al. (2021b)

Parameter	Sweet potato	Taro
Maximum root depth (m)	1.00-1.20	0.30-0.40
Maximum crop height (m)	0.50	1.20
Maximum ground cover (%)	98	
K_c (mid-season)	1.10	1.10
K_c (end-season)	0.60	1.05
K_{CB} (mid-season)	1.05	1.05
K_{CB} (end-season)	0.50	1.00

Table 16-14 Phenological growth stages observed in calendar day (CD) format for OFSP and taro, which were then converted to growing degree-day (GDD) format

Phenological period	OFSP		Taro	
	CD	GDD	CD	GDD
From transplanting to recovered transplant	6	81	14	198
From transplanting to maximum rooting depth	93	1,435	35	492
From transplanting to start of senescence	150	2,377	170	2,677
From transplanting to physiological maturity	160	2,533	180	2,824
From transplanting to start of yield formation	68	1,001	130	2,038
Canopy growth coefficient (CGC)	0.11139	0.007509	0.24736	0.017242
Canopy decline coefficient (CDC)	0.03000	0.001923	0.03000	0.002041

Table 16-15 Comparison of sweet potato parameters derived by Rankine et al. (2015) with those obtained in this project

*No.	Parameter	Rankine et al. (2015)	This project	Source
08	Base temperature (°C)	15	10	
11	Soil water depletion fraction for: - canopy expansion	0.26	0.25	Calibrated
14	- stomatal control	0.65	0.30	
16	- canopy senescence	0.69	0.80	
13	Shape factor for: - canopy expansion	3.3	6.0	Calibrated
15	- stomatal control	3.4	6.0	
17	- canopy senescence	2.7	3.0	
35	Basal crop coefficient	1.10	1.05	Pereira et al. (2021b)
38	Maximum rooting depth (m)	1.60	1.20	Pereira et al. (2021b)
43	Soil surface area covered by seedling at 90% emergence	15	50	Calibrated
45	Number of plants per hectare	90,000	55,556	Measured
50	Maximum canopy cover (CC _x)	0.94	0.91	Measured
46	Canopy growth coefficient (CGC in % day ⁻¹)	13.420	11.139	Calibrated
51	Canopy decline coefficient (CDC in % day ⁻¹)	9.529	3.000	Calibrated
52	Phenological period (days): from transplanting to - recovered transplant	6	6	Observation & calibrated
53	- maximum rooting depth	56	93	
54	- start of senescence	80	150	
55	- maturity (length of crop cycle)	96	160	
56	- start of yield formation	31	68	
60	- length of HI buildup period	65	92	
61	Normalised water productivity (WP* in g m ⁻²)	20.0	20.0	Unchanged
64	Reference harvest index (HI ₀)	55	78	Measured

*Denotes line number in AquaCrop parameter file (version 6; March 2017)

Table 16-16 Comparison of taro parameters derived by Mabhaudhi et al. (2016a) with those obtained in this project

*No.	Parameter	Mabhaudhi et al. (2016a)	This project	Source
11	Soil water depletion fraction for: - canopy expansion	0.10	0.25	Calibrated
14	- stomatal control	0.45	0.45	
16	- canopy senescence	0.45	0.80	
13	Shape factor for: - canopy expansion	3.0	0.0	Calibrated
15	- stomatal control	3.0	3.0	
17	- canopy senescence	3.0	3.0	
35	Basal crop coefficient	1.15	1.05	Pereira et al. (2021b)
37	Minimum rooting depth (m)	0.10	0.30	Pereira et al. (2021b)
38	Maximum rooting depth (m)	0.30	0.40	
43	Soil surface area covered by seedling at 90% emergence	25	5	Calibrated
45	Number of plants per hectare	20,000	55,556	Measured
50	Maximum canopy cover (CC _x)	0.78	0.69	Measured
46	Canopy growth coefficient (CGC in % day ⁻¹)	7.730	24.736	Calibrated
51	Canopy decline coefficient (CDC in % day ⁻¹)	3.000	3.000	Calibrated
52	Phenological period (days): from sowing to - recovered transplant	42	14	Observation
53	- maximum rooting depth	140	35	
54	- start of senescence	199	170	
55	- maturity (length of crop cycle)	258	180	
56	- start of yield formation	137	130	
60	- length of HI buildup period	110	50	
61	Normalised water productivity (WP* in g m ⁻²)	15.0	15.0	Unchanged
64	Reference harvest index (HI ₀)	83	81	Measured
65	Possible increase in HI due to water stress before start of yield formation (%)	10	0	Observation
66	Coefficient describing positive impact on HI due to restricted vegetative growth during yield formation	10	0	Observation
67	Coefficient describing negative impact on HI of stomatal closure during yield formation	8	10	Observation

*Denotes line number in AquaCrop parameter file (version 6; March 2017)

17 APPENDIX H

17.1 MINIMISING COMPUTATIONAL EXPENSE IN 2015

17.1.1 Background

According to Jones (2018), model performance can be dramatically improved on most computers by:

- running the model on a desktop PC as opposed to a laptop computer,
- dividing the simulation run into smaller tasks, so that each smaller task is handled by a single core of the computer's CPU,
- instructing the model to read inputs from and write outputs to a small virtual disk drive defined in the computer's random access memory (called a RAM drive),
- post-processing model output whilst it is temporarily stored on the RAM drive, and
- executing large runs in "batch" mode using scripts designed for Windows- or Linux-based PCs.

Kunz et al. (2015b) used some of the suggestions listed above to improve the performance of complex model simulations. Since then, further improvements were made by Kunz et al. (2020) and (Kunz and Mabhaudhi (2023)). A summary of the improvements is provided next.

17.1.2 Desktop PC vs laptop

It is well understood that laptops are typically slower than desktop PCs. This is mainly due to cooling issues that result from the need for laptops to be portable (i.e. as thin and light as possible). Hence, a laptop CPU typically has a reduced number of CPU cores compared to a desktop PC. For this reason, model runs should be done on desktop PCs, not laptops. For this project, a high-end computer was used, which comprised of 32 GB of RAM and a Core i9 CPU with 10 cores (20 threads) that handles AVX-512 instruction sets. This CPU can process twice the number of data elements than an Intel AVX2 CPU and four times that of an SSE-based CPU.

17.1.3 RAM drive size

A freely available software tool was used to create a RAM drive that assigns a drive letter (e.g. R:\) to a certain portion of RAM that is allocated for exclusive use by the model runs. Using RAM as temporary "disk" storage is much faster than a hard drive, especially one using spinning disks/platters. The size of the required RAM drive was calculated as follows: For each HRZ, AquaCrop requires input files containing climate data, soil data and a project file that instructs the model when to start and end each seasonal simulation. AquaCrop outputs a file of seasonal data, from which statistics are generated. Hence, a national run involving all 5,838 HRZs requires a RAM drive of 8 GB for a 50-year simulation (**Table 17-1**). All input files were copied to the RAM drive to speed up the model runs and all output files were temporarily stored on the RAM drive.

Table 17-1 File size of input and output files required to run AquaCrop with 50 years of historical climate data

Input/Output	File type	File size (KB)
Input	Climate	968
	Soils	1
	Project	57
Output	Seasonal output	236
	Statistics	132
Sub-total (KB)		1,394
Total (GB)		7.76

17.1.4 Automation procedure

In 2015, the computational automation of sequential AquaCrop runs across all 5,838 HRZs was developed in a Unix for WINDows emulator (called UWIN developed by AT&T) that run on Microsoft's Windows 7 operating system. It was written in Unix so that one day the code could be ported to a PC cluster running a Linux operating system.

The automaton was designed to run AquaCrop sequentially for all HRZs using a multiple profile (.prm) file, which instructed the model to simulate consecutive seasons, each with a common start date (i.e. 1st of November), but varying end dates, where the physiological maturity date was calculated using thermal time. A utility called "genprm.exe" was developed in the Fortran programming language to automate this process.

When AquaCrop was run at the national scale for all HRZs, the model sometime "crashed" (with a "division-by-zero" error) when simulating zones not suited to crop growth (i.e. too cold and/or too dry). The model required the user to click the "OK" to acknowledge this error, which unfortunately halted the model runs. This presented a significant challenge, which unless solved, prevented the automation of the model runs. Significant effort was spent on creating a solution where a specialised software utility was run in the background that constantly monitored for any errors to be generated by the model. When this was detected, the utility automatically acknowledged the error message, which caused AquaCrop to stop running, i.e. "crash". The automation process was then designed to re-start the model run for the next HRZ. For more information, the reader is referred to Kunz et al. (2015b).

The above-mentioned issue mainly occurred because AquaCrop was run for all 5,838 HRZs, regardless of whether or not the zone is suitable for rainfed crop production. This was done so that model output can be used to identify areas best suited to crop cultivation (cf. **Chapter 8**).

17.1.5 Model run time

Kunz et al. (2015a) reported that sequential runs of AquaCrop at the national scale took 62 and 90 hours to complete for grain sorghum and soybean, respectively. Run time was not only dependent on crop cycle, but also planting date. For example, sugarcane planted on 1st April and 1st February took 250 and 388 hours to complete, respectively. Such long runs are impossible without a UPS (uninterruptable power supply) and a diesel generator to cope with power failures, especially those related to regular load shedding events.

17.2 FURTHER IMPROVEMENTS MADE IN 2019

17.2.1 Desktop PC

Initial tests were conducted on a slower desktop PC (Core i7 CPU with 12 threads and 32 GB of RAM). This was the same PC used since 2015, which ensured more accurate benchmarking. However, tests were also conducted on a faster desktop PC (Core i9 CPU with 20 threads and 64 GB of RAM). Model runs were done with the same taro crop parameter file used by Kunz and Mabhaudhi (2023).

17.2.2 Derivation of smaller tasks

For parallel processing, I/O performance remains the main bottleneck compared to CPU speed. Temporary memory (RAM) usage for data storage (both reading and writing data) provides the smallest bottleneck when compared to solid state drives and especially spinning hard drives. In other words, a typical spinning hard drive cannot cope with the I/O required for parallel processing.

For the slower PC with 12 threads, two threads were utilised by the Windows operating system, to prevent the PC from becoming too unresponsive to input (via the keyboard and mouse). The remaining 10 threads were used to run 10 simultaneous AquaCrop runs (i.e. one model run per thread). Hence, instead of running one task involving 5,838 sequential model runs, 10 smaller tasks of 584 runs were started in parallel. This significantly reduced the overall model run time. However, performance is compromised by the need to write 10 output files simultaneously. Hence, this “bottleneck” strongly depends on the read/write speed of the RAM drive. Since the faster PC has 20 CPU threads, four were set aside for use by the operating system. The remaining 16 threads ran AquaCrop as 16 simultaneous simulations, where each task handled ~365 HRZs (i.e. 5,838/16).

17.2.3 Load balancing

An initial attempt was made to load balance the parallel runs by grouping HRZs in such a manner so that each task completed at the same time. However, this task proved difficult to perfect so no progress was made.

17.2.4 Maximum crop cycle

AquaCrop runs the slowest for long growing seasons that occur in cold regions where there is insufficient heat units (growing-degree days) for the crop to reach physiological maturity. The model typically simulates zero or very low seasonal yields and thus, the average yield is often 0 dry t ha⁻¹. Kunz and Mabhaudhi (2023) recommended that the model should not be run if the crop cycle exceeds 396 days. For HRZs with a crop cycle exceeding 396 days, the decision was made not to run the model and to flag the zone as unsuitable (i.e. too cold for production). This reduced the model run time to zero for such zones, resulting in reduced run times. The decision to not run the model for cold seasons has affected the calculation of average yields by eliminating zero (or close to zero) yields that skew the average towards zero and the calculation of high Y_{CV} values.

17.2.5 Automation procedure

AT&T stopped maintaining their UWIN emulator, and thus it was not compatible with Windows 10. However, Microsoft also developed a Unix emulator called Windows Subsystem for Linux (WSL). Version 1 (WSL 1) was first released in 2016, which underwent a significant change in 2019 when version 2 (WSL 2) became available. Since version 2 was relatively new in 2019, the decision was made to port the Unix (and Fortran) automation code to work on WSL 1. Much effort was spent on checking that the automation procedure worked correctly on WSL 1.

In 2019, the automation code was extensively modified to run AquaCrop concurrently (i.e. parallel processing) in WSL 1. Approximately 8,600 lines of code (in Unix and Fortran) was developed to automate the national model runs for AquaCrop. In addition, over 1,400 lines of code were written to convert the climate and soil input files into the format required by the model.

17.2.6 Model run time

The ability to run AquaCrop in parallel mode significantly reduced the time to complete national model runs. Kunz et al. (2020) reported that running AquaCrop simultaneously on a RAM drive reduced the national run time for grain sorghum to approximately 25 hours for on the slower PC, which was further reduced to 13 hours when run on the faster PC. This represented a significant reduction in computational expense compared to a sequential run that took 62 hours (cf. **Section 17.1.5**).

17.3 ADDITIONAL IMPROVEMENTS IN 2023

As part of another WRC-funded project, further improvements were made by Kunz and Mabhaudhi (2023). Inspired by the recognition for this effort, which is regarded as innovative, additional improvements were made in this project. Reducing model run time is deemed important, as it saves valuable time that allows for additional modelling scenarios to be considered. Hence, efforts are continuing to further minimise AquaCrop's run time as part of a four-year WRC-funded project that started in April 2023. These improvements are described next in more detail.

17.3.1 Climate file length

Analysis of the model runs undertaken by Kunz and Mabhaudhi (2023) revealed that AquaCrop ran considerably slower using 139 years of projected climate data from 1961 to 2099. Further investigation revealed that model run time increased with each consecutive season, and thus ran fastest for the first season (1961/62) and slowest for the last season (2098/99). The reason was due to the model reading the climate file from the beginning (i.e. 1 January 1961) for each consecutive season, until the required planting date was found (i.e. sequential access). This was proven when climate data from 1 January 2098 to 31 December 2099 was manually extracted from the climate file for the model to use, which resulted in a similar run time as the first season.

Prior to version 7 of AquaCrop, the model developers (FAO) had not made the source code publicly available. Hence, the inefficient (i.e. sequential) reading of climate data could not be fixed in the model, which is the ideal scenario. A workaround involved the development of a utility called "getcli.exe" in the Fortran programming language to automate the extraction of climate data for each season from the 139-year climate file. Considerable effort was spent on checking this utility as it needs to "trim" the rainfall (.PLU), temperature (.TNX) and reference evapotranspiration (.ETO) files correctly.

To make this utility run as fast as possible, the original climate files were reduced to a width of 12 characters. However, the time required to trim 17,514 (i.e. $5,838 \times 3$) climate files was considerable, taking approximately 19 minutes for historical climate files with 50 years of data, and 49 minutes for projected climate files with 140 years of data. The trimmed climate files were then compressed into one .RAR file, making it easier and quicker (< 1 minute) to copy to the RAM drive and to uncompress all the climate files.

Since each line of the climate file was now the same length (12 characters), climate data was extracted using a method called direct access, which is substantially faster than sequential access. Hence, the time required to extract the first or last season of data from the climate file was identical. This provided a considerable performance boost to the automation process, and thus was well worth the effort to implement.

17.3.2 Seasonal simulations

The automation procedure was then modified to run the model separately for each season, instead of grouping all seasons into one multiple AquaCrop project (.PRM) file. This was necessary to incorporate the “getcli.exe” utility, which was run before AquaCrop to extract the required rainfall, temperature and ET_O data from the climate files for a particular season. As explained previously, this was necessary so that the model run time was the same for the first and last season.

Tests were then carried out to determine the overall impact of this significant modification to the automation procedure. Although running the model one season at a time (in a loop) slowed down the automation, it was offset by the faster model run time. More importantly, comparison of yield simulations with older runs (i.e. before the change was implemented) highlighted some differences. As noted in **Section 17.1.4**, since AquaCrop was run for all HRZs, many of which are too cold and/or too dry for rainfed crop production, the model sometimes “crashes” with a “division-by-zero” error. Further investigation revealed that when this error occurred in a particular season, all subsequent seasons were not simulated. In other words, when AquaCrop was run in the past for multiple sequential seasons via a .PRM file, if an error occurred during the simulation of, for example, the first few seasons, the remaining seasons were not simulated. This would result in no seasonal yield average being calculated, since four or more yield values were required for the average to be calculated. Hence, the HRZ was flagged as totally unsuitable for crop production. However, since the model was now run separately for each season, if an error occurred in a particular season, the yield was set to zero, and the model was automatically run for the next season, until all seasons had been simulated (i.e. using a seasonal loop). This had a significant impact on the total number of zero yields, and the total number of seasons simulated, from which the risk of crop failure was calculated as the ratio, then expressed as a percentage. Results showed a reduction in this metric for certain HRZs where the model “crashed” early on a particular season. Overall, running the model separately for each season has resulted in more accurate simulations for multiple sequential seasonal runs.

17.3.3 RAM drive size

The “trimming” of the climate files to 12 characters (cf. **Section 17.2.2**) resulted in a reduction in amount of RAM required to temporarily store each climate file from 968 to 756 KB. Statistics were generated from each AquaCrop seasonal output file, which was then further processed to create “GIS-ready” files to simplify the mapping of certain variables, such as yield, crop water productivity and crop cycle. RAM drive space was also required to store the compressed versions of all output files, which made it faster to move them from the RAM drive to permanent disk storage. Hence, a national run involving all 5,838 HRZs, each with 50 years of climate data, required a total of 7 GB (**Table 17-2**).

Table 17-2 Size of input and output files when running AquaCrop with 50 years of climate data

Input/ Output	File type	File size (KB)
Input	Climate	756
	Soils	1
	Project	24
Output	Seasonal output	228
	Additional output	12
	Statistics	132
Sub-total per HRZ (KB)		1,153
Total for 5,838 HRZs (KB)		6,721,214
Processed statistics (KB)		23,504
Compressed files (KB)		122,544
Grand total (GB)		6.56

17.3.4 RAM drive type

The specialised software used to create a RAM drive was updated to the latest version, which provided a new feature of emulating a “logical” and not a “physical” drive. Speed tests showed that logical emulation was faster than physical emulation as shown in **Table 17-3**. Hence, this software upgrade helped to speed up the model runs.

Table 17-3 Increase in RAM drive read and write performance using logical (new) vs physical (old) disk emulation

Speed (MB s ⁻¹)	Older PC (12 threads)			Newer PC (20 threads)		
	Physical	Logical	Increase (%)	Physical	Logical	Increase (%)
Sequential read	3,881	4,488	15.6	5,370	5,389	0.4
Sequential write	2,530	4,121	62.9	5,750	6,969	21.2
Random read	202	569	181.7	446	882	97.8
Random write	129	310	140.3	378	732	93.7

17.3.5 Maximum crop cycle

As noted in **Section 17.2.4**, the crop cycle was limited to 396 days to reduce model run times in higher altitude HRZs, where insufficient growing degree-days exist for the crop to reach physiological maturity within an economically viable time frame. This prevented the model from simulating unrealistically long crop cycles. This problem was first noticed when AquaCrop was first run for sugarcane, a crop that requires 3,150 GDDs to reach physiological maturity. In cold HRZs, the model ran for more than 720 days (2 years) in 1,071 HRZs, with the worst case scenario being 8,195 days, i.e. 22.4 years. Hence, the maximum crop cycle for sugarcane was limited to 720 days, which improved model performance.

Owing to the cold climate, the AquaCrop model would often crash with a “division-by-zero” error or simulate zero (or close to zero) yields. The automaton code was therefore changed to prevent the model from running if the crop cycle exceeded 396 days. However, this decision impacted the calculation of the average seasonal yield. Prior to this change, AquaCrop simulated zero yield for 47 seasons in HRZ no. 13 (for example) and yields of 0.097 and 2.274 dry t ha⁻¹ for two seasons. From this, an average yield of 0.048 dry t ha⁻¹ was calculated across all 49 seasons. After the change, AquaCrop only ran for one season, since the crop cycle was less than 396 days and simulated a yield of zero dry t ha⁻¹, from which no average was calculated (< 4 data points). This zone was then flagged as totally unsuitable for taro production, instead of having a low average yield of 0.048 dry t ha⁻¹.

The automation code was modified to determine the range in taro’s maximum crop cycle for each HRZ. An analysis of the results showed that this threshold could be reduced to 334 days. However, it is also important to understand the impact this change has on average yields calculated for each HRZ. A national run was undertaken for taro, where the maximum allowable crop cycle was reduced from 396 to 365 days. This increased the total number of seasons deemed too cold for taro production from 154,426 to 155,680, i.e. by 1,254 seasons. Since the model is no longer run for these seasons, it provided a small improvement in reducing overall model run time. However, this decision had a larger impact on average yield estimates.

A comparison of the 396 vs 365 day national runs showed no change in average yields for 5,520 HRZs, i.e. zero difference. For 50 HRZs, the difference in average yields was 0.15 t ha⁻¹. However, the largest difference of 1.12 dry t ha⁻¹ occurred in HRZ no. 3,375 (**Figure 17-1**). In nine HRZs, the crop cycle exceeded 365 days across all seasons, and thus the model was not run for any season. These zones were then flagged as unsuitable for taro production.

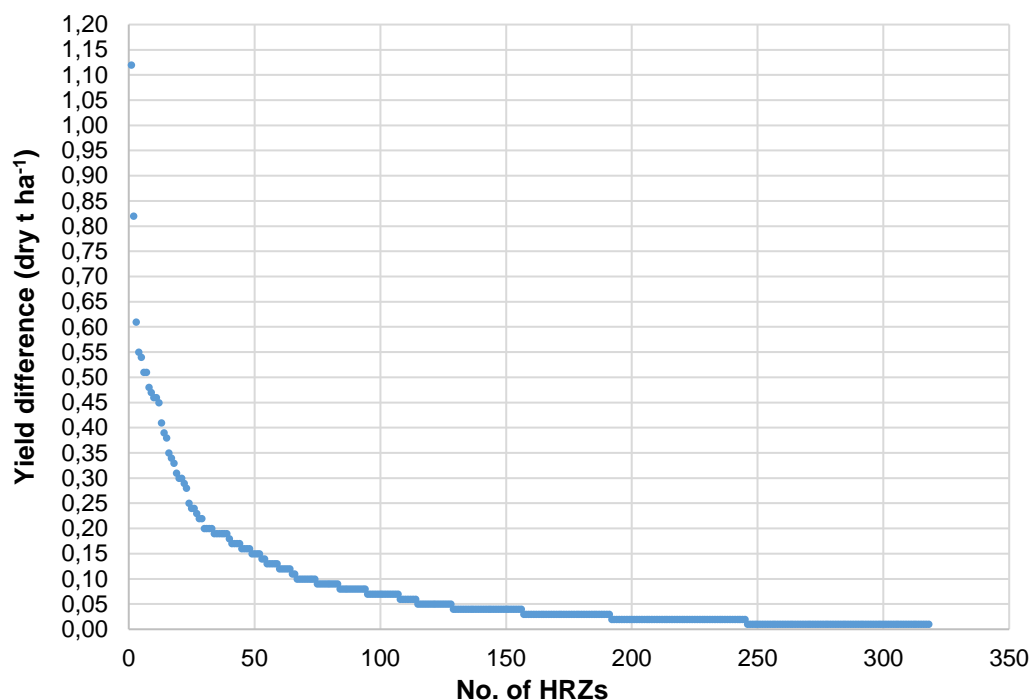


Figure 17-1 Difference in average taro yield simulated by AquaCrop when the maximum allowable crop cycle was reduced from 396 to 365 days

17.3.6 Sequential vs parallel runs

A sequential run was undertaken for all 5,838 HRZs for taro with 50 years of climate data input, which took 26.2 hours to complete. The model ran for 7.8 hours, whereas the pre- and post-processing of data took 18.4 hours (**Table 17-4**). Hence, more time was spent of data processing than model simulations. AquaCrop run times ranged from 14 to 22 seconds per zone.

The model run time was divided by 12 (number of CPU threads) and was used to group HRZs together so that each grouping would complete in a similar time. The number of zones varied from 259 to 876, with an average of 487. The model run time increased to 17.3 hours, with each zone taking 28-59 seconds to complete. However, since the 12 tasks were started simultaneously, the overall run time was determined by the task that took the longest to complete, i.e. 6.8 hours. Hence, running 12 parallel tasks reduced the overall run time from 26.2 to 6.8 hours, even though AquaCrop ran slower due to the parallel execution (**Table 17-4**).

Table 17-4 Sequential vs parallel run time tests with 50 years of input climate data

Run type	Model run time (h)	Pre- and post-processing (h)	Total (h)	Overall (h)
Sequential	7.8	18.4	26.2	26.2
Parallel	17.3	48.4	65.6	6.8

17.3.7 Derivation of smaller tasks

As noted previously, AquaCrop ran slower in parallel mode than in sequential mode. Further tests were conducted to better understand the impact of simultaneous model runs on overall completion time. Only 14 HRZs were used for testing, each with only 10 years of input data (1950-1960). **Figure 17-2** shows that the total run time doubled from 20 to 40 seconds when 9 simultaneous model runs were executed. Similar run times were noted when 4 or less threads were used (i.e. one model run per thread). When all 12 threads were utilised, the run time increased to 48 seconds. Hence, **Figure 17-2** explained why

the model run times ranged from 14-22 seconds for the sequential run and from 28-59 seconds for the parallel run of 12 tasks.

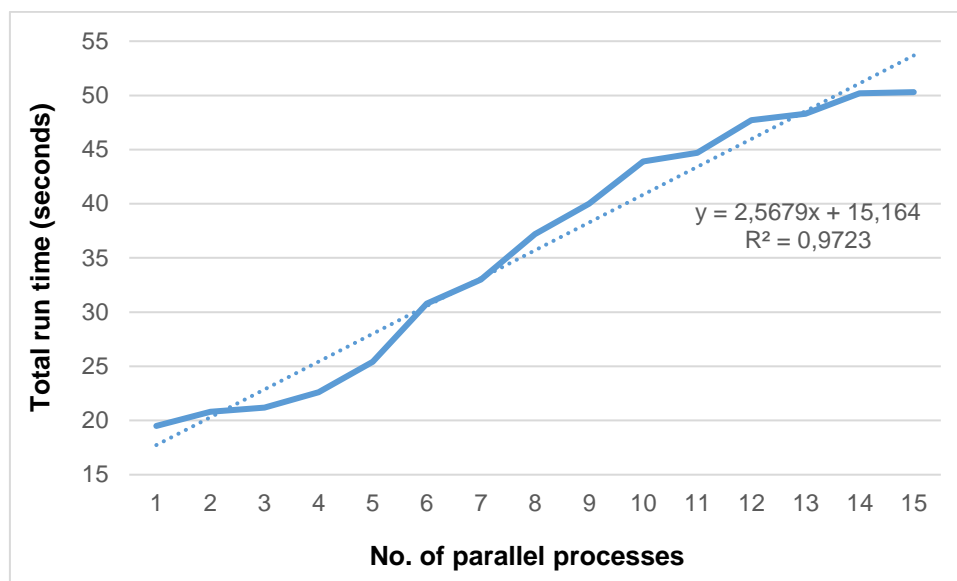


Figure 17-2 Increase in AquaCrop run time to complete simulations for 14 HRZs, each with 10 years of input climate data, using the slower PC with 12 threads

The above graph shows there was no benefit in running more than one task per thread, i.e. more than 12 parallel model runs. However, as the number of parallel tasks increased, the PC became progressively more unresponsive. Further tests were done to determine the maximum number of simultaneous runs that could be performed, before the PC became too unresponsive. Based on the results, the decision was made to reduce the number of threads used for simultaneous model runs from 12 to 10. Hence, two threads were used by the PC's operating system to improve response to keyboard and mouse input.

17.3.8 Load balancing: slower PC

Although the parallel tasks were expected to finish with similar times, this was not the case, since the fastest task finished in 4.3 hours. The range in completion times of 2.5 hours (6.8-4.3 hours) was much larger than expected. A deeper analysis highlighted a problem for HRZs where temperatures were too cold for taro production and the crop cycle exceeded 396 days. Since AquaCrop was no longer run for these cold regions (cf. **Section 17.3.5**), the model run time for all 49 seasons was zero. Since these altitude zones were often located next to each other in mountainous regions, they resulted in a large grouping of 876 zones, which took the longest time to complete (6.8 hours).

Since the groupings of HRZs were based on model run time only, it excluded the pre- and post-processing times. For example, pre-processing time was spent on (i) extracting 365 days of climate data for each season, and (ii) determining the crop physiological maturity date (i.e. end season date). Post-processing involved generating statistics of each AquaCrop output variable and extraction of specific values from the statistics files, e.g. mean, median and coefficient of variation. However, as shown in **Table 17-4**, far more time is spent on data processing compared to the model run time. Therefore, the automation code was modified to record the total run time for each HRZ, which included not only the model run time, but the time required for all data processing. Hence, the total run time provided a more accurate method to load balance the runs, with the intention to further reduce computational expense.

An initial run was undertaken to provide the total run time per HRZ, which was then used to determine 10 groupings of HRZs, i.e. each group was handled by a separate CPU thread. The run times were used for the second national model run and produced excellent results, considering the last task completed in 6.99 hours, only 25 minutes after the first task (**Table 17-5**).

It became apparent that small gains were achieved via this iterative process, where the total run times per HRZ from the 2nd run were used to update the groupings. For the 3rd national run test, the groupings changed slightly and ranged from 403 to 761 zones, resulting in a 23 minute difference between the first and last tasks. The total run time per HRZ from the 3rd national run was analysed to provide new groupings that ranged from 411 to 762 zones. From **Table 17-5**, the number of zones in the smallest grouping had increased to 411 zones, whereas the largest grouping decreased and stabilised at ~760 HRZs. Using these groupings, the 4th national model run produced a 15-minute difference between the fastest and slowest, but the overall time was not improved. Hence, there was no need to continue this iterative process to further refine the HRZ groupings.

Table 17-5 HRZ groupings to reduce the time difference between the fastest and slowest tasks (10 in total) running simultaneously on the slower PC with 30 years of input climate data

Task no.	No. of HRZs in each task		
	2 nd	3 rd	4 th
1	397	403	411
2	481	476	478
3	534	527	524
4	543	548	548
5	558	565	568
6	602	607	601
7	621	627	626
8	630	629	627
9	694	695	693
10	778	761	762
Time diff. (min)	25	23	15
Total run time (hrs)	6.99	6.79	6.95

17.3.9 WSL 1 vs WSL 2

As noted in **Section 17.2.4**, the automation procedure is mostly written in Unix, which ran on WSL version 1. Microsoft re-designed WSL version 2 to run on a “lightweight” virtual machine that provided both advantages and disadvantages when compared to WSL 1. The decision was made to test the performance of WSL 2 vs WSL 1. This required the Windows operating system on both PCs to be upgraded (i.e. from a 2019 to a 2021 build), which was a time-consuming process.

Much effort was then spent on testing the automation code on WSL 2, which required certain modifications due to differences in the behaviour of certain commands in WSL 2 vs WSL 1. For example, “wslpath” is an important utility that converts Windows path to Linux paths and vice versa. For WSL 2, this utility does not convert the path if the file name does not exist, whereas the WSL 1 version does. Hence, code changes were required to remove the filename from the path before “wslpath” is run.

17.3.9.1 RAM utilisation

Microsoft reported that WSL 2 used far less RAM than WSL 1. Tests showed that a national run with AquaCrop consumed ~5.2 GB of memory using WSL 1, compared to only 258 MB for WSL 2. The virtual machine was therefore limited to using only 1 GB of RAM. This difference in RAM usage was

substantial and highlighted the memory efficiency of WSL 2, thus allowing more RAM to be allocated to the RAM drive. This was particularly important for the slower PC with 12 threads, which only had 32 GB of RAM. Hence, the upgrade to WSL 2 would be beneficial due to the improved memory usage.

17.3.9.2 Parallel processing

Although WSL 2 requires at least one CPU thread and a portion of RAM to be dedicated to the virtual machine, it can utilise more than 64 threads. Further testing showed that there were no performance gains whether one or all threads were allocated to the WSL virtual machine. Hence, no changes were made to the configuration of using only one CPU thread and only 1 GB of RAM. Since one thread was required by the WSL virtual machine and another for the Windows operating system, 10 threads were still used for running AquaCrop in parallel sessions. However, On the faster PC with 20 threads, utilising an equivalent 18 threads resulted in a very unresponsive PC. The number of parallel model runs needed to be reduced from 18 to 12 for the PC to become adequately responsive to keyboard and mouse input.

17.3.9.3 Performance tests

According to Microsoft’s website, I/O performance in WSL 2 is faster in comparison to WSL 1. However, this does not apply when accessing data “outside” of the virtual machine, e.g. data stored in a RAM drive. In WSL, the version can easily be set to either 1 or 2, thus facilitating simple switching between the two versions for testing purposes.

Using the final load balancing obtained from the iterative runs (cf. **Table 17-5** in **Section 17.3.8**), WSL was set to version 2 and AquaCrop was again run for taro using historical climate input on the slower PC with 12 threads (of which only 10 were utilised for model runs). From **Table 17-6**, the results showed that the national run was 2.2 hours faster for WSL compared to WSL 1. Furthermore, the fastest (275 minutes) and slowest (281 minutes) tasks finished only 6 minutes apart. This outcome was not expected, since the full I/O performance benefit provided by WSL 2 cannot be realised as the model runs are not performed within the virtual machine. A similar test was conducted on the faster PC, where WSL 1 running 12 parallel tasks took 13 minutes longer than WSL 2. Hence, the effort required to upgrade the operating system, which facilitated the upgrade to WSL version 2, proved to be beneficial.

Table 17-6 Performance of version 2 of WSL compared to version 1 for taro using historical climate data input

Parallel tasks	WSL 1		WSL 2	
	Grouping	Time (min)	Grouping	Time (min)
1	411	397	626	275
2	478	399	627	275
3	548	401	693	277
4	627	403	762	278
5	568	404	548	279
6	601	405	601	280
7	524	405	568	280
8	626	406	411	280
9	693	408	478	280
10	762	412	524	281
Time diff. (min)		15		6
Total run time (hrs)		6.95		4.77

17.3.10 Load balancing: faster PC

The above iterative tests were repeated on the faster PC with 20 threads, of which only 12 were used, as explained in **Section 17.3.9.2**. Instead of using 50 years of climate data input (1950-1999), tests were conducted using 30 years of projected climate data. The national runs undertaken by Kunz and Mabhaudhi (2023) showed that the slowest overall run time for taro was achieved for one particular GCM (Norwegian Earth System Model) and time period (2070-2099). It is important to remember that an initial run was required to obtain the total run times per zone, which were then analysed to develop the HRZ groupings used for the 2nd national run. The latter run times were then used to refine the groupings for the 3rd national run, and so on. The overall results shown in **Table 17-7** again highlight the success of the load balancing exercise, where the fastest national run time was achieved in the 3rd national run (i.e. similar to **Table 17-5**).

Table 17-7 HRZ groupings to reduce the time difference between the fastest and slowest tasks (12 in total) running simulatenously on the faster PC with 30 years of input climate data

Zonal grouping	Time (min) to run each zonal grouping		
	2 nd	3 rd	4 th
1	449	451	452
2	457	460	463
3	462	466	469
4	466	468	471
5	466	472	476
6	476	472	503
7	476	475	469
8	489	479	507
9	495	502	476
10	514	506	522
11	516	525	474
12	572	562	556
Time diff. (min)	7	3	2
Total run time (hrs)	3.04	2.72	2.89

For the above two tables, a comparison of the 3rd and 4th iterative runs showed that as the time difference between the fastest and slowest task was reduced, the total run time increased. This occurs because almost all of the tasks are running concurrently, which means they all run slower (cf. **Figure 17-2** in **Section 17.2.2**). Hence, there is no benefit in perfecting the load balancing to reduce the time difference to almost zero.

The model was also re-run for another crop and from an analysis of the total run times, it became apparent that load balancing would need to be performed for each crop. Since this represents a time-consuming process involving three iterative runs, the decision was made to stop all load balancing work and continue with what had been achieved for taro. In other words, the HRZ grouping obtained from the 3rd national runs for taro was used for all other crops.

17.3.11 Automation procedure

A national run on the faster PC was now reduced to under three hours, allowed more modelling scenarios to be considered. For example, Kunz and Mabhaudhi (2023) completed national runs for four crops using climate projections from 6 GCMs for three 30-year time periods (1961-1990; 2015-2044; 2070-2099). These 72 (4 x 6 x 3) national runs took 157.1 hours of computational time to complete,

thus averaging 2.2 hours each run. Since it took 49 minutes to trim the climate files with 140 years of daily data for one GCM to 12 characters, the model runs were done for each GCM at a time, but for all three time periods. Hence, each GCM run took ~6.6 (3 x 2.2) hours on average, after which the next GCM run was manually started. This resulted in time being “wasted” in-between GCM runs, especially when model runs finished in the early hours of the morning. Hence, the total time taken to complete the simulations was 190.4 hours.

The automation code has since been modified (and thoroughly tested) to automatically run all the crops in succession. Hence, one a single GCM climate dataset has been trimmed and copied to the RAM drive, the model runs are then completed for all crops and all time periods, thus (i) reducing the “idle” time between each national run to zero, and (ii) making the most efficient use of the climate dataset. Owing to the amount of RAM required to store the climate files, they are deleted immediately after all the model runs have been completed. This frees up space in the RAM drive to store the post-processed data and to compress all output that has been generated, i.e. by AquaCrop and the statistics utility.

Since the faster PC has 32 GB more RAM than the slower PC, other changes were made to further improve the performance of the model runs. For example, instead of calculating statistics and compressing model output immediately after AquaCrop has finished running in each thread, these two procedures are now run only once, after all parallel model runs have been completed, i.e. for all crops and all time periods. This important change could only be implemented due to the additional RAM, allowing for the RAM drive to be sized accordingly. The stats utility is written in Fortran and is multi-threaded, and thus automatically splits the analysis equally over all available CPU threads. The statistics only take 67 seconds to generate data for all 5,838 HRZs. Certain statistics (e.g. mean, median and coefficient of variation) required for mapping purposes are then extracted from the statistical output files to create .CSV files. Thereafter, the WinRAR utility is used to compress all model output, which also utilises all CPU threads, taking 142 seconds to finish.

On the slower PC with only 32 GB of RAM, the (i) generation of statistics, and (ii) extraction of certain statistical values, could only be after the model runs had been completed for each crop and time period (due to the limited size of the RAM drive) and AquaCrop’s output had been compressed and moved to permanent disk storage. The process involved (i) copying the compressed AquaCrop output files to the RAM drive, (ii) uncompressing them, (iii) then generating the statistics, and finally (iv) extracting various statistical values. Thereafter, the AquaCrop output files were deleted from the RAM drive to free up space for compressing the statistical and extracted statistical files. This highlights the need to have sufficient RAM so that the model runs can be efficient as possible, since it facilitates the generation of statistics and data extraction immediately after the model runs have been completed.

The various utilities that were developed to run AquaCrop for multiple seasons and HRZs also require input parameters read in from a file. These input files are re-created each time the model runs, even though the HRZ and season year are the only variables that change. To further improve performance, file templates were created, thus preventing static information (e.g. storage paths) from being re-created. Hence, the zone and season numbers are the only variables being changed in the template files before each model run.

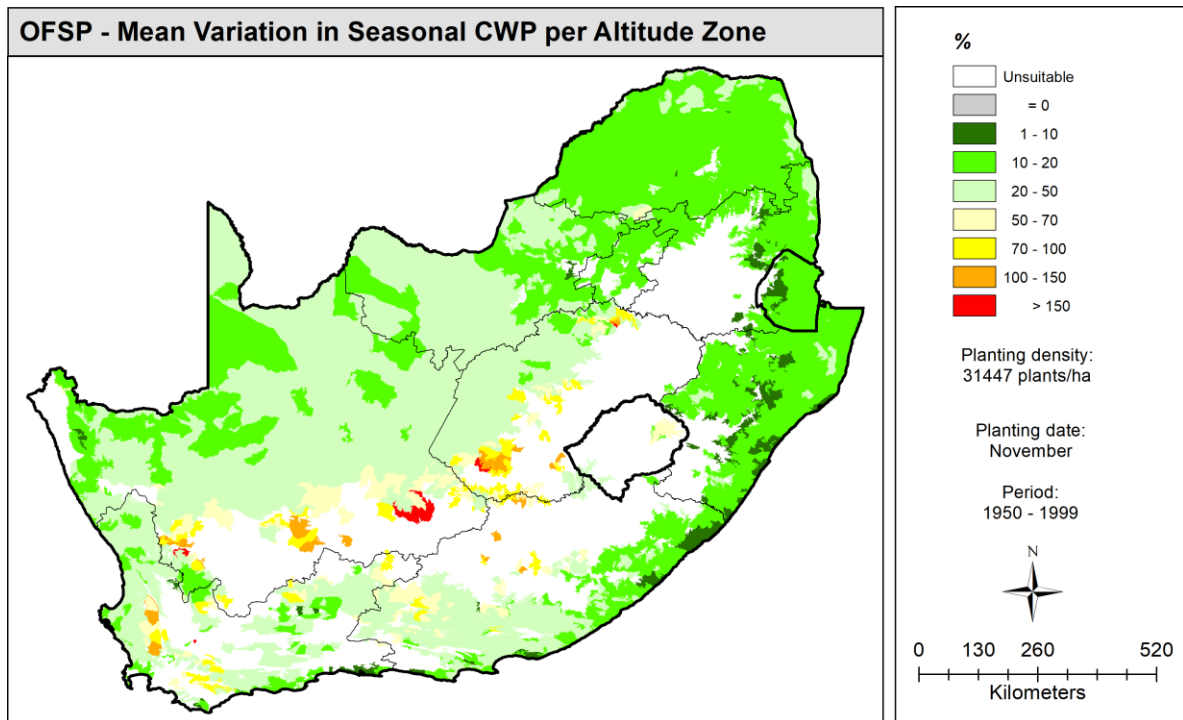
When AquaCrop generates an error (e.g. “division-by-zero” error) message, the user is required to click the “OK” button, thus acknowledging this error message. AquaCrop then “hangs” and needs to be manually terminated and re-started. Since 2015, various techniques were used to automatically close the error message window, then to stop and re-start the model runs (cf. **Section 17.1.4**). In 2019, separate tasks were started to monitor AquaCrop runs by each CPU thread (i.e. 10 or 12 tasks in total). In 2023, this was reduced to only one task that monitors all simultaneous model runs. Since this single task runs more efficiently than 12 separate tasks, model crashes are detected quicker, thus resulting in improved performance.

17.3.12 Model run time

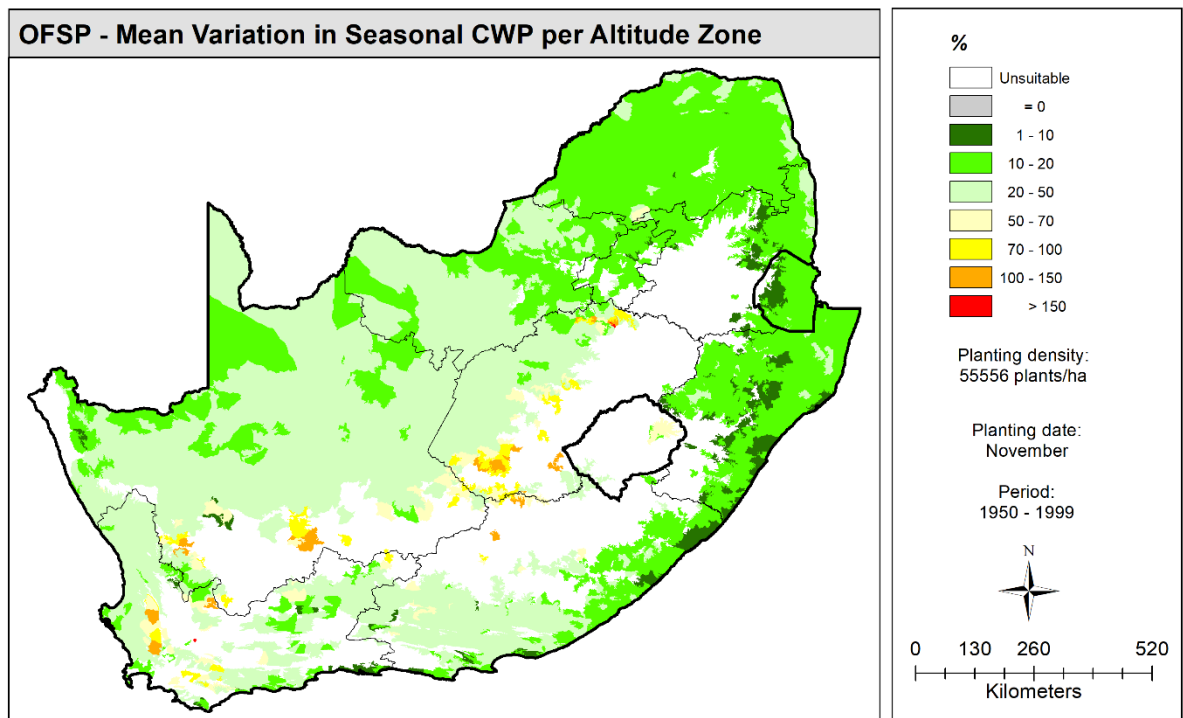
As highlighted in **Table 17-7**, a national run using 30 years of climate input data for one crop takes ~2.8 hours to complete, which increases to ~3.4 hours with 50 years of climate input data. This represents a substantial improvement compared to the first runs in 2015 that took over 62 hours. The effort has allowed additional modelling scenarios to be considered, such as multiple GCMS, planting dates and/or plant densities.

18 APPENDIX I

18.1 INTER-SEASONAL VARIATION IN CWP: OFSP

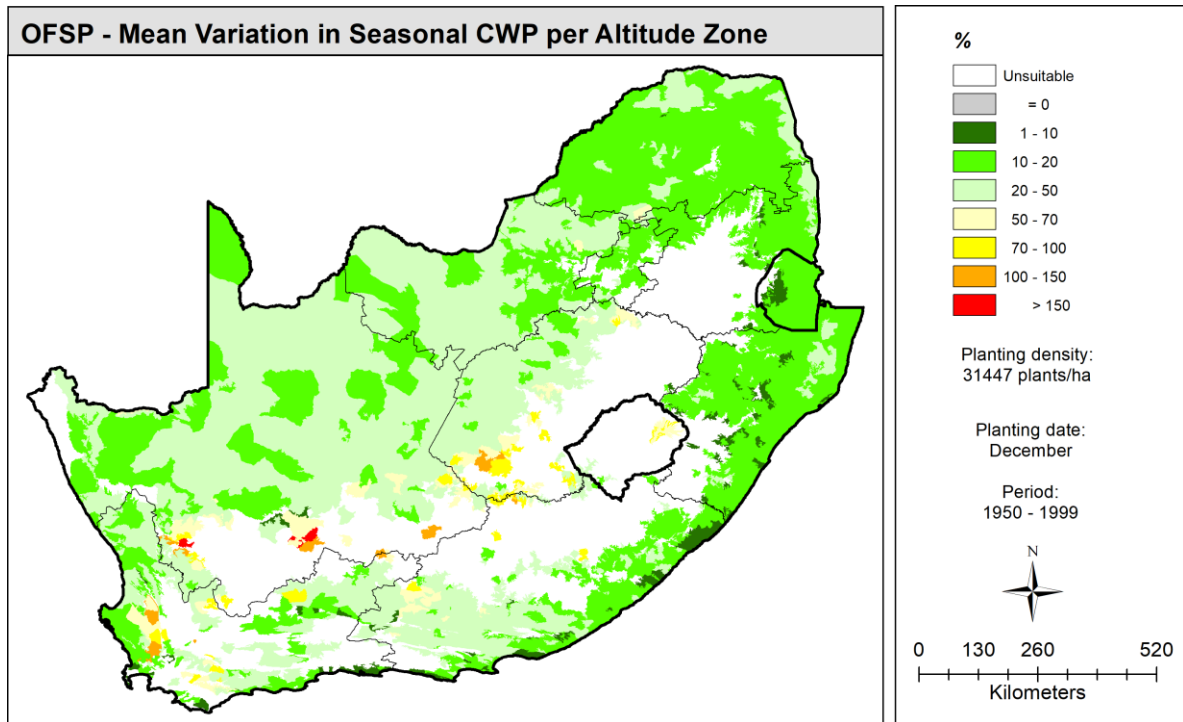


(a)

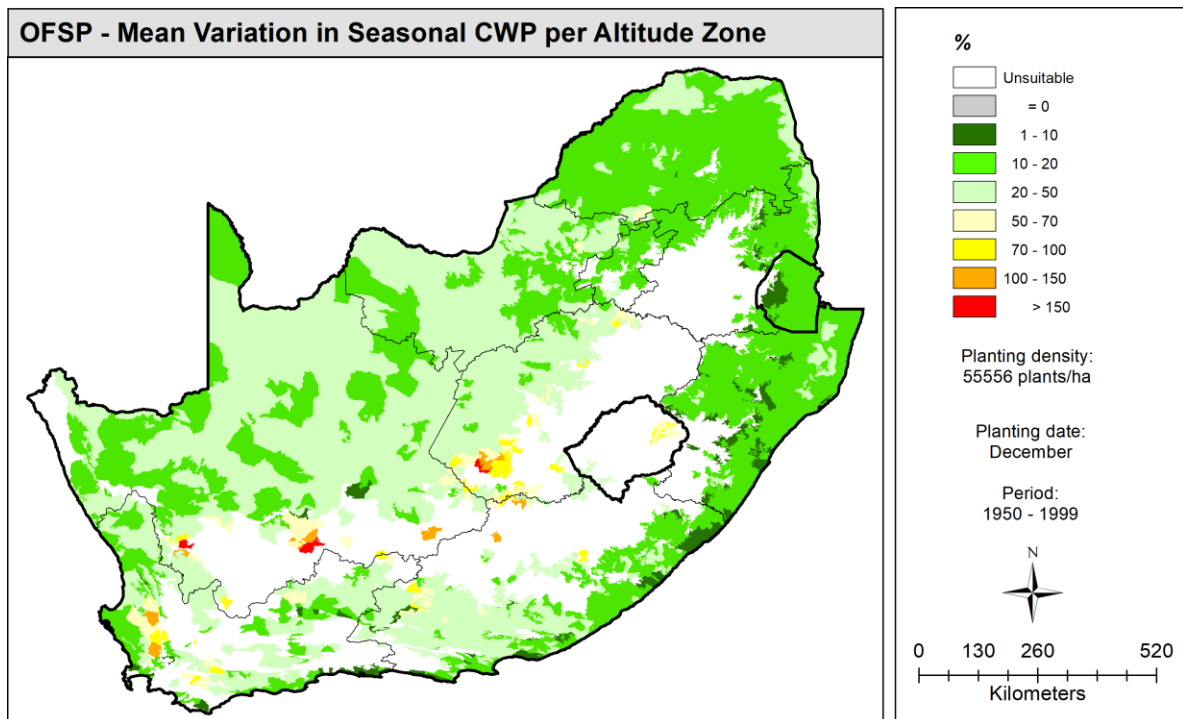


(b)

Figure 18-1 Inter-seasonal variation in CWP for OFSP planted in November at a density of (a) 31,447 and (b) 55,556 plants ha⁻¹



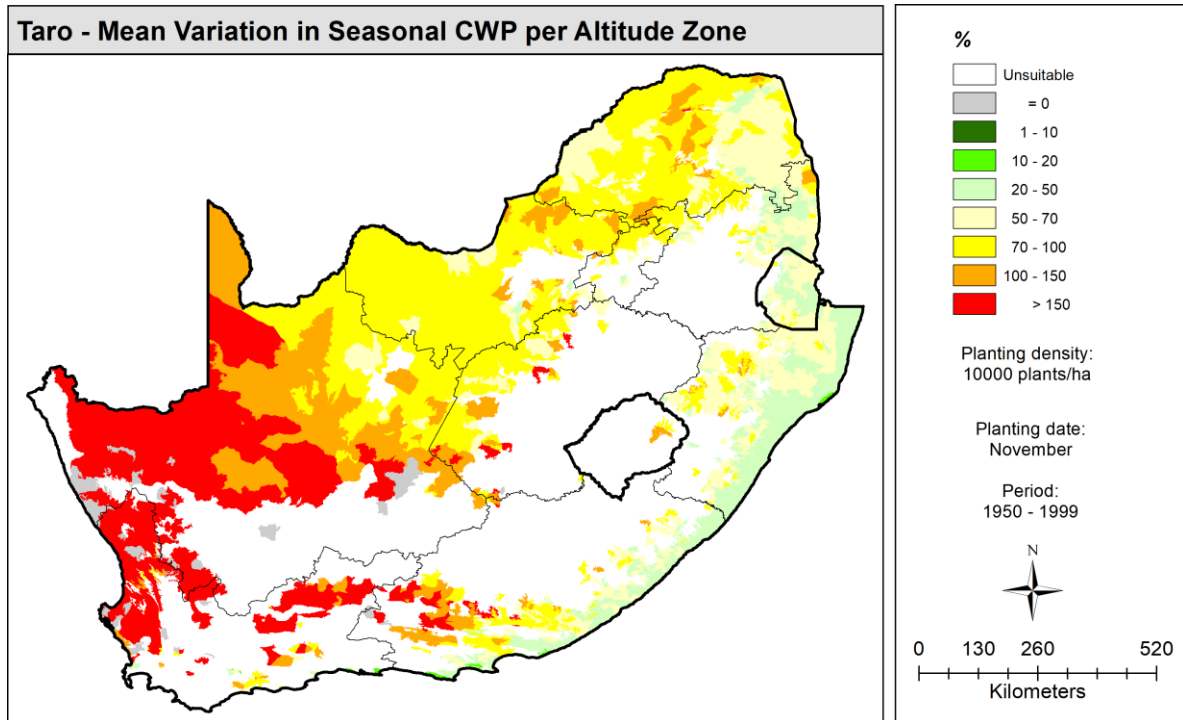
(a)



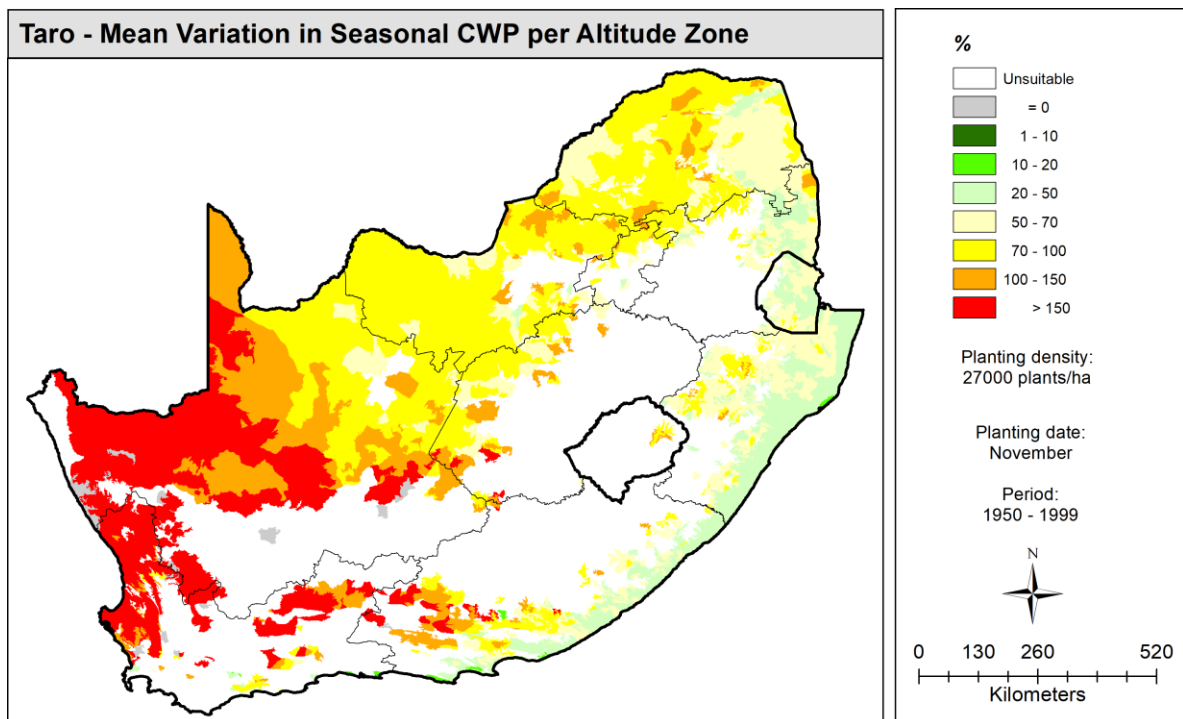
(b)

Figure 18-2 Inter-seasonal variation in CWP for OFSP planted in December at a density of (a) 31,447 and (b) 55,556 plants ha⁻¹

18.2 INTER-SEASONAL VARIATION IN CWP: TARO

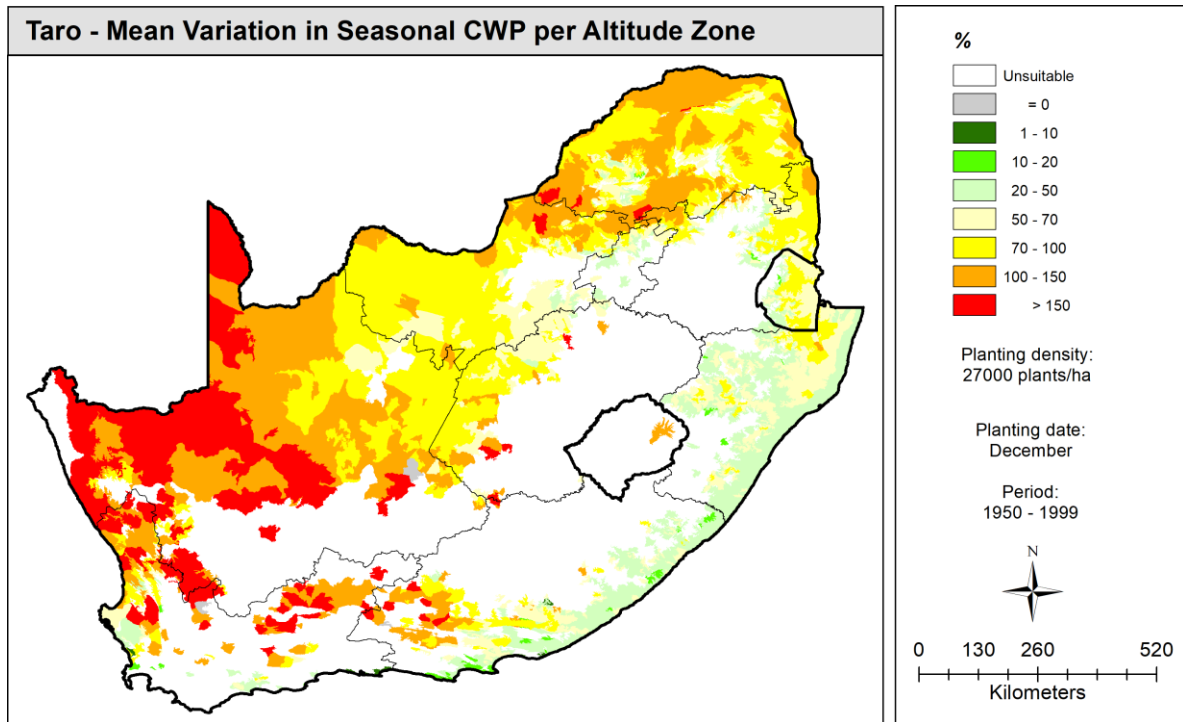


(a)

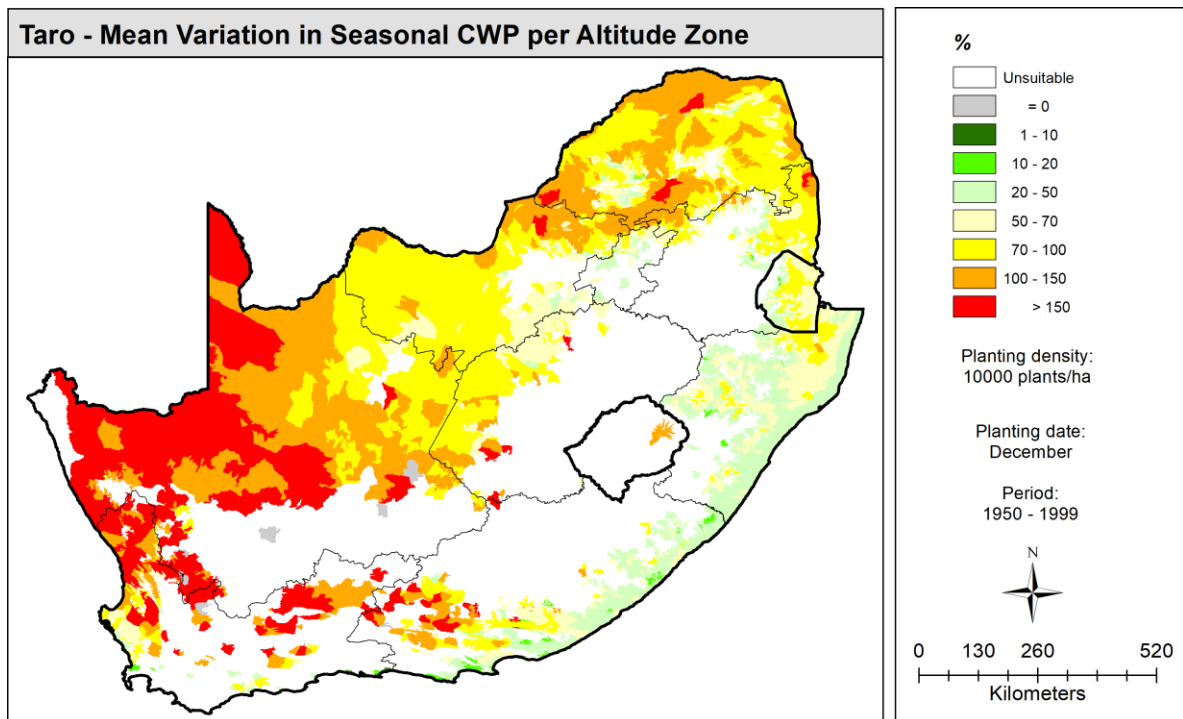


(b)

Figure 18-3 Inter-seasonal variation in CWP for taro planted in November at a density of (a) 10,000 and (b) 27,000 plants ha⁻¹



(a)



(b)

Figure 18-4 Inter-seasonal variation in CWP for taro planted in December at a density of (a) 10,000 and (b) 27,000 plants ha⁻¹

19 APPENDIX J

Based on a review undertaken by Lake (2022), different methods have been used to develop land suitability maps, which have been classified as either (i) traditional, or (ii) modern methods (Akpoti et al., 2019). The traditional methods mainly involve the use of GIS and are typically qualitative, quantitative and parametric based. The modern techniques consider multi-criteria evaluation, remote sensing and machine learning approaches (Akpoti et al., 2019).

19.1 TRADITIONAL METHODS

The majority of land suitability mapping is undertaken using traditional methods that are based on overlays of certain optimum growth criteria. These criteria are typically based on (i) the crop, and (ii) the availability of spatial and temporal datasets. Traditional methods assess crop options using qualitative, quantitative and parametric methods based on biophysical characteristics (Mugiyo et al., 2021a). These methods are categorised by lack of categorical data as well as socio-economic data. A number of case studies are presented next in chronological order. These case studies provide a brief description of the methodology used to develop the land suitability maps.

19.1.1 Case study 1: Holl et al. (2007)

Holl et al. (2007) considered the production of *Jatropha curcas* in South Africa, assessing its water use and bio-physical potential. For the latter, a land suitability map was produced by applying thresholds (i.e. cut-off values) to five criteria, namely rainfall, temperature, soils, frost and slope. The following three-tiered approach was used:

- 1) elimination of areas that are unsuitable for crop production,
- 2) yield estimates were then calculated using a weighted modelling approach based on climate and other data, and
- 3) a formal equation-driven analysis was used to produce estimates of potential yield.

The method used by Holl et al. (2007) provided a more detailed description of areas suitable for production. The three-tiered approach allowed unsuitable areas to be removed first and thus, only remaining areas deemed suitable were further divided into land suitability classes. For step 2, the selected criteria (e.g. rainfall and temperature) were weighted according to their relative importance in determining crop yield. With the aid of GIS (Geographic Information System), the weightings were then used to calculate spatial estimates of initial yield. At the time of the study, there was no *jatropha* yield equation for South African growing conditions. As a result, sunflower yield and tree growth equations were combined and then adjusted according to the sensitivities and tolerances for *jatropha* (Holl et al., 2007). The equation was then used to estimate *jatropha* yield. Yield categories were developed using statistical properties, assuming that yield follows a normal distribution. The final map identified areas suitable for *jatropha* production based on the estimated yields.

19.1.2 Case study 2: Jewitt et al. (2009a)

Jewitt et al. (2009a) developed land suitability maps identifying potential growing areas for selected biofuel crops such as cassava, canola, *jatropha*, sweet sorghum, sugarbeet, soybean (**Figure 19-1**) and sunflower. The study involved simple overlays of rainfall and temperature data using a GIS that highlighted optimum growing areas. Climatic thresholds for optimum growth were sourced from the available literature. These thresholds were then applied to spatial datasets of rainfall and temperature to identify areas deemed suitable and unsuitable for growth.

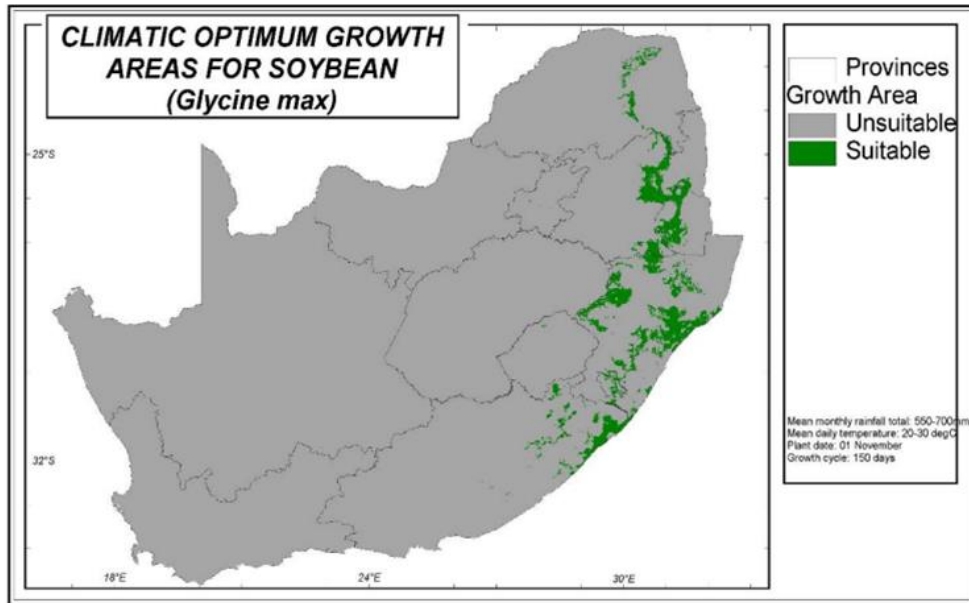


Figure 19-1 Land suitability map for soybean production (Jewitt et al., 2009a)

19.1.3 Case study 3: Kunz et al. (2015b)

Kunz et al. (2015b) also developed land suitability maps that identified areas suitable for biofuel crop cultivation. The study focused on sugarcane, sugarbeet, grain sorghum, soybean (Figure 19-2) and canola. The maps were created by applying five criteria, namely rainfall, temperature, relative humidity, soil depth and slope. The selection of these criteria was based on a study undertaken by Khomo (2014) for soybean. The criteria were then applied to distinguish between suitable (highly suitable (S1), marginally suitable (S2), moderately suitable (S3) and unsuitable (N1) growing areas.

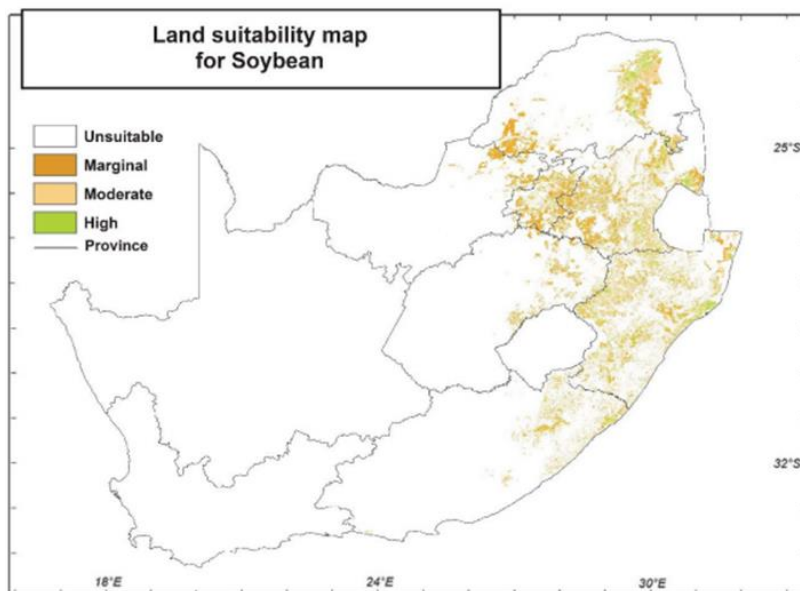


Figure 19-2 Land suitability map for soybean production (Kunz et al., 2015c)

The study followed the first two phases from Holl et al. (2007) (cf. Section 19.1.1). Firstly, permanently unsuitable areas for production (N2) were eliminated such as urban and protected areas, as well as water bodies. Thereafter, criteria were then ranked according to their relative importance in determining crop growth. The latter weightings were based on expert opinions and thus, were subjective. Rainfall was considered most important for crop growth (weighted at 40%), followed by temperature and slope

(each 20%) and relative humidity and soil depth (each 10%). Kunz et al. (2015b) stated that the distribution of rainfall during the growing season and temperature stresses impact the crop's growth. Since rainfall is not distributed evenly over the growing season, a monthly crop coefficient (K_C) approach was used to determine the crop's rainfall requirement in each month (or growth stage). Finally, currently unsuitable areas (N1) such as degraded lands and commercial forestry plantations were removed.

19.1.4 Case study 4: Khalid et al. (2021)

Khalid et al. (2021) identified and mapped suitable sites for bioenergy production using *Jatropha curcas* in the northern region of Pakistan. The study applied a fairly unique approach to mapping land suitability and adopted the following two methods as follows:

- 1) The first applied selected thresholds to climate, elevation and slope data to determine three suitability classes (more, moderate and less suitable). This was similar to previous studies involving *Jatropha curcas* that predominantly used climate (rainfall and temperature), elevation and slope data (e.g. Holl et al., 2007; cf. **Section 19.1.1**). The study area was divided into smaller sub-regions using the Thiessen polygon method based on climate and soil data input.
- 2) The second method used FAO's AquaCrop model (Steduto et al., 2009) with inputs of, *inter alia*, crop density, canopy cover, harvest index and threshold temperature, to estimate the expected yield of jatropha. Owing to the lack of reliable information on jatropha yield, the study used simulated yield (Y in $t\ ha^{-1}$) in order to fill this knowledge gap. The model was also used to estimate the water productivity (WP in $t\ m^{-3}$) of jatropha. From the modelled output, the water footprint (WF in $m^3\ t^{-1}$) was calculated as $1/WP$. The study undertook a simple overlay of Y and WF within each of the suitability classes, which showed that, as expected, the most suitable areas were associated with high Y and low WF .

19.2 MODERN TECHNIQUES

Akpoti et al. (2019) described modern land suitability methods as those that consider more complex methods that require additional input datasets, compared to the simpler, traditional methods (cf. **Section 19.1**), as they. Mugiyo et al. (2021a) highlighted three main categories of modern methods, namely those that made use of:

- computer assisted (e.g. GIS, remote sensing and cloud computing) technologies,
- machine learning (e.g. species distribution models such as MaxEnt, fuzzy rule-based systems and artificial neural networks), and
- multi-criteria decision analysis (MCDA), in particular the Analytical Hierarchy Process (AHP).

Mugiyo et al. (2021a) also identified a fourth category involving the use of crop simulation models. An analysis of 101 papers related to land suitability assessment showed that the most common method involved machine learning (25.7%), followed by AHP (14.9%), fuzzy logic (12.9%) and crop simulation models (9.9%). Based on this, a number of case studies are presented next, which focus on the two most common methods used in land suitability studies.

19.2.1 Machine learning

The Maximum Entropy (MaxEnt) model is a general-purpose machine learning approach with an intuitive and exact mathematical formulation (Phillips et al., 2006; Phillips and Dudik, 2008) that was designed to predict species distributions. However, it has also been used to identify suitable areas for crop cultivation (Mugiyo et al., 2022). A presence dataset is used to train MaxEnt, which represents a list of geographical coordinates (i.e. point locations) where the target species (or crop) has been successfully grown in the past. The presence points, together with selected predictor variables (e.g. rainfall and temperature), are used by MaxEnt to predict the suitability of other locations to species/crop

growth. Hence, MaxEnt can be used to create land suitability maps by predicting the probability of current crop growth at a specific location, which ranges from 0 (unsuitable for growth) to 1 (ideally suited for growth). Two case studies are presented next that used MaxEnt to develop land suitability maps for crops grown in South Africa.

19.2.1.1 Case study 5: Estes et al. (2013)

Estes et al. (2013) used the MaxEnt model to create a land suitability map for the cultivation of maize in South Africa. The study made use of both presence and absence data points. The absence points represented unsuitable maize growing areas. In total, 11,390 presence points and 11,390 absence points were used. Five criteria (minimum and maximum temperature, seasonal precipitation, soil depth and topsoil organic carbon) were used to predict maize suitability. MaxEnt was also trained with high-productivity occurrence points, which improved the prediction considerably. Estes et al. (2013) also used the DSSAT crop model to produce a land suitability map using the climate and soil databases available for the quinary sub-catchments. The study showed that both MaxEnt and DSSAT were equally successful in predicting overall crop suitability when compared to a land suitability map produced from observed maize yield data. It is important to note that this study demonstrated the ability of crop yield models to predict land suitability.

19.2.1.2 Case study 6: Taghizadeh-Mehrjardi et al. (2020)

Other types of machine learning algorithms that are used for land suitability mapping include Random Forest (RF) and Support Vector Machine (SVM). Taghizadeh-Mehrjardi et al. (2020) used these two algorithms to develop land suitability maps for rainfed wheat and barley in western Iran. The RF and SVM algorithms were chosen because they work well when large amounts of training data are not available. A square root method was used to calculate land suitability, which considered 11 criteria, namely rainfall, temperature, slope, soil texture, soil depth, gravel, CaCO₃, soil pH, organic carbon, electrical conductivity and exchangeable sodium percentage. The study also followed the land suitability classes developed by the FAO (1976), where N₂, N₁, S₃, S₂ and S₁ were given ranges of 0-12.5, 12.5-25, 25-50, 50-75 and 75-100, respectively. The map generated using the two machine learning algorithms was then compared to a traditional land suitability map.

19.2.1.3 Case study 7: Mugiyo et al. (2022)

Mugiyo et al. (2022) also used MaxEnt to identify suitable growing areas for selected indigenous crops (i.e. sorghum, cowpea, amaranth and taro). The study used 240 coordinates representing indigenous crop growing areas in KwaZulu-Natal, of which half were used for model training and the other half for model validation. The predictor variables were as follows:

- four climatic (seasonal precipitation, maximum temperature, minimum temperature & length of growing period),
- seven soil (available soil water capacity, soil pH, soil depth, soil texture & fraction of clay, silt and sand),
- two topographic (elevation & slope), and
- two socio-economic variables, namely 1 distance along road network (ACCESS) and distance to metro cities (EUCDIST).

The maps were then produced using the mean and 95th percentile of 1,000 model runs that were conducted for crop suitability. The suitability classes were defined as highly suitable (S₁; suitability index > 0.80, moderately suitable (S₂; 0.60-0.79), marginally suitable (S₃; 0.20-0.59) and unsuitable (N₁; < 0.19). The map produced for taro in KZN is shown in **Figure 19-3**.

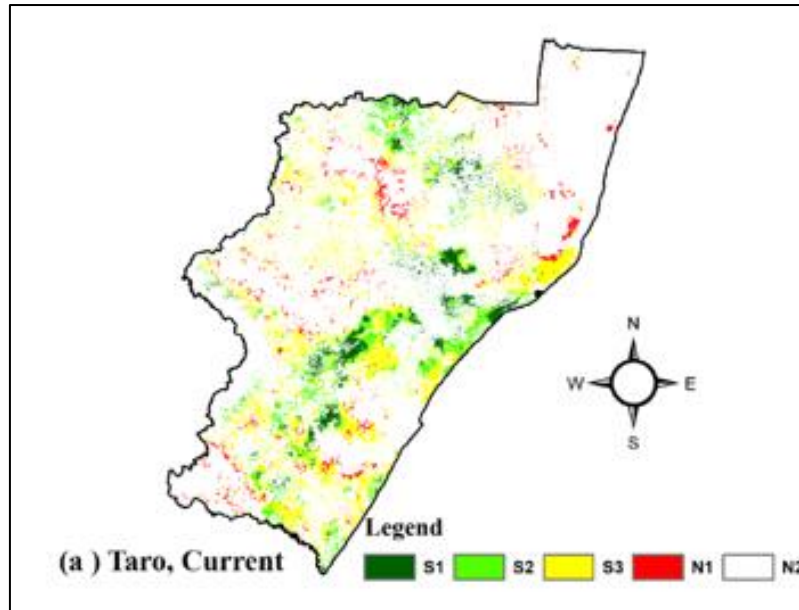


Figure 19-3 Land suitability map for taro in KZN using MaxEnt (Mugiyo et al., 2022)

MaxEnt also outputs the contribution of each predictor variable to the overall suitability index. These contributions are displayed as jack-knife plots (Figure 19-4). The plot showed the importance of precipitation in predicting taro suitability, followed by length of growing period and temperature. Soil depth, soil pH and slope provided the least contributions to overall suitability. Similarly, the two socio-economic variables (EUCDIST and ACCESS) did not contribute much to predictability (Figure 19-4).

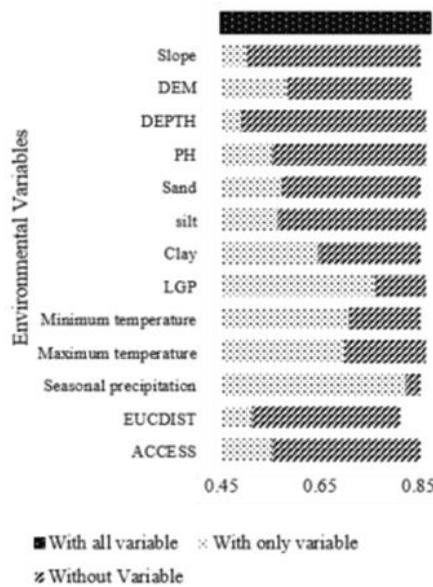


Figure 19-4 Jack-knife plot evaluating the relative importance of environmental variables for predicting suitability for taro cultivation (Mugiyo et al., 2022)

19.2.2 Analytical hierarchy process

One of the most widely used and most reliable MCDA methods is AHP (Mugiyo et al., 2021a). The AHP method developed by Saaty (2008) has been used to deal with complex decision making (Mugiyo et al., 2021a). The method uses pairwise comparisons to capture both subjective and objective components of decision making and then synthesises the outcome into a single index (Saaty, 2008).

AHP uses a nine-point scale that weights each criterion according to its importance (Mugiyo et al., 2021a). A score of 1 means that each of the two criteria have equal importance, whereas 9 means one of criterion is far more important than the other (**Table 19-1**). Two case studies are presented next that used AHP to develop land suitability maps.

Table 19-1 The fundamentals for pairwise comparison (Saaty, 2008)

Intensity of importance	Definition	Explanation
1	Equal importance	Two activities contribute equally to the objective
3	Moderate importance of one over another	Experience and judgement slightly favour one activity over another
5	The strong or essential importance	Experience and judgement strongly favour one activity over another
7	Very strong or demonstrated importance	One activity is strongly favoured, and its dominance showed in practice
9	Extreme importance	The evidence favouring one activity over another is of the highest possible order of affirmation
2, 4, 6 & 8		Even numbers represent intermediate values between the two adjacent judgements

19.2.2.1 Case study 8: Mufungizi et al. (2020)

Mufungizi et al. (2020) also developed land suitability maps using AHP for maize and sorghum in the Vhembe district of South Africa. The study used (i) the AHP method to determine the criteria weightings as described by Saaty (2008), and (ii) the weighted linear combination method to synthesise the preference information (Chou, 2013). The maps were created by applying six criteria identified from a literature review, namely soil pH, soil structure, elevation, rainfall, maximum and minimum temperature. For both crops, soil pH and soil structure were found to be the most important criteria for growth, which differs to the weightings produced by MaxEnt for taro (cf. **Figure 19-4**). Some crops need more acidic soils, whereas others (e.g. maize) prefers a neutral soil for optimum growth. Hence, the soil pH criterion for sorghum was assigned a slightly higher weighting than compared to maize. Since maize requires between 450 to 600 mm of water per season (du Plessis, 2003), rainfall for maize was assigned a higher ranking (3rd) compared to sorghum, which is considered a drought resistant crop. Maximum temperature for maize is the least important variable (ranked 6th), compared to a ranking of 3 for sorghum.

19.2.2.2 Case study 9: Mugiyo et al. (2021b)

Mugiyo et al. (2021b) used AHP to create a land suitability map for four indigenous crops, namely sorghum, cowpea, taro and amaranth. The nine criteria used in the pairwise comparison were as follows: rainfall, temperature, reference evapotranspiration, length of growing period, elevation, slope, land use land cover, soil depth and distance from road. Mugiyo et al. (2021b) assigned the highest pairwise weighting to rainfall, whereas distance from the road had the lowest weighting. AHP then calculates the overall weighting for each criterion using Eigenvectors. For each pairwise comparison, a consistency ratio and random index were used to calculate a consistency index, which must be below 0.1 in order to be accepted. After the weightings were determined, the weighted linear combination method was applied. The final suitability index was determined using Liebig's law of the minimum. The study also followed the land suitability classes developed by the FAO (1976), where N2, N1, S3, S2 and S1 were assigned a final suitability index 0-29, 30-44, 45-59, 60-80 and > 80, respectively. The map produced for taro is shown in **Figure 19-5**, which identifies very few areas deemed highly suitable

for taro cultivation (Mugiyo et al., 2021b). This is in contrast to the map produced by Mugiyo et al. (2022) using the MaxEnt model (cf. **Figure 19-3**).

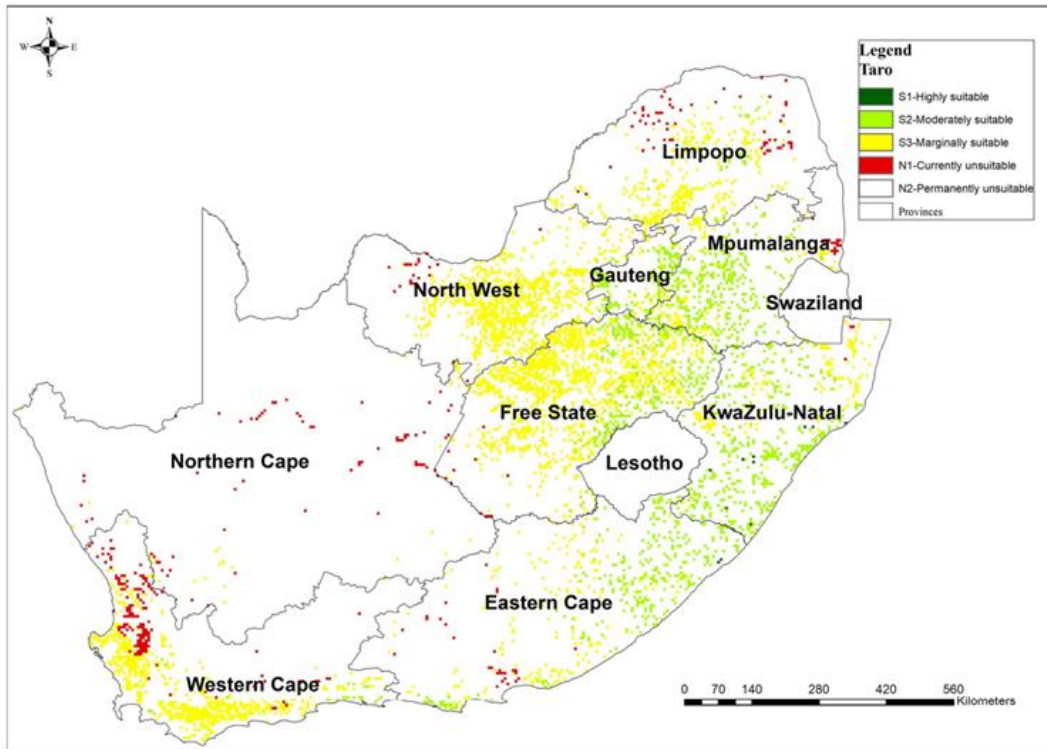


Figure 19-5 Land suitability map for taro based on AHP (Mugiyo et al., 2021b)

19.3 DISCUSSION AND CONCLUSIONS

Various methods exist to develop land suitability maps that range from (i) traditional methods involving simple overlays of spatial data (e.g. climate and soils), to the (ii) more complex modern methods involving remoted sensing, machine learning, AHP and computer simulation models. The advantages of using traditional methods for land suitability assessment is that they (i) are simple, (ii) less time consuming to apply, and (iii) can provide relatively accurate results. This accuracy is, however, dependent on the number of variables used, i.e. in general, the more variables, the greater the accuracy of the map. The disadvantages are that the (i) thresholds are not always known for a particular crop (especially for neglected and underutilised crops), (ii) the weightings of each variable are subjective, and (iii) some variables are not independent (i.e. collinear). The advantages of using the modern methods are that (i) they tend to provide more accurate results, and (ii) methods such as MaxEnt provide objective (rather than subjective) criteria weightings. However, such methods are more complex and time consuming to implement (Lake, 2022).

Of the nine case studies presented, two traditional approaches utilised crop yield data. Firstly, Holl et al. (2007; cf. **Section 19.1.1**) developed a simple yield equation for jatropha and then applied it to identify areas deemed suitable for production. Secondly, Khalid et al. (2021; cf. **Section 19.1.4**) used AquaCrop yield estimates to verify land suitability classes derived using a traditional approach. Their results showed that, as expected, the most suitable areas were associated with high yield and low water footprint. For the modern methods, Estes et al. (2013; cf. **Section 19.2.1.1**) produced a land suitability map for maize using a large database of observed yield data, which was then compared to maps developed using (i) MaxEnt, and (ii) yield data simulated by the DSSAT model. The comparison showed that both approaches produced similar results to that obtained using observed yield data. Taghizadeh-Mehrjardi et al. (2020; cf. **Section 19.2.1.2**) compared potential crop yield to actual yield to determine input efficiencies. Therefore, only four of the nine case studies utilised crop yield data to determine land

suitability for crop production, which is surprising considering the fact that suitability class and yield are closely related, i.e. high suitability equates to high yields. Of these, two case studies utilised output from crop simulation models (AquaCrop and DSSAT), which Mugiyo et al. (2021a) identified as the fourth category of modern methods (Lake, 2022).

20 APPENDIX K

20.1 NATIONAL LAND COVER OF 2009

Khomo (2014) obtained spatial datasets of (i) protected areas (formal), and (ii) national land cover (2009) from SANBI's Biodiversity-GIS [data portal](#). These two spatial datasets were combined to identify the following land covers/uses deemed unsuitable areas for crop production:

- protected areas (e.g. nature reserves, national parks, world heritage sites and protected natural forests),
- urban (built-up) areas, rural clusters and smallholdings,
- water bodies (lakes, dams and wetlands),
- natural (indigenous forest, woodland, bushland, shrubland, hermland, Fynbos),
- commercial forest plantations, and
- bare rock/soil and degraded land.

All areas that were classified as suitable for soybean cultivation that overlapped with the unsuitable areas (**Figure 20-1**) were excluded using GIS.

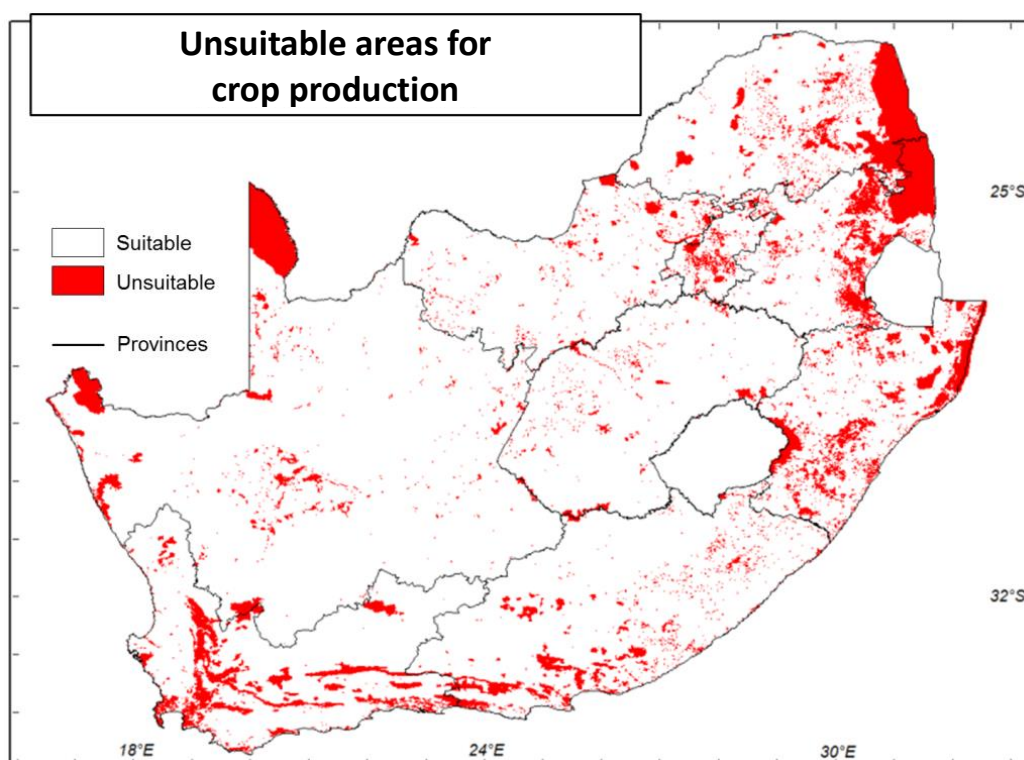


Figure 20-1 Location of areas considered unsuitable for crop production in South Africa (after Khomo, 2014)

20.2 NATIONAL LAND COVER OF 2018

In this project, a similar approach to that adopted by Khomo (2014) was used. Land uses that are permanently unsuitable (N2) for crop production were identified, i.e. mining, water bodies, wetlands, protected and urban areas. Similarly, areas that are currently not suitable (N1) were also identified, such as indigenous forests, orchards, commercial forestry and sugarcane production areas. Well established industries are unlikely to switch to RTC production. The clearing of indigenous forests for

crop cultivation should be avoided to protect their high biodiversity potential. The 2018 national land cover map (1 km² resolution) and the 2022 protected areas dataset were obtained from [SAEON](#) and [DFFE](#), respectively. The latter dataset was imported into ArcGIS and converted from vector to raster format. If the land cover occupied more than 50% for each 1 km² grid cell (or pixel), it was assumed the entire pixel had the same land use. The land use raster layers were then combined and reclassified as 1 (N1) and 2 (N2), as shown in **Figure 20-2**.

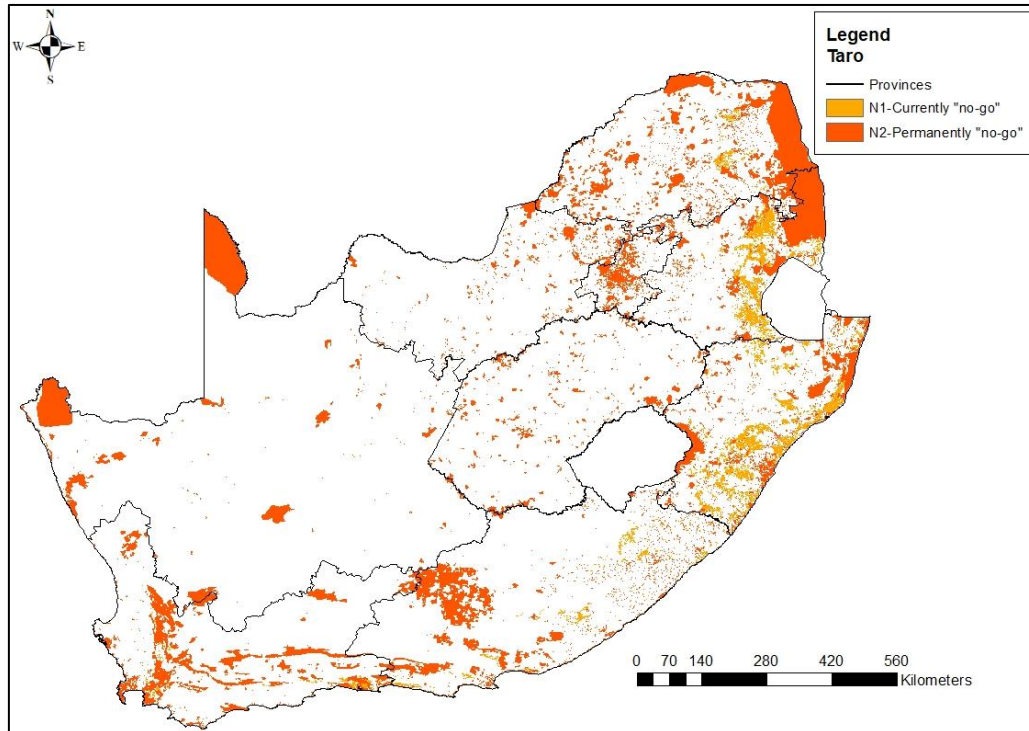


Figure 20-2 Unsuitable land uses for crop production based on the 2018 national land cover dataset (Lake, 2022)